

4. GUAYMAS BASIN: SITES 477, 478, AND 481¹

Shipboard Scientific Party²

BACKGROUND AND OBJECTIVES

Introduction

The Guaymas Basin sites constitute the second area of investigation by Leg 64 in the Gulf of California. Sites 477, 478, and 481, included within this cluster, represent the combined interest of the Ocean Crust, Passive Continental Margin, and Ocean Paleoenvironment Advisory Panels. Drilling was proposed for Guaymas Basin because the high rate of influx of sediment makes it possible here to drill both into very young ocean crust and into "zero-age" crust of the spreading axis itself. The Guaymas Basin offers an opportunity to examine the kind of ocean crust which is formed when volcanic rocks of the spreading axis are not extruded on the sea floor, but are instead intruded into young, soft sediments with high water content. This type of oceanic crust may be important in the early stages of opening of new oceans and formation of new rift-origin continental margins.

Structure, Tectonics, and Geophysics

A plate-tectonic model and the geological history have already been presented for the Gulf as a whole. Guaymas Basin (Figs. 1 and 2) includes two short segments of spreading axis, separated by a short transform fault, and flanked by long transform faults which extend to the northwest to San Pedro Mártir or Sal Si Puedes Basins and to the southeast to Carmen Basin.

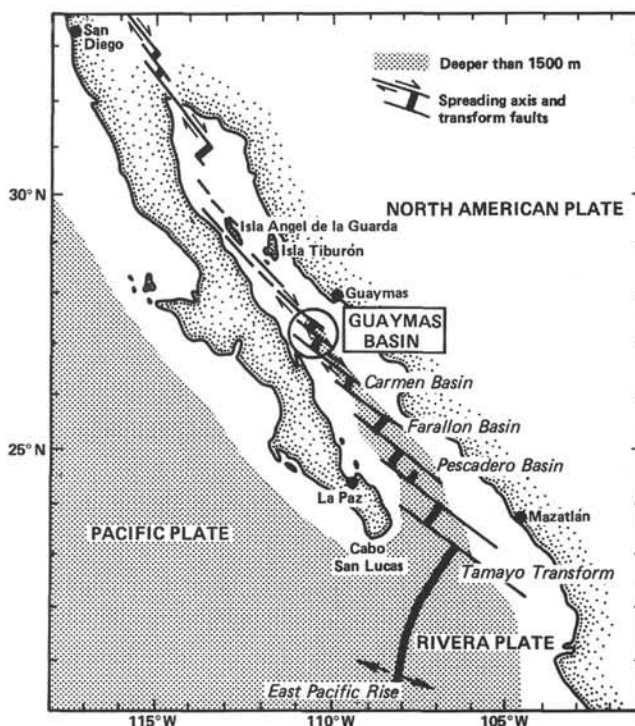


Figure 1. Tectonic features of the Gulf of California. Location of Guaymas Basin Sites.

These long transform faults presumably separate the ocean crust accreted during the present phase of opening of the Gulf from either continental crust or proto-Gulf oceanic crust.

Sharman (1976) examined details of spreading axes and transform faults in several deep basins of the Gulf, including Guaymas Basin. He proposed a scenario of evolution of spreading axes and transforms modeled after a laboratory analog of freezing paraffin. He postulated that the evolution consists of an initial resolution of arbitrary rift boundaries to a set of orthogonal spreading axes and transform faults. The segments of spreading axes and transform faults become fewer with time, and larger through coalescence.

Magnetics in these basins of the Gulf cannot be resolved into identifiable oceanic anomalies. Larson et al. (1972) followed a suggestion of Vogt et al. (1970) in suggesting that normal thermal remnant magnetism would not be acquired as readily in basaltic rocks intruded into sediment, in contrast to those extruded on the sea floor. Sharman (1976) suggested in addition that plate-edge jumps would further inhibit formation of correlatable oceanic magnetic anomalies.

¹ Curry, J. R., Moore, D. G., et al., *Init. Repts. DSDP*, 64: Washington (U.S. Govt. Printing Office).

² Joseph R. Curry (Co-Chief Scientist), Geological Research Division, Scripps Institution of Oceanography, La Jolla, California; David G. Moore (Co-Chief Scientist), Deep Sea Drilling Project, Scripps Institution of Oceanography, La Jolla, California (present address: Geological Research Division, Scripps Institution of Oceanography, La Jolla, California); J. Eduardo Aguayo, Instituto Mexicano del Petróleo, México 14, D. F., México; Marie-Pierre Aubry, Woods Hole Oceanographic Institution, Woods Hole, Massachusetts, and Laboratoire de Géologie des Bassins Sédimentaires, Université Pierre et Marie Curie, Paris, France; Gerhard Einsele, Geologisches Institut der Universität Tübingen, Tübingen, Federal Republic of Germany; Daniel Fornari, Lamont-Doherty Geological Observatory, Columbia University, Palisades, New York (present address: Department of Geology, State University of New York at Albany, Albany, New York); Joris Gieskes, Ocean Research Division, Scripps Institution of Oceanography, La Jolla, California; José Guerrero-García, Instituto de Geología, Universidad de México, México, D. F., México; Miriam Kastner, Geological Research Division, Scripps Institution of Oceanography, La Jolla, California; Kerry Kelts, Deep Sea Drilling Project, Scripps Institution of Oceanography, La Jolla, California (present address: Eidgenössische Technische Hochschule, Geologisches Institut, Zürich, Switzerland); Mitchell Lyle, Department of Geology, Stanford University, Stanford, California (present address: School of Oceanography, Oregon State University, Corvallis, Oregon); Yasumochi Matoba, Department of Geology, Stanford University, Stanford, California (present address: Institute of Mining Geology, Mining College, Akita University, Akita, Japan); Adolfo Molina-Cruz, Instituto de Geología, Universidad de México, México, D. F., México; Jeffrey Niemitz, Department of Geology, Dickinson College, Carlisle, Pennsylvania; Jaime Rueda-Gaxiola, Tecnología de Exploración, Instituto Mexicano del Petróleo, México, D. F., México; Andrew Saunders, Department of Geological Sciences, The University, Birmingham B15 2TT, United Kingdom (present address: Department of Geology, Bedford College, London, United Kingdom); Hans Schrader, School of Oceanography, Oregon State University, Corvallis, Oregon; Bernd R. T. Simoneit, Department of Geophysics and Planetary Physics, University of California, Los Angeles, California (present address: School of Oceanography, Oregon State University, Corvallis, Oregon); and Victor Vacquier, Graduate Division, Scripps Institution of Oceanography, La Jolla, California.

Seismic-refraction work by Phillips (1964) (Fig. 3) shows that the Guaymas Basin lies north of apparently normal oceanic crust in the axis of the Gulf. At this latitude in mid-Gulf, the structure starts to show a marked deviation from "normal oceanic" section: Layer 1 (sediment), Layer 2 (4.2-4.5 km/s basement of basalts, possibly with some sediments), Layer 3 (6.5-6.9 km/s, "ocean crust"), and mantle. Here in contrast, a more-gradational increase in velocity occurs, and the lower layer, with a velocity of 6.5 to 6.7 km/s, is more deeply buried beneath "sediments" and is thicker than the oceanic counterpart. Thickening also increases markedly to the north. The extreme deviation is in the northern end of the Gulf, where possible Layer 3 lies at a depth of 10 km, and mantle lies at 20 to 25 km. Moore (1973) explained the mid-Gulf deviation from normal oceanic and the northern Gulf lower layer thickening by the concept of clastic compensation, by which crustal growth and resulting structure are controlled by the balance between rate of separation, with intrusion of magma, and the flow of sediments into the gaps. He pointed out that very great supplies of clastic sediments in the northern Gulf preclude the formation of oceanic-type crust as a result of plate separation, and lead instead to the formation of intermediate crust, typical neither of oceanic nor continental realms. Another possible reason for the apparently anomalous velocity structure in the northern Gulf may, however, be that those refraction lines (Phillips, 1964) were run before bathymetry, structure, and tectonics of the Gulf had been delineated. These lines cross many major structural boundaries.

Seismicity, both in regional and detailed local studies, confirms the general pattern of the rectilinear spreading axis-transform system. Sykes (1968) confirmed the transform-fault concept in the Gulf and suggested that the troughs such as the two rift valleys in the Guaymas Basin were loci of sea-floor spreading, a concept previously anticipated for this area by Rusnak et al. (1964). Moore (1973) showed the Northern Guaymas Basin trough to be an active tensional feature with normal growth faults cutting the partial sedimentary fill, and Brune and his colleagues (Figs. 4 and 5) have demonstrated the seismically active nature of the spreading axes and transforms in the Guaymas Basin.

Heat flow is generally high in the entire Gulf and is locally very high in the Guaymas Basin Rifts. Special attention has been given to the Guaymas Basin in heat-flow studies, partly because the spreading axes are so clearly defined. General distribution of heat-flow values is shown in Figures 6 and 7. In addition, during the March 1978 site survey (Moore et al., 1978), a large number of additional heat-flow measurements were made. The following discussion is adapted from Becker (1978, in Moore et al., 1978).

A total of 54 new heat-flow measurements were made in the Guaymas Basin (Figs. 8-10) at two proposed drilling sites, GCA-12 (Site 477) and GCA-30 (Site 481). Fifty-four new and ten previously reported (Lawver et al., 1975) conductive-heat-flow measurements showed isolated peak values of > 30 HFU in each of the two axial grabens of the Guaymas Basin. The spatial pattern of measurements indicates quite different styles of crustal

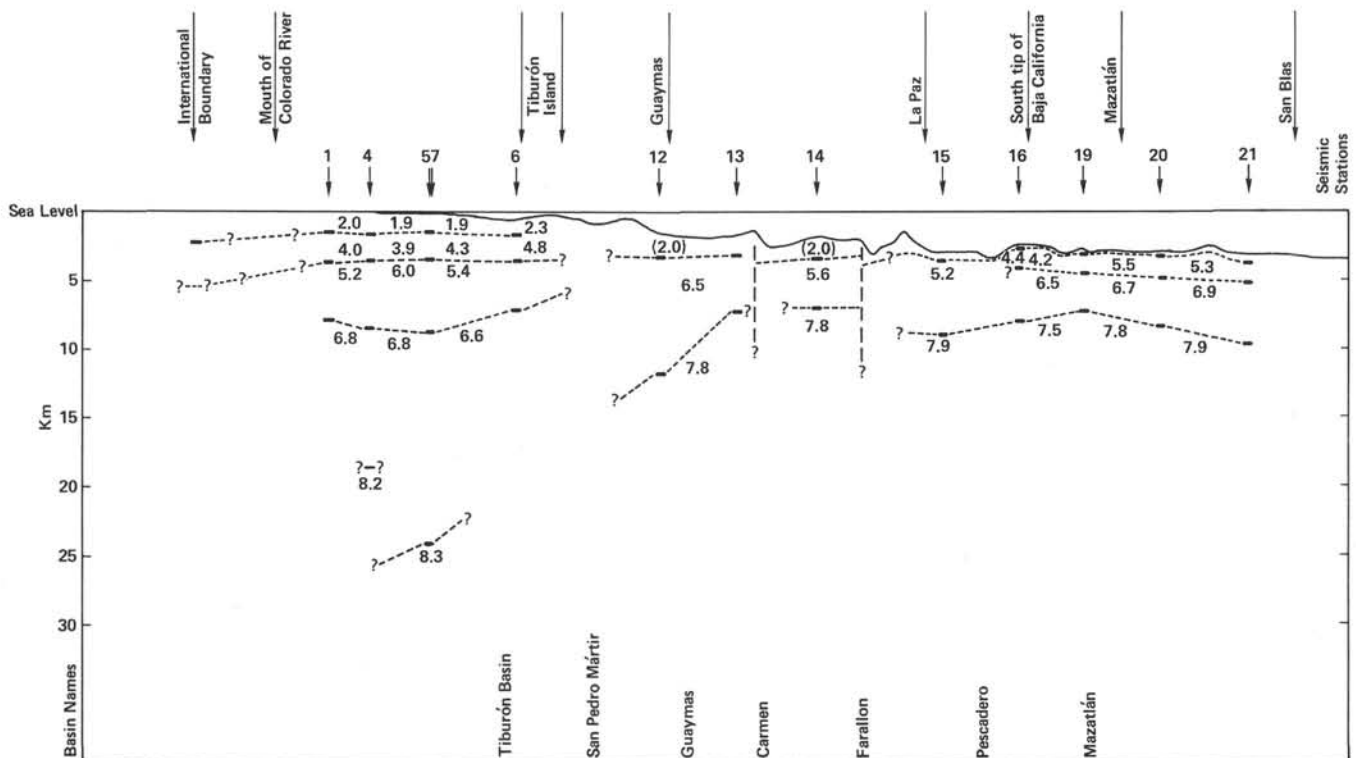


Figure 3. Structure section of the Gulf of California (after Phillips, 1964). International Boundary station from Kovach et al. (1962). (Velocities in km/s.)

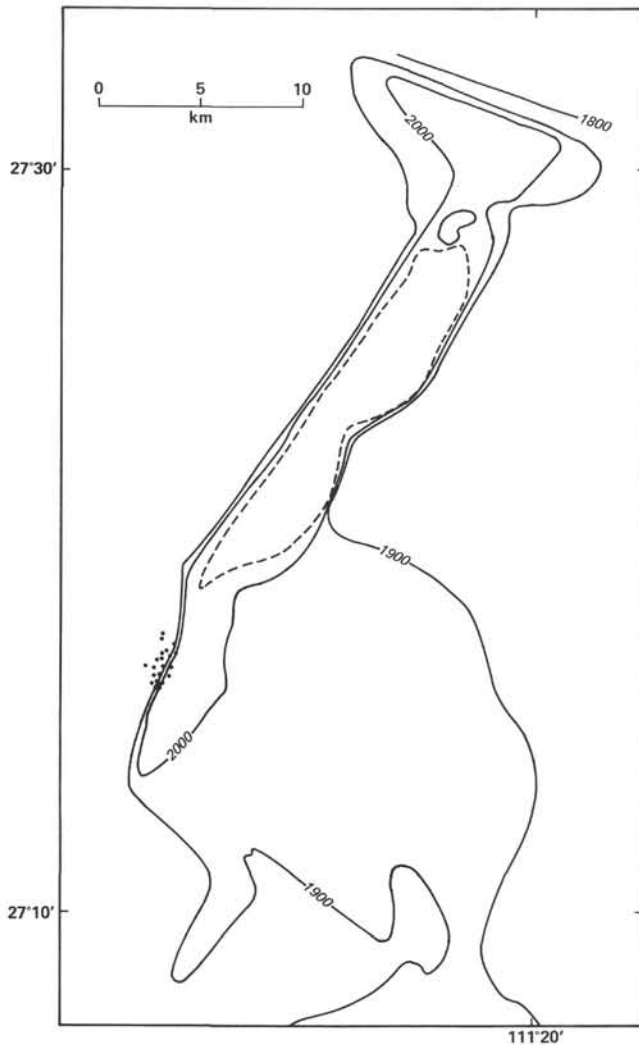


Figure 4. Epicenters in the Guaymas Basin from earthquake swarms of 1972 (from Reichle and Reid, 1977).

heat transport in these apparent spreading centers: largely conductive transfers in the southern trough (Site 477) and dominantly convective transport at the southwestern end of the northern trough (Site 481). In addition, about 40 previous measurements (Lawver and Williams, 1979) at the northern end of the northern trough at a third planning site (GCA-13) define a mostly conductive system, of far less power than that in the southern trough.

In the southern trough—the site of a large anomaly modeled by conduction from a near-surface, linear, intrusive source by Lawver et al. (1975)—32 new stations were taken in profiles across the rift (Fig. 8). These profiles generally display peak values centered over the rift, with nearly monotonically decreasing values to the side (Fig. 10, profiles d, e, and f). Site 477 is near the small region of highest heat flow in the Southern Rift (Figs. 8 and 10). The smooth spatial pattern is consistent with an intrusive source, but the added two-dimensional control suggests that this source might better be modeled as a point source (i.e., a vertical magma pipe, rather than a

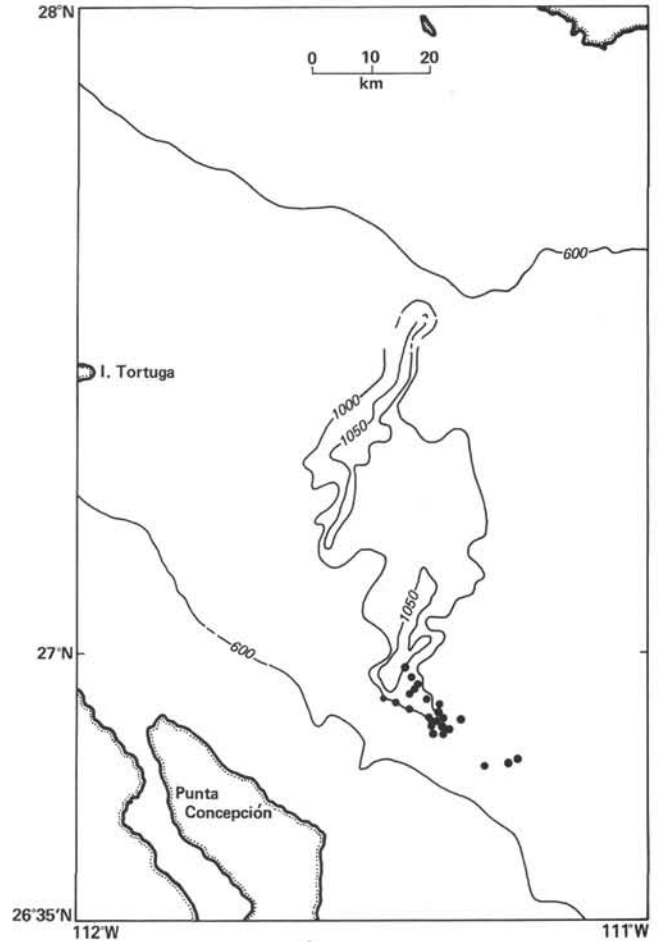


Figure 5. Epicenters in the Guaymas Basin from earthquake swarms of 1974 (from Reichle et al., 1976).

linear dike). There are a few exceptions (isolated high values) to the trend of decreasing heat flow away from the center of the southern rift. These may suggest relatively small-scale hydrothermal venting, particularly at the normal-faulted borders of the rift.

Twenty-two heat-flow measurements were taken in three profiles across the southern end of the northern trough (Fig. 9), around a hydrothermal site directly observed from a submersible (Lonsdale, 1978). Site 481 was located in this trough. These display both a closely spaced variability and association with tectonic structures (Fig. 10), which strongly suggest that hydrothermal convection is the major mechanism for heat transport from the crust at this site. Very high heat flow was recorded at the western boundary fault (Line b, Figs. 9 and 10), implying that this fault system is a major hydrothermal discharge site. Low heat flow in the center of the rift, away from boundary faults, suggests either deep-seated lateral advection of heat toward the boundary fault, or hydrothermal recharge through the rift floor.

Lawver et al. (1975, p. 23) had suggested previously that the southern rift of the Guaymas Basin might be underlain “by a 1-km wide basaltic intrusion which is roughly 100 m deep and less than 18,000 yr. old.” We

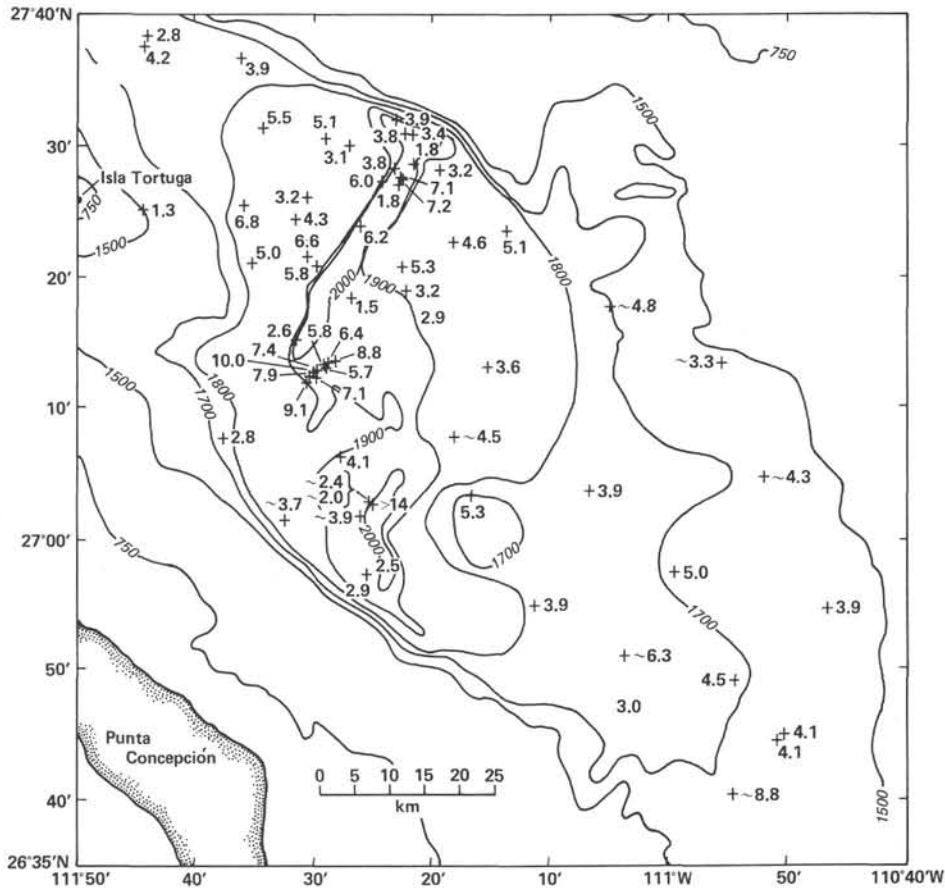


Figure 6. Heat flow values in the Guaymas Basin (from Lawver and Williams, 1979).

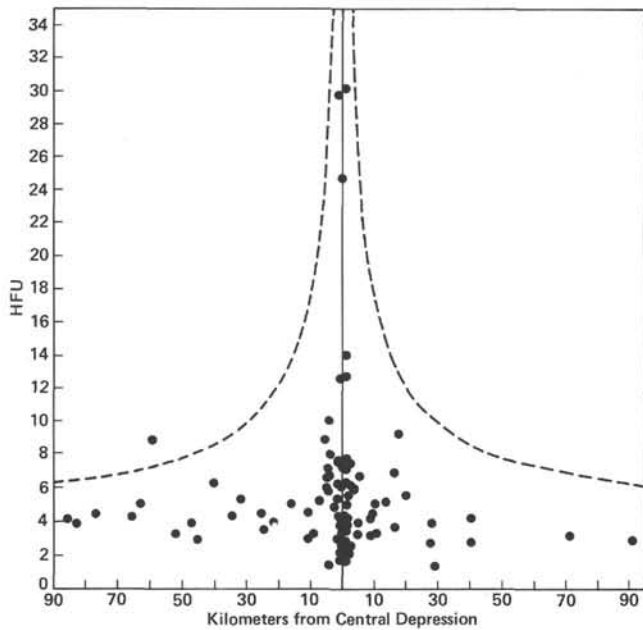


Figure 7. Heat flow values in the Guaymas Basin, plotted against distance from the spreading axes (from Lawver and Williams, 1979).

will comment later on the outcome of this prediction in the light of Leg 64 drilling results.

Sediments, Stratigraphy, and Basement

The Guaymas Basin is characterized as having a higher rate of sediment accumulation than the mouth of the Gulf, but considerably less than the extreme rates in the north, where the Colorado River delta apparently has filled the structural Gulf to sea level. Study of a piston core from the Guaymas Basin (van Andel, 1964) gave a rate of $2.7 \text{ m}/10^3 \text{ yr}$ ($2700 \text{ m}/\text{m.y.}$). These high rates—as well as seismic-reflection, magnetic, and other data—suggested to us that newly formed oceanic basement in the Guaymas Basin and farther north may never come directly into contact with sea water. Instead it is formed under a thick sediment pile intercalated with basaltic intrusions. Lawver et al. (1975) used a rate of $2 \text{ m}/10^3 \text{ yr}$ to conclude that the intrusion they postulated had always been buried under sediment. They also concluded that intrusion events in this basin are episodic, rather than continuous. This type of oceanic crust may be important in many young ocean basins formed by rifting of continental crust, and it therefore may be the oldest oceanic basement to be found under the thick sediment wedges of older continental margins (Vogt,

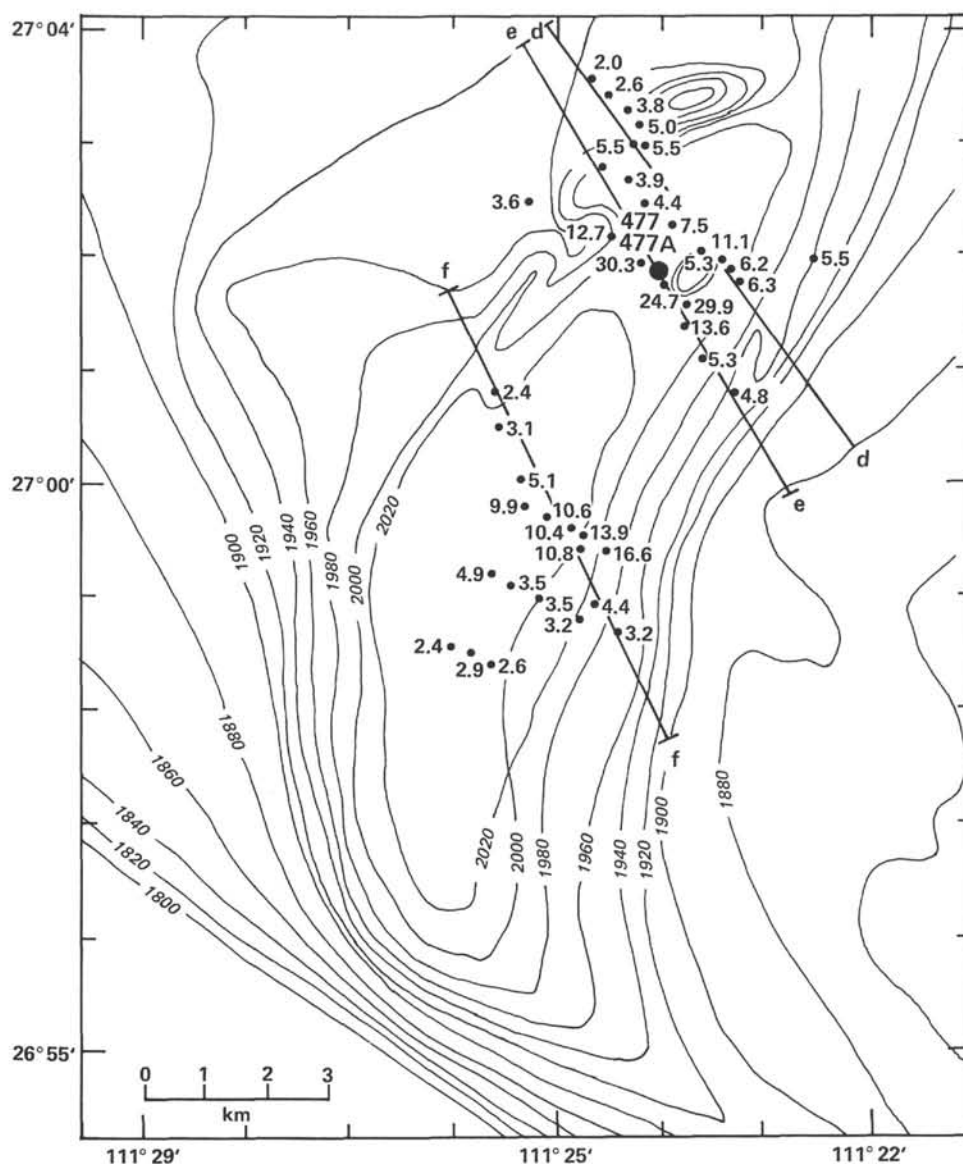


Figure 8. Location of heat-flow transects across the southern trough of Guaymas Basin (from Williams et al., 1979). (Values in HFU.)

Lorentzen, and Dennis, 1970; Vogt et al., 1970; Larson et al., 1972; Moore, 1973).

Sites were proposed both in the actively spreading rifts in "zero-age" sea floor and on the flank of one of the rifts in the otherwise flat-bottom basins. Seismic-reflection records in the Guaymas Basin (see later figures in this chapter) show an acoustic basement under the relatively thin, flat-lying turbidites. One of these rift-flank sites was drilled (478, GCA-25) to penetrate acoustic basement and to determine the nature of the crust and basement rock formed in such an environment. We anticipated that the section would consist of young, wet, rapidly deposited, diatom-rich turbidites intruded by basaltic composition sills. The sills and their feeder dikes would increase in proportion and in grain size with depth, although we could not predict the depth at which this transition would occur. The acoustic basement, therefore, could be either hydrothermally altered

intrusives or hydrothermally altered sediments—or a mixture of the two. The question could be resolved only by drilling.

The Guaymas Basin holes are also important because they were planned in the only basin in the Gulf where direct evidence for hydrothermal activity has been found. Helium is leaking from the mantle into the bottom waters (H. Craig, pers. comm.; Lupton, 1979), and hydrothermal precipitates have been found on fault ledges (Lonsdale, 1978). The basin is being faulted actively, and it appeared likely that one or more faults, possible pathways for hydrothermal fluxes, would be sampled in the sediments by the drilling.

Because heat flow is high within the Guaymas Basin rifts, very young, shallowly buried sediments have been heated relatively rapidly to higher temperatures. For geochemists working on the time-temperature effects on organic-maturation indicators, this combination is

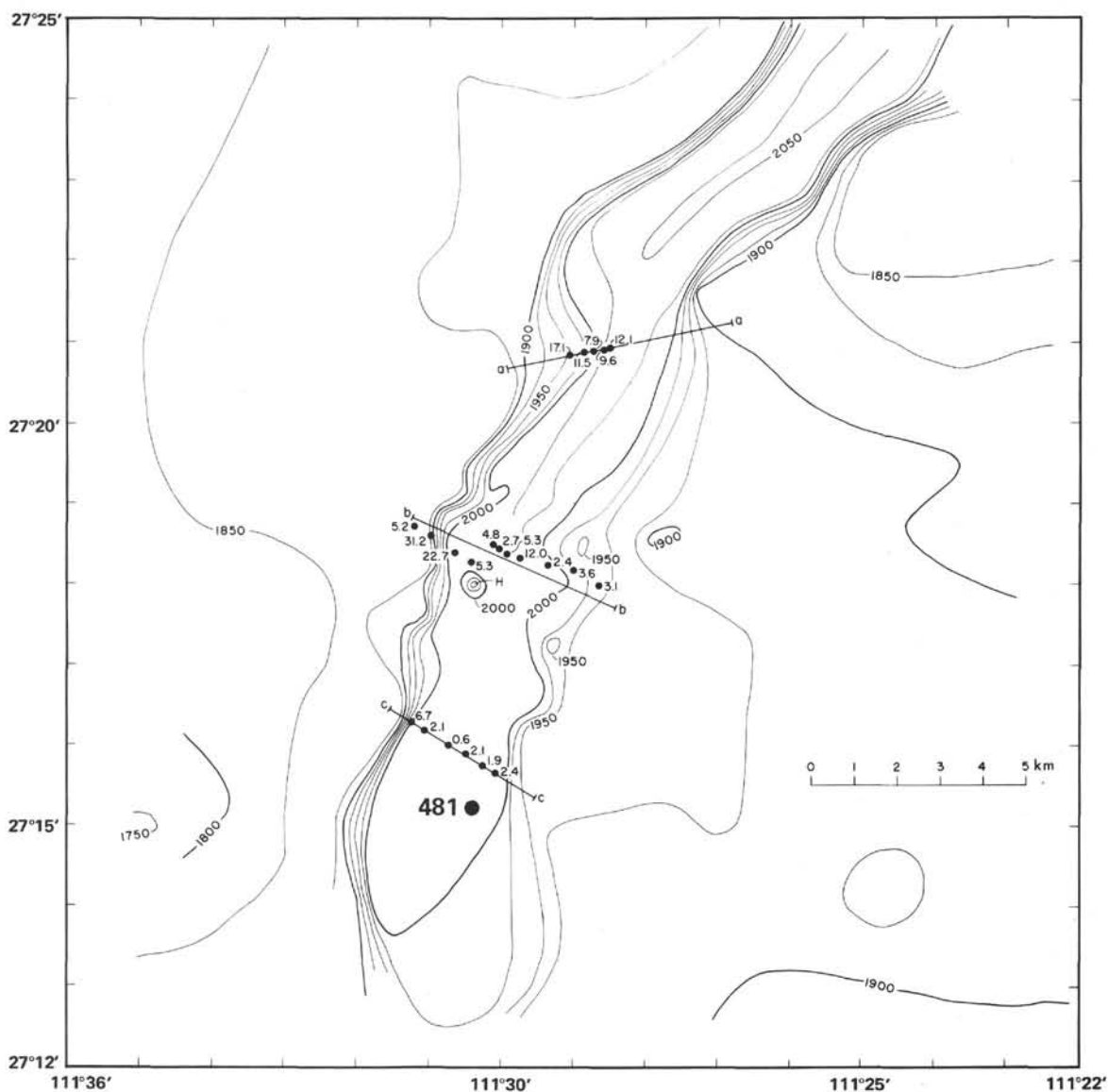


Figure 9. Location of heat-flow transects across the northern trough of the Guaymas Basin (from Williams et al., 1979). (Values in HFU.)

an ideal and rare "end member" representing heating to relatively high temperatures in short times. Detailed analysis of the diagenetic products of biological marker compounds could indicate whether high heat flow in young sediments can considerably influence the rates of competing chemical reactions and thus change the diagenetic pathway of such molecules. The results of these investigations will be compared to the extremely "mild" diagenesis conditions found at other deep-sea sites. A single gravity core, collected in 1972 by the Scripps Institution of Oceanography, contained biogenic hydrocarbons in detectable, but small amounts up to C_8 (Simoneit, Mazurek, et al., 1979). Subsequent attempts to duplicate this core or to detect such hydrocarbons in other cores had failed. One of our objectives was to evaluate this significant find.

Detailed sampling of interstitial waters using conventional shipboard squeezing techniques and the *in situ*

water sampler (with heat-flow attachment) was planned. The aim of these studies in the Guaymas Basin sites was to test the occurrence of reaction zones in the sediments and the influence of underlying oceanic rocks on interstitial-water composition.

The inorganic geochemical program in the Guaymas Basin sites was directed specifically to:

- 1) Study of possibly hydrothermal events in the rift zones from the point of view of interstitial-water changes and interactions with the sediments. A special sampler was on board to collect any hydrothermal fluids encountered.

- 2) Placement of major emphasis on the study of silica diagenesis in high-heat-flow sediments, in which recrystallization of silica may occur at much younger ages than normally occurs in marine sediments.

- 3) Study of interstitial waters and sediment mineralogy in the layered diatomites of the oxygen-mini-

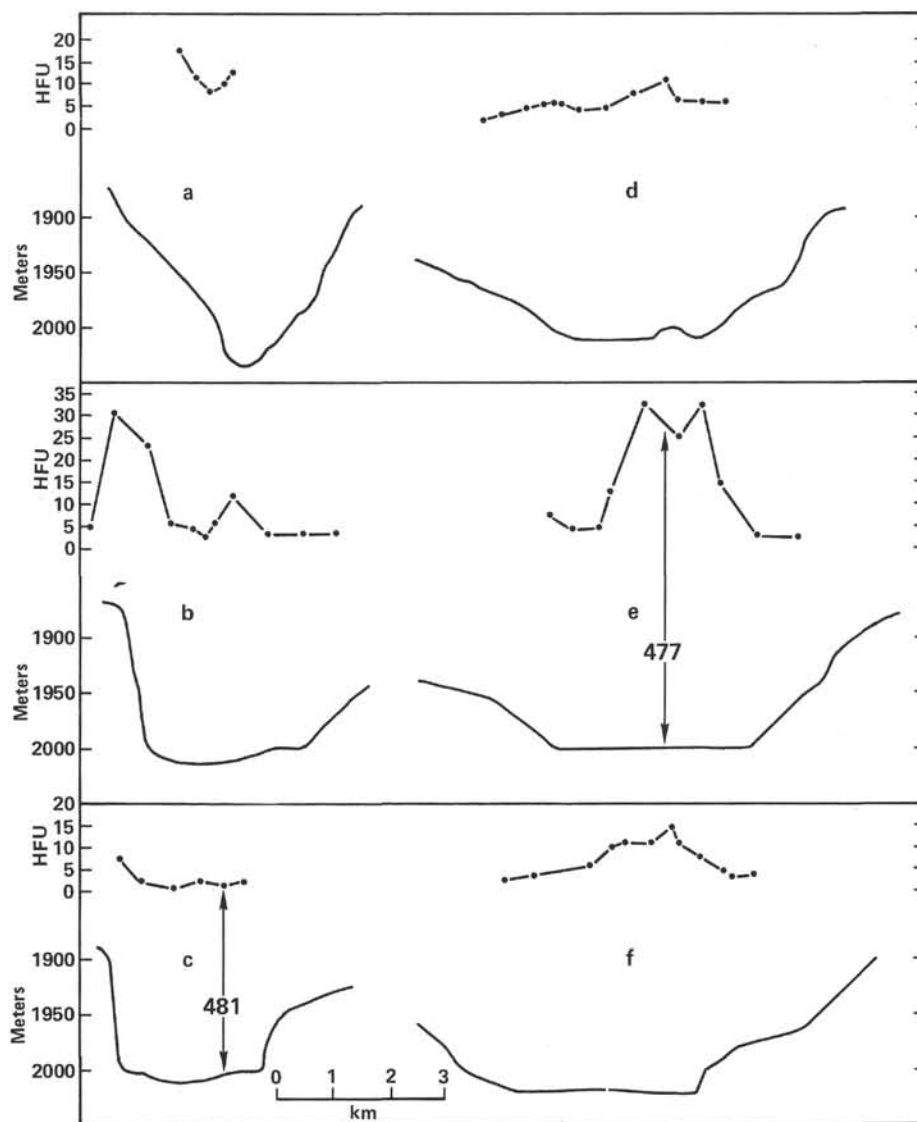


Figure 10. Heat-flow profiles and bathymetric profiles across the Guaymas Basin (from Moore et al., 1978) on transects a-f of Figures 8 and 9.

mum layer on the basin flanks, to better understand diagenetic processes that have affected similar sediments now exposed on land.

In general, the inorganic-geochemistry program aimed at a more complete understanding of chemical processes in the sediments and underlying basalts, including work by a group of shore-based investigators.

Three sites were selected for drilling in the Guaymas Basin. Site 477 was located in the high-heat-flow area of the Southern Rift, on "zero-age" crust. Site 481 was in the low-heat-flow, hydrothermal area of the northern rift, also on "zero-age" crust. Site 478 was on the flank of the southern rift, in crust with predicted age of 400,000 years.

PRINCIPAL RESULTS

Sites 477 and 481 were drilled in the southern and northern rifts of the Guaymas Basin, respectively. Both

penetrated late Quaternary, very soft diatomaceous sediments with high water contents, each intruded by several dolerite bodies (presumably sills). Heat flow was high (20 HFU) at Site 477, and the sediments adjacent to the sills showed thermal metamorphism. At each site, the sediments above and below the sills have higher bulk densities and reduced water contents, demonstrating expulsion of pore water during intrusion of the sills.

Site 478 was drilled in crust approximately 400,000 years old according to a plate-tectonic model. The section is likewise diatomaceous sediments, including turbidites, intruded by dolerite sills. The only biostratigraphic time horizon encountered was approximately 260,000 years. We do not believe that any of the sites was drilled deep enough to have reached the bottom of the oldest sediments in the respective localities.

The lithologic and seismic sections are shown in Figure 11.

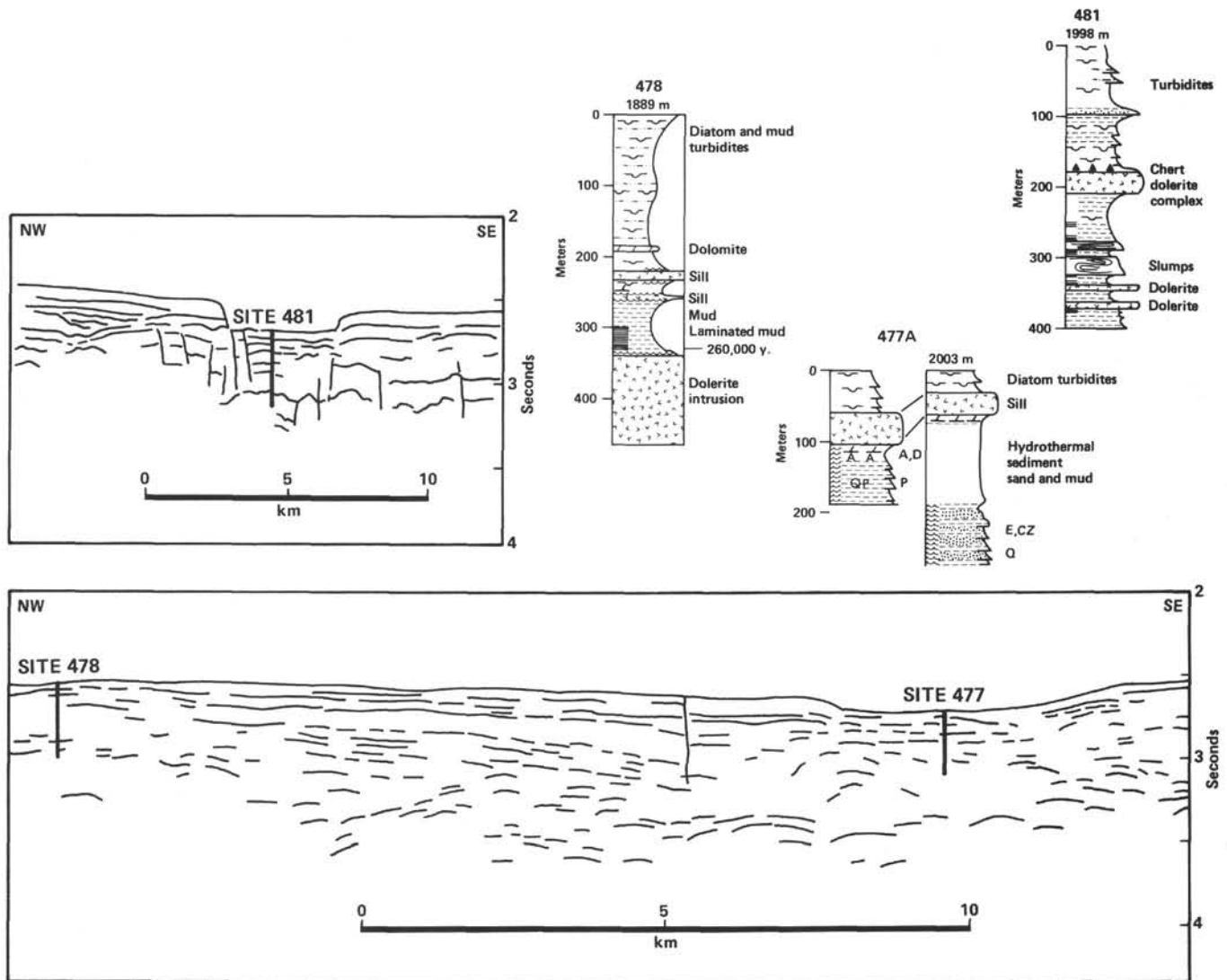


Figure 11. Simplified principal lithologic results and line drawing of seismic section through the Guaymas Basin rift transect.

HOLE 477

Date occupied: 18 December 1978
Date departed: 20 December 1978
Time on hole: 2 days
Position: 27°01.85' N; 111°24.02' W
Water depth (sea level; corrected m, echo sounding): 2003
Water depth (rig floor; corrected m, echo sounding): 2013
Bottom felt (m, drill pipe): 2020
Penetration (m): 191.0
Number of cores: 23
Total length of cored section (m): 191.0
Total core recovered (m): 52.46
Core recovery (%): 27.5
Oldest sediment cored:
 Depth sub-bottom (m): 191.0
 Nature: Claystone
 Age: Holocene/late Quaternary
Basement: Not reached

Principal results: This site in the southern rift of the Guaymas Basin was drilled and continuously cored to a depth of 191 meters. A dolerite sill was encountered and cored between 58 and 105.5 meters. Sediments above the sill are rapidly deposited, moderate-olive-brown, hemipelagic diatom oozes and mud turbidites, some with sands. Below the sill, these types of sediments have been pervasively hydrothermally altered to gray claystones and sandstones, with newly formed dolomite, pyrite, dolerite, and quartz. Recovery was 27% in the sediments, and 20% in the dolerite. Features of the sediment and intercalated dolerite are summarized under Hole 477A. Hole 477 was logged through the drill pipe with gamma-ray, neutron, and temperature tools.

HOLE 477A

Date occupied: 20 December 1978
Date departed: 22 December 1978
Time on hole: 2 days, 5 hours, 35 minutes
Position: 27°01.80' N; 111°23.93' W
Water depth (sea level; corrected m, echo sounding): 2003
Water depth (rig floor; corrected m, echo sounding): 2013
Bottom felt (m, drill pipe): 2020

Penetration (m): 207

Number of cores: 12

Total length of cored section (m): 120.5

Total core recovered (m): 16.03

Core recovery (%): 13.3

Oldest sediment cored:

Depth sub-bottom (m): 267.5

Nature: Altered clayey sand turbidites

Age: Holocene/late Quaternary

Basement: Not reached

Principal results: This continuation of Site 477 in the southern rift of Guaymas Basin was washed to 32.5 meters, where a dolerite sill was encountered. This sill was cored to its termination at 62.5 meters. Washing was then resumed to reach a depth of 181.5 meters, 9.5 meters above total depth in Hole 477. Continuous coring was then resumed to 267 meters, where drilling was discontinued for safety reasons. Recovery in the indurated sediments alternating with softer sediments below 181.5 meters was only 6%. The age of the entire drilled section, both sediments and dolerite intrusions, is Quaternary to Recent (50,000 years or less, if accepted spreading rates are used). Two lithologic units are recognized for combined Holes 477 and 477A. Unit 1 is diatomaceous turbidites above the sill. A dolerite sill was encountered at 48 to 105.5 meters in Hole 477 and 32.5 to 62.5 meters in Hole 477A. The lithologies of the sills of these two holes cannot be correlated directly. Unit 2 comprises hydrothermally altered and indurated diatomaceous turbidites ranging from clay and claystone to sandy siltstone and silty sandstone. A full suite of logs was successfully run at Hole 477A. Heat flow was extremely high (14–20 HFU).

SITE 477

Site 477 Background and Objectives

This site (planning site GCA-12), located in the center of the southern rift in the Guaymas Basin, was the first site to be drilled in this transect. It was the exploratory hole to determine the nature of the sediment and rock column in the basin. Specific objectives included:

A. Sediments.

1. Sedimentary facies and organic constituents.
2. Diagenesis and the effects of high heat flow on both inorganic and organic material.
3. Hydrothermal effects and/or deposits.

B. Basement.

1. Composition and comparison with MORB, especially at proposed site GCA-1 (Site 482, Leg 65).
2. Mode of emplacement of intrusions and lateral continuity.
3. Depth below sea floor.
4. Maximum depth of sediments in relation to intrusive bodies.
5. Effects of hydrothermal activity.

C. Chronology. Confirmation or denial of the tectonic model. The rift at this site is 3 km wide and should not contain sediments older than 50,000 years.

Site 477 Operations

On departing the mouth of the Gulf of California, we set course by the most direct route to the southern rift of the Guaymas Basin and Site 477. In general, our route took us along the southwestern flanks of the basins as we progressed northward. At 0455Z on 18 December we changed course to 312°T to make our crossing perpendicular to the strike of the southern rift (Fig. 12). We

crossed the rift trough, went beyond the northern wall, and then made a 180° turn to starboard to return to the site selected for the beacon drop. We were surprised to find that, in the short distance required to make the turn to starboard and return on a reciprocal course, the nature of the terrain in the trough had changed completely from a smooth-floored trough with layered, ponded sediments to a hummocky surface of very disturbed appearance (see section on correlation of drilling and seismic results). We found that there are abrupt lateral changes in the trough floor over short distances. After reaching the south flank of the trough again, we corrected course to attempt to recross the flat bottom of the trough. At 0739Z on 18 December, we located a suitable site and dropped the beacon. On returning to the drop site by radar fixes, we acquired only a faint signal, not good enough for positioning. At 0920Z we began to resurvey the trough site with the 3.5-kHz system only, and at 1011Z we dropped a second beacon with a 12-ft tether to allow the beacon to float above the very soft surface mud layer we believed to be present. The ship was positioned over this beacon in automatic at 1130Z, and we commenced running in the hole. A mechanical bit release was used to avoid the problems experienced with the hydraulic unit at earlier-drilled sites. The hole was spudded in at 2003 meters water depth at 1530Z, and our first core was on deck at 1637Z. The mud line was recorded at 2020 meters from the derrick floor; thereafter, we continuously cored to a total depth of 191 meters, including an altered dolerite sill from 58 to 105.5 meters. The lower few cores contained a dark-gray, oil-like hydrocarbon in the sediment, and methane/ethane ratios increased. Very high temperatures were encountered below the sill to this depth. A reading from the cut core *on deck* was 40°C. At 1930Z we decided to delay coring ahead until readings from the Hewlett-Packard GC could be taken. Because the Hewlett-Packard GC needed repairing, we decided to utilize waiting time to run the Neutron Gamma Ray Log and Temperature Log through the pipe. The Gearhart-Owen logging engineer taped a maximum reading thermometer to their lower tools. The tape melted and it fell to the plug placed in the bit to prevent logging tools from passing through the flap valve. The steel case of the thermometer wedged alongside the plug, preventing our latching onto it for recovery. Fishing efforts were unsuccessful, and at 1130Z on 19 December we had to pull the drill string, abandon the hole, and offset 165 meters to the northwest to begin Hole 477A. The thermometer was recovered and gave a reading of 87.78°C. A third beacon with 25-ft tether was dropped at 1238Z because the 13.5-kHz beacon was fading fast. We spudded in Hole 477A at 1200Z and began washing. The drill encountered and cored a hard dolerite sill from 32.5 to 62.5 meters. Thereafter, we washed to 181.0 meters and then cored sediments to a total depth of 267 meters before the hole was terminated at 1515Z on 21 December for safety reasons. Our concerns were increased gas content in porous sands, increased incidence of fluorescence, and dark-gray to black, oil-like substance increasing (see organic geochemistry section, this volume, Pt. 2).

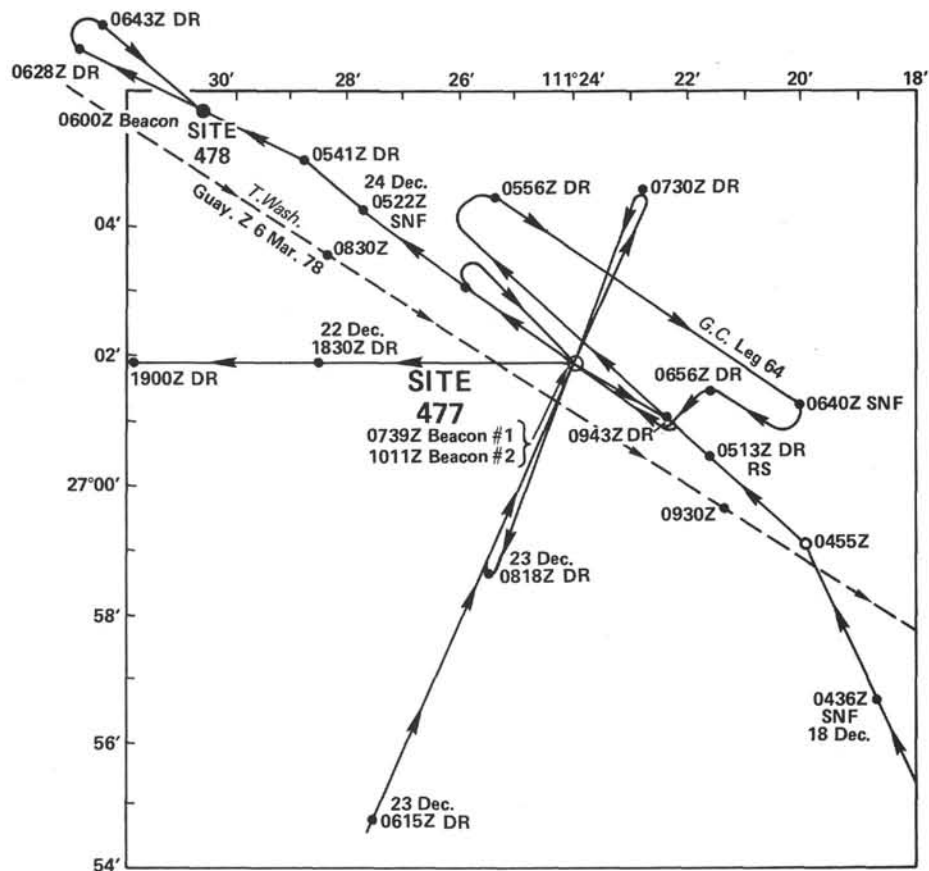


Figure 12. Track chart of *Glomar Challenger* survey, Site 477.

Recovery at Site 477 was 27% in sediments and 20% in igneous rocks in the first hole; 29% in the dolerite sill of Hole 477A; and only 6% in the sediments of Hole 477A cored from 181.5 to 267.0 meters. Hole 477A then was logged after dropping the bit, filling the hole with 150 barrels of 11-lb mud, and pulling the pipe to 2151 meters. The first logging run was for temperature, density, gamma ray, and calipers; the second run was for sonic, variable density, gamma ray, and calipers; the third run was for guard, neutron, and gamma ray; the fourth run was for induction and gamma ray; the fifth run was for temperature. Logging was completed at 1245Z on 22 December. We commenced plugging the hole with 168 sacks of 14-lb cement at 1345Z from 2151 to 2025 meters. We were out of the hole at 1705Z and underway on 270° at 1750Z on 22 December to a rendezvous in the lee of Isla Santa Inés, Bahía Concepción, with a Mexican Navy vessel carrying our piston corer and replacement scientists for the second half of our leg. After completing personnel and equipment transfer and other business at anchorage, we were underway on 085° at 0317Z on 23 December for Site 477, again to test the piston corer and attempt to core an undisturbed shallow section there. At 0610Z we changed course to 020° to survey up the axis of the trough (Fig. 12). We then crossed the beacon at Site 477 on NNE and SSW headings while seismic profiling and conducting sonobuoy surveying in the vicinity of the Site. We ended the survey at the site at 0845Z and began to position in automatic over the bea-

con left from Hole 477A. By 1514Z we had made up the bottom-hole assembly for the piston corer and had set pipe for a piston-coring attempt at Hole 477B. From 1730Z to 2330Z, operations were concerned with testing the piston core. After loss of inner core barrel on first lowering and inability to seat and seal properly on second run, the third run successfully recovered a 3.6-meter section of relatively undisturbed core (together with a piece of steel from lost barrel of first run). We then pulled out of the hole and at 0428Z on 24 December began the short run to Site 478.

Table 1 summarizes Site 477 coring.

Site 477 Sediment Lithology

We recognize two distinct sedimentary units based primarily on mineralogical composition and induration (Fig. 13). They are separated by thick dolerite intrusions. The age of the entire sedimentary column is late Pleistocene, although sediments below the sills are barren. The site is characterized by exceptionally high accumulation rates and high heat flow which has caused extensive alteration to sediments below the sills (Table 2).

Unit 1: Muddy Diatom Oozes and Mud Turbidites (477-1 through 477-7, 0.0–58.0 m) and 477A (0–32.5 m)

Cores 477-1 and 477-2 are dominated by moderate-olive-brown to grayish-olive diatomaceous oozes and silty sands. These sediments have high water content

Table 1. Coring summary, Site 477.

Core No.	Date (Dec. 1978)	Time	Depth from Drill Floor (m)		Length Cored (m)	Length Recovered (m)	Recovery (%)
			Top	Bottom			
477-1	18	0937	2020.0	-2021.0	1.0	1.00	100
2	18	1017	2021.0	-2030.5	9.5	5.15	54
3	18	1055	2030.5	-2040.0	9.5	1.89	20
4	18	1133	2040.0	-2049.5	9.5	1.64	17
5	18	1243	2049.5	-2059.0	9.5	2.99	31
6	18	1320	2059.0	-2068.5	9.5	0.00	0
7	18	1544	2068.5	-2078.0	9.5	2.40	25
8	18	1645	2078.0	-2080.0	2.0	0.03	1
9	18	1830	2080.0	-2087.5	7.5	0.40	5
10	18	2015	2087.5	-2097.0	9.5	0.81	81
11	18	2139	2097.0	-2106.5	9.5	1.80	19
12	18	2310	2106.5	-2116.0	9.5	6.44	68
13	19	0329	2116.0	-2121.5	5.5	2.74	50
14	19	0427	2121.5	-2125.5	4.0	0.08	2
15	19	0515	2125.5	-2135.0	9.5	1.50	16
16	19	0612	2135.0	-2144.5	9.5	9.11	75
17	19	0708	2144.5	-2154.0	9.5	4.03	42
18	19	0758	2154.0	-2163.5	9.5	0.00	0
19	19	0844	2162.5	-2173.0	9.5	3.76	40
20	19	0935	2173.0	-2182.5	9.5	2.60	27
21	19	1023	2182.5	-2192.0	9.5	0.53	6
22	19	1115	2192.0	-2201.5	9.5	2.39	25
23	19	1203	2201.5	-2211.0	9.5	1.15	12
477A-1	20	1344	2052.5	-2062.0	9.5	1.28	13
2	20	1700	2062.0	-2075.0	13.0	4.43	47
3	20	2045	2075.0	-2087.5	12.5	4.90	39
(wash)	20	2230	2087.5	-2201.5	114.0	0.18	—
4	20	2320	2201.5	-2211.0	9.5	0.00	0
5	21	0013	2211.0	-2220.5	9.5	1.20	13
6	21	0105	2220.5	-2230.0	9.5	0.13	1
7	21	0209	2230.0	-2239.5	9.5	0.86	9
8	21	0305	2239.5	-2249.0	9.5	0.18	2
9	21	0409	2249.0	-2258.5	9.5	1.00	11
10	21	0515	2258.5	-2268.0	9.5	1.30	14
11	21	0705	2268.0	-2277.5	9.5	0.60	6
12	21	0815	2277.5	-2287.5	9.5	0.15	2
477B-P1	23	1620	2020.0	-2024.6	4.6	3.46	75

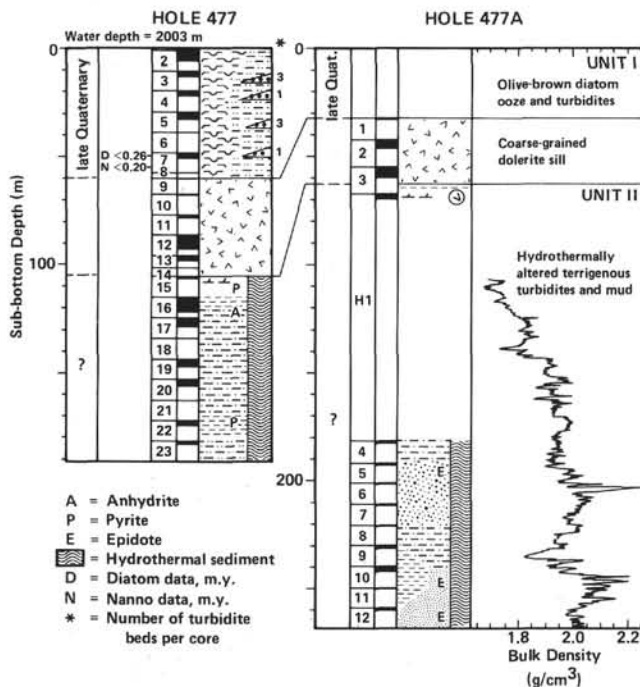


Figure 13. General lithology, lithologic units, core recovery (shown in black), and bulk-density logs from Site 477.

(> 60%) and generally low percentages of terrigenous material (< 15%), which consists mostly of quartz and plagioclase grains, rare pyrite framboids, and clay minerals. Consequently, the sediments exhibit a gelatinous

consistency and appear quite uniform in texture. Drill disturbance is pervasive, and sedimentary structures generally are not observed. Diatom frustules are commonly well preserved and form ~ 60% of the sediment. Calcareous nannofossils, sponge spicules, silicoflagellates, and terrigenous plant debris constitute the remaining 25% of the bulk sediment. Slight compaction of sediments occurs with depth; hydrogen sulfide and dark-gray streaks are present in minor amounts.

Cores 477-3 through 477-7 contain a series of muddy turbidites 40 to 70 cm thick with medium-gray to dark-medium-gray sandy silt at the base of each, 2 to 3 cm thick (Fig. 13). Each mud turbidite grades upward to lighter grayish-olive colors and finer-grained diatomaceous clay-silt. Diatoms increase in abundance from < 5% in basal sand layers to > 60% in the top of each turbidite. The clay fraction (~ 20–25%) and pyrite (~ 5%) remain uniform. Nannofossils constitute up to 10%. Where drilling disturbance is moderate, contacts are sharp, distinguished by color and texture. H₂S odor increases down-hole to the top of the dolerite sills. Exsolution of gases causes surface pimples or partings.

Section 1 of Core 477-7 contains diatomaceous ooze along with glassy basaltic pebbles and cobbles, and chips and pebbles of hard dolomitic siltstone above a thick, dark-gray to light-gray, well-sorted basal sand layer. These exotic components are well rounded, suggesting redeposition. Evidence suggests that most of the unconsolidated sediment at this site comprises turbidites or mass flows.

A chill margin forms the contact between Unit 1 and the dolerite sills. In Hole 477A, bits of vermilion claystone are entrapped and baked along with a vesicular margin. (See igneous section for description of the altered dolerite sill.)

Unit 2: Hydrothermally Altered and Indurated Mud Turbidites (105.0–267.0 m)

Unit 2 is poorly recovered, but characterized by hard, brownish-gray to medium-dark-gray clay and claystone and medium-gray to light-gray sandy siltstone and silty sandstone. The sediments are hard, but friable, and brecciate easily.

Logging results suggest the presence of interbedded sandy and shaley sediments. Unit 2 is barren of microfossils, with the exception of Core 477-19, where some rare, recrystallized, shallow-water, Quaternary benthic foraminifers occur in the core catcher.

Recovery is very poor, but where whole chunks occur some faint bedding or other sedimentary structures are preserved. Two small pieces of laminated and cross-bedded sands occur in Cores 477A-7, CC (Fig. 14) and 477A-11-1, 2–9 cm (Fig. 15). These exhibit grading, parallel laminations, convoluted beds, carbonized wood chips, and extensive iron sulfide patches in the slightly bioturbated upper portions. These turbidite sedimentary structures suggest that sedimentary processes in the Guaymas Basin were similar before and after sill emplacements.

Unit 2 sediments have undergone extensive high-temperature propylitic alteration. The replacement mineral-

Table 2. Summary of major lithologies, Holes 477 and 477A.

Lithologic Unit	Cores	Sub-bottom Depth (m)	Thickness (m)	Lithology	Paleoenvironment	Age	Approximate Accumulation Rate (m.y.)
1	477-1 through 477-7	477: 0.0-58.0 477A: 0.0-32.5	58.0 32.5	Moderate olive-brown (5Y 4/4) to grayish-olive (10Y 4/2), diatomaceous ooze; medium-gray (N5) to dark-medium-gray (N4) sandy silts and silty clays as turbidites	Rapid deposition of basin-plain turbidites, either diatomaceous or sandy-silty muds	Late Pleistocene (<0.20 m.y.)	> 1000
	477-8 through 477-14 and 477A-1 through 477A-3	477: 58.0-105.5 477A: 32.5-62.5	47.5 30.0	Coarse-grained, altered dolerite with ~20% plagioclase phenocrysts (see igneous petrology section for details)	Intrusion (sill).		
2	477-15 through 477-23 and 477A-4 through 477A-12	477: 105.5-191.0 477A: 62.5-267.0	85.5 104.5	Brownish-gray (5YR 4/1-5/1) to medium-dark-gray (N4) clay and claystone and medium-gray (N5) to light-gray (N7), sandy siltstone to silty sandstone with current laminations and grading; epidote-chlorite-quartz-albite-pyrite-pyrrhotite-dolomite-anhydrite mineralogy	Hydrothermally altered basin-plain turbidites and diatomaceous muds		Very rapid

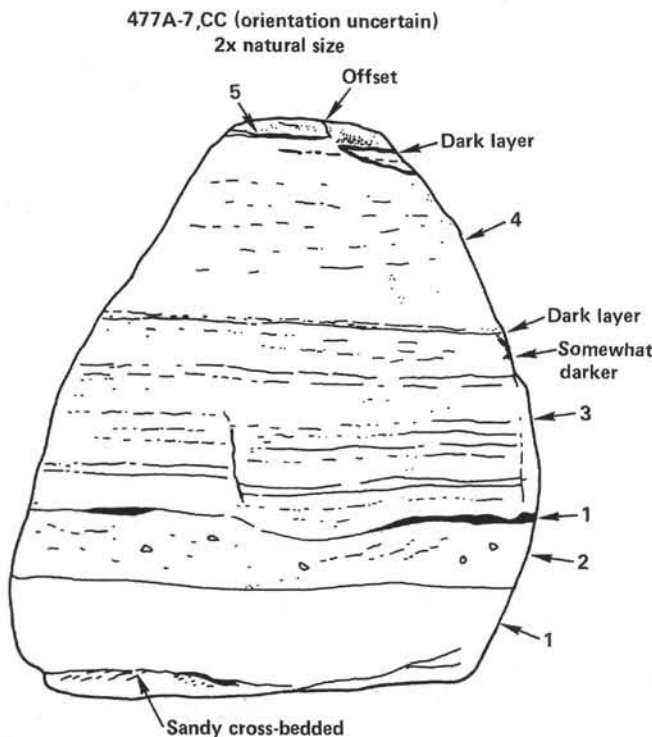


Figure 14. Line drawing from 477A-7,CC. Indurated, hard mudstone layer: (1) dark gray mudstone (no carbonate); (2) dirty, poorly-sorted, gray, fine sand, some cross-bedding; (3) light-gray, parallel-laminated, fine-grained siltstone, well sorted (no carbonate); (4) like 3, but lamination indistinct; (5) dirty, very fine-grained sand.

ogy is variable and exhibits a progressive pattern down-hole indicative of increasing temperature (Table 3).

Dolomite occurs just below the sills as scattered euhedral (16-40 μm) rhombs in Core 477-15, and as rhombs in hard, silicic dolostones in Section 477A-14-1. Below these depths (100 m and 70 m, respectively), scattered relict carbonate may have been calcite, dolomite, or siderite rhombs. Dolomite ranges from 5 to 30% in upper sediments to 75% in indurated dolostones.

Pyrite is ubiquitous in these holes, but varies in habit, commonly occurring as framboids (2-10 μm) above the sills in unaltered sediments, and as scattered cubes or thin veins in claystone just below the sills. Lower in the section, pyrite is absent, reappearing in Core 477-22 as 8 to 10% of the bulk sediment. At this depth, the pyrite is present as large (2-4 mm), bulging cubes with corroded corners and curved, striated crystal faces. Toward the bottom of Hole 477A, pyrite disappears as H₂S concentration increases, and in Cores 477A-6 to 12 pyrrhotite is the common iron sulfide phase in sandstones.

In Cores 477-15 and 477-16, anhydrite occurs in claystones as equidimensional (1-2 mm), round, fuzzy, white clusters dotting the freshly cut core surfaces. As much as 40% anhydrite is observed in some sections of Cores 477-15 through 477-21. Zeolites and possibly K-feldspar are also present.

Below ~ 191.0 meters, the assemblage includes zoisite and epidote, microcrystalline quartz, abundant chlorite, and some albite. Eight gray, hard, but porous and friable sandstones from the base of Hole 477A (Cores 477A-5-477A-12) have radial clusters, or fan-shaped ag-

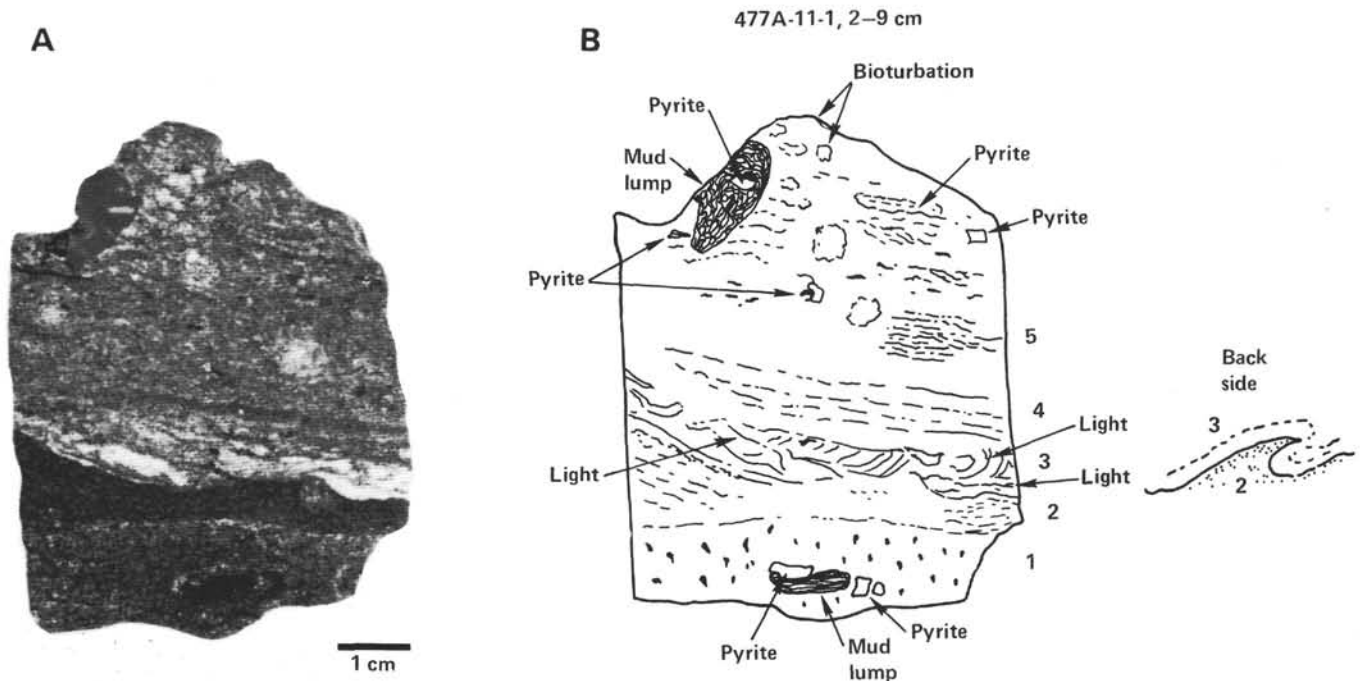


Figure 15. Photograph (A) and line drawing (B) of 477A-11-1, 2-9 cm, indurated piece of turbidite with sedimentary structures: (1) massive, medium sand, gray, with some pyrite; (2) laminated, dark-gray, fine sand; (3) cross-laminated, somewhat convoluted, fine sand, alternating light and gray laminae; (4) more-or-less parallel-laminated, gray, fine sand; (5) gray, fine sand, with many small platy mud lumps and dark windows, very small-scale cross-bedding.

Table 3. Hydrothermal mineral zones in Unit 2, Holes 477 and 477A.

Zone	Assemblage	Sub-bottom Depth (m)
1	Major: dolomite Minor: anhydrite, pyrite (zeolites?)	105.0-115.0
2	Major: clay minerals Minor: dolomite, (zeolites?), anhydrite Rare: pyrite	115.0-143.5
3	Major: hydrocarbon (zeolites?) Minor: dolomite Rare: anhydrite, pyrite	143.5-172.0
4	Major: pyrite (large, cuboctahedral) Minor: hydrocarbons Trace: dolomite	172.0-191.0
5	Major: authigenic quartz, (feldspar?), chlorite Minor: epidote minerals, pyrite, pyrrhotite	191.0-248.0
6	Major: epidote-zoisite, chlorite Minor: authigenic quartz + albite, authigenic quartz + sphene Rare: (increased H ₂ S), pyrrhotite	248.0-267.0

gregates of elongate prisms of epidote. In thin-section, the prisms are clear, pale yellow-green, 0.04 to 0.20 meters long, and terminated, with parallel extinction, high birefringence, and an index of refraction of 1.71 to 1.72. A few prisms contain black (sulfide?) inclusions. Epidote constitutes up to 30% of the rock in Cores 477A-5 through 477A-12. Epidotes increase toward the bottom of the hole, and epidote at the very bottom shows signs of corrosion. Relict minerals are abundant, with only a rim of alteration minerals.

Quartz is ubiquitous, and much of it is detrital; however, thin-sections show significant amounts of clear,

large flakes which have euhedral terminations along one margin, which suggests that quartz is being newly formed, partly growing into pore spaces. Albite and/or K-feldspar are observed as very small (10-15 μm), monoclinic-looking, clear chips with low birefringence, no cleavage, and an index of refraction of 1.55. Many of the detrital feldspars are altered; commonly, euhedral epidote prisms have grown out of plagioclase crystals.

Site 477 Organic Geochemistry

No gas pockets formed in any core liner upon arrival on deck, but the sections were probably too short, because of poor recovery of sediments.

C₁-C₅ Hydrocarbon Analyses

Methane and ethane (also CO₂) were monitored on the Carle GC as drilling proceeded and C₂-C₅ hydrocarbons were measured intermittently on the Hewlett-Packard GC. H₂S was detectable by odor from about 15 to 50 meters and it is of a biogenic origin. H₂S was observed again near the upper surface of the sill, and it increased with depth below the sill to about 270 meters; this H₂S is thermogenic.

All gas samples were derived from pressure build-up under the core caps about 15 to 30 minutes after closure. The normalized concentrations of methane (CH₄) and ethane (C₂H₆), are plotted versus depth in Figure 16A and B. The CH₄ shows a decrease toward the dolerite sill from 30 to 50 meters, and an increase (about 10-90%) with depth below the sill. Essentially, no C₂H₆ is present in the shallow sediment, and below the sill it first increases with depth to about 0.5%, followed by a decrease to an approximately constant level of 0.15%.

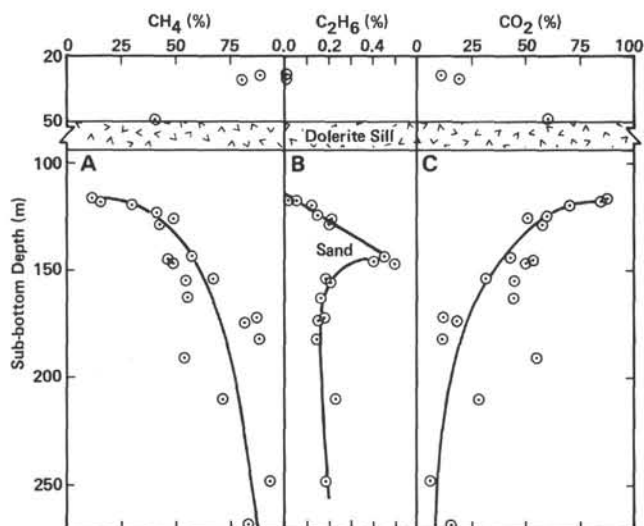


Figure 16. Concentrations of methane (A), ethane (B), and carbon dioxide (C) versus depth at Site 477 (data normalized after correction for air).

This decrease in C_2H_6 content below about 145 meters may reflect a steep increase in the thermal gradient (cf. C/N data).

Carbon dioxide (CO_2) is present as a major component of the gas and the normalized data are plotted in Figure 16C. This is the first site of this leg where the CO_2 exhibits a depth gradient. The values increase toward the sill from 30 to 50 meters and then decrease below with depth from about 90 to 10%.

The ratios of ethane to methane (C_2/C_1) are plotted in Figure 17A. The values are low above the sill, and a rapid increase (Cores 16 and 17) is observed below the sill to a maximum value of 1×10^{-2} in Core 19, followed by a sharp decrease with depth. No sediment was recoverable for Core 18; it was suspected to consist of sands. Selected samples were also analyzed for C_2 - C_5 hydrocarbon contents. The concentrations of ethane and propane (assuming 100% CH_4 by volume) are plotted in Figure 17B. The concentrations of both hydrocarbons are scattered, but indicate an increase below the sill, followed by a decrease after Core 18 at about 140 meters. The maximum amounts of C_2 - C_4 hydrocarbons on an air-free basis are: $C_2 = 0.50\%$, $C_3 = 0.04\%$, and $C_4 = 0.003\%$. The ratio of *n*-butane to *iso*-butane increases to 1.6 in Core 17 just above the inferred sand layer, indicating a contribution from hydrocarbons of a more petroliferous composition; however, the absence of thermogenic hydrocarbons (low temperature) such as *neopentane* and 2,2-dimethylbutane, with greater excess of normal hydrocarbons, should be noted.

Black Slick

In Hole 477, Cores 19 to 23, and Hole 477A, Cores 5 to 10, the sediment was very disturbed and gassy, with a black slick permeating voids, cracks, and spaces along the core liner (Fig. 18). This slick had hydrophobic properties and was less dense than water; it formed an emulsion and had no odor or fluorescence. It had visual characteristics of an odorless condensate and was there-

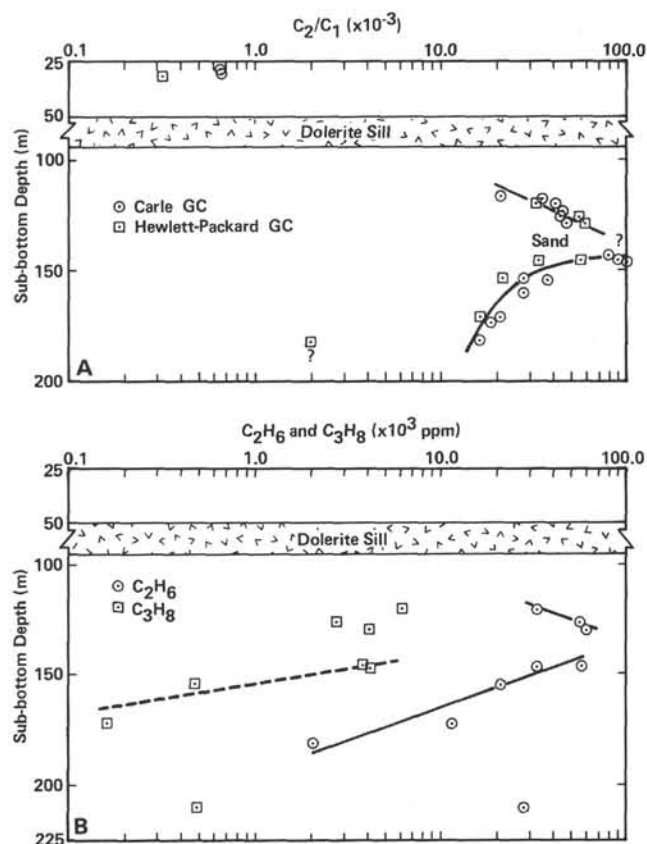


Figure 17. Ratios and concentrations of hydrocarbon gases versus depth for Site 477. A. Ethane to methane. B. Ethane and propane concentrations.

fore sampled extensively and analyzed. A toluene-ethanol extract showed no fluorescence, and there was no *in situ* fluorescence. The black particulate matter could be burned in a flame, leaving a gray ash, indicating that it may be asphaltic or amorphous residual carbon on fine minerals. A sample (~20 ml) of slick with water was removed by syringe from the split core about 1 hr after recovery and sealed with 5-ml head space. The gas in the head space above the sample was analyzed by GC and was found to consist predominantly of methane, ethane, and propane (Fig. 19). No hydrocarbons $> C_3$ were detectable, and the CH_4 had suffered loss by some diffusion, resulting in the C_2/C_1 ratio of 7×10^{-2} (Sample 20-1). This black slick appears to be a fine particulate mixture of clay-sized minerals and amorphous carbon, with adsorbed or included C_1 - C_3 hydrocarbons produced from organic matter in the sediments under high thermal stress.

The black material of the slick is less dense than water and thus was separated by floatation. The two fractions then were analyzed for total C and N content. The carbon content of the black material ($d < 1.0$) from Section 477-23-1 is 14%, with a C/N of 86. This organic matter has been heated to high temperatures.

Fluorescence

Fluorescence data were measured on (1) dried sediment samples, and on tetrachloroethylene extract solu-

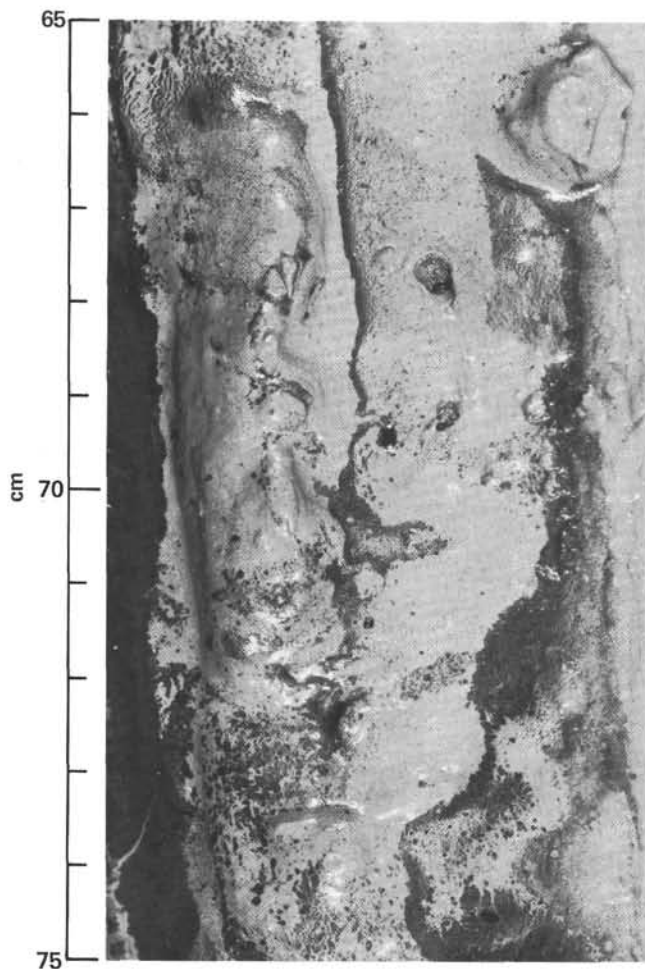


Figure 18. Photograph of "black slick," the pyrolyzed carbonaceous residue in the split core (477-19-2, 65-75 cm).

tions of (2) dried sediment samples and (3) pyrolyzed samples (red heat). None of the dried sediment samples exhibited any fluorescence; however, the deeper cores in Hole 477A exhibited strong yellow fluorescence in small spots, predominantly along the core liner. The extracts of the dried sediments exhibited a yellow to yellow-white fluorescence near the upper boundary of the sill and in Section 477A-5-1. The fluorescence in the sill vicinity is due to the thermal stress of that intrusion on the organic matter, which resulted in limited *in situ* pyrolysis. The fluorescence in Section 477A-5-1 and predominantly along the liner in the deeper cores is due either to pipe dope or to bearing lubricant from the drill bit (the retrieved bit from Hole 477 had two leaking bearings). A cluster of synthetic bristles with grease (strong yellow fluorescence) was found in the top of Section 477A-5-1. It is suspected that the high hole temperature melts some of the pipe joint grease (dope) as the drill string descends, and thus introduces small grease droplets into the core barrel. Some of this material may also have come from bits of grease dropping off the sand line or from the drill bit. All these contaminants and respective fluorescent spots in the cores were sampled for future examination on shore.

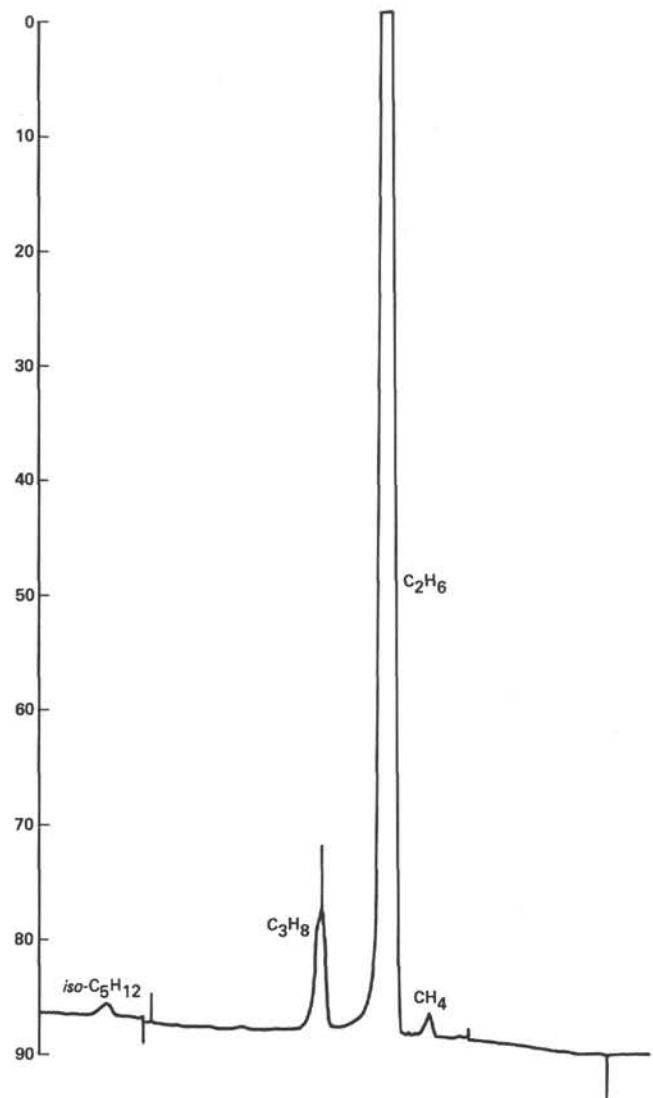


Figure 19. Gas chromatographic trace for adsorbed gas from "black slick" in Section 477-22-1 (Hewlett-Packard GC data).

The pyrolyzed samples exhibited a yellow-white fluorescence in the shallow samples above the sill, and fainter yellow fluorescence near the upper boundary of the sill and in Section 477A-5-1. This indicates that the upper sediment is thermally unaltered and contains immature organic matter which can yield petroliferous material under pyrolytic conditions. In the proximity of the sill, some of the organic matter has been expelled by that thermal event. Section 477A-5-1 probably is contaminated by pipe grease. Below the sill, all the organic carbon is dead; it has been pyrolyzed *in situ*. The sediment does not change its gray color under pyrolysis (a darkening is observed for the upper sediments below the sill).

Organic Carbon and Nitrogen

The samples were prepared as described before, and the results from the CHN analyzer are summarized in Appendix II, this volume, Pt. 2. Total-carbon and organic-carbon contents and the organic-nitrogen content

are plotted in Figure 20. The organic-carbon content ranges from about 0 to 3%, with two maxima down the hole. The highest values are observed in the unaltered upper section of diatomaceous ooze and silty clay above the sill. A distinct decrease of carbon content is observed toward the top of the sill, with a further decrease below it to about 150 meters sub-bottom; then both organic and total carbon increase to maxima of 1 and 1.5%, respectively, followed by a steady decrease. The organic-nitrogen content ranges from about 0 to 0.35% and parallels that of the organic carbon above the sill, showing a steady decrease without a second maximum below the sill. These data, coupled with the sediment lithology and fluorescence analyses, indicate that the dolerite intruded a sediment sequence which was already baked from below (>250 m). The second maximum of carbon content (150–200 m) represents residual carbon from a baked organic-rich section. These inferences are further supported by the C/N ratios (Fig. 20). In the shallow sediments above the sill, the ratios range from 11 to 15, which is typical of immature Recent sediments (Ryther, 1956), followed by a sharp increase toward the sill, indicating thermal alteration during intrusion. Below the sill, the C/N values decrease slightly to about 150 meters sub-bottom, which may indicate that these sediments were relatively cool and were mainly altered by sill emplacement. However, below 150 meters there is a steep increase of the C/N ratio to essentially infinity, confirming the effect of the high thermal gradient on the conversion of the organic matter to dead carbon and expulsion of all the organic nitrogen.

The course of events at Site 477 from an organic geochemical point of view consists of the following: The sedimentary column was subjected to a high thermal gradient, as indicated by fluorescence analyses, the C

and N contents and C/N ratio, and the absence of petrogenic gas and liquid products. The latter were probably removed by the hydrothermal circulation. The high proportion of CO₂ in the gas below the sill, as well as the increase of H₂S, may also indicate that the C₁–C₄ hydrocarbons could represent cracking products from biogenic organic matter or from petrogenic gas and liquid products. A thermal origin was the interpretation given for similar gas distributions at Site 368 (Dooze et al., 1978); however, the absence of any petroliferous odor is puzzling and does not support that conclusion for Site 477. It appears that the gas below the sill is both indigenous and thermally derived from primary biogenic organic matter and was concentrated by the recent thermal event, whereas above the sill most of that gas has diffused out of the sediment. After the emplacement of the upper sill, sedimentation of further biogenic ooze was continued, and these upper sediments are unaltered.

The organic matter of this sediment sequence poses only a limited safety and pollution hazard. The C₂/C₁ ratio approached 100 × 10⁻⁴, but in view of the low pressure of total gas and its limited occurrence with a high C₂/C₁ ratio (probably in sand of Core 18 and top of Core 19), the seepage was considered safe and biodegradable. The black slick found from Core 19 down was a "condensate" of C₁–C₄ hydrocarbons (same distribution as in free gas) adsorbed on fine clays and amorphous carbon; thus, that material was not considered a hazard. The increase with depth of oily material (high fluorescence) caused some concern, but that material was derived from melting of pipe-joint grease which got into the liners. In retrospect, the results from the fluorescence and C and N analyses, coupled with the presence of bristles and grease in Section 477A-5-1 and the leakage of grease from the Hole 477 drill bit, indicate

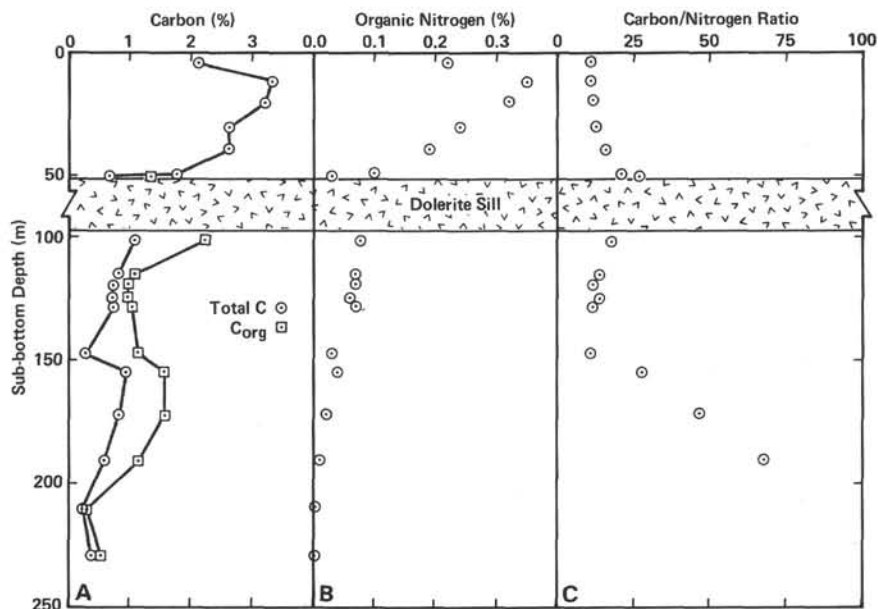


Figure 20. Total-carbon and organic-carbon content (A), organic-nitrogen content (B), and atomic ratio of carbon to nitrogen (C).

that we were observing only ship contamination at depth caused by the elevated hole temperature, and it would have been safe to drill on.

Site 477 Inorganic Geochemistry

Interstitial-Water Chemistry

Interstitial-water concentration-depth profiles (Fig. 21) at this high-heat-flow site show complex patterns. Alkalinity and ammonia show maxima above the doleritic sill, which can be explained by biochemical oxidation of organic matter in these rapidly deposited sediments. Toward the doleritic sill, however, concentrations rapidly decrease as a result of alteration reactions in the basalts.

Below the sill, the influence of the hydrothermal system at greater depths is clearly reflected by the disappearance of dissolved magnesium and by the rapid increases in calcium, chloride, and ammonia. The increase in ammonia must be the result of thermal decomposi-

tion of organic carbon. The rise in chloride is probably the result of hydration of the sediments and/or basalts during hydrothermal alteration. The shape of the dissolved-chloride profile implies an upward advection of water.

Site 477 Biostratigraphy

Nannofossils

At Site 477, only the Unit 1 diatom muds and turbidites contained calcareous nannofossil assemblages. These have common, well-preserved coccoliths of late Pleistocene age, as indicated by the presence of *Emiliana huxleyi*. No datum planes were crossed.

Diatoms

Open marine tropical to subtropical planktonic diatoms are abundant and well preserved, to rare and poorly preserved, in the hemipelagic sediment sequence of Hole 477, Cores 1 through 7. Samples below are barren

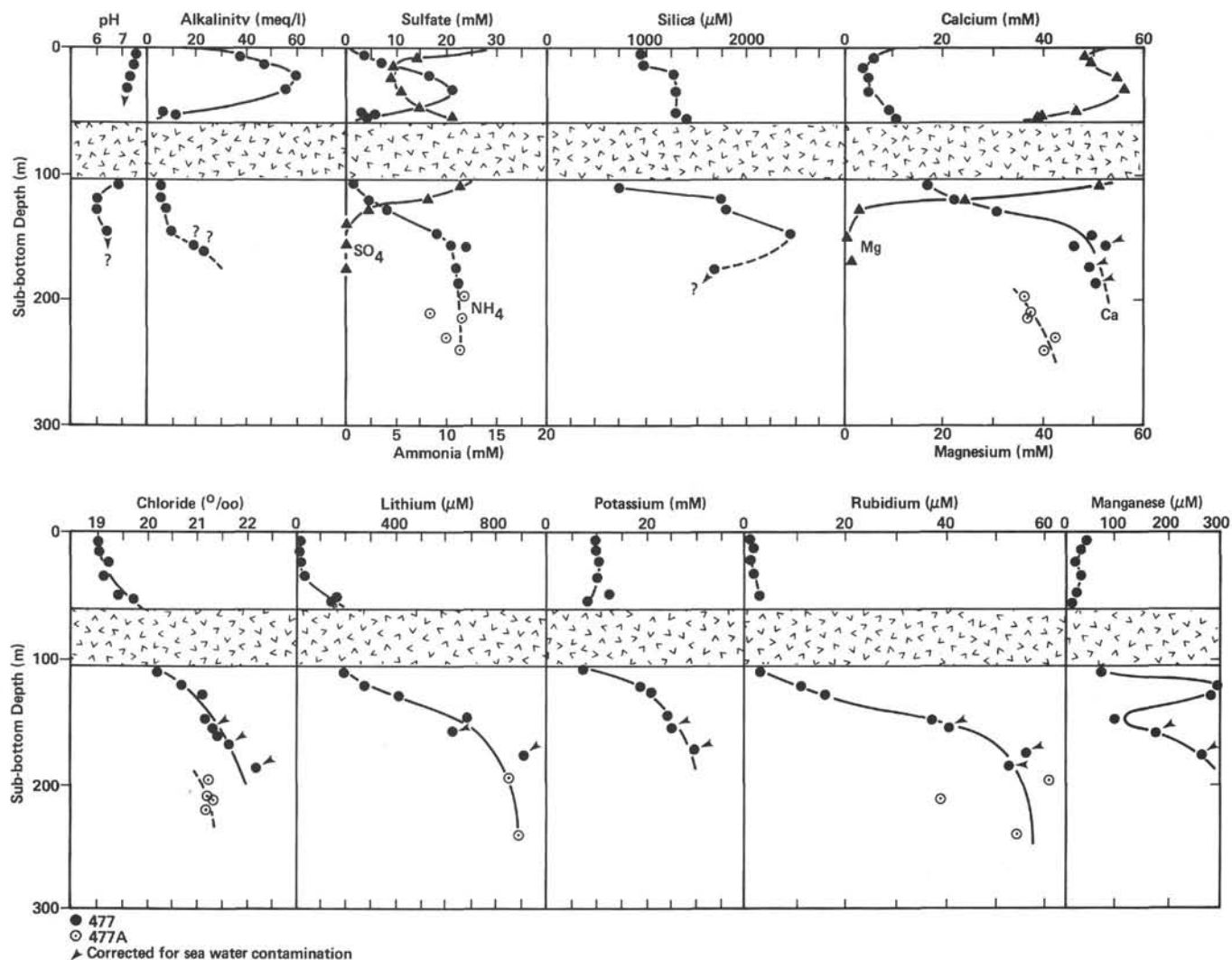


Figure 21. Composite results from interstitial-pore-water analysis, Site 477.

of opal phytoplankton remains. No diatom or silico-flagellate datum was identified, suggesting that the sediment above Core 7 is not older than 260,000 years.

Radiolarians

The dominant radiolarians in the sediments of Holes 477 and 477A are *Dupptractus* sp. cf. *D. pyriformis*, *Dupptractus irregularis*, *Ommatodiscus* sp. (Benson, 1966), *Anomalacantha dentata*, and *Thecosphaera* sp. In the Gulf of California, this specific suite of radiolarians is characteristic of a water mass largely influenced by coastal upwelling.

The 267 meters of drilled sediment do not show evidence of being older than latest Pleistocene age. This argues for a very high sedimentation rate, which precludes establishment of a radiolarian zonation.

Foraminifers

As in the radiolarian thanatocoenoses, the planktonic-foraminifer thanatocoenoses at Holes 477 and 477A appears to have been deposited from a water mass influenced by coastal upwelling. Both above and below the "sill" (see Fig. 11), species characteristic of temperate water masses (Bé, 1977) are dominant. These are *Globigerina bulloides*, right-coiling *Globoquadrina pachyderma*, and *Globigerinoides ruber*. In 477-22, CC a slight increase in the relative abundance of *G. ruber* is observed.

Because of the high sedimentation rate, it was not possible to establish a planktonic-foraminifer zonation.

Samples above Core 7 of Hole 477 yield foraminifers which are moderately well preserved. Samples below Core 7, however, are almost barren, and foraminifers are rare in Cores 20 and 22 of Hole 477 and Core 5 of Hole 477A, in which they are very poorly preserved and affected by strong alteration. The planktonic fauna in Core 7 of Hole 477 indicates cooler conditions than do the faunas in cores above. Benthic foraminifers are dominated by *Cassidulina* spp., *Uvigerina* spp., *Bolivina seminuda*, and *Buliminella tenuata*.

Site 477 Sediment-Accumulation Rates

The diatom oozes recovered above the dolerite sill from Hole 477 (the sediments above the sill were washed at Hole 477A, and the contact between the upper sediments and the sill was not recovered) belong to nannofossil zone NN21, which corresponds in time to less than 200,000 Ma. No age determinations are possible for the hydrothermally altered sands and muds beneath the sill. Except for some benthic foraminifers, all the siliceous and calcareous microfossils and nannofossils have been obliterated. From the well-preserved chitinous fossils, no age information has yet been obtained; thus, it is difficult to estimate sedimentation rates at this site. Certainly they are high when compared to other oceanic deposits proximal to a mid-ocean-ridge segment. In the diatom oozes, calcareous and siliceous fossils are beautifully preserved; chitinous microfossils are abundant and well preserved; chlorophyll and filamentous algae are also exceptionally abundant and well preserved. Such a good preservation implies that the organisms

have been buried quickly and thus protected against oxidation. Additionally, the sediments in the hydrothermally altered zone seem to comprise a sequence of dominantly thick turbidites ranging from a few decimeters to some meters in thickness, with terrigenous detritus. This supports the conclusion that continuous, rapid sedimentation is and has been occurring at this site. If we assume that only pelagic diatom oozes have been deposited during the last 200,000 years, the rate at which they accumulated is greater than 300 m/m.y. This is the minimum rate at which the datable Pleistocene sediments have accumulated at this site. The rate is probably higher, and if we refer to the estimates of van Andel (1964) and Calvert (1966) for the Recent sediments in the Guaymas Basin, we would reach values of 1000 to 2500 m/m.y. Such an estimate would suggest that the entire section represents less than 100,000 years.

Site 477 Igneous Petrology

Hole 477

Small pebbles of basalt (Igneous Unit 1) with glassy rinds and baked clay selvages were recovered embedded in silty clay in Core 477-7 (Table 4). The basalt contains phenocrysts of plagioclase (10%) and subhedral to euhedral olivine (5%), frequently intergrown to form glomerocrysts up to 3 mm in diameter, in a fine-grained groundmass of pyroxene, olivine, pilotaxitically aligned feldspar microlites, and disseminated opaques. The origin of these pebbles is uncertain, but the absence of any localized thermal alteration of the adjacent silty clay suggests that they are not *in situ*, but rather have been derived from a nearby flow, perhaps as a slump deposit.

The dolerite unit is petrographically variable, with textures ranging from aphyric to feldspar-phyric varieties. Consequently, the unit has been subdivided into three sub-units on the basis of the presence or absence of feldspar phenocrysts. Other textural variations (e.g., grain size) tend to be gradational and are not easily delineated.

Subunit 2a comprises the uppermost 0.2 meters of the dolerite unit, recovered from 477-8, CC through 477-9-1, 14 cm. It is friable, water-permeated dark-gray (N3/N4), coarse-grained dolerite containing abundant (up to 15%) plagioclase (An₆₀₋₇₀) phenocrysts, and is mineralogically and texturally indistinguishable from the upper portion of Subunit 2c.

Igneous Subunits 2a and 2c are separated by Subunit 2b, an aphyric dolerite, of which only 0.5 meters were recovered from 477-9-1, 15 cm through 477-10-1, 15 cm. As with Subunit 2a, the rock is very friable and permeated by water. In thin-section, anhedral clusters of pale-brown augite (29%) sub-ophitically enclose plagioclase (50%). There are minor amounts of olivine (3%) and titanomagnetite (5%). Alteration is restricted to the development of zeolites (natrolite?) and soft, green clays in interstitial cavities; individual mineral grains appear quite fresh.

Subunit 2c forms the major part of Igneous Unit 2, representing about 11.6 meters of recovery through the interval 477-10-1, 16 cm to 477-14, CC. Subunit 2c is

Table 4. Igneous lithologic units, Site 477.

Unit	Top ^a (m sub-bottom)	Base ^a (m sub-bottom)	Thickness ^a (m)	Recovery ^b (m)	Type of Cooling Unit	Phenocryst Assemblage	Vertical Extent
Hole 477							
1	Core 477-7		—	Dispersed pebbles	Basalt	Pl, Ol	477-7-1, 50 cm to 477-7-2, 2 cm
2	58.0	100.0	42.0	12.3	Massive dolerite	Pl (and aphyric)	477-8, CC to 477-14, CC
Hole 477A							
1	34.0	41.0	7.0	1.7	Massive dolerite	Pl, Ol	477A-1-1, 0 cm to 477A-1-2, 40 cm
(sedimentary intercalation)							
2	45.5	60.0	14.5	10.2	Massive dolerite	Pl	477A-2-1, 0 cm to 477A-3-5, 18 cm

^a Determined from downhole log.
^b Determined from core log and corrected for spacers.

texturally and mineralogically variable, ranging from strongly feldspar-phyric (up to 30% plagioclase phenocrysts) to more sparsely phyric dolerite (~10% plagioclase phenocrysts), and having coarse-grained basaltic to coarse-grained doleritic (almost gabbroic) textures. Plagioclase phenocrysts range in size from 1 to 5 mm, and the groundmass olivine and pale-brown augite from 0.5 to 4 mm, olivine being subordinate to augite in both size and abundance. There is, however, an apparent slight increase in olivine content in the lower part of Subunit 2c. The interstices between the individual mineral grains are filled with soft, pale-green clay minerals as in Subunits 2a and 2b, and again the individual mineral grains are unaltered. Up to 15% of the rock may be made up of these alteration minerals.

The basaltic textures developed towards the base of Subunit 2c, and the gabbroic textures in the center of the body, suggest that the textural variations have resulted from differential cooling rates, the center cooling more slowly than the margins. Although neither the upper nor the lower contact of Igneous Unit 2 was recovered, it is evident from the thermal alteration in the overlying sediments that Unit 2 is at least in part intrusive, and is possibly a sill. Petrographically, Subunits 2a and 2c appear to have been derived from a single, plagioclase-rich magma type.

Hole 477A

The recovered rocks have been divided into two igneous units on the basis of downhole gamma-ray and neutron logs, macroscopic descriptions, and petrographic and modal analyses (Table 4). The presence of chilled margins at the top of Cores 477A-1 and 477A-2 and the distinct textural change from doleritic to gabbroic between the base of Core 477A-2 and the top of Core 477A-3 are the principal petrographic criteria used to delineate the two igneous units.

Several glassy chill zones and one baked sediment selva were recovered in the upper part (Sections 477A-1-1, 477A-2-1) of what appears to be an intrusive body (Unit 1; see Table 4). The base of a second body (Unit 2) occurs in Core 477A-H-1 (H designation indicates a wash-core) and is located at approximately 60 meters sub-bottom.

Unit 1 consists of the sparsely phyric to plagioclase-phyric basalt of Section 477A-1-1, and the plagioclase-phyric dolerite present in Section 477A-1-2. Section 477A-1-1 has two chill zones. The first occurs in Piece 1 (Fig. 22) and consists of very fresh basaltic glass with some small, ropy surface-flow structures and stringers of baked, light-pink, silicified sediment and cavities containing small (~1 mm) euhedral natrolite(?) crystals. The second chill zone occurred in Piece 4. Both zones exhibit fresh, glassy surfaces; little or no palagonitization of the glass has taken place. The chill zones consist of quenched groundmass of clinopyroxene and plagioclase microlites (80%), olivine and plagioclase phenocrysts (5% each), and disseminated opaque phases. Minor clay and carbonate minerals are present as fillings in radial fractures and veinlets and as olivine re-



Figure 22. Section 477A-1-1, Piece 1. Upper chill margin from doleritic sill.

placements. Small, unfilled, spherical vesicles are present near the chill zone, but do not extend into the main body of the rock for more than a few centimeters. The basalt in Section 477A-1-1 becomes progressively more plagioclase-phyric until the base of Section 477A-1-1 and through Section 477A-1-2, where the rock is a medium-grained, intergranular, plagioclase-phyric dolerite (or coarse basalt). The doleritic section of Unit 1 consists of plagioclase phenocrysts (20%), plagioclase groundmass crystals (40%), clinopyroxene (30%), olivine phenocrysts (5%), and minor opaque phases and clay minerals. All of the rocks are very fresh and show only small effects of sea-water or hydrothermal alteration.

A sedimentary intercalation between Units 1 and 2 is indicated by the bulk-density downhole log. In addition, a glassy chill zone present in Piece 3 and the aphanitic texture of the first three pieces of basalt in Section 477A-2-1 have been used to define the break between Units 1 and 2. The basalts have large (up to 10 mm) plagioclase phenocrysts that make up 15% of the rock volume. Below 15 cm, Section 477A-2-1 becomes doleritic, although the plagioclase phenocryst phase is still present. A vesicular zone occurs within the dolerite of Unit 2 between 477A-2-2, 20 cm, and 477A-2-3, 66 cm. It consists of vesicular (6% mode), inequigranular to subophitic, coarse-grained basalt or dolerite. The vesicularity is very pronounced, and there is little or no filling by clay minerals of the round, 0.75- to 5-mm diameter, randomly dispersed vesicles. Occasional clusters of natrolite crystals are nested within some of the vesicles (Fig. 23). The porphyritic nature of the rock continues unaffected by the vesicular zone and the unaltered plagioclase ($\sim \text{An}_{50}$) phenocrysts make up $\sim 15\%$ of the rock.

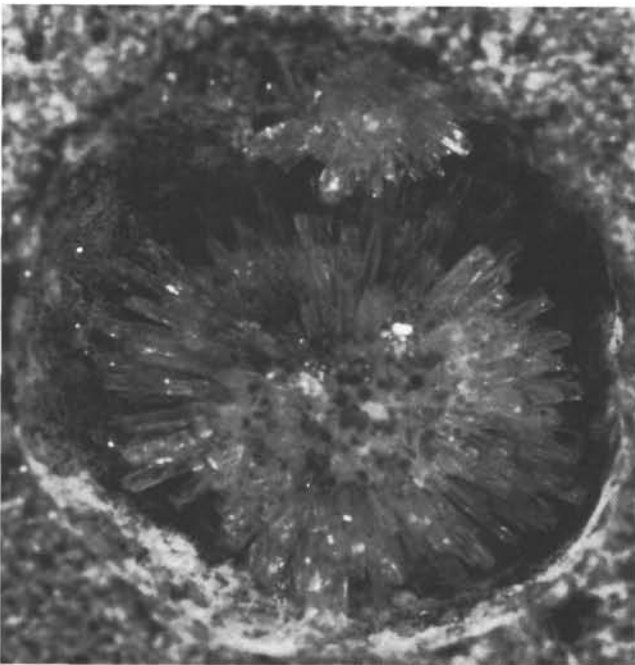


Figure 23. Close-up photograph of natrolite crystal clusters in a vesicle in dolerite at 477A-2-2, 20 cm.

Unit 2 seems to continue into Core 477A-3, where it becomes texturally and mineralogically variable. In Core 477A-3, Unit 2 consists of a medium-dark-gray, subophitic to inequigranular gabbro with large (1–4 mm), tablate plagioclase ($\sim \text{An}_{50}$) laths, often strongly normally zoned, and smaller clinopyroxene and olivine phenocrysts, set in a matrix of plagioclase microlites, abundant euhedral to subhedral opaque phases (with occasional cruciform [magnetite] and trellis-type [ilmenite] habit), and minor clay minerals deposited along intergrain boundaries. A short (~ 40 -cm long) interval of small (~ 1 -mm diameter) vesicles occurs at 477A-3-1, 65–105 cm. The rock is slightly finer grained in this interval. Unit 2 becomes increasingly olivine-rich in Section 477A-3-3, although an abrupt transition occurs near the bottom of Section 477A-3-3, where the rock becomes a plagioclase ($\sim \text{An}_{60}$) phyric dolerite, similar in many respects to the upper part of Unit 2. Unit 2 continues to the end of Section 477A-3-5, 20 cm, and is present again in wash core H-1, which recovered a small (~ 10 -cm long) drilled piece of plagioclase-phyric dolerite and a silicified dolomite (5-cm-long piece) intercalation above the basal dolerite.

Correlation Between the Igneous Lithologies of Holes 477 and 477A

Because of the close proximity (~ 165 m) of Holes 477 and 477A, it is important to compare and contrast the igneous lithologies which occur within these holes. In particular, it would be useful to assess the extent of lateral continuity of individual sills by showing that identical lithologies occur in both holes (Fig. 24).

The salient points of any comparison between the lithologies and petrographies of the igneous rocks of the two holes are:

1) The top of the igneous units in Hole 477 is at 58.0 meters sub-bottom, whereas the top of the igneous units in Hole 477A is at 34 meters sub-bottom.

2) A total of 42 meters of igneous rock was drilled in Hole 477, whereas only 21.5 meters was drilled in Hole 477A; however, because of the probability of considerable lateral variations in thickness, this may not be a significant factor; what is important is that the igneous rocks in Hole 477A show a greater textural range.

3) The igneous body in Hole 477 appears, on mineralogical and textural grounds, to be one major sill (Subunits 2a and 2c), with a minor sill (Subunit 2b) intruding the upper part of the main sill. The lithology at Hole 477A, however, comprises at least three distinct units, two of which are characterized by glassy chill zones on their upper surfaces. No glassy chill zones are observed in Hole 477 rocks. Nor are there any vesicular zones in Hole 477, unlike that in the upper zone in Unit 2 of Hole 477A.

4) Although there are considerable textural differences between the two igneous lithologies, their mineralogies do not differ significantly. Indeed, it would appear that the mineralogical variations within, say, Subunit 2a of Hole 477, which are probably due to gravitational crystal settling, are greater than the observed dif-

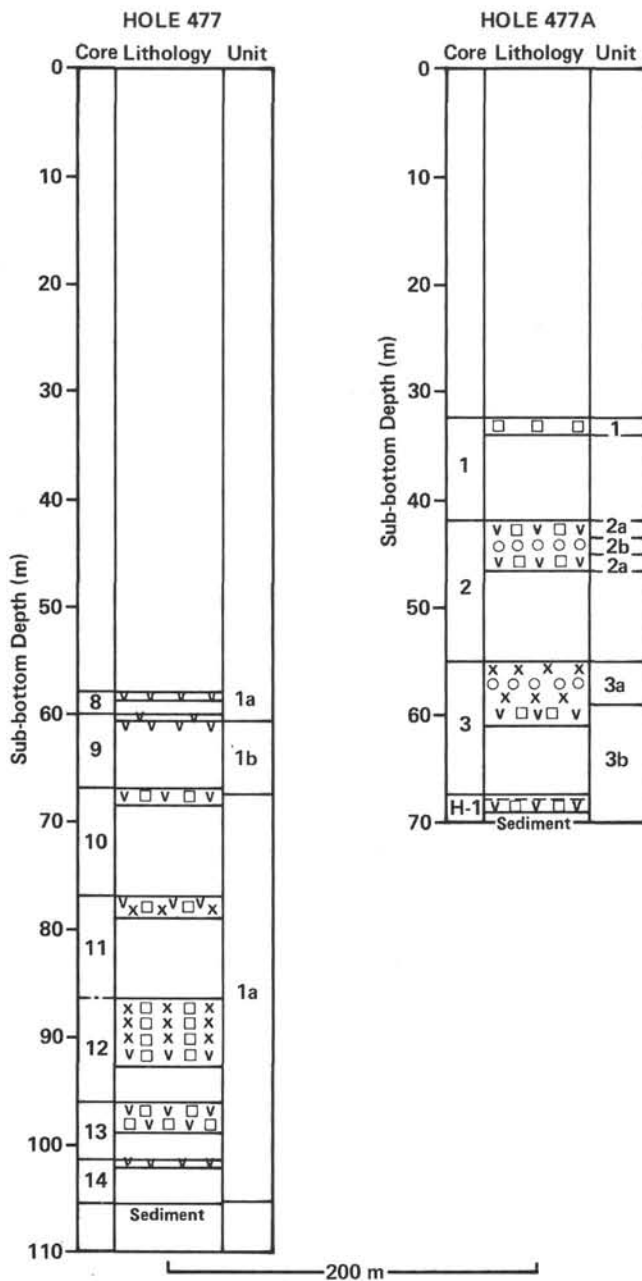


Figure 24. Correlation of igneous rocks in Holes 477 and 477A.

ferences between comparable units in Holes 477 and 477A.

5) The dolerite sills of Hole 477 show considerable alteration, with the development of clay minerals in the crystal interstices, but the sills of Hole 477A show much less evidence of alteration.

It is therefore apparent from a cursory examination of the lithologic data in Table 4 that the two lithologies of Holes 477 and 477A cannot be correlated directly. The number of units, their textures, and the degree of alteration, vary considerably; however, the lithologies are not dissimilar on mineralogical grounds, and possibly they were derived from the same magma chamber; they differ slightly in timing and mode of emplacement only.

Site 477 Physical Properties

Core 477-1, and parts of 477-2, 477-5, 477-7, as well as 477-19 through 477-23, were so badly disturbed by drilling or by expanded gas (Sections 477-5-1 and 477-23-1) that samples could be taken only for water content and as small chunks for the determination of bulk density and porosity. Core barrels 477-6 and 477-18 were empty. Data from the dolerite sill (Cores 477-8 through 477-14) are not included in Figure 25, which shows data obtained from these samples. Unfortunately, the sediment contacts of the dolerite could not be sampled. Although the original depth of the sediments recovered in Core 477-7 is not known, the plotted data for this core may characterize a layer close to the top of the dolerite sill. On Cores 477-16 and 477-17, the hand-operated soil-test shear-strength apparatus was used, because the sediments were too hard for the Wykeham-Farrance machine. From Hole 477A, only a few small undisturbed chunk samples could be taken (Cores 477A-8 through 477A-12). The data are also presented in Figure 25, together with those of Hole 477. In Figure 25, only the data for the sedimentary units are plotted.

In Unit 1, above the dolerite sill, the physical-property data and their depth gradients correspond approximately to those measured at the previous sites at this depth interval. Near the sediment surface, water content is about 65%, porosity 80%, and wet-bulk density 1.3 g/cm³. The somewhat deviating results from Core 477-2 cannot be explained. According to the visual core description, the sediments of this core are diatomaceous ooze in which very high water contents and low bulk densities are to be expected. The trend lines of Figure 25 for the uppermost meters of Unit 1 are confirmed by the results on the piston core taken later near this site (Hole 477B, Fig. 26).

Because of poor core recovery, the change of physical properties near the contact with the underlying dolerite is not clear. The data for 477-7, CC seem to indicate a marked change, but this sample has been taken from a silty layer and is therefore not characteristic of the clayey sequence represented by the trend lines in Figure 25. As at Sites 478 and 481, it is however assumed that the physical properties of the sediments above the dolerite are also affected considerably by heat.

Below the dolerite sill of Hole 477 (Unit 3), the sediments are much more compacted than those of Unit 1 of the same hole or those of the other holes in the corresponding depth range (100-165 m). In the summary of physical properties (Einsele, this volume, Pt. 2), it is demonstrated that the load of the 45-meter-thick dolerite sill can replace a sedimentary column of about 140 meters. This effect is, however, not quite sufficient to produce the high degree of compaction (water content 35%, porosity 55%, bulk density 1.7 g/cm³, vane shear strength > 1.5 × 10⁵ Pa = ~1500 g/cm²) observed at shallow depth (110 m sub-bottom) below the basaltic sill; therefore, we assume that, in addition to the loading effect of the sill, water content and porosity are also reduced by high temperature and its influence on diagenesis, including the formation of authigenic minerals described above. The unusually strong gradient of all

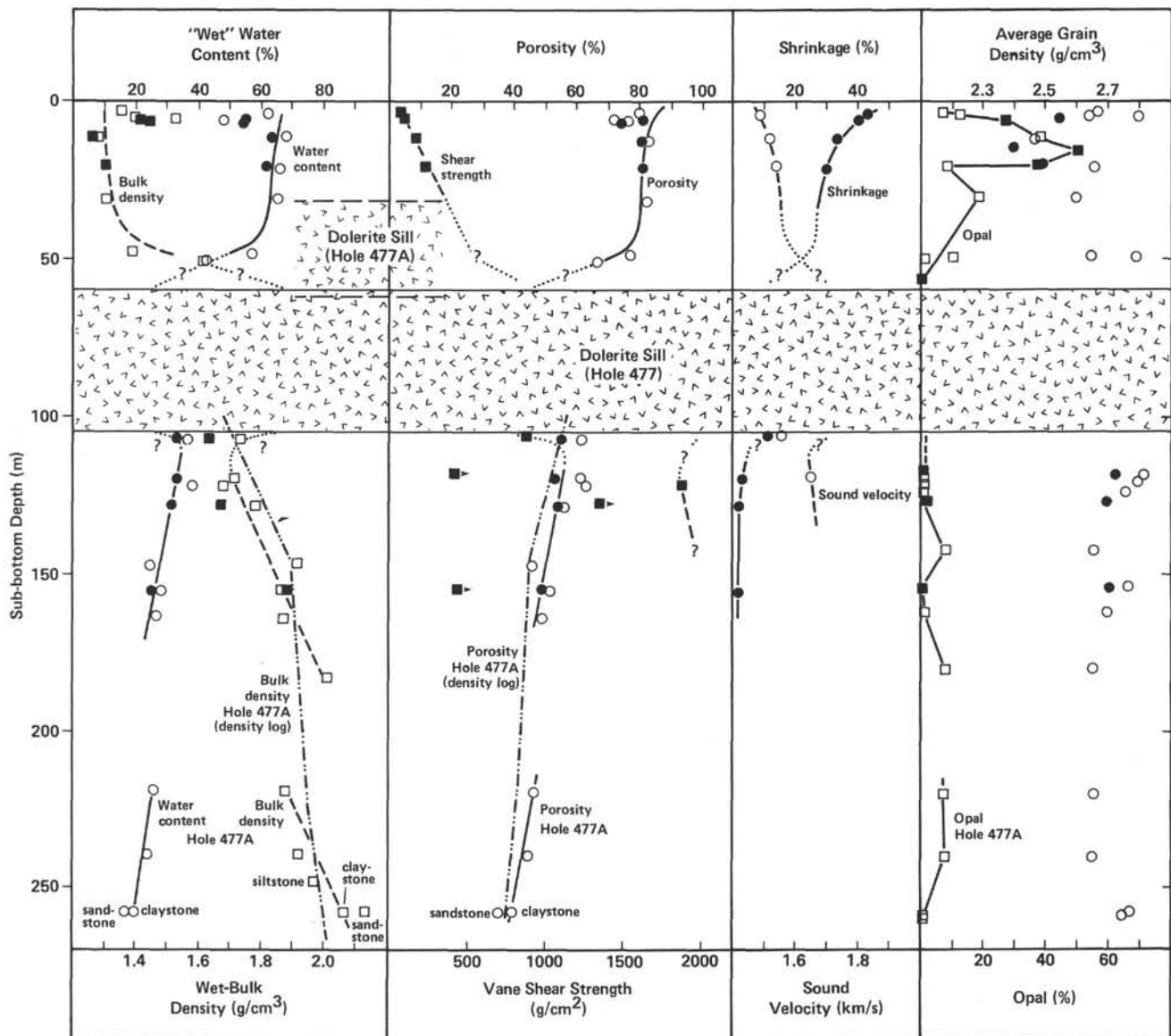


Figure 25. Mass physical properties, shrinkage, and proportion of opaline silica of sediments from Holes 477 and 477A. Note that in Hole 477A only the section from 220 to 260 meters was cored. Below 100 meters, bulk density and porosity of this hole are, therefore, inferred from the density log. Because of poor core recovery, the contacts of the sill are uncertain. (Solid symbols are cylindrical samples. Open symbols are chunk samples.)

physical properties below 110 meters indicates a heat source deeper than the depth explored by drilling.

Hole 477A revealed a higher, somewhat thinner (30 m) sill than Hole 477. Nevertheless, the density log of Hole 477A, starting at about 100 meters depth, shows about the same bulk densities and porosities as found in Hole 477. Below 150 meters, the gradients become smaller. For that reason, the mass physical properties determined on core samples from 220 to 260 meters depth are about the same as those of Hole 477 at shallower depth (~150 m). Possibly this is caused by differences in heat flow during and after sill intrusion.

The data on average grain densities indicate that in both holes, 477 and 477A, opaline silica, if it was present in higher quantities, has been transformed to chal-

cedony or quartz below the basaltic sill, and also to some extent above the sill of Hole 477. Here, from Core 477-7 downhole, average grain density always is equal to or higher than 2.64 g/cm^3 .

At Hole 477B, a piston corer recovered 3.46 meters in sediment near the sea bottom, although it is not known exactly how deep the piston corer penetrated below the mudline. From geochemical evidence, it may be assumed that the top of the sediment recovered was about 0.5 meters below the sea floor. The upper and lowermost parts of the core were rather disturbed and could not be tested adequately (see Fig. 26). The physical-property data for the middle part of the core are surprisingly consistent and show that the diatomaceous ooze is rather homogeneous and probably little disturbed by cor-

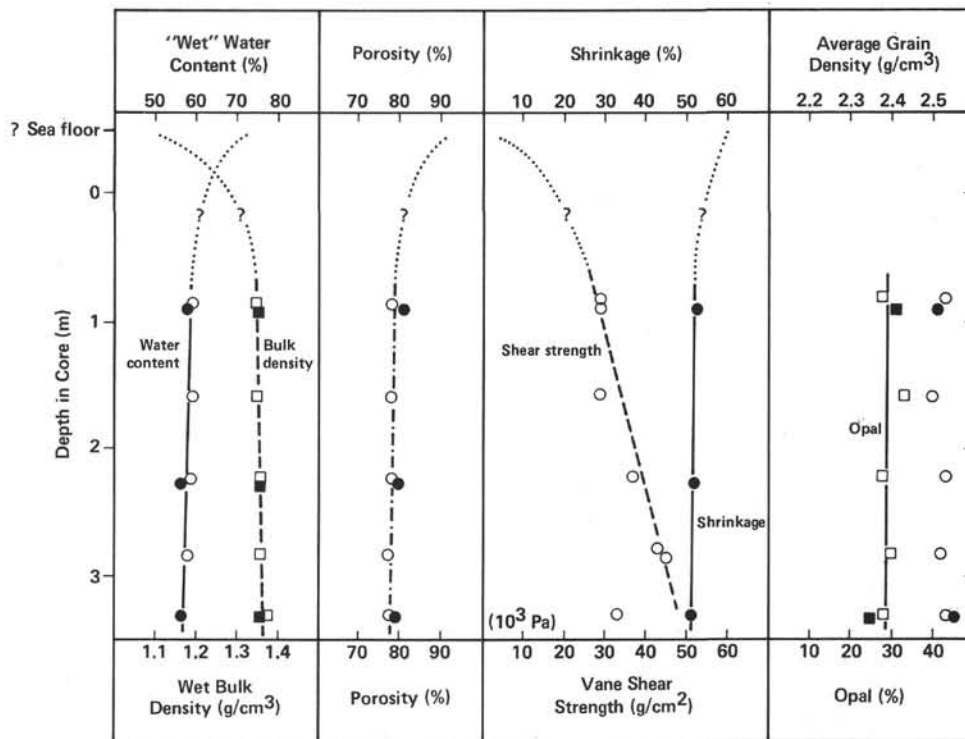


Figure 26. Mass physical properties, shrinkage, and content of opaline silica of sediments from a piston core (Hole 477B). Penetration below mudline uncertain. Upper part of core strongly disturbed. (Solid symbols are cylindrical samples. Open symbols are chunk samples.)

ing. Water content, porosity, bulk density, and shrinkage have only very small depth gradients. In contrast to these results, shear strength distinctly increases.

The physical-property data of this piston core confirm and supplement the data gained from Core 477-2. The extrapolation to the sediment surface in Figure 25 is purely tentative, but takes into account the extreme values found for very soft diatomaceous ooze at Sites 478 through 481.

Some data on sound velocity and acoustic impedance of soft-rock samples from Holes 477 and 477A are plotted in Figure 25. Data for hard-rock samples are listed in Table 5.

Site 477 Heat Flow and Thermal Conductivity

Thermal conductivities (*K*) measured in Hole 477 are listed in Table 6. The drilled section can be divided into

three major sub-units: the upper diatom ooze (*K* ≅ 2.1 mcal/cm s °C), the altered dolerite sill (*K* ≅ 3.9), and the claystones beneath the sill (*K* ≅ 3.2).

Only one temperature measurement was made with the Uyeda downhole temperature probe, at 48.5 meters. The temperature did not equilibrate completely during the run, but extrapolation suggests an equilibrium temperature of 50°C. Using a measured bottom-water temperature of 3.3°C and thermal conductivity of 2.1 mcal/cm s °C, heat flow at this site is 20 HFU. A second temperature measurement made with a maximum-recording thermometer at 173 meters sub-bottom depth recorded a temperature of 87.8°C 16 hours after drilling stopped. The hole was too hot to use the thermistor on the Uyeda probe. A three-layer model of thermal conductivity (see Beck, 1963) and this temperature yields a heat flow of 14 HFU. The lower heat flow calculated

Table 5. Some physical properties of hard-rock samples from Holes 477 and 477A.

Section	Interval (cm)	Rock Description	Orientation	<i>v_s</i> (km/s)	Bulk Density (g/cm ³)	Acoustic Impedance × 10 ⁵ (g/cm ² s)
477-9-1	Piece 49	Dolerite, fine-grained		3.36	—	—
477-10-1	Piece 5	Dolerite, coarse-grained		3.31	—	—
477-13-2	10	Gabbro	=	4.88	—	—
477-13-2	70-72	Plagioclase-phyric dolerite		—	2.89	—
477A-1-1	143	Dolerite	=	4.98	2.84	14.14
477A-2-3	Piece 5	Vesicular, coarse-grained basalt or dolerite		5.42	—	15.54
				5.94	2.76	—
					5.53	—
477A-2-4	85	Dolerite (Piece 10)		4.60	2.81	13.09
				4.72	—	—
477A-3-3	59	Gabbro	?	4.89 ^a	2.83	13.84
477A-11-1	15	Sandstone	=	1.79	1.97	3.53

^a Poor signal.

Table 6. Thermal conductivities, Hole 477.

Core	Section	Interval (cm)	K (mcal/cm s °C)
2	4	16-18	2.45
3	2	92-94	2.04
4	1	9-11	2.03
7	1	17-19	2.16
9	1	#4 (dolerite sill)	3.90
12	2	72-76	3.88
16	3	14-16	2.91
17	1	29-31	2.86
19	3	19-21	3.56
20	2	68-70	3.19

from this measurement may indicate that the hole had not yet approached equilibrium conditions, despite the long period after drilling stopped before taking the temperature. Alternatively, it may indicate that the emplacement of the sill has modified the geothermal gradient slightly.

The two temperature measurements taken at Hole 477 (50° at 49 m and 87°C at 168 m sub-bottom) confirm that the high heat flow in the southern Guaymas Basin is primarily conductive and at shallow depths is not an artifact of water convecting through the sediments. The data also show that the high geothermal gradient extends well below the sill encountered at 55.5 meters. Although the emplacement of the sill probably has modified the geothermal regime at Hole 477, the data suggest that the high conductive heat flow primarily is from the basement.

Site 477 Correlation of Drilling Results with Seismic Data

Many seismic-reflection lines have been run over or near the location of Site 477. Sharman (1976) reported on a network of single-channel analog records. The SIO IPOD Site Survey cruise (Guaymas expedition) ran two multichannel records over the site, one perpendicular to the rift and the other down its axis, and final selection of the site was based on the location of this crossing. We ran several crossings of the rift with *Glomar Challenger* before dropping the first and second beacons. On our return from a personnel transfer between drilling Holes 477 and 477A, we ran single-channel lines northeastward and southwestward in the axis of the rift, and we attempted a sonobuoy run in order to obtain wide-angle reflection and velocity.

The sonobuoy failed to produce any refractors, probably because the sills which would ordinarily refract are of very limited continuity. The sonobuoy record furthermore does not contain any usable wide-angle reflection, because "acoustic basement" surfaced during parts of the run. As a result, our information on velocity comes from the downhole sonic log, from the multichannel moveout velocity analyses, and from a limited number of laboratory measurements. From these various sources, we were able to compile a detailed velocity structure which applies principally to Hole 477A. Even

with this information, however, we are unable to correlate in a meaningful way with any of the single-channel analog records. We conclude that the principal reason for the apparent lack of correlation is the extreme variability of geology over short distances within the rift. Some correlation is suggested, however, with the processed multichannel record crossing the rift and with the 3.5-kHz records.

Holes 477 and 477A are only about 165 meters apart, but the sections they penetrated were very different. Study of petrology of the sills leads to the conclusion that the sills encountered at about 58 to 105 meters and 32.5 to 62.5 meters represent different intrusive events. The several lines run across the rift with the 3.5-kHz system are especially revealing because of the extreme variability from line to line, separated only by a total of about 3 km (see Fig. 12; Fig. 27). The 3.5-kHz line run along the axis before we attempted the sonobuoy run (Fig. 28) furthermore suggests that the southwestern end of this rift does not contain shallow intrusive bodies (sills?), and that northeast of Site 477 some of the magmas may have extruded above the sea floor to form the mounds and hills. Relative locations of all these lines are only approximate, hence the difficulty in correlating. Finally, Figure 29 shows a section of 3.5-kHz recording with *Glomar Challenger* stationary over the beacon at Hole 477A. Even with a presumably stationary position, there appears to be sufficient ship movement and sub-bottom variability to show changes with time in the record. We can correlate drilling results with lithology in this hole and the location of the sill is indicated. The prominent dark reflector about 15 meters below the very soft sea floor is apparently the change from diatomaceous ooze (Holocene?) to the uppermost turbidites of sands and sandy silts (pre-Holocene, late Pleistocene deposits of lower sea level or early transgression, Core 477-3).

The section of processed multichannel seismic-reflection record we had on *Glomar Challenger* during the leg could not be correlated with drilling results. After completion of the leg, however, we had this line reprocessed, running NW-SE across the rift, crossing Sites 477 and 478. Some correlations can be suggested between this reprocessed record and drilling results (Fig. 30).

The sea floor is very faint in this record, as it is in 3.5-kHz records cited previously. Prominent sub-bottom reflectors appear to be rather discontinuous. Location of Holes 477 and 477A cannot be determined precisely in this line, because of positioning uncertainties, but reflectors of about 40 to 80 meters sub-bottom could correlate with the sills encountered at about 32 and 58 meters in Holes 477A and 477, respectively. A strong, rather continuous reflector at about 200 meters sub-bottom is not explained so easily. It appears to correlate, however, with a sandstone section at 190 meters, with a higher-velocity section in the sonic velocity log of 195 to 214 meters, and with a kick in the bulk-density log at about 200 meters. Continuity of this reflector suggests that this may be a sand turbidite, flat-ponded in the rift during a low sea-level stand of late Pleistocene age.

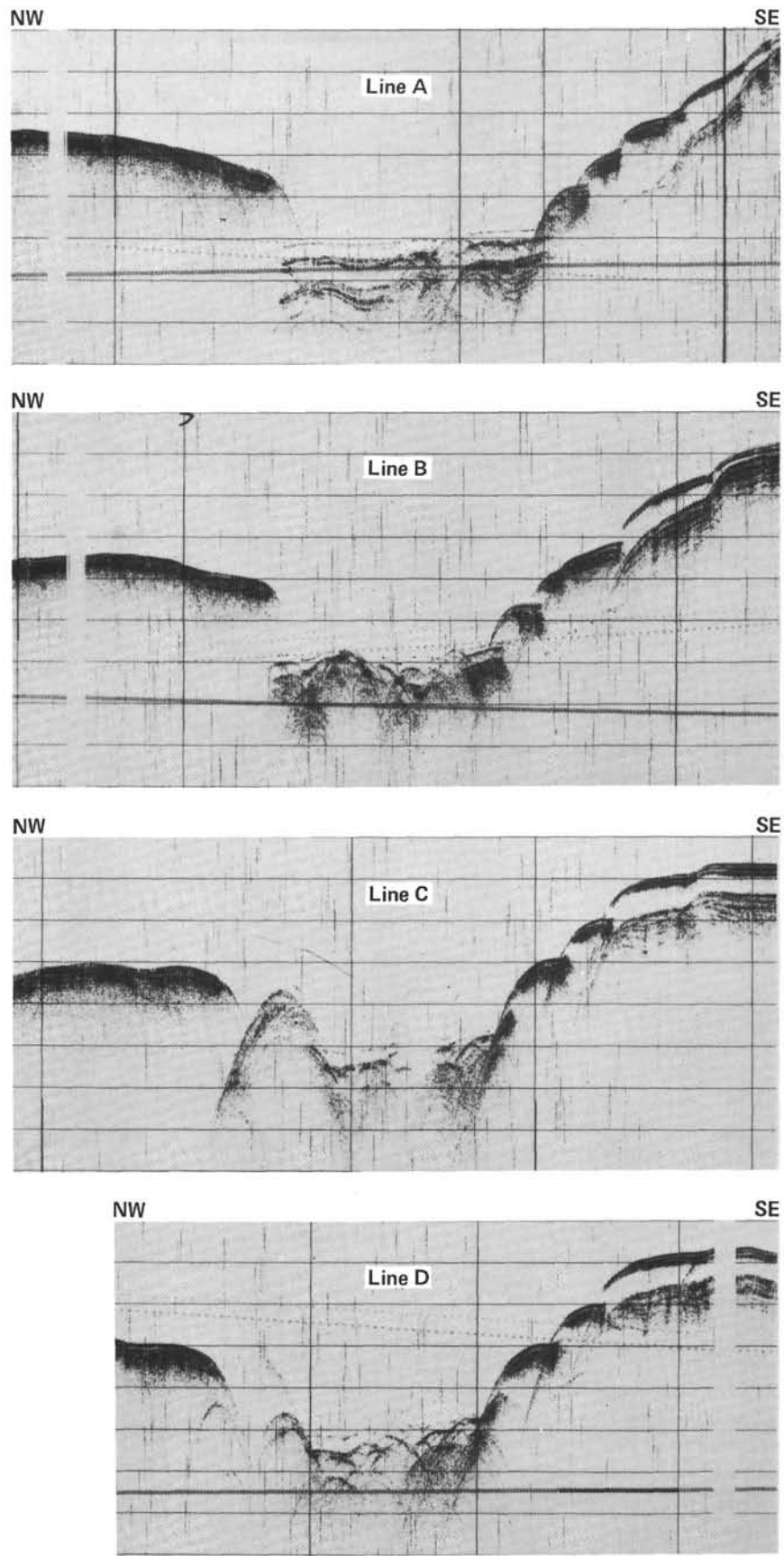


Figure 27. Composite of 3.5-kHz records across the southern rift of Guaymas Basin near Site 477.

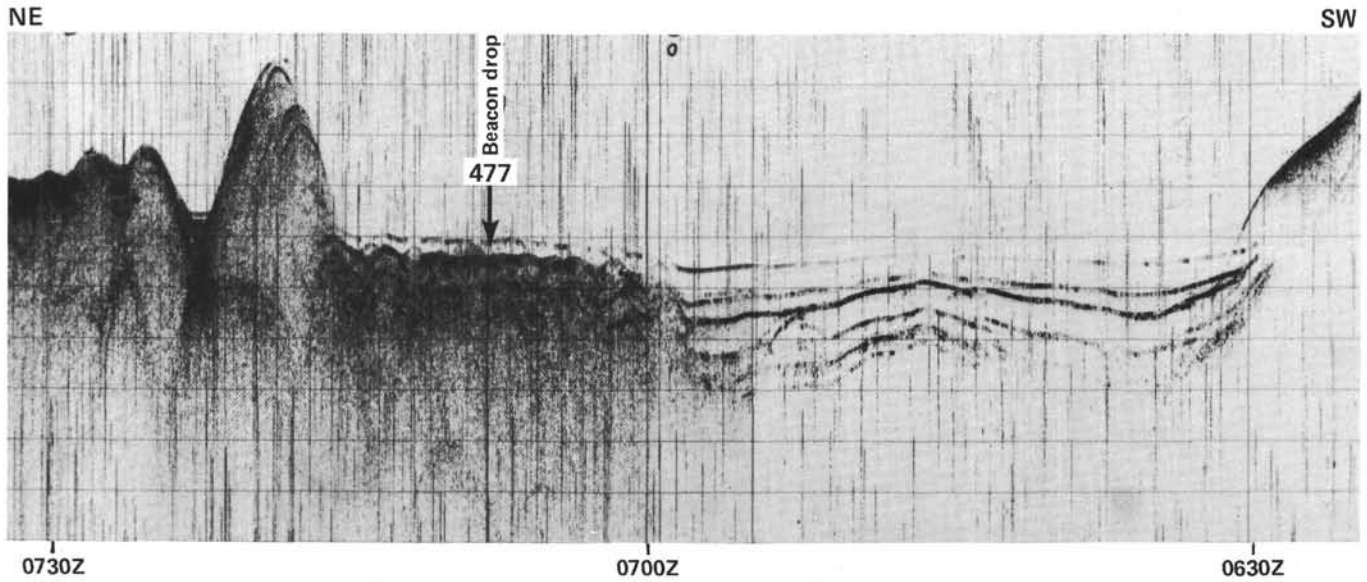


Figure 28. Guaymas Basin 3.5-kHz record longitudinally along the axis of southern rift, across Site 477.

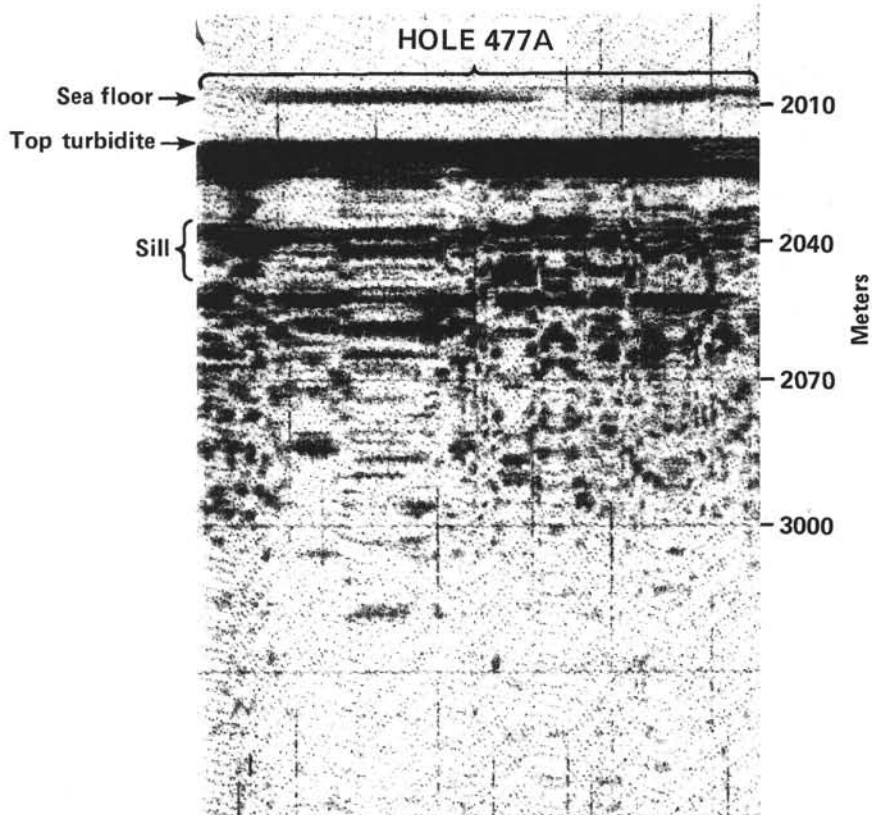


Figure 29. Correlation of drilling lithology with 3.5-kHz records, Hole 477A.

Site 477 Summary and Conclusions

Drilling at this site in the southern active rift of Guaymas Basin was not without technical difficulties and safety concerns for possible pollution problems, the latter eventually causing abandonment of the site. Nevertheless, it was a scientific success, and most of our objectives were met. Several previously untested hypoth-

eses were verified. For example, the emplacement of an igneous intrusion within very rapidly deposited sediments of late Quaternary age (NN21) was confirmed by drilling. This also substantiated the concept that, in newly formed basins flanked by large continental sediment supplies, upwelling of magma in response to rifting results in mixing of sediments and igneous intrusive bodies, rather than extrusion of pillow basalts onto the sea floor. High

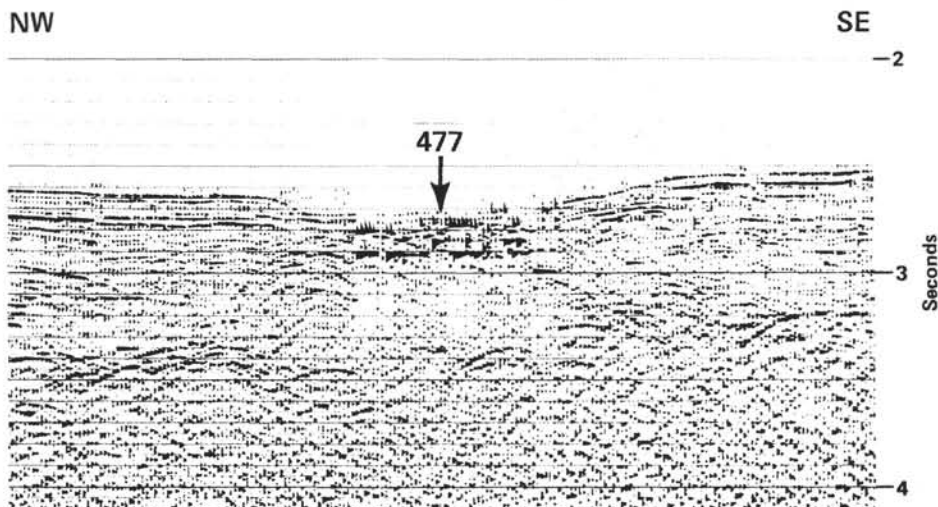


Figure 30. Section of processed multichannel seismic-reflection record across southern rift, Guaymas Basin and Site 477, from Guaymas Expedition, Scripps Institution of Oceanography Site Survey.

heat flows measured at the sea floor and a hypothesis of conductive flow to account for the anomalies also were given added credence by our two downhole temperature measurements. These showed that the heat flow in the trough is primarily conductive, and not an artifact of water convecting through sediments at shallow depths. The measurements also show that the high gradients extend well below the intrusive body penetrated by the drill. The very fundamental assumption required of the sea-floor-spreading hypothesis, that sediments in the rift must be of an age related to the rift dimension and spreading rate ($\sim 50,000$ years old in this case) was supported by the lack of sediments older than NN21.

The site is, as expected, characterized by exceptionally high heat flow, which is responsible for the very young and unusual alteration mineralogy and geochemical properties not previously observed in deep-sea cores. The mineralogical and chemical effects of mixing young sediments of high water content with intrusive basalts or dolerites was studied in a preliminary way aboard ship and will be given thorough post-cruise examination. The effects of this mixture on the organic constituents was particularly intense, and is related to the chronology of sill intrusion. Before emplacement of the sill, the lower sediments were subject to high thermal gradients, as indicated by fluorescence, C and N contents, and absence of petrogenic gas, which was probably removed by hydrothermal circulation. Later emplacement of the dolerite sill imposed a second thermal stress on the sediments above. This resulted in higher concentrations of biogenic hydrocarbon gas (C_1 - C_4) below the sill only. The high proportion of CO_2 in the gas below the sill and an increase in H_2S may also indicate that the C_1 - C_4 hydrocarbons could be cracking products of petrogenic gas and liquids, but this is not supported by the puzzling absence of petroliferous odor. It appears that the gas below the sill is both endogenous and thermally derived from primary biogenic organic matter. The black "slick" which was found in and below Core 477-19 appears to be a "condensate" of C_1 - C_4 hydrocarbons having the same distribution as in the gas and adsorbed in fine clays.

Two main sediment units were recognized. The youngest is the section of unaltered diatomaceous turbidites. A dolerite sill lies below these sediments, and the second unit comprises altered and indurated diatomaceous turbidites. A high-temperature hydrothermal assemblage of minerals beneath the sill is the first of its kind found in deep-sea drilling. This discovery is unique in its shallow (60-260 m), intense alteration of extremely young terrigenous turbidites, mixed with a pelagic rain of reactive opaline frustules, in temperatures of over $135^\circ C$ at 260 meters. Sediments above the sill remain pristine, suggesting that the sill has formed a closed or restrictive system. Tentative shipboard determinations record a mineral assemblage which includes dolomite, anhydrite, at least two zeolites, varieties of epidote, pyrite masses, quartz, anatase, traces of siderite, possible albite or K-feldspars, and clays. The envisaged hydrothermal system has minimal circulation of sea water, low water/rock ratios, and sea-water-basalt/sediment interactions significantly different from hydrothermal systems postulated for mid-ocean ridges.

Pore-water chemistry also is affected strongly by the intrusion into the young sediments. A sharp decrease in alkalinity and magnesium occurs as the intrusion is approached. Below the sill, the hydrothermal alteration of the sediments is reflected by depletion in magnesium and gains in calcium in the fluid phase. A large increase in dissolved chloride is interpreted best by water removal, either within the sediment column or at depth. The latter case involves upward advection of water from deeper, hydrothermally altered strata. Upward advection of hydrogen sulfide could account for the high concentrations of sulfide minerals near the base of the intrusion (Core 477-22).

Diagenetic affects of the encountered high temperatures are expressed in the physical properties of the sediments as well. Rough calculations of effective bulk densities of sediments and dolerite suggest that the loading effect of the dolerite is insufficient to replace the 200-meter sediment column which would be necessary to account for densities and porosities at this site compared

to those not influenced by intrusives or abnormal heat flow. Interstitial-water loss from high heat flow at depth and basal effects of the sills probably account for the divergence from normal or expectable bulk densities.

An expectable result of a combination of high sedimentation rate in a confined rift trough, subject to active intrusion of magmas and tensional faulting, is structural chaos. This expectation was confirmed by attempts at correlation of drilling results with seismic data. Extensive study of the many seismic-reflection records taken over or in the vicinity of this site, together with velocity data from downhole logging, revealed no meaningful correlations between the two. It is concluded that the reason for this lack of correlation is the extreme variability of the geology over very short distances within the rift trough.

SITE 478

Site 478 Background and Objectives

General background and objectives of the Guaymas Basin sites were explained previously. Site 478 (GCA-25) was the first and only site to be drilled on the flank of one of the spreading rifts in the floor of the basin. It is approximately 12 km northwest of the axis of the southern rift. Assuming a spreading half-rate of 3 cm/yr, this site should be approximately 400,000 years old, unless spreading-axis jumps have complicated formation of new crust in this area. Specific objectives of this site included the following:

- A. Sediments.
 1. Sedimentary facies and organic constituents.
 2. Diagenesis and the effects of early very high heat flow and subsequent moderately high heat flow.
 3. Hydrothermal effects and/or deposits.
 4. Evidence for climatic, sea-level, subsidence, or other environmental changes.
- B. Basement and other igneous rocks.
 1. Intrusions into the sediment column.
 2. Depth of "basement" as compared to acoustic basement in multichannel and other seismic records.
 3. Composition of basement and comparison with MORB, especially Site 482, Leg 65 (GCA-1).
 4. Mode of emplacement of basement.
 5. Effects of hydrothermal activity.
- C. Chronology. Confirmation or denial of tectonic model and predicted age.

Site 478 Operations

To complement Site 477 drilling in the active south rift of Guaymas Basin, we planned to drill a site on the flank of the rift to compare geology and processes and test the spreading hypothesis for Guaymas Basin. The selected site, Site 478, lies 12 km northwest of the south rift. Previous site-survey multifold seismic (*T. Washington*, Guaymas 2, 6 Mar 78) suggested that low-velocity seismic basement at that site is contiguous to that of the presently active rift. A simple pre-drilling seismic line to connect the two sites using *Glomar Challenger* seismic equipment was begun at 0440Z on 24 December, as we

were under way from Site 477 toward Site 478 on course 302° (see Fig. 12). At 0600Z the beacon was dropped in 1889 meters water depth, and after continuing about 3 km on course we retrieved the seismic gear at 0630Z and returned to the beacon. The 3.5-kHz record shows our site to be on the outer edge of a natural levee flanking the south side of an east-trending turbidity-current channel. The channel appears to be inactive now and partially filled. Bathymetry in the area suggests that the channel connects to a canyon originating on the eastern margin of the Concepción Peninsula. At 0700Z we began lowering hydrophones for positioning over the beacon, and at 0745Z we began running-in the hole.

The drill was spudded in at 1400Z, and the mudline was recorded at 1913 meters, corresponding to the PDR depth of 1899 meters. Our first core was on deck at 1435Z. Thereafter, we cored continuously to 342.5 meters at 0753Z on 26 December before encountering massive, altered basalt. Overall recovery was very good, with 72% of the sediments retained despite the poor recovery in some hard, dolomitic sandstones. Two other dolerite sills were penetrated (220–232 m and 253–257 m) within this sediment section. We attribute this good recovery rate in both sediments and igneous rocks to the use of a bit with a smaller-than-normal throat required for use of the pressure core barrel. The heat probe was deployed at 70, 136, and 159 meters, with one success and two failures. The pressure core barrel was lowered at 159 meters and again at 322 meters. Both of these attempts were unsuccessful; the first returned with gas, but no core, and the second returned with a sandstone core, but was not closed to pressure.

Drilling at this site was reluctantly terminated for time considerations based on overall priorities of our remaining objectives. We believed additional sediments might lie below the sill, but the unknown thickness of the sill, slow drilling rates, and low probability of recovering thin intercalations of soft sediment argued against continued operations at this site at the expense of our last three planned sites.

On termination of drilling, we conditioned the hole for logging, dropped the bit, and pulled up the pipe to log. Logging began at 0700Z on 28 December and continued until 0100Z on 29 December.

The first logging run was for density, gamma ray, caliper, and temperature; the second run was for sonic, gamma ray, and caliper. On this run, the sonic tool stuck in a bridge of hard material on its return trip, and the connecting head parted in our attempt to free it. It was then necessary to rig-down the logging gear, run the drill pipe down to above the lost tool, and attempt to fish it out. The fishing met with no success, and logging gear was then re-rigged and logging resumed to a level above the bridged section, from 2250 meters to the mudline. Run number three was for guard, neutron, and gamma ray. Run number four was for induction and gamma ray. We then cemented a plug in the hole from 2113 to 2050 meters, pulled out of the hole, and prepared for departure. At 0700Z on 29 December, we departed Site 478 enroute to Site 479.

A coring summary is given in Table 7.

Table 7. Coring summary, Site 478.

Core No.	Date (Dec. 1978)	Time	Depth from Drill Floor (m)		Depth below Sea Floor (m)		Length Cored (m)	Length Recovered (m)	Recovery (%)
			Top	Bottom	Top	Bottom			
478-1	24	0735	1913.0	1916.5	0.0	3.5	3.5	2.10	60
2	24	0815	1916.5	1926.0	3.5	13.0	9.5	8.30	87
3	24	0855	1926.0	1935.5	13.0	22.5	9.5	6.88	72
4	24	0938	1935.5	1945.0	22.5	32.0	9.5	8.91	94
5	24	1043	1945.0	1954.5	32.0	41.5	9.5	9.56	101
6	24	1102	1954.5	1964.0	41.5	51.0	9.5	8.97	94.5
7	24	1156	1964.0	1973.5	51.0	60.5	9.5	9.54	100
8	24	1303	1973.5	1983.0	60.5	70.0	9.5	6.14	65
9	24	1500	1983.0	1992.5	70.0	79.5	9.5	6.93	73
10	24	1543	1992.5	2002.0	79.5	89.0	9.5	3.67	39
11	24	1621	2002.0	2011.5	89.0	98.5	9.5	8.38	88
12	24	1703	2011.5	2021.0	98.5	108.0	9.5	5.88	62
13	24	1753	2021.0	2030.5	108.0	117.5	9.5	6.36	67
14	24	1835	2030.5	2040.0	117.5	127.0	9.5	8.18	86
15	24	1927	2040.0	2049.5	127.0	136.5	9.5	6.62	70
16	24	2025	2049.5	2059.0	136.5	146.0	9.5	6.43	68
17	24	2217	2059.0	2068.5	146.0	155.5	9.5	9.93	104
18	24	2312	2068.5	2072.5	155.5	159.5	4.0	0.18	5
19	25	0005	2072.5	2078.0	159.5	165.0	5.5	9.73	177
20	25	0223	2078.0	2087.5	165.0	174.5	9.5	7.71	81
21	25	0315	2087.5	2097.0	174.5	184.0	9.5	9.42	99
22	25	0420	2097.0	2106.5	184.0	193.5	9.5	4.62	49
23	25	0518	2106.5	2116.0	193.5	203.0	9.5	0.00	0
24	25	0620	2116.0	2125.5	203.0	212.5	9.5	0.03	1
25	25	0734	2125.5	2135.0	212.5	222.0	9.5	0.10	1
26	25	0925	2135.0	2144.5	222.0	231.5	9.5	1.20	13
27	25	1023	2144.5	2154.0	231.5	241.0	9.5	0.83	9
28	25	1145	2154.0	2163.5	241.0	250.5	9.5	9.58	101
29	25	1325	2163.5	2169.0	250.5	256.5	6.0	3.05	51
30	25	1420	2169.0	2173.0	256.5	260.0	3.5	3.20	91
31	25	1515	2173.0	2182.5	260.0	269.5	9.5	8.63	91
32	25	1605	2182.5	2192.0	269.5	279.0	9.5	6.17	65
33	25	1656	2192.0	2201.5	278.0	288.5	9.5	7.83	82
34	25	1752	2201.5	2211.0	288.5	298.0	9.5	7.53	79
35	25	1902	2211.0	2220.5	298.0	307.5	9.5	6.91	73
36	25	1950	2220.5	2230.0	307.5	317.0	9.5	4.89	50
37	25	2055	2230.0	2235.5	317.0	322.5	5.5	0.00	0
38	25	2212	2235.5	2239.0	322.5	326.5	4.0	0.21	2
39	25	2304	2239.0	2249.0	326.5	336.0	9.5	4.44	47
40	26	0053	2249.0	2258.5	336.0	345.5	9.5	4.32	45
41	26	0409	2258.5	2268.0	345.5	355.0	9.5	9.70	102
42	26	0650	2268.0	2277.5	355.0	364.5	9.5	5.04	53
43	26	0927	2277.5	2287.0	364.5	374.0	9.5	5.60	59
44	26	1209	2287.0	2296.0	374.0	383.0	9.0	8.01	89
45	26	1433	2296.0	2305.0	383.0	392.0	9.0	8.35	93
46	26	1742	2305.0	2314.0	392.0	401.0	9.0	7.18	80
47	26	2115	2314.0	2323.0	401.0	410.0	9.0	0.00	0
48	26	2340	2323.0	2332.0	410.0	412.0	2.0	1.36	68
49	27	0300	2332.0	2332.0	412.0	419.0	7.0	3.91	56
50	27	0540	2332.0	2341.0	419.0	428.0	9.0	8.72	97
51	27	0820	2341.0	2350.0	428.0	437.0	9.0	8.77	97
52	27	1129	2350.0	2359.0	437.0	446.0	9.0	9.00	100
53	27	1425	2359.0	2368.0	446.0	455.0	9.0	5.50	61
54	27	1753	2368.0	2372.0	455.0	464.0	9.0	5.77	64

Site 478 Sediment Lithology

Although the entire sediment column penetrated at Site 478 (Table 8; Fig. 31) is probably less than 300,000 years old, we have selected three sedimentary units within a sequence dominated by olive-drab, muddy, diatomaceous oozes. These are differentiated by the type and frequency of redeposited beds in Unit 1; the occurrence of dolerite sills and contact zones with dolomite in Unit 2; and diatomaceous mudstones, some with varve-like laminations, in Unit 3 between the second sill and the basal dolerite intrusion.

Subunit 1A: Diatomaceous Muds and Silty Turbidites (478-1 through 478-14, CC, 0-127 m);

The upper part of Unit 1 is characterized by a mixture of moderate-olive-brown (5Y 4/4), muddy, diatomaceous oozes, interlayered with redeposited beds grading from pale-olive-gray (10Y 4/2) diatom muds to gray (N4-7), silty sands. Some scattered, thin, pale-olive diatom oozes occur, mainly on top of graded silts. Cores are

moderately to intensely disturbed, which obliterated any burrow mottling, laminations, or bedding other than some faint banding. Calvert (1966), however, has demonstrated that surface cores from the deep Guaymas Basin are pervasively burrowed.

In Core 478-1 the consistency of the diatom oozes is gelatinous, but firms rapidly. The first cores are rich in H₂S, which diminishes below Core 478-7. The diatom oozes to muds contain abundant diatoms (20-60%), with common quartz, feldspar, and clays. Minor components include some radiolarians and foraminifers (2%). Nanofossils remain persistently 5 to 10% of a sample, increasing slightly in Cores 478-11 to 478-13. Pyrite is ubiquitous (2-5%); it is typically concentrated within diatom frustules.

Sandy turbidites are initially rare, but then dominate from Cores 478-2 through 478-12. Repetitive graded beds of gray sand to clayey silt turbidites, some 200 to 400 cm thick, occur. Several lines of evidence suggest that these are redeposited from a single, possibly deltaic, source. Basal zones have limited size ranges, from silt to fine sand, independent of thickness of turbidites. The clasts are subangular. Feldspars and rounded volcanic rock fragments are as common as quartz, and there is little clay. The beds grade from well-washed fine sand to thick, homogeneous sections of grayish-olive, clayey silt. The top part of a bed contains little clay, but blends into the host lithology. The main body is massive, structureless. Extremely thick beds occur from 478-2-3, 76 cm to 478-2-5, 40 cm (265 cm thick), 478-3-1, 0 cm to 478-3-3, 50 cm (350 cm), 478-7-5, 6 cm (210 cm), and 478-11 (490 cm).

Interspersed throughout Subunit 1A, thin (1-3 cm), pale-olive (10Y 6/2) pulses of pure diatom ooze typically occur at the tops of another kind of turbidite, which grades downward to darker, less-diatom-rich sediments—an olive-brownish sandy silt. In contrast to the host lithology of muddy diatom ooze, these pale layers contain more of the less-resistant, fragile, small diatoms and almost none of the larger, round, robust types. In some places, thin laminae of coarse sands occur at the base of these beds (e.g., Fig. 32; 478-2-2, 120 cm). They contain mostly angular rock fragments, some quartz, and mixed shallow-water carbonate hash. A lack of clay in source regions and hydraulic equivalent behavior of the fragile diatom frustules would tend to concentrate them at the top of turbidites.

Subunit 1B: Diatomaceous Silty Mud (478-15-1 through 478-23-3, 120 cm; 127.0-188.2 m)

Subunit 1B is separated to distinguish a zone with possibly higher rates of accumulation. The contact with Subunit 1B is gradational from Core 478-14, as the interlayered beds of moderate-olive-brown, muddy diatom oozes dwindle and vanish. Abundances of both gray sand and moderate-olive-brown layers decrease. Although cores are disturbed, the sediments clearly change to more-uniform, massive, grayish-olive (10Y 4/2), diatomaceous, silty mud. Any bedding, mottles, or bioturbation are rare and very faint, although a few sand wisps persist. H₂S is absent. In general, the composition

Table 8. Sediment lithology, Site 478.

Lithologic Unit	Cores	Sub-bottom Depth (m)	Thickness (m)	Lithology	Paleoenvironment	Age	Average Accumulation Rate
1	478-1 to 478-22-3	0-188.20	188.20	Muddy diatomaceous ooze to diatom mud with episodic graded, gray sands	Basinal turbidites	NN21	Rapid
1A	478-1 to 478-14,CC	0-127.0	127.0	Moderate-olive-brown, muddy, diatomaceous ooze with frequent gray, sandy interlayers		NN21	Rapid
1B	478-15-1 to 478-22-3, 120 cm	127.0-188.2	61.2	Grayish olive diatomaceous silty mud	Mass flows and mud turbidites	(?)	Very rapid (slumping?)
2	478-22,CC to 478-30,CC	188.2-260.0	71.8	Dolomitic siltstones, two dolerite sills with contact aureoles, diatomaceous mudstone	Hemipelagic with basinal turbidites	NN20	Slow to rapid
3	478-31-1 to 478-40-3, 10 cm	260.0-342.5 ^a	82.5	Olive-brown, diatomaceous, silty claystones		NN20	Slow to rapid
3A	478-31 to 478-34,CC	260.0-288.0	28.0	Diatom mudstone with some sandy interlayers	Redeposited muds interlayered with hemipelagic host	NN20	Moderate
3B	478-35-1 to 478-40-3, 10 cm	288.0-342.5 ^a	54.5	Laminated diatom mudstone with dolomite and siltstone	Small basinal high with low-oxygen environment; contact zone to lowermost dolerite intrusion	NN20 (Core 36, 0.26 m.y.) (<0.45 m.y.) late Pleistocene	Moderate seasonal (overall 1200 m/m.y.)

^a Basement depth 342.5 meters, based on driller's records.

shifts toward fewer diatoms (<20%), nannofossils (3%), and clay (30%). Plant remains increase (7%). Pyrite is present partly as cubes. Most of the carbonate is unspecified and very fine-grained. Most sections do not react with HCl.

More-differentiated basin sediments occur at the base of the subunit, marked by two well-defined, thick, gray (N5) sand turbidites (Fig. 33; Cores 478-19-6, 120 cm and 478-20-5, 300 cm) before interlayered moderate olive-brown diatom oozes and muds reappear. Carbonate nannofossils and diatoms increase in abundance.

Unit 2: Diatomaceous Muds Intruded by Dolerite Sills (478-22,CC through 478-30,CC; 188.2-260.0 m)

Recovery in this unit was very poor, because of hard and soft interlayers. Induration of some beds is related to the effect of the two sill complexes within this unit. The upper sill (12-13 m thick) contains two separate igneous units and evidence from logging of a sediment intercalation which was not recovered. The lower sill is about 4 meters thick, based on logging, and also has a thin contact zone (see igneous petrology section).

Above the upper sill, the only sediments recovered from 188 to 222 meters sub-bottom were lithified light-olive-gray to tan siltstones with a dolomitic cement. Drilling and logging records indicate, however, that softer sediments were intercalated between hard layers encountered at 190 meters (1.5 m thick), two thin ones at 201 to 202 meters and 204 to 205 meters, and the last just above the sill, at about 219 to 220 meters. Presumably, these softer sediments were similar to those diatomaceous muds to oozes recovered above and below. Smear-slide evidence from the dolomitic siltstones includes abundant diatom relics and quartz and feldspar grains. These indurated rocks preserve many of the sedimentary structures not otherwise visible in the softer

sediments, such as oblong burrows or parallel laminations and cross-beds in coarse-grained sands.

Between the sills, sediments are partially indurated, but friable, diatomaceous claystones. They have been much brecciated by drilling, but seem to be without sandy interlayers according to logs. Smear slides show abundant diatoms (up to 50%), along with some nannofossils (5-7%), pyrite (1-3%), and the ubiquitous quartz-feldspar terrigenous overprint, with 20 to 40% clay.

A more or less symmetrical contact aureole is present around the second sill; 60 cm were recovered above the sill and 90 cm below. Bulk density increases in the last meter toward the contact from both directions. Sediments grade from dark-yellow-brown (10YR 3/2), diatomaceous mudstones, to black (N1), silty claystone. Scattered dolomite rhombs are a common constituent on both sides—from 20 to 30% of the sediment. The black claystones are hard, without evidence of calcium carbonate or H₂S. Smear-slide compositions are mostly clay (50-60%), along with minor quartz and feldspar and pyrite. Some clays show ferruginous coatings, but the black color must result from reduction of organic matter.

Subunit 3A: Diatom Mudstones (478-31-1 through 478-34,CC; 260.0-288 m)

Below the second sill, sediments grade to uniform light-olive-gray mudstone to muddy diatomite. The induration of the claystones is greater than expected for silty clays at this burial depth, suggesting that the emplacement of the sills and/or high heat flow contributed to early lithification.

Unit 3 designates the renewed occurrence of moderate-olive-brown (5Y 4/4), uniform diatomites to diatomaceous claystones, with some interlayered softer gray sands. Distinct sand layers with bulk densities around

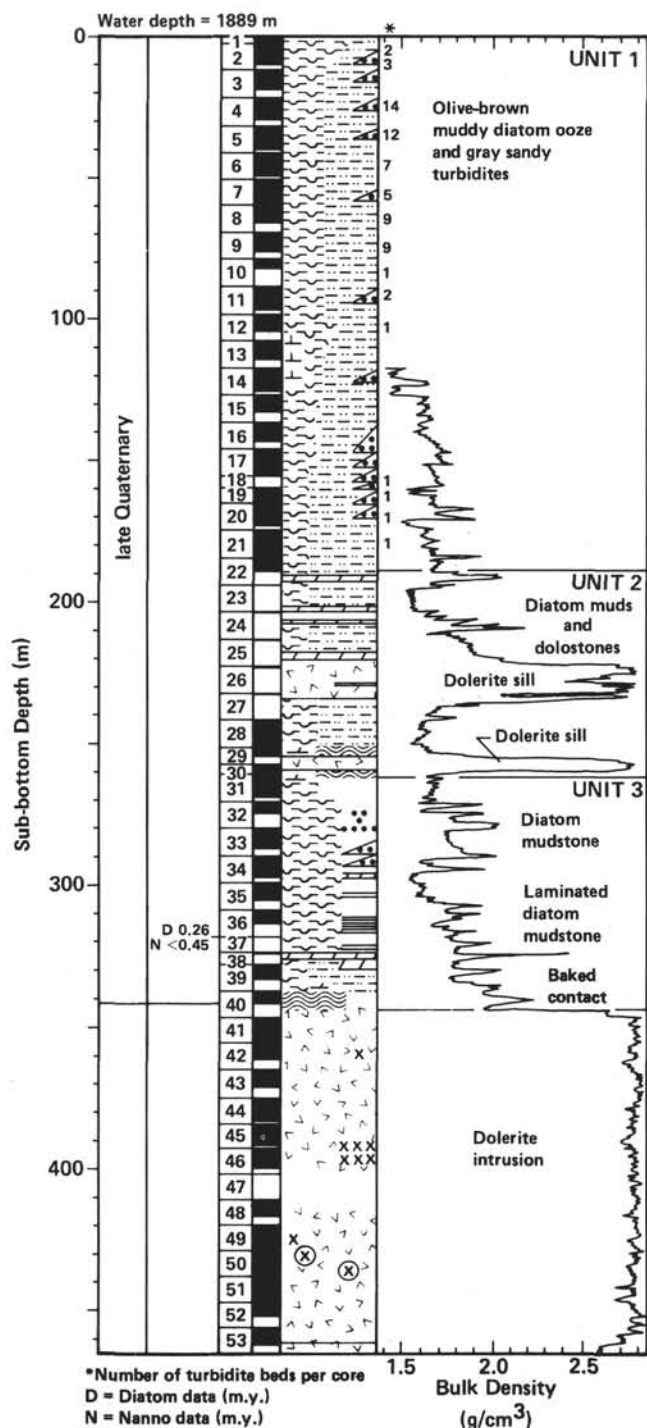


Figure 31. General lithology, lithologic units, core recovery (shown in black), and bulk density, Site 478.

2.0 g/cm³ are seen as peaks on logging records at 272, 275, and 278 meters sub-bottom. Diatoms decrease from as much as 50% in Core 478-31 to less than 6% in Core 478-33, where they are poorly preserved, but the sediment type remains similar. Calcite reappears, as well as more common, well-sorted, but thin, gray sands which are typically dominated by feldspar grains and rounded volcanic fragments. Foraminifers and radiolarians again are present. Drilling has shattered most original sedi-

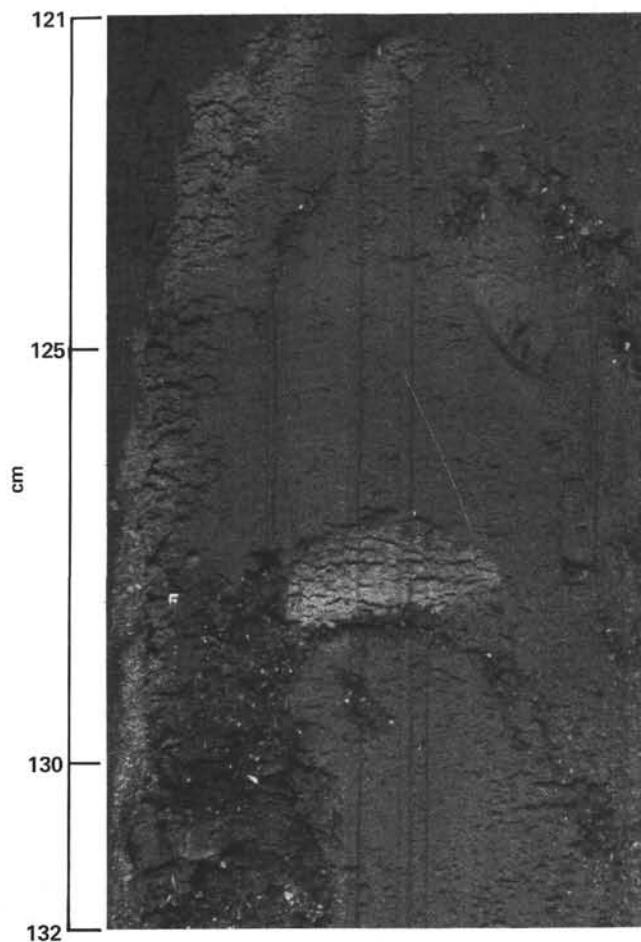


Figure 32. Photograph of 478-2-2, 121-132 cm (Unit 1). Example of two redeposited beds of coarse, well-sorted, angular, feldspar-rich sand, with volcanic-rock fragments and some shelly hash capped by lighter, pale-olive layers of pure diatom ooze. Interpreted as turbidites from offshore banks of the western slopes of the Guaymas Basin.

ment structures, but based on sand abundance the rate of accumulation is less than that of Unit 1.

Subunit 3B: Laminated Diatomites, Dolomitic Siltstone, and a Contact Zone to Dolerite Intrusion (478-35-1 through 478-40-3, 10 cm; 288.0-342.5 m)

The sediment character in Subunit 3B is similar to that above, and distinct sand layers are again seen as peaks on logging records at 290, 291, and 294 meters sub-bottom, but two aspects change. Varve-like, light and dark diatomite laminations are observed in some of the more-indurated pieces in Cores 478-35 and 478-36, and diatom abundance increases drastically in Core 478-35 to values of 40 to 70%. This is shown on the density log by a drop to below 1.6 g/cm³. In Section 478-35-1 (Fig. 34) a slightly indurated layer contains mud clasts of tilted, millimeter-scale, laminated diatomite which may derive from a slump. Light layers are richer in diatoms, containing almost monospecific warm-water forms (Schrader, pers. comm.), whereas darker layers contain more silty clay. These harder pieces also show burrowing, mostly large *Planolites* (Fig. 35). Nanofossils increase to 20% of some samples in Core

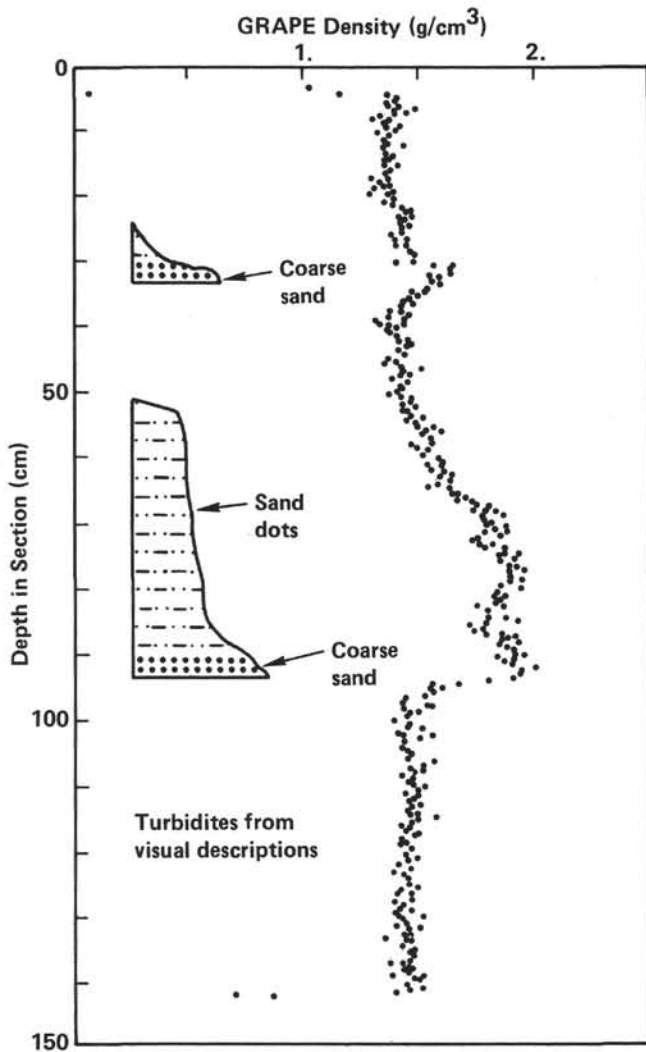


Figure 33. Turbidite signature of massive, gray, sandy silt on GRAPE measurements of density, 478-3-4, 1-140 cm, indicating that these sediments are intercalated into uniform hemipelagic host lithology.

478-36. Most of the core is developed in a laminated or lineated facies. A few thin layers of gray turbidite sand occur. A homogeneous dolomitic mudstone was encountered in Section 478-36-4, about 43 meters above the basaltic intrusive body. Laminated dolomites were also recovered in Cores 478-38 and 478-39. They show alternately burrowed and finely laminated original sediment (Fig. 35). Many of the diatom frustules are filled with pyrite framboids.

From Core 478-32 (322.5 m) downward, diatoms and nannofossils gradually diminish toward the lower dolerite. In the last core, sediments compositionally and sedimentologically similar to those above show a gradational change in color and in organic carbon as a result of baking at the contact (Fig. 36). Colors grade from olive-brown mudstones (with diatoms and calcite) to olive-black to black, barren claystones and laminated sands, and finally light-gray, bleached claystone bordering a thin (2-5 cm), glassy, basaltic chill margin. Pyrite-filled seams and large (0.1-0.4 cm) crystals are common in the last 70 cm. Some vertical veins thought to result

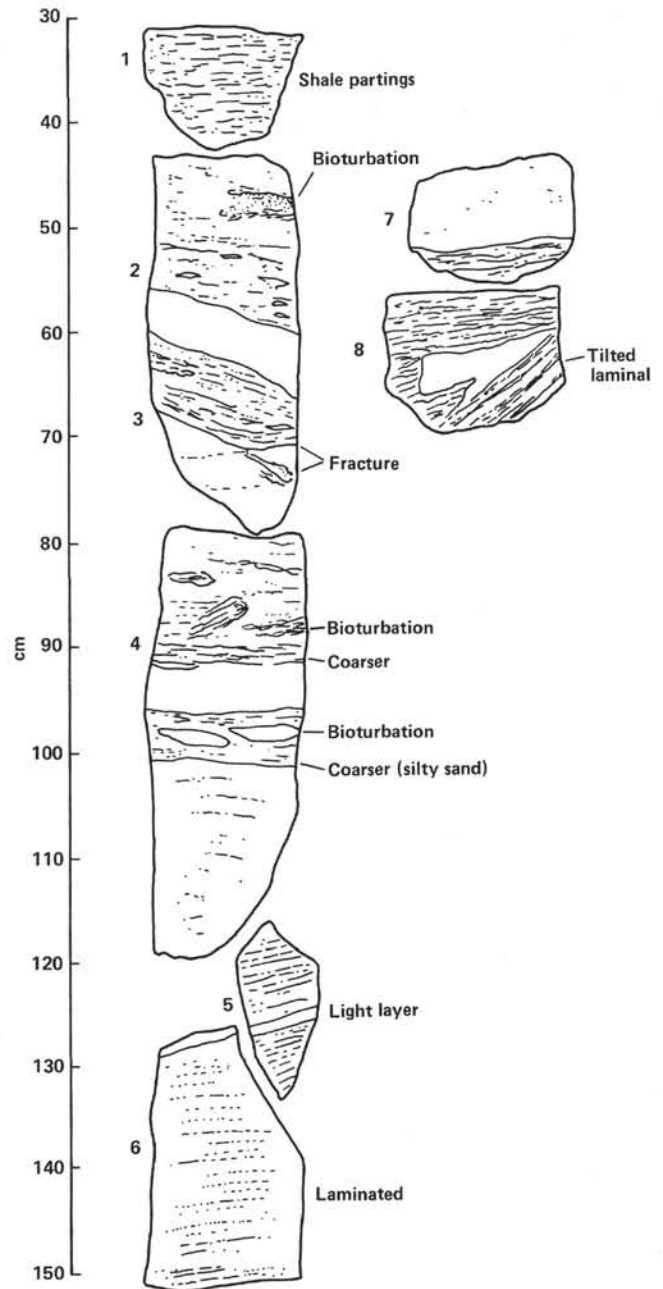


Figure 34. Line drawing of Section 478-35-1, Pieces 1 to 8. Lithified diatomaceous claystones illustrating sedimentary structures that suggest some creep or mass flows.

from thermal expansion and cooling are lined with black coatings (soot?). It is not certain, although likely, that some older sediments may occur deeper, intercalated between thick sills. Contact zones for the three sill complexes are wider for the topmost sills and narrowest for the lowermost.

Depositional Environment

Much of the sediment at Site 478 shows evidence of rapid deposition by mass flow. The basin was already deep when the lowermost dolerite was intruded. Perhaps the thin contact zone is an indication of thin sediment cover at that time.



Figure 35. Hard, dolomite-cemented mudstone, showing primary laminations and a contact to a basal sand of a turbidite (478-39-1, 60-64 cm).

Varve-like laminations in Cores 34 to 37, near the lower dolerite intrusion, indicate that there were times when this site received much less turbidite. Rhythmites require a seasonal input and no infauna. Microlaminations show that conditions similar to the present-day O_2 minimum zone of the outer hemipelagic slopes must have been recurrent also in the deep basin during the late Pleistocene. During these periods basin and accumulation rates must have slowed to rates similar to those of slope sites. Claystones, lithified by silica or dolomite diagenesis, preserve some sedimentary structures which indicate syngenetic movements. These include soft-sediment deformation, pinch and swell, pull-apart and microfractures. They also show that the original sediments have centimeter-scale alternations of laminated zones and burrowed zones, microlaminations, and even thin sands showing current cross-laminations.

The laminated oozes of Unit 3 could be related to topography. The site is located over a basement high which must have been smoothed by turbidite ponding before coarse sand accumulated. Another possibility is that the locus of sedimentation shifted with respect to land sources, because of transform movements.

The gray, silty sands intercalated throughout the section seem to derive from a similar source area. Although this site is presently on the levee of a submarine canyon from Baja, many characteristics of these massive layers

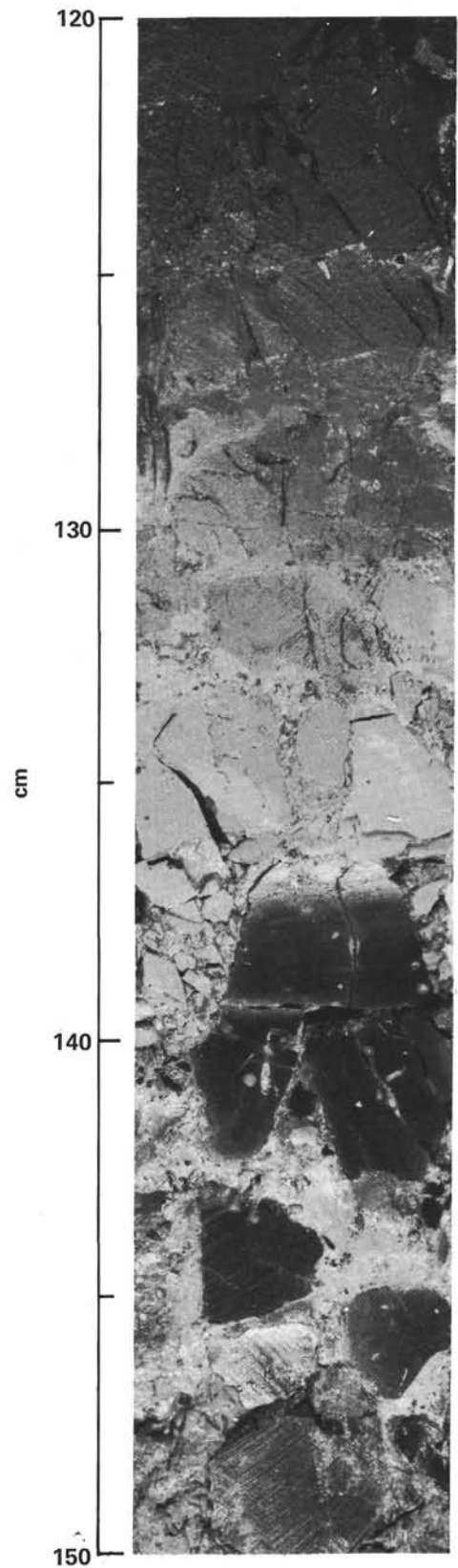


Figure 36. Chill zone and baked contact with the bottom dolerite intrusion (478-40-2, 120-150 cm).

match a source area from the Yaqui Delta. Reworked Cretaceous nannofossils are common. Grains are subrounded and moderately well-sorted, and include about equal proportions of plagioclase and quartz with volcanic-rock fragments (Appendix III, this volume, Pt. 2).

There are several reasons for thinking that Subunit 1A sediments accumulated at exceptionally high rates, although sand layers are not very common. Bulk-density logs show 10-meter-thick graded muds in Cores 16 and 17. Gas pockets, cracks, and ruptures are produced by the abundant methane and CO_2 derived from the rapid burial of organic matter. Jumps and breaks in interstitial-water data (e.g., alkalinity) suggest that original gradients are partially preserved. These grayish-olive, diatomaceous, clayey silts may be interpreted as a continuous dumping from a uniform source area. One might speculate that during a Quaternary epoch of lowered sea level the outer fringe of the prograding Yaqui Delta was rapidly denuded of silty deposits. There is evidence from logging that some of the empty cores were from intervals containing sands. Gelatinous diatomaceous oozes of Cores 1 and 2 might result from a shift of source areas because of rising Holocene sea levels.

Diagenesis

The most conspicuous feature of low-temperature diagenesis in Hole 478 is the cementation of some beds by dolomite. The first traces of diagenetic carbonate are tufted clots of magnesian calcite at 478-5-1, 120 cm. Cores and logging indicate at least isolated beds (Cores 22, CC, 23, 24, 38, 39), generally decimeter-thick. These may cement either sands (as Core 22, CC) or homogeneous and laminated sections (see Kelts and McKenzie, this volume, Pt. 2). Dolomite seems also to have formed in response to the higher-temperature sill intrusions; it occurs as scattered rhombs in the contact zones. Sills have also caused extensive silica remobilization, as indicated by the loss of diatom frustules and the formation of authigenic silicates (Kastner, this volume, Pt. 2). In the contact zone above the lowermost intrusion, the following mineralogical observations indicate alteration at elevated temperatures:

- 1) The clay minerals are strongly recrystallized, and have acquired a fibrous texture (smectite?).
- 2) Fine-grained (5–10 μm), euhedral crystals of authigenic quartz and/or feldspar are present.
- 3) Many of the detrital quartz grains are coated and show distinct undulatory extinction.
- 4) Many of the detrital feldspar grains are altered.
- 5) Syntaxial overgrowth on quartz and overgrowth around feldspar grains is observed. The overgrowths probably fill pore spaces, which could be observed only in thin sections, not in smear slides.

Site 478 Organic Geochemistry

The shipboard monitoring program was carried out upon arrival on deck of each core, which was sampled for gas if active bubbling and pockets developed. The bottom section or core catcher was split and inspected for petroleum shows by fluorescence, and the maturation of organic matter down-section was followed by the

fluorescence of a toluene-ethanol extract from a small amount of pooled sediment taken from the lower core section or core catcher.

C_1 – C_5 Hydrocarbon Analysis

Methane, ethane, and carbon dioxide were monitored, and because the ethane remained at low concentrations, only a few samples were analyzed for C_2 – C_5 hydrocarbons. H_2S was detectable by odor from about 10 to 50 meters at medium strength, then faintly to about 100 meters; it is biogenic. No H_2S was detected near the sills.

The gas samples were derived from the core caps (approximately 30 minutes after closure) where no gas pressure had built up or no gas pockets had formed in the liner (sea bed to ~100 m and ~240–330 m), and from partially over-pressured gas pockets in the liners as the core arrived on deck (~100–180 m). The normalized data for CH_4 and C_2H_6 versus depth are plotted in Figure 37; CH_4 shows an increase commencing at about 80 meters to about 100 meters, followed by an average content of 75%. From about 180 meters to the upper sill, no gas was recovered, probably reflecting the poor re-

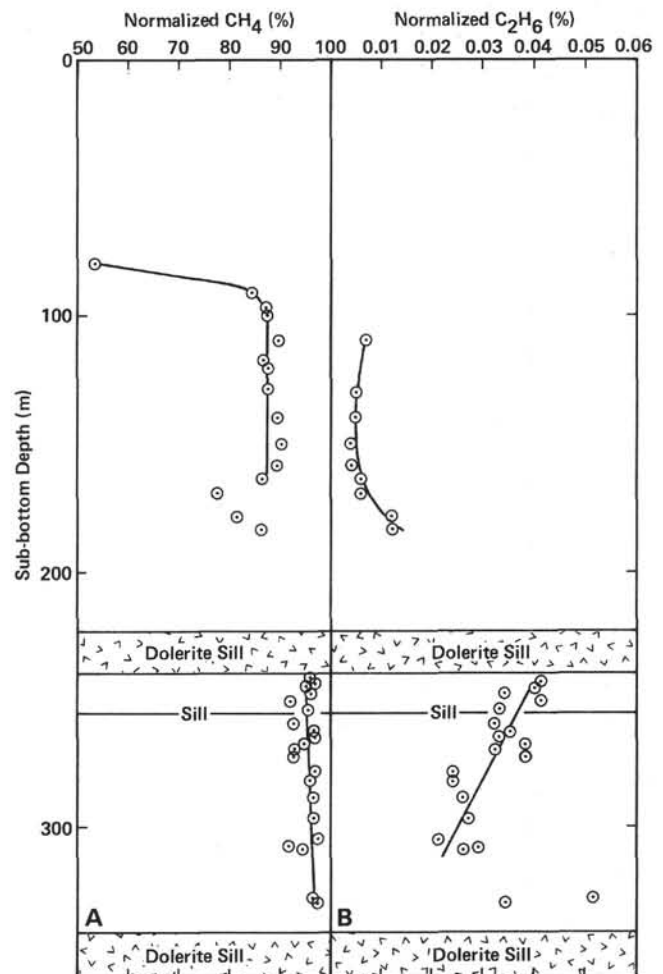


Figure 37. Concentrations of interstitial methane (A) and ethane (B) versus depth for Hole 478 (data normalized after correction for air).

covery of more lithified sediments. Below and between the sills, the CH₄ values are >90% and show a slight increase with depth. The C₂H₆ values are somewhat more scattered between the sills, but cluster for a decreasing trend with depth, two points at about 330 meters showing an increase. These data indicated that the higher-weight (>C₂) hydrocarbons have undergone thermal cracking to CH₄ because of the sill emplacements. The minor sill at about 356 meters and the upper sill did not have significant effects on the CH₄ and C₂H₆ content. From about 100 to 180 meters, C₂H₆ shows a gradual increase in concentration. The ratio of ethane to methane (C₂/C₁) is plotted in Figure 38, and from about 100 to 180 meters the C₂/C₁ ratio increases, corroborating the C₂H₆ increase. Between the sills, the C₂/C₁ ratio goes through a minimum with depth, with maximum values near the sills. The overall values are low, and, coupled with the minor content of >C₂ hydrocarbons, a minimal thermal stress is indicated. The C₂-C₅ hydrocarbons had a typically biogenic distribution pattern, consisting of CH₄, C₂H₆, propane, *iso*-butane, and a trace of *iso*-pentane. The absence of petrogenic hydrocarbons >C₄ should be noted. The maximum concentrations of the C₂-C₄ hydrocarbons are: C₂ = 0.10%, C₃ = 0.007%, and C₄ = 0.001%.

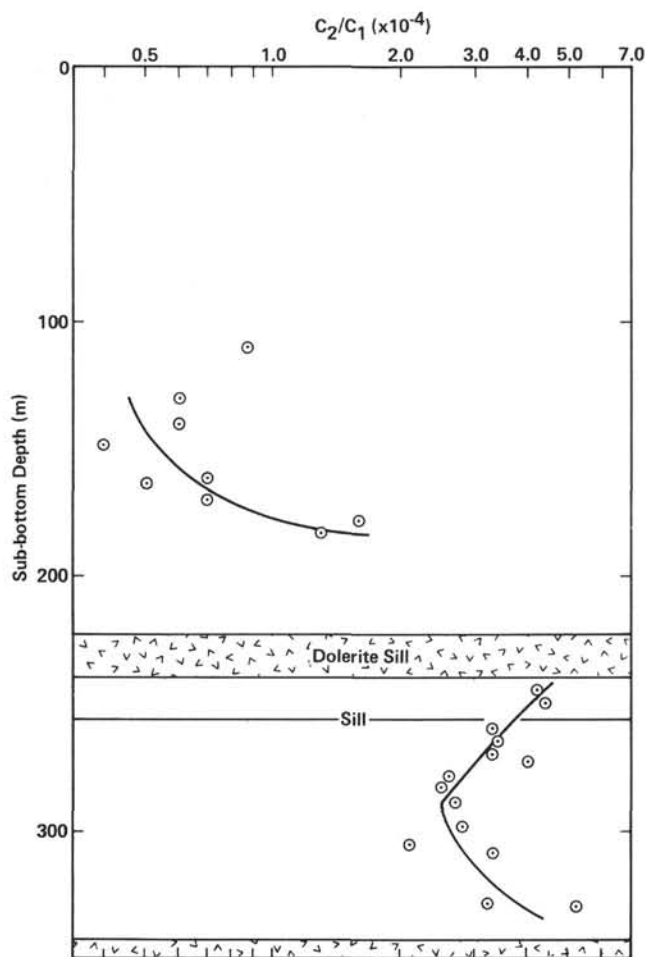


Figure 38. Ratio of ethane to methane versus depth for Hole 478.

Carbon dioxide (CO₂) is present as a major gas component, and the data are plotted versus depth in Figure 39. The values are low in the top section, increase sharply from about 80 to 120 meters to a level of 10 to 12% (120–160 m), followed by a narrow maximum and decrease above the lithified zone. Between the sills, the values show a maximum across the minor sill at about 256 meters and a mean value of about 0.3%, followed by a decrease near the lowest sill. This curve is essentially the same in the upper section as the data for calcium content and alkalinity (cf. inorganic geochemistry section, p. 248, Fig. 49).

Black Slick

A black-brown slick permeated most cores from about 250 meters to the bottom sill. It was similar to the slick observed in cores from Site 477. This material was extensively sampled and analyzed. Samples of slick and water (~20 ml) were removed by syringe about 1 hour after recovery and sealed. The head space (~3–4 ml) above the samples was analyzed by GC and found to consist predominantly of methane and carbon dioxide,

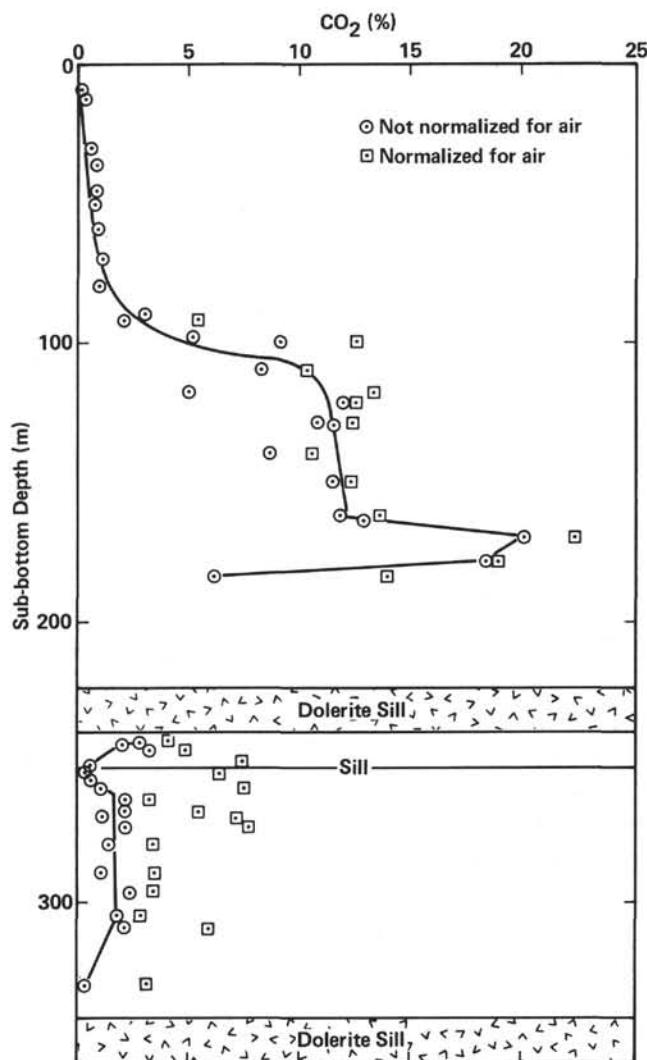


Figure 39. Concentration of CO₂ versus depth for Hole 478.

with only traces of ethane and propane. This material had the interstitial gas adsorbed and differs from the slick of Site 477 in that adsorbed-gas composition. The total slick material from Site 478 was dried and analyzed for total C and N. The C and N contents of material from 478-30-1 is about the same as the bulk sediments, and the C/N is 22, slightly higher than the trend. This indicates that the organic carbon of the slick has been subjected to moderately high temperatures (cf. 477-23-1).

Organic Carbon and Nitrogen

The samples were prepared as described before, and the results are summarized in Appendix II (this volume, Pt. 2). The organic carbon and nitrogen contents are plotted versus depth in Figure 40. The organic-carbon content ranges from about 0.5 to 3.6%, with a single maximum just below the bottom and considerable scatter. Between the sills, the data are also scattered, with a decrease toward the lower sill. The organic-nitrogen values range from 0.06 to about 0.4% and exhibit a distribution parallel to that of organic carbon. The carbon-to-nitrogen ratios (C/N) are also plotted versus depth in Figure 40C. The upper section to about 200 meters sub-bottom exhibits a scattered range from 11 to 17, which fits for the approximate C/N value of 12 for Recent immature sediments (Ryther, 1956).

The sill emplacements (224–242 m and 256–257 m) did not have a strong thermal effect on the nitrogen content of the organic matter, i.e., the C/N ratios show no dramatic increases near the sills (except for two isolated samples). The lower sill may have brought the organic matter to a higher temperature than the upper sills, but in all cases this effect was operative only near the sill (within a few centimeters).

Fluorescence

Composite sediment samples from either the core catcher or the lower section were shaken with toluene

and ethanol mixture (1:1) and allowed to settle. The color of the extract and the color and intensity of the fluorescence were used as approximate guides for the estimation of the nature and quantity of the lipid and/or petroliferous (bituminous) organic matter.

The extract colors ranged from yellow-green in the upper section (to about 170 m) to light yellow-brown between the sills; near the sills the color was a very pale yellow. The yellow-green is immature lipid matter, and the yellow-brown is mature bitumen; however, the light colorations indicated no allochthonous influx nor endogenous large concentrations of petroliferous material. This was further substantiated by the fluorescence of these extracts. The colors ranged from orange to yellow (immature) in the upper section and blue-white, white, and yellow-white (mature) between the sills.

Further fluorescence data were measured on (1) dried sediment samples and on tetrachloroethylene-extract solutions of (2) dried sediment samples and (3) pyrolyzed samples (red heat) None of the dried samples exhibited bulk fluorescence, indicating no major accumulation of heavy petroleum. Pipe-dope fluorescence was observed at random throughout the sections along the core liners.

The extracts of the dried sediments exhibited a yellow or yellow-white fluorescence, or no fluorescence. Tetrachloroethylene extracts the more non-polar lipid or bituminous material; thus, this test can be utilized as a qualitative indicator for petroliferous material. The data are presented in Figure 41 on a relative-intensity scale versus depth. A low level of fluorescence is observed to a depth of about 160 meters, then a maximum and back to none at 190 meters. Between the sills, three maxima are present, one on either side of the minor sill at about 256 meters, and one above the third sill. The maxima are indicative of petroliferous distillate which was cooked out of the sediments by the sill emplacements. It has been observed at DSDP Site 367 (Simoneit et al., 1978) that this distillation, migration, and concentration of petroliferous material proceeds farther upward than downward away from a sill intrusion. This is the case here for the upper two sills, indicating that they were intruded into the sediment; however, the close proximity of a maximum in fluorescence to the thickest third sill may reflect the deposition of the sediment (~290–342 m) directly onto the sill (flow?), and the effects of the thermal gradient from the sill generated the fluorescence maximum at 330 meters.

The fluorescence data of the pyrolyzed samples above the sills indicate that the sediment is thermally unaltered and can yield petroliferous material under pyrolytic conditions from the endogenous immature organic matter. Between the sills the organic matter still has a petrogenic potential (except near the sills, where the organic carbon is dead, i.e., it has been pyrolyzed *in situ*), indicating that the sill emplacements did not bring the entire sediment column to high temperatures.

Conclusions

The geologic events at Site 478 interpreted from organic geochemical data are as follows. The major bottom sill was emplaced into the lower sediment column,

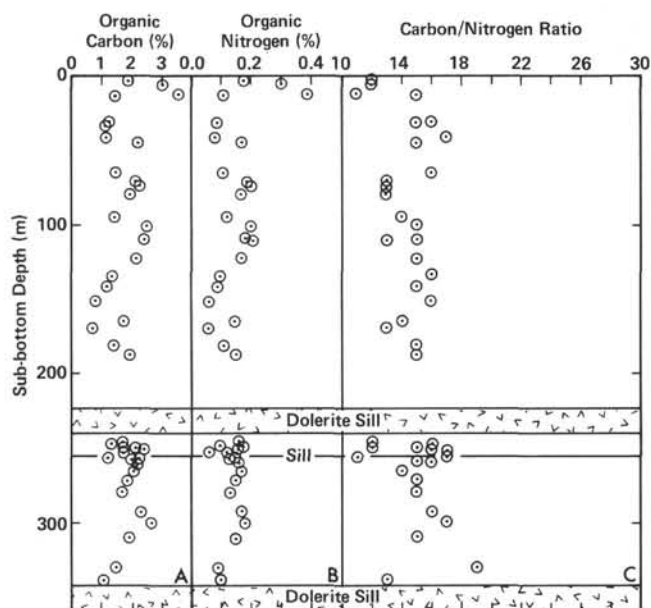


Figure 40. Organic-carbon (A) and organic-nitrogen (B) contents and carbon/nitrogen atomic ratios (C) of Hole 478 sediments.

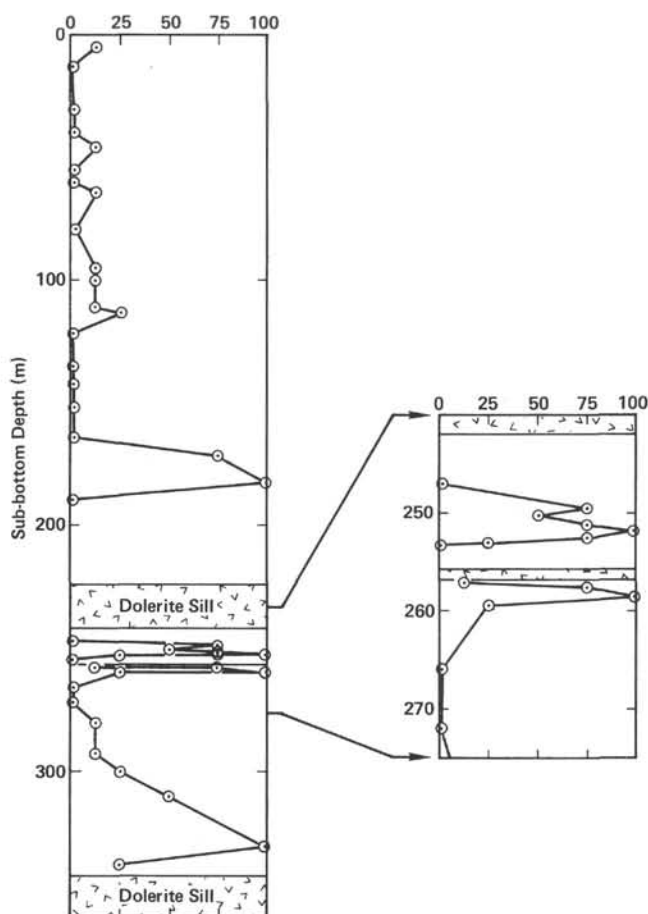


Figure 41. Fluorescence of petroliferous organic matter versus depth in Hole 478 (qualitative scale).

or, as some of these data indicate, the sediment was deposited onto the sill or flow, which still propagated a high thermal gradient (high enough to generate petroliferous material from the sedimentary organic matter, minimum about 150°C). Sedimentation continued rapidly, then the upper sills were emplaced as intrusions into the sediment. However, their high-temperature influence was limited to the vicinity of the immediate contact (within a few centimeters), and their lower-temperature thermal gradient expelled petroliferous organic matter from the sediment, leaving behind some viable organic matter. The sediment column between the three sills was not completely pyrolyzed. Further rapid sedimentation continued, and the upper part of the column contains immature, unaltered organic matter.

The brown-black "slick" permeating the deeper sediment section (between the sills) consists predominantly of fine-grained minerals, with residual carbonaceous matter and adsorbed interstitial gases. The gases of this sediment column consist of predominantly biogenic CH_4 , CO_2 , and H_2S , with traces of C_2H_6 and a minor component of thermally generated ethane, propane, and *iso*-butane at depth. In terms of pollution and safety hazards, this site posed no problems.

Site 478 Inorganic Geochemistry

Interstitial-Water Chemistry

Depth distributions of alkalinity, ammonia, and phosphate, as well as calcium and magnesium, show a complex pattern in the upper 150 meters. Processes of decomposition of organic matter must occur at different rates in these sediments, methane production becoming important below 60 meters. In addition, possible differences in accumulation rates may affect the non-steady-state distribution profiles.

Below 150 meters, the concentration profiles of calcium and magnesium indicate that alteration reactions in the sills and underlying sediments affect these constituents.

Dissolved-silica values show a steady increase with depth, but below 300 meters silica diagenesis has led to a lower dissolved-silica concentration (Fig. 42).

Site 478 Biostratigraphy

Paleontological Summary

All major microfossil groups (calcareous nannofossils, diatoms and silicoflagellates, planktonic and benthic foraminifers, and radiolarians) occurred in the pelagic-hemipelagic sequences drilled at Site 478 to a depth of 342.5 meters sub-bottom. Diatoms, and to a lesser amount calcareous nannofossils, formed the major component of the sedimentary sequence, whereas foraminifers and radiolarians formed only a minor component (Fig. 43). Microplankton and nannoplankton assemblages were generally well preserved.

Under the assumption that equatorial Pacific datum levels also occur synchronously in the Gulf of California, tentative age assignments are as follows: Cores 478-1 to 478-15 are within NN21; Cores 478-16 to 478-20 have not been defined yet; Cores 478-21 to 478-40 are within NN20. The *Nitzschia fossilis* extinction datum (~0.26 m.y.) was found in Core 478-36. Planktonic foraminifers indicate a general cooling of surface waters below Core 478-18; other microfossil groups did not support this observation. Benthic foraminifers indicate a middle-bathyal condition, similar to the present water depth of this site, throughout the sequence.

Diatoms

Diatoms are abundant in all pelagic-hemipelagic sequences in Site 478. They are mostly excellently preserved, and delicate species (*Skeletonema costatum*) are found throughout. Diatom abundance decreases sharply in Core 478-39, and at the same depth preservation grades to poor, only strongly silicified valves being present in Core 478-40.

Displaced fresh-water and benthic marine species occur throughout, but never exceed 1% of the total diatom population, indicating a constant supply of terrigenous and/or shallow-water marine debris to this site.

Assemblages consist of pelagic subtropical to tropical species with *Pseudoeunotia doliolus*, *Coscinodiscus nod-*

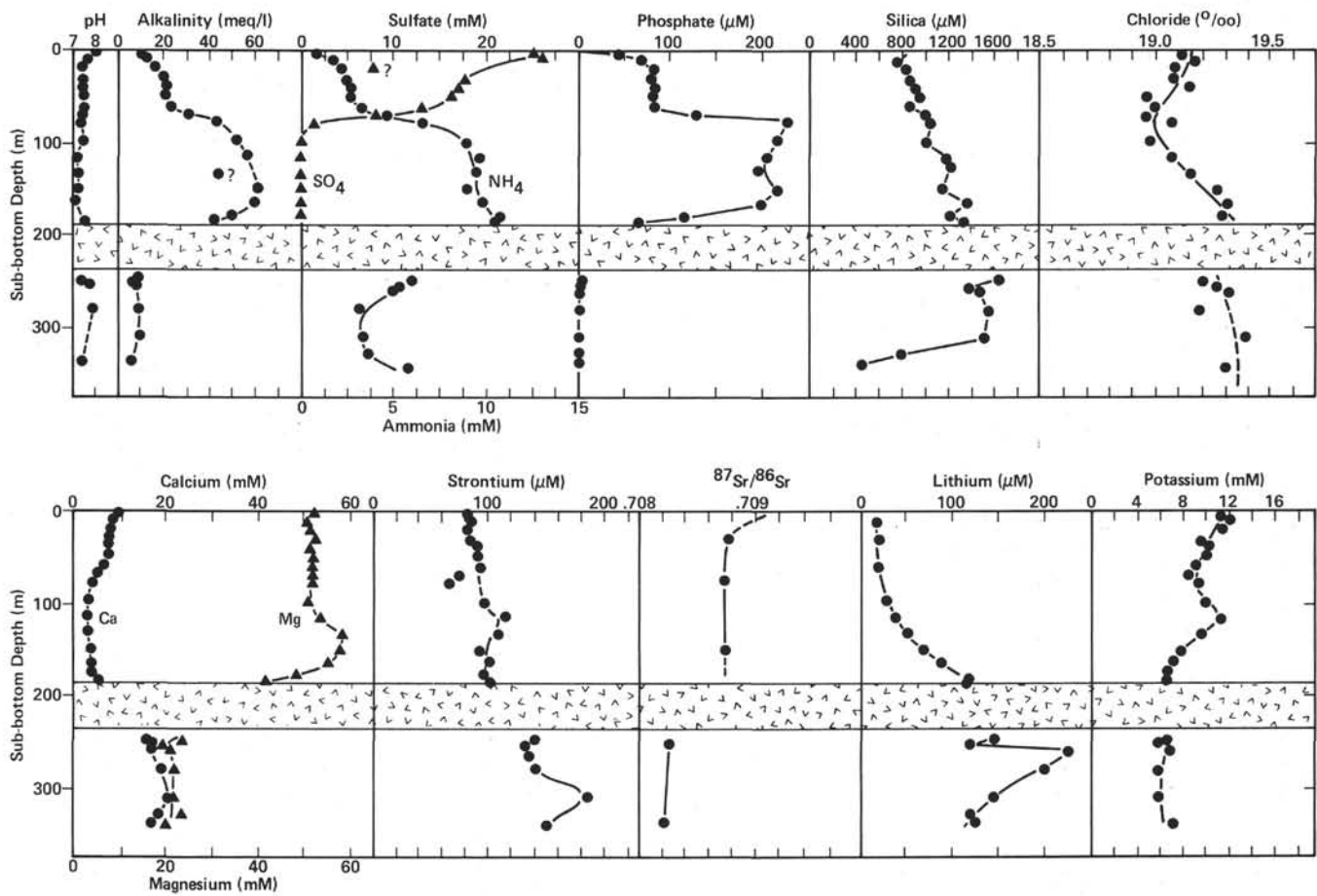


Figure 42. Composite diagram of pore-water chemistry, Site 478.

ulifer, *Thalassionema nitzschioides* and var. *parva*, and *Thalassiothrix longissima*, a minor component in the meroplanktonic group with *Actinocyclus ehrenbergii*, *Actinopterychus undulatus*, *Cyclotella striata*, and others. Occasionally, two distinct assemblages could be differentiated: one (A) with dominant *Thalassionema nitzschioides* s.l. and one (B) with dominant *Coscinodiscus nodulifer* and *Thalassiosira oestrupii*. Assemblage (A) might be interpreted to represent more-vigorous mixing of surface waters (increased upwelling), whereas assemblage (B) might represent more-stable surface-water conditions. The varved intervals in Core 478-37 are dominated by the tropical species *Thalassionema nitzschioides* var. *parva*.

Reworked older species were not encountered and indicate that no older strata are exposed along the flanks of this basin. On the basis of rare occurrences of *Nitzschia fossilis* in Core 478-36, CC, the sequence above Core 478-36 is dated as being younger than 0.26 m.y., and the sequence below Core 478-36, CC older than 0.26 m.y. The *N. fossilis* datum is defined in both the North Pacific and the equatorial Pacific and is thought to be synchronous. Since neither the *Thalassiosira nidulus* nor *N. reinholdii* data, which are slightly older, were observed, the foregoing interpretation might be correct (Burckle, 1977; Barron, pers. comm.; Schrader, in prep.).

Detailed floral analysis will provide definition of distinct assemblages, which in turn can be correlated to environmental parameters (cf. Baumgartner et al., 1979).

Nannofossils

The late Pleistocene sediments recovered at Site 478 yielded abundant and well-preserved calcareous nannofossils. The coccolith assemblages are very constant in composition and of low diversity throughout the section. Coccoliths reworked from the Upper Cretaceous were common at most levels.

Radiolarians

Radiolarian remains in the sediments from Hole 478 are strongly diluted by diatom frustules; nevertheless, in the size fraction greater than 62 μm , radiolarians occur in most samples taken throughout the sedimentary sequence of the hole (0–346 m sub-bottom). Turbidite layers are barren of radiolarians (e.g., Core 478-34, CC and 478-39, CC).

The preservation of the radiolarians which do occur in the cores from Hole 478 is moderate, and *Botryostrobus auritus-australis* group, *Drupptractus* sp. cf. *D. pyriformis*, *D. irregularis*, *Ommatodiscus* sp. (Benson, 1966), *Teocalyptra davisiana*, and *Stylodictia validispina* are the dominant species of the radiolarian population. This composition of the population is similar to

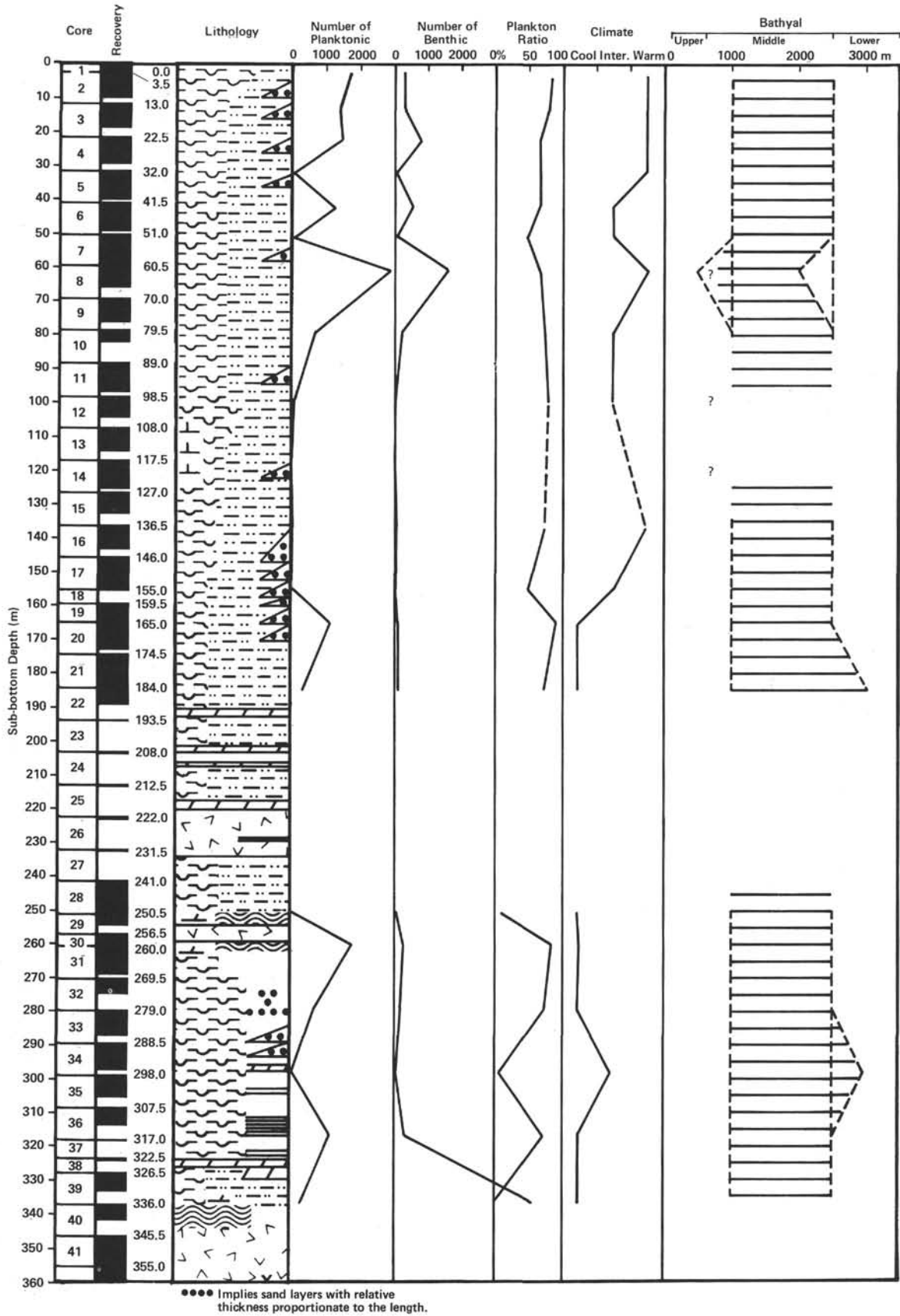


Figure 43. Correlation of lithology with counts of planktonic and benthic foraminifers, plankton ratio, climatic variations, and interpretation of depth of deposition, Site 478.

the one found in coastal upwelling areas in the central Gulf of California. The relative abundance of *C. davisiana* is increased in Core 478-36, CC.

Because the sedimentary sequence at Hole 478 is younger than 300,000 years (see diatom datums), no radiolarian biozonation has been established for this hole.

Foraminifers

Although no indicator species older than late Pleistocene can be found, at least four cooler intervals are seen within the section, based on planktonic foraminifers, indicated by the abundant occurrence of *Neogloboquadrina pachyderma* s.l. and the occurrence of *N. pachyderma* s.s. In the benthic fauna, *Epistominella smithi*, *Uvigerina* spp., and *Cassidulina* spp. are abundant throughout the section at this site.

Site 478 Sediment-Accumulation Rates

The estimated sediment-accumulation rate for Hole 478, using the calcareous-nannoplankton zone boundary NN21/20, is 780 meters/m.y., and using the datum provided by the extinction of the diatom *Nitzschia fossilis* it is 1220 meters/m.y. The average of these two estimated sediment accumulation rates is 1000 meters/m.y. This accumulation rate is adopted for this report.

For an alternative method of calculating accumulation rates, the zonal boundary between NN21 and NN20 is placed at the most conservative point on the range at 175 meters. Regardless of where this point is selected, it appears that there has been a change in accumulation rate with time, but that the mean rate for this 310-meter section is almost 1200 m/m.y., or 1.2 m/10³ yr, or 1.2 km/m.y. With only one datum plane, there also remains the possibility of redeposition of older nannofossils.

Site 478 Igneous Rocks

The igneous lithology at Site 478 has been divided into six units (Table 9; Fig. 44). Although only 1 meter of aphyric basalt was recovered in Core 26, bulk-density logging measurements indicate that Unit 1 is an igneous body approximately 10.5 meters thick, and that the lower part of Unit 1 may comprise three thin basaltic

layers and intercalated sediments. Unit 2 may be the lowermost of these basaltic layers. No direct sediment/basalt contacts were recovered, but the presence of a contact zone of altered sediments up to about 38 meters above Unit 1 is indicated by the bulk-density log and mineralogy of the sediments. This suggests that Unit 1 is intrusive.

In hand specimen, the basalt of Unit 1 is dark gray (N4), medium grained, and slightly weathered. Minor veins and occasional vesicles are filled with carbonate; a dusting of pyrite is present on some fracture surfaces. The aphyric texture of the basalt is confirmed in thin-section. The mineralogy comprises normally zoned plagioclase laths (An₄₅₋₆₅), interstitial feldspar, intergranular pale-brown augite, and minor opaque phases. The plagioclase laths range up to about 1.5 mm long, whereas pyroxene rarely exceeds 0.5 mm. Approximately 10% of the rock consists of green clay minerals replacing both the mesostasis and possibly olivine, although no olivine was seen in thin-section.

Unit 2 represents a small igneous body beneath Unit 1. A fragment of dolomitized and pyritized silty claystone in the top of Core 478-27 shows that Units 1 and 2 are separated by a sediment intercalation. From the bulk-density logs, it can be seen that Unit 2 is approximately 1.5 meters thick, and that it is separated from Unit 1 by approximately 1 meter of sediment. No contacts or baked sediments were recovered, so it is not possible to say unequivocally whether Unit 2 represents a sill or a flow; however, Units 1 and 2 are mineralogically very similar, suggesting a similar time and mode of emplacement.

In hand specimen, the basalt of Unit 2 is medium light gray (N6), aphanitic, and, in the upper 60 cm of the recovered section, vesicular. The vesicles are between 1 and 10 mm in diameter, and usually lined or filled with calcite, pyrite, clay minerals, and possible dolomite. Occasional narrow veins are also calcite-filled.

In thin-section, the basalt of Unit 2 is much finer grained than that of Unit 1, which may be because of the limited vertical extent of the body. Olivine again appears to be absent. Skeletal laths of plagioclase, less than 0.8 mm in length, and intergranular, anhedral

Table 9. Igneous lithologic units, Site 478.

Unit	Top ^a (m sub-bottom)	Base ^a (m sub-bottom)	Thickness ^a (m)	Recovery ^b (m)	Type of Cooling Unit	Phenocryst Assemblage	Vertical Extent
1	221.0	231.5	10.5	1.2	Massive Basalt	Aphyric	478-26-1, 0 cm to 478-26-2, 15 cm
(sedimentary intercalation)							
2	232.0	233.5	1.5	1.0	Massive Basalt	Aphyric	478-27-1, 0 cm to 478-27-1, 120 cm
(sedimentary intercalation)							
3	254.5	259.0	4.5	0.2	Basalt	Aphyric	478-29, CC
(sedimentary intercalation)							
4	342.5	455.0	112.5	82.6	Massive Dolerite	Minor Pl	478-40-2, 140 cm to 478-53-4, 98 cm
5	455.0	459.5	4.5	2	Massive Basalt	Aphyric	478-54-1, 0 cm to 478-54-2, 85 cm
6	459.5	463.5	4.0	3.8	Massive Basalt	Minor Pl	478-54-2, 86 cm to 478-54-4, 110 cm

^a Determined from downhole log.

^b Determined from core log and corrected for spacers.

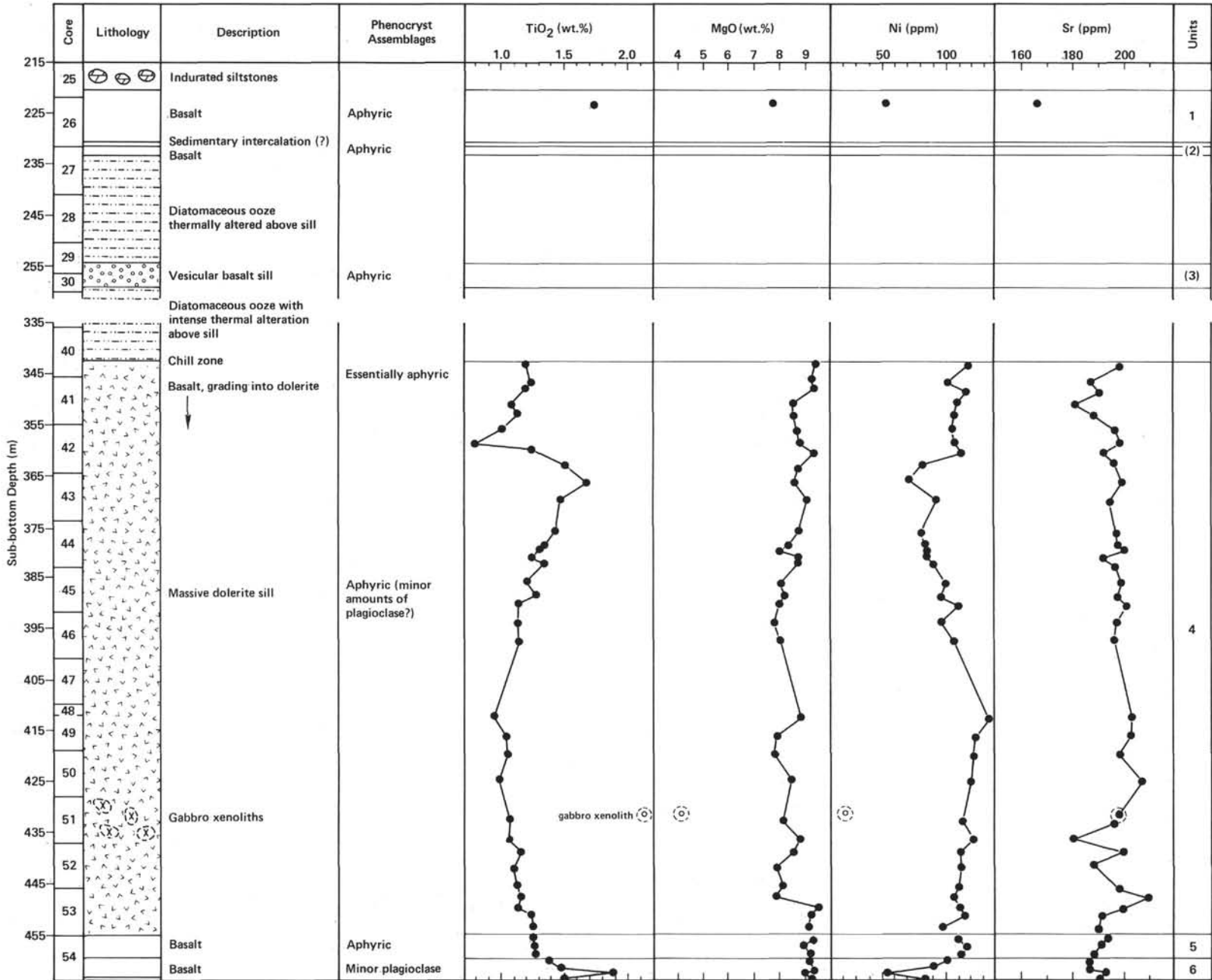


Figure 44. Summary of igneous units, Hole 478.

clinopyroxene lie in a mesostasis completely replaced by green clay minerals. Any groundmass olivine, if present, has been altered to clay minerals, but the pyroxenes and feldspars are fresh. In the studied thin-sections, vesicles constitute less than 5% of the rock. They are usually spherical, 1 to 1.5 mm in diameter, with partially preserved carbonate fillings. One large vesicle (~10 mm in diameter) contains a residue of medium-grained basalt, consisting of plagioclase, pyroxene, and an iron-rich mesostasis which in turn contains several micro-vesicles.

The bulk-density logging data indicate that there is a 4.5-meter-thick igneous unit (Unit 3) between 253.5 and 258.0 meters sub-bottom; unfortunately, only 20 cm of aphyric, medium-gray (N6) basalt fragments were recovered in the core catcher of Core 478-29. The basalt contains calcite-, pyrite-, and clay-mineral-lined vesicles up to 1 cm in diameter, and in hand specimen resembles the rock from the uppermost part of Core 478-27 (i.e., Unit 2). The extensive altered zones within the sediments above and below Unit 3 confirm an intrusive origin for this unit, and suggest that it is a sill.

Core 478-40 (336.0–345.5 m sub-bottom) contains approximately 3 meters of silty clay that is brown for the top 10 cm, and then dark gray to black for the remaining 290 cm, as a result of heating and breaking down of organic compounds. At the base of the sediment column, a 10- to 20-cm-thick, light-gray clay horizon is succeeded by a zone of brecciated, aphyric, aphanitic basalt with chilled (not glassy) margins lying in a light-gray clay matrix. The brecciated zone (~10–20 cm thick) rapidly grades into aphyric basalt, and finally into aphyric, coarse basalt or dolerite. The top of this igneous unit (Unit 4), assumed to be a sill, is placed at 342.5 meters sub-bottom by the drilling record.

Core 478-54, near the base of the hole, recovered 5.77 meters of aphyric basalt that is petrographically distinct from the overlying dolerite. The contact between the dolerite and the basalt was not recovered. The basalt has been divided into two units (5 and 6) separated by a contact zone in Section 2 of Core 54.

Unit 4 is the thickest internally consistent igneous body sampled in Hole 478. The top of Unit 4 consists of sparsely vesicular, coarse-grained basalt and extends down to ~80 cm in Section 478-41-1. In hand specimen, this uppermost part of Unit 4 is aphyric, with small (1–2 mm diameter) vesicles randomly dispersed throughout (about 3% total volume) and filled with green clay minerals and little, if any, calcite. The rock is medium gray (N5); in thin-section, the major mineral phases are plagioclase (~40%) and clinopyroxene (augite, ~35%), with minor opaque phases (~5%) and some clay and zeolite minerals (~15%). The texture, as seen in thin-section, is ophitic to intergranular, although occasionally the clinopyroxene phenocrysts completely enclose small plagioclase laths in an ophitic, almost poikilitic fashion. This poikilitic texture persists to the base of the dolerite body, although its abundance varies down the section.

From ~80 cm in Core 478-1 to ~1 cm in Section 478-53-4, Unit 4 is doleritic; however, discrete textural changes occur throughout this section and are princi-

pally related to the occurrence of poikilitic clinopyroxene-plagioclase glomerocrysts, gabbroic xenoliths, and vertical and horizontal zones of alteration associated with silica- and clay-filled veins. In hand specimen, the dolerite of Unit 4 is remarkably unfractured, medium gray (N5-N6), and substantially weathered, with between 30 and 50% secondary clay and zeolite minerals. The unfractured nature probably is a function of the siliceous nature of the vein fillings; if the fillings had been calcite the rock likely would have fractured along the veins, severely reducing the recovery rate and possibly interfering with the drilling.

A very pronounced blotchy or mottled appearance characterizes the rocks in Cores 478-45 to 478-59. This mottling is caused by poikilitic clinopyroxene phenocrysts, few of which are altered, that contain ophitic inclusions of small plagioclase laths. At times the clinopyroxene phenocrysts coalesce to form lighter-colored glomerocrysts bordered by zones of darker, fresher clinopyroxene, and opaque phases and plagioclase. Below Core 478-49, the dolerite becomes significantly fresher (only 5 to 15% clays and zeolites), and by Core 478-50 the rocks are no longer mottled; however, some poikilitic clinopyroxene persists to the base of the dolerite. The other major textural change occurs within Core 478-51 and consists of 1- to 10-cm, irregular gabbro xenoliths, many showing signs of extensive alteration.

In thin-section, the texture of the Unit 4 dolerite is predominantly subophitic to intergranular, with abundant but restricted areas of ophitic to poikilitic texture. Mineralogically, the unit is uniform, despite the textural variations. Plagioclase (An_{45-65}) constitutes between 20 and 40% of the rock and occurs as small laths between 0.1 and 0.5 mm in size in the groundmass and as tabular laths, 1 to 3 mm long, which often are strongly normally zoned. The plagioclase is usually fresh, although in the altered rocks it is partially sericitized, and is found (1) enclosing intergranular clinopyroxene and rare anhedral to subhedral olivine crystals, (2) as an intergranular matrix surrounding clinopyroxene and rare olivine, and (3) as ophitic inclusions in large clinopyroxene aggregates. Clinopyroxene (augite) constitutes between 20 and 40% of the rock and is usually found in subhedral to anhedral, optically continuous aggregates, either intergranular to plagioclase or ophitically and frequently poikilitically enclosing small plagioclase laths. The clinopyroxene ranges in size from small, 0.5-mm, anhedral fragments to subhedral aggregates up to 5 mm long. The larger clinopyroxene crystals often are fresh; however, in the more-weathered portions of the dolerite they show more serious effects of alteration, second only to olivine.

Olivine is rare and constitutes at most 5% of the rock. Much of the olivine may have been altered to green clay minerals ("bowlingite"), although no persistent pseudomorphing was observed. Opaque minerals are common and much of the rock has 5% opaque phases. Both magnetite and ilmenite occur, the identification being based mainly on crystal habit. The opaque phases often occur along intergrain boundaries and commonly are associated with altered clinopyroxene. Brown

to green clay minerals and amorphous to clear-fibrous zeolite account for between 10 and 50% of the rock. The wide range in abundance reflects the different degrees of alteration in the upper and central portions of the dolerite, as opposed to the fresher rock recovered in Cores 478-50 to 478-53.

The gabbro xenoliths that commonly occur in the rocks of Core 478-51 have a predominantly ophitic texture, 1- to 10-mm clinopyroxene phenocrysts accounting for 50% of the xenolith. Tabular laths of plagioclase (~30%; 0.5–3 mm) are optically enclosed in the clinopyroxene aggregates with between 10 and 20% clay and zeolite minerals in the matrix. Opaque phases are randomly dispersed, but often are represented by long needles (up to 7 mm long) of ilmenite which occasionally intrude into the plagioclase and clinopyroxene phenocrysts. Very little or no olivine is present in the xenoliths. Some of the gabbro xenoliths (e.g., Section 42-2, 116 cm) show clear evidence of cumulate texture.

The basalt in Core 54 has been divided into two units (5 and 6) on the basis of a contact within the recovered basalt at 478-54-2, 80–95 cm. It is apparent from textural considerations that Unit 5 is chilled against Unit 6. The contact between Unit 5 and the overlying dolerite Unit 4 was not recovered, but the slight variation in the bulk-density record suggests that the two units are adjacent and that they are not separated by a sediment intercalation.

In hand specimen, the basalts of Units 5 and 6 are very similar. Medium-gray (N5), aphyric, and having an altered appearance, the basalt of Unit 5 progressively decreases in grain size from medium grained at the top of Core 478-54 to aphanitic at the contact with Unit 6 in Section 478-54-2. The actual contact is preserved within a small pebble (Piece 3a), and although the basalt of Unit 5 is aphanitic adjacent to the contact, a proper chill zone is not seen. The basalt within Unit 6 is slightly more coarse grained than that in Unit 5; however, there is considerable variation, and the grain size ranges from fine grained near the contact in Section 478-54-2 to medium grained in Section 478-54-4. The basalt of Unit 6 appears to be increasingly mafic toward the base of the core. Texturally, the basalt of Section 478-54-1 (Unit 5) is not distinguishable from that of Section 478-54-4 (Unit 6).

The basalt is generally more fractured than the dolerite of Unit 4. Green clay minerals and dustings of pyrite coat many fracture surfaces, and calcite occurs in several veins.

In thin-section, the basalt of Unit 5 is aphyric, with an intersertal to intergranular texture. Clinopyroxene is present as small (<0.4 mm) intergranular crystals, and as occasional, slightly larger (0.5–0.6 mm) crystals which subophitically enclose plagioclase laths. No olivine is seen, but it easily could be mistaken for clinopyroxene because of the small grain size. As much as 50% of the rock consists of an altered mesostasis, now completely replaced by clay minerals, zeolites, and possibly calcite. No vesicles are present.

Unit 6 consists of a sparsely plagioclase-phyric basalt. Resorbed and zoned plagioclase phenocrysts (less

than 1% of the whole rock) between 2.5 and 3.0 mm in length lie in an intersertal to intergranular matrix of plagioclase, clinopyroxene, and altered mesostasis. The clinopyroxene is partly equidimensional to and partly intergranular to the plagioclase. Some of the pyroxene may be misidentified olivine.

The similar mineralogies and textures seen in Units 5 and 6, and the absence of a chill zone between the two units, suggest that they are contemporaneous igneous bodies. Probably they are intrusive, but the absence of baked sediments above Unit 5 means that this cannot be confirmed. It is not possible to say with any degree of certainty whether Unit 4 postdates Units 5 and 6, but the extensive alteration of Units 5 and 6 suggests that this is the case.

Site 478 Paleomagnetism

Twenty-one specimens of basalt were processed in the DIGICO spinner and the Bison Susceptibility Meter. The results are given in Table 10. From experiments on two specimens, it appeared that a demagnetizing field of 75 Oe is about right for removing the unstable magnetization, if any. Actually, the "declination" and the dip angle did not change appreciably by demagnetization up to 200 Oe. The treatment merely reduced the magnitude of the magnetization. The mean value of the NRM is 0.0014 emu/cm³, omitting the largest and smallest values. The average paleolatitude given by the NRM is 25°. After demagnetization, it dropped to 23°—an insignificant difference. The present latitude is 27°. It differs also insignificantly from the paleolatitude. The average magnetic susceptibility is 366 × 10⁻⁶ emu/cm³ Gauss. The ambient field of the location is 0.45 Gauss. The ratio of the NRM to the induced magnetization (the Koenigsberger ratio) is 10.3, a relatively high value, which accounts for the small standard deviation of the inclination, only 3°.

Table 10. Paleomagnetic results, Site 478.

Sample (interval in cm)	Susceptibility × 10 ⁻⁶ (emu/cm ³ G)	NRM (emu × 10 ⁻⁶ / cm ³)	Inclination (degrees)	After Demagnetization	
				<i>I_r</i> (emu × 10 ⁻⁶ / cm ³)	Inclination (degrees)
478-26-1, 114-116	—	8393	52.8	—	—
41-1, 100-102	379	2231	37.2	2107	37.0
41-2, 15-17	417	1919	42.3	—	—
41-5, 56-58	—	1107	39.7	1065	39.8
42-1, 15-12	200	812	40.1	—	—
42-4, 10-12	532	3112	39.2	2801	40.5
43-1, 124-126	597	2251	46.6	1489	41.0
43-3, 20-22	557	2272	42.1	1795	38.5
44-1, 103-105	383	2353	39.8	1901	36.1
44-5, 121-123	293	2616	39.1	2512	40.1
45-4, 35-37	249	1217	44.0	1073	40.7
45-5, 107-107	317	1557	38.7	1208	38.7
49-3, 56-58	—	1008	41.2	—	—
50-1, 84-86	185	845	36.3	806	36.9
51-1, 94-96	161	536	44.3	487	42.0
51-6, 100-102	133	145	53.3	86	40.8
52-5, 129-131	388	499	51.3	245	46.5
53-4, 70-72	574	637	49.3	287	38.7
54-1, 92-94	347	777	46.5	484	38.1
54-3, 109-110	452	791	42.8	620	38.4
54-4, 45-47	450	801	49.4	702	47.3
	< 367 > ± 141	< 1694 > ± 1742	< 42.63 > ± 4.3	< 1224 > ± 799	< 40.6 > ± 3.0

Note: Omitting extreme values, NRM = 0.0014 emu/cm³, *I_r* = 0.0012 emu/cm³; induced magnetization = 0.45 × 367 = 165 emu/cm³; Koenigsberger ratio = 1694/165 = 10.3; A.F. demagnetizing field = 75 Oe; paleolatitude = 25° or 23°.

Site 478 Physical Properties

Small sections of Cores 478-1 through 478-9, 478-11 through 478-14, and 478-19 through 478-22 were moderately or little disturbed by drilling and could be sampled and tested for physical properties. Cores 478-10, 478-15 through 478-18, 478-28, 478-29, and 478-31 through 478-36 were intensively disturbed by drilling or by expanding gas (e.g., Cores 478-10 and 478-19), so that either no samples or only small chunks could be taken. Core barrels 478-23 and 478-37 were empty, and Cores 478-24 through 478-27, as well as 478-38, recovered only small pieces of cemented siltstones or basalt. From Cores 478-28 and 478-29 downhole, the cores had to be cut by saw. Measurements of the sound velocity with the Hamilton Frame were possible only in Cores 478-1 through 478-8, and on some chunk samples from Cores 478-30 through 478-32.

Figure 45 shows the general trends of physical properties of the fine-grained "background" sediments versus depth. Data from turbidites, which often differ considerably from those of the "background" sediments, are treated separately (see Einsele and Kelts, this volume, Pt. 2). Sometimes it was, however, difficult or impossible to distinguish between sediments from the uppermost part of mud turbidites and those from "background" sedimentation, especially when the cores were rather disturbed.

From the sediment surface down to about 170 meters, the physical properties change in a manner rather similar to that found in Holes 474 through 476, but because of the high percentage of siliceous biogenic material, water content and porosity are about 10% higher and wet-bulk density is 0.1 to 0.2 g/cm³ lower than at the previous sites near the tip of Baja California. This is true for the total sequence down to about 170 meters depth. Similarly, as in Hole 476 (145–180 m), an increasing percentage of diatoms in the sediments of Hole 478 (90–120 m) exerts some influence on the physical properties, but as in Hole 476, at this depth range shrinkage is not affected any more by a high content of biogenic silica (Fig. 45). All the other physical properties show a very small gradient versus depth down to 170 meters, particularly vane shear strength.

At about 170 meters, the first marked change of physical properties can be observed. Water content and porosity decrease by at least 10%, and bulk density increases by 0.2 g/cm³. At the same depth (lower part of Subunit 1B), preservation of diatoms becomes poor, and the first silica-cemented and dolomite-bearing pieces of siltstone were recovered here (Cores 478-24 and 478-25). These rapid changes cannot be explained by the slightly increased overburden pressure in comparison to cores taken from depths shallower than 170 meters. As can be seen from the density log of this site, and also at Sites 477 and 481, the first dolerite sill, at 222 to 235 meters depth, has influenced the physical properties of the overlying sediments (Fig. 31). It appears that up to 40 meters of the sediment column are affected above the top of the sill, but because of the lack of core material for the sequence between 190 and 240

meters, as well as for the contact to the sill, the evidence is mainly based on the density log.

Below the dolerite sill, at about 240 meters depth, two samples again have relatively high water contents and porosities, which correspond to those at 170 meters depth in this hole. A sample taken from Core 478-31 below the second dolerite sill (264 m depth) was even less compacted. This indicates that thin basaltic sills do not strongly change the general normal depth relationship of the physical properties in the underlying sediments. According to grain-density determinations and visual descriptions of smear slides, opaline silica (mainly diatoms) is still present in considerable quantities. The sediment contact below a sill appears to be thinner than above the sill. At the only 3-meter-thick sill at about 255 meters depth, both the upper and lower contacts with the sediments were recovered. Although the sampling was not as densely spaced as desirable, the data show that water content and porosity near the contact are lower by about 15%, and bulk density higher by about 0.2 g/cm³ than 2 to 3 meters above or below the sill.

At 260 to 280 meters depth (Subunit 3A), little-compacted sediments appear to prevail, with water contents, porosities, and bulk densities similar to those at 240 to 250 meters. Then, at about 300 meters depth, at the transition from Subunit 3A to 3B, a second marked change to more-compacted material takes place (Fig. 45). Ten centimeters above the contact of the lowermost thick dolerite body, water content and porosity decrease by about 10%, and bulk density increases by more than 0.2 g/cm³.

The sound velocities measured in the uppermost 50 meters were 1.49 to about 1.53 km/s. In the deeper part of the hole, few determinations of sound velocity could be carried out, because of strong drilling disturbance and expanding gas. At about 270 meters depth, the sound velocity through undisturbed chunks of mudstone reached values between 1.61 and 1.63 km/s. A value of 2.21 km/s measured on a chunk from Section 478-31-1 below the thin dolerite sill appears to be too high, because the bulk density of this mudstone is rather low (1.57 g/cm³). Some values for sound velocity, wet-bulk density, and acoustic impedance of hard-rock samples from the dolerite sills are listed in Table 11.

The following general conclusions can be drawn from physical-property measurements:

- 1) If the contact zones of the dolerite sills are excluded, the sediments in Hole 478 are no more compacted than in Holes 474A through 476. The gradients of physical properties versus depth are low—much lower than in Holes 477 and 477A, located in the present spreading center of the Guaymas Basin. From physical-property measurements we have, therefore, no indications of abnormally high heat flow or another mechanism which may have accelerated compaction in the sediments above the thick dolerite body at 340 meters depth.

- 2) The contact zones of the intruding basaltic sills appear to be asymmetric. A much thicker sediment sequence (up to 40 meters above the thick sills) is influenced above rather than below the sills, but very strong

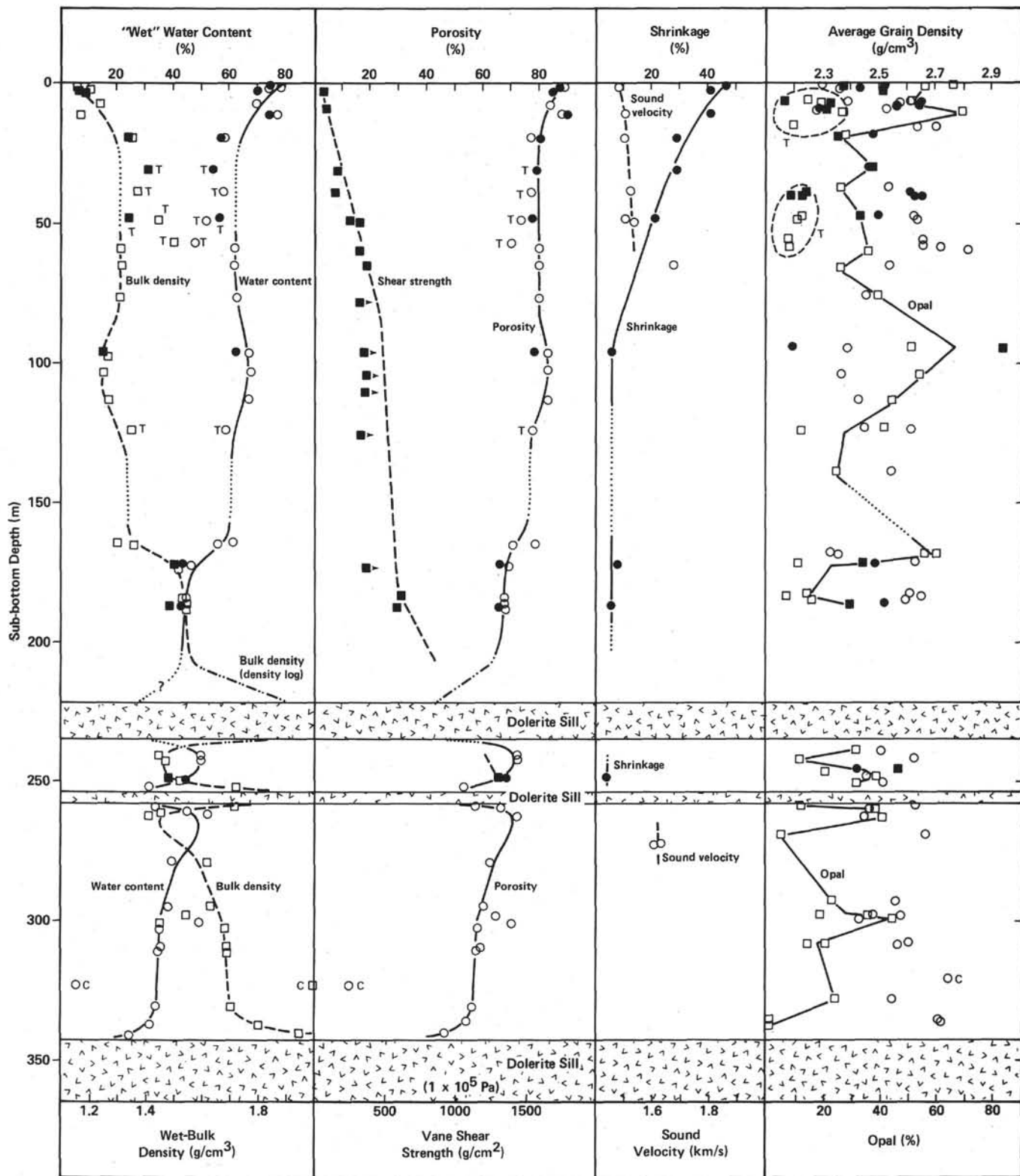


Figure 45. Mass physical properties, shrinkage, and content of opaline silica of sediments from Hole 478. Mud turbidites (T) often deviate from the general trend lines. Marked changes in bulk density and porosity on top of the uppermost contact are inferred from density log. (C = cemented dolomitic siltstone. Solid symbols are cylindrical samples. Open symbols are chunk samples.)

Table 11. Sound velocity, wet-bulk density, and acoustic impedance of hard rocks from dolerite sills, Site 478.

Core Section	Top of 2-cm Intervals	Rock Description	Orientation	Sound Velocity (km/s)	Wet-Bulk Density (g/cm ³)	Acoustic Impedance × 10 ⁵ (g/cm ² s)
478-26-1	123	Coarse-grained basalt	=	4.25	2.83	12.03
478-41-3	51	Aphyric dolerite	⊥	5.70	2.79	15.90
478-43-3	65	Dolerite	⊥	4.90	2.76	13.52
478-44-4	92	Dolerite, coarse-grained	⊥	5.11	2.78	14.21
478-45-2	65	Aphyric dolerite	⊥	5.25	2.77	14.54
478-50-5	62	Dolerite	⊥	5.36	2.80	15.01
478-51-2	62	Gabbro xenolith (weathered) in dolerite	⊥	4.55	2.81	12.79
478-51-2	62	Gabbro xenolith (weathered) in dolerite	=	4.09	2.81	11.49
478-53-1	72	Aphyric dolerite	⊥	4.45	2.85	12.68
478-54-1	81	Coarse aphyric basalt	⊥	3.91	2.77	10.83
478-54-1	81	Coarse aphyric basalt	=	3.74	2.77	10.36
478-54-4	47	Aphyric basalt	=	3.91	2.66	10.40

changes of the physical properties are limited to a sediment thickness of one to a few meters above and below the sills.

3) The apparently similar contact zone on top of the uppermost sill and the lowermost, thick dolerite body indicates that both have formed in about the same way. Both have intruded a sedimentary sequence of normal compaction which probably never was influenced by as high a temperature gradient as the sediments in Holes 477 and 477A. Such sediments might be expected farther below the sill at the bottom of Hole 478.

Site 478 Heat Flow

Temperature was measured at 70 meters down the hole by the Uyeda/Kinoshita instrument, and at the bottom by the first temperature-logging run. The second temperature run was not made, because the hole caved in, causing the loss of the logging tool. Unfortunately, no maximum thermometers were carried by the other tools, so we have only one temperature at the bottom. From past experience, when both temperature runs were made about 22 hours apart under similar conditions the second measured temperature was 10°C higher than the first, and the extrapolated temperature rise to infinite time from the second run would add another 2°. Applying these corrections, the formation temperature is $50 + 12 = 62^\circ\text{C}$. Subtracting the mudline temperature of 3.4° leaves a temperature differential of 58.6° . Dividing by the depth, 0.464 km, gives a gradient of $126.3^\circ\text{C}/\text{km}$. From the lithology of the hole and measurements of thermal conductivity of samples from this and other holes, the average conductivity of the total length of the hole is $2.9 \text{ mcal}/\text{cm s } ^\circ\text{C}$. Multiplying by the gradient gives the heat flow, 3.66 HFU.

It is difficult to assign a greater value of conductivity than 2.1 to the first 70 meters of this hole, because of the diatomaceous ooze in the upper part of the section, the conductivity of which is only 1.75. When this sediment is brought up, it swells from expanding H₂S and methane. The *in situ* conductivity should be higher. The temperature gradient given by the Uyeda instrument is $(12.5-3.4)/0.070 = 130^\circ/\text{km}$, which when multiplied by the conductivity gives 2.73 HFU, only 75% of the value

obtained from the bottomhole temperature. A similar discrepancy (25%) is more firmly established for Hole 481A because both temperature logs were run in that hole.

The value 3.66 HFU is the preferred one for Site 478.

Site 478 Correlation of Drilling Results, Seismic Data, and Logging

Although a close network of seismic-reflection lines had been run previously in the Guaymas Basin, this site was selected mainly for its location on one of the multi-channel lines run during the SIO site survey cruise. In this chapter we will correlate drilling and downhole logging results with that multichannel record (Fig. 46), and with 3.5-kHz and 5-second-sweep air-gun records made while arriving on this site.

We have some velocity information for this site from a few laboratory measurements on core samples, from the multichannel move-out velocities, and from a sonobuoy which was permitted to drift away from the ship while sitting on this site. The wide-angle-reflection data from this sonobuoy record were analyzed after this cruise by R. T. Bachman, USNOSC, San Diego, to provide velocity information; no refraction information was obtained from this record. Here, as at Site 477, we suspect that the surface of the acoustic basement and any deeper possible refracting layers may be too irregular and our run was not long enough to get refraction arrivals. The sonic downhole log was not completed, because the tool was lost in the hole where some bridging or caving had occurred.

Each of the types of seismic-reflection records used in this comparison is illustrated: Figure 47 is the 3.5-kHz record over this station; Figure 48 is the 2-second-sweep seismic-reflection record, collected with 120-in³ and 20-in³ air guns firing at 7-second repetition rate and signals received through a 40- to 80-Hz bandpass filter; Figure 49 is the 5-second-sweep record collected at the same time, but with a 20- to 40-Hz bandpass; and Figure 46 is the processed 24-channel record collected during the SIO site survey, using 300-in³, 120-in³, and 40-in³ air guns firing at 15-second intervals.

Correlations between some lithologic changes in the drilling results and reflectors in these various records are shown in Table 12, as reconstructed using the combined velocity information from the various sources.

Site 478 Summary and Conclusions

The presently active rifts, or spreading centers, in the Guaymas Basin are steep-walled topographic depressions elongated in the northeast-southwest direction. As these rift troughs grow by spreading in a northwest-southeast direction, their walls of Quaternary sediments and sedimentary rocks slump into the low trough, and turbidity currents seek this lowest level within the basin. But we are living in a period of glacial minimum and high sea levels, and wide shelves trap the sediment loads of the rivers to form large deltas. It seems likely that during times of glacial maxima and low sea levels these same rivers must flow directly onto the slope and virtually all of their loads are transferred to the basin fans and

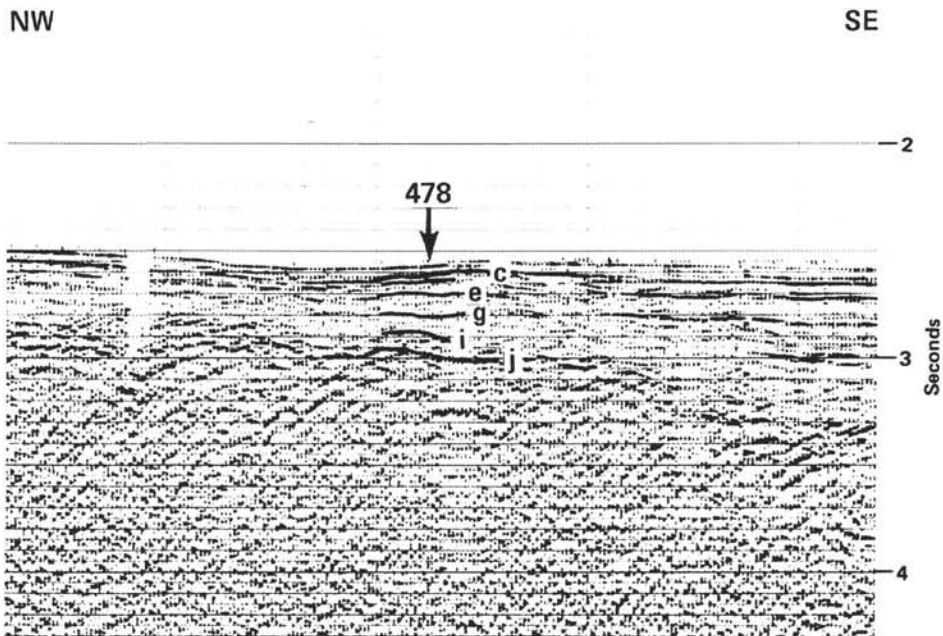


Figure 46. Correlation of drilling lithology with section of processed multichannel seismic-reflection record across Site 478. Seismic record from Guaymas Expedition, Scripps Institution of Oceanography site survey. Reflectors c, e, g, i, and j are listed in Table 12.

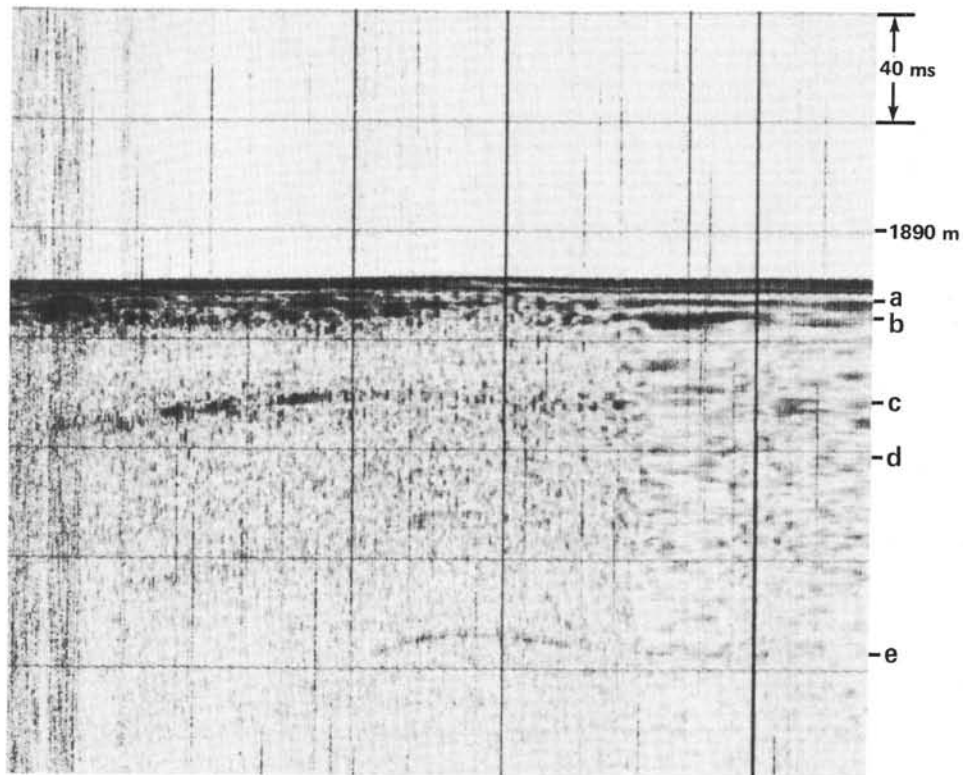


Figure 47. Correlation of drilling lithology with 3.5-kHz record on Site 478. Reflectors a, b, c, d, and e listed in Table 12.

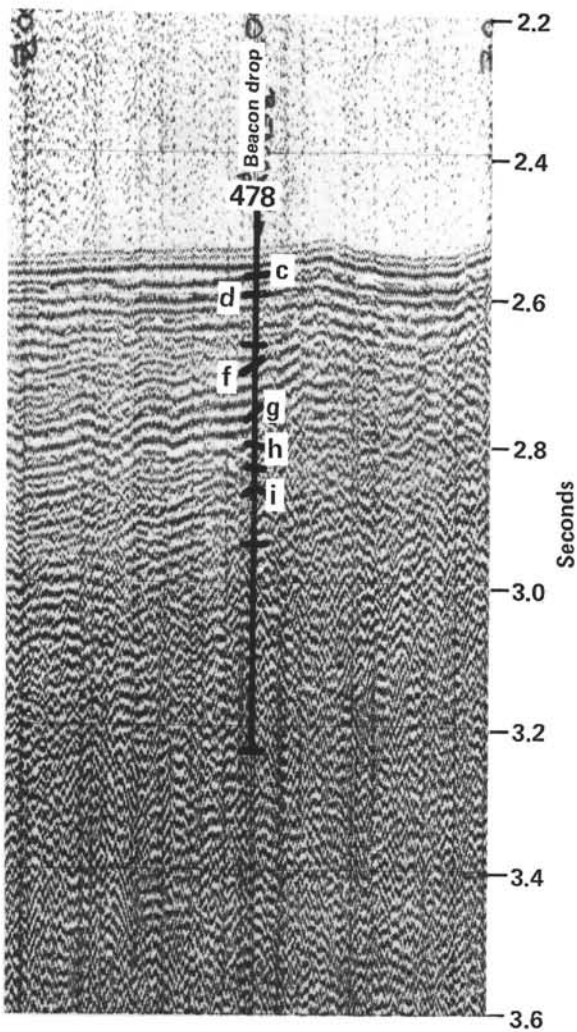


Figure 48. Correlation of drilling lithology with 2-second air-gun seismic-reflection record across Site 478.

plains, completely filling the rift troughs, forming a single depositional basin plain. This and many other variations must occur at these spreading centers through time as climatic and sedimentary influences change. Site 477, drilled in the present active south rift trough, gave us invaluable information on the interplay between sediment deposition and intrusion of basaltic magmas. Site 478, 12.1 km northwest of the southern rift, was drilled to compare these conditions with a site that was itself located over the active center about 400,000 years ago (assuming validity of the plate-tectonics model within Guaymas Basin, uniform spreading rates, and relatively constant plate-edge geometry through time). Multifold seismic lines from the SIO site survey at this basin show that acoustic basement is of low velocity and apparently contiguous from the present rift to Site 478, and extends well beyond this locality to the farthest points beneath the relatively flat floor of Guaymas Basin both northwest and southeast of the active rift. We believe this acoustic basement to be the expression of the non-coherent mixture of intrusive bodies and intercalated, faulted sediments that were drilled at Site 477. Overlying the entire basin plain, other than the rifts, is another

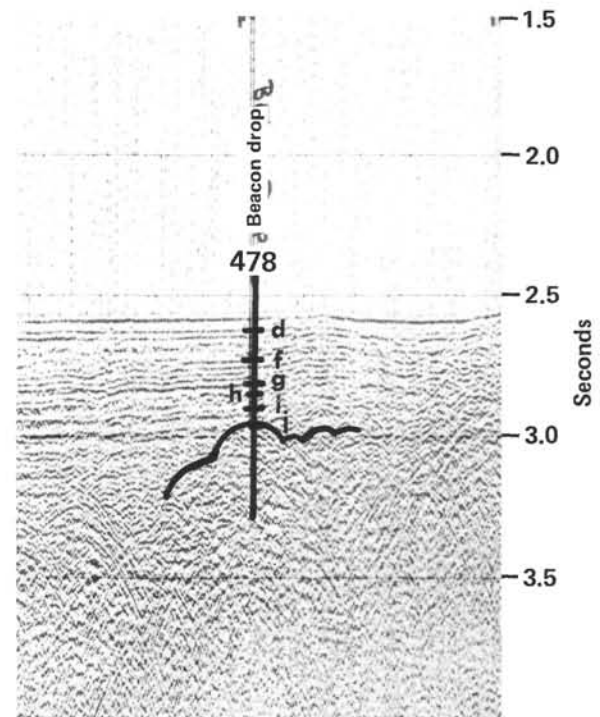


Figure 49. Correlation of drilling lithology with 5-second air-gun seismic-reflection record across Site 478.

Table 12. Correlation of lithology and seismic-reflection data, Site 478.

Reflector	Reflection Time (ms)	Sub-bottom Depth (m)	Reflection Velocity (km/s)	Record	Figure	Lithologic Unit	Lithology
a	8	6	1.50	3.5 kHz	47		Diatom ooze/Turbidite
b	15	11	1.50	3.5 kHz	47	1a	Sand
c	43	32	1.50	3.5 kHz	47		
				2 sec	48		
				mcs	46		
d	67	51	1.52	3.5 kHz	47		Sand
				2 sec	48		
				5 sec	49		
				mcs	46		
e	130	101	1.55	3.5 kHz	47		Turbidite/diatom ooze
				2 sec	48		
				mcs	46		
f	162	127	1.57	2 sec	48	1b	Onlap 1A/1B diatom mud
				5 sec	49		
				mcs	46		
g	236	188	1.59	2 sec	48		Contact 1B/2 dolomitic siltstones
				5 sec	49		
				mcs	46		
h	273	219	1.60	2 sec	48	2	
				5 sec	49	1	dolerite sill?
				2 sec	48	2	dolerite sill?
				5 sec	49		
				mcs	46	3	
i	304	253	1.66	2 sec	48		
				5 sec	49		
				mcs	46		
j	405	342	1.69	5 sec	49		dolerite
				mcs	46	3	

sedimentary unit that shows relatively good coherence over considerable distances and appears to be a 2- to 600-meter-thick section of turbidites, perhaps deposited largely during the last eustatic low stand of the sea. The section drilled at Site 478 was intended to include about 300 meters of the presumed turbidites overlying acoustic basement and the upper part of the acoustic basement itself. We hoped in this way to compare lithologies and properties of the rifting phase to those of the post-rifting basin-plain deposits. Our site, in fact, was located on the distal southern edge of a natural levee on the south side of a channel now partially filled and perhaps

a relic of turbidity-current activity of late Pleistocene time.

Total penetration of the drill at this site was 464 meters. The upper 342.5 meters is predominantly a sedimentary section that we subdivided into three main units. The lower 121.5 meters is a complex intrusion of basaltic to doleritic texture. The sediments above the major intrusion are differentiated on the basis of the type and frequency of redeposited beds in Unit 1; on the presence of some calcareous cemented interlayers and altered sediment around two dolerite intrusive bodies in Unit 2; and, in Unit 3, on the delineation of some diatomaceous mudstones near the base which show indications of primary varve-like laminations, as well as a contact zone with a thick underlying intrusion. Unit 1 (0–188 m) is composed of muddy diatomaceous ooze to diatom mud with episodic gray, sandy turbidites. The section from 188 to 260 meters is Unit 2, comprising dolomitic sandstones, two dolerite sills with contact aureoles, and diatomaceous mudstone. Unit 3 extends from 260 to 342.5 meters and is made up of uniform diatom mudstone overlying laminated diatom mud with dolomite, overlying siltstone and a basal contact with the basaltic intrusion below. All of these sequences are considered to be of moderate to very rapid deposition. Based on the nannoplankton zone boundary NN21/20 and a diatom datum, the rate of accumulation must have been at least 1000 m/m.y. Based on the datum provided by the extinction of the diatom *Nitzschia fossilis*, most of the sediment section (0–310 m) is no older than 260,000 years.

This extremely high rate of deposition makes it possible to detect non-steady-state conditions in the pore-water chemistry of the sediments. Using a reasonable diffusion coefficient, one can calculate a mean diffusion length in the section of 30 meters over a period of 100,000 years in these sediments. Thus, non-steady-state inclinations in the profiles of dissolved calcium, alkalinity, ammonia, and phosphate are well established below about 50 meters beneath the sea floor.

Comparison of this site 12 km out on the flank of the axis of rifting to Site 477 in the present rift reveals some rather strong contrasts, suggesting that our drilling has stopped short of penetration into a true Guaymas Rift-type section. Physical-properties measurements show that, if contact zones with the dolerite sills are excluded, the sediments in Hole 478 are no more compacted than those of our more-normal sections at Hole 474A through 476. The gradients of physical properties with depth are much lower than those measured in the southern Guaymas Basin Rift. Studies of the mineralogy of the sediments also suggest that the sediments recovered from Site 478 were warm, but never very hot. If our assumption that a high-temperature regime existed at the time of zero age of the crust at this site is correct, then the existence of deeper sediments below the lowest drilled thick sill is required. Organic geochemistry also shows that the contacts of penetrated intrusive bodies record that the high-temperature influence was limited to the immediate vicinity of the contact (within a few centimeters). Lower-temperature thermal gradients propagated

by the intrusive expelled petroliferous organic matter from the sediment, but left behind viable organic matter, and the sediment between the intrusions was not completely pyrolyzed. Finally, the age of the sediments intruded by the igneous bodies is, by nannofossil assemblages and diatom-extinction datum, about 260,000 years old—well short of the 400,000-year age required by extrapolation of the 3-cm/yr half-rate of measured spreading. Thus, in summary, the age, thermal history, and physical properties of the penetrated sediments all suggest the probability of an extensive sediment section below the lower igneous intrusion.

Tentative correlations of lithology with available seismic data are hampered by the lack of reliable velocity data. Nevertheless, it is relatively clear that the lower intrusion into which we drilled for 121 meters, without fully penetrating it, can be equated to the “acoustic basement” of the 24-channel seismic record of the SIO site survey. If this correlation is correct, it has important implications for the timing of intrusive events and genetic processes involved in developing the abnormally thick intermediate layer overlying Layer 3 in the Guaymas Basin, and perhaps in similar sections of very young ocean basins. Specifically, the seismic correlation together with the youth and thermal histories of the encountered intrusive units demonstrate that the process of intrusion of magma into rapidly deposited sediments is not limited to a narrow zone corresponding to the average 3-km width of the present rift troughs. Similarly, the time of intrusion is not restricted to the first 50,000 years of rifting represented by the modern troughs, but apparently spans a much longer time—at least 140,000 years, and possibly as much as 200,000 years.

SITE 481

Site 481 Background and Objectives

The general background and objectives for the Guaymas Basin sites were discussed previously. Site 481 is a second attempt to drill a presumed active spreading rift in the basin floor. Site 477 was located in a high-heat-flow portion of the southern rift, where heat flow had previously been assumed to be largely conductive (Lawver and Williams, 1979). Site 481 is located in the northern rift near where a submersible dive (Lonsdale, 1978) had permitted observations of hydrothermal deposits on the flank of the rift. Heat flow is very spotty in this rift, as in the southern rift, but is generally lower and was presumed to be largely convective (Lawver and Williams, 1979). This site has therefore been known as the “hydrothermal site,” and much of the support and enthusiasm for drilling it came from the hydrothermal faction of both the Gulf of California working group and the shipboard scientists. Other objectives for this site were basically the same as for 477. These specific objectives were itemized previously for Site 477. Most of those objectives, unfortunately, were not achieved, because the holes were both terminated at shallower depths than we would have wished. In addition, more new problems and questions were introduced than were

answered. These new questions, which may form the objectives of future drilling, include:

1) How deep beneath the sea floor are sediments intercalated with sills? Were these sediments emplaced by lateral infilling within the rift, as envisioned by the model, and as suggested by the lack of continuity of stratification as shown by the seismic-reflection records? Can this deformation structure predicted by this model be confirmed by observation on cores? Will these deepest and presumably oldest sediments contradict the age predicted by the plate-tectonic model for the origin of the rifts?

2) Are all of the igneous intrusions really sills, or are many dikes and shapeless intrusions also present? The probability of encountering sills is greater than the probability of encountering dikes. The model predicts approximately as many dikes as sills within the stratified part of the section, and an increasing frequency of sills and proportion of dikes with depth down to the sheeted dike complex beyond the lowest sediments.

3) Would the increase in higher hydrocarbon compounds continue with depth, and if so would it constitute a pollution hazard if drilled? Hydrocarbons up to pentane were detected in a shallow surface piston core from near Site 481, but Site 477 did not reach a significant level of hydrocarbons higher than C_4 .

4) Will hydrothermal alteration of sediments be found at this site, where present heat flow is lower, or is the hydrothermal activity at this site being vented to the sea-floor by the faults of the northwest flank of the rift valley? Hydrothermal activity may be spotty in location as well as in time. Is the hydrothermal activity produced by the intrusive events driving out sediment pore water, or is it caused by sea water recharging and circulation?

Site 481 Operations

Upon getting under way from Site 480 at 1658Z on 2 January, we had time for only one additional site in the Guaymas Basin before ending Leg 64 drilling and setting course for San Pedro and the drydock to work on *Glomar Challenger's* thrusters. There was much enthusiasm among the scientific party (and the geothermal lobby ashore) for drilling the north rift of the basin where earlier submersible dives had revealed the presence of hydrothermal deposits above a fault scarp near the north wall of the trough. We were now aware of the great irregularity of topography and structure over short distances within the active rifts, and we therefore decided that a pre-drilling air-gun and 3.5-kHz survey was necessary to locate the optimum drill site. Accordingly, we departed on course 160° to a point northwest of the area of the proposed site, where our survey would begin. At 2112Z we changed course to start the survey, a series of crossings normal to the strike of the rift (Fig. 50). After five crossings, working along the rift from northeast to southwest, it became evident that our first crossing appeared to be the best place to locate the site. We therefore proceeded up the axis of the rift in a northeasterly direction to the vicinity of the first crossing and swung out of the trough to the northwest, then back in to drop a beacon at 0452Z on 3 January. We then re-

trieved our seismic gear to search for the beacon, but found no coherent signal from the beacon (the ninth bad beacon of this leg). Because it was blowing a gale and we were receiving only intermittent weak beacon signals, we then began an interminable wait for a satellite navigation fix and a continuing search for the errant beacon. Finally, at 0835Z on 3 January, we began a further survey with the 3.5-kHz alone for another suitable site in this locality, and at 0926Z we let go a beacon at our chosen position. By 1120Z we had positioned over the beacon in 1998 meters and began running in the hole. We earlier had decided to use the hydraulic piston corer the first 50 meters of this hole to allow optimum measurement of shallow structure, chemistry, and physical properties. From 1600 to 1800Z, before beginning the piston coring, we washed to 100 meters to assure that we would not destroy the corer by banging an intrusive. That finished, we began HPC operations, and at 2210Z our first core was on deck—the usual excellent undisturbed core. Ten additional piston cores then were obtained, until we had cored to a depth of 52.75 meters by 1508Z on 4 January.

We then pulled out of the hole and rigged up the standard bottomhole assembly and mechanical bit release for normal operations. From 1900 to 0100Z on 5 January we deployed the drill string and began Hole 481A (same location and depth as Hole 481) by washing to 2058.5 meters, just above the level of our deepest piston core. The combination heat-flow-pore-water tool was then used, with good results. Normal coring operations followed, our first core arriving on deck at 0327Z on 4 January. Thereafter, until 0630Z on 7 January, we continuously cored to a depth of 384 meters below the sea floor in 37 cores. Another successful run of the heat-probe-pore-water tool was accomplished after Core 481A-4. We encountered complex hydrocarbon assemblages and gas accumulations associated with intrusive dolerite bodies, but our experience in drilling in these conditions had broadened considerably and we correctly assessed the situation as posing no threat to safety or environment. At 1200Z on 5 January we had to drop another 13.5-kHz beacon to replace the rapidly fading 16-kHz instrument we were using. This was the tenth bad beacon of this leg. From 1500Z on 6 January to our last coring attempt at 0630Z of 7 January, we recovered only 1 meter of sample in seven cores. The bit was plugged, the float valve was stuck open, and we were unable to properly seat the core barrel. Repeated attempts to clear by dropping the center bit failed, and at 0815Z on 7 January we decided to secure drilling and log the hole. Preparations for logging lasted until 1130Z. Logging then began and continued until 0700Z on 8 January. Five logs were successfully run. First run: density, caliper, gamma, and temperature; second run: sonic, caliper, and gamma; third run: guard, neutron (misrun, no good); fourth run: same as last, but good this time; fifth run: induction, gamma; and, sixth run: temperature. We then secured the logging equipment and cemented the hole from 2220 to 2150. From 0830 until 1732Z we pulled out of the hole, magnafluxed drill collars and other equipment, and completed operations

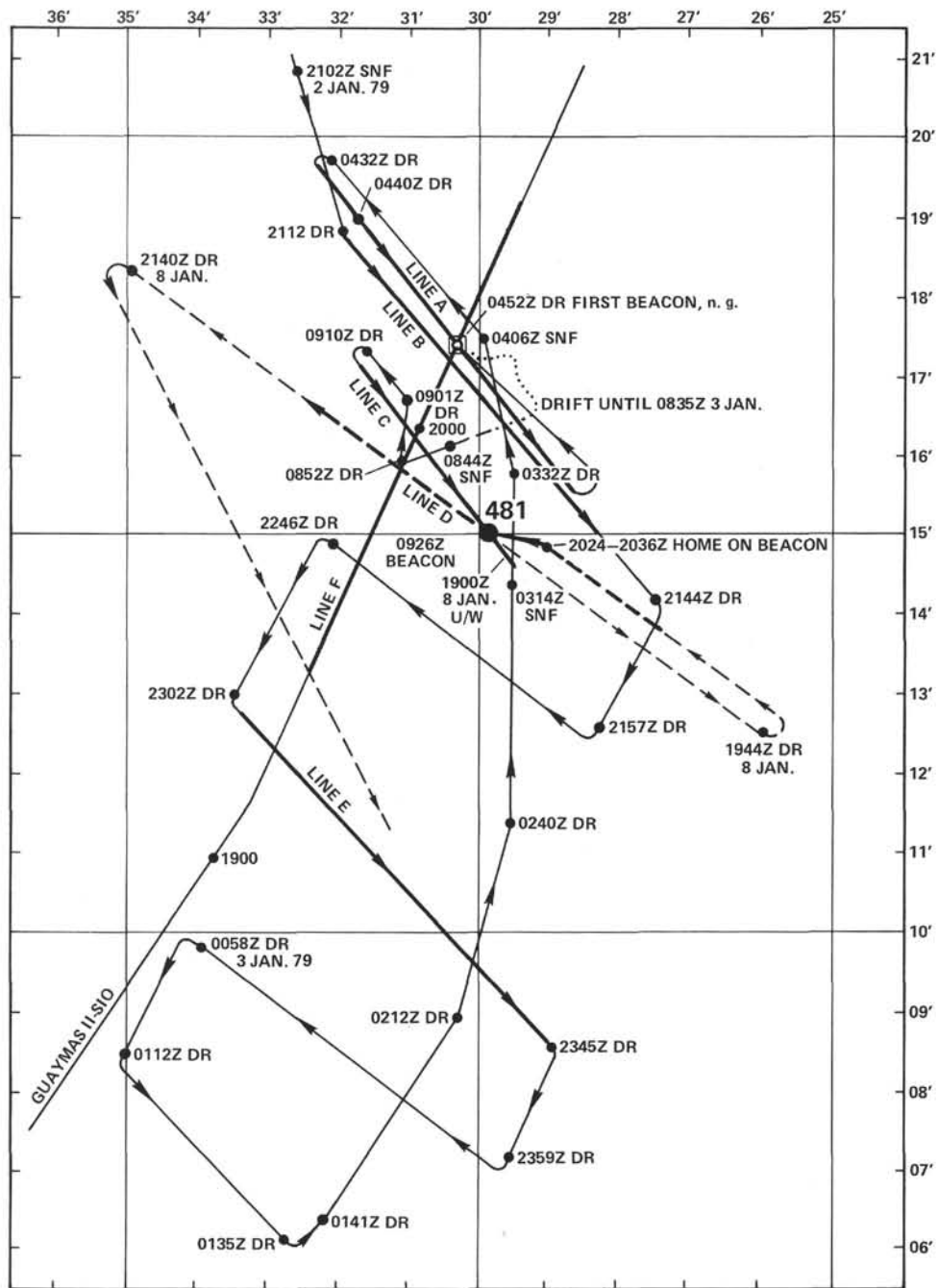


Figure 50. Track chart of *Glomar Challenger* survey on approach (solid lines) and departure (dashed lines), Site 481. Also, one track from Guaymas expedition of S.I.O. (Heavy sections of lines are illustrated in figures as follows: Line A, Fig. 70; Line B, Fig. 71; Line C, Fig. 72; Line D, Fig. 73; Line E, Fig. 74; and Line F, Fig. 75.)

connected with the hole. At 1900Z we were under way toward the southeast to run one additional crossing of the rift with air guns and 3.5-kHz seismic to tie the beacon and our site correctly into our previous survey. At 1944Z we changed course back toward the northwest and our beacon, and at 2140Z, 8 January, we departed the Guaymas Basin north rift area and set a southeasterly course for a survey off Cabo San Lucas, which would be the last operational activity of Leg 64.

A coring summary is presented in Table 13.

Site 481 Sediment Lithology

The location of this site along the marginal fault of the northern rift is reflected by the extremely high accumulation rates (> 1500 m/m.y.) of redeposited diatomaceous muds intercalated into minor amounts of host hemipelagic, muddy, diatomaceous, basinal oozes which may be either laminated or massive as the result of fluctuating bottom-water oxygen levels. The undisturbed sections recovered in the hydraulic-piston-core

Table 13. Coring summary, Site 481.

Core No.	Date (Jan. 1979)	Time	Depth from Drill Floor (m)		Depth below Sea Floor (m)		Length Cored (m)	Length Recovered (m)	Recovery (%)
			Top	Bottom	Top	Bottom			
—	3	—	2007.00–2011.75		—		—	—	—
—	3	—	2011.75–2016.50		—		—	—	—
481-P1	3	1510	2016.50–2021.25	2011.75–2016.50	0.00–4.75	4.75	2.66	56	
P2	3	1615	2021.25–2026.00	2016.50–2021.25	4.75–9.50	4.75	4.55	96	
P3	3	1725	2026.00–2030.75	2021.25–2026.00	9.50–14.25	4.75	4.45	95	
P4	3	1830	2030.75–2035.50	2026.00–2030.75	14.25–19.00	4.75	1.70	36	
P5	3	2336	2035.50–2040.25	2030.75–2035.50	19.00–23.75	4.75	0.00	0	
P6	4	0059	2040.25–2045.00	2035.50–2040.25	23.75–28.50	4.75	0.20	4	
P7	4	0211	2045.00–2049.75	2040.25–2045.00	28.50–33.25	4.75	4.57	96	
P8	4	0412	2049.75–2054.50	2045.00–2049.75	33.25–38.00	4.75	4.58	96	
P9	4	0522	2054.50–2059.25	2049.75–2054.50	38.00–42.75	4.75	2.08	42	
P10	4	0655	2059.25–2064.00	2054.50–2059.25	42.75–47.50	4.75	4.43	93	
P11	4	0808	2064.00–2068.25	2059.25–2064.00	47.50–52.25	4.75	4.48	94	
481A-1	4	2027	2058.5–2068.0	2064.00–2068.25	42.0–51.5	9.5	3.20	34	
2	4	2112	2068.0–2077.5	2068.00–2068.25	51.5–61.0	9.5	1.29	14	
3	4	2200	2077.5–2087.0	2077.5–2077.5	61.0–70.5	9.5	1.33	14	
4	4	2241	2087.0–2096.5	2087.0–2087.0	70.5–80.0	9.5	3.81	40	
5	4	2332	2096.5–2106.0	2096.5–2106.0	80.0–89.5	9.5	9.62	101	
6	5	0028	2106.0–2115.5	2106.0–2115.5	89.5–99.0	9.5	9.55	100	
7	5	0126	2115.5–2125.0	2115.5–2125.0	99.0–108.5	9.5	9.54	100	
8	5	0221	2125.0–2134.5	2125.0–2134.5	108.5–118.0	9.5	9.65	102	
9	5	0322	2134.5–2144.0	2134.5–2144.0	118.0–127.5	9.5	9.17	97	
10	5	0420	2144.0–2153.5	2144.0–2153.5	127.5–137.0	9.5	6.43	68	
11	5	0513	2153.5–2163.0	2153.5–2163.0	137.0–146.5	9.5	7.78	82	
12	5	0621	2163.0–2172.5	2163.0–2172.5	146.5–156.0	9.5	5.95	63	
13	5	0725	2172.5–2182.0	2172.5–2182.0	156.0–165.5	9.5	6.02	63	
14	5	0850	2182.0–2191.5	2182.0–2191.5	165.5–175.0	9.5	5.09	54	
15	5	1117	2191.5–2201.0	2191.5–2201.0	175.0–184.5	9.5	4.92	52	
16	5	1500	2201.0–2210.5	2201.0–2210.5	184.5–194.0	9.5	3.48	37	
17	5	1637	2210.5–2220.0	2210.5–2220.0	194.0–203.5	9.5	1.85	19	
18	5	1751	2220.0–2229.5	2220.0–2229.5	203.5–213.0	9.5	0.49	5	
19	5	1907	2229.5–2239.0	2229.5–2239.0	213.0–222.5	9.5	0.00	0	
20	5	2118	2239.0–2248.5	2239.0–2248.5	222.5–232.0	9.5	2.07	22	
21	5	2238	2248.5–2258.0	2248.5–2258.0	232.0–241.5	9.5	0.00	0	
22	5	2349	2258.0–2267.5	2258.0–2267.5	241.5–251.0	9.5	7.09	75	
23	6	0102	2267.5–2277.0	2267.5–2277.0	251.0–260.5	9.5	0.66	7	
24	6	0203	2277.0–2286.5	2277.0–2286.5	260.5–270.0	9.5	9.89	104	
25	6	0308	2286.5–2296.0	2286.5–2296.0	270.0–279.5	9.5	8.80	93	
26	6	0407	2296.0–2305.5	2296.0–2305.5	279.5–289.0	9.5	8.12	85	
27	6	0505	2305.5–2315.0	2305.5–2315.0	289.0–298.5	9.5	8.13	86	
28	6	0612	2315.0–2324.5	2315.0–2324.5	298.5–308.0	9.5	6.61	70	
29	6	0706	2324.5–2334.0	2324.5–2334.0	308.0–317.5	9.5	1.45	15	
30	6	0800	2334.0–2343.5	2334.0–2343.5	317.5–327.0	9.5	8.13	86	
31	6	0950	2343.5–2353.0	2343.5–2353.0	327.0–336.5	9.5	0.53	6	
32	6	1045	2353.0–2362.5	2353.0–2362.5	336.5–346.0	9.5	0.00	0	
33	6	1441	2362.5–2372.0	2362.5–2372.0	346.0–355.5	9.5	0.45	5	
34	6	1650	2372.0–2381.5	2372.0–2381.5	355.5–365.0	9.5	0.00	0	
35	6	1825	2381.5–2382.5	2381.5–2382.5	365.0–366.0	1.0	0.00	0	
36	6	2130	2382.5–2391.0	2382.5–2391.0	366.0–374.5	8.5	0.02	< 1	
37	6	2330	2391.0–2400.5	2391.0–2400.5	374.5–384.0	9.5	0.00	0	

Hole 481 (Fig. 51) allowed us to distinguish the end members for two general types of mud turbidites (Type I, Type II) as well as recognize a pebbly mud flow (I). The subdivision between turbidite Types I and II is based mainly on color, texture, and relative amounts of biogenic (mainly diatoms) and terrigenous components. Turbidites seem to derive from hemipelagic slope drape along the basin margins (Type I) or outer deltaic slopes of the Rio Yaqui fan (Type II). Where recovery was limited, successful logging was essential to distinguish some levels with early diagenesis, as well as the gradational character of two large mass flows (II, III).

Although the sediment column is very young (less than 250,000 years old) and has been intruded by multiple sills, we have divided it at 200 meters sub-bottom into two informal units marked by the base of a chert-and-sill complex. Above this complex, accumulation of unit sediments may be more rapid, punctuated by more frequent intercalations of thick, delta-derived sandy silts. Holes 481 and 481A can be correlated by the presence of sand layers in the 10.25-meter overlap 45 meters sub-bottom.

Unit 1: Late Quaternary (< 250,000 yr)
(481-1 through 11, 481A-1 through 17-2; 0–200 m)

The upper part of the sediment column (Fig. 51) is extensively disturbed but comprises generally moderate-olive-brown, diatomaceous muds with common intercalations of gray, graded, muddy sands. Sedimentary structures revealed in the 52 meters of undisturbed section from HPC Hole 481 show that much of the diatomaceous mud is also organized as faintly graded mud turbidites with only rare intervals of mostly homogeneous, bioturbated, hemipelagic, muddy, diatomaceous ooze. This hole best illustrates the general end-member types of redeposited beds, although intermediate varieties also occur. Turbidites of Type I are generally thinner beds, from a few centimeters to a few decimeters thick, and

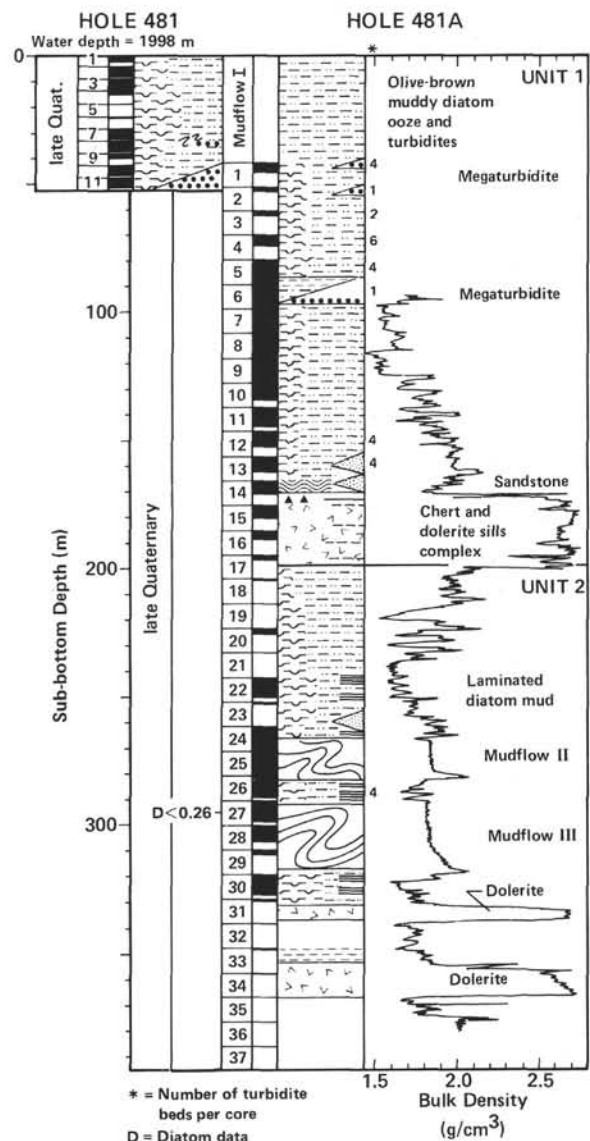


Figure 51. General lithology, lithologic units, core recovery (shown in black), and bulk density, Site 481.

show very faint grading of color and texture. Typical beds are recognized at first glance by a very pale band of diatom ooze at the top and a thin basal sand, commonly coarse; the color parallels composition and grades downward from dusky-yellow (5Y 6/4) to pale-olive (10Y 6/2) diatomaceous ooze; the body is moderate-olive-brown (5Y 4/4), muddy, diatomaceous ooze to olive-gray (5Y 3/2), diatomaceous muds or clayey silts, to a thin, dark, medium-gray (N4) basal sand. The thin layer (1–5 cm) of very pale diatom ooze at the top of these beds commonly consists of diatom frustules from very fragile upwelling species (Fig. 52). These layers are thought to occur by hydraulic sorting during sluggish turbidity-current transport. If they were diatom blooms, then similar layers also should have been recovered at HPC Site 480 along the slope (see discussion in Einsele and Kelts, this volume, Pt. 2). At 2 meters sub-bottom there is a unique layer with dark-gray (5Y 3/2) iron monosulfide pigment preserved in a thick diatom-ooze layer at the top of one of the Type I turbidites (Sample 481-2-2, 0–14 cm). An irregular, diffuse redox boundary separates gray from pale olive below. Preservation of frustules and calcareous nannofossils seems better in the gray zone. Long-term preservation of metastable monosulfides in marine sediments is rare, and indicates very rapid burial of the layer.

The thin basal-sand layer commonly contains higher concentrations of bathyal benthic foraminifers, and plagioclase-rich rock fragments. The average composition of these turbidites is 35 to 50% frustules, 35 to 40% clays; 10% calcareous nannofossils, 3 to 7% feldspars, and 1 to 3% quartz. Pyrite is ubiquitous and commonly occurs within frustules.

Where undisturbed, the hemipelagic host sediment is distinguished from Type I turbidites by a slightly darker brownish hue and a faint mottling which results from bioturbation.

Turbidites of Type II are generally thicker (0.5 to > 10 m) and characterized by a greater proportion of terrigenous components. The body is rather structureless, with a subtle but uniform downward grading of color and components. The smoothly cut surface is dotted with gas-expansion pimples. Beds are generally grayish olive (10Y 4/2) but may grade downward from moderate-olive-brown (5Y 4/4), diatomaceous muds, to gray-olive (10Y 4/2), clayey silt, to gray (N4–N5). Rather than a distinct thin, sorted, sandy base, there is a gradual downward increase in sand grains, accompanied by a muddy matrix. The incompletely recovered, but over 10-meter thick graded “megaturbidites” of Cores 481-10 and 11 and 481A-5 and 6 are of this type, with thick basal portions of muddy, fine sand. The tops are uniform clayey lutite.

The average composition includes diatoms (20–35%), calcareous nannofossils (10–15%), clay minerals (30–45%), feldspars (10–18%), quartz, (4–10%), and pyrite (1–3%). Wood debris, benthic foraminifers, and shelly debris occur in some beds.

Type I and II beds are interbedded with non-cyclic frequency. Because of their greater thicknesses, Type II varieties appear to dominate the section.



Figure 52. Core photograph. Pale-olive tops of Type I mud turbidites.

A 70-cm-thick olive-gray (5Y 4/1) mud flow (I) with gas-expansion partings recovered between 33.85 and 34.55 meters (HPC 481-8-1, 50–121 cm) has a matrix with abundant terrigenous silts and 10 to 15% diatom frustules, with floating soft-sediment mud clasts. A double convolute fold (Fig. 53) indicates that the distance of transport of this flow was modest; it probably was derived from the nearby rift-wall fault scarp.

An unusual grayish-white (N8–N6) claystone with indurated lumps occurs in Core 481-8, 36.2 to 36.6 meters

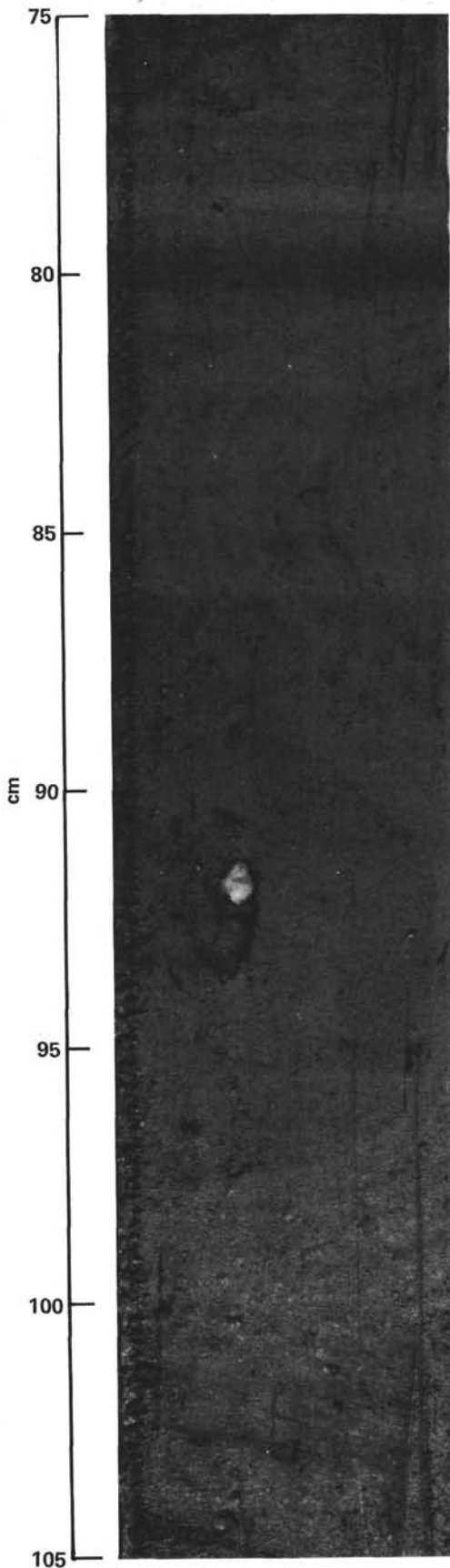


Figure 53. Photograph of HPC Sample 481-P8-1, 75-105 cm. Convolute fold in diatomaceous muds.

sub-bottom. It consists of mainly quartz and chlorite, and includes concentrations of broken and single valves of bathyal clam species.

**Unit 2: late Quaternary (< 250,000 yrs)
(481A-18 through 37; 200-384.0 m)**

Recovery was not so good below the first sill complex, although the diatomaceous muds show a higher degree of induration than their depth of burial would suggest, mainly because of the effects of interlayered sills. Interlayered turbidite Types I and II are common, as above, but Unit 2 is characterized by longer sections showing laminated and homogenous hemipelagic beds and two giant mud flows (II, III), which are delineated on the bulk-density log (Fig. 51).

Laminated muds occur as host sediment in small intervals and as some clasts in mud flows, first appearing at 241.5 meters sub-bottom (481A-22) and extending to about 330 meters (481A-30). Two main types were observed: (a) regular millimeter couplets of light-olive-gray (5Y 4/2), muddy diatom ooze and pale-olive (10Y 6/2), diatomaceous ooze, and (b) couplets of finely laminated, silty claystones, commonly with dark (Mn?, organic matter) pigment and calcareous mudstone. Type (b) occurs only in Core 481A-26. Diatom laminae of type (a) commonly show 15 to 21 couplets per centimeter. The calcareous mudstone includes monospecific-nannofossil laminae indicating episodic coccolith blooms. Where baked by intrusions, the diatoms in type (a) couplets are commonly absent, as in Core 481A-31.

In various cores (e.g., 481A-26 and 30) laminated zones alternate with homogeneous zones on a decimeter scale. Some of the homogeneous beds appear to be mud turbidites, but others show evidence of pervasive burrow mottling, suggesting episodes of fluctuating oxygen supply in the deep basin.

The two large mud flows (II, III) are similar in composition, color, and texture to the one (I) in Unit 1. Floating mud clasts, some with laminated couplets, shells, and wood fragments are more common near the base, where they tend to show gradually increasing sand content. The upper portions of these beds are massive, uniform, only slightly diatomaceous, olive-gray (5Y 4/1) clayey silts. Grading is indicated by the density log. Pumice pieces and a few hard calcareous clasts occur in the mudflows and a few sandy layers.

Depositional Environment

The alternations of laminated and bioturbated hemipelagic muddy diatomaceous ooze which characterize the lowermost 142.5 meters are similar to the slope Sites 480 and 479. This pattern represents changing levels of oxic and anoxic conditions in the basinal region, as a result of fluctuations in the lower boundary of the oxygen-minimum zone following changes in productivity or circulation patterns in the bottom water.

This prevailing regime was periodically interrupted by a few decimeter-thick turbidites of Types I and II, but in particular by the large mud flows (II, III), and the intrusion of basaltic sills and/or flows. High heat flow

contributes to early consolidation of oozes that are initially very water-rich, almost gelatinous.

Benthic foraminifers and the clam-valve debris found in mud flows and turbidites indicate source areas at bathyal depths not significantly different from the present basin depths. Tectonic movement along the transform segments or boundary faults of the rift trough probably initiate multiple-phase, local mass flows.

The upward increase in amount and thickness of delta-derived sands suggests increased accumulation rates and may partly be due to changing bottom configuration at this site, such as down-faulting of the narrow northern rift-trough concomitant with the intrusion of the upper sill complex. Fan feeder systems of the Río Yaqui also may have shifted in the late Quaternary as a result of changing sea levels. A mineralogical change about 50 meters sub-bottom does suggest a shift in the main source area on land.

The difference in matrix and hydraulic sorting between Type I and II turbidites suggests that the delta-derived Type II sediments perhaps were carried by higher-concentration flows.

Drill disturbance in Unit 1 limits comparisons, but in the upper portions of the hole there seem to have been fewer periods of basin-wide anoxia.

Contact Zones

Diagenesis in the rapidly deposited, muddy, diatomaceous oozes is mainly a result of basaltic intrusions (see section on igneous units). Only one contact zone was recovered fairly completely, that above the sill complex beginning at 168.7 meters (481A-14-4; Fig. 51). Bulk-density logging indicates a broad zone of induration which begins rather abruptly at 127.5 meters sub-bottom (Core 481A-10-1), 42 meters above the sill. The color of the sediment changes in 481A-11 to olive black (5Y 2/1), which grades to brownish black (5Y 2/1) in Cores 481A-12 and 13 as a result of heating of organic carbon. The dissolution of diatom frustules is indicated about 38 meters above the sill, and at 20 meters above all diatoms have completely dissolved (Fig. 54). The released silica formed cement and authigenic quartz crystals. Clays became strongly fissile. Ten centimeters above the sill, a sand layer composed 30% of quartz and 52% of feldspar is bleached to light gray and cemented by silica and calcite. A few large, brecciated calcite crystals occur. Dissolution of calcareous nannofossils is observed 7 meters above the sill (Fig. 54). This pattern indicates that the hydrothermal solutions involved with sediment alteration were not as acidic as at ridge crests, but rather derived from heated pore waters (see Kastner, this volume, Pt. 2). Porous sands are more affected than clay-rich sediments, because they serve as conduits.

Strongly baked sediment is intercalated in the sill complex of Core 481-14 (Fig. 55A). These are highly indurated, with a quartzose metachert cement and irregular contact zones. The rock contains highly birefringent micaceous sheaths in a meshwork around feldspar and quartz grains with epitaxial overgrowths.

Several pieces of baked, silicified sediment, some with rhythmic couplets, and one piece of glassy stringer

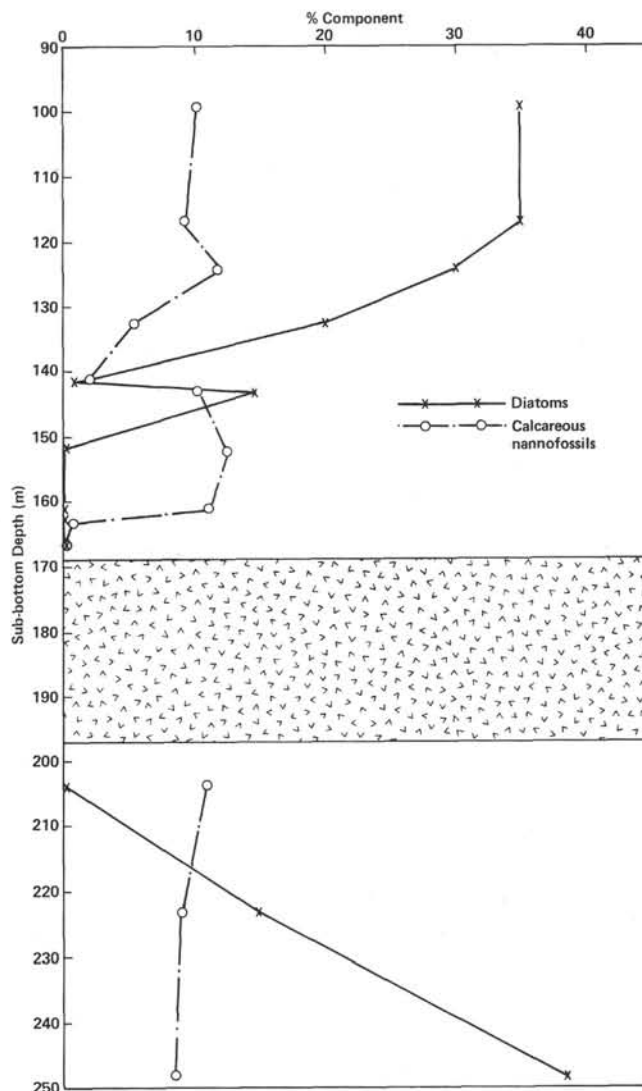


Figure 54. Contact zone around upper sill complex at Site 481. Effects of dissolution on diatoms and calcareous nannofossils.

were recovered with vesicular basalt pieces in Core 481-33 (Fig. 55B). Diatoms are recrystallized to euhedral quartz (~10 μm) and quartz overgrowths, whereas feldspar grains do not seem strongly affected.

The character of the lowermost igneous rocks, the logging record, and the basinal sediment character suggest that deeper drilling probably would penetrate more sediment intercalated with basaltic sills.

Site 481 Organic Geochemistry

Gas pockets formed in the liners from 80 to 175 meters and 222 to 327 meters. The gases were analyzed with the Carle GC and the Hewlett-Packard GC. The maturation of the organic matter was monitored by the fluorescence of toluene-ethanol extracts of small, composited sediment samples.

C₁-C₅ Hydrocarbon Analyses

Methane, ethane, carbon dioxide, and hydrogen sulfide were monitored, and selected samples were further

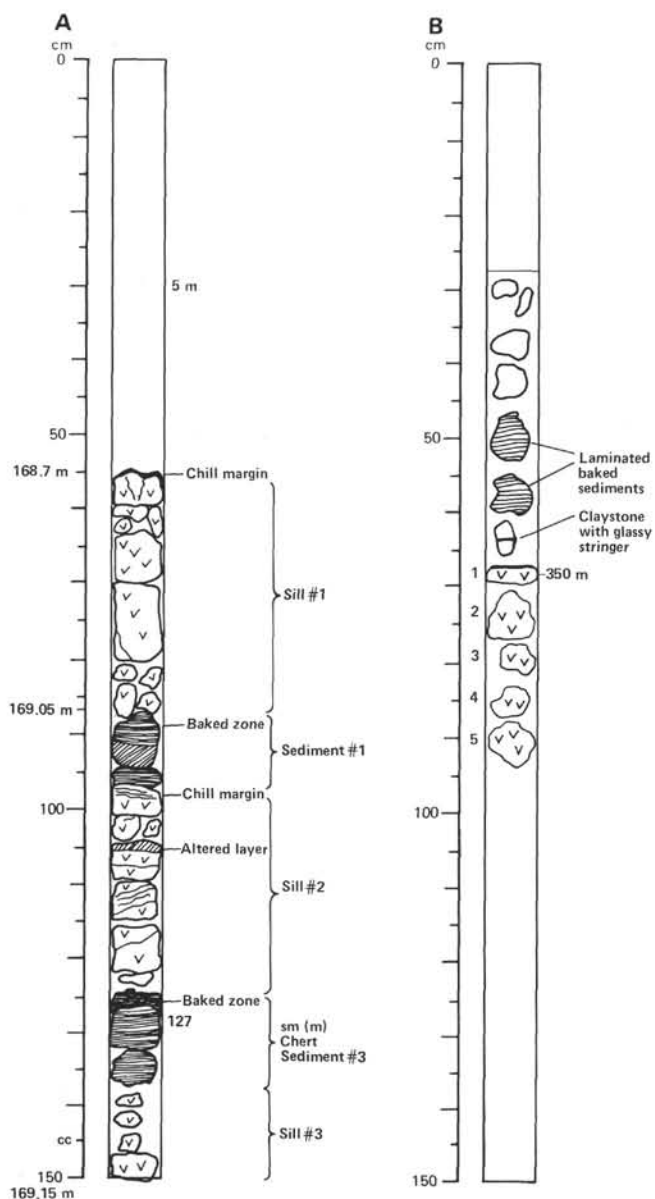


Figure 55. Core descriptions for baked sediment in contact with sills in Sections 481A-14-4 (A) and 481A-33-1 (B).

analyzed for C_2 - C_5 hydrocarbons. The normalized CH_4 and C_2H_6 concentrations versus depth are shown in Figure 56. The CH_4 concentration shows a decrease to about 40 meters sub-bottom, followed by an increase to a level of about 95% that remains essentially constant to about 140 meters. It increases further to > 98% near the upper sill. Between the upper sill complex and the small sill at about 336 meters, CH_4 shows a steady increase, with a possible decrease just above the minor sill. The upper portion (probably to 40 m) of the CH_4 distribution represents biogenic respiration products (cf. CO_2) (Claypool and Kaplan, 1974). Hydrogen sulfide was observed only intermittently from about 6 to 20 meters, indicating that biogenic activity ceases at shallower depths than at Sites 479 and 480. The CH_4 below about 40 meters probably has a dual origin. The ethane concentration increases gradually with depth to about 0.07%,

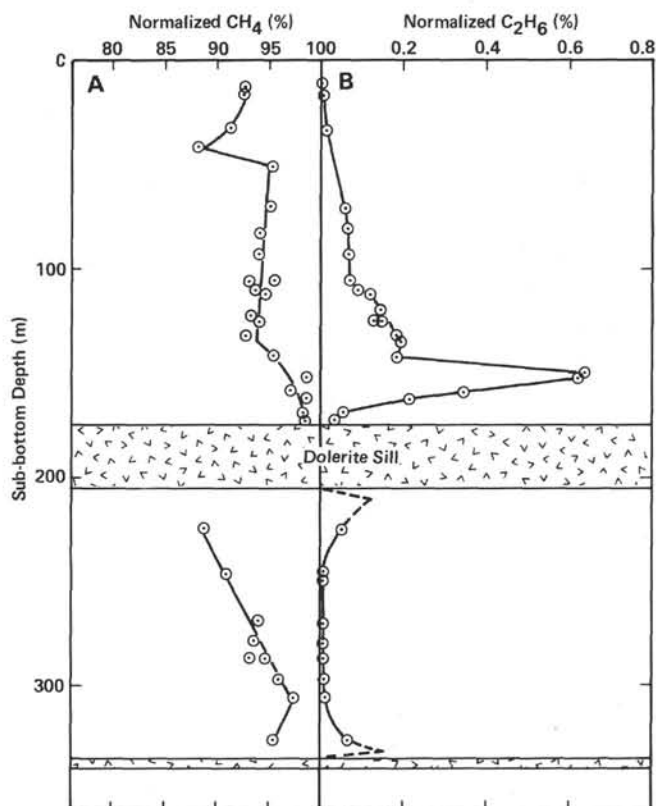


Figure 56. Concentrations of methane (A) and ethane (B) versus depth for Hole 481A. (Depth data are normalized after correction for air. Dashed line is inferred trend toward sill.)

then more rapidly to 0.2% at 140 meters, and to a maximum of 0.64% at about 150 meters, followed by a rapid decrease to the sill complex. Between the sills, C_2H_6 is at a maximum concentration of about 0.06%, near the sills and at 0.01% between them. The implied further increasing and decreasing trends toward the sills are indicated by the dashed lines in Figure 56B.

The ethane-to-methane ratio (C_2/C_1) is plotted versus depth in Figure 57. It exhibits a similar trend, with an increase to about 70 meters, a steady level to 106 meters, a further increase to a maximum at 150 meters, and a sharp decrease to the vicinity of the upper sill. Between the sills, the ratio decreases and increases with depth. The inferred maxima (dotted line in Fig. 57) were not observed, because of lack of samples.

The carbon dioxide normalized concentration versus depth is shown in Figure 58. It exhibits a complex distribution, and the upper portion (to about 50 m) may be the result of biogenic respiration (Claypool and Kaplan, 1974). Below that, it remains level at about 6% to 140 meters, and then decreases toward the upper sill complex. Between the sills, CO_2 shows a steady decrease from about 11 to 9% with depth, followed by a slight increase. The trends of the CO_2 distribution do not follow the calcium concentration or the alkalinity.

The $>C_2$ -hydrocarbon concentrations were observed to increase with depth in the Hewlett-Packard GC analyses. For example, the gas of 481A-5-3 (~83 m) consists predominantly of biogenic hydrocarbons, i.e., $C_1 \gg C_2$

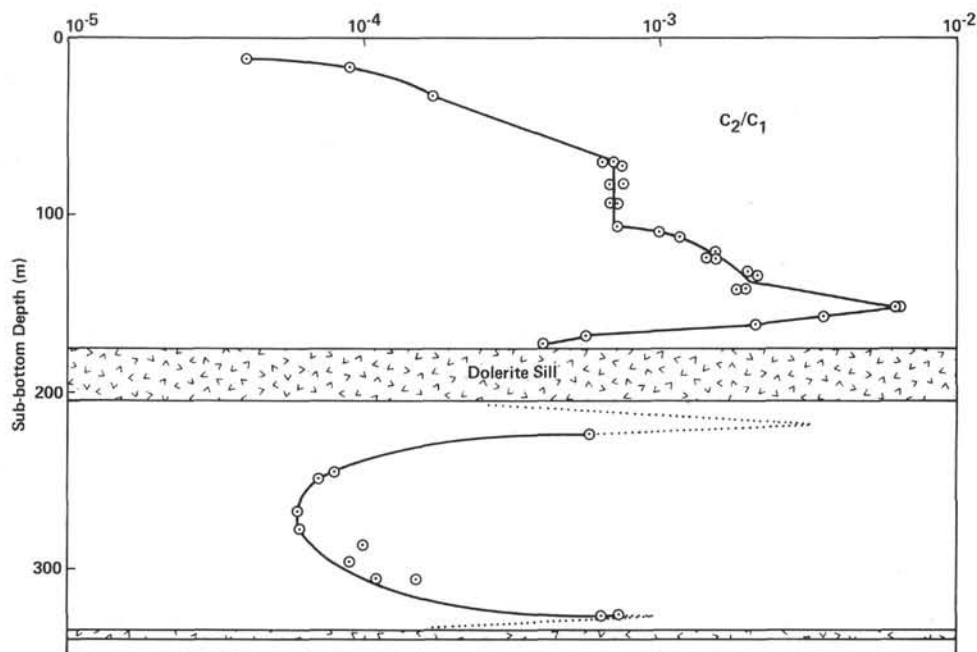


Figure 57. The ratios of ethane to methane versus depth for Hole 481A. (Dotted line is inferred trend.)

$\gg C_3 > iso-C_4 \gg C_5$ (Fig. 59A); in 481A-7-6 (~106 m), the contribution of thermogenic hydrocarbons has increased, i.e., $C_1 \gg C_2 > C_3 < n-$ and $iso-C_4 > C_5$ (Fig. 59B); and in 481A-13-4 (~162 m), the gasoline-range hydrocarbons predominate, besides methane and ethane, i.e., $C_1 \gg C_2 > C_3 < C_4 < C_5 < C_6$ (Fig. 59C). Material from 481A-13-4 and to some extent 481A-30-7 (~326 meters) contain significant amounts of various C_6H_{14} and C_7H_{16} isomers. *Neo*-pentane (2,2-dimethylpropane, C_5H_{12}) is also found in both samples. The odor of the gas from about 80 meters downward was strongly petroliferous, and at about 150 to 170 meters and between the two upper sills it had the same characteristic petroliferous odor as the gravity core recovered in 1972 about 8 km from this site in the northern basin ($27^\circ 23.0' N$, $111^\circ 26.9' W$) (Simoneit et al., 1979). The composition of the C_2 - C_7 hydrocarbons of 481-13-4 also matches the concentrations of those same compounds in the gravity core (Simoneit et al., 1979). Between the upper sill complex and the next minor sill at about 335 meters, the C_2 - C_5 hydrocarbons exhibit a distribution with a dominance of the lower weight homologs, i.e., $C_1 \gg C_2 \gg C_3 > iso-C_4 > iso-C_5 > n-C_4 > n-C_5$. These hydrocarbons probably are predominantly thermogenic (Doose et al., 1978).

The ethane and propane concentrations are plotted versus depth in Figure 60. The C_2H_6 trend in concentration is essentially the same as that obtained with the Carle GC. The propane increases rapidly from about 50 meters sub-bottom to three maxima at about 110, 135, and 150 meters, with three minima at about 125, 140, and 170 meters. Between the sills, the propane concentration exhibits a broad minimum, with the maximum near the sills. The concentrations of the C_2 - C_5 hydrocarbons are plotted in Figure 61. The *iso*-butane and *iso*-pentane follow essentially the same maxima and

minima in concentration as propane, except that their relative concentrations vary, i.e., at 160 meters $C_3 > C_4 < C_5$, and at 135 meters $C_3 = C_4 > C_5$. The relationship of the normal versus the *iso*- C_4 and *iso*- C_5 hydrocarbons is shown in Figure 62. Again, the *n*-butane and *iso*-pentane have the same distribution as propane and *n*-pentane occurs in significantly lesser amounts. The C_2 - C_5 hydrocarbons in the sediment from about 80 to 170 meters represent a condensate of gasoline-range homologs. The three maxima can be interpreted in two ways: (1) the upper sill complex (~75-250 m) happened in three pulses, resulting in three distinct distillations of hydrocarbon material upward, or (2) the sediment lithology at 125 and 142 meters may be indurated and/or organic-rich to the extent that it acts as an adsorbant or absorbant of the higher-weight (liquid) hydrocarbons, which then out-gas slower in those regions.

Fluorescence

Composited sediment samples from the core catcher or the lower section were shaken with a toluene-and-ethanol mixture (1:1) and allowed to settle. The color of the extract and the color and intensity of the fluorescence were used as an approximate guide for estimation of the nature and quantity of the lipid and/or petroliferous organic matter. The extract colors ranged from yellow in the upper section (to ~60 m) to pale yellow-brown between and near the sills. The yellow color represents more-immature lipid matter and the yellow-brown is mature bitumen; however, the low concentrations indicate no allochthonous influx, nor endogenous large concentration of petroliferous material. This is further substantiated by the fluorescence of these extracts. The colors ranged from orange to yellow (immature) in the upper section and blue-white and yellow-green to yellow-white (mature) between and near the

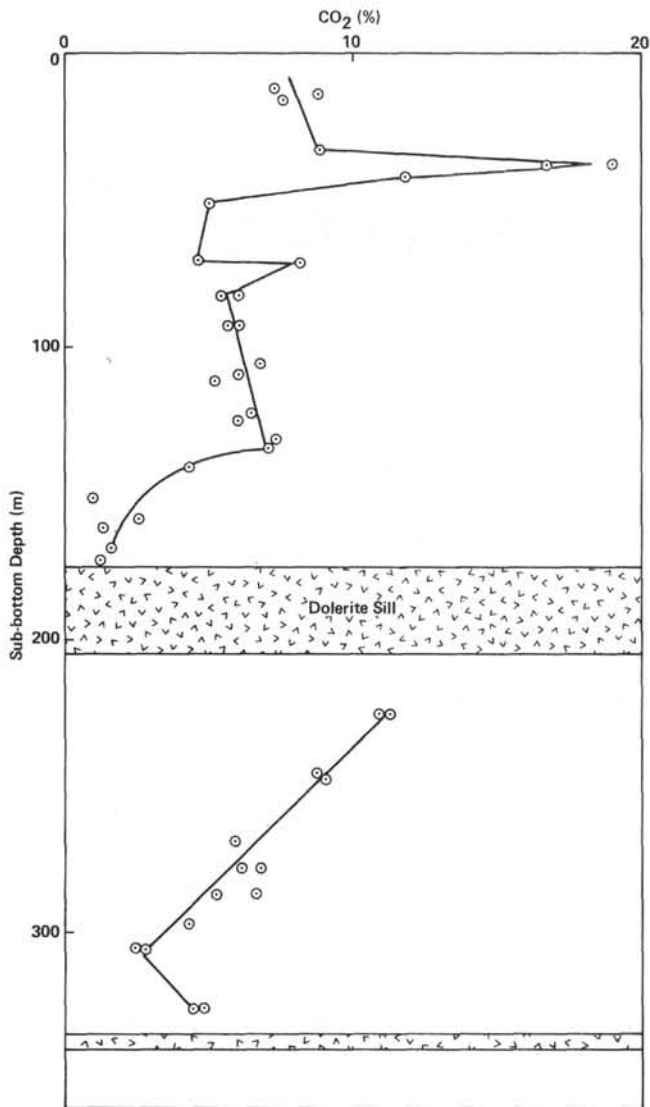


Figure 58. Concentration of CO_2 versus depth for Hole 481A (data are normalized after correction for air).

sills. Pipe-dope fluorescence was observed at random throughout the sections along the core liners.

Further fluorescence data were measured on (1) dried sediment samples, and on tetrachloroethylene-extract solutions of (2) dried sediment samples and (3) pyrolyzed samples (red heat). None of the dried samples exhibited bulk fluorescence, indicating no major accumulation of heavy petroleum.

The extracts of the dried sediments exhibited a yellow, yellow-green, or no fluorescence. Tetrachloroethylene extracts the more nonpolar lipid or bituminous material; thus this test can be utilized as a qualitative indicator of petroliferous material. The data are presented in Figure 63 on a relative-intensity scale versus depth. An increase in fluorescence is observed from 60 meters to a maximum at 145 meters, followed by a decrease to the sill. Between the sills, there are two maxima at 248 and 324 meters, respectively. These maxima

are indicative of petroliferous distillate expelled from the sediments by the sill emplacements. It has been observed at Site 478 and at DSDP Site 367 (Simoneit et al., 1978) that this distillation, migration, and concentration of petroliferous material proceeds farther upward than downward away from the sill intrusion. This may be the case here for the upper sill, and it appears to be the case for the minor lower sill.

The fluorescence data of the pyrolyzed samples above the upper sill indicate that the sediment is thermally unaltered to a depth of about 63 meters and can yield petroliferous material under pyrolytic conditions from the endogenous organic matter. Above the upper sill, the carbon is dead (~130–170 m), i.e., it has been pyrolyzed *in situ*. Between the sills, the organic matter has a petrogenic potential (except very near the sills, where the organic carbon is dead), indicating that the sill emplacements did not bake the total sediment column to higher temperatures.

Organic Carbon and Organic Nitrogen

The samples were prepared as described before, and the results are given in Appendix II of this volume, Pt. 2. The organic-carbon and organic-nitrogen contents are plotted versus depth in Figure 64A,B. The organic-carbon content ranges from 4.3 down to 0.4% and shows an overall decrease toward the upper sill, interspersed with two carbon-rich zones. Between the sills, the organic-carbon content exhibits considerable variation, from 0.9 to 2.5%. The organic-nitrogen content exhibits a trend versus depth approximately parallel to that of carbon, and ranges from 0.03 to 0.45%. The carbon-to-nitrogen ratios (C/N) are plotted versus depth in Figure 64C; the upper section is within the range typical of Recent, immature sediments (~12; Ryther, 1956). It then exhibits an increase to 15 at about 100 meters, indicating a slight maturation trend, followed by a decrease from 120 to 160 meters, which may indicate the influx of immature organic matter (turbidite flow). The values near the upper sill are also low (immature?). Between the sills, C/N is about 15, with an increase toward the second sill, indicating localized heating by that thin sill.

Conclusions

The geologic events at this site are relatively complex, as indicated by the organic geochemical data. The upper sill complex intruded the sediments which existed at the time to about 60 meters sub-bottom (cf. Fig. 63, limit of upward expulsion of petroliferous material). Based on the C_2 – C_5 hydrocarbon content, this sill intrusion may have happened in three pulses. The minor sill at 335 to 340 meters also intruded the sediment column, distilling petroliferous material upward. However, the high-temperature influence of these sills was limited to their immediate vicinity (about 10 meters in the case of the upper sill, and 5 meters for the lower). Their lower temperature gradient did not expel all petroliferous material from the sediment between the sills; some viable carbon still remains. Subsequent deposition of immature sediment has continued in the upper column.

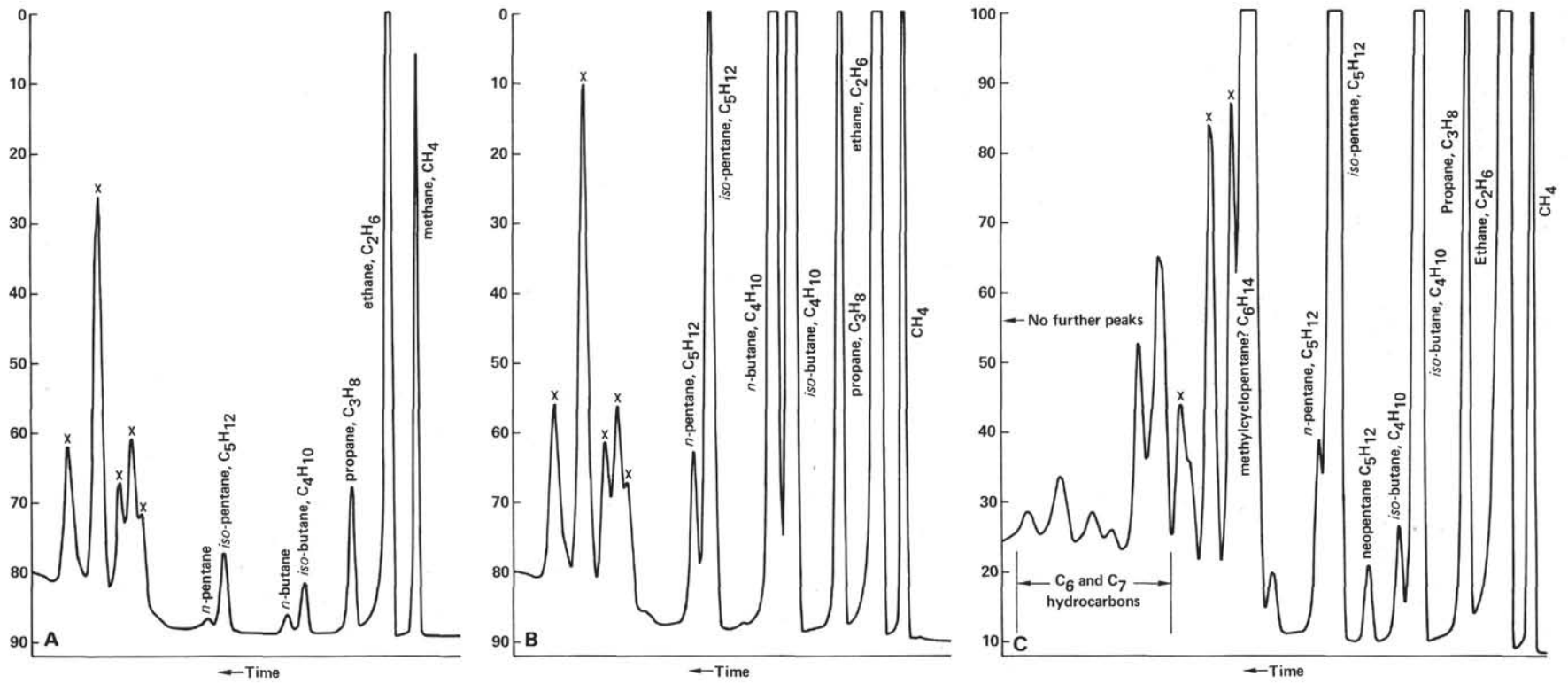


Figure 59. Gas chromatographic traces for hydrocarbon gases in Hole 481A (Hewlett-Packard GC data). A. 481A-5-3, core-liner gas. B. 481A-7-6, core-liner gas. C. 481A-13-4, core-liner gas (X designates contaminants from vacutainer).

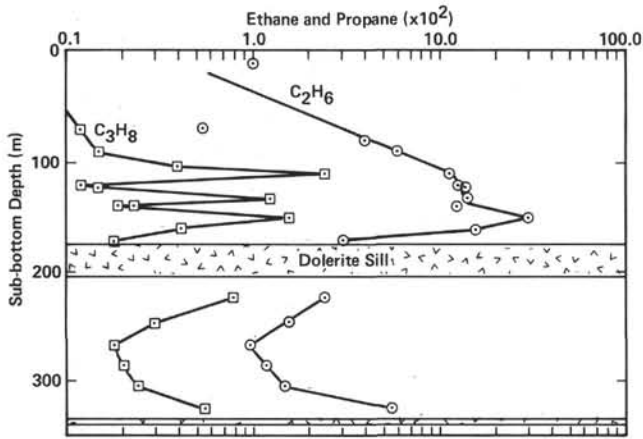


Figure 60. Concentrations of ethane and propane versus depth for Hole 481A.

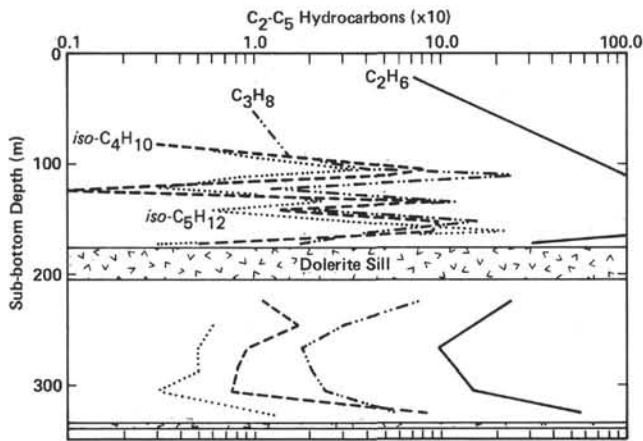


Figure 61. Concentrations of C₂-C₅ hydrocarbons versus depth for Hole 481A.

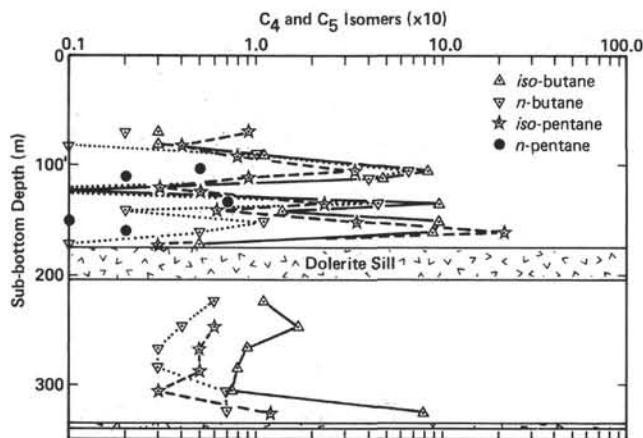


Figure 62. Concentrations of the C₄ and C₅ hydrocarbon isomers versus depth for Hole 481A.

The gases of this sedimentary column consist predominantly of biogenic CH₄, CO₂, and H₂S, with traces of C₂H₆, and in the zone from about 80 to 170 meters and between the sills a large thermogenic component is

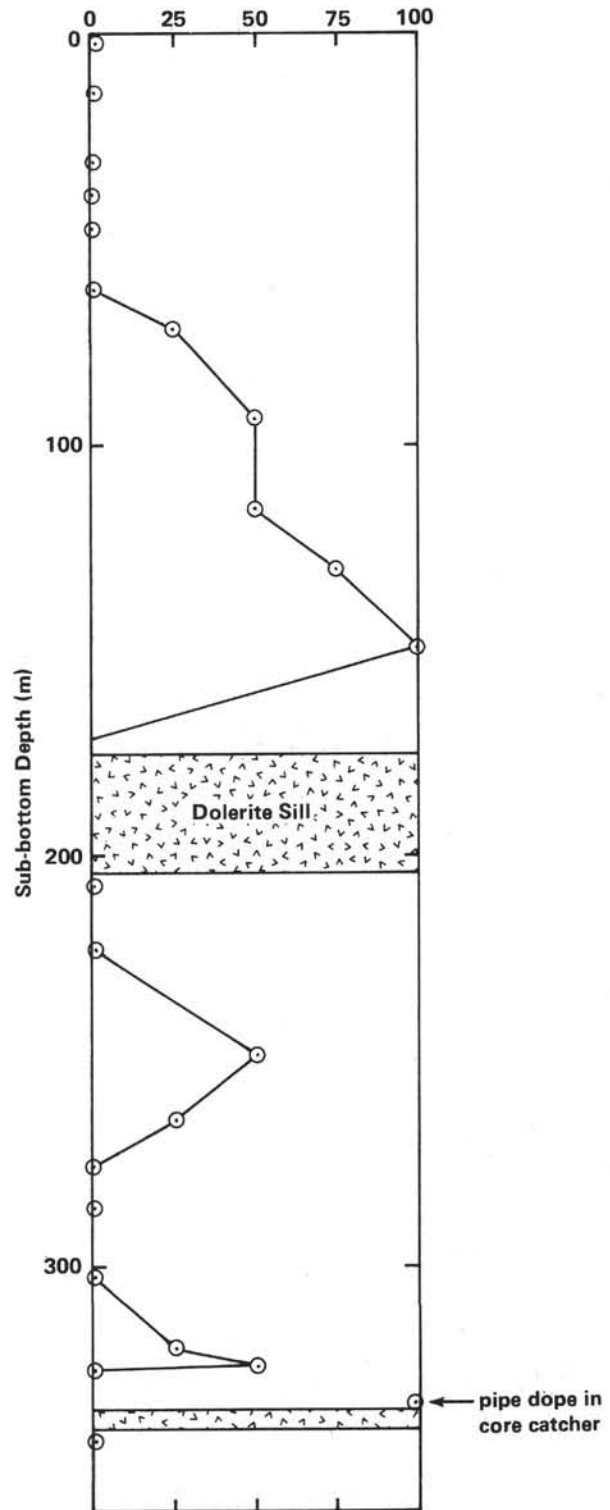


Figure 63. Fluorescence of petroliferous organic matter versus depth at Site 481 (qualitative scale).

superimposed on the biogenic gas. This thermogenic component consists of the C₂ to C₇ homologs above the upper sill, and predominantly C₂H₆, C₃H₈, and *iso*-C₄H₁₀ between the sills. The absolute amounts of gas posed no problem in terms of safety and pollution hazards.

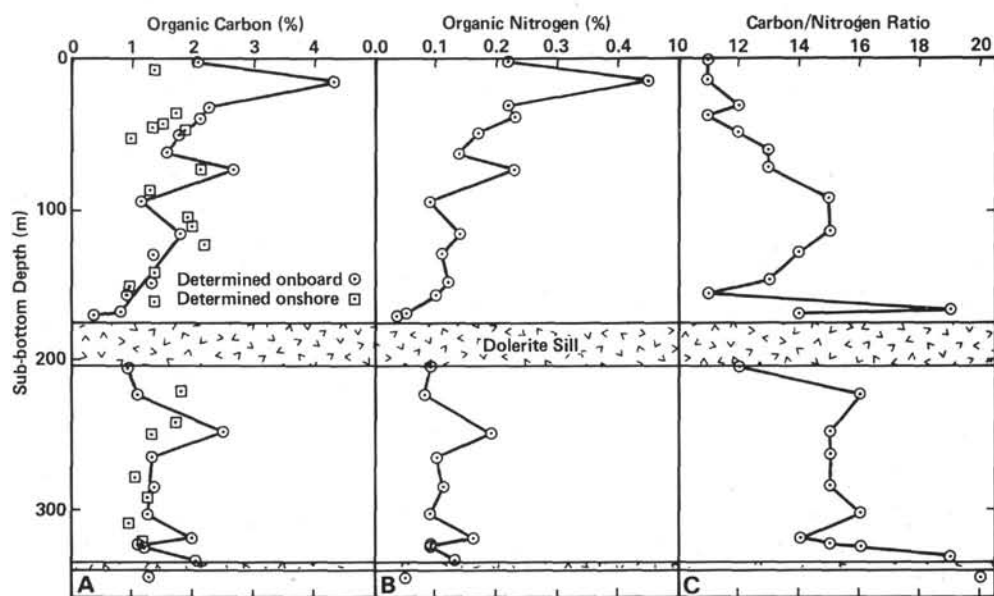


Figure 64. Contents of organic carbon (A) and organic nitrogen (B) and (C) atomic ratios of carbon to nitrogen versus depth for Site 481.

Site 481 Inorganic Geochemistry

Interstitial-Water Chemistry

At this site, characterized by high sedimentation rates and the deposition of thick turbidites and mud flows, complex concentration–depth patterns of all pore-water constituents are observed (Fig. 65).

The influence of the doleritic sill complex is clearly noticeable in the increases in chloride above and below the sills. Low-temperature and high-temperature alteration have led to decreases in magnesium and increases in calcium.

Dissolved-silica values also decrease around the sills as a result of the disappearance of biogenic silica.

Site 481 Biostratigraphy

Diatoms and Silicoflagellates

Siliceous phytoplankton skeletons were abundant and mostly well preserved in the hemipelagic sequence cored at Site 481. Turbidite and mud-flow sequences contained less-abundant and moderately well-preserved diatom assemblages. Oldest recovered sediments from 481-31-1, 134–135 cm contained common diatoms, which were well preserved. *Pseudoenotia doliolus* was common in this sample; about 500 individuals could be studied, and not one was found resembling the shape of its ancestor, *Nitzschia fossilis*. This is the basis for interpreting all recovered sediments as younger than the *N. fossilis* datum at 0.26 m.y. Diatoms together with silicoflagellates were the first microfossils observed to disappear above the sill contact in Core 481-12 (contact is in Core 481-14); they occurred in trace amounts in Core 481-18 and constituted ~15% in Core 481-20.

Laminated pieces of hemipelagic sediments were observed in Cores 481-29 and 481-30. The lamination might indicate stagnant basin conditions, depleted oxygen near the bottom preventing the sediments from be-

ing bioturbated. Around 28 laminae were counted in available pieces from 481-30-5, 27–29 cm within 1 cm, representing about 14 years per 1 cm sediment. Detailed floral analysis on individually separated white and greenish laminae revealed that the white laminae contained a diatom floral assemblage almost identical to the greenish ones. The only obvious difference between the white and the greenish laminae was the clay content, about 60% in the greenish laminae and around 10% in the white laminae. Both laminae contained calcareous nannofossils. It is concluded that different mechanics of varve formation must be applied here as compared to those at Site 480.

Diatom assemblages in the hemipelagic sequences of Hole 481 consisted mostly of *Coscinodiscus nodulifer*, *Pseudoenotia doliolus*, *Thalassionema nitzschioides*, *Cyclotella striata*, *Actinopterychus undulatus*, *Octactis pulchra*, *Thalassiosira oestrupii*, and rare *Rhizosolenia bergonii*, *Thalassiosira lineata*, and others. Diatom assemblages in the hemipelagic sequences of Hole 481A carried mostly similar assemblages, and in only a few cases was an enrichment of the oceanic component with *Coscinodiscus nodulifer*, *Nitzschia marina*, *Roperia teselata*, *Thalassionema nitzschioides* var. *parva* observed (481-4,CC, 481-9,CC, 481-11,CC). Another laminated piece, from 481-30-4, 2–4 cm, showed 16 white and greenish laminae in 1 cm. Planktonic foraminifers were enriched in the white layers and could easily be detected in broken surface pieces. Occasionally white to greenish-white bands of diatomaceous ooze were observed within a muddy diatomaceous ooze (Fig. 66). There, bands, sometimes 1 cm thick, contained an excellently well-preserved diatom assemblage with floods of delicate *Chaetoceros* bristles and thin *Thalassionema nitzschioides*.

Core 481-P2 contained numerous layers of redeposited muddy diatomaceous ooze grading from a silty texture to a diatomaceous ooze on top. There, white top

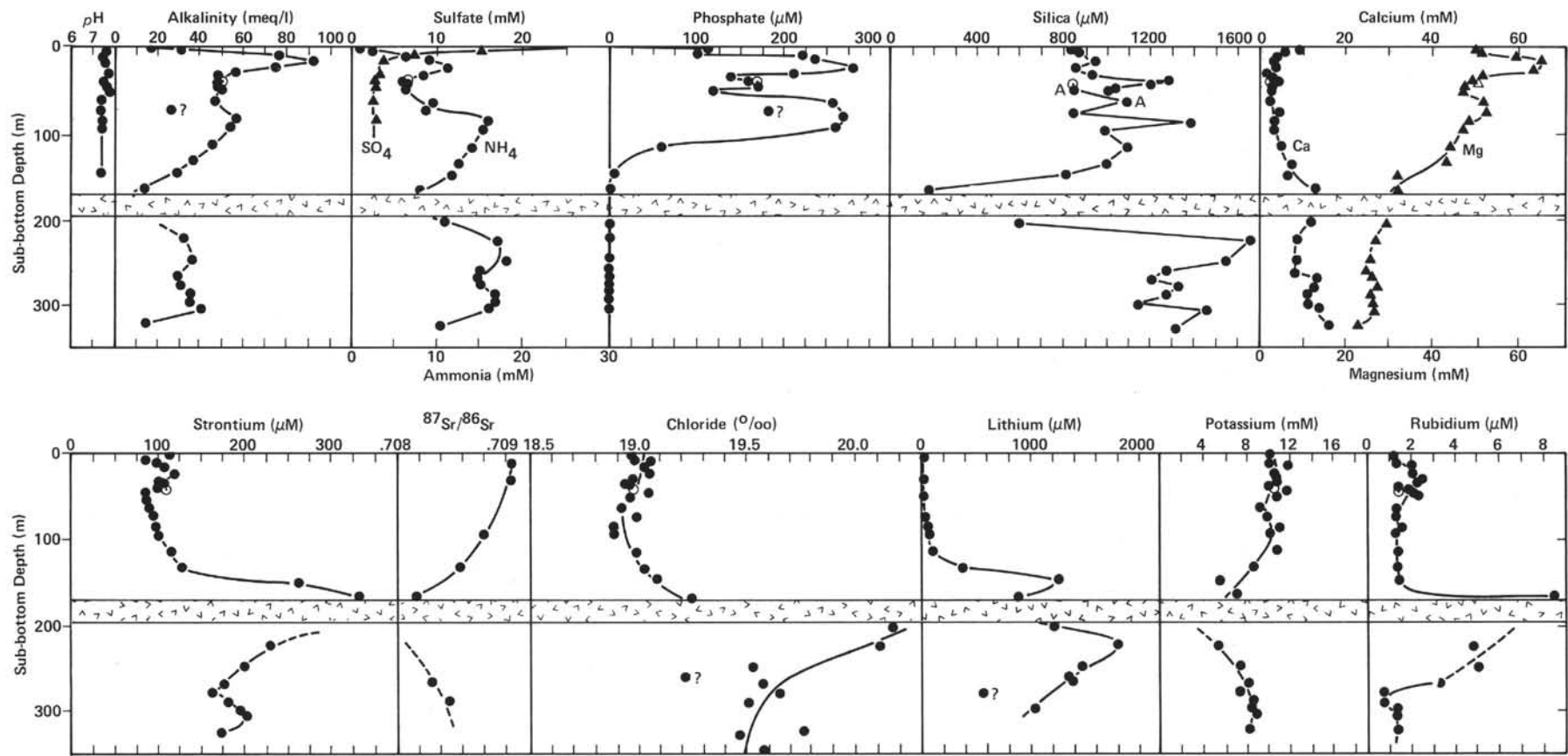


Figure 65. Composite plots of pore-water chemistry, Site 481. (Symbol A in silica plot designates Hole 481A. Open circles are samples from *in situ* pore-water sampler.)

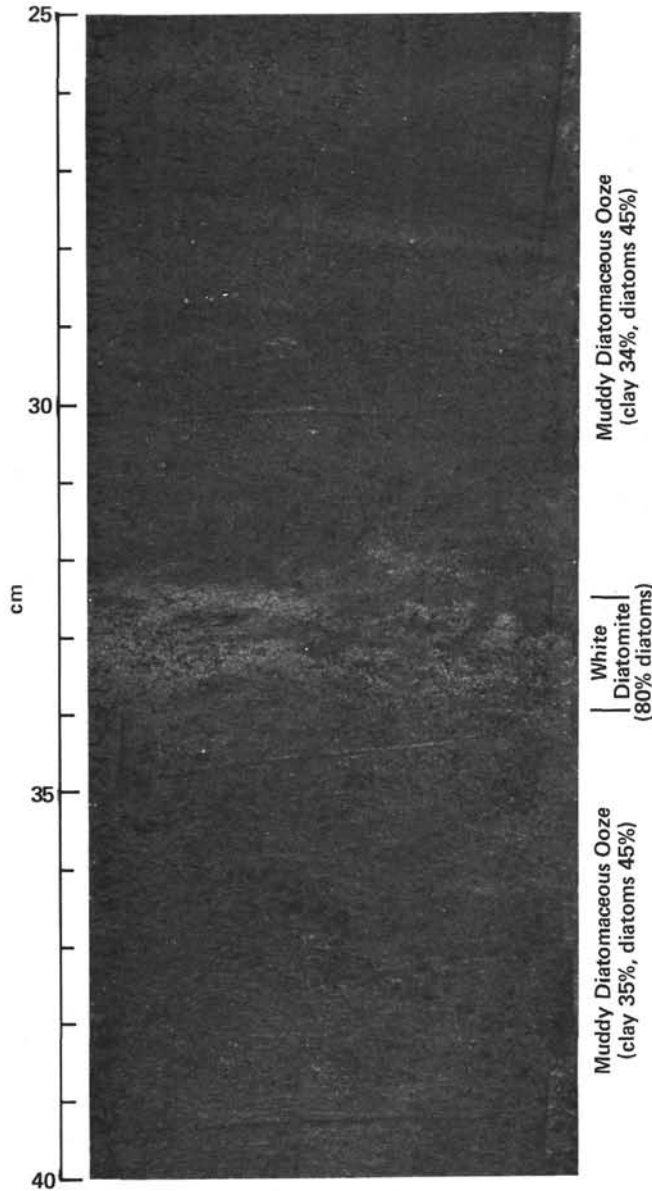


Figure 66. Photograph of 481-P8-3, 25–40 cm, showing muddy diatomaceous ooze, with intercalated white, massive diatomite layer.

layers contained about 75% diatoms and only about 10% clay. Diatom assemblages again were excellently preserved. The absence of any marine benthic species and the preservation of fragile diatomaceous fragments may indicate an autochthonous character.

As at Sites 479 and 480, the well-preserved diatom assemblages of *Chaetoceros* bristles, *Thalassionema* spp., and *Thalassiothrix* spp. are mechanically broken into small fragments because of grazing by zooplankton. This disaggregation, together with downwelling fronts and increased settling rates, accounts for the rapid sedimentation through the water column and quick burial through the sediment/water surface. Surprisingly, no diatomaceous layer containing excellently preserved assemblages contained visible fecal pellets. Rapid oxidation and predation of organic matter at the sediment/water interface might be responsible for this fact. No

sedimentation rates are calculated for this site, because no diatom datum levels were observed.

Nannofossils

At Site 481, nannofossils are diluted by diatoms and are not found in great abundance, except in Sample 481-P2-2, 9–10 cm, where a single species (probably *Cyclcoccolithus leptoporus*) is abundant but badly dissolved. The preservation decreases downhole, being moderate to good to Core 22, and rather poor below. Coccolith assemblages are of low diversity and almost constant. Reworked Upper Cretaceous species occur in abundance in some samples (e.g., 481A-22-3, 65–66; 481-P8-3, 56–57; 481-P10-1 and -2). Reworked discoasters are also found (Samples 481-P2-2, 19–20; 481-P3-3, 94–95). Below Core 481A-22, *Coccolithus pelagicus* increases in abundance, and the diversity of the assemblages decreases strongly. Because of the generally poor preservation of the assemblages, any age assignment is uncertain.

Radiolarians

In the size fraction coarser than 62 μm , radiolarian remains occur in most of the core-catcher samples from Holes 481 and 481A, although they are strongly diluted by diatoms and/or terrigenous debris. Generally, the abundance of radiolarians ranges from few (0–40 m below the sea floor) to rare (from 40 m to the bottom of the sedimentary sequence at 328 m). Also, there is more diversity of species in the upper 40 meters of the hole than below that interval.

The most common species at Site 481 are *Druppa-tractus* sp. cf. *D. pyriformis*, *D. irregularis*, *Siphocampe aquilonaris*, *Lithomelissa* spp., *Ommatodiscus* sp. (Benson), and *Stylodictya validispina*.

The oldest sediments recovered were above the *Stylactrus universus* extinction level, which has been dated as occurring about 0.41 Ma.

Foraminifers

No index species older than Pleistocene are found, but four cooler intervals are seen within the section of this site based on planktonic foraminifers. The benthic fauna is dominated by *Epistominella smithi*, *Uvigerina* spp., *Bolivina* spp., *Buliminella tenuata*, and *Cassidulina* spp. throughout the section.

Summary

Moderately well to well-preserved siliceous and calcareous microfossils are present through the sedimentary sequence of Site 481 (Holes 481 and 481A); however, radiolarians and foraminifers are common only in the upper half of the site (0–150 m sub-bottom) (Fig. 67). Also, the diversity of radiolarian species is larger in the upper half of the site.

The planktonic foraminifers indicate that a warmer pelagic environment has occurred during the deposition of the upper 40 meters of the site.

Laminations (varves) were observed at several levels of the core. These varves generally consist of alternate white and greenish laminae. White laminae are consti-

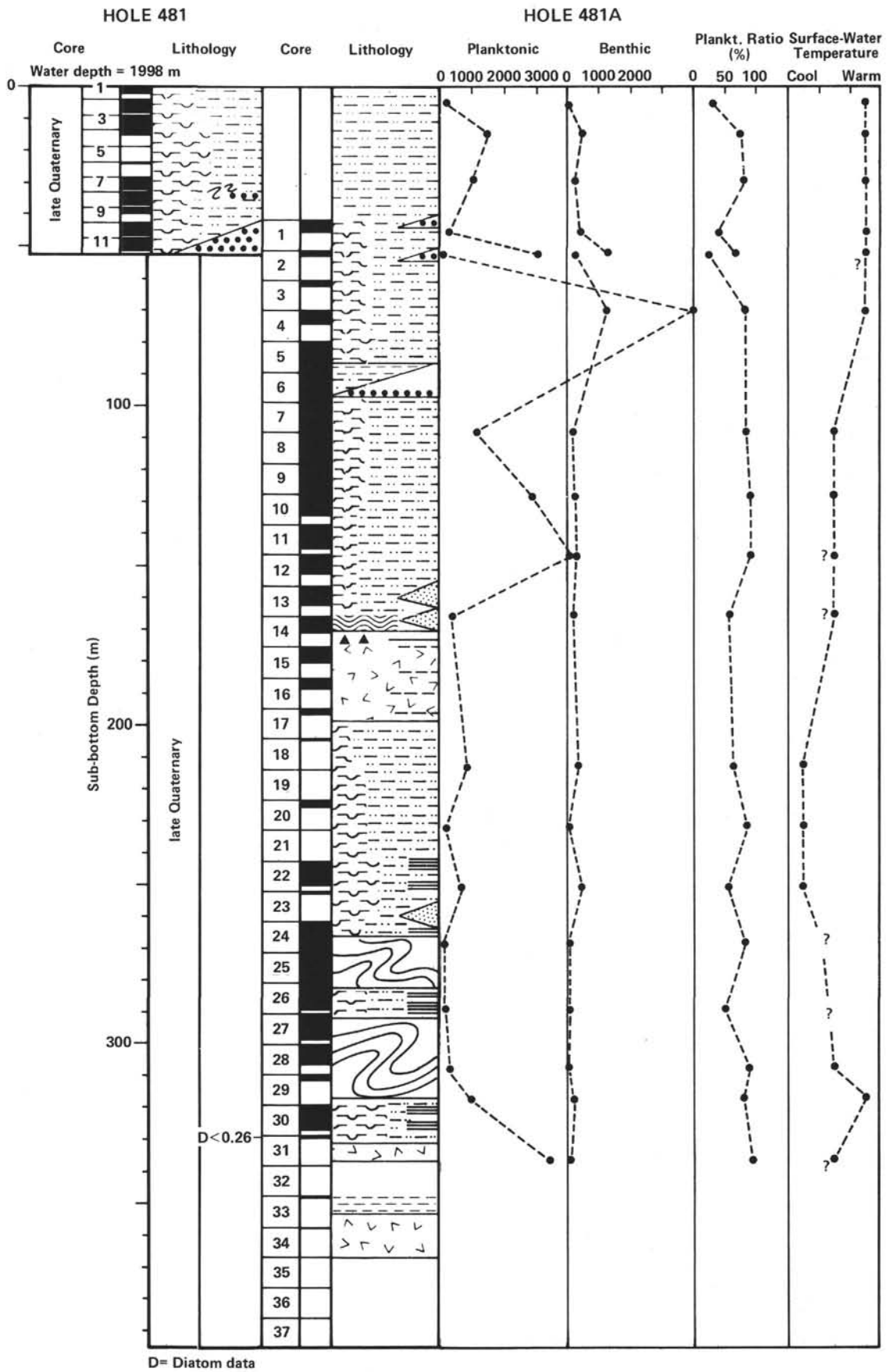


Figure 67. Correlation of drilling lithology and microfossil abundance, Site 481.

tuted mostly by diatoms, the greenish ones by clays. Analysis of one of these laminated intervals (481-30-5, 27-29 cm) shows that the species composition of the diatom assemblages in the white laminae is similar to that in the greenish laminae.

Calcareous-nannoplankton and foraminifer populations showed evidence of reworking, but the siliceous microfossils (radiolarians and diatoms) did not.

The oldest sediments recovered at Hole 481 have a mixture of calcareous nannofossils representing Zones NN21 and NN20. These sediments are above the *Nitzschia fossilis* extinction level, which has been dated at about 0.26 m.y. in the Pacific Ocean.

Hole 481A Igneous Rocks

Four main igneous units were drilled at Hole 481A (Table 14). Recovery rates from each of these units were variable, ranging from about 46% from Unit 1 to less than 1% from the other three units.

Unit 1 has a total recorded thickness of 28 meters, although this value includes at least 4.5 meters of intercalated sediments. A total of 18 igneous sub-units have been identified and many of these are separated by thin, chertified sedimentary intercalations (Table 15). Most of the sub-units are intrusive, with both upper and lower contacts against earlier igneous rocks or sediments. The contact zones usually consist of aphanitic, not glassy, basalt, and aphanitic dark-colored, iron-rich basalt veins can be seen cross-cutting intrusive Sub-units 1-13 to 1-18 (e.g., Section 481A-17-1).

Mineralogically, the sub-units of Unit 1 are practically indistinguishable; in hand specimen they tend to be aphyric. However, most sub-units contain minor (generally < 5%) amounts of plagioclase and altered olivine microphenocrysts. The groundmass texture exhibits considerable variation, ranging from variolitic through intersertal to doleritic and even gabbroic. Sub-unit 1-10, for example, has a gabbroic center which shows development of prismatic pyroxene crystals up to 30 mm long. Many of the sub-units are visibly altered in hand specimen, discrete intervals of more extensive alteration occurring in some of the basalts. Calcite veining is also common.

There are a few basalt/basalt contacts that allow positive identification of the emplacement history of some of the intrusions: Sub-unit 1-7 intrudes sub-unit 1-6; Sub-unit 1-10 is chilled against 1-11; Sub-unit 1-15 is chilled against 1-16; and the dark-colored, iron-rich veins cut Sub-units 1-13 to 1-18.

Only two pieces of medium-gray (N5), aphanitic, aphyric vesicular basalt were recovered from Unit 2. No chilled contact was recovered, and the absence of evidence of thermal alteration in the overlying sediments means that it is not possible to determine whether this unit is intrusive or extrusive.

The top of Unit 3 is marked by a devitrified chill zone about 1 cm thick below a sequence of baked, finely laminated, varved sediments which contain very thin (<1 mm) stringers of devitrified basaltic glass. The baked varves grade from black to whitish-gray at the contact. The contact (Piece 1) exhibits a ropy-textured, devitrified surface that grades into aphanitic basalt with rare phenocrysts of plagioclase. The other four pieces in Section 481A-33-1 are rounded fragments of vesicular (vesicles 1-5 mm), partially aphyric to aphanitic, medium-gray (N5) to medium-dark-gray (N4) basalt. The contact in Piece 1 has a variolitic to pilotaxitic texture, with about 95% relatively fresh basaltic glass containing pyroxene wheat-sheave structures and spherulites. Several 0.2- to 3-mm plagioclase phenocrysts are randomly oriented in the glassy mesostasis. Only minor clays and zeolites are found in the mesostasis, usually replacing microlites of clinopyroxene and olivine. The remaining four pieces are hyalopilitic, vesicular (~5% vesicles) basalt with 15% plagioclase phenocrysts and microlites set in a mesostasis of 65% basaltic glass (little altered) and olivine and plagioclase and 3% disseminated opaque phases. The feldspar often has a pilotaxitic alignment around the roughly ellipsoidal to coarsely rounded vesicles. Some of the vesicles are filled or lined with calcite and/or zeolites and pyrite.

A 2-cm vesicular, aphyric, aphanitic basalt pebble was recovered from Unit 4 in Core 481-36,CC. In hand specimen the rock appears to be similar to the aphanitic vesicular basalts recovered in Units 2 and 3. Unit 4 may be intrusive or extrusive.

Table 14. Igneous lithologic units, Hole 481A.

Unit	Top ^a (m sub-bottom)	Base ^a (m sub-bottom)	Thickness ^a (m)	Recovery ^b (m)	Type of Cooling Unit	Phenocryst Assemblages	Vertical Extent
1	168.7	196.7 m	28.0 (including >4.5 m sediment)	10.9	Massive dolerite, basalt, and gabbro	Minor Ol, Pl	481A-14-4, 55 cm to 481A-17-2, 25 cm
(sedimentary intercalation)							
2	328	332.8	4.8	0.08	Basalt	?Aphyric	481A-31,CC
(sedimentary intercalation)							
3	350	363.2	31.2 (including 0.5 m sediment intercalation)	0.20	Basalt	Aphyric, Pl	481A-33-1
(sedimentary intercalation)							
4	365.7	366.1	0.6	1 pebble	Basalt	Aphyric	481A-36,CC
(sediments)							

^a Determined from downhole logs.

^b Determined from core logs and corrected for spacers.

Table 15. Detailed igneous lithology, Hole 481A.

Sub-unit	Estimated Thickness ^a (m)	Recovery ^a (m)	Type of Cooling Unit	Phenocryst Assemblage	Vertical Extent
1-1	0.3-0.4	0.3	Basalt	Minor Pl	481A-14-4, 55 cm to 481A-14-4, 86 cm
(sedimentary intercalation)					
1-2	0.25-0.3	0.25	Basalt	Aphyric	481A-14-4, 96 cm to 481A-14-4, 123 cm
(sedimentary intercalation)					
1-3	0.7-0.9	0.70	Massive basalt-dolerite-basalt	Minor Pl, Ol	481A-14, CC to 481A-15-1, 50 cm
(sedimentary intercalation)					
1-4	0.4	0.4	Massive basalt-dolerite-basalt	Minor Pl, Ol	481A-15-1, 65 cm to 481A-15-1, 109 cm
(sedimentary intercalation)					
1-5	0.5-0.6	0.45	Massive basalt-dolerite-basalt	Minor Pl, Ol	481A-15-1, 119 cm to 481A-15-2, 22 cm
(sedimentary intercalation)					
1-6	0.6-0.7	0.59	Massive basalt-dolerite-basalt	Minor Pl, Ol	481A-15-2, 32 cm to 481A-15-3, 11 cm
1-7	0.65	0.63	Massive basalt-dolerite-basalt (intrudes Sub-unit 1-6)	Minor Pl, Ol	481A-15-2, 77 cm to 481A-15-2, 138 cm
1-8	0.3	0.30	Massive basalt-dolerite-basalt	?Aphyric	481A-15-3, 12 cm to 481A-15-3, 47 cm
1-9	(unknown)	0.10	Dolerite	?Aphyric	481A-15-3, 48 cm to 481A-15-3, 59 cm
1-10	2.3-2.5	2.25	Massive basalt-dolerite-gabbro-dolerite-basalt	?Aphyric	481A-15-3, 61 cm to 481A-16-1, 77 cm
1-11	0.09	0.09	Basalt	Aphyric	481A-16-1, 77 cm to 481A-16-1, 86 cm
(sedimentary intercalation)					
1-12	0.5	0.48	Massive basalt	Minor Pl	481A-16-1, 90 cm to 481A-16-1, 138 cm
(sedimentary intercalation)					
1-13	1.7-1.9	1.65	Massive basalt and dolerite	Minor Pl	481A-16-1, 146 cm to 481A-16-3, 27 cm
(sedimentary intercalation)					
1-14	Unknown	20.27	Basalt and dolerite	Minor Pl	481A-16-3, 31 cm to 481A-17-1, 10 cm
(sedimentary intercalation)					
1-15	0.6	0.57	Massive basalt-dolerite-basalt	?Aphyric	481A-17-1, 25 cm to 481A-17-1, 67 cm
1-16	>0.3	0.3	Massive basalt	?Aphyric	481A-17-1, 68 cm to 481A-17-1, 88 cm
(sedimentary intercalation)					
1-17	0.25	0.23	Basalt	Minor Pl	481A-17-1, 89 cm to 481A-17-1, 109 cm
1-18	>0.6	0.6	Massive basalt and dolerite	Minor Pl	481A-17-1, 110 cm to 481A-17-2, 25 cm

^a Determined from core log.

Hole 481 Paleomagnetic Measurements

Five specimens from a basalt sill encountered between 170 and 199 meters were measured. The results are given in Table 16. The direction of magnetization is normal and was not affected by a demagnetizing field of 175 Oe. The remanent magnetization is 5.4, the induced one in the present Earth's field (Koenigsberger ratio).

The paleolatitude is 31°, as against 23° for the specimens of Site 478. The difference can be accounted for by secular variation, departure of the hole from the vertical, and tilt of the formation after emplacement. It is likely that the two bodies were emplaced at times differing by a few hundred years.

Site 481 Physical Properties

Piston coring down to about 52 meters sub-bottom at Site 481 was not quite as successful as at Site 480. Cores

481-P4-P6 and 481-P9 had little recovery; Core 481-P5 was empty; and Cores 481-P1-P3 were partly disturbed.

At Hole 481A, many cores were intensively disturbed by drilling and expanding gas (Cores 481A-1, 2, 7 through 10, 20, 22, 29); some consisted entirely of drilling breccia (Core 481A-14); and some had little recovery (Cores 481A-3, 4, 18, 33). Core barrels 481A-19, 21, 32, and 34 through 37 were empty. Wherever possible, small disturbed samples were taken, or small undisturbed chunks from drilling breccia were selected. From Core 481A-14, immediately above the first dolerite sill, very small chunks were separated by wet sieving from the soft drilling breccia.

Results for Hole 481

Special care was taken to get many physical-property data on the well-preserved piston cores at this site, in order to check the data from the previous sites, which may be partly affected by the strong drilling disturbance, especially in the uppermost 50 meters of soft sediments. In general, vane shear strength probably is most influenced (i.e., reduced) by coring. Therefore, many measurements of shear strength in the different types of sediments were carried out.

The data are plotted in an enlarged vertical scale (Figure 68) to demonstrate minor variations due to changing lithology. The lithologic column (Fig. 51) shows three major types of sediments, as described above:

- 1) Host "background" pelagic sediments (muddy diatomaceous ooze), often laminated or bioturbated, brownish light-olive-gray, rich in diatoms;
- 2) Turbidites, Type I: similar to (1), but homogeneous, sometimes with a grayish yellow top layer;
- 3) Turbidites, Type II: olive-gray diatomaceous silty mud, distinctly darker than (2), homogeneous.

Some of the turbidites, especially Type II, contain sand at their base, which often was disturbed by coring, even in the piston cores. There is a marked difference in physical properties between turbidites of Type II and those of the "background" sediments and turbidites of Type I. Turbidites II contain less water and have higher bulk densities than the other sediments (Cores 481-P10 and P11); therefore, the data from Core 481-P1 are not representative for host background sediments near the sea bottom. In comparison with data from the previous sites, near the surface the muddy diatomaceous ooze may start with water contents of 85 to 90%, porosities of 90 to 95%, and bulk densities of 1.1 to 1.2 g/cm³, and reach values of ~65%, ~80% and ~1.45 g/cm³, respectively, at about 50 meters sub-bottom. According to average grain densities (background sediments, 2.14-2.45 g/cm³; turbidites Type I, 2.33 to maximum 2.55 g/cm³; turbidites Type II, 2.48-2.69 g/cm³), background sediments and turbidites of Type I contain considerably more opaline silica than turbidites of Type II. Furthermore, most of the turbidites Type I and II show a decrease of grain densities from bottom to top and therefore an increase of the content of biogenic silica. The grading of other physical properties within turbidites is discussed in more detail in the chapter on turbidite sedimentation and physical properties (Einsele and Kelts, this volume, Pt. 2).

Table 16. Paleomagnetic measurements of Hole 481A basalts.

Sample (interval in cm)		NRM (10^{-6} emu/ cm ³)	Inclination (degrees)	Susceptibility (10^{-6} emu/ cm ³ G)	Demagnetizing Field (Oe)	After Demagnetization	
						Ir	Inclination
481A-15-1, 68-70	1K	1233	50.2	604	75	1196	51.2
						175	793
15-2, 86-88	10	1418	52.9	425	75	1246	50.5
15-2, 86-88	1-1	1014	49.9	963	175	537	52.7
15-3, 80-82	1-1	2044	47.9	734	175	1609	48.7
16-2, 122-124	2D	4725	52.0	1129	75	4145	51.8
		<2086> ±1524	<50.7> ±2.2	<771> ±280			<50.4> ±1.4

Notes: Induced magnetization is 0.45 Gauss = 347×10^{-6} emu/cm³; Koenigsberger ratio = 2086/347 = 5.4; paleolatitude = 31.0°.

Vane shear-strength measurements have been carried out at least twice at the same depth in the cores, where they yielded surprisingly consistent results; therefore, these data can be regarded as reliable. Shear strength increases from 3 to 4×10^3 Pa (30–40 g/cm²) near the sea bottom to about 5×10^4 Pa (500 g/cm²) at 50 meters depth. Shear strength of the silty mud turbidites Type II is somewhat lower than in the other sediment types. Shrinkage probably starts at about 40% near the surface and drops to 20 to 30% at 50 meters depth. Sound-velocity measurements with the Hamilton Frame show a slight increase versus depth from 1.49 to 1.53 km/s. In layers rich in diatoms, sound velocity appears to be somewhat lower than in silty muds (turbidites Type II).

Results for Hole 481A

In Figure 69 representing the relationship of physical properties versus depth for Hole 481A, the trend lines from Hole 481 for the upper 50 meters of sediments, but not the data points, are included. From 50 meters downward to about 130 meters sub-bottom, the gradients of physical properties may be somewhat stronger than usual, but because several data points represent turbidites (Type II, Cores 481A-5, 6, 8) and maybe also Cores 481A-7 and 481A-10, which deviate considerably from the "host" sediments, no special trend can be ascertained. At about 130 meters sub-bottom, about 40 meters above the first dolerite sill, the physical properties show, however, a drastic change. Fortunately, core recovery was fairly good in this section of the hole, so we got a sufficient number of samples to study the influence of the basaltic intrusion on the overlying sediments. Approaching the sill, water content and porosity drop to less than 20% and 30 to 40%, respectively. Bulk density increases to more than 2.0 g/cm³ near the contact with the sill, in good agreement with the results from the density log. Average grain densities are raised to values of 2.6 to 2.7 g/cm³ in the zone 40 meters above the sill, indicating that most of the opaline silica has been dissolved or used up to form other minerals. This is confirmed by the smear-slide descriptions. Also, shear strength appears to increase considerably, whereas about 20 meters above the sill shrinkage was found to be only 7%. Two samples at greater depth below the sill (~250 and 300 m depth) showed little shrinkage (2%); therefore, it can be assumed that shrinkage near the sill contact approaches zero.

Unfortunately, most of the samples selected for sonic-velocity measurements yielded no result, although they were soaked in salt water. Since sonic velocity at 50 meters sub-bottom (~80% porosity) was already about 1.5 km/s and at 243 meters sub-bottom (below the sill, sediments of <60% porosity) 1.66 km/s, values in the neighborhood of the sill were probably much higher (>1.6 to 1.7 km/s) than recorded by the sonic log. However, it can be also deduced from the log that sonic velocity increases toward the sill.

Below the sill, from 200 meters downhole, the compaction of the sediments appears also to be strongly affected by the basaltic intrusion. According to the density log and measurements on some samples, about 20 meters below the contact bulk density is about as high as on top of the sill. Then, farther downhole at about 250 meters depth, water content again increases to about 35%, and porosity to more than 55%; finally all physical properties regain more or less normal gradients versus depth down to about 320 meters (Fig. 69). Bulk density, however, remains higher (by about 0.1 g/cm³)—and water content and porosity lower (both by about 10%)—than in sequences not influenced by sills with comparable sediments in the corresponding depth range (Site 479). This is also true of varved layers which deviate in their properties from the general trend lines in Figure 68. Thick mass flows, as found in Cores 481A-24 and 25, as well as in Cores 481A-27 through 29, show a distinct grading of all physical properties, similar to thick turbidites with a sandy base. This can also be seen on the density log, but the density values of the log are higher by 0.1 g/cm³ than those determined by gravimetric methods.

Shear strength below the sill, from 200 to 320 meters, was too high for measurements with the Wykeham Farrance apparatus. By means of the hand-operated Soil-test vane, values between 1.2 and 1.8×10^5 Pa (1200 and 1800 g/cm²) were determined. It is assumed that the higher values are more reliable than the lower ones. Because of poor recovery, it remains open whether there is a further marked contact zone above the sill at 330 meters. According to the density log, about 5 meters of sediments on top of the sill may be somewhat more compacted than normal sediments. If the single small chunk sample from 347 meters (Core 481A-33) is representative, this thin sill had only a narrow contact zone at its base, comparable to the thin sill in Hole 478 (253–256 m). Similarly, the sill at 353 to 365 meters affected the

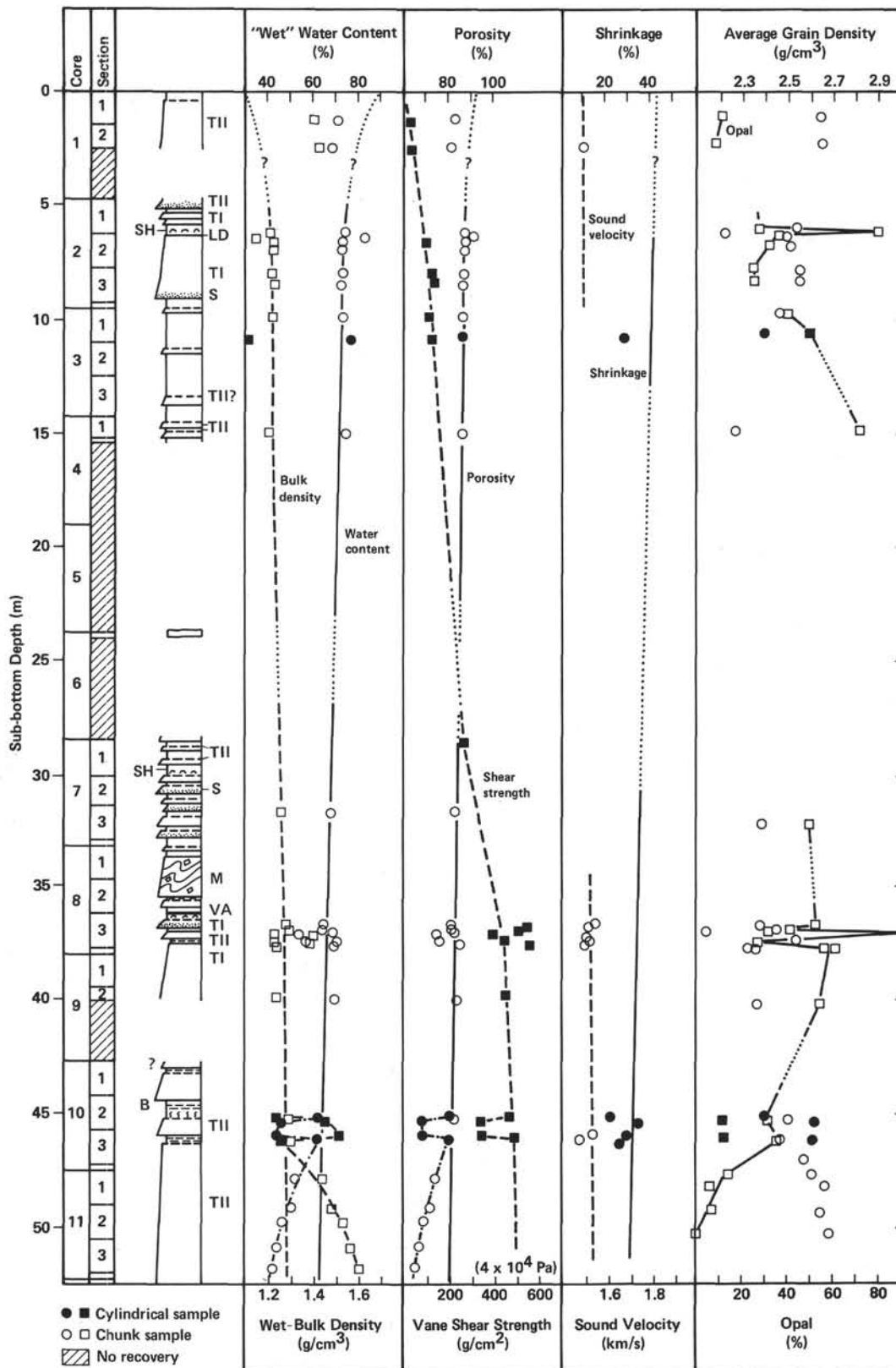


Figure 68. Mass physical properties, shrinkage, and content of opaline silica, as determined on exceptionally well-preserved piston cores from Hole 481. Note the enlarged vertical scale and the lithologic column, showing minor changes of sediments, especially mud turbidites of two types (TI and TII), with or without a sandy base (S), bioturbation (B), shell beds (SH), mass-flow deposits (M), light diatomaceous layers (LD), and a volcanic-ash layer (VA). Curves for physical properties should show only general trends.

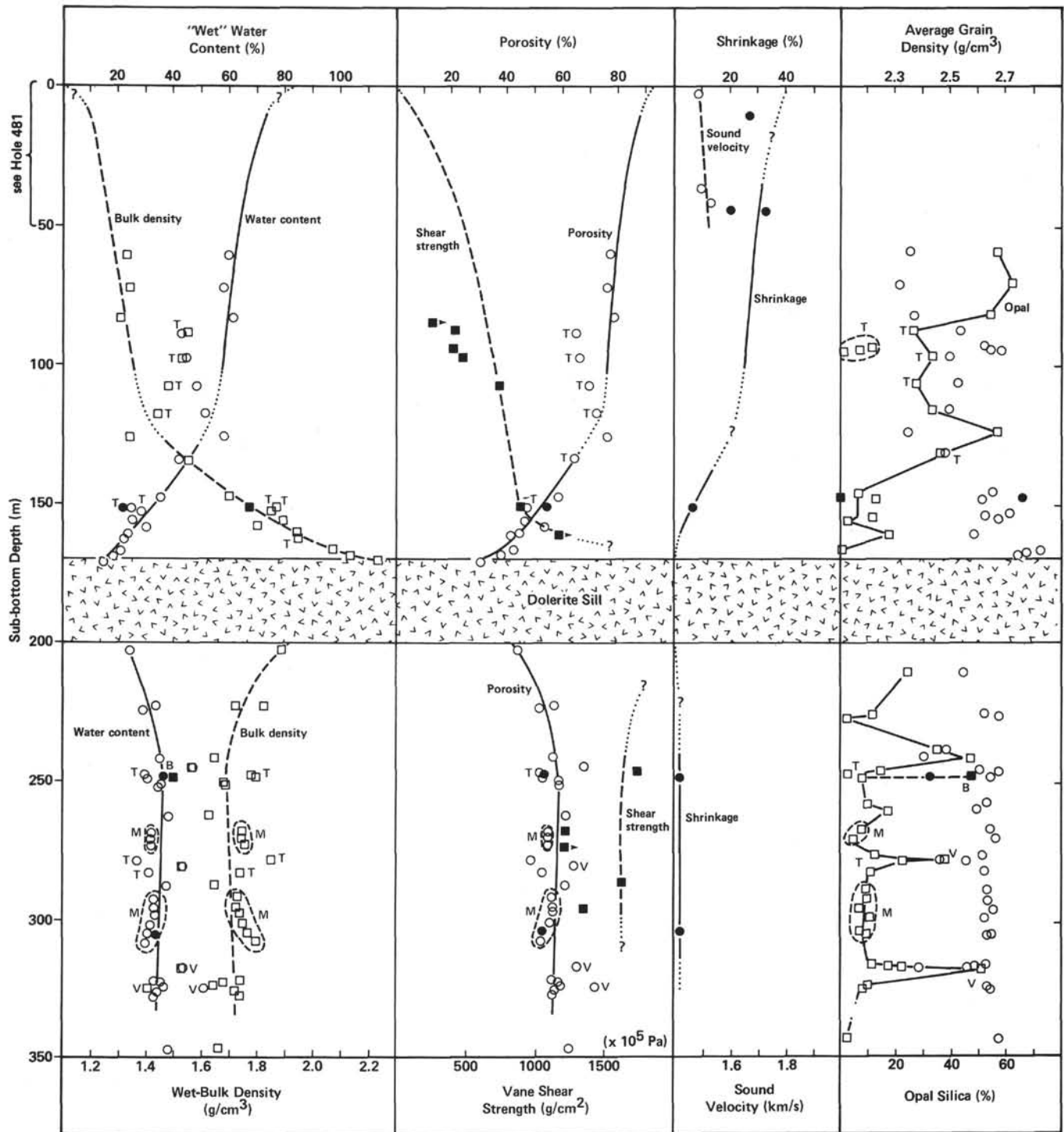


Figure 69. Mass physical properties, shrinkage, and content of opaline silica sediments from Hole 481A. The trend lines for the uppermost 50 meters represent the results from Hole 481. Samples from mud turbidites (T) and from mass flows (M) as well as from varved layers (V) rich in diatoms usually deviate from the general trend lines representing mainly "background" sediments (B). Sediments on top of the uppermost sill are strongly affected by the contact. (Solid symbols are cylindrical samples. Open symbols are chunk samples.)

neighboring sediments much less than the thick uppermost sill.

Some values of sound velocity and bulk density for hard-rock samples from the upper sill and its contact are listed in Table 17. Further inferences from the physical properties affected by basaltic intrusions with respect to the intrusion mechanism and the initiation of hydro-

thermal activity are discussed separately (Einsele, this volume, Pt. 2).

Site 481 Heat Flow

The Uyeda-Kinoshita instrument measured temperatures of 3.6°C at the mudline and 9.0°C at 42 meters, giving a gradient of 128.6°C/km. From two samples in

Table 17. Sound velocity and wet-bulk density of some hard-rock samples from Hole 481A.

Section	Interval or Top (cm)	Rock Description	Orientation	v_s (km/s)	Bulk Density (g/cm ³)
481A-14-4	126	Indurated sediment from contact to basalt	=	4.03	2.55
481A-15-1	45	Sparsely phytic basalt	⊥	4.33	2.75
481A-15-3	30	Dolerite, fine grained	⊥	3.58 3.29	2.73
481A-15-4	34	Gabbro, altered	⊥	(no signal)	2.68

the same hole and interval, a conductivity of 2.1 was measured; this makes a heat flow of 2.70 HFU.

Two temperature logs were made. The temperatures measured at the bottom were:

Run 1, 26.2°C, 3.5 hr. after circulation ceased;

Run 2, 51.0°C, 20 hr. after circulation ceased;

Taking one hour for the circulation time, using the method described for Site 479, we obtain a bottomhole temperature of 56.8°C. Subtracting the mudline temperature of 3.6° leaves 53.2° for the temperature differential, and the gradient is

$$\frac{53.2}{0.33} = 161^\circ\text{C}/\text{km}.$$

The lithology of this site was divided thus:

Depth	Lithology	K
0-170 m	Soft sediments	2.1
170-199 m	Vesicular basalt (2 specimens)	3.25
199-330 m	Firm hard silt	2.4
	Claystone	4.0
	65 m of each are	3.00

The conductivity for the whole interval 0 to 330 meters is

$$\begin{aligned} \langle K \rangle &= \left[\left(\frac{170}{2.1} + \frac{29}{3.25} + \frac{131}{3.00} \right) \frac{1}{330} \right]^{-1} \\ &= 2.47 \text{ mcal/cm s } ^\circ\text{C} \end{aligned}$$

therefore

$$q = 1.612 \cdot 10^{-3} \times 2.47 \cdot 10^{-3} = 3.98 \cdot 10^{-6} = 3.98 \text{ HFU}$$

This time, the Uyeda instrument gave only 0.67 of the heat flow. The operations manager believes that circulation of sea water for 5 or 6 minutes to clear the hole lowers the temperature indicated by the instrument.

Site 481 Correlation of Drilling Results and Seismic Reflection

Site 481, like the other sites in the Guaymas Basin, lies within a dense network of seismic lines. In addition,

we ran a survey of the site locality before dropping our first two beacons for the chosen location. The track of this survey is shown in Figure 50. The first beacon drop, indicated by the square, was especially carefully selected and is shown in Figure 70. Unfortunately, as at so many other sites on Leg 64, this beacon failed after we had pulled in all underway geophysical gear; we lost position in near-gale-force winds, and no satellites were received. We therefore dropped the second beacon, using 3.5 kHz only, in another favorable location. After drilling the site, we made another complete crossing of the rift directly over the beacon (Fig. 50).

Our conclusion from study of all available records, as at Site 477, is that we cannot very satisfactorily correlate the drilling with the seismic. The geology is apparently too variable, sediments must be somewhat deformed, and intrusions are very local. Only the 3.5-kHz records made while stationary over the site correlate well. We recommend that if any future drilling is to be done in an environment like this, a means be developed or the time be devoted to collection of both high-resolution and deeper-penetration records directly over the hole. We were unable to do this while the stern thrusters were in use maintaining position.

In this chapter, we will present 3.5-kHz records from portions of this survey to demonstrate the variability both transverse to and longitudinal to the axis of this northern rift. We will then show correlations which we are able to make with 3.5-kHz records while on the drilling site, and conclude with only a very tenuous suggestion of a correlation with 2-second analog seismic-reflection record crossing the site.

The survey lines in Figure 50 were all run from *Glomar Challenger*, except for one longitudinal line run from Guaymas Expedition, part of which ran up the axis of the rift. Note the variation in transverse sections, starting with Line A at the north, proceeding to Line E at the south (Figs. 70-74), and correlation with crossings marked in the longitudinal section of Line F (Fig. 75). The southwestern end of Line F deviates from the axis of the rift. The northeastern end, on the other hand, shows a hill which may be either an intrusion bulging up the sea floor or extrusive volcanics. The sea floor in most of the rift is covered with sediment, with at least one strong internal reflector, probably correlating with a prominent sand in a turbidite. The acoustic basement in these lines probably represents the uppermost intrusive body (or sill?). Stratification below the acoustic basement is shown only in Line F, northeast of the crossing with Line A, and appears to be the dipping basement from the surficial hill at the northeast end of the line. Diffractors throughout the record within the acoustic basement are probably indicative of irregularities and complexities within the deeper part of the section as drilled, with deformed sediments and intrusive bodies.

Some of the shallow reflectors of Figure 76 may correlate with hydraulic piston core samples from Site 481: a = sea floor; b = 4 meters = bottom of ooze, top of turbidite; c = 6 to 7 meters = turbidite?; d = 43 meters = turbidite; e = 53 meters = sand at base of turbidite;

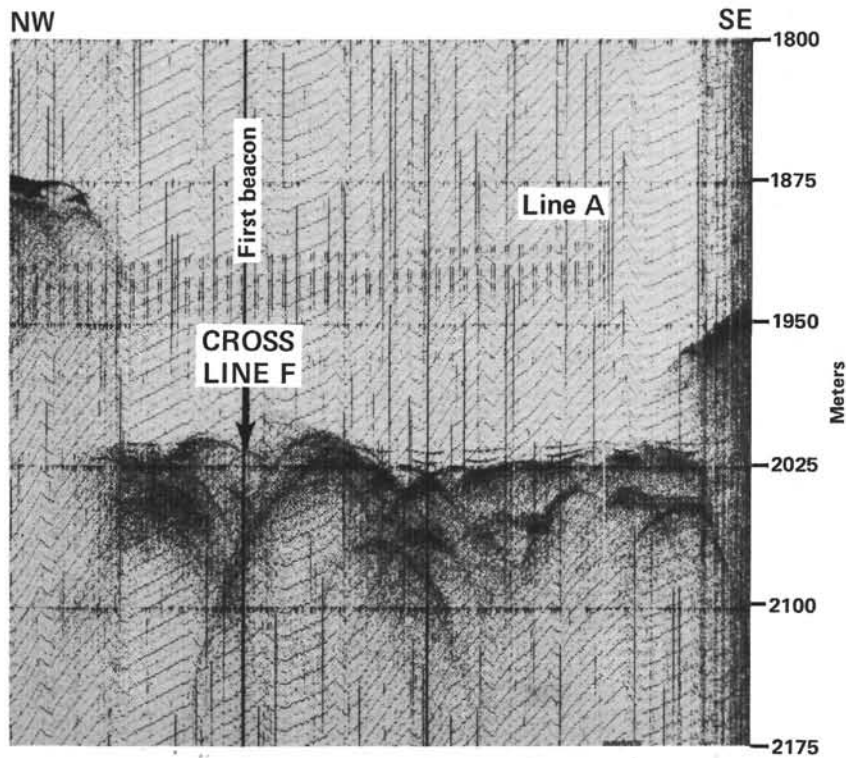


Figure 70. 3.5-kHz echo-sounding line crossing the rift along Line A shown in Figure 50.

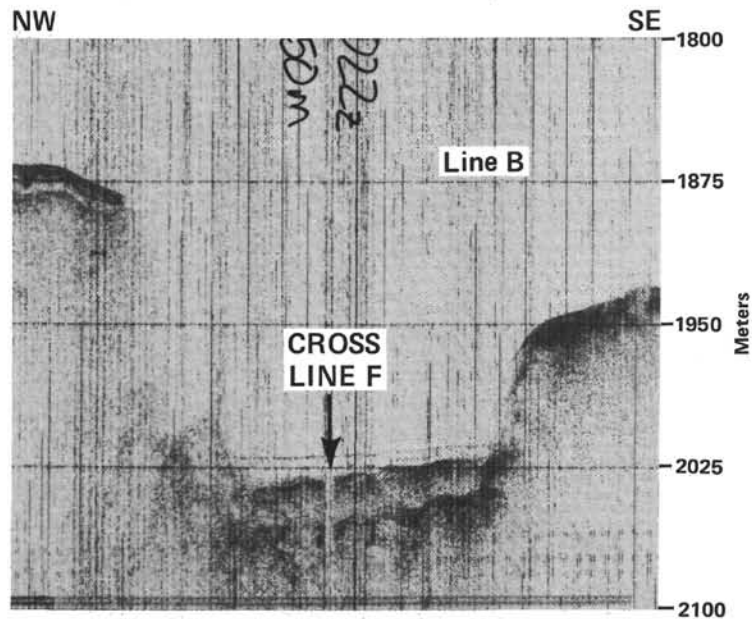


Figure 71. 3.5-kHz record along Line B (Fig. 50).

$f = 97$ meters = sand at base of turbidite. No reflections in the other records can be correlated directly, even with the sill at 169 meters, with the possible exception of the reflector marked in Figure 77. That is at approximately the correct reflection time to be the sill at 169 meters, using a reflection velocity of between 1.5 and 1.6 km/s.

The northwest wall of the rift is higher than the southwest side, the floor is generally shoaler at the southwest

end, and there appears to be more sediment fill proceeding toward the northeast or mainland-Mexico end.

Several multichannel seismic-reflection records were run near this site during Guaymas Expedition of Scripps Institution. Funding was available for processing only one of these, however, and this line crossed the rift obliquely, too far from the drilling site to be of use in correlation with drilling results.

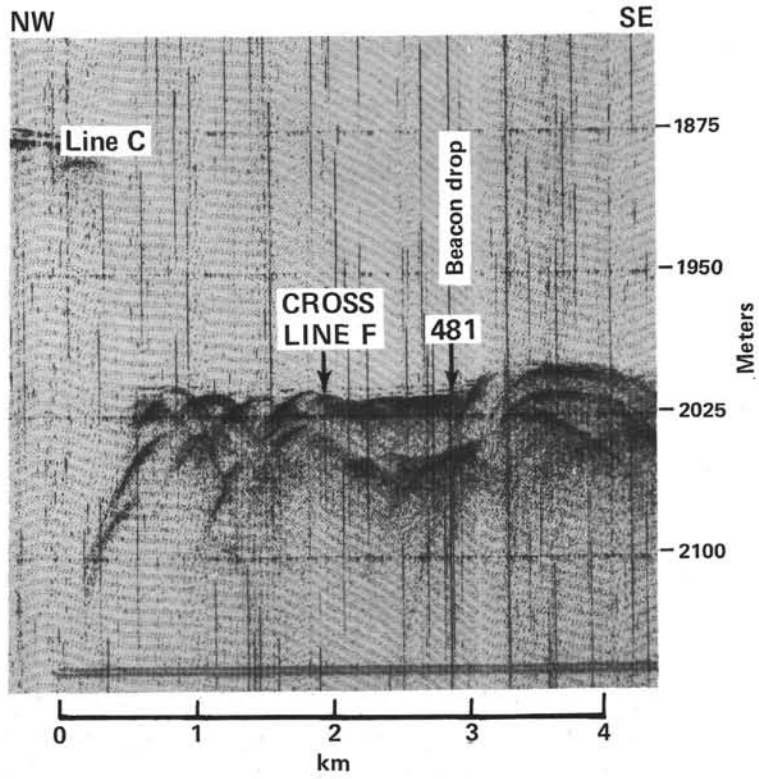


Figure 72. 3.5-kHz record along Line C (Fig. 50).

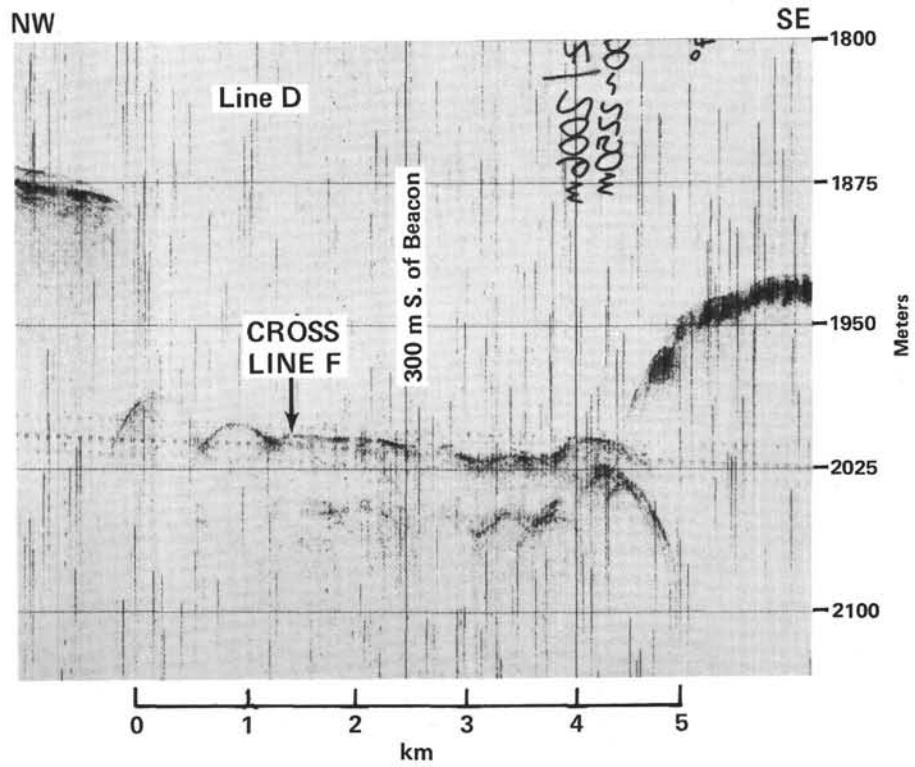


Figure 73. 3.5-kHz record along Line D (Fig. 50).

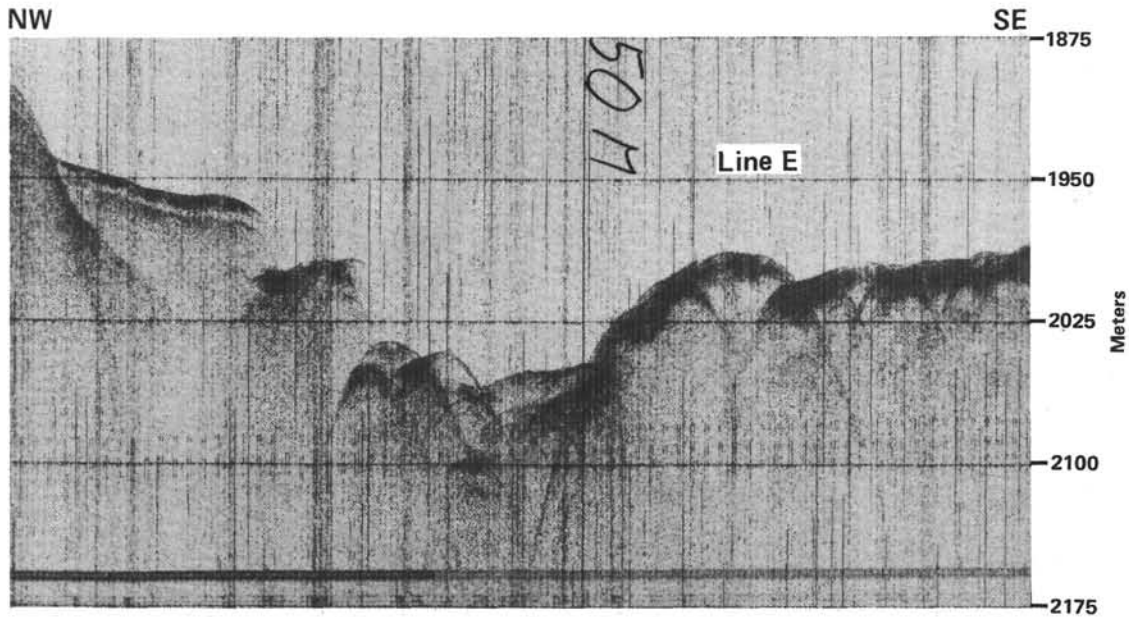


Figure 74. 3.5-kHz record along Line E (Fig. 50).

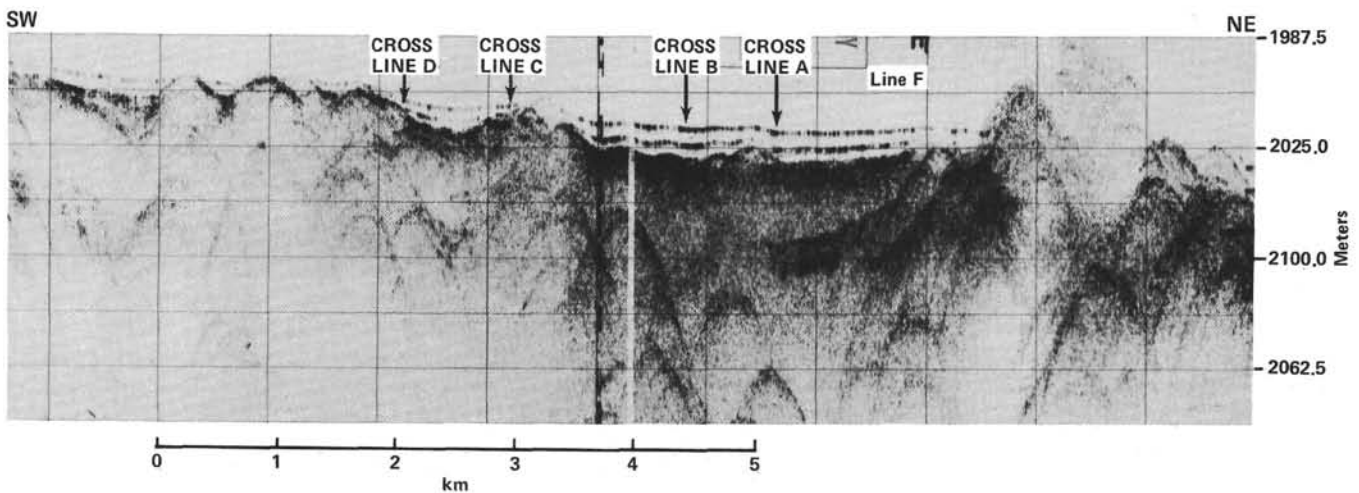


Figure 75. 3.5-kHz record of Line F (Fig. 50) longitudinally southwest-northeast along the axis of the rift, showing crossings with Lines A through D (Fig. 50).

Site 481 Summary and Conclusions

Drilling at Site 481 in the southwestern part of the northern rift of Guaymas Basin was a second attempt to drill into what is believed to be an active spreading rift. Our first attempt at Site 477 was located in a high-heat-flow zone of the southern rift, where heat flow was believed to be largely conductive. Heat flow in the northern rift is very spotty and, although high in places, it is generally lower than that of the southern rift and believed to be largely convective. Site 481 is located near where a submersible dive allowed observations of hydrothermal deposits on the rift flank above a fault scarp. The site thus has become known as the “hydrothermal site,” although our objectives were essentially the same as those for Site 477: to study the nature of sediment and igneous rock accumulation, the effects on

both of their admixtures at high temperatures, and to define the kinds and proportions of rock types at depth.

Seismic-reflection studies show that this site, like that in the south rift, is characterized by a general lack of coherent reflections in the rift and general difficulty in correlating lithology with seismic. This is not a surprising result in view of the active tectonic nature of the setting. The 3.5-kHz records again show great variation over relatively small distances. The rift floor changes from flat, ponded sediments to very irregular, hummocky topography in distances of less than a kilometer.

Two holes were drilled at this site. Hole 481 is a series of 11 Serocki-Storms-Cameron hydraulic piston corer samples from 0 to 52 meters. These were recovered to allow detailed studies of early changes in physical properties and chemistry in the shallow section. Hole 481A was washed to 42 meters and then continuously cored to

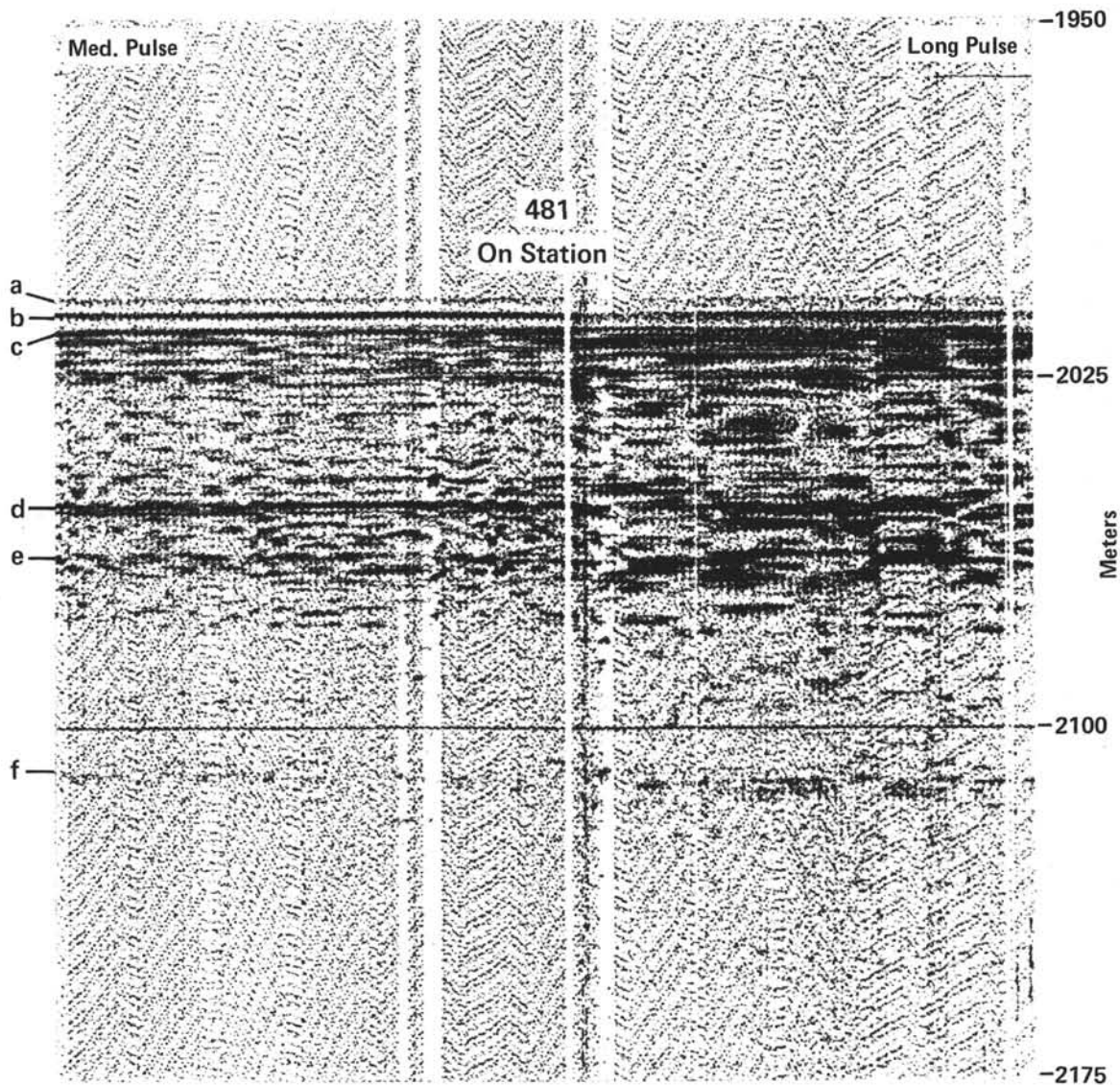


Figure 76. 3.5-kHz record made while *Glomar Challenger* sat stationary over Site 481. Left-hand side of the record was made with medium-pulse length on the recorder, right-hand half of the record with long pulse length. Horizons a through f identified in the text.

384 meters. Recovery was a respectable 56% through Core 30 at 327 meters. Thereafter, we had big problems in the alternating thin sills and baked sediments, apparently of a fractured nature, that we encountered to total depth. The hole finally was stopped by a clogged bit and float valve in these rocks at 384 meters. Recovery in the last seven cores was only 1 meter.

One sediment unit comprising two types of turbidites (Type I and Type II), mass flows, laminated sediments, and "host" or "background" sediments was sampled. In addition, four complexes of sills and/or flows were recovered. The sediment types within the one unit alternate with depth. The subdivision between turbidite Types I and II is primarily on relative amounts of biogenic versus terrigenous components. Type I turbidites have components less terrigenous and mainly hemipelagic; upward grading from sand or silt is a result of differential settling velocities. Type II turbidites appear

to have a more distant source, grading is less pronounced, generally no basal sands are present, and shallow-water components are evident. Turbidites of Type II have less water, higher bulk density and sonic velocity, and somewhat lower shear strength than do Type I turbidites or mass flows. Three mass flows were recovered at 33.8 to 34.5 meters, 268 to 279 meters, and 289 to 317 meters. No grading or basal sands are observed in these, and convolute bedding is present. They are composed mainly of terrigenous material, with some clasts. Laminated sediments were first encountered at 241 meters; they increase in frequency with depth and are intercalated between turbidites and mass flows. Most are diatomaceous ooze and mudstone.

Moderately well- to well-preserved siliceous and calcareous microfossils are present through the cored section, but radiolarians and foraminifers are common only in the upper 150 meters. The planktonic foramini-

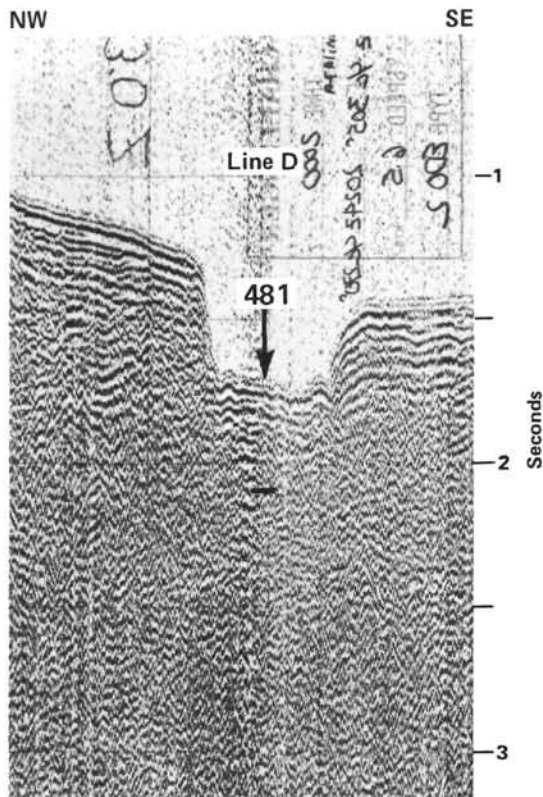


Figure 77. Two-second analog seismic-reflection record crossing the rift very near Site 481. The indicated reflector correlates approximately with the depth of the uppermost sill at 169 meters.

fers indicate that a warmer pelagic environment has prevailed during deposition of the upper 40 meters. Oldest sediments cored have a mixture of calcareous nannofossils of Zones NN21/20. The sediments are above the *Nitzschia fossilis* diatom extinction level, dated at about 0.26 m.y. in the Pacific. No depositional rates were calculated, as no fossil boundaries were crossed, but the rate is presumed to be very high (> 1000 m/m.y.), and all deposition is within the latest Quaternary. These very high sedimentation rates have resulted in very high values of alkalinity and ammonia in interstitial water, with consequent complex distributions of dissolved magnesium.

Four distinct igneous bodies were sampled at Hole 481A. Forty-six percent of Unit 1 was recovered. It consists of 18 individual intrusive units between 0.23 and 2.25 meters thick. Sediment intercalations were common. Units 2 through 4 were drilled with great difficulty and only about 1 to 5% recovery. These rock units are all similar vesicular basalt and are separated by sediment sequences. They are believed to be thin extrusive basalt flows or intrusives from a gas- or water-rich magma.

Contact zones between sediment and igneous sills and/or flows are represented by several recovered pieces of strongly baked sediments intercalated between Igneous Units 1 and 2. Contacts were not parallel to bedding, and two have contorted sediments in the vicinity of the contact. These observations suggest that the sills intruded cold and rather soft sediments, unlike those of

Site 478. One true contact was recovered above Igneous Unit 1 at 169.7 meters. The altered zone above the igneous unit is 40 meters, and below about 2 meters. The recovered altered zone shows the following features:

- 1) Induration increases abruptly at 41 meters above the sill, as shown in the density log and measured physical properties; bulk density and shear strength increase; water content decreases; below the sill the physical properties tend to become normal again, but bulk density remains higher by about 0.1 gm/cm³, and water content and porosity are lower by about 10% than in sequences unaffected by intrusion at similar depths.

- 2) Colors change to olive-black to brownish black as a result of baking of organic matter.

- 3) Clays become strongly fissile.

- 4) Sand layers may be cemented by silica.

- 5) Dissolution of diatom frustules starts at about 38 m above the sill; 20 meters above the sill all diatoms are dissolved; released silica formed cement and authigenic quartz crystals; large increases in dissolved chloride are also observed, presumably a result of intensive hydration of the sills during alteration to zeolites and/or smectites; the dissolution of calcareous nannofossils is observed only in a 7-meter-thick zone above the sill, indicating that solutions involved in sediment alterations were not acidic as in convective hydrothermal systems at ridge crests, but were probably heated pore waters; sands, the most porous sediments, were most strongly affected by these pore-water hydrothermal fluids, and probably acted as conduits through which the solutions flowed to escape.

Organic geochemical parameters preserve the temperature history of the sill intrusions and allow some reconstruction of geologic history. The upper sill was intruded while 60 meters less sediment was present than now exists, based on upper limit of expulsion of petroliferous material. Subsequently, deposition of immature sediment was continued. Based on C₂-C₅ hydrocarbon content, this sill intrusion may have happened in three pulses. A minor sill at 335 to 340 meters also intruded sediments, distilling petroliferous material upward. High-temperature influence of the sills was limited to their immediate vicinity (~10 m for the upper sill, 5 m for the lower). Lower-temperature influences did not expel all petroliferous material from between the sills, and some viable carbon remains. The gases of the sampled sediment section consist predominantly of biogenic CH₄, CO₂, and H₂S, with traces of C₂H₆. In the zone between the sills, a large thermogenic component is superimposed on the biogenic component.

Drilling at Site 481 as well as Site 477 in the north and south rifts of Guaymas Basin has given us new insight into the processes of deposition and emplacement of the sediments and rocks and the chemical and physical effects of mixing young, wet sediments and molten igneous rock, but, because both sites were stopped prematurely, the drilling has also left unattained many of our original objectives and created new problems for future drilling. New questions and unsolved problems include:

- 1) How deep beneath the sea floor will sediments be found? Will they be older than the plate-tectonics model

predicts? Are they predominantly emplaced by lateral infilling, by vertical settling of previously deposited beds, or by primary deposition?

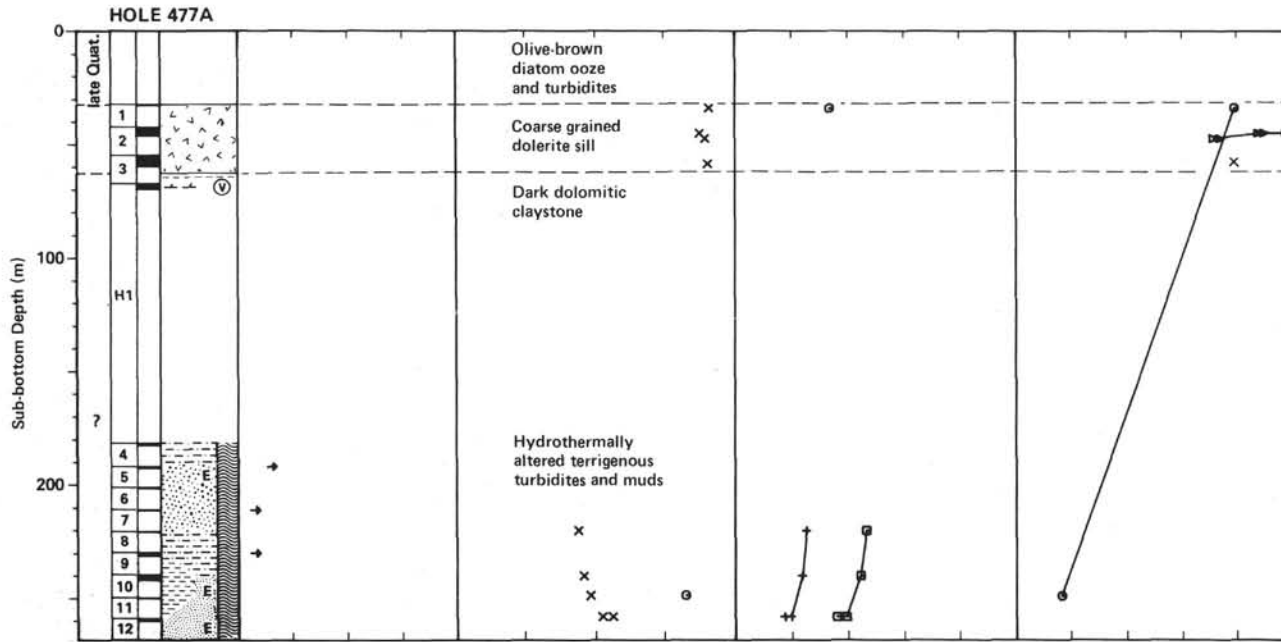
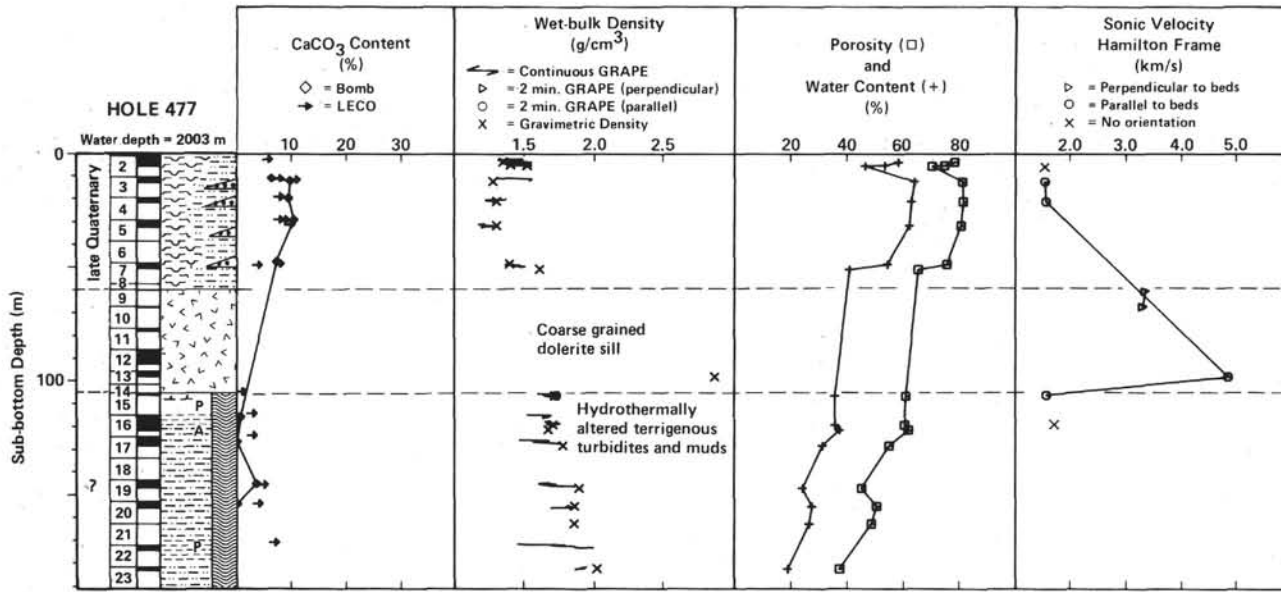
2) Are the igneous intrusions all sills, or do we have equally large numbers of dikes and irregular intrusive bodies? What is the quantitative importance of extrusive lavas? How do these features vary in quantity with depth.

SUMMARY OF DOWNHOLE LOGGING FOR GUAYMAS BASIN SITES

Results of downhole logging, compared to lithology, calcium carbonate, and physical properties, are shown in Figures 78–80. (Original tapes are available from storage at the DSDP Information Handling Group.) The logs provide significant information on the depth relationships of sills and their sub-unit boundaries, the position and thickness of various mass flow beds, the onset of diagenesis, the width of contact zones around sills, and clues to hard and soft lithologies that for some reason or another were not recovered or at least not undisturbed.

REFERENCES

- Bé, A. H., 1977. An ecological, zoogeographic and taxonomic review of Recent planktonic foraminifera. In Ramsay, A. T. S. (Ed.), *Ocean Micropaleontology*: New York (Academic Press), pp.
- Benson, R. N., 1966. Recent radiolaria from the Gulf of California [Ph.D. dissert.]. University of Minnesota, Minneapolis.
- Burckle, L., 1977. Pliocene and Pleistocene diatom datum levels from the equatorial Pacific. *Quat. Geol.*, 7:330–340.
- Baumgartner, T. R., Christensen, N., Jr., Fok-Pun, L., and Quinn, W., 1979. Sources of interannual climate variation in the Gulf of California and evidence for biological response. CALCOFI Ann. Conf., Idylwild, Calif. (Abstract)
- Calvert, S. E., 1966. Accumulation of diatomaceous silica in the sediments of the Gulf of California. *Geol. Soc. Am. Bull.*, 77: 569–596.
- Doose, P. R., Sandstrom, M. W., Jodele, R. Z., and Kaplan, I. R., 1978. Interstitial gas analysis of sediment samples from Site 368 and Hole 369A. In Lancelot, Y., Seibold, E., et al., *Init. Repts. DSDP*, 41: Washington (U.S. Govt. Printing Office), 861–863.
- Kovach, R. L., Allen, C. R., and Press, F., 1962. Geophysical investigation in the Colorado Delta region. *J. Geophys. Res.*, 67:2845–2871.
- Larson, P. A., Mudie, J. D., and Larson, R. L., 1972. Magnetic anomalies and fracture-zone trends in the Gulf of California. *Geol. Soc. Am. Bull.*, 83:3361–3368.
- Lawver, L. A., and Williams, D. L., 1979. Heat flow in the central Gulf of California. *Geophys. Res.*, 84:3465–3478.
- Lawver, L. A., Williams, D. L., and Von Herzen, R. P., 1975. A major geothermal anomaly in the Gulf of California. *Nature*, 257:23.
- Lonsdale, P., 1978. Submersible exploration of Guaymas Basin: a preliminary report of the Gulf of California 1977 operations of DSV-4 *Seacliff*. *Scripps Inst. Oceanogr. Ref.*, 78-1.
- Lupton, J. E., 1979. Helium-3 in the Guaymas Basin: evidence for injection of mantle volatiles in the Gulf of California. *J. Geophys. Res.*, 84:7446–7452.
- Moore, D. G., 1973. Plate-edge deformation and crustal growth, Gulf of California structural province. *Geol. Soc. Am. Bull.*, 84: 1883–1906.
- Moore, G. F., Becker, K., Bibee, L. D., Crane, K., Curray, J. R., Guerrero, J., Hawkins, J. W., Kastens, K., Kastner, M., Lawver, L. A., Melchior, J., Vacquier, V., and Williams, D. L., 1978. Gulf of California IPOD site summary, final report. [unpublished manuscript]
- Phillips, R. P., 1964. Seismic refraction studies in Gulf of California. In van Andel, Tj. H., and Shor, G. G. (Eds.), *Marine Geology of the Gulf of California*. Am. Assoc. Pet. Geol. Mem., 3:90–121.
- Reichle, M. S., and Reid, I., 1977. Detailed study of earthquake swarms from the Gulf of California. *Bull. Seismol. Soc. Am.*, 67:159–171.
- Reichle, M. S., Sharman, G. F., and Brune, J. N., 1976. Sonobuoy and teleseismic study of Gulf of California transform fault earthquake sequences. *Bull. Seismol. Soc. Am.*, 66:1623–1641.
- Rusnak, G. A., Fisher, R. L., and Shepard, F. P., 1964. Bathymetry and faults of Gulf of California. In van Andel, Tj. H., and Shor, G. G. (Eds.), *Marine Geology of the Gulf of California*: Am. Assoc. Pet. Geol. Mem., 3:59–75.
- Ryther, J. H., 1956. Photosynthesis in the ocean as a function of light intensity. *Limnol. Oceanogr.*, 1:6–70.
- Sharman, G., 1976. The plate tectonic evolution of the Gulf of California [Ph.D. dissert.]. University of California, San Diego.
- Simoneit, B. R. T., Brenner, S., Peters, K. E., and Kaplan, I. R., 1978. Thermal alteration of Cretaceous black shale by basaltic intrusions in the eastern Atlantic. *Nature*, 273:501–504.
- Simoneit, B. R. T., Mazurek, M. A., Brenner, S., Crisp, P. T., and Kaplan, I. R., 1979. Organic geochemistry of Recent sediments from Guaymas Basin, Gulf of California. *Deep-Sea Res.*, Pt. A, 26:879–891.
- Sykes, L. R., 1968. Seismological evidence for transform faults, sea-floor spreading, and continental drift. In Phinney, R. A. (Ed.), *The History of the Earth's Crust—A Symposium*: Princeton (Princeton Univ. Press), pp. 120–150.
- van Andel, Tj. H., 1964. Recent marine sediments in the Gulf of California. In van Andel, Tj. H., and Shor, G. G. (Eds.), *Marine Geology of the Gulf of California*: Am. Assoc. Petrol. Geol. Mem., 3:216–310.
- Vogt, P. R., Lorentzen, G. R., and Dennis, L. S., 1970. An aeromagnetic survey of the Keathly magnetic anomaly sequence between 34°N and 40°N in the western North Atlantic [abs.]. *Am. Geophys. Union Trans.*, 51:274.
- Vogt, P. R., Anderson, C. N., Bracey, D. R., and Schneider, E. D., 1970. North Atlantic magnetic smooth zones. *J. Geophys. Res.*, 75:3955–3968.
- Williams, D. L., Becker, K., Lawver, L. A., Von Herzen, R. P., 1979. Heat flow at the spreading centers of the Guaymas Basin, Gulf of California. *J. Geophys. Res.*, 84:6757–6796.



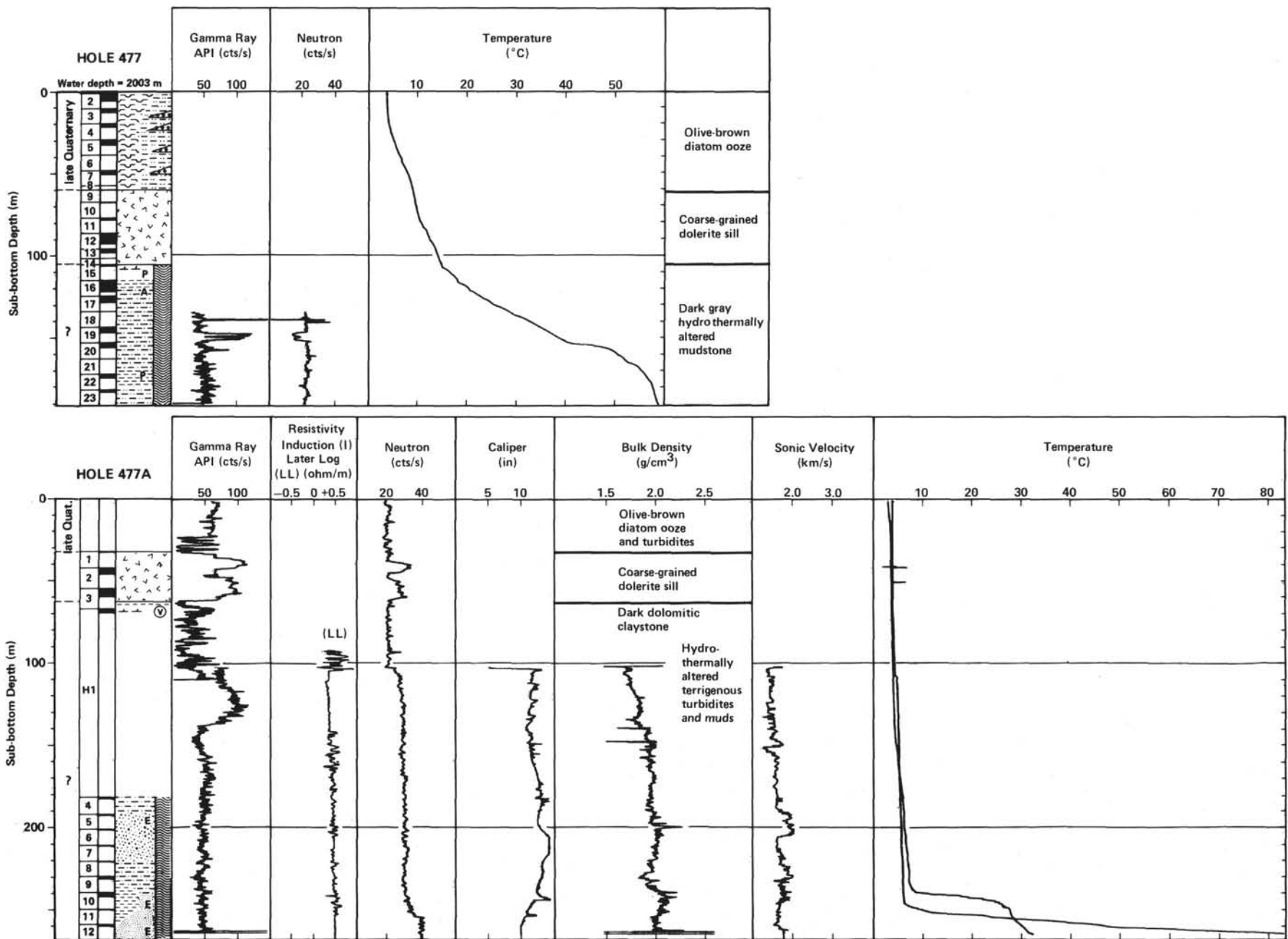
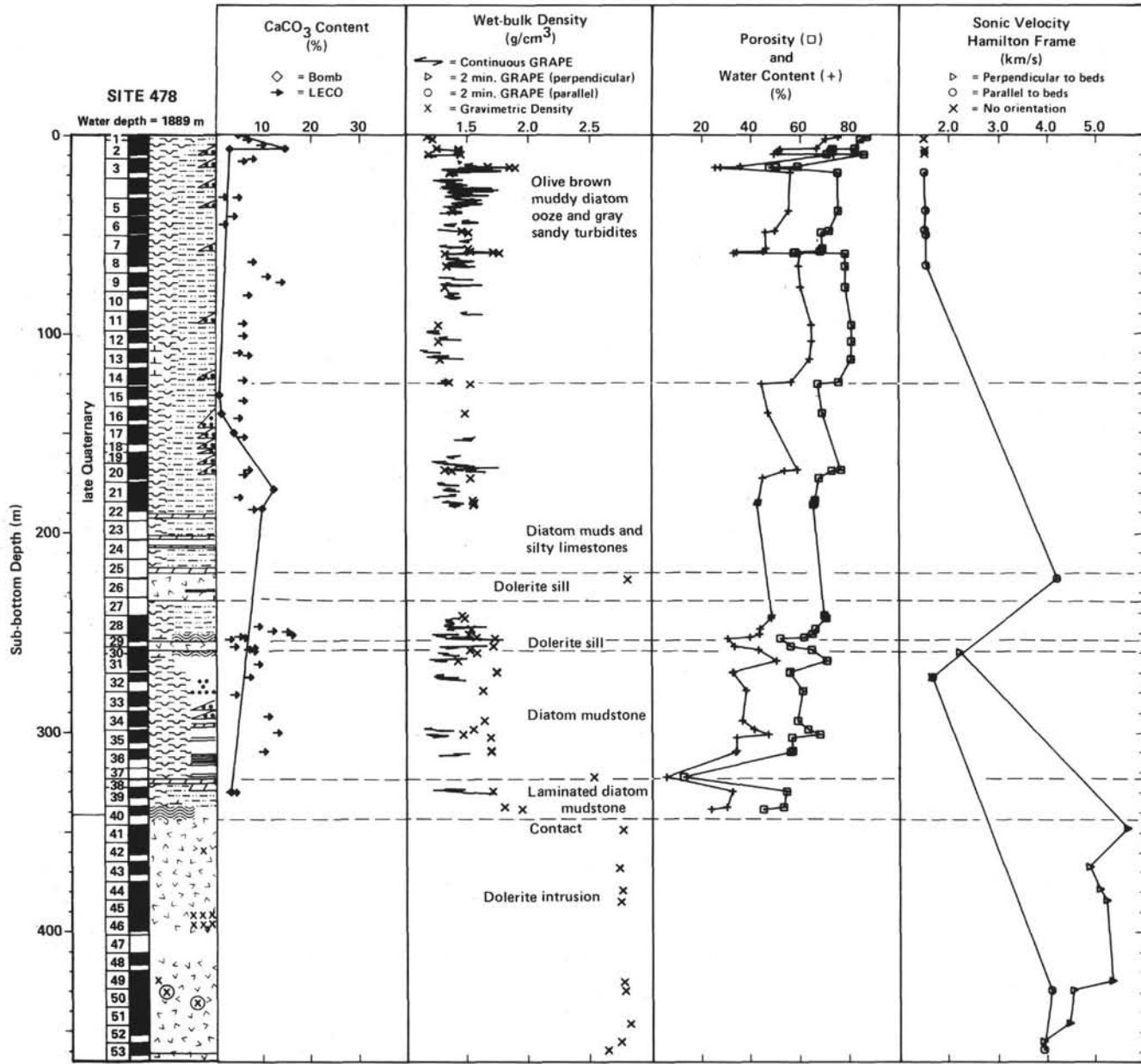


Figure 78. Results of downhole logging compared to lithology, calcium carbonate, and physical properties for Holes 477 and 477A.



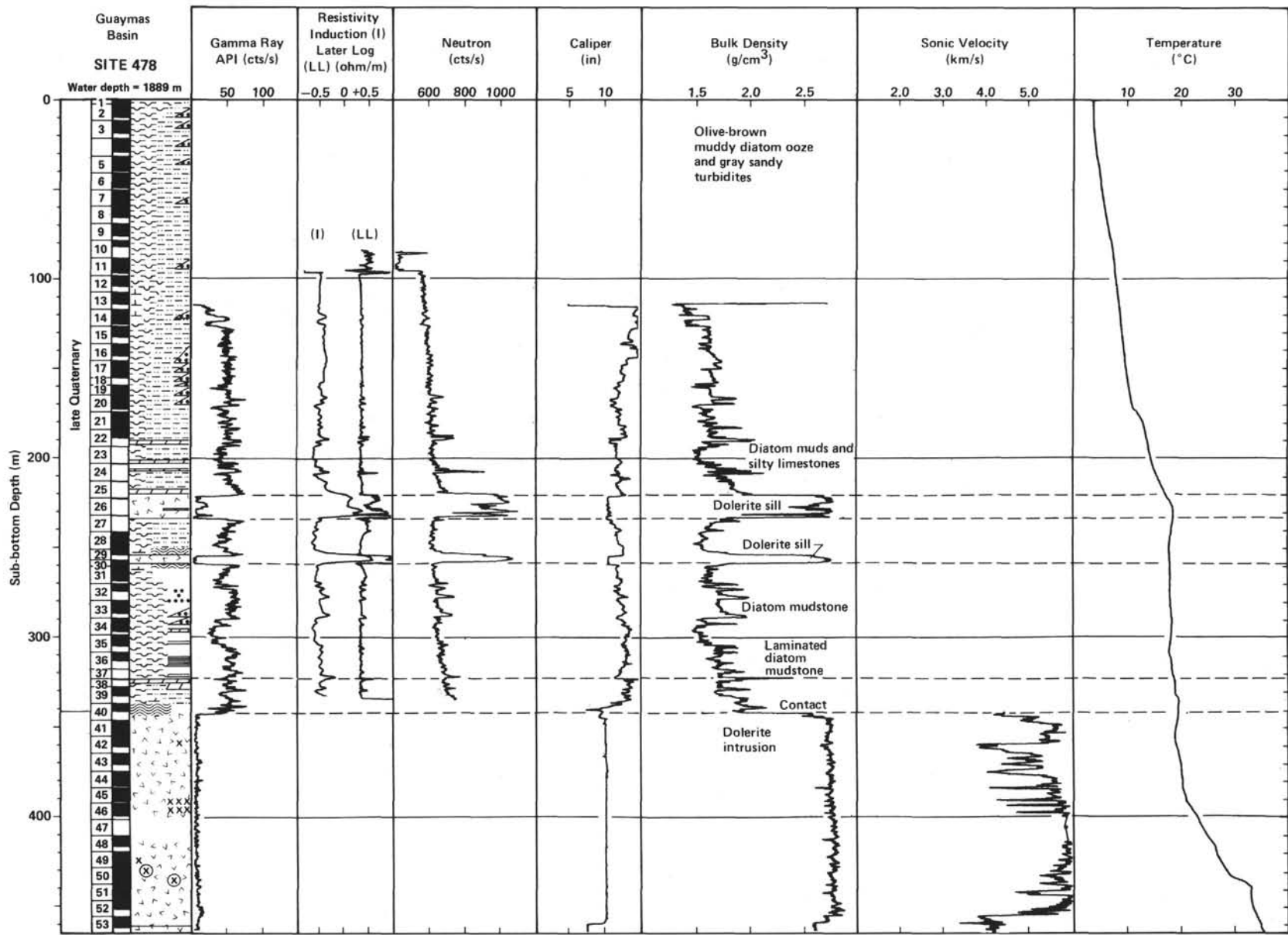
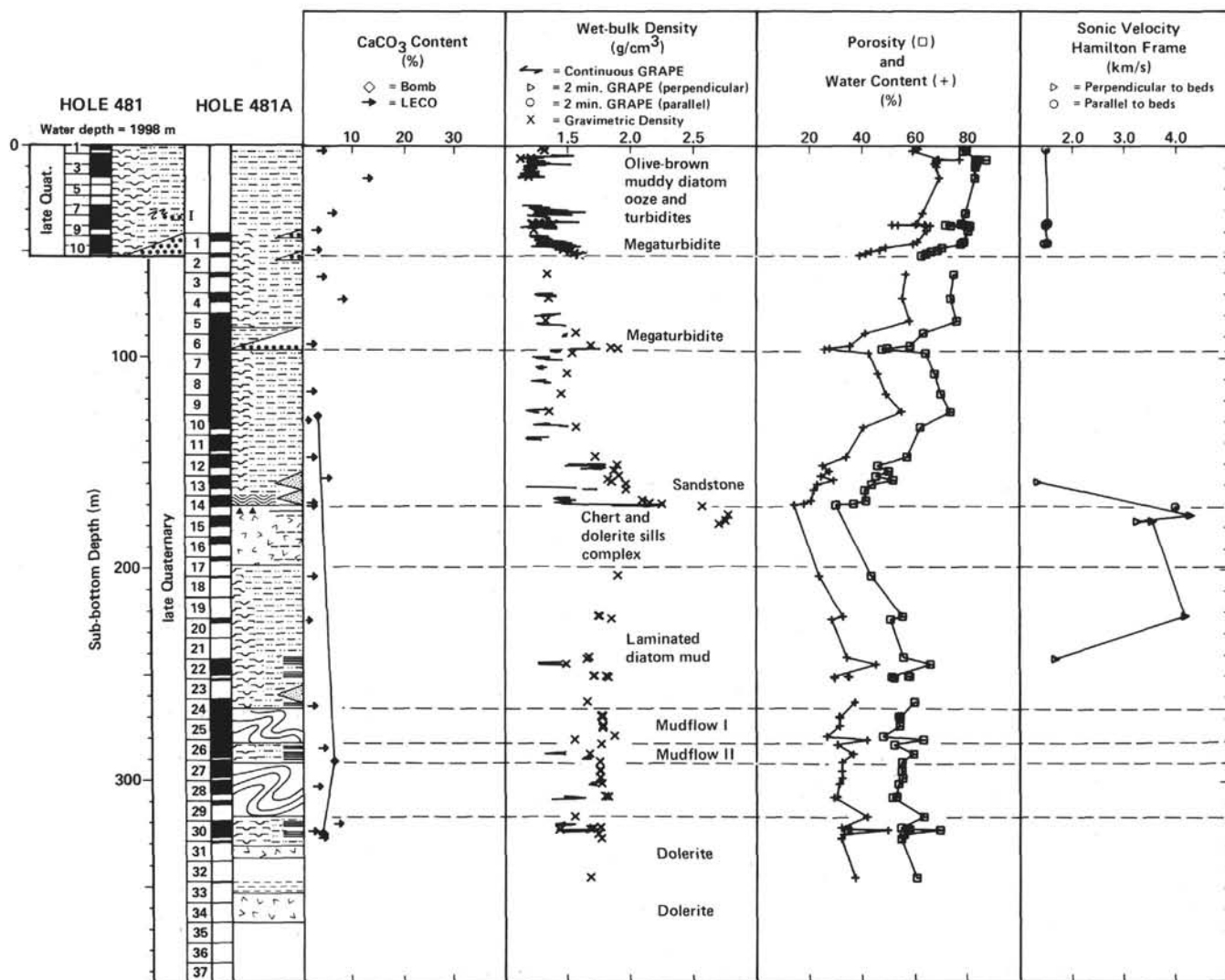


Figure 79. Results of downhole logging compared to lithology, calcium carbonate, and physical properties for Hole 478.



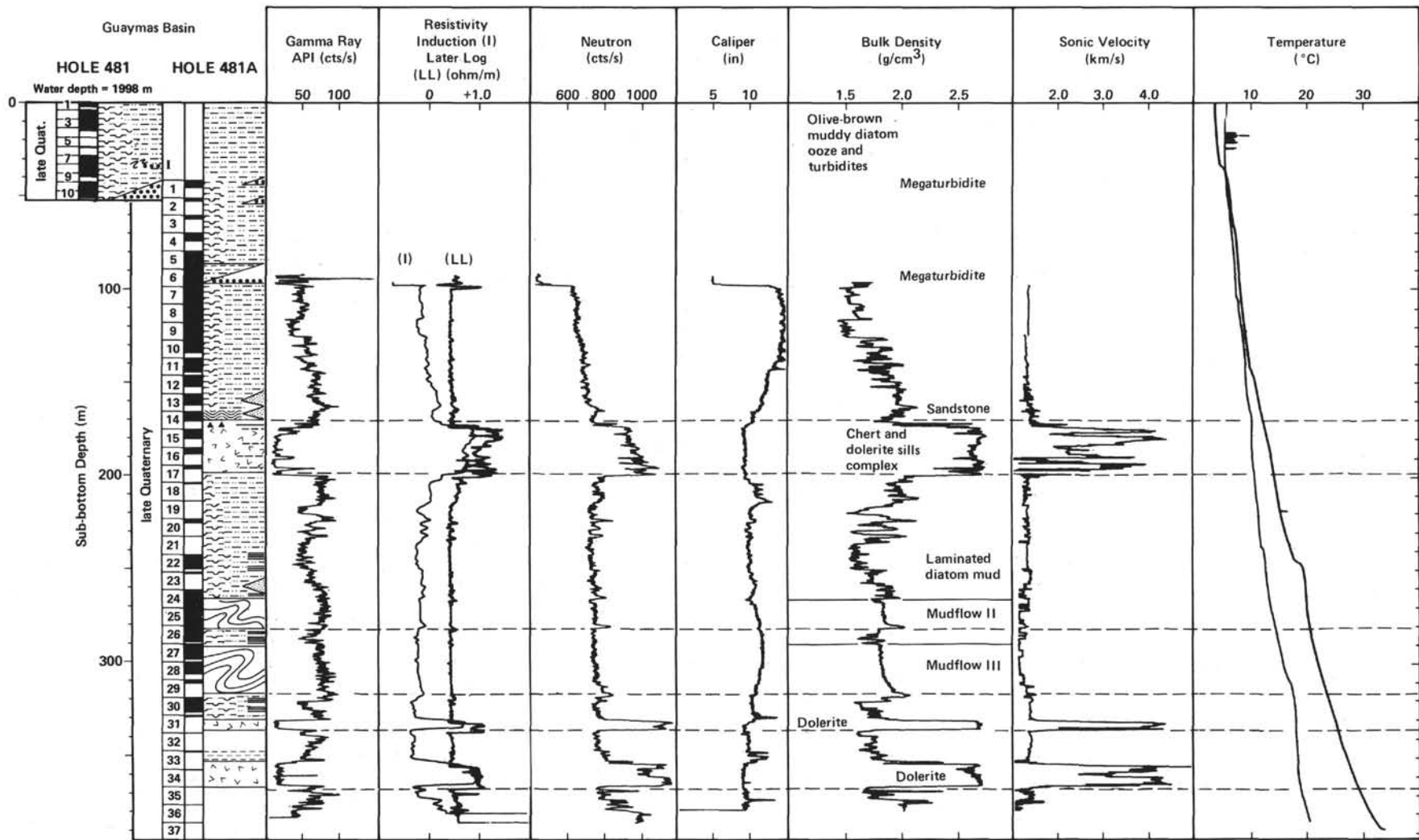
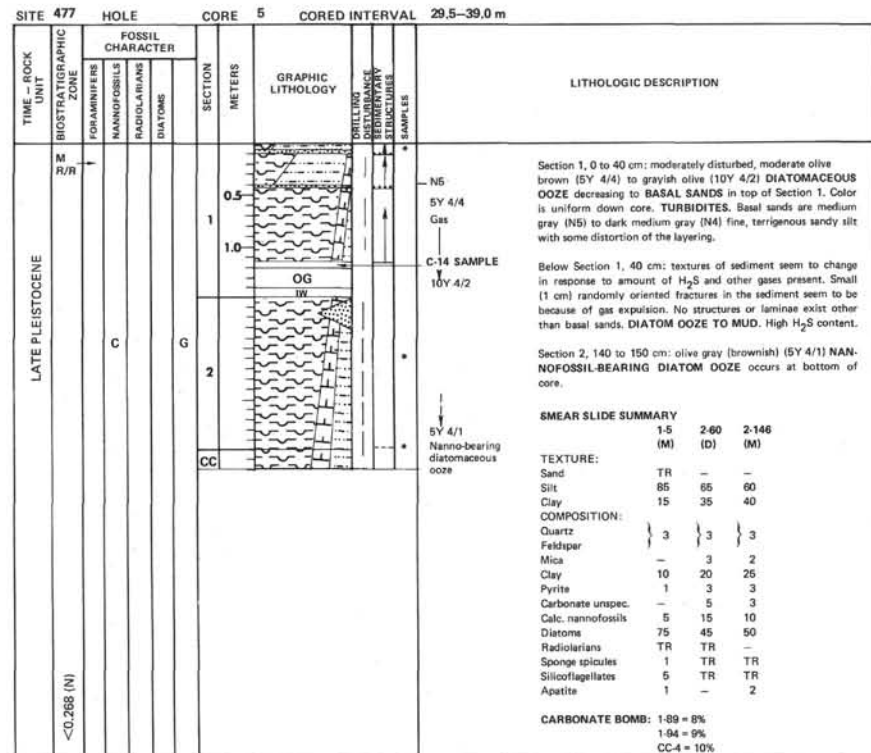
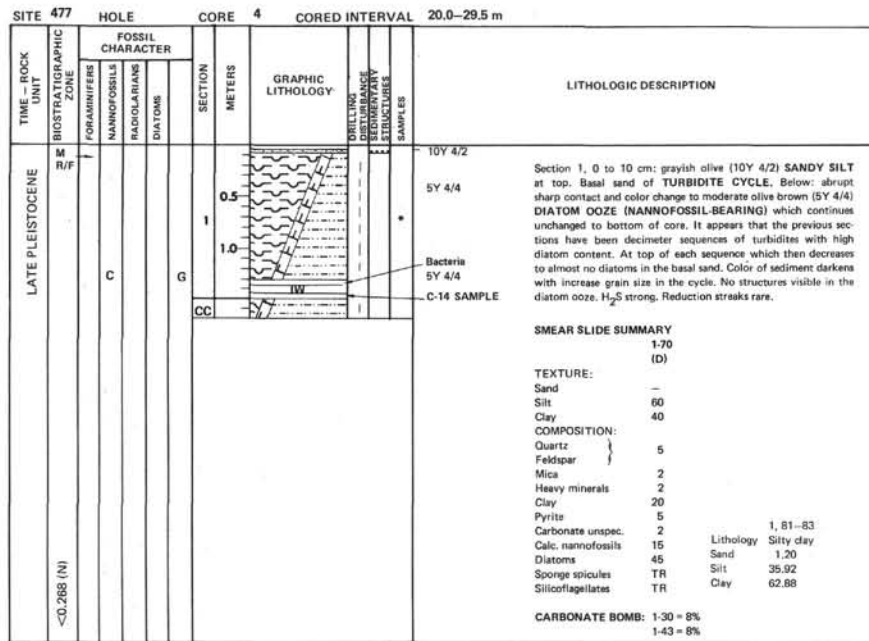


Figure 80. Results of downhole logging compared to lithology, calcium carbonate, and physical properties for Holes 481 and 481A.

SITE 477		HOLE		CORE 1		CORED INTERVAL		0.0-1.0 m	
TIME - ROCK UNIT	BIOSTRATIGRAPHIC ZONE	FOSSIL CHARACTER			SECTION METERS	GRAPHIC LITHOLOGY	DRILLING DISTURBANCE	TEMPORARY STRATIGRAPHIC SAMPLES	LITHOLOGIC DESCRIPTION
		FORAMINIFERS	NANNOFOSSILS	RADIOLARIANS					
LATE PLEISTOCENE	<0.268 (N)				CC				VOID
									Moderate olive brown (5Y 4/4) to grayish olive (10Y 4/2), uniform DIATOMACEOUS OOZE. Some terrigenous plant matter cuticles in coarse fraction = 30% of total sample. High water content; jelly-like consistency. Faint H ₂ S smell. Diatoms are silt-size, well-preserved. Translucent hematite conspicuous.
									SMEAR SLIDE SUMMARY CC-26 (D)
									TEXTURE: Sand 2 Silt 80 Clay 20
									COMPOSITION: Quartz 3 Feldspar 3 Clay 10 Pyrite 3 Hematite 1 Carbonate unsp. 5 Calc. nannofossils 7 Diatoms 60 Radiolarians TR Sponge spicules 1 Silicoflagellates 2 Organics 6

SITE 477		HOLE		CORE 2		CORED INTERVAL		1.0-10.5 m	
TIME - ROCK UNIT	BIOSTRATIGRAPHIC ZONE	FOSSIL CHARACTER			SECTION METERS	GRAPHIC LITHOLOGY	DRILLING DISTURBANCE	TEMPORARY STRATIGRAPHIC SAMPLES	LITHOLOGIC DESCRIPTION
		FORAMINIFERS	NANNOFOSSILS	RADIOLARIANS					
LATE PLEISTOCENE	<0.268 (N)				0.5				
					1				Moderate olive brown (5Y 4/4) to grayish olive (10Y 4/2) DIATOMACEOUS OOZE; homogeneous. Little or no coarse TERRIGENOUS fraction. Silt-size grains all well-preserved diatoms. Slight H ₂ S smell. Some black reduction streaks. Slight compaction with depth. High water content with jelly-like consistency. No structures or laminae. Very rapid sediment rate inferred.
					1.0				CF
					2				5Y 4/4
					2				10Y 4/2
					3				SMEAR SLIDE SUMMARY 1-125 (CF) 1-125 (CF) 2-70 (D) (>144 μm) (63 μm)
					3				TEXTURE: Sand - - - Silt - - - 70 Clay - - - 30
					3				COMPOSITION: Quartz 10 30 15 Feldspar 20 20 Heavy minerals - - 3 Clay - - - 20 Glauconite 107 157 - Pyrite - - - 2 Carbonate unsp. - - - 3 Foraminifers 2 (benthic) 1 (benthic and planktonic) -
					4				10Y 4/2
					4				Calc. nannofossils - - - 5 Diatoms 70 30 45 Radiolarians 1 2 1 Sponge spicules - - 1 Silicoflagellates - 1 2 Plant debris - 1 - Wood 3 - -
					CC				VOID
									CARBONATE BOMB: 2.136 = 6%

SITE 477		HOLE		CORE 3		CORED INTERVAL		10.5-20.0 m	
TIME - ROCK UNIT	BIOSTRATIGRAPHIC ZONE	FOSSIL CHARACTER			SECTION METERS	GRAPHIC LITHOLOGY	DRILLING DISTURBANCE	TEMPORARY STRATIGRAPHIC SAMPLES	LITHOLOGIC DESCRIPTION
		FORAMINIFERS	NANNOFOSSILS	RADIOLARIANS					
LATE PLEISTOCENE	<0.268 (N)				0.5				10Y 4/2
					1				Moderately disturbed, uniform color grayish-olive (10Y 4/2) DIATOM OOZE at top of core which grades to a darker (slightly) DIATOM CLAYEY SILT at 70 cm in Section 1 implying a MUD TURBIDITE with medium grayish to dark medium gray (N4). Fine sandy silt at the base. Diatom content drops significantly within a turbidite cycle being <10% at or near the basal sand. Section 1, 117 cm: start of moderate olive brown (5Y 4/4) section which coarsens into Section 2, another turbidite large section of diatom ooze in section. H ₂ S content; water content high, contacts below basal sands are sharp, although distorted moderately basal sands 2 to 3 cm thick. Turbidites are 40 to 70 cm thick. C ¹⁴ and bacteria samples from Section 1.
					1.0				5Y 4/4
					2				10Y 4/2
					2				CF (sandy silt)
					2				5Y 4/4
					CC				SMEAR SLIDE SUMMARY 154 (D) 2-9 (CF) 2-20 (D)
									TEXTURE: Sand 5 40 TR Silt 65 40 70 Clay 30 20 30
									COMPOSITION: Quartz 50 65 15 Feldspar - 3 - Mica - 3 1 Heavy minerals 2 3 1 Clay 20 10 20 Glauconite - 27 - Pyrite 2 5 2 Carbonate unsp. 5 3 3 Foraminifers 2 ^(a) - - Calc. nannofossils 3 3 7 Diatoms 15 5 45 Radiolarians - - TR Sponge spicules - - TR Silicoflagellates - - 2 Plant debris - 1 -
									(a) Benthic and planktonic Lithology Silty clay Sand 2.68 Silt 40.32 CARBONATE BOMB: 2.28 = 8% Clay 56.80 2.83 = 11%



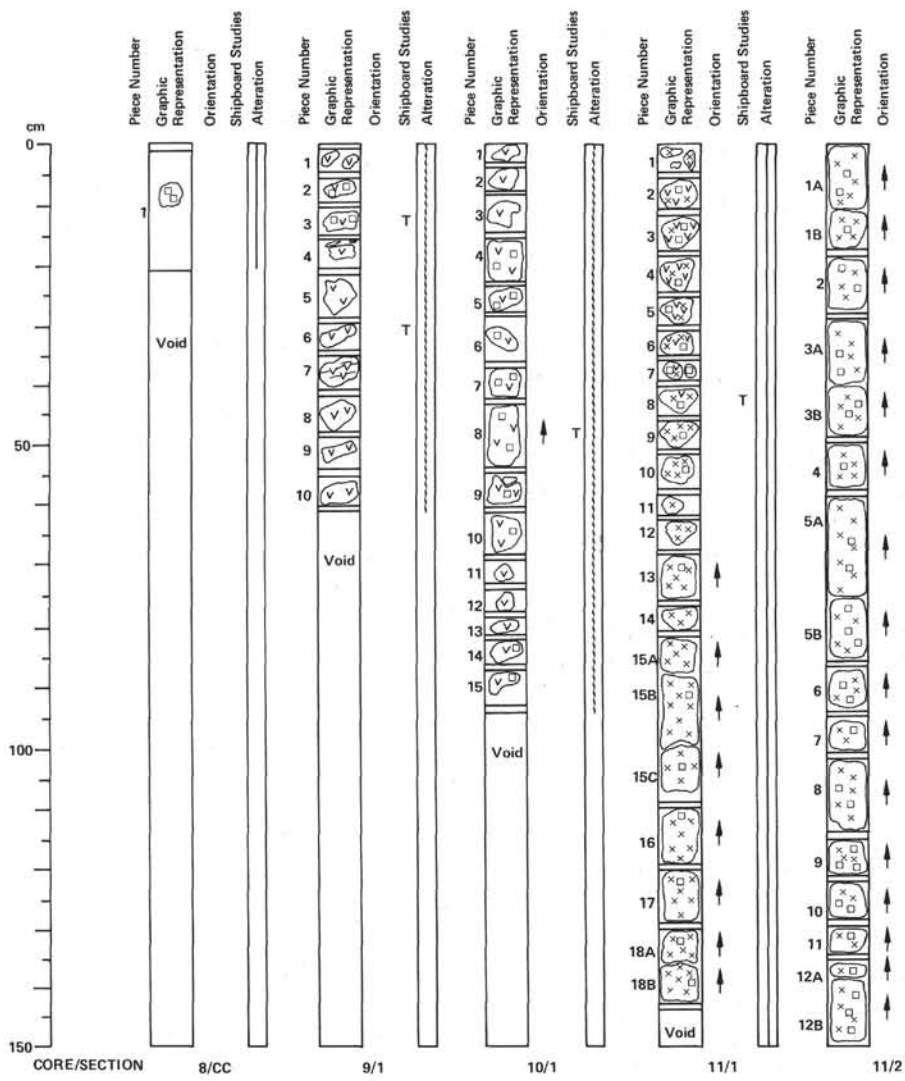
SITE 477 HOLE		CORE 6		CORED INTERVAL 39.0-48.5 m		
TIME - ROCK UNIT	BIOSTRATIGRAPHIC ZONE	FOSSIL CHARACTER			SECTION METERS	LITHOLOGIC DESCRIPTION
		FORAMINIFERS	NANNOFOSSILS	RADIOLARIANS		
					0.5	Only trace of recovery. SMEAR SLIDE SUMMARY From sample collected off heat flow - interstitial water sampler TEXTURE: Sand - Silt 70 Clay 30 COMPOSITION: Quartz 20 Feldspar 1 Clay 30 Pyrite 10? (not framboidal) Opakes 10 Diatoms TR Apatite 40 (or drilling mud) R. I. ~ 1.65
					1.0	
					2	

SITE 477 HOLE		CORE 7		CORED INTERVAL 48.5-58.0 m							
TIME - ROCK UNIT	BIOSTRATIGRAPHIC ZONE	FOSSIL CHARACTER			SECTION METERS	LITHOLOGIC DESCRIPTION					
		FORAMINIFERS	NANNOFOSSILS	RADIOLARIANS			DIATOMS				
LATE PLEISTOCENE	<0.268 (N)	M F/C	C	G	0.5	Pebble	Section 1: highly disturbed to marbled, light olive gray (5Y 4/2) nannofossil-bearing DIATOMACEOUS OOOZE grades at Section 1, 43 cm to a DIATOMACEOUS OOOZE with dispersed GLASSY BASALT PEBBLES and small dark medium gray (N4) SANDY SILT blebs.				
					1.0	5Y 4/2					
					P A/F	C	G	2	N4 N3 Light gray (N6)	Section 2, 70 to 80 cm: at bottom of core thick but disturbed layer of dark to light (N4-N7) gray sandy silt is found. May have been interlayered sands of different colors. Sands represent a diverse source terrain with zircon, garnet, epidote, and K-feldspar. Strong H ₂ S smell. May be seeing a disturbed turbidite with diatom ooze at top. Debris flow of basaltic pebbles with small well-rounded siltstone (fibrous cement) followed by and grading into a thick basal sand. Fresh basalt pebbles may be derived from basin flanks (lava flows that have brecciated) and then been incorporated into turbidite flow.	
								CC	N4 N7 Sandy clay		
										3	SS 1, 42 cm: light gray, poorly-indurated siltstone pebble. Components: 15% 5 to 15 micron, opaque crystals and framboids (pyrite) 15% weathered feldspars (twinned and untwinned) (0.03 to 0.06 mm) many subhedral 5% very altered pyroxene (0.03 to 0.05 mm) 1% carbonate silt 2% diatoms 5% diverse 5% quartz (0.04 to 0.1 mm) Matrix: 30% thin ragged fibrous mineral (up to 0.02 mm long, 0.002 mm wide), isotopic, banded in sprays, R. I. ~ 1.48 (mordenite?)
										4	TS 2, 2 cm: basalt pebble fragment in sediment. Quenched, porphyritic: PHENOCRYSTS: 5% olivine (0.5 to 1 mm) sub-hedral, fresh and 10% plagioclase, lath-shaped. Frequently intergrown in glomerocrystic aggregates up to 30 mm across. GROUNDMASS: 5% olivine, <0.1 mm, skeletal; 30% plagioclase, up to 0.2 mm, skeletal microlites, pilotaxitic alignment, 50% clinopyroxene and opakes, plus mesostasis, quenched. No alteration observed. No vesicles.
										5	SMEAR SLIDE SUMMARY
					6						
					7						
					CC						

	1-39 (D)	1-69 (M)	2-23 (M)	2-32 (M)	2-37 (M)	CC (M)
TEXTURE:						
Sand	5	-	10	25	45	30
Silt	60	20	30	25	30	30
Clay	35	80	60	50	25	40
COMPOSITION:						
Quartz	5	10	8 (a)	40 (a)	10	10
Feldspar	-	-	5	-	35 (a)	5
Mica	-	-	-	-	-	4
Heavy minerals	2	2	2	-	3	-
Clay	25	70	50	50	25	38
Magnetite	-	-	-	-	1	-
Pyrite	3	-	5	?	3	-
Opakes	-	15	-	-	-	-
Zecolite	-	40?	-	-	-	-
Carbonate unspc.	5	-	2	-	-	TR
Foraminifers	1	-	2	-	-	-
Calc. nannofossils	10	-	TR	-	-	-
Diatoms	45	-	15	-	5	5
Radiolarians	-	-	1	-	-	-
Silicoflagellates	1	-	-	-	5	1
Plant debris	3	-	3	-	-	-
Plagioclase	-	-	5	-	15	-
Ferruginous coatings	-	-	TR	-	-	-
Clay coated grains	-	-	-	-	30	-

(a) most grains coated by ferruginous clay

CARBONATE BOMB: 1-124 = 8% and 2-14 = 4% (hard, sandy)



64-477-8 Depth: 58.0 to 60.0 m
CORE-CATCHER: DOMINANT LITHOLOGY: feldspar phryic basalt/dolerite.

Macroscopic Description
 Soft, sea-water permeated, dark gray (N3-N4) coarse-grained basalt containing about 20% plagioclase phenocrysts (0.5-3.5 mm). Vague greenish-tint indicates (clay-mineral) alteration. May be more doleritic than basaltic, but the rock is too soft (altered) to make a thin section.

64-477-9 Depth: 60.0 to 67.5 m
SECTION 1: DOMINANT LITHOLOGY: SEVERELY ALTERED DOLERITE.

Macroscopic Description
 Two distinct rock varieties can be seen. Both are very friable, and permeated by water and altered with green clay minerals.

Type 1 (Pieces 1, 2, and 3): plagioclase phryic (crystals 0.5-4 mm), up to 15% plagioclase, in a medium- to coarse-grained doleritic, dark gray matrix of feldspar and pyroxene and possibly olivine. Similar to the dolerite recovered in the Core-Catcher of Core 8.

Type 2 (Pieces 4-8): medium-grained dark gray aphyric dolerite. Matrix of feldspar and pyroxene, and possibly olivine.

In both types, although the rock is very friable and shot through with clay minerals, the pyroxenes appear fairly fresh. This suggests low-grade alteration. The hole temperature at the depth has been estimated at 80°C. The olivines are also very fresh.

Vesicles (Pieces 9-10): contain about 4% irregular cavities which may be vesicles or diptyctaxitic cavities. They are about 1 mm across, and contain acicular needles of white zeolite (? natrolite).

Alteration: the samples are all permeated by water, and about 20% of the rock consists of green, very soft clay minerals (or zeolites). This has led to a loss of integrity in the samples. The individual mineral grains appear to be very fresh.

TS *13 cm (Piece 3): PORPHYRITIC DOLERITE, 13.2% plagioclase phenocrysts (1-5 mm), seriate gradation into groundmass. Groundmass of olivine (6.4%); plagioclase (44.3%); and augite (17.2%); magnetite (4.0%); grain size 0.5-4 mm, subophitic texture. No alteration of minerals seen, but interstices filled with green clay (~10.9%).

*Mineral proportions determined by point counting.

TS 32 cm (Piece 6): DOLERITE (subophitic texture). No phenocrysts. Groundmass of olivine (3.2%); plagioclase (50.4%); clinopyroxene (28.6%); magnetite (7.3%). No alteration of minerals but interstices filled with clay (6.5%) and zeolite (0.3%).

64-477-10 Depth: 67.5 to 77.0 m
SECTION 1: DOMINANT LITHOLOGY: dolerite.

Macroscopic Description
 Friable, dark green gray (5G 2/1) water-permeated medium- to coarse-grained dolerite. As in Core 9, there are two distinct lithologies.

Type 1 (Pieces 1-3): medium-grained altered dolerite, dark greenish gray, aphyric. Vesicles occur in Piece 3*. Zeolites in cavities. Constituent minerals (olivine?, pyroxene and feldspar) appear fresh but are easily separated from one another due to alteration.

Type 2 (Pieces 4-15): coarse-grained, feldspar-rich dolerite. Phenocrysts of feldspar, up to 1 cm across, in a coarse matrix of olivine(7), pyroxene and feldspar. Again, severe alteration indicated by friable nature and presence of ~10-20% clay minerals, although constituent minerals are not visibly altered. Groundmass grains range in size from about 0.5 mm (olivine) up to about 5 mm (feldspar). Zeolites again present in cavities.

*Piece 3 may represent a chill zone.

64-477-11 Depth: 77.0 to 86.5 m
SECTION 1: DOMINANT LITHOLOGY: coarse dolerite or GABBRO.

Macroscopic Description

Dark greenish gray coarse-grained dolerite or medium-grained gabbro. The top of the core is very similar to Core 10, Pieces 4-15, with medium-grained dolerite containing ~15% plagioclase phenocrysts. After about Piece 9, the rock becomes more coarse, all crystals appear to attain the size of the plagioclase phenocrysts seen in Pieces 1-9 (i.e. approximately 3-6 mm across).

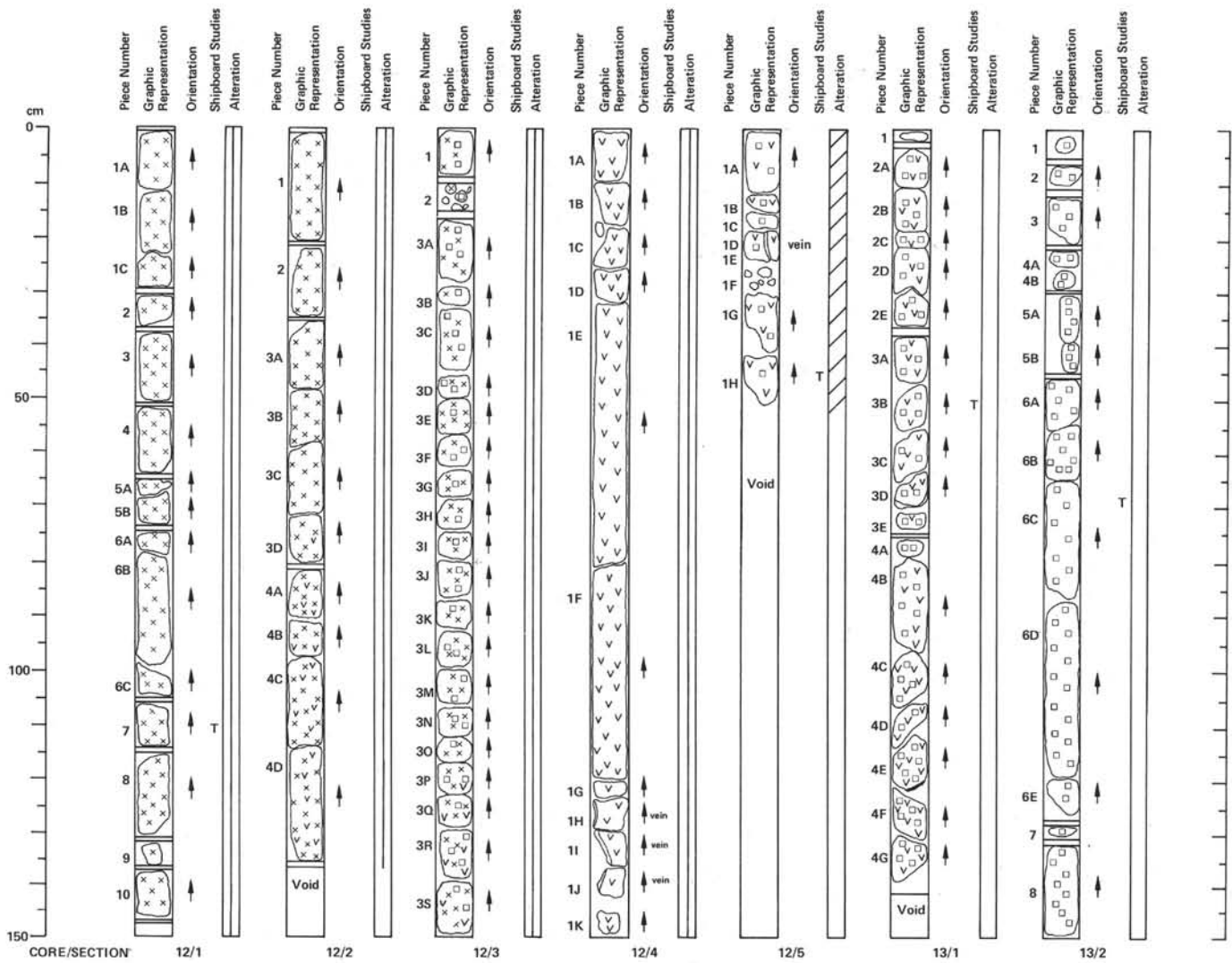
The rock comprises fresh olivine, pyroxene and plagioclase, with abundant soft, light green clay minerals (about 20-30%) in the mineral interstices. The rock is again permeated by water. Occasional large plagioclase phenocrysts occur in the coarse, gabbroic section (Piece 10 onwards); they are up to 10 mm across. Generally, the grain size in the gabbro is from about 1-6 mm.

TS 43 cm (Piece 8): COARSE DOLERITE OR GABBRO. Strongly inequigranular/porphyritic, with subophitic groundmass. Phenocrysts: plagioclase (~An₆₀), up to 6 mm, 29% of rock, large, lath-shaped and tabular crystals, seriate in size from groundmass, zoned, and frequently aggregated. Groundmass: olivine 6.3%, anhedral crystals up to 2 mm may be phenocrystic (i.e. pre-eruptive); augite; 15.3%, anhedral crystals up to 6 mm, subophitically and ophitically enclosing plagioclase laths; plagioclase 35.3%, laths, about 0.5-2 mm long; Titanite 3.6%. Distinction between groundmass-phenocrysts difficult (cavities 3.2% interstitial to crystals). Alteration: minerals not altered but about 7.2% of rock comprises clays and zeolites in interstices.

SECTION 2: DOMINANT LITHOLOGY: ALTERED GABBRO.

Macroscopic Description

Coarse-grained equigranular by gabbro with fresh euhedral-pyroxene phenocrysts, 2-5 mm and fresh plagioclase phenocrysts 2-5 mm in size. Smaller olivines 1-2 mm in size and pale yellow also present. Major phenocrysts minerals have been separated along grain boundaries which are filled with a greenish turquoise blue clay mineral and a zeolite that is acicular where found in vugs. All pyroxenes and feldspars are very fresh and have not been altered. About 20% of the rock consists of the clay minerals.



64-477-12 Depth 86.5 to 96.0 m

SECTION 1: DOMINANT LITHOLOGY: GABBRO.

Macroscopic Description

Medium-grained dark green gray altered gabbro. Inequigranular, slightly porphyritic, with grains between 1–6 mm, comprising fresh crystals of plagioclase, pyroxene and olivine. Interstitial to these grains is an abundant light green clay mineral, about 20% of rock. Rock is less friable than in previous cores, but is otherwise very similar to Core 11, Section 2. Occasional plagioclase phenocrysts present.

TS 110 cm (Piece 7): COARSE DOLERITE OR GABBRO. Texture: subophitic, with seriate plagioclase texture. Phenocrysts: plagioclase about 7.4% (up to 4 mm), tabulate, frequently broken. Seriate from groundmass so division between phenocrysts and groundmass fairly arbitrary. Groundmass: olivine: 11.4%, up to 1.5 mm across, anhedral to subhedral crystals; augite: 17.2%, up to 2 mm across, irregular crystals suboptically enclosing plagioclase; plagioclase: 47.2%, up to 2 mm across, elongate, lath-shaped; and magnetite 2.8%. Cavities ~2.2%, <0.5 mm across. Lying in interstices between crystals, these are effectively diktytaxitic cavities. Although they are now empty, they probably were filled with very soft clay minerals. Alteration: about 11.5% of the rock consists of green clays and zeolite in interstitial cavities. There is slight alteration of the olivine to clay.

64-477-12 Depth 86.5 to 96.0 m

SECTION 2: DOMINANT LITHOLOGY: altered GABBRO AND COARSE DOLERITE.

Macroscopic Description

Dark green gray medium-grained inequigranular to porphyritic gabbro (to dolerite).

Piece at the upper half of the core tend to have coarse texture, similar to Section 1 of Core 12, with a slight gradation to a medium-grained doleritic texture in the lower half of the core. Plagioclase crystals tend to be prominent, and about 10% remain at ~6 mm grain-size throughout the section, producing a porphyritic texture in the lower half of the core. The main transition occurs in Sections 3 and 4. Main minerals are fresh clinopyroxene, olivine and plagioclase.

Alteration is a 20% pale green clay mineral and zeolites. Matrix rather than mineral grains altered. Pale green clay minerals face the joint surfaces (upper and lower) on several pieces.

SECTION 3: DOMINANT LITHOLOGY: GABBRO TRANSITIONAL TO PLAGIOCLASE PHYRIC DOLERITE at base of section.

Macroscopic Description

Medium-grained gabbro similar to Sections 1 and 2, however a subtle transition is discernable through Sections 2 through 3 until at the base of Section 3 (this section) the rock has become fine-grained to the point where it grades into a doleritic texture with the plagioclase phenocrysts predominant. In the upper part of the section plagioclase and pyroxene are of approximate equal size, however plagioclase is 1.5 times more abundant. Olivine is still present as a smaller phenocryst phase. All phenocrysts are very fresh and alteration is restricted to intergrain surfaces which are completely filled with bluish green clay minerals and fibrous acicular zeolite.

SECTION 4: DOMINANT LITHOLOGY: FELDSPAR PHYRIC DOLERITE.

Macroscopic Description

A continuation of Section 4. Dark green gray medium- to fine-grained doleritic rock. Phenocrysts of plagioclase (about 10%) (1–5 mm) is in a fine- to medium-grained groundmass of plagioclase, clinopyroxene and olivine. Abundant clay minerals in groundmass. Mineral grains not altered. Clay mineral coatings on several pieces indicating small scale veining. Pieces 1E to F were continuous prior to sawing

(no calcite veining). The base of the section tends to a basaltic texture.

Although the alteration is rather severe, there is less clay mineral present than in previous sections (now about 10%). The rock is therefore grayer in color.

SECTION 5: DOMINANT LITHOLOGY: PORPHYRITIC DOLERITE OR BASALT.

Macroscopic Description

Dark gray, fine-grained plagioclase phyric dolerite or basalt. Phenocrysts: plagioclase, lath-shaped and irregular tabulate crystals up to 6 mm, about 10% of rock. Groundmass: less than 0.5 mm grain-sized. Gradational in Sections 4 and 5. Alteration: moderate. Development of clay minerals as in previous sections not seen. Veining in Pieces 1A–D. No vesicles.

TS 47 cm (Piece 1H): subophitic to intergranular PLAGIOCLASE PHYRIC BASALT. Large – up to 4 mm laths (sometimes broken) of plagioclase (An₄₉) in a matrix of smaller plagioclase phenocrysts and clinopyroxene and olivine phenocrysts surrounded by plagioclase microlites and abundant opaques (Ti-rich magnetite). Some alteration of clinopyroxene and olivine contributes to 13% clay mineral (greenish) content. Modal content is: plagioclase phenocrysts 26%, olivine phenocrysts and groundmass 11%, clinopyroxene phenocrysts and groundmass 12%, plagioclase groundmass 27%, magnetite 11%, and clay minerals 13%. Many of the larger plagioclase laths are strongly zoned and some contain brownish-bleb shaped inclusions. Larger olivines are often fractured with alteration taking place along the fracture boundaries.

64-477-13 Depth: 96.0 to 101.5 m

SECTION 1: DOMINANT LITHOLOGY: PLAGIOCLASE-PHYRIC DOLERITE.

Macroscopic Description

Medium light gray dolerite with plagioclase phenocrysts from 1–4 mm in size. Pyroxene and opaques and possibly olivine are other components. Rock appears fresh and unfractured and is not veined.

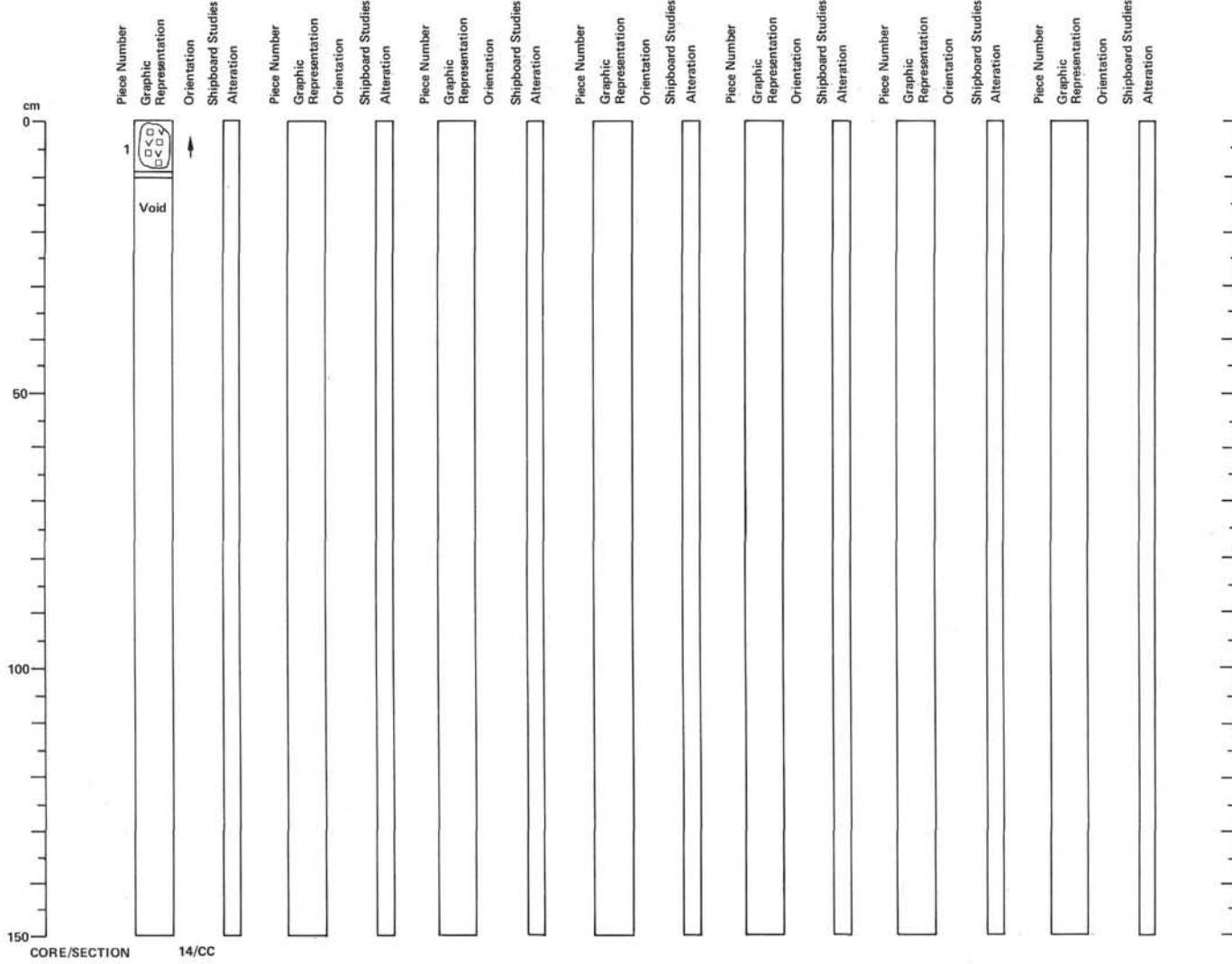
TS at 53 cm (Piece 3B): Sub-ophitic to intergranular plagioclase-phyric dolerite. Large plagioclase (~An₄₅) phenocrysts (0.5–2 mm) surrounded by smaller clinopyroxene and olivine microphenocrysts and groundmass composed of plagioclase laths and clinopyroxene and olivine. Abundant titanomagnetite in groundmass which shows well-developed cruciform habit. Modal content is: plagioclase phenocrysts 20%, olivine 14%, clinopyroxene 13%, groundmass plagioclase 31%, and magnetite 11%.

SECTION 2: DOMINANT LITHOLOGY: PLAGIOCLASE-PHYRIC DOLERITE.

Macroscopic Description

Medium light gray (N6) dolerite with plagioclase phenocrysts in a matrix of finer plagioclase laths, pyroxene, olivine and opaques. No fracturing in pieces and no veining – rock appears fresh. Similar in all respects to Section 1 of Core 13.

TS at 69 cm (Piece 6C): Sub-ophitic to intergranular medium-grained dolerite. Large plagioclase phenocrysts up to 4 mm (~An₅₀) surrounded by smaller plagioclase laths enclosing or partially enclosing anhedral to subhedral grains of clinopyroxene and olivine. Rock has approximately 15% plagioclase phenocrysts, 15% small olivine phenocrysts and ~10% clinopyroxene. Groundmass is principally plagioclase microlites (~30%) plus equal amounts of olivine and clinopyroxene (~10% each). Abundant (Ti-rich?) magnetite exhibiting well-developed cruciform (~5%) habit. Slight alteration is restricted to intergrain spaces and rarely after olivine and clinopyroxene phenocrysts. Clinopyroxene phenocrysts. Clinopyroxene and olivine are fresh but are commonly fractured along cleavage planes and orthogonal to them.



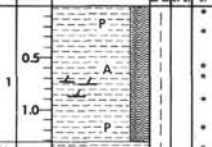
64-477-14

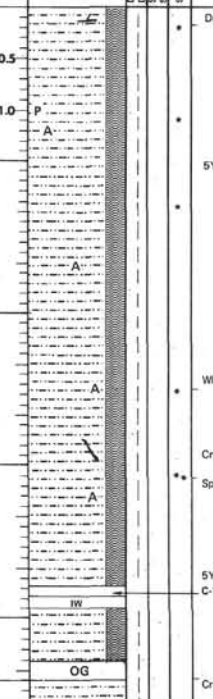
Depth 101.5 to 105.5 m

CORE-CATCHER: DOMINANT LITHOLOGY: PLAGIOCLASE PHYRIC DOLERITE.

Macroscopic Description

Nine cm piece of dolerite similar in all respects to Sections 1 and 2 of Core 13. Thin piece was found jammed in the Core-Catcher and consequently the contact, between the dolerite sill above and the claystone below in Core 15, was not recovered but is inferred to be located within the drilled interval 101.5-105.5 m sub-bottom.

SITE 477		HOLE		CORE 15		CORED INTERVAL 105.0-115.0 m																																																																																																																																																																																															
TIME - ROCK UNIT	BIOSTRATIGRAPHIC ZONE	FOSSIL CHARACTER			SECTION METERS	GRAPHIC LITHOLOGY	LITHOLOGIC DESCRIPTION																																																																																																																																																																																														
		FORAMINIFERS	NANNOFOSSILS	RADIOLARIANS				DIAZONIA																																																																																																																																																																																													
7							<p>Hard lump Silty claystone 5YR 4/1 White concretion soft anhydrite Tan dolomite silt Sulfide wisp</p> <p>Waxy clay</p> <p>Uniform, coherent, very hard brownish, waxy gray (5YR 4/1 to 5/1), CLAY TO SILTY CLAY with purple cast. Surface scattered with tiny specks of varying composition. Anhydrite clusters (1-3 mm) around 51-59 cm. No bedding or sedimentary structures visible. Appears to be baked; no fossils preserved. Hydrothermal sediment. Some sulfide concretions along thin seams (pyrite).</p> <p>Coarse fractions contain dolomite rhombs and pyrite cubes, euhedral white crystals, quartz, a platy black minerals and clay lumps. In smear slides clay minerals are chlorite or illite. Pyrite as 4 to 15 micron cubes. Dolomite rhombs (4 to 16 microns) surfaces a little uneven clouded with inclusions; may be ferroan. Many feldspars altered, zeolite or albite. Sandy parts include euhedral, heavy minerals, zircon, apatite, and sphene.</p> <p>SMEAR SLIDE SUMMARY</p> <table border="1"> <thead> <tr> <th></th> <th>1-2 (D)</th> <th>1-24 (D)</th> <th>1-59 (M)</th> <th>1-68 (M)</th> <th>1-90 (D)</th> </tr> </thead> <tbody> <tr> <td>TEXTURE:</td> <td></td> <td></td> <td></td> <td></td> <td></td> </tr> <tr> <td>Sand</td> <td>5</td> <td>-</td> <td>-</td> <td>-</td> <td>1</td> </tr> <tr> <td>Silt</td> <td>35</td> <td>20</td> <td>-</td> <td>75</td> <td>15</td> </tr> <tr> <td>Clay</td> <td>60</td> <td>80</td> <td>-</td> <td>25</td> <td>84</td> </tr> <tr> <td>COMPOSITION:</td> <td></td> <td></td> <td></td> <td></td> <td></td> </tr> <tr> <td>Quartz</td> <td>30</td> <td>-</td> <td>-</td> <td>5</td> <td>10</td> </tr> <tr> <td>Feldspar</td> <td>2</td> <td>10</td> <td>-</td> <td>3</td> <td>12</td> </tr> <tr> <td>Mica</td> <td>-</td> <td>-</td> <td>-</td> <td>-</td> <td>-</td> </tr> <tr> <td>Heavy minerals</td> <td>-</td> <td>-</td> <td>-</td> <td>-</td> <td>1</td> </tr> <tr> <td>Clay</td> <td>55</td> <td>30</td> <td>-</td> <td>15</td> <td>75</td> </tr> <tr> <td>Coated grains</td> <td>-</td> <td>50</td> <td>-</td> <td>-</td> <td>-</td> </tr> <tr> <td>Pyrite</td> <td>5</td> <td>5</td> <td>-</td> <td>5</td> <td>5</td> </tr> <tr> <td>Zeolite</td> <td>1</td> <td>-</td> <td>-</td> <td>2</td> <td>3</td> </tr> <tr> <td>Carbonate unsp. c.</td> <td>2</td> <td>-</td> <td>-</td> <td>-</td> <td>TR</td> </tr> <tr> <td>Calc. nannofossils</td> <td>1</td> <td>-</td> <td>-</td> <td>-</td> <td>-</td> </tr> <tr> <td>Plant debris</td> <td>-</td> <td>2</td> <td>-</td> <td>4</td> <td>5</td> </tr> <tr> <td>Dolomite rhombs</td> <td>5</td> <td>5</td> <td>-</td> <td>70</td> <td>-</td> </tr> <tr> <td>Anhydrite</td> <td>-</td> <td>-</td> <td>100</td> <td>-</td> <td>-</td> </tr> <tr> <td>Apatite</td> <td>-</td> <td>2</td> <td>-</td> <td>-</td> <td>-</td> </tr> </tbody> </table> <p>SMEAR SLIDE SUMMARY</p> <table border="1"> <thead> <tr> <th></th> <th>1-119 (D)</th> <th>CF (a) (silt)</th> <th>CF (a) (fine)</th> <th>CC (D)</th> </tr> </thead> <tbody> <tr> <td>TEXTURE:</td> <td></td> <td></td> <td></td> <td></td> </tr> <tr> <td>Sand</td> <td>TR</td> <td>-</td> <td>-</td> <td>-</td> </tr> <tr> <td>Silt</td> <td>65</td> <td>-</td> <td>25</td> <td>25</td> </tr> <tr> <td>Clay</td> <td>35</td> <td>-</td> <td>75</td> <td>75</td> </tr> <tr> <td>COMPOSITION:</td> <td></td> <td></td> <td></td> <td></td> </tr> <tr> <td>Quartz</td> <td>10</td> <td>30</td> <td>10</td> <td>10</td> </tr> <tr> <td>Feldspar</td> <td>40</td> <td>5</td> <td>10</td> <td>15</td> </tr> <tr> <td>Clay</td> <td>35</td> <td>-</td> <td>80</td> <td>60</td> </tr> <tr> <td>Glauconite</td> <td>-</td> <td>TR</td> <td>-</td> <td>-</td> </tr> <tr> <td>Pyrite</td> <td>5</td> <td>3</td> <td>2</td> <td>8</td> </tr> <tr> <td>Zeolite</td> <td>1</td> <td>3</td> <td>TR?</td> <td>5</td> </tr> <tr> <td>Plant debris</td> <td>2</td> <td>-</td> <td>15</td> <td>5</td> </tr> <tr> <td>Dolomite rhombs</td> <td>7</td> <td>50</td> <td>15</td> <td>-</td> </tr> </tbody> </table> <p>(a) composite sample Section 1</p> <p>CARBONATE BOMB: 1-26 = 1%</p>		1-2 (D)	1-24 (D)	1-59 (M)	1-68 (M)	1-90 (D)	TEXTURE:						Sand	5	-	-	-	1	Silt	35	20	-	75	15	Clay	60	80	-	25	84	COMPOSITION:						Quartz	30	-	-	5	10	Feldspar	2	10	-	3	12	Mica	-	-	-	-	-	Heavy minerals	-	-	-	-	1	Clay	55	30	-	15	75	Coated grains	-	50	-	-	-	Pyrite	5	5	-	5	5	Zeolite	1	-	-	2	3	Carbonate unsp. c.	2	-	-	-	TR	Calc. nannofossils	1	-	-	-	-	Plant debris	-	2	-	4	5	Dolomite rhombs	5	5	-	70	-	Anhydrite	-	-	100	-	-	Apatite	-	2	-	-	-		1-119 (D)	CF (a) (silt)	CF (a) (fine)	CC (D)	TEXTURE:					Sand	TR	-	-	-	Silt	65	-	25	25	Clay	35	-	75	75	COMPOSITION:					Quartz	10	30	10	10	Feldspar	40	5	10	15	Clay	35	-	80	60	Glauconite	-	TR	-	-	Pyrite	5	3	2	8	Zeolite	1	3	TR?	5	Plant debris	2	-	15	5	Dolomite rhombs	7	50	15	-
	1-2 (D)	1-24 (D)	1-59 (M)	1-68 (M)	1-90 (D)																																																																																																																																																																																																
TEXTURE:																																																																																																																																																																																																					
Sand	5	-	-	-	1																																																																																																																																																																																																
Silt	35	20	-	75	15																																																																																																																																																																																																
Clay	60	80	-	25	84																																																																																																																																																																																																
COMPOSITION:																																																																																																																																																																																																					
Quartz	30	-	-	5	10																																																																																																																																																																																																
Feldspar	2	10	-	3	12																																																																																																																																																																																																
Mica	-	-	-	-	-																																																																																																																																																																																																
Heavy minerals	-	-	-	-	1																																																																																																																																																																																																
Clay	55	30	-	15	75																																																																																																																																																																																																
Coated grains	-	50	-	-	-																																																																																																																																																																																																
Pyrite	5	5	-	5	5																																																																																																																																																																																																
Zeolite	1	-	-	2	3																																																																																																																																																																																																
Carbonate unsp. c.	2	-	-	-	TR																																																																																																																																																																																																
Calc. nannofossils	1	-	-	-	-																																																																																																																																																																																																
Plant debris	-	2	-	4	5																																																																																																																																																																																																
Dolomite rhombs	5	5	-	70	-																																																																																																																																																																																																
Anhydrite	-	-	100	-	-																																																																																																																																																																																																
Apatite	-	2	-	-	-																																																																																																																																																																																																
	1-119 (D)	CF (a) (silt)	CF (a) (fine)	CC (D)																																																																																																																																																																																																	
TEXTURE:																																																																																																																																																																																																					
Sand	TR	-	-	-																																																																																																																																																																																																	
Silt	65	-	25	25																																																																																																																																																																																																	
Clay	35	-	75	75																																																																																																																																																																																																	
COMPOSITION:																																																																																																																																																																																																					
Quartz	10	30	10	10																																																																																																																																																																																																	
Feldspar	40	5	10	15																																																																																																																																																																																																	
Clay	35	-	80	60																																																																																																																																																																																																	
Glauconite	-	TR	-	-																																																																																																																																																																																																	
Pyrite	5	3	2	8																																																																																																																																																																																																	
Zeolite	1	3	TR?	5																																																																																																																																																																																																	
Plant debris	2	-	15	5																																																																																																																																																																																																	
Dolomite rhombs	7	50	15	-																																																																																																																																																																																																	

SITE 477		HOLE		CORE 16		CORED INTERVAL 115.0-124.5 m																																																																																																																																						
TIME - ROCK UNIT	BIOSTRATIGRAPHIC ZONE	FOSSIL CHARACTER			SECTION METERS	GRAPHIC LITHOLOGY	LITHOLOGIC DESCRIPTION																																																																																																																																					
		FORAMINIFERS	NANNOFOSSILS	RADIOLARIANS				DIAZONIA																																																																																																																																				
7							<p>Dolomite</p> <p>Hydrothermal sediment, uniform, hard, light brownish-gray to brownish-gray (5YR 6/1-4/1) CLAY TO CLAYEY SILTSTONE with some coarse authigenic minerals scattered on the core surface. Gritty when scraped. Abundant pyrite in coarse fractions and filling thin seams. Together with anhydrite. Anhydrite(?) also occurs as fuzzy nodules or small (1 to 2 mm) specks in clay and claystone. Occasional twinned zeolite. No sedimentary structures or bedding visible.</p> <p>5YR 6/1</p> <p>Section 1, 10 cm: large brown dolomitic claystone nodule.</p> <p>Section 3, 150 cm: coarse translucent mineral filling vein seam.</p> <p>SS: dolomite, very fine-grained, irregular, wood bits dark brown to black common. Clays clear with R. I. -1.56 illite chlorite. Feldspar grains altered to clay.</p> <p>SMEAR SLIDE SUMMARY</p> <table border="1"> <thead> <tr> <th></th> <th>1-10 (M)</th> <th>1-108 (D)</th> <th>2-45 (D)</th> <th>3-78 (D)</th> <th>4-14 (D)</th> <th>4-17 (M)</th> </tr> </thead> <tbody> <tr> <td>TEXTURE:</td> <td></td> <td></td> <td></td> <td></td> <td></td> <td></td> </tr> <tr> <td>Sand</td> <td>-</td> <td>-</td> <td>2</td> <td>-</td> <td>-</td> <td>-</td> </tr> <tr> <td>Silt</td> <td>-</td> <td>60</td> <td>30</td> <td>-</td> <td>30</td> <td>-</td> </tr> <tr> <td>Clay</td> <td>-</td> <td>40</td> <td>70</td> <td>-</td> <td>60</td> <td>-</td> </tr> <tr> <td>COMPOSITION:</td> <td></td> <td></td> <td></td> <td></td> <td></td> <td></td> </tr> <tr> <td>Quartz</td> <td>-</td> <td>5</td> <td>30</td> <td>15</td> <td>10</td> <td>-</td> </tr> <tr> <td>Feldspar</td> <td>-</td> <td>5</td> <td>-</td> <td>10</td> <td>15</td> <td>-</td> </tr> <tr> <td>Mica</td> <td>-</td> <td>1</td> <td>-</td> <td>-</td> <td>-</td> <td>-</td> </tr> <tr> <td>Heavy minerals</td> <td>-</td> <td>2</td> <td>-</td> <td>-</td> <td>1</td> <td>-</td> </tr> <tr> <td>Clay</td> <td>20</td> <td>40</td> <td>65</td> <td>-</td> <td>70</td> <td>-</td> </tr> <tr> <td>Pyrite</td> <td>2</td> <td>5</td> <td>3</td> <td>5</td> <td>5</td> <td>-</td> </tr> <tr> <td>Zeolite</td> <td>3</td> <td>2</td> <td>-</td> <td>5</td> <td>-</td> <td>-</td> </tr> <tr> <td>Carbonate unsp. c.</td> <td>-</td> <td>-</td> <td>2</td> <td>-</td> <td>-</td> <td>-</td> </tr> <tr> <td>Fish remains</td> <td>-</td> <td>-</td> <td>TR</td> <td>-</td> <td>-</td> <td>-</td> </tr> <tr> <td>Plant debris</td> <td>-</td> <td>1</td> <td>1</td> <td>-</td> <td>TR</td> <td>-</td> </tr> <tr> <td>Dolomite</td> <td>75</td> <td>30</td> <td>-</td> <td>-</td> <td>-</td> <td>-</td> </tr> <tr> <td>Chalcedony cement</td> <td>-</td> <td>10</td> <td>-</td> <td>-</td> <td>-</td> <td>-</td> </tr> <tr> <td>Anhydrite</td> <td>-</td> <td>-</td> <td>-</td> <td>70</td> <td>-</td> <td>100</td> </tr> </tbody> </table> <p>CARBONATE BOMB: 1-36 = 3% 2-71 = 0% 3-99 = 0%</p> <p>White nodule</p> <p>Crystal vein</p> <p>Speck</p> <p>5Y 5/1</p> <p>C-14 SAMPLE</p> <p>Crystal vein</p>		1-10 (M)	1-108 (D)	2-45 (D)	3-78 (D)	4-14 (D)	4-17 (M)	TEXTURE:							Sand	-	-	2	-	-	-	Silt	-	60	30	-	30	-	Clay	-	40	70	-	60	-	COMPOSITION:							Quartz	-	5	30	15	10	-	Feldspar	-	5	-	10	15	-	Mica	-	1	-	-	-	-	Heavy minerals	-	2	-	-	1	-	Clay	20	40	65	-	70	-	Pyrite	2	5	3	5	5	-	Zeolite	3	2	-	5	-	-	Carbonate unsp. c.	-	-	2	-	-	-	Fish remains	-	-	TR	-	-	-	Plant debris	-	1	1	-	TR	-	Dolomite	75	30	-	-	-	-	Chalcedony cement	-	10	-	-	-	-	Anhydrite	-	-	-	70	-	100
	1-10 (M)	1-108 (D)	2-45 (D)	3-78 (D)	4-14 (D)	4-17 (M)																																																																																																																																						
TEXTURE:																																																																																																																																												
Sand	-	-	2	-	-	-																																																																																																																																						
Silt	-	60	30	-	30	-																																																																																																																																						
Clay	-	40	70	-	60	-																																																																																																																																						
COMPOSITION:																																																																																																																																												
Quartz	-	5	30	15	10	-																																																																																																																																						
Feldspar	-	5	-	10	15	-																																																																																																																																						
Mica	-	1	-	-	-	-																																																																																																																																						
Heavy minerals	-	2	-	-	1	-																																																																																																																																						
Clay	20	40	65	-	70	-																																																																																																																																						
Pyrite	2	5	3	5	5	-																																																																																																																																						
Zeolite	3	2	-	5	-	-																																																																																																																																						
Carbonate unsp. c.	-	-	2	-	-	-																																																																																																																																						
Fish remains	-	-	TR	-	-	-																																																																																																																																						
Plant debris	-	1	1	-	TR	-																																																																																																																																						
Dolomite	75	30	-	-	-	-																																																																																																																																						
Chalcedony cement	-	10	-	-	-	-																																																																																																																																						
Anhydrite	-	-	-	70	-	100																																																																																																																																						

SITE 477		HOLE		CORE 17		CORED INTERVAL 124.5-134.0 m																																																																																																	
TIME - ROCK UNIT	BIOSTRATIGRAPHIC ZONE	FOSSIL CHARACTER			SECTION METERS	GRAPHIC LITHOLOGY	LITHOLOGIC DESCRIPTION																																																																																																
		FORAMINIFERS	NANNOFOSSILS	RADICULARIANS				DIATOMS																																																																																															
?	X	Barren			0.5	A	Anhydrite Disturbed, uniform, brownish-gray (5YR 4/1) SILTY CLAYSTONE TO CLAYEY SILTSTONE. Brecciated somewhat by drilling. Hydrothermal sediments. Gritty texture due to authigenic minerals, anhydrite(?) and pyrite seams (numerous) lined with pyrite or anhydrite. Dolomitic silts in gray brown (5YR 5/1) to medium gray (N4) clayey siltstone in bottom of core. Some parallel laminac present, faint evidence of phacoids.																																																																																																
					1.0		5YR 4/1																																																																																																
					1.0		C-14 SAMPLE																																																																																																
					2		<p>SMEAR SLIDE SUMMARY</p> <table border="1"> <tr> <td></td> <td>1-29</td> <td>2-28</td> <td>2-69</td> <td>3-23</td> <td>3-83</td> </tr> <tr> <td></td> <td>(D)</td> <td>(M)</td> <td>(D)</td> <td>(D)</td> <td>(D)</td> </tr> </table> <p>TEXTURE:</p> <table border="1"> <tr> <td>Sand</td> <td>-</td> <td>-</td> <td>-</td> <td>-</td> <td>5</td> </tr> <tr> <td>Silt</td> <td>-</td> <td>-</td> <td>40</td> <td>40</td> <td>65</td> </tr> <tr> <td>Clay</td> <td>-</td> <td>-</td> <td>60</td> <td>60</td> <td>30</td> </tr> </table> <p>COMPOSITION:</p> <table border="1"> <tr> <td>Quartz</td> <td>15</td> <td>5</td> <td>10</td> <td>10</td> <td>10</td> </tr> <tr> <td>Feldspar</td> <td>15</td> <td>5</td> <td>15</td> <td>10</td> <td>20</td> </tr> <tr> <td>Mica</td> <td>-</td> <td>-</td> <td>-</td> <td>-</td> <td>1</td> </tr> <tr> <td>Heavy minerals</td> <td>-</td> <td>2</td> <td>-</td> <td>2</td> <td>-</td> </tr> <tr> <td>Clay</td> <td>25</td> <td>65</td> <td>60</td> <td>60</td> <td>30</td> </tr> <tr> <td>Pyrite</td> <td>2</td> <td>8</td> <td>5</td> <td>5</td> <td>3</td> </tr> <tr> <td>Zeolite</td> <td>-</td> <td>5</td> <td>-</td> <td>3</td> <td>-</td> </tr> <tr> <td>Calc. nannofossils</td> <td>-</td> <td>-</td> <td>TR</td> <td>-</td> <td>-</td> </tr> <tr> <td>Organics</td> <td>-</td> <td>5</td> <td>-</td> <td>10</td> <td>-</td> </tr> <tr> <td>Anhydrite</td> <td>40</td> <td>-</td> <td>1</td> <td>-</td> <td>TR</td> </tr> <tr> <td>Dolomite</td> <td>-</td> <td>-</td> <td>5</td> <td>-</td> <td>25</td> </tr> </table> <p>3, 21-23 Lithology Clayed silt Sand 4.85 Silt 59.71 Clay 35.44</p> <p>CARBONATE BOMB: 1.41 = 3% 3.44 = 0%</p> <p>NOTE: Site 477, Core 18, 134.0-143.5 m: NO RECOVERY.</p>		1-29	2-28	2-69	3-23	3-83		(D)	(M)	(D)	(D)	(D)	Sand	-	-	-	-	5	Silt	-	-	40	40	65	Clay	-	-	60	60	30	Quartz	15	5	10	10	10	Feldspar	15	5	15	10	20	Mica	-	-	-	-	1	Heavy minerals	-	2	-	2	-	Clay	25	65	60	60	30	Pyrite	2	8	5	5	3	Zeolite	-	5	-	3	-	Calc. nannofossils	-	-	TR	-	-	Organics	-	5	-	10	-	Anhydrite	40	-	1	-	TR	Dolomite	-	-	5	-	25
	1-29	2-28	2-69	3-23	3-83																																																																																																		
	(D)	(M)	(D)	(D)	(D)																																																																																																		
Sand	-	-	-	-	5																																																																																																		
Silt	-	-	40	40	65																																																																																																		
Clay	-	-	60	60	30																																																																																																		
Quartz	15	5	10	10	10																																																																																																		
Feldspar	15	5	15	10	20																																																																																																		
Mica	-	-	-	-	1																																																																																																		
Heavy minerals	-	2	-	2	-																																																																																																		
Clay	25	65	60	60	30																																																																																																		
Pyrite	2	8	5	5	3																																																																																																		
Zeolite	-	5	-	3	-																																																																																																		
Calc. nannofossils	-	-	TR	-	-																																																																																																		
Organics	-	5	-	10	-																																																																																																		
Anhydrite	40	-	1	-	TR																																																																																																		
Dolomite	-	-	5	-	25																																																																																																		
					3		<p>IW</p> <p>5YR 5/1</p> <p>N4, dolomitic</p> <p>CC</p>																																																																																																

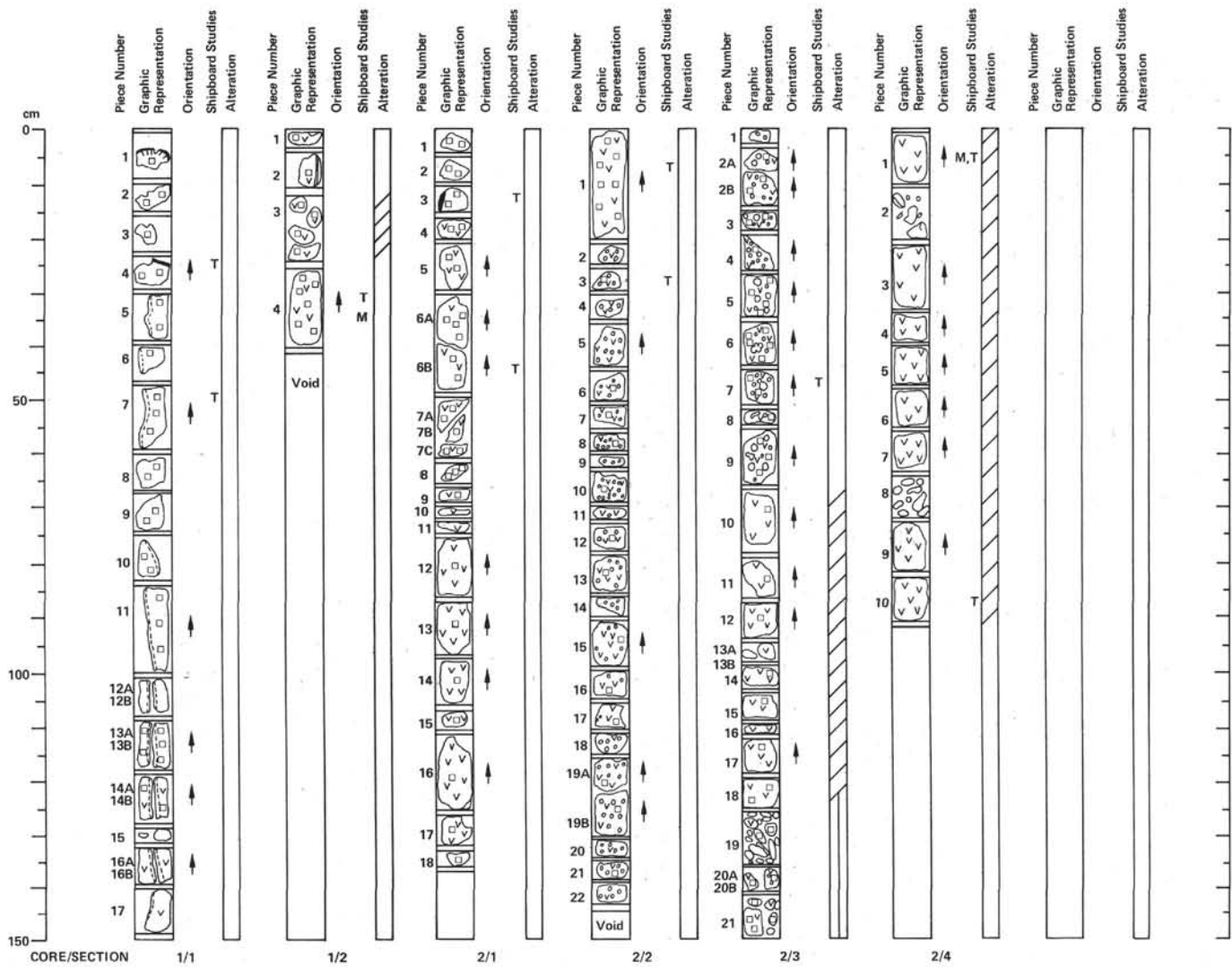
SITE 477		HOLE		CORE 19		CORED INTERVAL 143.5-153.0 m																																																																																						
TIME - ROCK UNIT	BIOSTRATIGRAPHIC ZONE	FOSSIL CHARACTER			SECTION METERS	GRAPHIC LITHOLOGY	LITHOLOGIC DESCRIPTION																																																																																					
		FORAMINIFERS	NANNOFOSSILS	RADICULARIANS				DIATOMS																																																																																				
?		Barren			0.5	VOID	Sand Drill breccia to soup of uniform, medium light gray (N6) to medium gray (N5) HARD CLAYEY TO SANDY SILTSTONE TO "SOOTY" SILTSTONE. Hydrothermal sediment. Silt includes many authigenic minerals. Pyrite common. No bedding preserved. Hard chunks very friable.																																																																																					
					1.0		N6-N6 Section 1: dolomitic pebbles at top of core (dusky yellow, 5Y 6/4). Section 2: siltstone becomes coated with fine light brown carbon particules similar to soot which seeps from fractures at the base of the core, does not permeate the siltstone.																																																																																					
					1.0		Silty clay Some rare benthic (shallow water?) foraminifers in Core-Catcher. SS notes: Terrigenous grains only partially altered, large feldspars with serrated edges. Very few replaced or large authigenic grains. Organic bits black. Very little clay. Some scattered subhedral feldspars. Pyrite cubes or framboids.																																																																																					
					3		<p>SMEAR SLIDE SUMMARY</p> <table border="1"> <tr> <td></td> <td>1-56</td> <td>2-138</td> <td>3-27</td> <td>CC</td> </tr> <tr> <td></td> <td>(D)</td> <td>(D)</td> <td>(D)</td> <td>(D)</td> </tr> </table> <p>TEXTURE:</p> <table border="1"> <tr> <td>Sand</td> <td>2</td> <td>TR</td> <td>30</td> <td>30</td> </tr> <tr> <td>Silt</td> <td>60</td> <td>40</td> <td>30</td> <td>30</td> </tr> <tr> <td>Clay</td> <td>40</td> <td>60</td> <td>40</td> <td>40</td> </tr> </table> <p>COMPOSITION:</p> <table border="1"> <tr> <td>Quartz</td> <td>5</td> <td>10</td> <td>20</td> <td>20</td> </tr> <tr> <td>Feldspar</td> <td>25</td> <td>20</td> <td>10</td> <td>15</td> </tr> <tr> <td>Mica</td> <td>-</td> <td>-</td> <td>2</td> <td>2</td> </tr> <tr> <td>Heavy minerals</td> <td>-</td> <td>-</td> <td>4</td> <td>-</td> </tr> <tr> <td>Clay</td> <td>35</td> <td>50</td> <td>40</td> <td>50</td> </tr> <tr> <td>Pyrite</td> <td>5</td> <td>8</td> <td>8</td> <td>8</td> </tr> <tr> <td>Zeolite</td> <td>-</td> <td>7</td> <td>-</td> <td>-</td> </tr> <tr> <td>Carbonate unspc.</td> <td>-</td> <td>1</td> <td>10</td> <td>5</td> </tr> <tr> <td>Plant debris</td> <td>5</td> <td>2</td> <td>3</td> <td>-</td> </tr> <tr> <td>Anhydrite</td> <td>1</td> <td>TR</td> <td>-</td> <td>-</td> </tr> <tr> <td>Apatite</td> <td>TR</td> <td>-</td> <td>-</td> <td>-</td> </tr> <tr> <td>Dolomite</td> <td>12</td> <td>5</td> <td>-</td> <td>-</td> </tr> </table> <p>2, 135-137 Lithology Sand-silt-clay Sand 41.21 Silt 34.76 Clay 24.03</p> <p>CARBONATE BOMB: 3.29 = 5%</p>		1-56	2-138	3-27	CC		(D)	(D)	(D)	(D)	Sand	2	TR	30	30	Silt	60	40	30	30	Clay	40	60	40	40	Quartz	5	10	20	20	Feldspar	25	20	10	15	Mica	-	-	2	2	Heavy minerals	-	-	4	-	Clay	35	50	40	50	Pyrite	5	8	8	8	Zeolite	-	7	-	-	Carbonate unspc.	-	1	10	5	Plant debris	5	2	3	-	Anhydrite	1	TR	-	-	Apatite	TR	-	-	-	Dolomite	12	5	-	-
	1-56	2-138	3-27	CC																																																																																								
	(D)	(D)	(D)	(D)																																																																																								
Sand	2	TR	30	30																																																																																								
Silt	60	40	30	30																																																																																								
Clay	40	60	40	40																																																																																								
Quartz	5	10	20	20																																																																																								
Feldspar	25	20	10	15																																																																																								
Mica	-	-	2	2																																																																																								
Heavy minerals	-	-	4	-																																																																																								
Clay	35	50	40	50																																																																																								
Pyrite	5	8	8	8																																																																																								
Zeolite	-	7	-	-																																																																																								
Carbonate unspc.	-	1	10	5																																																																																								
Plant debris	5	2	3	-																																																																																								
Anhydrite	1	TR	-	-																																																																																								
Apatite	TR	-	-	-																																																																																								
Dolomite	12	5	-	-																																																																																								
					CC																																																																																							

SITE 477 HOLE		CORE 20		CORED INTERVAL 153.0-162.5 m																																																															
TIME - ROCK UNIT	BIOSTRATIGRAPHIC ZONE	FOSSIL CHARACTER			SECTION METERS	GRAPHIC LITHOLOGY	LITHOLOGIC DESCRIPTION																																																												
		FORAMINIFERS	NAUPOFOSSILS	RADIOLARIANS				DIATOMS																																																											
7	VP R/R	Barren			0.5		<p>Brecciated, dark grayish-black (N2) CARBONACEOUS CLAYSTONE TO SILTY CLAYSTONE. Drill brecciated with a soupy matrix. Some small pieces of sandy siltstone (moderate induration) scattered through the breccia. Pyrite fragments throughout core. Pyrite crystals common, mostly euhedral cubes.</p> <p>Smear slides are dominated by iron sulfides, irregular black specks (4 to 20 microns) from coaly fragments(?), large (4 to 8 microns) low birefringence clay flakes and altered, relict feldspar grains. Scattered aggregates of (2%) highly dispersive, high R. I. and birefringence? minerals. Only rare euhedral outlines.</p> <p>SMEAR SLIDE SUMMARY</p> <table border="1"> <thead> <tr> <th></th> <th>1-70 (D)</th> <th>2-70 (D)</th> <th>CC (D)</th> </tr> </thead> <tbody> <tr> <td>TEXTURE:</td> <td></td> <td></td> <td></td> </tr> <tr> <td>Sand</td> <td>-</td> <td>10</td> <td>-</td> </tr> <tr> <td>Silt</td> <td>35</td> <td>30</td> <td>25</td> </tr> <tr> <td>Clay</td> <td>65</td> <td>60</td> <td>75</td> </tr> <tr> <td>COMPOSITION:</td> <td></td> <td></td> <td></td> </tr> <tr> <td>Quartz</td> <td>8</td> <td>10</td> <td>20</td> </tr> <tr> <td>Feldspar</td> <td>5</td> <td>-</td> <td>10</td> </tr> <tr> <td>Mica</td> <td>-</td> <td>2</td> <td>-</td> </tr> <tr> <td>Clay</td> <td>60</td> <td>50</td> <td>45</td> </tr> <tr> <td>Pyrite</td> <td>12</td> <td>8</td> <td>10</td> </tr> <tr> <td>Zeolite</td> <td>-</td> <td>30</td> <td>-</td> </tr> <tr> <td>Carbonate unspc.</td> <td>10</td> <td>5(a)</td> <td>5</td> </tr> <tr> <td>Plant debris</td> <td>-</td> <td>3</td> <td>-</td> </tr> <tr> <td>Opaque organics</td> <td>12</td> <td>-</td> <td>10</td> </tr> </tbody> </table> <p>(a) Dolomite</p> <p>CARBONATE BOMB: 2.51 = 4% 2.61 = 4%</p>		1-70 (D)	2-70 (D)	CC (D)	TEXTURE:				Sand	-	10	-	Silt	35	30	25	Clay	65	60	75	COMPOSITION:				Quartz	8	10	20	Feldspar	5	-	10	Mica	-	2	-	Clay	60	50	45	Pyrite	12	8	10	Zeolite	-	30	-	Carbonate unspc.	10	5(a)	5	Plant debris	-	3	-	Opaque organics	12	-	10
								1-70 (D)	2-70 (D)	CC (D)																																																									
					TEXTURE:																																																														
Sand	-	10	-																																																																
Silt	35	30	25																																																																
Clay	65	60	75																																																																
COMPOSITION:																																																																			
Quartz	8	10	20																																																																
Feldspar	5	-	10																																																																
Mica	-	2	-																																																																
Clay	60	50	45																																																																
Pyrite	12	8	10																																																																
Zeolite	-	30	-																																																																
Carbonate unspc.	10	5(a)	5																																																																
Plant debris	-	3	-																																																																
Opaque organics	12	-	10																																																																
1.0	OG																																																																		
2	IW																																																																		
CC																																																																			

SITE 477 HOLE		CORE 21		CORED INTERVAL 162.5-172.0 m																																													
TIME - ROCK UNIT	BIOSTRATIGRAPHIC ZONE	FOSSIL CHARACTER			SECTION METERS	GRAPHIC LITHOLOGY	LITHOLOGIC DESCRIPTION																																										
		FORAMINIFERS	NAUPOFOSSILS	RADIOLARIANS				DIATOMS																																									
7	Barren				0.5		<p>Drill brecciated, medium gray (N5) to medium dark gray (N4) SILTY CLAYSTONE TO SILTSTONE. Carbon permeates sediments giving them a darker color. Sediment firmer in Core-Catcher. Scattered claystone chips imbedded in drill soup.</p> <p>SMEAR SLIDE SUMMARY</p> <table border="1"> <thead> <tr> <th></th> <th>1-30 (D)</th> <th>CC (D)</th> </tr> </thead> <tbody> <tr> <td>TEXTURE:</td> <td></td> <td></td> </tr> <tr> <td>Sand</td> <td>-</td> <td>-</td> </tr> <tr> <td>Silt</td> <td>25</td> <td>40</td> </tr> <tr> <td>Clay</td> <td>75</td> <td>60</td> </tr> <tr> <td>COMPOSITION:</td> <td></td> <td></td> </tr> <tr> <td>Quartz</td> <td>5</td> <td>30</td> </tr> <tr> <td>Feldspar</td> <td>10</td> <td>12</td> </tr> <tr> <td>Heavy minerals</td> <td>2</td> <td>TR</td> </tr> <tr> <td>Clay</td> <td>75</td> <td>50</td> </tr> <tr> <td>Pyrite</td> <td>3</td> <td>5-8</td> </tr> <tr> <td>Zeolite</td> <td>-</td> <td>2-3?</td> </tr> <tr> <td>Carbonate unspc.</td> <td>TR</td> <td>1</td> </tr> <tr> <td>Plant debris</td> <td>5</td> <td>10</td> </tr> </tbody> </table>		1-30 (D)	CC (D)	TEXTURE:			Sand	-	-	Silt	25	40	Clay	75	60	COMPOSITION:			Quartz	5	30	Feldspar	10	12	Heavy minerals	2	TR	Clay	75	50	Pyrite	3	5-8	Zeolite	-	2-3?	Carbonate unspc.	TR	1	Plant debris	5	10
								1-30 (D)	CC (D)																																								
					TEXTURE:																																												
Sand	-	-																																															
Silt	25	40																																															
Clay	75	60																																															
COMPOSITION:																																																	
Quartz	5	30																																															
Feldspar	10	12																																															
Heavy minerals	2	TR																																															
Clay	75	50																																															
Pyrite	3	5-8																																															
Zeolite	-	2-3?																																															
Carbonate unspc.	TR	1																																															
Plant debris	5	10																																															
1.0	VOID																																																
CC																																																	

SITE 477 HOLE		CORE 22		CORED INTERVAL 172.0-181.5 m				
TIME - ROCK UNIT	BIOSTRATIGRAPHIC ZONE	FOSSIL CHARACTER			SECTION METERS	GRAPHIC LITHOLOGY	LITHOLOGIC DESCRIPTION	
		FORAMINIFERS	NAUPOFOSSILS	RADIOLARIANS				DIATOMS
7	VP R/R	Barren			0.5		<p>Drill-brecciated medium dark gray (N4) SILTY CLAY, hydrothermally altered. Abundant pyrite disseminated throughout the silty clay-dodecahedra and cubes (1 to 3 mm diameter). Edges of pyrite crystals corroded, crystal faces curved. Pyrite appears concentrated but this may be partly a drilling effect. Some sandy siltstone chips are dispersed throughout the core. These are quite friable. Carbon particles in water permeate the sediment producing an oil slick appearance.</p> <p>SS 22-1, slick: very fine-grained, many with serrated edges</p> <p>10% quartz</p> <p>20% feldspars, relict shapes, ragged, no twinning preserved (albite? or K-feldspar) patchy extinction R. I. < 1.55. Possible pseudomorphs</p> <p>40% clay, large flakes, low b.f., R. I. = 1.54</p> <p>8% sphene or epidote(?), high b.f., extreme dispersion, aggregate grains yellow</p> <p>2% hexagonal iron sulfides (pyrrhotite?)</p> <p>2% epidote; small prisms, euhedral sprays, low b.f.</p> <p>10% opaques</p> <p>Coarse fraction is 50% large (1 to 5 mm) pyrite crystals; 50% clay clumps.</p> <p>SM 22-1, 140 IW: feldspar (60%) sand, numerous feldspars, show evidence of replacement by epidote prisms (20%). Surfaces altered to chlorite.</p> <p>CARBONATE BOMB: 1.26 = 7% (with pyrite)</p>	
					1.0			VOID
					2			
CC								

SITE 477 HOLE		CORE 23		CORED INTERVAL 181.5-191.0 m																															
TIME - ROCK UNIT	BIOSTRATIGRAPHIC ZONE	FOSSIL CHARACTER			SECTION METERS	GRAPHIC LITHOLOGY	LITHOLOGIC DESCRIPTION																												
		FORAMINIFERS	NAUPOFOSSILS	RADIOLARIANS				DIATOMS																											
7	Barren				0.5		<p>Moderately disturbed, medium dark gray (N4) to dark gray (N3) SILTY CLAY TO SILTSTONE. Indurated, friable soft, sediment surface on split core has random fractures indicative of abundant gas pockets, H₂S smell is present. Pyrite crystals and sandy siltstone chips are abundant, dispersed throughout the core. Pyrite occurs as 1 to 3 mm diameter dodecahedra and cubes. Hydrothermally altered. Siltstone may derive from redeposited and cemented basal turbidite sands.</p> <p>SS 23-1, 50 cm (M): sandy clump, light gray (0.1 to 0.2 m 50% feldspars, partially euhedral; some ragged, no twinning; irregular extinction, inclusions, R. I. 1.55; replace(?) relicts without overgrowth rims</p> <p>15% epidote, low b.f. prisms; some replacing feldspars (0.03 mm)</p> <p>3% dispersive aggregates (sphene?) (0.02 mm)</p> <p>5% opaques; some hexagonal platelets</p> <p>20% quartz, diverse</p> <p>2% dolomite</p> <p>SMEAR SLIDE SUMMARY</p> <table border="1"> <thead> <tr> <th></th> <th>1-75 (D)</th> </tr> </thead> <tbody> <tr> <td>TEXTURE:</td> <td></td> </tr> <tr> <td>Sand</td> <td>-</td> </tr> <tr> <td>Silt</td> <td>15</td> </tr> <tr> <td>Clay</td> <td>85</td> </tr> <tr> <td>COMPOSITION:</td> <td></td> </tr> <tr> <td>Quartz</td> <td>5</td> </tr> <tr> <td>Feldspar</td> <td>15</td> </tr> <tr> <td>Heavy minerals</td> <td>5</td> </tr> <tr> <td>Clay</td> <td>65</td> </tr> <tr> <td>Pyrite</td> <td>3</td> </tr> <tr> <td>Zeolite</td> <td>?</td> </tr> <tr> <td>Carbonate unspc.</td> <td>?</td> </tr> <tr> <td>Plant debris</td> <td>30</td> </tr> </tbody> </table>		1-75 (D)	TEXTURE:		Sand	-	Silt	15	Clay	85	COMPOSITION:		Quartz	5	Feldspar	15	Heavy minerals	5	Clay	65	Pyrite	3	Zeolite	?	Carbonate unspc.	?	Plant debris	30
								1-75 (D)																											
					TEXTURE:																														
Sand	-																																		
Silt	15																																		
Clay	85																																		
COMPOSITION:																																			
Quartz	5																																		
Feldspar	15																																		
Heavy minerals	5																																		
Clay	65																																		
Pyrite	3																																		
Zeolite	?																																		
Carbonate unspc.	?																																		
Plant debris	30																																		
1.0	VOID																																		
CC																																			



64-477A-1

Depth: 32.5 to 42.0 m

SECTION 1: DOMINANT LITHOLOGY: BASALT (grading into DOLERITE).

Macroscopic Description

Dark to medium gray (N5–N6 dry, N2–N3 wet) feldspar-phyric basalt. Phenocrysts: plagioclase, 0.5–5 mm, about 10%, lath-shaped to tabulate.

Groundmass: fine-grained, with an apparent gradation from aphanitic chilled (top) to doleritic (bottom).

Alteration: very faint yellowish staining of the groundmass indicates presence of minor smectites. Veining parallel to core occurs in several pieces, and a 2 cm-wide alteration zone surrounds veins. Veins comprise zeolites; no calcite is present.

Glass selvages, up to 6 mm thick, occur in Piece 1 and 4. They have a distinct ropy texture. Baked, RED, SEDIMENT is found attached to the glass on Piece 1, and zeolites and dolomite line cavities beneath the glassy rind. The glass is very fresh; and contains phenocrysts of feldspar.

TS 28 cm (Piece 4): sparsely PHYRIC BASALT, sampled adjacent to glass rim. Phenocrysts: olivine 5%, up to 0.5 mm euhedral–subhedral crystals; plagioclase 5%, up to 1.0 mm lath-shaped and tabulate crystals, often intergrown with olivine to form glomerocrysts. The large plagioclase phenocrysts seen in hand specimen were not found in the thin section. Groundmass: olivine, plagioclase microlites, clinopyroxene (quenched), disseminated ore and mesostasis. About 5% of rock consists of aggregates and strings of opaques. Less than 2% vesicles, 3% calcite in veins and cavities and plus 2% clays. Some alteration of olivines.

TS 50 cm (Piece 7): PLAGIOCLASE PHYRIC BASALT, intragranular/porphyritic from sill interior. Phenocrysts: olivine 5%, 0.4–1.0 mm, anhedral crystals; plagioclase 20%, 1–4 mm, An_{65-75} , equant to tabulate unjoined resorbed crystals which frequently occur as aggregates. Groundmass: plagioclase 40%, up to 1 mm, An_{50-60} lath-shaped. Clinopyroxene 30%, <1 mm (augite) anhedral, intragranular. Magnetite and ilmenite, 0.05 to 0.4 mm, anhedral to cuboid, intragranular. Alteration: 5% interstitial mesostasis.

Smear Slides of alteration products:

Piece 1: white crystals: calcite 100%

Piece 1: red brown: devitrified glass, clay 100%, microlitic grains

Piece 1: brown: mostly carbonate, some quartz; reddish oxides

SECTION 2: DOMINANT LITHOLOGY: PLAGIOCLASE PHYRIC DOLERITE.

Macroscopic Description

Medium light gray dolerite with plagioclase phenocrysts 1–4 mm in size. Rock is fresh except areas proximal to veins containing zeolites and clay minerals.

TS 33 cm (Piece 4): FELDSPAR PHYRIC DOLERITE or coarse basalt. Fresh. Phenocrysts: olivine 5%, 0.5–1.5 mm, subhedral; plagioclase 15%, 2–4 mm, large equant crystals, strongly zoned. Groundmass: Olivine 5%, <1 mm – may be microphenocrysts; plagioclase 50%, 0.5–2 mm elongate laths, occasionally optically enclosed in clinopyroxene; Clinopyroxene: 15%, up to 4 mm – probably augite – anhedral crystals, generally elongate, and frequently intergranular; magnetite and opaques 5%. Vesicles: 5%, <1 mm, no filling, spherical. Little or no alteration.

64-477A-2

Depth 42.0 to 55.0 m

SECTION 1: DOMINANT LITHOLOGY: DOLERITE.

Macroscopic Description

Pieces 1–3: medium dark gray (N4) aphanitic basalt containing about 15% large (up to 1 cm) plagioclase phenocrysts. Very fresh, with glass selvage on Piece 3. Glass contains plagioclase phenocrysts. No vesicles. Occasional olivine microphenocrysts.

Pieces 4–9: medium light gray (N5–N6) medium-grained dolerite. Inequigranular, almost porphyritic, with 0.2–0.8 mm sized plagioclase crystals in groundmass of plagioclase, clinopyroxene (some large laths up to 5 mm) and occasional olivine. No recognizable alteration. No vesicles. Minute diktytaxitic cavities.

Pieces 10–18: Similar to Pieces 4–9 but fewer plagioclase phenocrysts. Fresh and nonvesicular.

TS 14 cm (Piece 3): GLASSY MARGIN of chill zone – hyalopilitic texture – moderately altered brownish-black basalt in glass (90%) with disseminated opaques (2%) and carbonate (1%) surrounding small 0.1–0.5 mm plagioclase microlites that show some quenched textures although it is not well-developed.

TS 45 cm (Piece 6B): dolerite or COARSE-GRAINED BASALT with subophitic texture. Tabulate-laths of plagioclase (An_{50}), 1–6 mm, and subhedral clinopyroxene (augite) 1–3 mm in size – surrounded by plagioclase microlites and clinopyroxene and olivine and abundant opaques (ilmenite [trellis-type] and magnetite). Very fresh appearance and only ~3% modal clay minerals. Modal per cent (600 point counts), plagioclase phenocrysts 26%, clinopyroxene phenocrysts and groundmass 18%, olivine 8%, plagioclase and groundmass 36%, opaques 9%, and clays 3%.

SECTION 2: DOMINANT LITHOLOGY: vesicular, coarse BASALT OR DOLERITE.

Macroscopic Description

Piece 1: medium light gray (N5–N6), medium-grained dolerite. Inequigranular with about 5–10 mm plagioclase phenocrysts. No discernible alteration. No vesicles. Very similar to Pieces 10–18 on Section 1, Core 2.

Pieces 2–17: Very similar to Piece 1 but vesicular. About 5% vesicles, spherical, ranging in size from 0.5 to 3 mm. Unfilled except for occasional clusters of white acicular crystals (?zeolites). Groundmass finer-grained than Piece 1?

Pieces 18–22: Similar to remainder of section but strongly vesicular, about 15% vesicles, up to 5 mm across, spherical and irregular in form. Unfilled except for occasional clusters of white acicular crystals, and rare, very thin lining of clay minerals. About 15% plagioclase phenocrysts, which is more than in Pieces 1–17.

TS 10 cm (Piece 1): inequigranular PORPHYRITIC DOLERITE or coarse basalt, 0.5–3.5 mm plagioclase laths in a matrix of olivine and clinopyroxene, microphenocrysts and plagioclase microlites and abundant opaques and some clay minerals along intergrain boundaries. Opaques tend to be concentrated on or around altering mafic minerals. Magnetite and ilmenite are present. Modal analysis = plagioclase phenocrysts 16%, clinopyroxene 15% and olivine 9% (phenocrysts plus groundmass of minerals), plagioclase and groundmass 38%, opaques 13%, and clays 9%.

TS ~28 cm (Piece 3): VESICULAR DOLERITE with subophitic to very fresh appearance, plagioclase (An_{54}) olivine-clinopyroxene phenocrysts in an intergranular matrix of plagioclase microlites and opaques. Round vesicles (6% modal) randomly dispersed (0.75–1.5 mm) with little or no filling except for occasional thin linings of claystone alteration (glass?). Modal analysis = plagioclase phenocrysts 14%, plagioclase groundmass 39%, clinopyroxene 9%, olivine 17%, opaques 9%, clays 6%, and vesicles 6%.

SECTION 3: DOMINANT LITHOLOGY: VESICULAR COARSE BASALT OR DOLERITE AND DOLERITE.

Macroscopic Description

Pieces 1–9 (1–67 cm): medium light gray (N5–N6) medium- to coarse-grained basalt (dolerite). About 15% plagioclase phenocrysts (1–4 mm) in groundmass of plagioclase, pyroxene and olivine. Appears to be very fresh. Very vesicular (about 15% vesicles, up to 5 mm across (spherical) and 1 cm across (irregular-coalesced). Vesicles unfilled but a few contain acicular crystals in clusters (?zeolites). Very similar to Pieces 18–22 of Section 2.

Pieces 10–21: medium gray dolerite with 5–10% plagioclase phenocrysts in a groundmass of clinopyroxene, plagioclase and olivine. Little alteration of the constituent minerals but rock groundmass appears to be hydrated. Numerous diktytaxitic cavities (0.5–1.0 mm). Pieces 19 and 21 comprise collections of drilling fragments, caused by friable nature of rock.

TS 48 cm (Piece 7): subophitic PLAGIOCLASE PHYRIC COARSE GRAINED BASALT with some vesicularity (rounded vesicles, 4% modal) (0.75–4.0 mm) plagioclase phenocrysts (~ An_{66}) 0.5–3.0 mm in size in tabulate crystals and laths. Many show strong zoning and some have small bleb-like inclusions of brownish mineral (may be glass?). Clinopyroxene crystals are very fractured. Some are altered. The phenocrysts phases are surrounded by plagioclase microlites, olivine and clinopyroxene and abundant magnetite and ilmenite. Some clay minerals present along intergrain boundaries and lining some vesicles and in fractures in clinopyroxene. Modal analysis based on 600 counts are: plagioclase phenocrysts 17%, olivine 4%, clinopyroxene 16%, opaques 12%, plagioclase and groundmass 38%, vesicles 4%, and clay 9%.

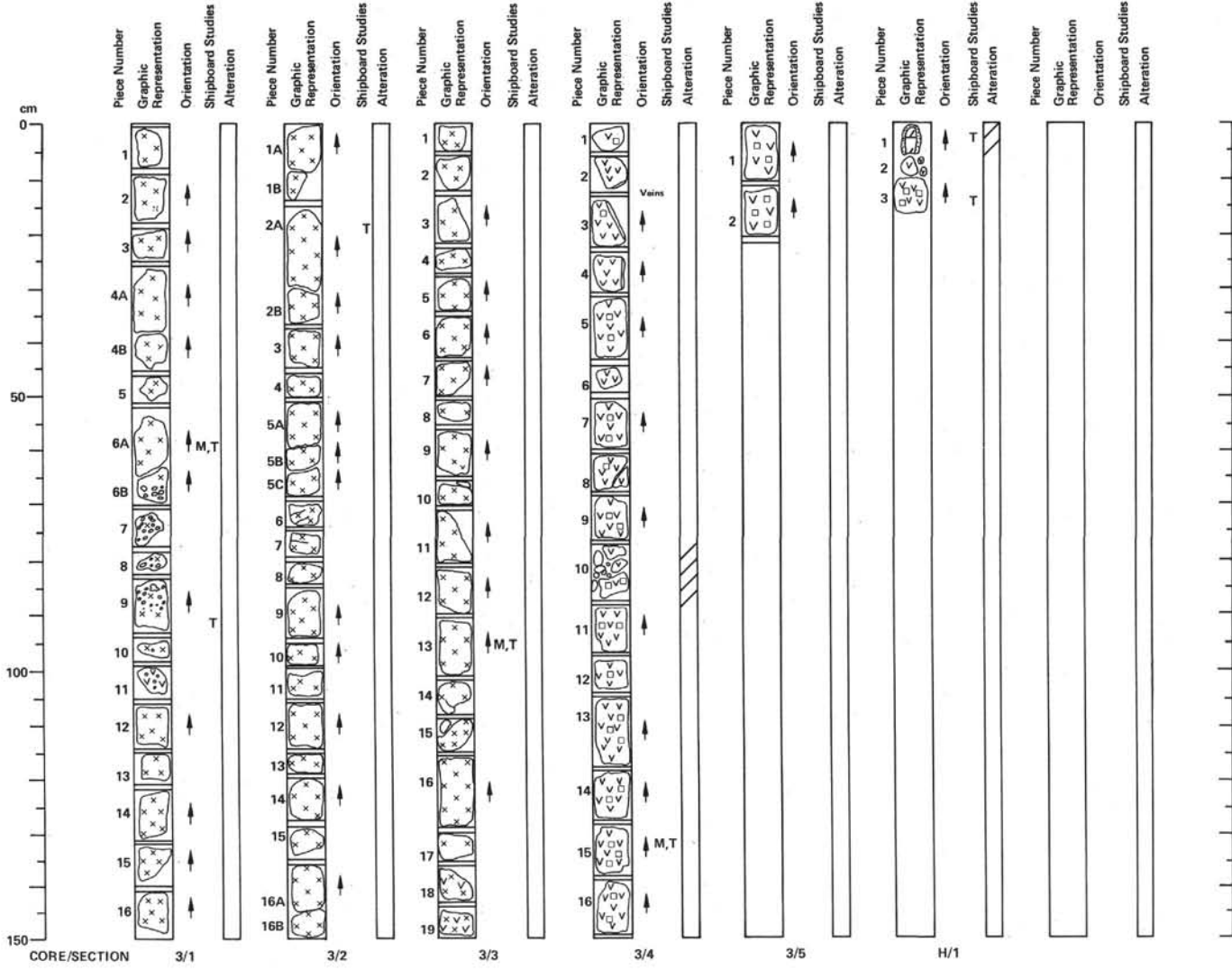
SECTION 4: DOMINANT LITHOLOGY: DOLERITE.

Macroscopic Description

Medium to dark gray medium-grained dolerite, containing about 5–10% plagioclase phenocrysts (up to 4 mm). A continuation of Section 3. The rock contains abundant small (<0.5 mm) diktytaxitic cavities, and it is permeated by water. However, the constituent minerals appear fresh. The rock appears to be more feldspathic from Piece 5 onwards, with a band of normal dolerite running across Piece 7.

TS 85 cm (Piece 10): inequigranular DOLERITE – tabulate laths – 1.5 mm (~ An_{50-60}) of plagioclase and olivine plus clinopyroxene microphenocrysts (euhedral–anhedral) set in matrix of plagioclase microlites and disseminated opaques with minor clays along intergrain boundaries. Modal analysis: plagioclase phenocrysts 17%, plagioclase and groundmass 39%, clinopyroxene 17%, olivine 15%, opaques 10%, and clay 2%.

TS 5 cm (Piece 1): inequigranular dolerite. Same as Piece 10 above, except slightly more altered with 5% clay minerals.



64-477A-3

Depth: 55.0 to 67.5 m

SECTION 1: DOMINANT LITHOLOGY: GABBRO (or coarse dolerite).

Macroscopic Description

Grayish black (N2) when wet, medium to medium dark gray (N4–N5) when dry, coarse-grained dolerite or GABBRO. Inequigranular, comprising plagioclase (1–4 mm, 50%), pyroxene (~40%, appears to be anhedral and optically enclosing the plagioclase) and olivine. The minerals are very fresh-looking.

Slight mineral segregation has led to pyroxene-rich areas in Piece 2. **VESICLES:** small 1 mm vesicles (<5%) in Pieces 1, 10, and 11. There is a zone diktytaxitic cavities and irregular vesicles in Pieces 6, 7, 8, and 9. Piece 11 is finer-grained, more doleritic in appearance. The entire rock has minute (numerous) diktytaxitic cavities.

TS 60 cm (Piece 6A): very fresh ophitic to subophitic GABBRO with clinopyroxene (augite) and plagioclase phenocrysts (~An₅₀) surrounded by clinopyroxene microphenocrysts, and plagioclase microlites and olivine microphenocrysts and abundant opaques — magnetite and ilmenite. Many large clinopyroxene are fractured along cleavage planes although ophitic texture is well-preserved. One large ~3 mm ocellus-filled with ilmenite laths and basaltic quench is present. Plagioclase phenocrysts are 1–3 mm in size and almost all are strongly zoned. Clinopyroxene phenocrysts are 0.5–4.0 mm in size and opaques tend to be concentrated around them. Modal analysis based on 600 counts is: plagioclase phenocrysts 32%, clinopyroxene phenocrysts and groundmass 23%, olivine groundmass and phenocrysts 6%, plagioclase groundmass 25%, opaques 10%, and clays and alteration products 4%.

SECTION 2: DOMINANT LITHOLOGY: GABBRO OR COARSE DOLERITE.

Macroscopic Description

A continuation of Section 1 (Piece 1 is connected to Piece 1b of Section 1).

Grayish black (N2) (wet), medium to medium dark gray (N4–N5) (dry) coarse dolerite or gabbro. Inequigranular, comprising plagioclase (about 35–40%) pyroxene (40%) and olivine (~15%). Plagioclase is larger than clinopyroxene and enclosed by it; olivine forms small (<1 m) green crystals.

Minute diktytaxitic cavities occur throughout rock.

The rock is very fresh.

TS 20 cm (Piece 2A): coarse-grained, inequigranular DOLERITE, or gabbro. Many of the olivine and plagioclase crystals may be phenocrysts, but because of the seriate textures there is no way of verifying this. Olivine: 6%, <1–5 mm anhedral. Plagioclase: 70%, two main grain sizes, a) 0.5–1.0 mm, An_{50–60} laths; and b) 1.0–6.0 mm, ?An₈₀ large tabulate crystals, strongly zoned. Augite: 19%, up to 5 mm, optically enclosing plagioclase. However, there is a low birefringence clinopyroxene present (about 0.5% of the total pyroxene). Mesostasis: about 5% microcrystalline interstitial material consisting of pyroxene, plagioclase and magnetite. Cavities: ~2%, 0.5–1.5 mm, irregular. No clays or alteration seen.

SECTION 3: DOMINANT LITHOLOGY: OLIVINE GABBRO, or coarse olivine dolerite.

Macroscopic Description

A continuation of Section 2.

Grayish black (N2) (wet), medium to medium dark gray (N4–N5) (dry) coarse dolerite or gabbro.

The dominant minerals are plagioclase (up to 6 mm), optically enclosed by dark clinopyroxene, and green olivine (<1 mm). The proportions of these vary slightly, olivine increasing in abundance towards the base of the section (especially Pieces 13–16), up to ~20%.

The rock is very fresh.

Diktytaxitic cavities are again abundant.

Pieces 18 and 19 are finer-grained than the remainder of the section, although feldspars are a similar size.

TS 95 cm (Piece 13): COARSE DOLERITE. Porphyritic and subophitic. Phenocrysts: 15%, up to 5 mm across, An₇₀ elongate, subhedral and strongly zoned crystals containing numerous inclusions. Groundmass: olivine: 10%, 0.5–2 mm, anhedral crystals; plagioclase: 50%, 1–2 mm laths; clinopyroxene 20%, up to 4 mm augite, irregular crystals subophitically enclosing plagioclase; magnetite and ilmenite 4%. Much of slide not preserved, so no mesostasis seen. Trace amounts of clay minerals.

SECTION 4: DOMINANT LITHOLOGY: PLAGIOCLASE PHYRIC DOLERITE.

Macroscopic Description

Dark grayish black (N2) (wet), medium to medium dark gray (dry) (N4–N5) plagioclase phyric dolerite.

Plagioclase phenocrysts, up to 8 mm across at top of section, decreasing in size abundance to ~4 mm at bottom of section. Set in groundmass of plagioclase, olivine, and clinopyroxene. Phenocrysts ~10–15% of rock.

Rock very fresh again, although veins consisting of calcite (HCl+) and zeolites are found on Pieces 2–4.

TS 130 cm (Piece 16): PORPHYRITIC basalt or DOLERITE. Dolerite to intergranular texture. Phenocrysts: olivine: 4%, up to 1 mm, subhedral to anhedral crystals; plagioclase: 20%, up to 5 mm, resorbed, rounded tabulate, zoned crystals. Groundmass: olivine, 5%, 0.2–0.5 mm, anhedral crystals; plagioclase, 44%, up to 1 mm, An_{60–65} laths; clinopyroxene: 18%, <1 mm, augite, anhedral, intergranular between plagioclase. Cavities, 2%, <1 mm, random, empty, irregular.

SECTION 5: DOMINANT LITHOLOGY: PLAGIOCLASE PHYRIC DOLERITE.

Macroscopic Description

Indistinguishable from the dolerite in Section 4.

64-477A-H

Depth 67.5 to 68.0 m

SECTION 1: DOMINANT LITHOLOGY: silicic DOLOMITE (Piece 1 (0–6 cm) and DOLERITE PLAGIOCLASE PHYRIC (6–16 cm).

Macroscopic Description

Piece 1: yellowish gray (5Y 7/2) to dusky yellow (5Y 6/4) very hard, indurated SILICIC DOLOMITE. Light olive patina (weathering?). Cut surface sprinkled with silt and holes. Smear Slide Section 1, 10 cm: 40% quartz and 60% fine-grained (0.02–0.1 mm) dolomite, anhedral.

Pieces 2 and 3: dolerite plagioclase phyric, with phenocrysts 1–3 mm in size, probably base of sill sampled in Cores 1–3.

Silicic dolomite occurs above the base of sill suggesting that it exists as an intercalation at the base of the sills. The actual interval sampled by this material is probably at ~67–70 m sub-bottom.

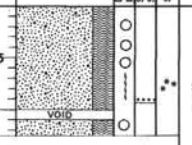
SITE 477 HOLE A CORE 5 CORED INTERVAL 191.0-200.5 m																																																																		
TIME - ROCK UNIT	BIOSTRATIGRAPHIC ZONE	FOSSIL CHARACTER			SECTION METERS	GRAPHIC LITHOLOGY	DRILLING DISTURBANCE	SEDIMENTARY STRUCTURES	SAMPLES	LITHOLOGIC DESCRIPTION																																																								
		FORAMINIFERS	NANNOFOSSILS	RADIOLARIANS							DIATOMS																																																							
7	VP/R				1					<p>Site 477A, Core 4, 181.5-191.0 m: NO RECOVERY.</p> <p>Medium light gray (N6-N5) friable SANDSTONE TO SILTSTONE. Sand comprises mostly deuterically altered feldspar. Epidote minerals prevalent in smear slides. Some light gray (N7) sandstone clumps contain many euhedral and altered minerals. Pyrite scattered throughout. Some speckled with a dark, sometimes zoned and thinly flaky mineral. Some zones enriched in tabular hornblende-like mineral. Traces of zirconite and talc. Epidotes: idiomorphic, mostly low b.f. prisms. R. I. 1.70-1.72 (0.04 mm x 0.01 mm). Feldspars: ragged to euhedral, no twinning, pitted, irregular extinction.</p> <p>SMEAR SLIDE SUMMARY</p> <table border="1"> <thead> <tr> <th></th> <th>1-90 (D)</th> <th>1-100 (D)</th> <th>1-102 (D)</th> </tr> </thead> <tbody> <tr> <td>TEXTURE:</td> <td></td> <td></td> <td></td> </tr> <tr> <td>Sand</td> <td>-</td> <td>10</td> <td>-</td> </tr> <tr> <td>Silt</td> <td>-</td> <td>60</td> <td>-</td> </tr> <tr> <td>Clay</td> <td>-</td> <td>30</td> <td>-</td> </tr> <tr> <td>COMPOSITION:</td> <td></td> <td></td> <td></td> </tr> <tr> <td>Quartz</td> <td>10 (a)</td> <td>20</td> <td>3</td> </tr> <tr> <td>Feldspar</td> <td>30 (b)</td> <td>50</td> <td>50</td> </tr> <tr> <td>Heavy minerals</td> <td>-</td> <td>2 (c)</td> <td>2</td> </tr> <tr> <td>Clay</td> <td>-</td> <td>15</td> <td>20</td> </tr> <tr> <td>Pyrite</td> <td>-</td> <td>2</td> <td>2</td> </tr> <tr> <td>Dolomite</td> <td>20</td> <td>-</td> <td>1</td> </tr> <tr> <td>Organics</td> <td>-</td> <td>3</td> <td>5</td> </tr> <tr> <td>Epidote</td> <td>40</td> <td>15</td> <td>30</td> </tr> </tbody> </table> <p>(a) Authigenic? (b) Albite? (c) 2% high bf. R.I., dispersion aggregate</p> <p>CARBONATE BOMB: 1.44 = 6%</p>		1-90 (D)	1-100 (D)	1-102 (D)	TEXTURE:				Sand	-	10	-	Silt	-	60	-	Clay	-	30	-	COMPOSITION:				Quartz	10 (a)	20	3	Feldspar	30 (b)	50	50	Heavy minerals	-	2 (c)	2	Clay	-	15	20	Pyrite	-	2	2	Dolomite	20	-	1	Organics	-	3	5	Epidote	40	15	30
	1-90 (D)	1-100 (D)	1-102 (D)																																																															
TEXTURE:																																																																		
Sand	-	10	-																																																															
Silt	-	60	-																																																															
Clay	-	30	-																																																															
COMPOSITION:																																																																		
Quartz	10 (a)	20	3																																																															
Feldspar	30 (b)	50	50																																																															
Heavy minerals	-	2 (c)	2																																																															
Clay	-	15	20																																																															
Pyrite	-	2	2																																																															
Dolomite	20	-	1																																																															
Organics	-	3	5																																																															
Epidote	40	15	30																																																															

SITE 477 HOLE A CORE 6 CORED INTERVAL 200.5-210.0 m																																								
TIME - ROCK UNIT	BIOSTRATIGRAPHIC ZONE	FOSSIL CHARACTER			SECTION METERS	GRAPHIC LITHOLOGY	DRILLING DISTURBANCE	SEDIMENTARY STRUCTURES	SAMPLES	LITHOLOGIC DESCRIPTION																														
		FORAMINIFERS	NANNOFOSSILS	RADIOLARIANS							DIATOMS																													
7					CC					<p>Three pieces of medium gray (N5) SILTY CLAYSTONE with sand-sized authigenic minerals (epidote, zoisite), very soft, friable claystone with pyrite and tiny white specks.</p> <p>Smear slides show mostly altered and replaced feldspars. Scattered quartz flakes (30%) and 10% feldspars (0.008 mm). Many tiny (2 microns) highly dispersive specks.</p> <p>SMEAR SLIDE SUMMARY</p> <table border="1"> <thead> <tr> <th></th> <th>CC (D)</th> </tr> </thead> <tbody> <tr> <td>TEXTURE:</td> <td></td> </tr> <tr> <td>Sand</td> <td>3</td> </tr> <tr> <td>Silt</td> <td>40</td> </tr> <tr> <td>Clay</td> <td>60</td> </tr> <tr> <td>COMPOSITION:</td> <td></td> </tr> <tr> <td>Quartz</td> <td>5</td> </tr> <tr> <td>Feldspar</td> <td>50</td> </tr> <tr> <td>Heavy minerals</td> <td>5</td> </tr> <tr> <td>Clay</td> <td>30</td> </tr> <tr> <td>Volcanic glass</td> <td>TR</td> </tr> <tr> <td>Zeolite</td> <td>27</td> </tr> <tr> <td>Opauques</td> <td>5</td> </tr> <tr> <td>Zoisite</td> <td>3</td> </tr> <tr> <td>Other epidote</td> <td>1</td> </tr> </tbody> </table>		CC (D)	TEXTURE:		Sand	3	Silt	40	Clay	60	COMPOSITION:		Quartz	5	Feldspar	50	Heavy minerals	5	Clay	30	Volcanic glass	TR	Zeolite	27	Opauques	5	Zoisite	3	Other epidote	1
	CC (D)																																							
TEXTURE:																																								
Sand	3																																							
Silt	40																																							
Clay	60																																							
COMPOSITION:																																								
Quartz	5																																							
Feldspar	50																																							
Heavy minerals	5																																							
Clay	30																																							
Volcanic glass	TR																																							
Zeolite	27																																							
Opauques	5																																							
Zoisite	3																																							
Other epidote	1																																							

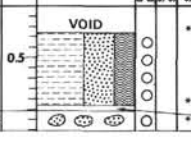
SITE 477 HOLE A CORE 7 CORED INTERVAL 210.0-219.5 m																																																	
TIME - ROCK UNIT	BIOSTRATIGRAPHIC ZONE	FOSSIL CHARACTER			SECTION METERS	GRAPHIC LITHOLOGY	DRILLING DISTURBANCE	SEDIMENTARY STRUCTURES	SAMPLES	LITHOLOGIC DESCRIPTION																																							
		FORAMINIFERS	NANNOFOSSILS	RADIOLARIANS							DIATOMS																																						
7					1					<p>Very disturbed medium gray (N5) QUARTZ-FELDSPAR SAND. Friable, hard lumps in drill matrix. Some H₂S. Evidence of hydrothermal alteration. Hard chunk in the Core-Catcher shows primary sedimentary structures: fine parallel lamination (wave-like) with scour marks in a sandstone. Appears to grade into massive sandstone to a medium gray claystone.</p> <p>Piece above from Core-Catcher (not calcareous):</p> <ol style="list-style-type: none"> 1) dark gray mudstone 2) "dirty" poorly sorted, gray fine sand, some cross-bedding 3) light gray, parallel laminated fine-grained siltstone, well sorted 4) as 3, but lamination indistinct 5) "dirty" very fine-grained sand <p>SMEAR SLIDE SUMMARY</p> <table border="1"> <thead> <tr> <th></th> <th>1.24 (D)</th> <th>CC (D)</th> </tr> </thead> <tbody> <tr> <td>TEXTURE:</td> <td></td> <td></td> </tr> <tr> <td>Sand</td> <td>60</td> <td>10</td> </tr> <tr> <td>Silt</td> <td>30</td> <td>60</td> </tr> <tr> <td>Clay</td> <td>10</td> <td>30</td> </tr> <tr> <td>COMPOSITION:</td> <td></td> <td></td> </tr> <tr> <td>Plagioclase (30% fine, subhedral flakes)</td> <td>10</td> <td>30</td> </tr> <tr> <td>Altered grains</td> <td>10</td> <td>20</td> </tr> <tr> <td>Scaly low bf epidote prisms</td> <td>10</td> <td>-</td> </tr> <tr> <td>Highly dispersed high R.I., bf aggregates</td> <td>10</td> <td>10</td> </tr> <tr> <td>Opauques/pyrite</td> <td>5</td> <td>10</td> </tr> <tr> <td>Quartz, microlites</td> <td>5</td> <td>10</td> </tr> <tr> <td>Fine-grained chlorite?</td> <td>15</td> <td>20</td> </tr> </tbody> </table> <p>CARBONATE BOMB: 1.43 = 3%</p>		1.24 (D)	CC (D)	TEXTURE:			Sand	60	10	Silt	30	60	Clay	10	30	COMPOSITION:			Plagioclase (30% fine, subhedral flakes)	10	30	Altered grains	10	20	Scaly low bf epidote prisms	10	-	Highly dispersed high R.I., bf aggregates	10	10	Opauques/pyrite	5	10	Quartz, microlites	5	10	Fine-grained chlorite?	15	20
	1.24 (D)	CC (D)																																															
TEXTURE:																																																	
Sand	60	10																																															
Silt	30	60																																															
Clay	10	30																																															
COMPOSITION:																																																	
Plagioclase (30% fine, subhedral flakes)	10	30																																															
Altered grains	10	20																																															
Scaly low bf epidote prisms	10	-																																															
Highly dispersed high R.I., bf aggregates	10	10																																															
Opauques/pyrite	5	10																																															
Quartz, microlites	5	10																																															
Fine-grained chlorite?	15	20																																															

SITE 477 HOLE A CORE 8 CORED INTERVAL 219.5-229.0 m																																				
TIME - ROCK UNIT	BIOSTRATIGRAPHIC ZONE	FOSSIL CHARACTER			SECTION METERS	GRAPHIC LITHOLOGY	DRILLING DISTURBANCE	SEDIMENTARY STRUCTURES	SAMPLES	LITHOLOGIC DESCRIPTION																										
		FORAMINIFERS	NANNOFOSSILS	RADIOLARIANS							DIATOMS																									
7					1					<p>Brecciated, small fragments of medium dark gray (N4) SILTY SANDSTONE TO SANDY SILTSTONE. Wisp of clay clast(?) appear. Sandstone appears to be a basal sand from a turbidite that has been hydrothermally altered. (Epidote group minerals). Feldspars have been altered or replaced. Quartz or feldspar silt.</p> <p>SMEAR SLIDE SUMMARY</p> <table border="1"> <thead> <tr> <th></th> <th>CC (D)</th> </tr> </thead> <tbody> <tr> <td>TEXTURE:</td> <td></td> </tr> <tr> <td>Sand</td> <td>2</td> </tr> <tr> <td>Silt</td> <td>60</td> </tr> <tr> <td>Clay</td> <td>38</td> </tr> <tr> <td>COMPOSITION:</td> <td></td> </tr> <tr> <td>Quartz</td> <td>70</td> </tr> <tr> <td>Feldspar</td> <td>20 (grains)</td> </tr> <tr> <td>Chlorite</td> <td>10</td> </tr> <tr> <td>Epidote/zoisite</td> <td>10 (many fine prisms [2-4 microns])</td> </tr> <tr> <td>Organic</td> <td>5</td> </tr> <tr> <td>Pyrite</td> <td>3</td> </tr> <tr> <td>Feldspar/zeolite?</td> <td>10 (low bf flakes [2-20 microns])</td> </tr> </tbody> </table>		CC (D)	TEXTURE:		Sand	2	Silt	60	Clay	38	COMPOSITION:		Quartz	70	Feldspar	20 (grains)	Chlorite	10	Epidote/zoisite	10 (many fine prisms [2-4 microns])	Organic	5	Pyrite	3	Feldspar/zeolite?	10 (low bf flakes [2-20 microns])
	CC (D)																																			
TEXTURE:																																				
Sand	2																																			
Silt	60																																			
Clay	38																																			
COMPOSITION:																																				
Quartz	70																																			
Feldspar	20 (grains)																																			
Chlorite	10																																			
Epidote/zoisite	10 (many fine prisms [2-4 microns])																																			
Organic	5																																			
Pyrite	3																																			
Feldspar/zeolite?	10 (low bf flakes [2-20 microns])																																			

SITE 477 HOLE A CORE 9 CORED INTERVAL 229.0-238.5 m

TIME - ROCK UNIT	BIOSTRATIGRAPHIC ZONE	FOSSIL CHARACTER			SECTION METERS	GRAPHIC LITHOLOGY	DRILLING DISTURBANCE	TEMPERATURE	STRUCTURES	SAMPLES	LITHOLOGIC DESCRIPTION																																																												
		FORAMIFERES	NANNOFOSSILS	RADIOLARIANS								DIATOMS																																																											
7		X			1 0.5						<p>Drilling breccia of medium gray (N5) SILTY SAND TO SANDSTONE. Patches of light gray (N7). Friable, porous; induration increases markedly upon drying. H₂S odor. Pyrite scattered throughout core. Numerous specks of fluorescence. Hydrothermally altered to quartz-epidote-chlorite-feldspar. Zeolite-like, low b.f., R. I., 45 degree extinction, laths common. Stubby to elongate epidote prisms (0.1 to 0.2 mm), subhedral, low b.f., some replacing feldspar grains. Feldspars (0.1 to 0.2 mm), subhedral, irregular extinction, no twinning, R. I. <1.55, altered, replaced; serated edges and neoformation. Sphene: abundant high R. I., b.f., extreme dispersion. Many fine-grained (0.01 to 0.02 mm) monoclinic, low b.f., R. I. laths. In dark gray, most relict feldspar grains are chloritized. Abundant small ragged grains.</p> <p>SMEAR SLIDE SUMMARY</p> <table border="1"> <thead> <tr> <th></th> <th>1-5 (D)</th> <th>1-9 (M)</th> <th>1-82 (M)</th> </tr> </thead> <tbody> <tr> <td>TEXTURE:</td> <td></td> <td></td> <td></td> </tr> <tr> <td>Sand</td> <td>-</td> <td>10</td> <td>-</td> </tr> <tr> <td>Silt</td> <td>40</td> <td>50</td> <td>-</td> </tr> <tr> <td>Clay</td> <td>60</td> <td>40</td> <td>-</td> </tr> <tr> <td>COMPOSITION:</td> <td></td> <td></td> <td></td> </tr> <tr> <td>Quartz</td> <td>30</td> <td>40</td> <td>30</td> </tr> <tr> <td>Feldspar</td> <td>25</td> <td>36</td> <td>40</td> </tr> <tr> <td>Epidote/zoisite</td> <td>30</td> <td>10</td> <td>5</td> </tr> <tr> <td>Clay</td> <td>5</td> <td>5</td> <td>5</td> </tr> <tr> <td>Sphene</td> <td>5</td> <td>5</td> <td>5</td> </tr> <tr> <td>Opauques</td> <td>10</td> <td>1</td> <td>10</td> </tr> <tr> <td>Pyrite</td> <td>2</td> <td>2</td> <td>2</td> </tr> <tr> <td>Zeolite</td> <td>10</td> <td>3</td> <td>-</td> </tr> <tr> <td>Unknown</td> <td>15</td> <td>5</td> <td>-</td> </tr> </tbody> </table> <p>CARBONATE BOMB: 1.39 = 3%</p>		1-5 (D)	1-9 (M)	1-82 (M)	TEXTURE:				Sand	-	10	-	Silt	40	50	-	Clay	60	40	-	COMPOSITION:				Quartz	30	40	30	Feldspar	25	36	40	Epidote/zoisite	30	10	5	Clay	5	5	5	Sphene	5	5	5	Opauques	10	1	10	Pyrite	2	2	2	Zeolite	10	3	-	Unknown	15	5	-
	1-5 (D)	1-9 (M)	1-82 (M)																																																																				
TEXTURE:																																																																							
Sand	-	10	-																																																																				
Silt	40	50	-																																																																				
Clay	60	40	-																																																																				
COMPOSITION:																																																																							
Quartz	30	40	30																																																																				
Feldspar	25	36	40																																																																				
Epidote/zoisite	30	10	5																																																																				
Clay	5	5	5																																																																				
Sphene	5	5	5																																																																				
Opauques	10	1	10																																																																				
Pyrite	2	2	2																																																																				
Zeolite	10	3	-																																																																				
Unknown	15	5	-																																																																				

SITE 477 HOLE A CORE 10 CORED INTERVAL 238.5-248.0 m

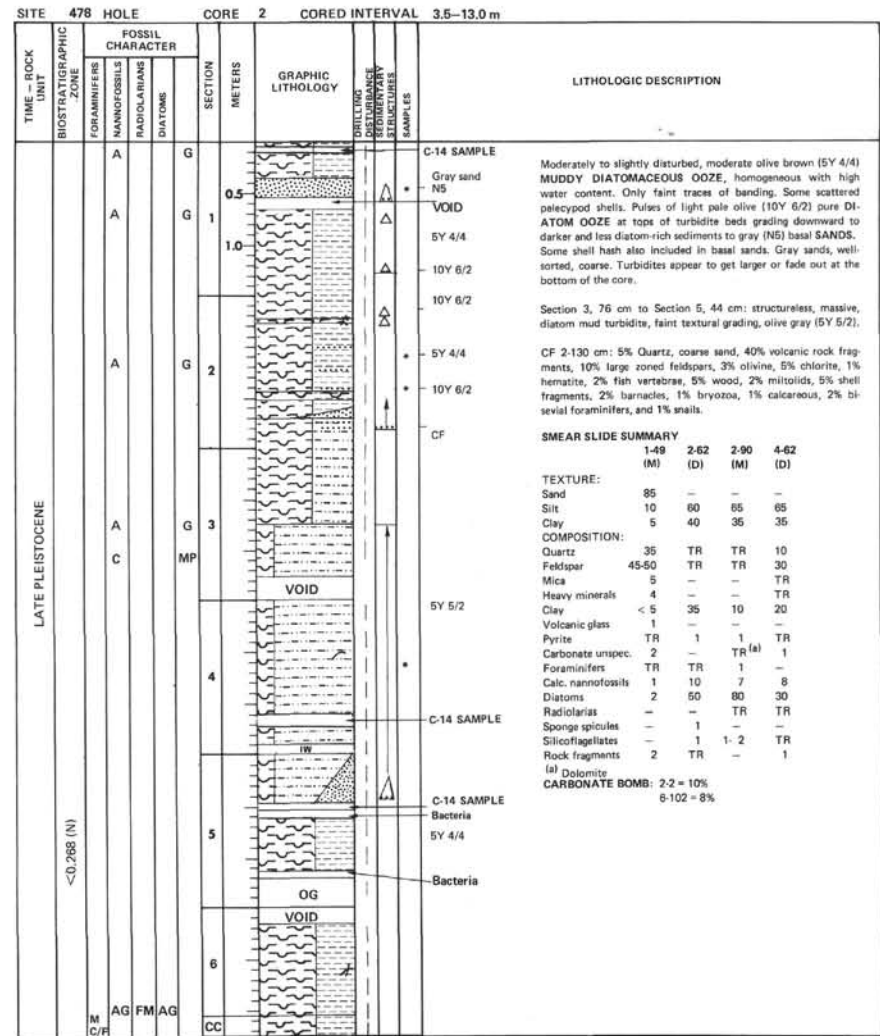
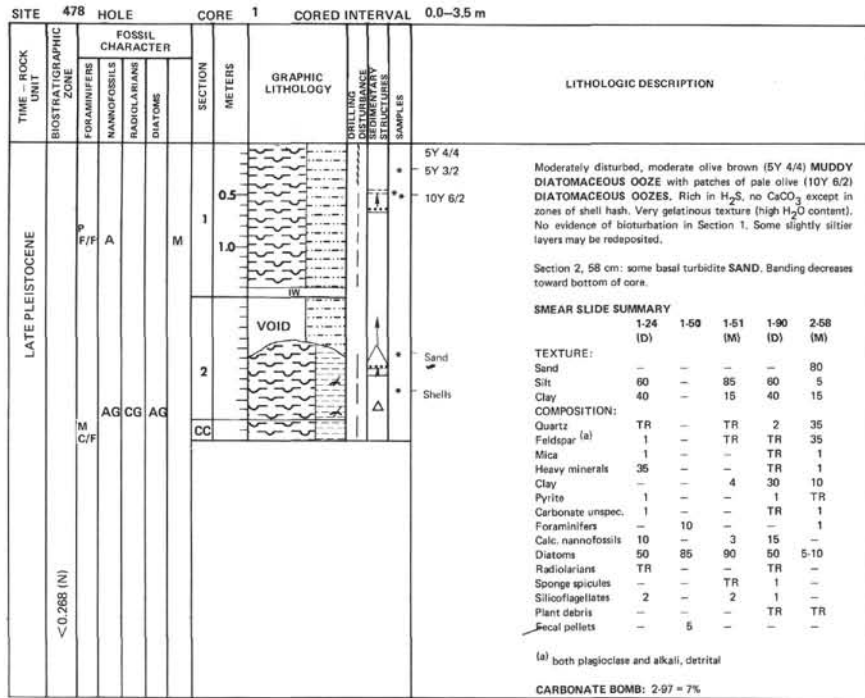
TIME - ROCK UNIT	BIOSTRATIGRAPHIC ZONE	FOSSIL CHARACTER			SECTION METERS	GRAPHIC LITHOLOGY	DRILLING DISTURBANCE	TEMPERATURE	STRUCTURES	SAMPLES	LITHOLOGIC DESCRIPTION																																																												
		FORAMIFERES	NANNOFOSSILS	RADIOLARIANS								DIATOMS																																																											
7		X			1 0.5						<p>Brecciated chips of hard, brittle, medium dark gray (N4), CLAYSTONE TO SANDSTONE. Hydrothermally altered, epidote-rich. Appears to have been layered in a cm-scale. Scattered carbon scum and fine-grained pyrite present but not abundant. Gas present. Sands become more indurated with depth in core. Three pieces of hard cemented, but friable coarse sandstone.</p> <p>Section 1, 0 to 10 cm: some downhole cavings from soft diatom oozes.</p> <p>Zeolite: long monoclinic laths (0.05 mm) R. I. ¹⁰ 1.53 Carbonate: rare rhombs Matrix: small (0.005 mm) subhedral epidote/chlorite/quartz Altered feldspar grains (0.1-2.0 mm): epidote along cleavages Sphene: extreme b.f., R. I., dispersion mineral aggregate (0.03 mm) In the clay fraction, low b.f., clear flakes with R. I. ¹⁰ 1.55 are dominant.</p> <p>SMEAR SLIDE SUMMARY</p> <table border="1"> <thead> <tr> <th></th> <th>1-20 (D)</th> <th>1-90 (D)</th> <th>CC (D)</th> </tr> </thead> <tbody> <tr> <td>TEXTURE:</td> <td></td> <td></td> <td></td> </tr> <tr> <td>Sand</td> <td>-</td> <td>10</td> <td>-</td> </tr> <tr> <td>Silt</td> <td>-</td> <td>10</td> <td>-</td> </tr> <tr> <td>Clay</td> <td>-</td> <td>80</td> <td>-</td> </tr> <tr> <td>COMPOSITION:</td> <td></td> <td></td> <td></td> </tr> <tr> <td>Quartz</td> <td>15</td> <td>-</td> <td>80 (authigenic)</td> </tr> <tr> <td>Feldspar</td> <td>25</td> <td>-</td> <td>-</td> </tr> <tr> <td>Sphene</td> <td>10</td> <td>1</td> <td>-</td> </tr> <tr> <td>Clay</td> <td>-</td> <td>70</td> <td>10</td> </tr> <tr> <td>Pyrite</td> <td>2</td> <td>2</td> <td>-</td> </tr> <tr> <td>Zeolite</td> <td>5</td> <td>-</td> <td>-</td> </tr> <tr> <td>Carbonate unspc.</td> <td>2</td> <td>-</td> <td>-</td> </tr> <tr> <td>Zoisite/epidote</td> <td>15</td> <td>2</td> <td>5-10</td> </tr> <tr> <td>Opauques</td> <td>2</td> <td>10</td> <td>-</td> </tr> </tbody> </table>		1-20 (D)	1-90 (D)	CC (D)	TEXTURE:				Sand	-	10	-	Silt	-	10	-	Clay	-	80	-	COMPOSITION:				Quartz	15	-	80 (authigenic)	Feldspar	25	-	-	Sphene	10	1	-	Clay	-	70	10	Pyrite	2	2	-	Zeolite	5	-	-	Carbonate unspc.	2	-	-	Zoisite/epidote	15	2	5-10	Opauques	2	10	-
	1-20 (D)	1-90 (D)	CC (D)																																																																				
TEXTURE:																																																																							
Sand	-	10	-																																																																				
Silt	-	10	-																																																																				
Clay	-	80	-																																																																				
COMPOSITION:																																																																							
Quartz	15	-	80 (authigenic)																																																																				
Feldspar	25	-	-																																																																				
Sphene	10	1	-																																																																				
Clay	-	70	10																																																																				
Pyrite	2	2	-																																																																				
Zeolite	5	-	-																																																																				
Carbonate unspc.	2	-	-																																																																				
Zoisite/epidote	15	2	5-10																																																																				
Opauques	2	10	-																																																																				

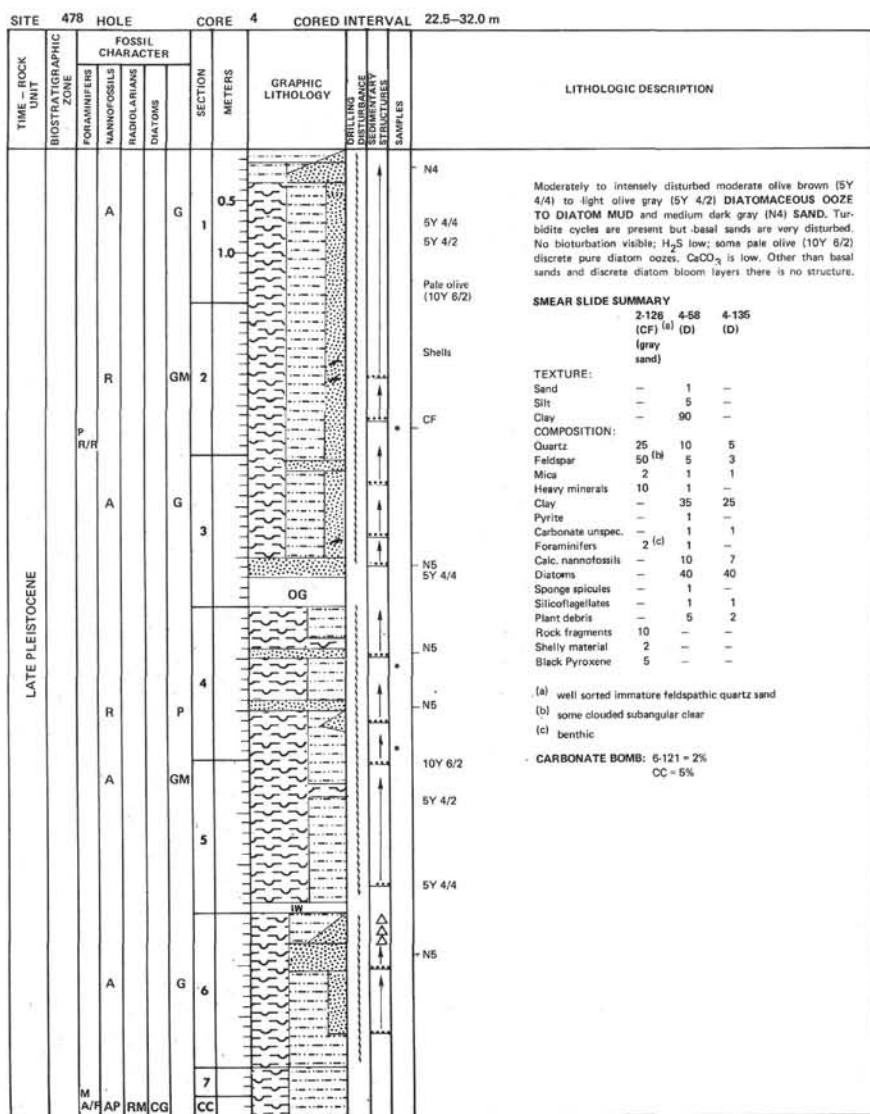
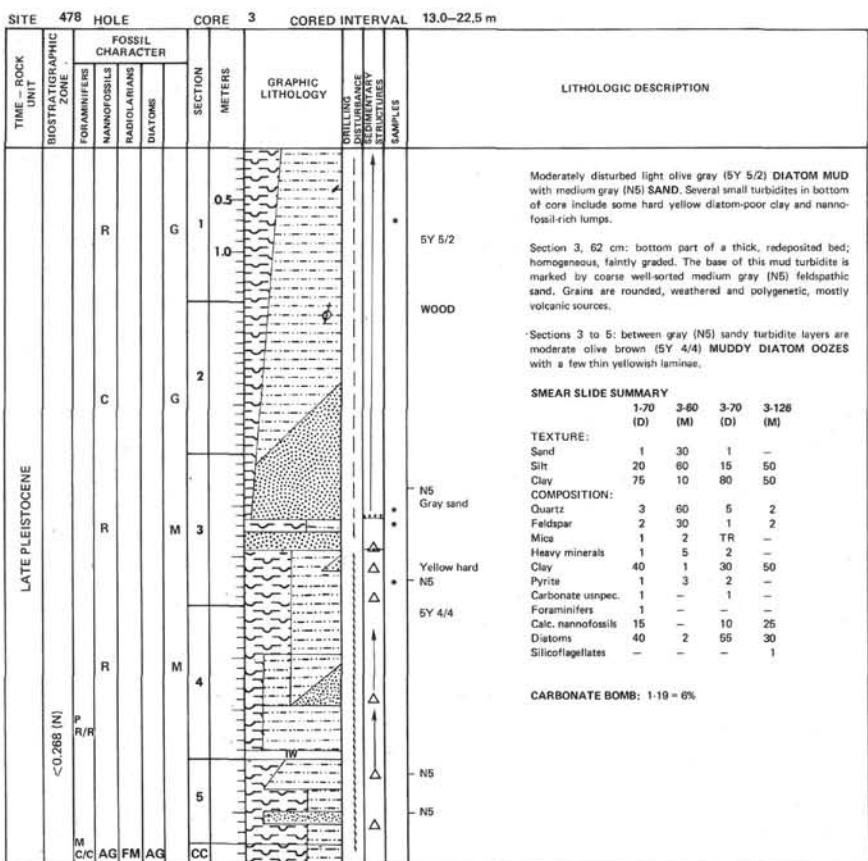
SITE 477		HOLE A			CORE 11		CORED INTERVAL 248.0-257.5 m																																										
TIME - ROCK UNIT	BIOSTRATIGRAPHIC ZONE	FOSSIL CHARACTER			SECTION METERS	GRAPHIC LITHOLOGY	DRILLING DISTURBANCE	LITHOLOGIC DESCRIPTION																																									
		FORAMINIFERS	NANNOFOSSILS	RADIOLARIANS					DIAZONES																																								
7					1		<p>N6 N2</p> <p>Mixture of drill "pebbles" of altered mud to sand.</p> <p>Type I: medium light gray (N6), coarse, very porous, friable, CEMENTED SANDSTONE. Bedding in pieces at top of core (3 to 9 cm). Indication of redeposition (see diagram with cross-bed, flame structures, laminations and grading). Strong H₂S odor with gas. Pyrite abundant.</p> <p>Type II: grayish black (N2), brittle, pyrite-rich SILTY CLAYSTONE chips scattered throughout core.</p> <p>One piece of black (N1) "hornfels" CLAYSTONE imbedded with large euhedral crystals. Difference between light and dark is mostly number of irregular opaque chips (0.01 to 0.05 mm) which are carbon not sulfides. Feldspars are K-feldspar or albite; clusters of euhedral epidote prisms.</p> <p>Piece above from Section 1, 3-9 cm (turbidite):</p> <ol style="list-style-type: none"> 1) massive medium sand, gray, with some pyrite (or pyrrhotite) 2) laminated dark gray fine sand 3) cross-laminated, somewhat convoluted fine sand, alternating light and gray laminae 4) plus or minus parallel laminated gray fine sand 5) gray fine sand with many small platy mud lumps and dark minerals, very small-scaled cross-bedding <p>SMEAR SLIDE SUMMARY</p> <table border="1"> <thead> <tr> <th></th> <th>1-3 (D)</th> <th>1-5 (D)</th> </tr> </thead> <tbody> <tr> <td>TEXTURE:</td> <td></td> <td></td> </tr> <tr> <td>Sand</td> <td>-</td> <td>-</td> </tr> <tr> <td>Silt</td> <td>-</td> <td>-</td> </tr> <tr> <td>Clay</td> <td>-</td> <td>-</td> </tr> <tr> <td>COMPOSITION:</td> <td></td> <td></td> </tr> <tr> <td>Quartz</td> <td>15</td> <td>10 (authigenic)</td> </tr> <tr> <td>Feldspar</td> <td>60</td> <td>3</td> </tr> <tr> <td>Clay</td> <td>5</td> <td>-</td> </tr> <tr> <td>Pyrite</td> <td>3</td> <td>3</td> </tr> <tr> <td>Zeolite</td> <td>10</td> <td>5</td> </tr> <tr> <td>Coal</td> <td>-</td> <td>15</td> </tr> <tr> <td>Zoisite/epidote</td> <td>10</td> <td>50</td> </tr> <tr> <td>Unidentified</td> <td>10</td> <td>15</td> </tr> </tbody> </table>		1-3 (D)	1-5 (D)	TEXTURE:			Sand	-	-	Silt	-	-	Clay	-	-	COMPOSITION:			Quartz	15	10 (authigenic)	Feldspar	60	3	Clay	5	-	Pyrite	3	3	Zeolite	10	5	Coal	-	15	Zoisite/epidote	10	50	Unidentified	10	15
	1-3 (D)	1-5 (D)																																															
TEXTURE:																																																	
Sand	-	-																																															
Silt	-	-																																															
Clay	-	-																																															
COMPOSITION:																																																	
Quartz	15	10 (authigenic)																																															
Feldspar	60	3																																															
Clay	5	-																																															
Pyrite	3	3																																															
Zeolite	10	5																																															
Coal	-	15																																															
Zoisite/epidote	10	50																																															
Unidentified	10	15																																															

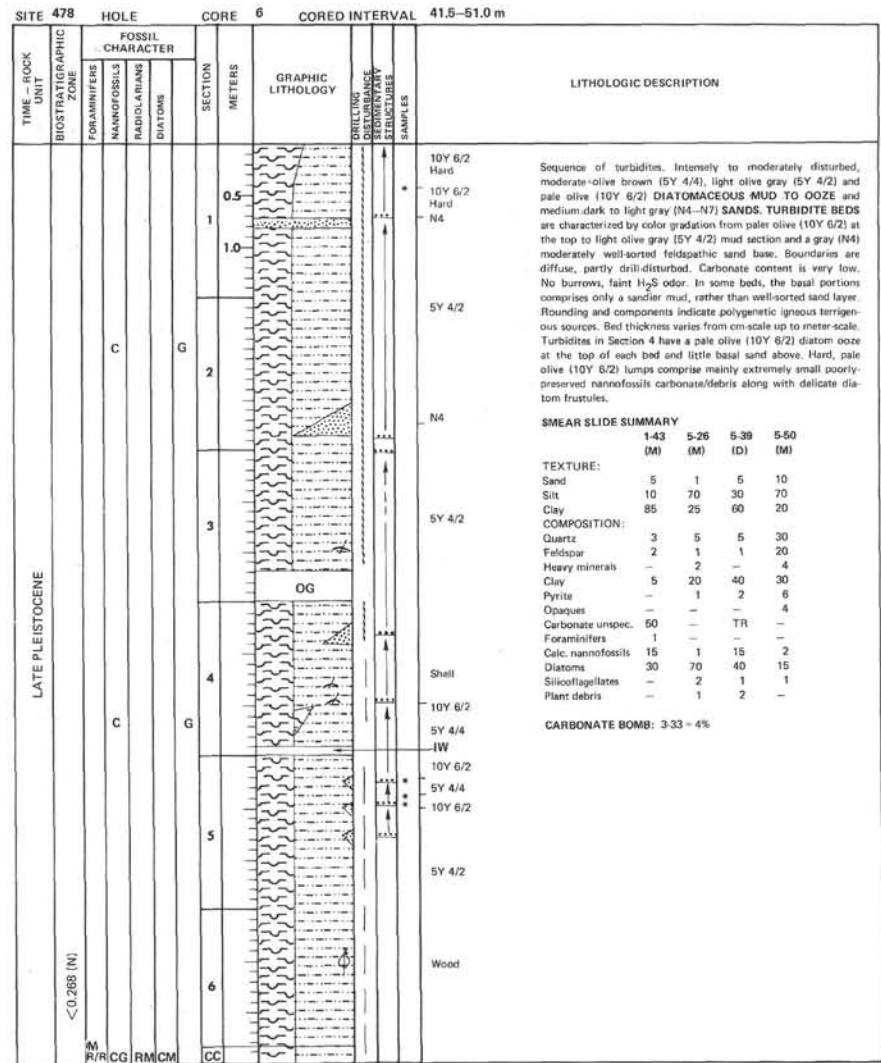
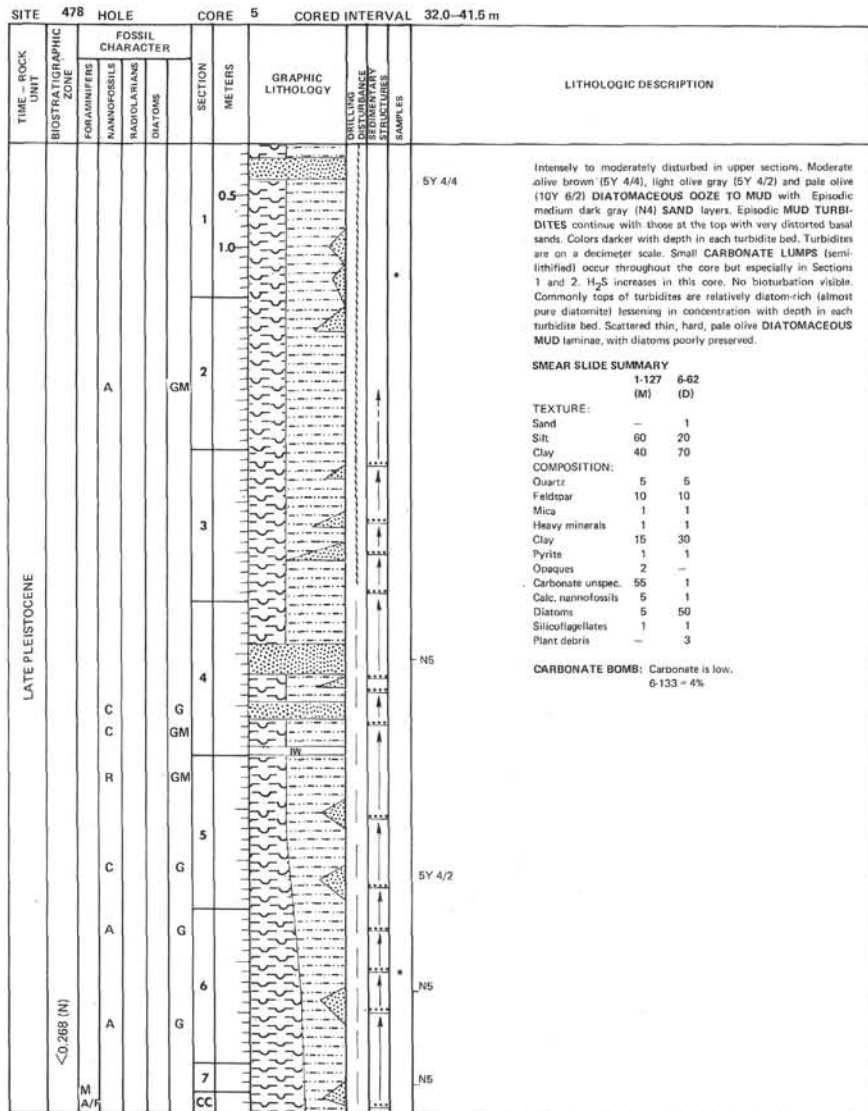
SITE 477		HOLE A			CORE 12		CORED INTERVAL 257.5-267.0 m	
TIME - ROCK UNIT	BIOSTRATIGRAPHIC ZONE	FOSSIL CHARACTER			SECTION METERS	GRAPHIC LITHOLOGY	DRILLING DISTURBANCE	LITHOLOGIC DESCRIPTION
		FORAMINIFERS	NANNOFOSSILS	RADIOLARIANS				
					1		<p>Light gray (N7) porous epidote-feldspar SANDSTONE with intercalated platy gray (N4) mud chips. Sandstone is very friable, porous with some laminations present in one drilling breccia piece.</p>	

SITE 477 HOLE B CORE 1 CORED INTERVAL 0.0-4.6 m

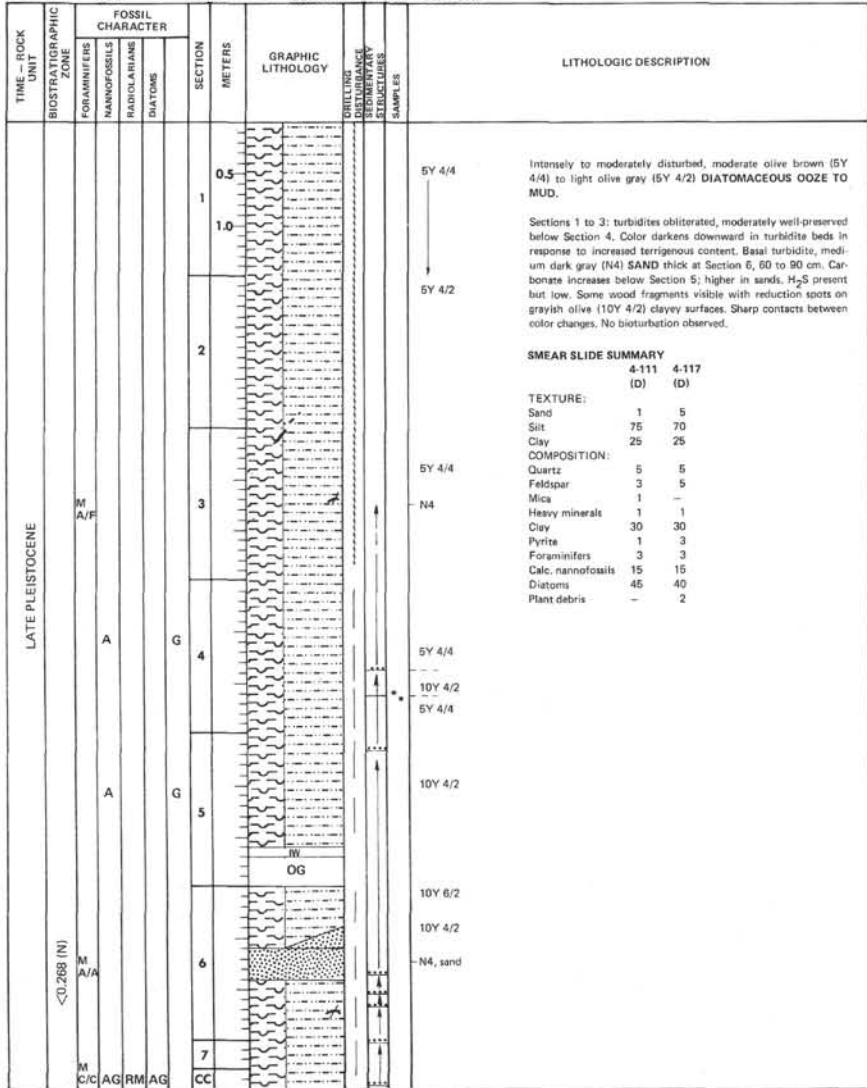
TIME - ROCK UNIT	BIOSTRATIGRAPHIC ZONE	FOSSIL CHARACTER			SECTION	METERS	GRAPHIC LITHOLOGY	ORILLINO SEDIMENTARY SAMPLES	LITHOLOGIC DESCRIPTION
		FORAMINIFERS	NANNIFOSSILS	RADIOLARIANS					
		X			0.5		IW	<p>Moderate olive brown (5Y 4/4) MUDDY DIATOMACEOUS OOZE. Intensely disturbed in the top of the core; slightly disturbed in the bottom of the core. Very uniform texture and color. No structures or bedding. No H₂S present. Pyrite seen as framboids in diatom frustules. Organic (terrigenous) consist of wood fragments and cuticles with high b.f.</p> <p>SMEAR SLIDE SUMMARY 1-75 (D)</p> <p>TEXTURE: Sand - Silt 40 Clay 60</p> <p>COMPOSITION: Quartz } 10 Feldspar } Mica 3 Clay 35 Pyrite 5 Foraminifers TR Calc. nannofossils 5 Diatoms 35 Radiolarians TR Silicoflagellates TR Plant debris 5</p> <p>CARBONATE BOMB: 1-14 = 5% 2-110 = 8%</p>	
				1	1.0		IW * IW		
				2		OG	IW		
				3			IW		
							Bacteria		



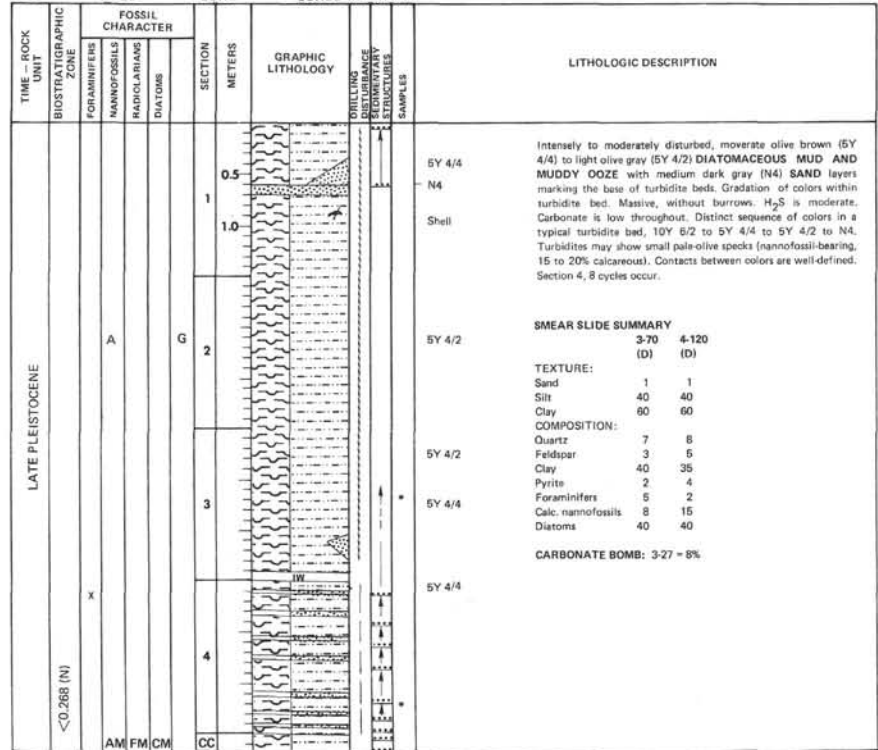


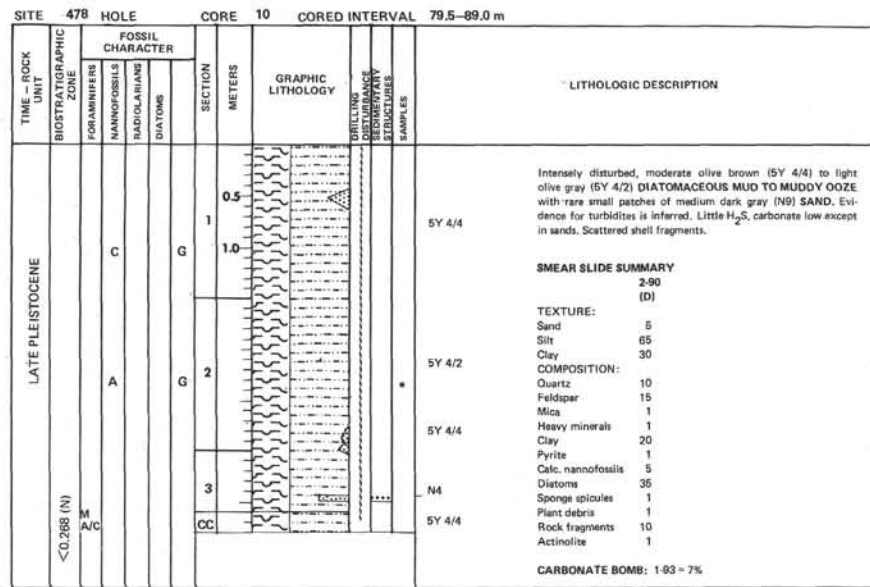
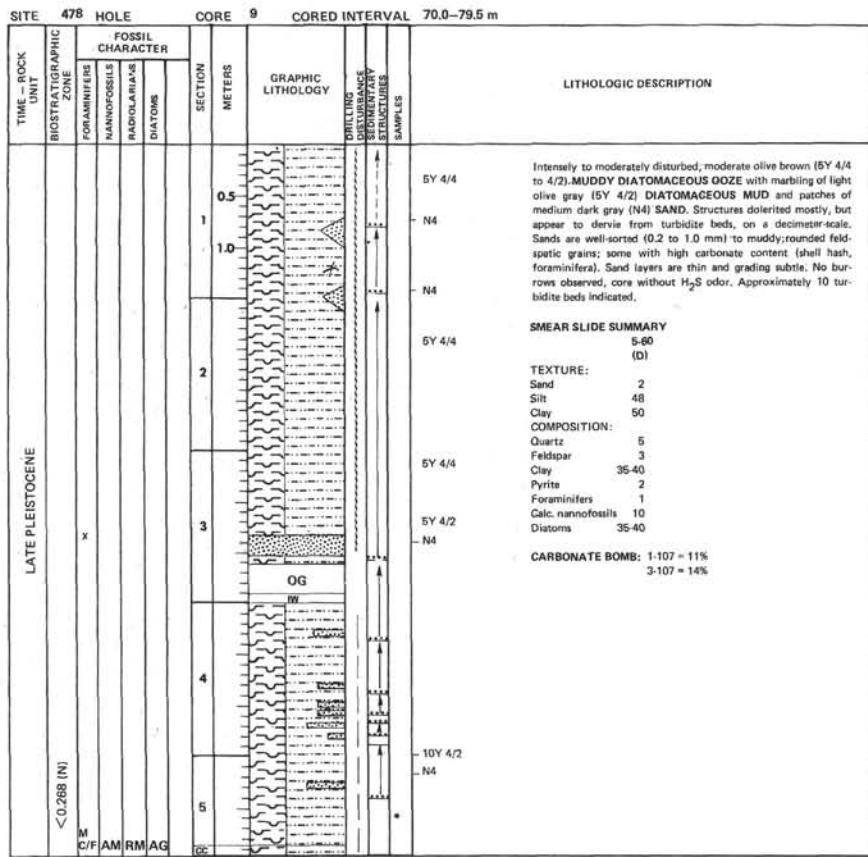


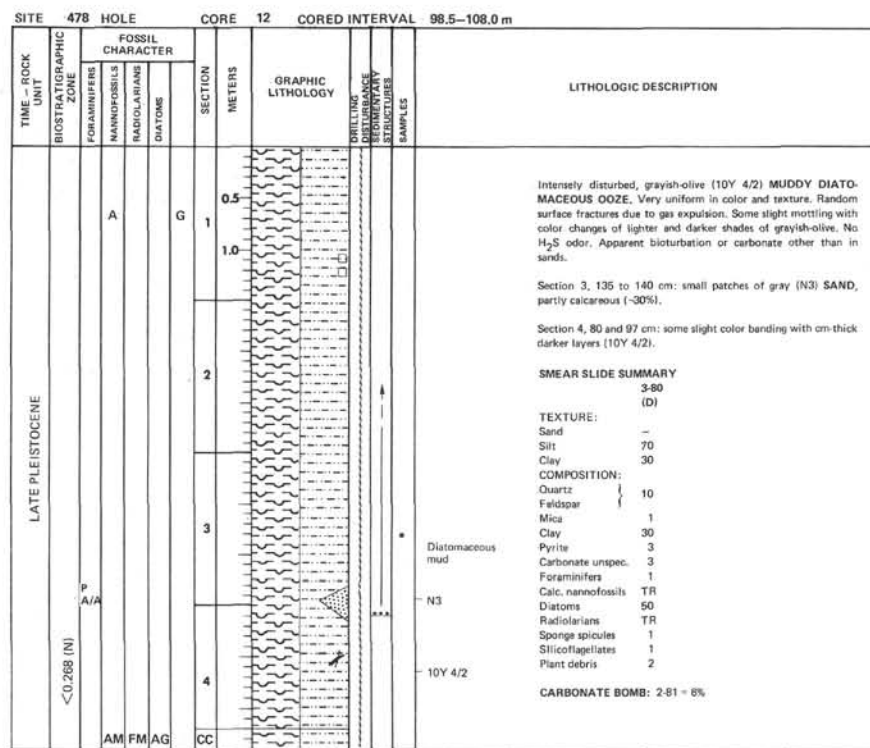
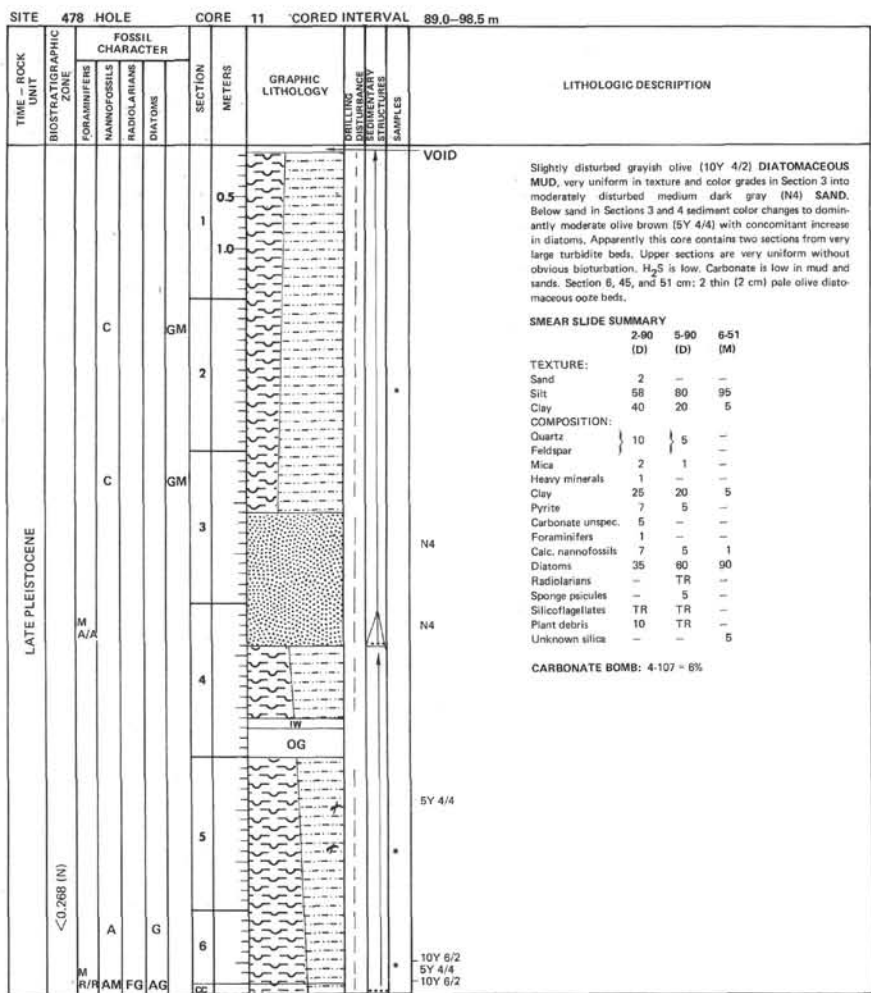
SITE 478 HOLE CORE 7 CORED INTERVAL 51.0-60.5

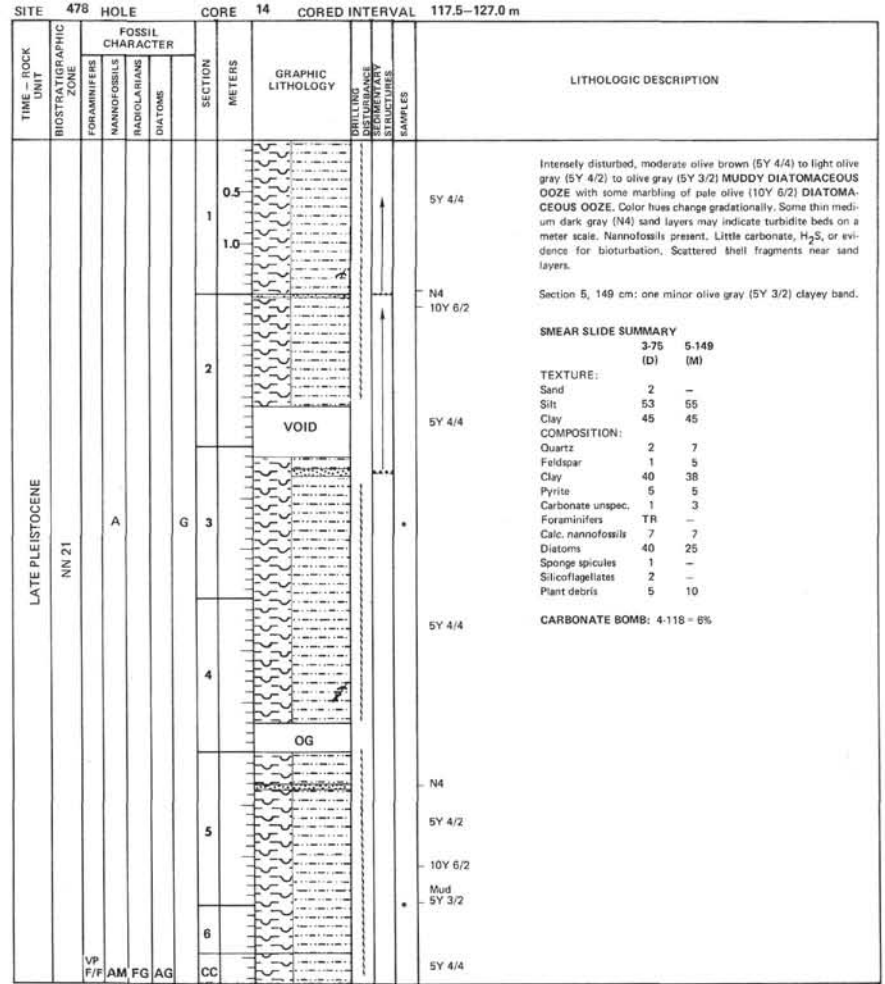
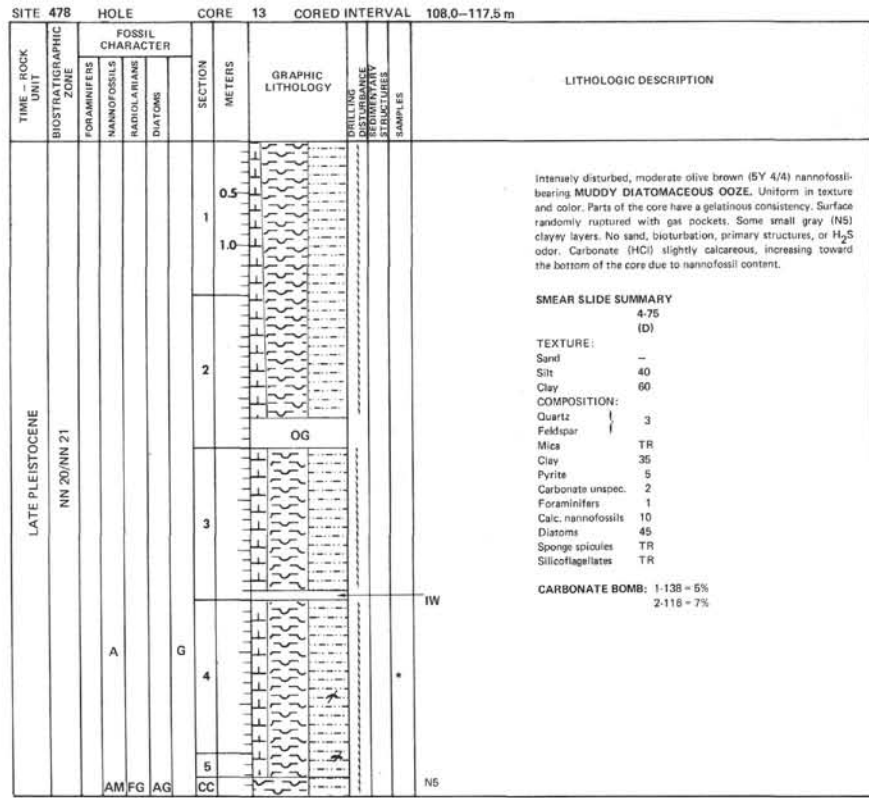


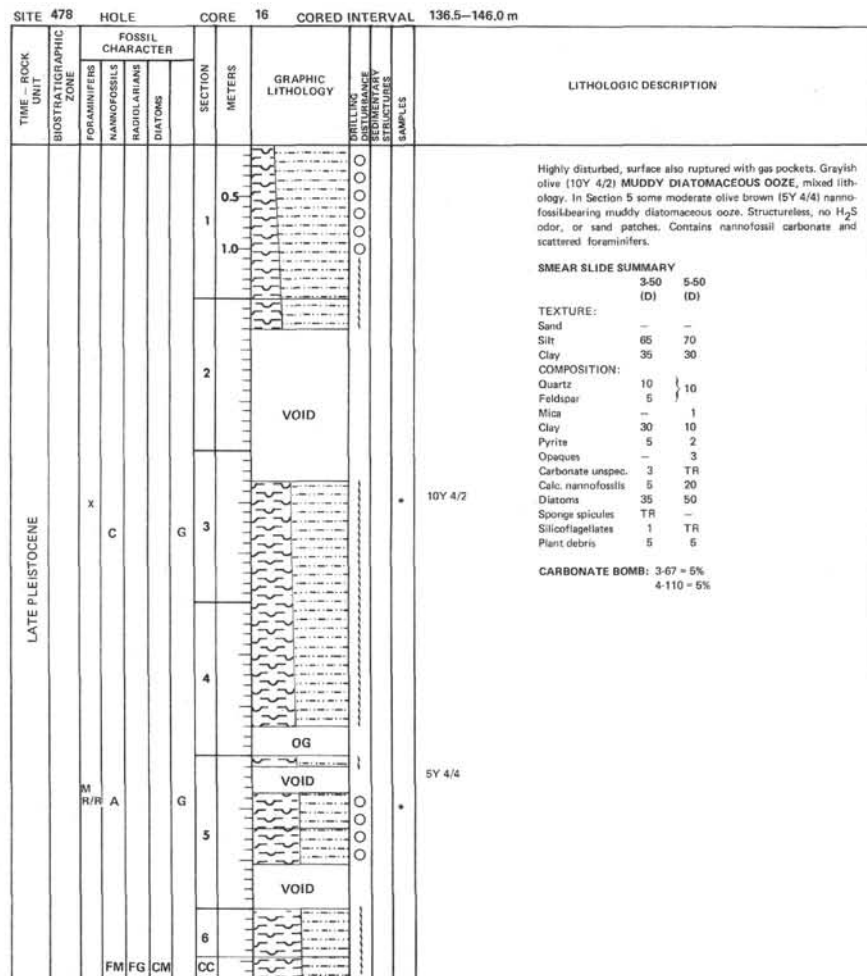
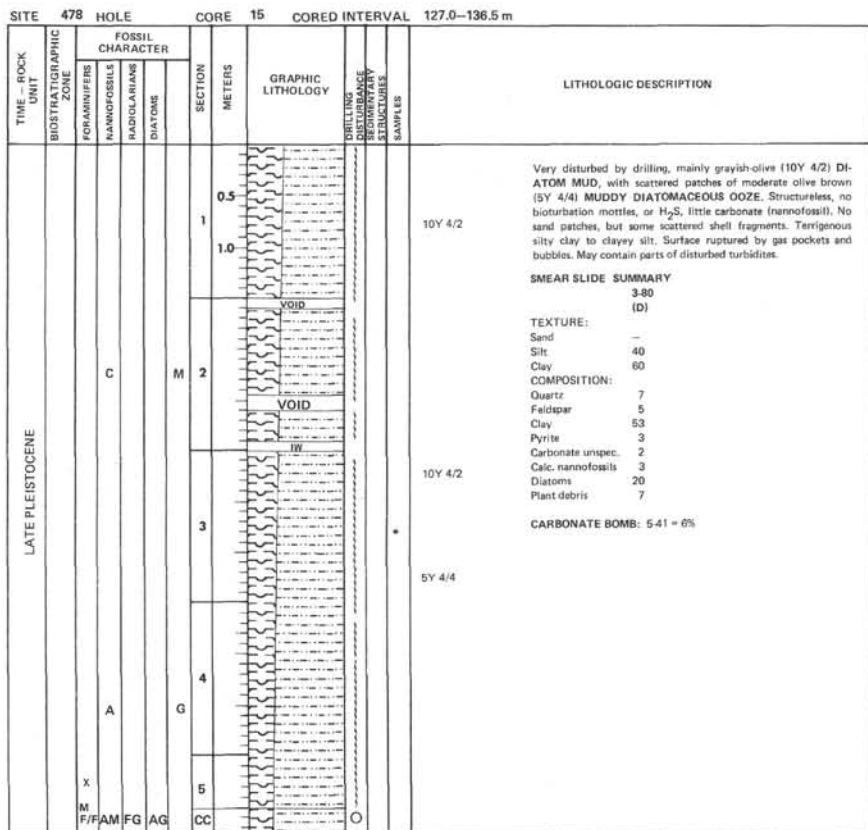
SITE 478 HOLE CORE 8 CORED INTERVAL 60.5-70.0 m





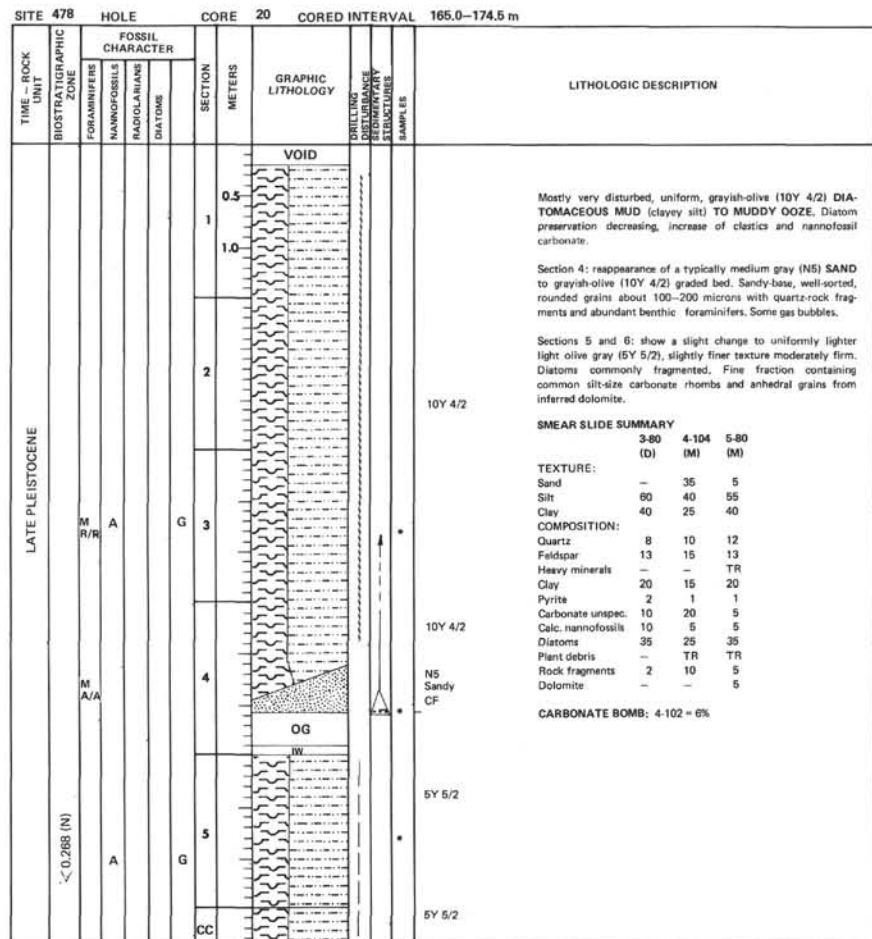
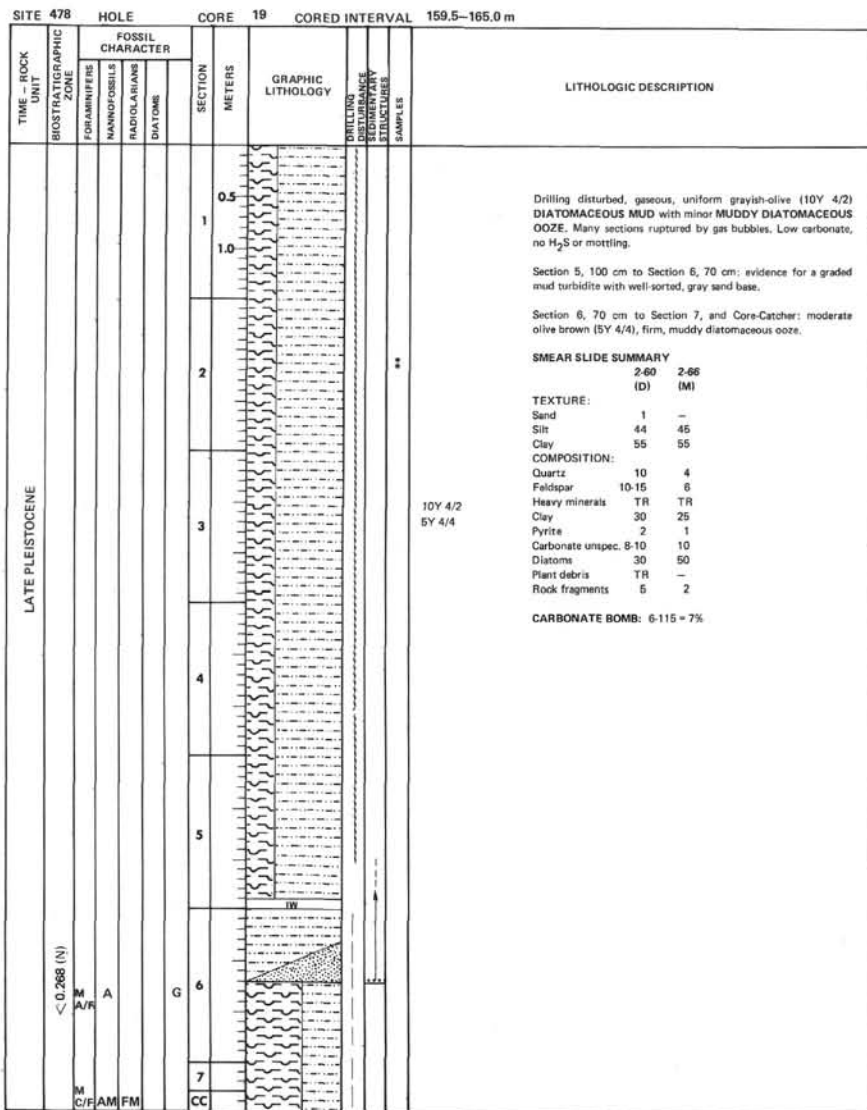


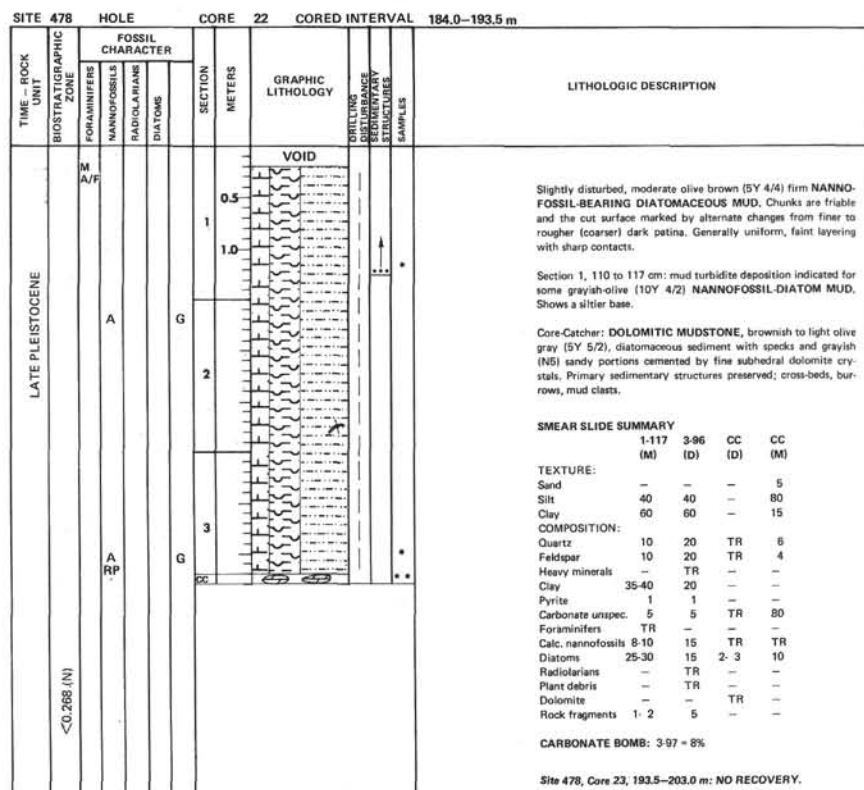
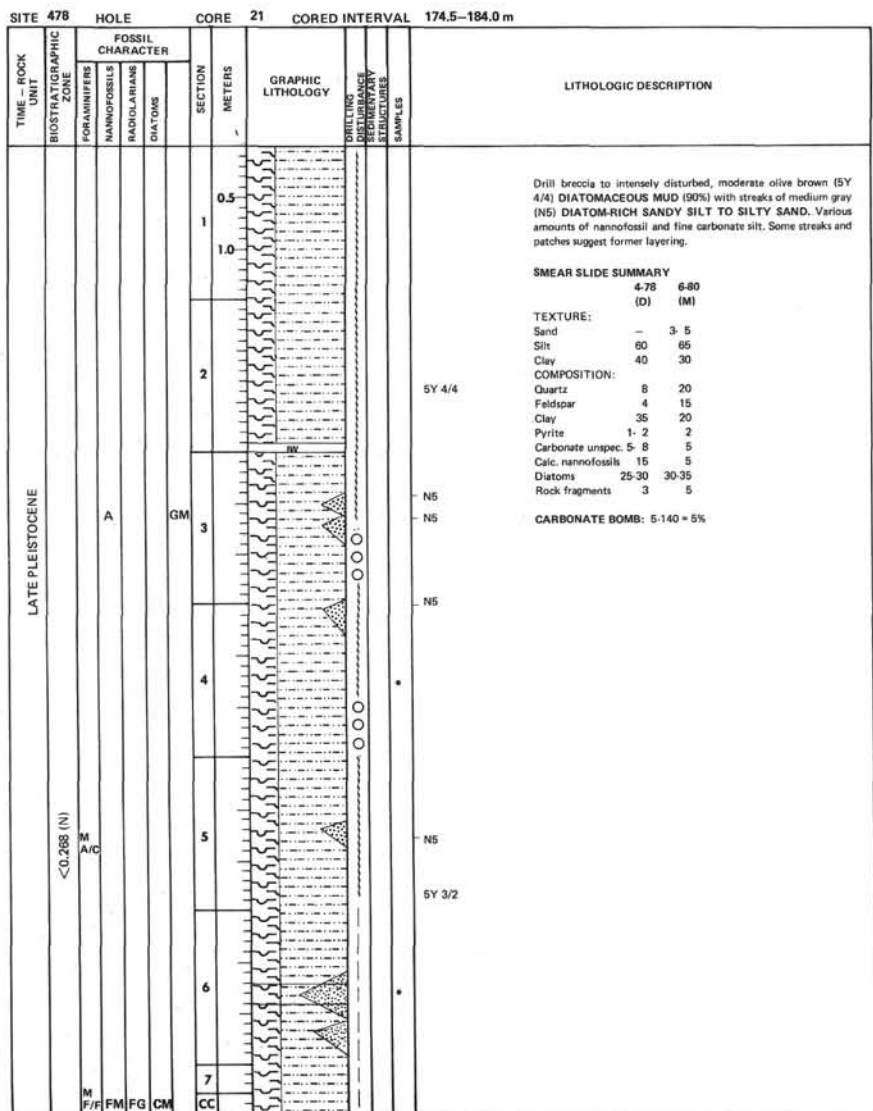




SITE 478		HOLE		CORE 17		CORED INTERVAL 146.0-155.5 m		
TIME - ROCK UNIT	BIOSTRATIGRAPHIC ZONE	FOSSIL CHARACTER			SECTION METERS	GRAPHIC LITHOLOGY	LITHOLOGIC DESCRIPTION	
		FORAMINIFERS	NANNOFOSSILS	RADICULARIANS				DIATOMS
LATE PLEISTOCENE	<0.268 (N)	P	R/R	FM	FG	CM	1	<p>Uniform, partly disturbed, firming below Section 3, grayish-olive (10Y 4/2) DIATOMACEOUS MUD, clayey silt. Carbonate, some gas speculation but few bubbles, very faint layering in lower part. No H₂S, sand or burrow mottles. Smear slide contains common 2 to 4 micron tiny carbonate grains, thought dolomitic.</p> <p>SMEAR SLIDE SUMMARY</p> <p>3-70 (D)</p> <p>TEXTURE:</p> <p>Sand 2 Silt 38 Clay 60</p> <p>COMPOSITION:</p> <p>Quartz 10 Feldspar 48 Clay 2 Pyrite 2 Calc. nannofossils TR Diatoms 20 Silicoflagellates 1 Fish remains 1 Plant debris 5 Dolomite 15</p>
							0.5	
							1	
							1.0	
							2	
							3	
							4	
5								
6								
7								
							CC	

SITE 478		HOLE		CORE 18		CORED INTERVAL 155.5-159.5 m	
TIME - ROCK UNIT	BIOSTRATIGRAPHIC ZONE	FOSSIL CHARACTER			SECTION METERS	GRAPHIC LITHOLOGY	LITHOLOGIC DESCRIPTION
		FORAMINIFERS	NANNOFOSSILS	RADICULARIANS			
LATE PLEISTOCENE	<0.268 (N)	P	R/R	CM	M	CC	<p>Diatomaceous clayey silt</p> <p>Uniform, grayish-olive (10Y 4/2) DIATOMACEOUS MUD, some nannofossils with considerable silt (clayey silt) (sand-silt-clay). No H₂S, sand patches. Smear slide contains some re-worked carbonate or recrystallized nannofossils, possibly dolomitic.</p> <p>SMEAR SLIDE SUMMARY</p> <p>1-12 (D)</p> <p>TEXTURE:</p> <p>Sand 2 Silt 58 Clay 40</p> <p>COMPOSITION:</p> <p>Quartz 10 Feldspar 15 Heavy minerals TR Clay 25 Pyrite 2 Carbonate unsp. 5 Calc. nannofossils 10 Diatoms 30 Plant debris TR Rock fragments 5</p>

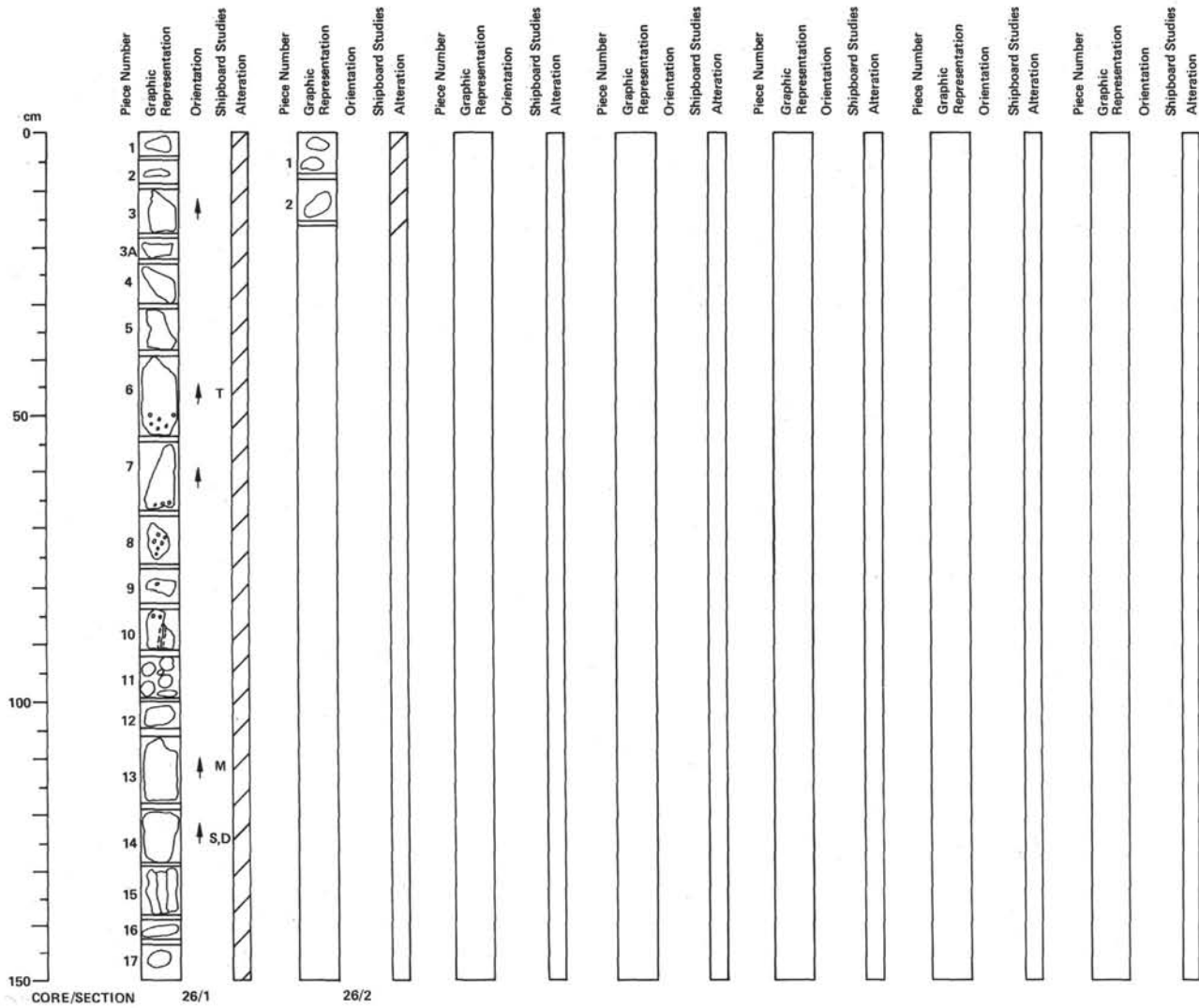




Site 478, Core 23, 193.5-203.0 m: NO RECOVERY.

SITE 478		HOLE				CORE 24	CORED INTERVAL 203.0-212.5 m		
TIME - ROCK UNIT	BIOSTRATIGRAPHIC ZONE	FOSSIL CHARACTER				SECTION METERS	GRAPHIC LITHOLOGY	FOSSILS OR DISTURBANCE STRUCTURES INCLUDED	LITHOLOGIC DESCRIPTION
		FORAMINIFERS	NANNOFOSSELS	RADIOLARIANS	DIAZONES				
						1		4	<p>Dolomite Scrape 1</p> <p>One indurated chunk of hard grayish-olive (10Y 4/2) DOLOMITIC SILTSTONE. Sandy at the base with possible cross-bedding preserved. Dolomite as cement in a redeposited bed. Dolomite as sub- to anhedral grains (0.02-0.04 mm).</p> <p>SMEAR SLIDE SUMMARY 1-2 (D)</p> <p>TEXTURE: Sand - Silt - Clay -</p> <p>COMPOSITION: Quartz 15 Feldspar 3 Clay 6 Dolomite 75</p>

SITE 478		HOLE				CORE 25	CORED INTERVAL 212.5-222.0 m		
TIME - ROCK UNIT	BIOSTRATIGRAPHIC ZONE	FOSSIL CHARACTER				SECTION METERS	GRAPHIC LITHOLOGY	FOSSILS OR DISTURBANCE STRUCTURES INCLUDED	LITHOLOGIC DESCRIPTION
		FORAMINIFERS	NANNOFOSSELS	RADIOLARIANS	DIAZONES				
						1		*	<p>Pieces of light olive gray, hard siltstone with dolomite cement. Massive, no primary structures visible.</p> <p>SS 1-1 cm: subhedral, silt-size quartz, feldspar 80% dolomite 10% detrital silt 3% opoques 7% other</p>



64-478-26

Depth 220.0 to 231.5 m

SECTION 1: DOMINANT LITHOLOGY: COARSE GRAINED BASALT.**Macroscopic Description**

Aphyric, coarse-grained (0.2–0.5 mm grain size) dark gray (N4) basalt. Slight weathering patina in Pieces 7 and 9 resulting in brown discoloration.

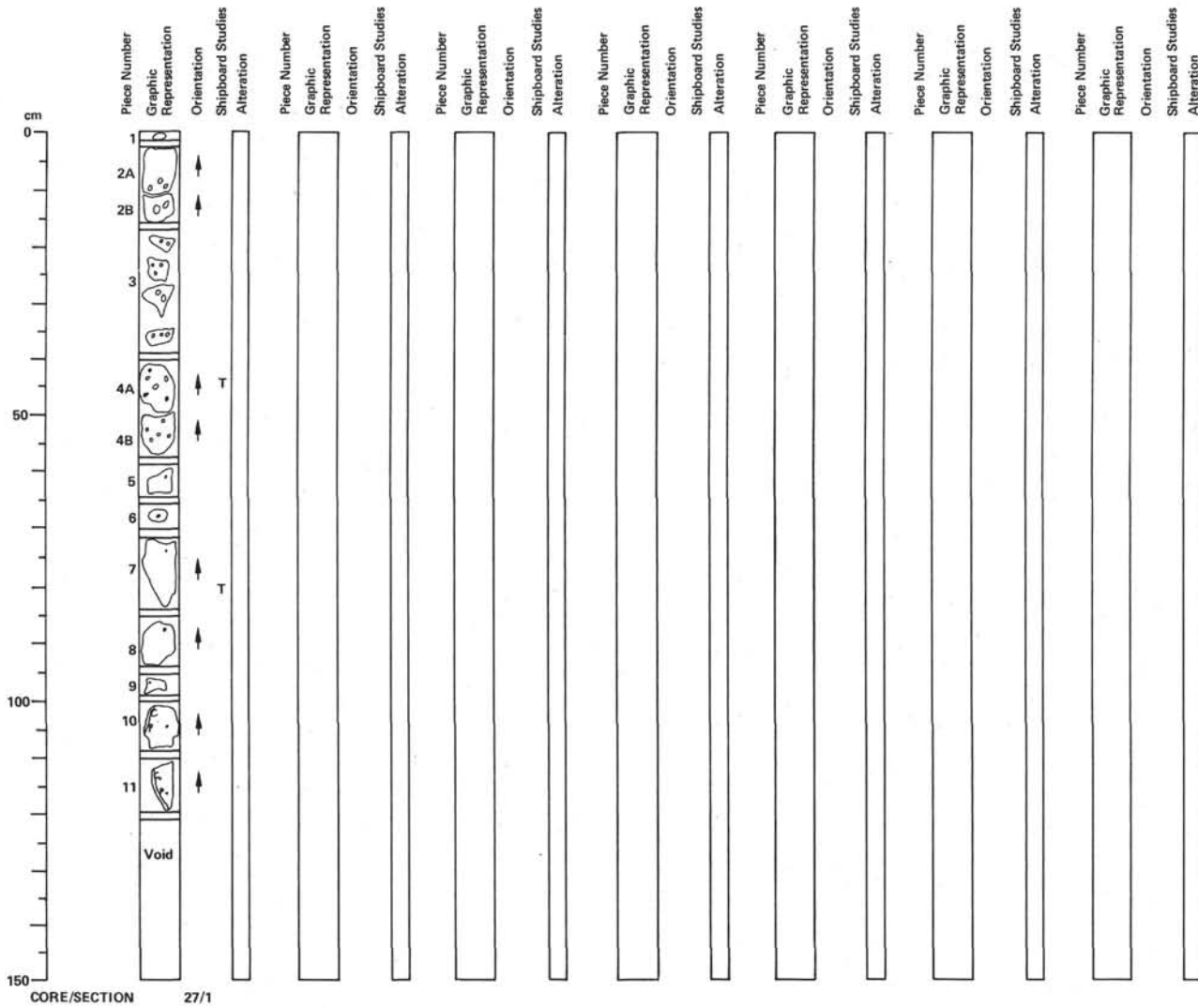
Small spherical vesicles, approximately 1 mm in diameter, occur in Piece 6 to 10. They are filled with white mineral, in part calcite. Veins in Pieces 10 and 15 calcite-filled.

Several pieces have pyrite dusting.

TS 6-48: 48 cm, aphyric basalt, intergranular texture. Plagioclase 60%, up to 1.5 mm long. An_{62-68} , lath-shaped crystals, but also occurs as anhedral interstitial fitting. Normally zoned. Clinopyroxene 25%, 0.1–0.5 mm, augite, anhedral, very pale brown, intergranular. Magnetite 3%, 0.1–0.3 mm cuboid and ilmenite 3%, up to 0.5 mm, elongate crystals (especially common in alteration areas). Alteration 10% green clay, occurring in interstitial areas, replacing mesostasis and possibly also olivine. No vesicles in this thin section.

SECTION 2: DOMINANT LITHOLOGY: coarse grained basalt.**Macroscopic Description**

Same as Core 26, Section 1.



64-478-27

Depth 231.5 to 241.0 m

SECTION 1: DOMINANT LITHOLOGY: VESICULAR BASALT grading to APHYRIC BASALT.

Macroscopic Description

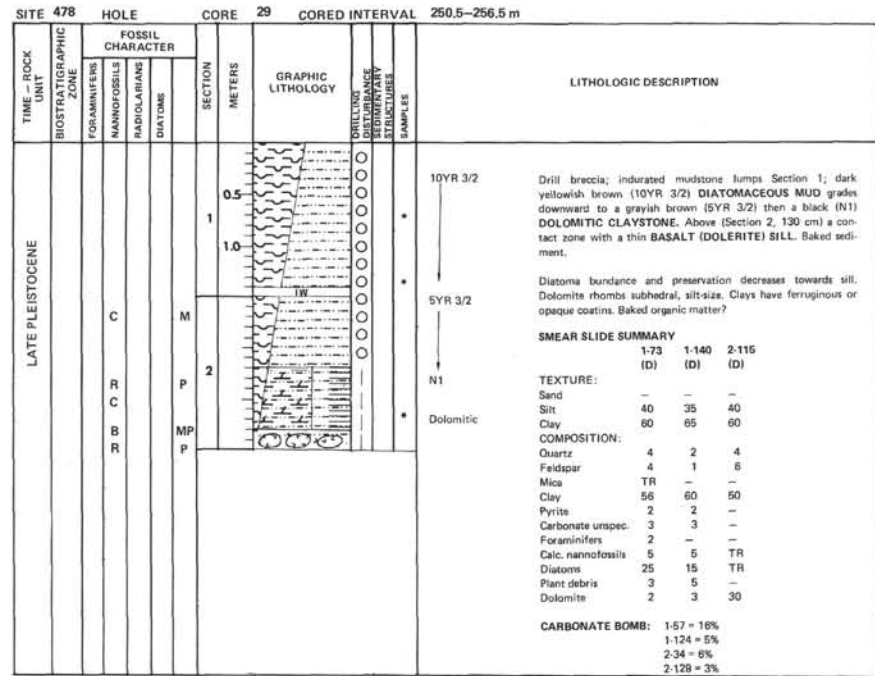
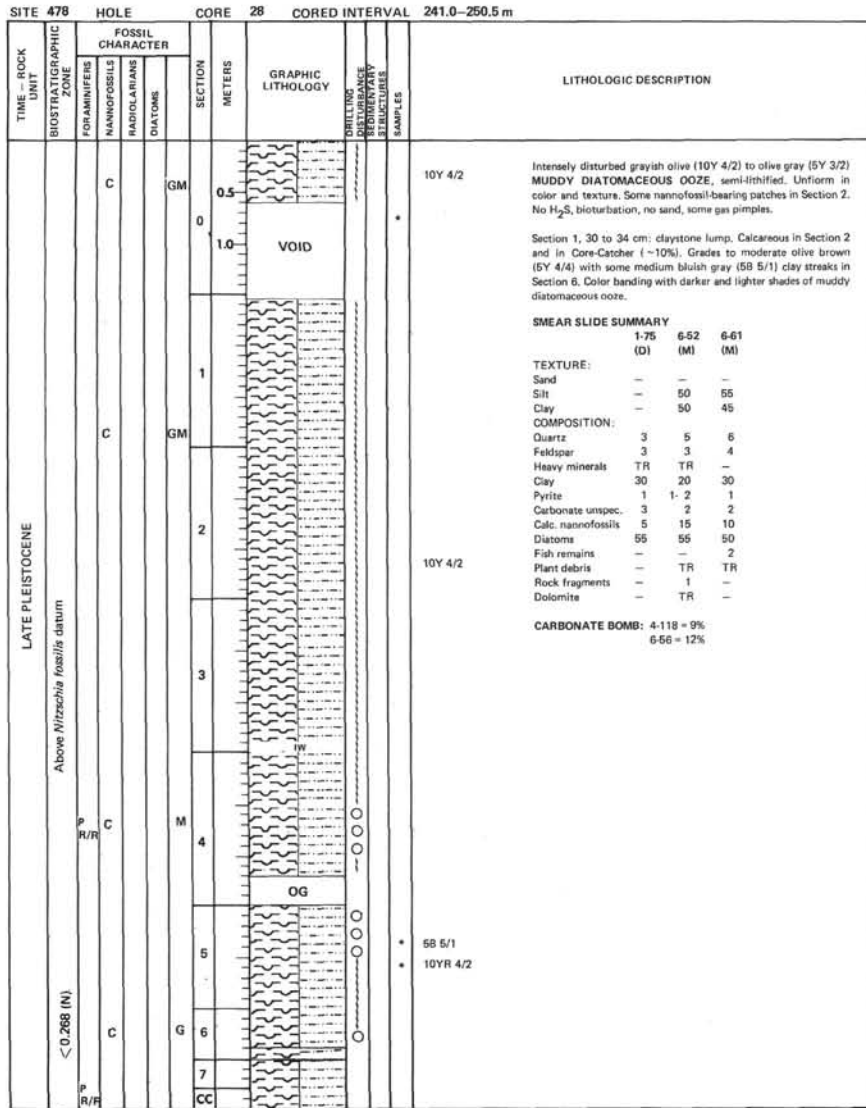
Piece 1 is a dolomite siltstone with pyrite.
 Pieces 2A-4B are vesicular aphyric basalt, medium dark gray (N6) color with 2-5 mm diameter vesicles. Most are lined with calcite and pyrite and clay minerals.
 Pieces 5-11 are medium gray (N6) aphanitic basalt with few small < 1 mm vesicles, some filled with calcite. Small veins (~1 mm thick) are pervasively filled with calcite and pyrite.

TS 45 cm, Piece 4A: Aphyric basalt with intersectoral, vesicular texture. Plagioclase 40%, 0.2-0.8 mm, skeletal laths, and interstitial crystals. Clinopyroxene 10%, <0.1 mm anhedral. Some may be olivine but the crystals are too small to be certain. Magnetite 3%, 0.01-0.1 mm. Ilmenite 3%, up to 0.1 mm. Vesicles less than 3%, 1-1.5 mm, spherical, no filling preserved. Alteration: severe alteration of mesostasis and possibly of olivines, 40% green clay minerals.

TS 82 cm, Piece 7: aphyric basalt. Similar to TS at 45 cm. Plagioclase 50% (?An₆₀), augite 10%, opaques 5%. Vesicles 1 large (up to 10 mm) compound vesicles containing smaller vesicles in a coarse-grained basalt of plagioclase, clinopyroxene and iron-rich mesostasis. Alteration: severe, ~35% clay minerals, 1% carbonate in vesicles.

SS 1-2:

- 33% Quartz
- 5% Feldspar (altered)
- 3% Mica
- 1% Heavy minerals
- 65% Clay
- 3% Pyrite
- 10% Carbonate unsp. spec.
- 1% Plant debris



0
50
100
150
CORE/SECTION

Piece Number

Graphic Representation

Orientation

Shipboard Studies

Alteration



29/CC

Piece Number

Graphic Representation

Orientation

Shipboard Studies

Alteration



Piece Number

Graphic Representation

Orientation

Shipboard Studies

Alteration



Piece Number

Graphic Representation

Orientation

Shipboard Studies

Alteration



Piece Number

Graphic Representation

Orientation

Shipboard Studies

Alteration



Piece Number

Graphic Representation

Orientation

Shipboard Studies

Alteration



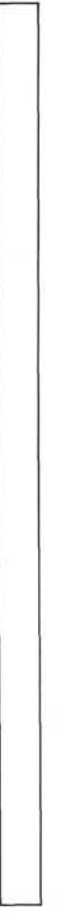
Piece Number

Graphic Representation

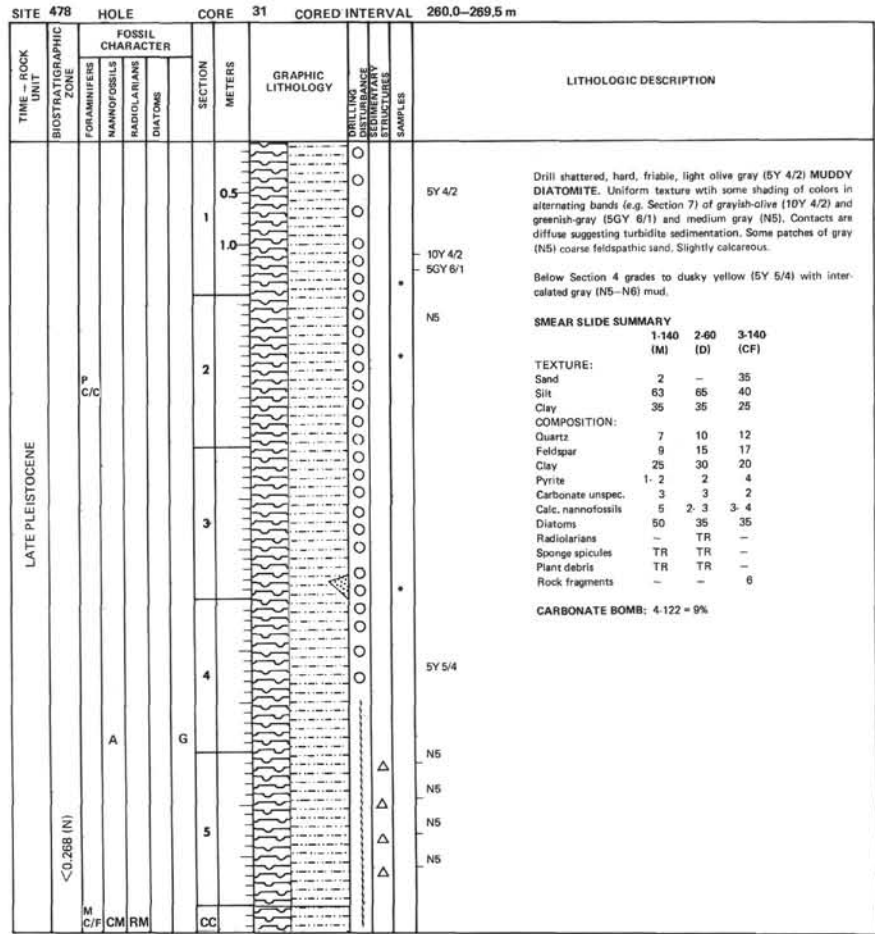
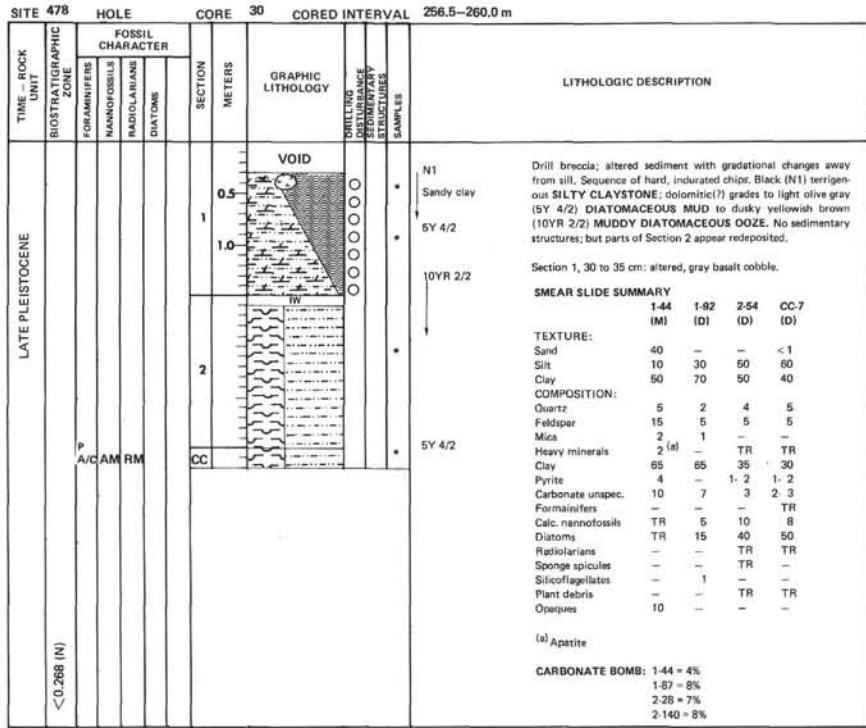
Orientation

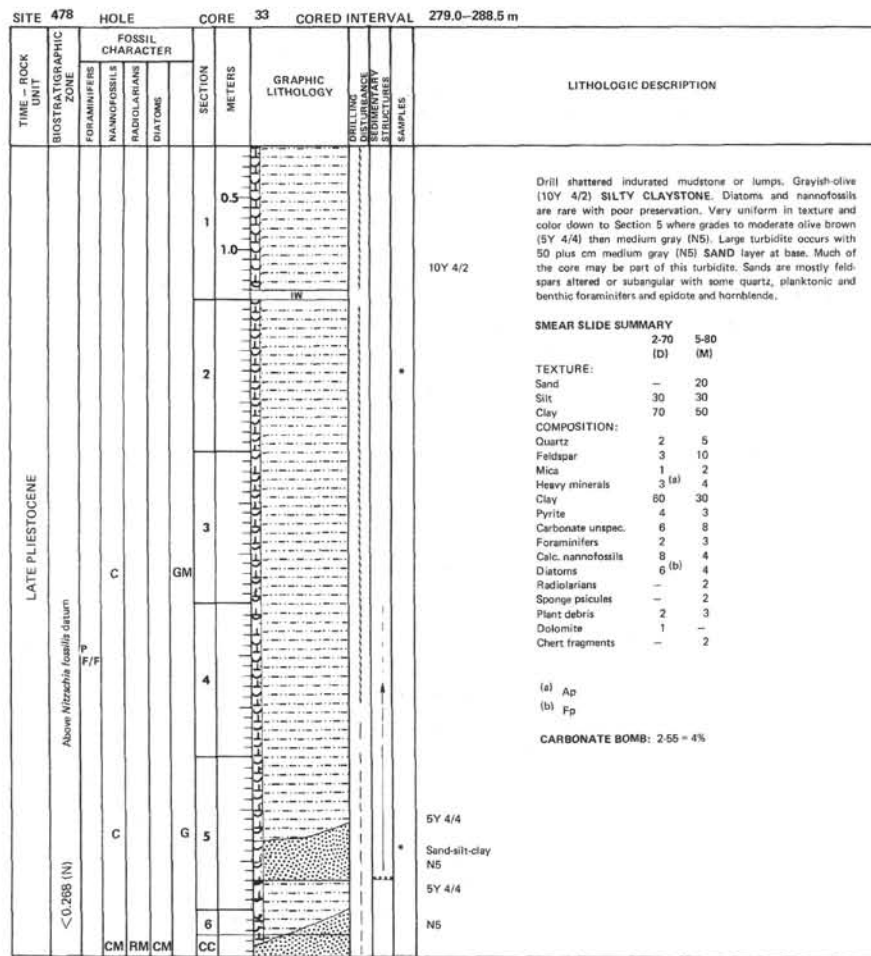
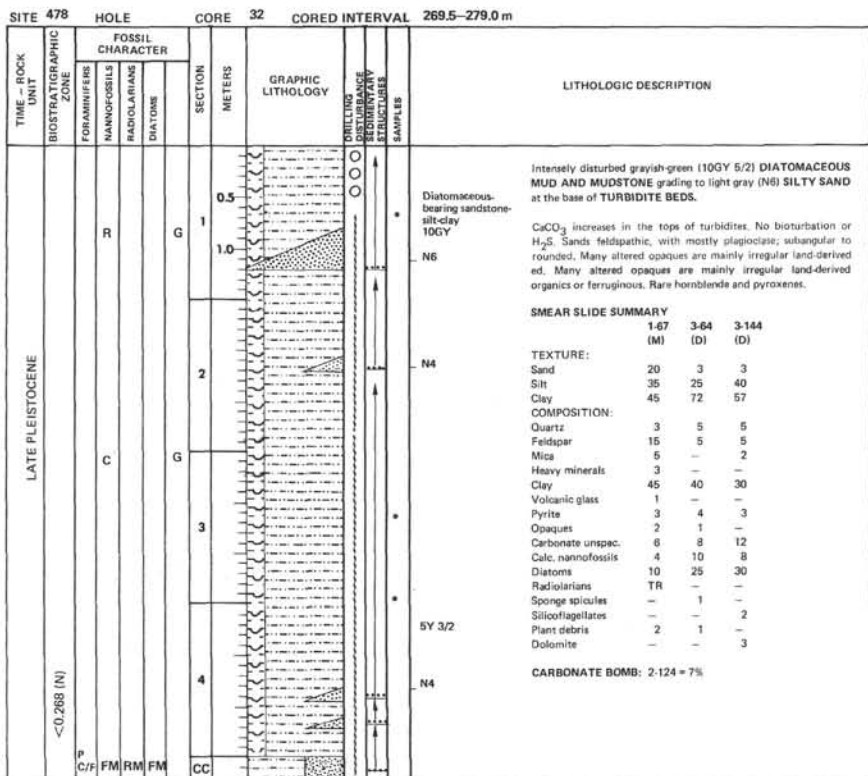
Shipboard Studies

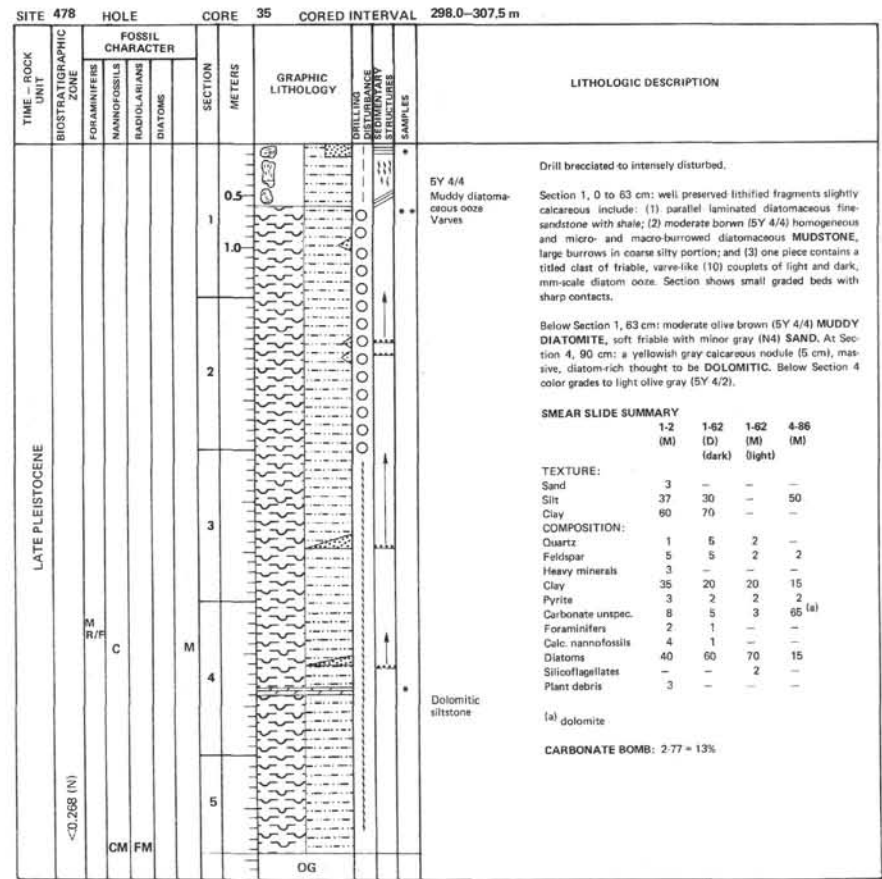
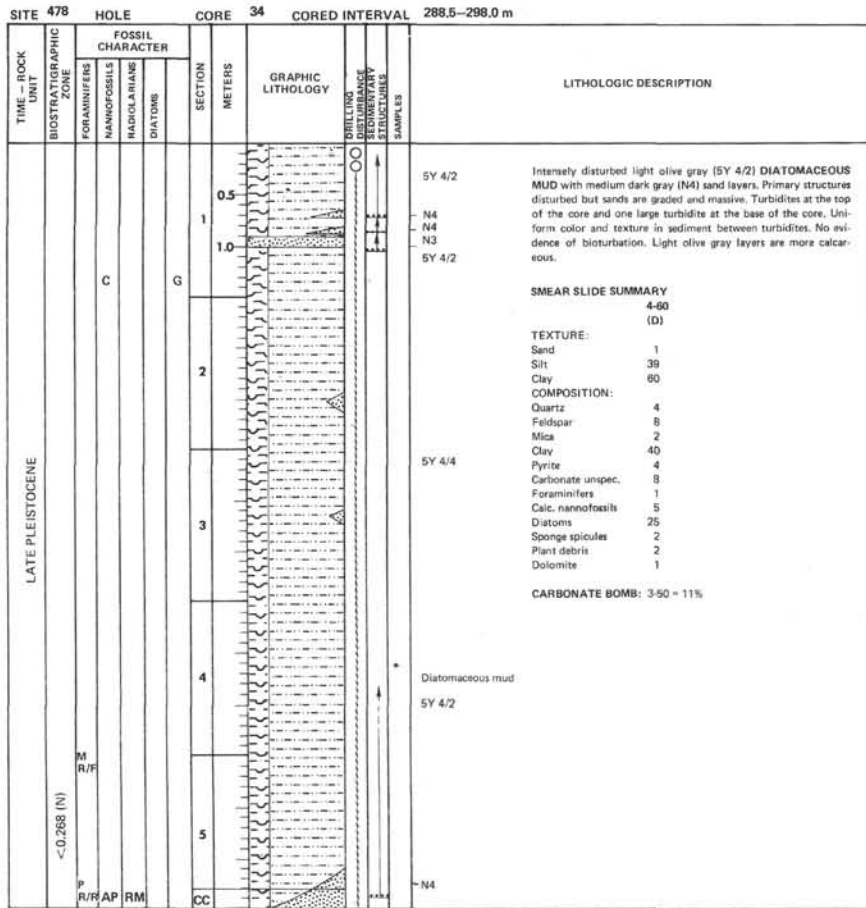
Alteration

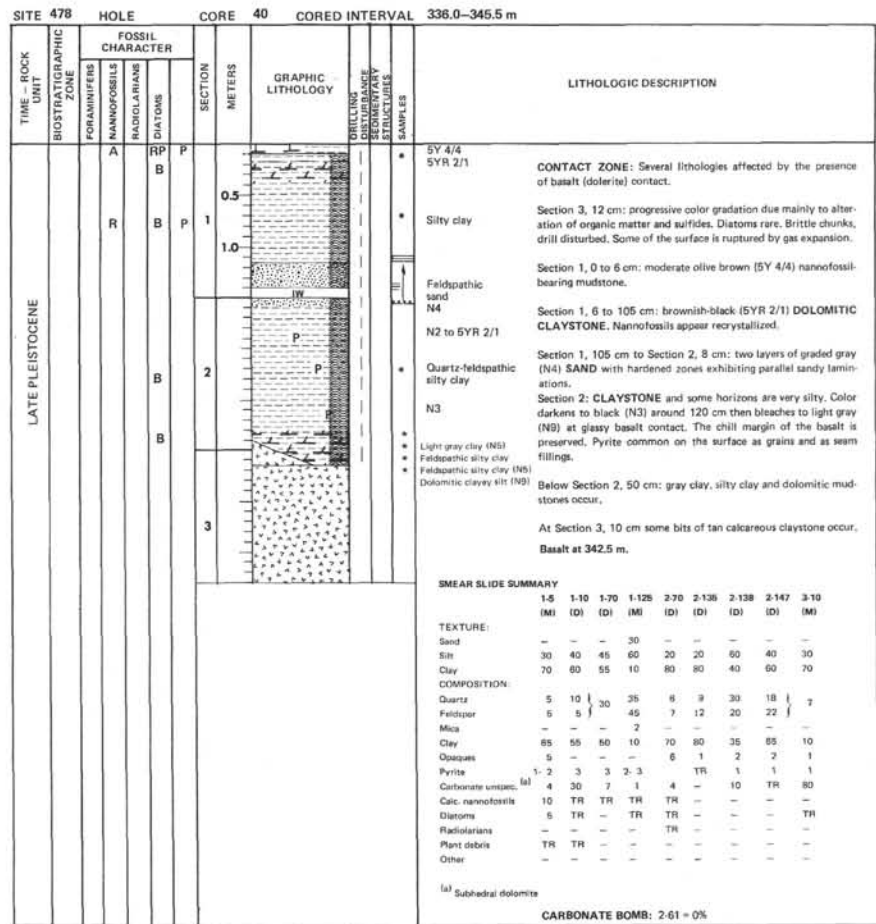
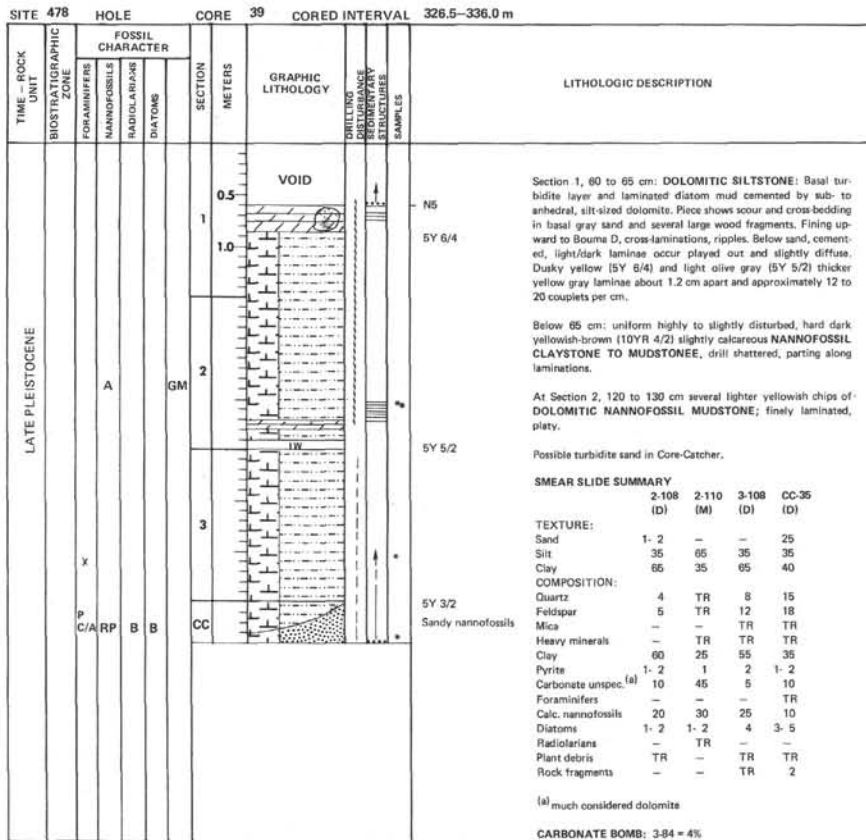


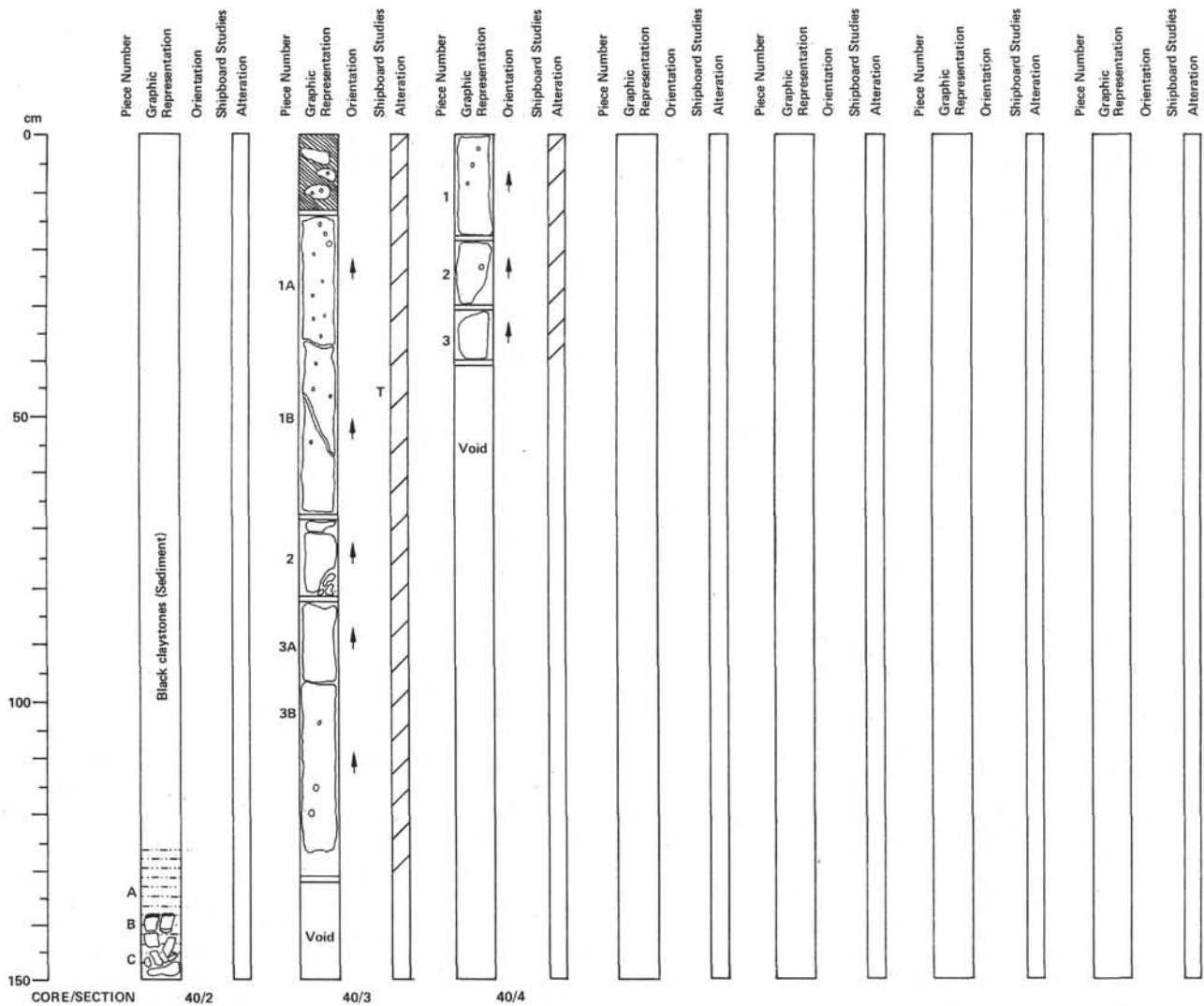
64-478-29 Depth: 250.5 to 256.5 m
CORE-CATCHER: DOMINANT LITHOLOGY: highly vesicular – APHYRIC BASALT.
Macroscopic Description
Medium gray (N8) aphyric-vesicular basalt with vesicles (1 cm) with calcite and pyrite and clay mineral linings. Similar to upper part of Core 27, Section 1.











64-478-40

Depth: 336.0 to 345.5 m

SECTION 2: DOMINANT LITHOLOGY: BLACK CLAYSTONE or mudstone. Upper SILL CONTACT in lower portion.

Macroscopic Description

Piece A (127–137 cm): medium gray (N6–N9) baked silty mudstone or claystone.

137–150 cm: fragments of aphyric, aphanitic basalt embedded in medium gray (N5–N6) silty mudstone.

Piece B: baked contact (no glass) with chilled basalt and baked selvage.

SECTION 3: DOMINANT LITHOLOGY: APHYRIC COARSE-GRAINED BASALT (or dolerite).

Macroscopic Description

0–15 cm: fragments (2–4 cm) of dark gray, sparsely vesicular, aphyric, aphanitic basalt; and lithified silty claystone in a clayey matrix. Pieces 1–3: coarse-grained (generally < 1 mm) aphyric basalt. Sparsely vesicular, the vesicles filled with green clay. No strong reaction with HCl on vesicle or vein filling so very little if any clastic. Constituent pyroxenes and olivines appear fresh but the feldspars show some green staining. The whole rock is medium-gray in color when dry (N5).

There is a distinct mottled appearance to the basalt in the lower part of the section; this is due to large, irregular pyroxene crystals, which contain plagioclase crystals – poikilitic texture.

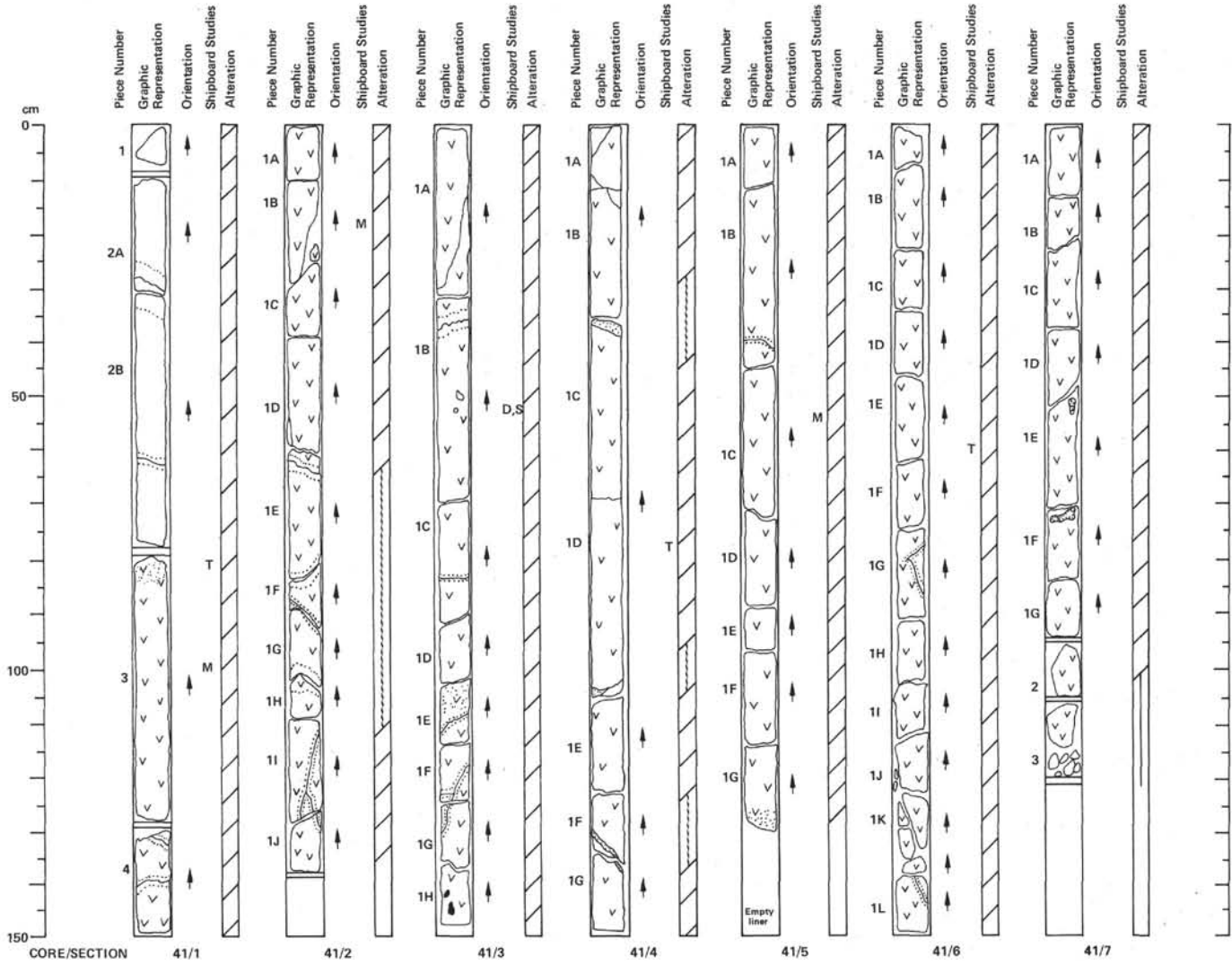
TS 50 cm, Piece 1B: subophitic to intergranular dolerite. Phenocrysts: plagioclase 1–2%, 2 mm size, equant to tabulate, resorbed, zoned. However, large clinopyroxene-plagioclase intergrowth may be considered phenocrysts or glomerocrysts. They are surrounded by smaller clinopyroxene and plagioclase and altered mesostasis. Groundmass: plagioclase 40%, 0.5–1.5 mm. Lath-shaped, occurring as ophitic inclusions in clinopyroxene and inbetween large clinopyroxene crystals. Pyroxene: 35%, up to 4 mm, large irregular crystals enclosing plagioclase, and smaller intergranular crystals, 5% opaques, 15% clays and zeolites, 3% vesicles.

SECTION 4: DOMINANT LITHOLOGY: aphyric coarse basalt.

Macroscopic Description

Medium gray (N5) coarse-grained aphyric basalt (or dolerite). Sparsely vesicular, vesicles now filled with white clay minerals. Constituent minerals (pyroxene, olivine) fairly fresh but feldspar shows greenish tint, and there are green clay minerals in the interstices.

The mottling effect seen in Section 3 continues into the top 10 cm of this section.



64-478-41

Depth: 345.5 to 355.0 m

SECTION 1: DOMINANT LITHOLOGY: COARSE BASALT OR DOLERITE.

Macroscopic Description

0–78 cm: medium dark gray (N4–N5), coarse-grained, APHYRIC BASALT. Contains olivine, clinopyroxene and green-tinted feldspar. Alteration is intense in the vicinity of clay- and zeolite-filled veins (25–35 cm; 62–64 cm). Calcite appears to be absent. Grain size (< 0.5 mm).

80–150 cm: medium dark gray (N4–N5), medium-grained DOLERITE, Aphyric. Consists of pyroxene, plagioclase and olivine (grain size ~0.5–1.0 mm). At the top of Piece 3 (80–84 cm) there is a concentration of felsic minerals which may be due to plagioclase accumulation, or part of a reaction aureole around a vein not recovered. The rock has a patchy appearance because of alteration.

TS 82 cm, Piece 3: DOLERITE, sampled in area of apparent alteration and feldspar accumulation. Olivine: ~5%, 0.3–0.8 mm, anhedral crystals. Plagioclase: 30%, plagioclase up to 2 mm elongate, lath-shaped. About 1/4 are enclosed in clinopyroxene crystals. Strongly zoned. Clinopyroxene: 25%, up to 3 mm augite. Optically encloses plagioclase and occurs at intergranular crystals. Larger crystals are merely optically continuous aggregates. Opaques: 3%, plus 2% aggregates in vein which may be pyrite. Alteration: 35%, fibrous clay minerals (green) and zeolites replacing mesostasis, olivine, some clinopyroxene and possibly some plagioclase.

SECTION 2: DOMINANT LITHOLOGY: aphyric dolerite.

Macroscopic Description

Medium-grained, aphyric, medium gray (N5, dry) dolerite, consisting of clinopyroxene, plagioclase, and olivine. Considerable alteration, especially in vicinity of 1–2 mm-wide veins of zeolite, clay, and quartz. Severe alteration in the 60–110 cm interval, with patches of quartz(?). At 103 cm, a 1 cm cavity lined with drusy, white crystals, possibly quartz.

SECTION 3: DOMINANT LITHOLOGY: aphyric dolerite.

Macroscopic Description

Medium-grained (1–1.5 mm), aphyric, medium gray (N4–N5) dolerite. Narrow 1–2 mm veins of white zeolite and silica; with reaction aureoles. Occasional blebs of white (?) silica or zeolite. No calcite detected.

102–108 cm: development of elongate (up to 1 cm) pyroxene crystals in a felsic groundmass. Probably an alteration area, but appears pegmatitic.

SECTION 4: DOMINANT LITHOLOGY: altered COARSE-GRAINED BASALT OR DOLERITE.

Macroscopic Description

Medium gray (N5) aphyric, medium-grained basalt/dolerite with clinopyroxene, plagioclase and olivine — appears equigranular alteration is moderate in most of section except near zones of calcite and clay minerals and veins where the alteration is more severe. Veins are up to 0.5 cm-thick and alteration zones are up to ~2 cm wide.

TS 80 cm, Piece 1D: DOLERITE. Ophitic texture with altered intergranular zones. Olivine: < 5%, ~0.5 mm, anhedral. Plagioclase: 30%, 0.5–3 mm, An_{54} (1 determination only), lath-shaped. Optically enclosed by clinopyroxene, and interstitial to clinopyroxene. Clinopyroxene: 40%, 1–4 mm anhedral crystals forming large crystals and smaller, interstitial grains. Opaques: 5%. Alteration: clays and zeolites replacing mesostasis and rimming (~20%) pyroxene and olivines. Slight alteration of intergranular plagioclase. Texture unusual — ophitic pyroxene and plagioclase appear to form what can be called large glomerocrysts — up to 6 mm across — in a minor, very fine-grained altered groundmass or mesostasis.

SECTION 5: DOMINANT LITHOLOGY: APHYRIC DOLERITE.

Macroscopic Description

Medium-grained (1–2 mm), medium gray (N4–N5) aphyric dolerite.

Consists of clinopyroxene, plagioclase, olivine, and is a continuation of Section 4.

Fairly badly altered, with occasional veins of zeolite and silica, and blebs of silica(?).

SECTION 6: DOMINANT LITHOLOGY: medium-grained DOLERITE.

Macroscopic Description

Medium-grained (0.5–1.5 mm grain size) medium gray (N4–N5) aphyric dolerite. Consists of plagioclase, pyroxene and olivine, with apparent segregation of mafics from felsics to give a blotchy appearance to the rock.

Veining less than in previous sections, but there is abundant secondary alteration with development of irregular blebs of zeolites and silica.

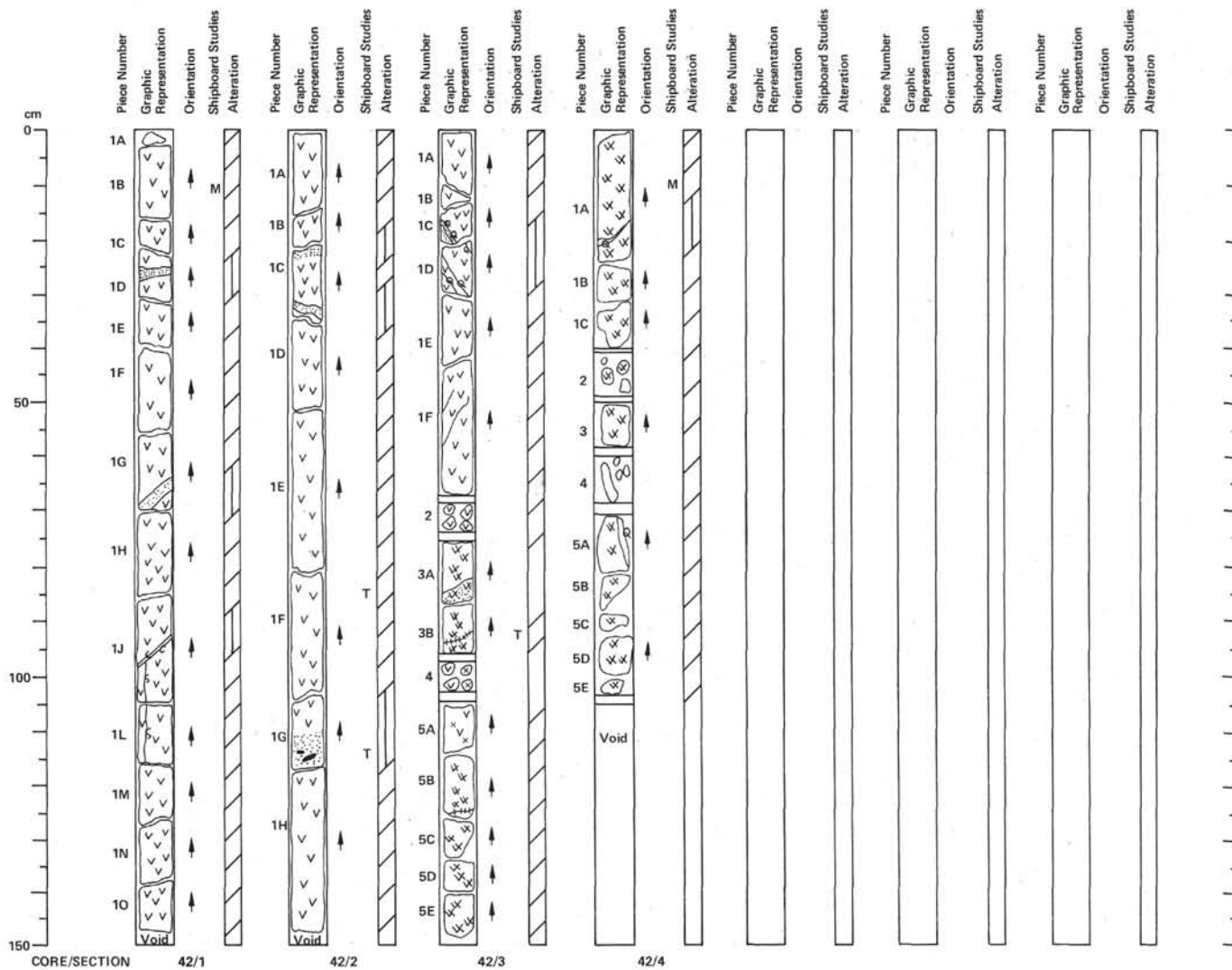
TS 60 cm, Piece 1E: SUBOPHITIC — GLOMEROCRYSTIC DOLERITE. The textures in this rock — and most of this dolerite unit — are unusual. The pyroxene and plagioclase crystals are intergrown to form sub-ophitic masses up to 5 mm across, which are surrounded by a fine-grained, altered basaltic matrix. This relationship suggests that the large clinopyroxene-plagioclase masses are phenocrysts (or glomerocrysts). Olivine: 3%, 0.5–1.0 mm, anhedral crystals, adjacent to or enclosed by clinopyroxene. Plagioclase: 20%, up to 3 mm, lath-shaped, intergrown with clinopyroxene and also intergranular to large clinopyroxene. Clinopyroxene: 20%, up to 5 mm, anhedral, semi-continuous augite crystals optically enclosing about 1/2 of plagioclase. Magnetite: ~3%. Altered mesostasis, now completely replaced by clay minerals and zeolites ~50%.

SECTION 7: DOMINANT LITHOLOGY: aphyric dolerite.

Macroscopic Description

Medium-grained (1–2 mm grain size) medium gray (N4–N5) dolerite. Aphyric. Comprises clinopyroxene, plagioclase, and olivine. Continuation of Section 6. Distinct segregation of mineral grains produces a blotchy appearance.

Blebs of amorphous, white zeolites and silica, especially in Pieces 1E and 1F (shown in column).



64-478-42

Depth 355.0 to 364.5 m

SECTION 1: DOMINANT LITHOLOGY: APHYRIC DOLERITE.

Macroscopic Description

Medium gray (N5) medium-grained aphyric dolerite. Moderately altered, grain size ~ 0.5-1 mm, clinopyroxene-plagioclase and opaques and olivine grains visible. Alteration is more extensive around several calcite-zeolite veins. Some veins and vugs filled with silicate material. Similar in all respects to previous core (41).

SECTION 2: DOMINANT LITHOLOGY: DOLERITE.

Macroscopic Description

Medium gray (N5-N6) aphyric basalt, medium-grained with clinopyroxene-olivine and plagioclase and opaques. Small mineral segregations separated by blebs of finer-grained material. Alteration is moderate except in zone of vein material, apparently siliceous and zeolitic. Not much calcite. Alteration zone in Piece 1G appears to have shards of glass (fresh) and may represent a chill zone.

TS 85 cm, Piece 1F: large 1-4 mm clinopyroxene (augite) phenocrysts, anhedral to subhedral, fractured, optically enclosing small (1 mm) plagioclase (~An₄₀) laths. Set in matrix of plagioclase (25%) and anhedral clinopyroxene and ~10% opaques. Magnetite and ilmenite ~20%. Alteration products mainly clay and zeolites concentrated in aphanitic (possibly quenched) areas.

TS 116 cm, Piece 1G: DOLERITE-GABBRO. Textures range from cumulate gabbro to plagioclase-phyric dolerite. The textures in the rock resemble those in Core 41, Section 6, 60 cm. However, the interstitial mesostasis is better preserved, and several of the xenocrystic fragments are gabbroic, one fragment (~12 mm long), comprises cumulate plagioclase, while another shows graphic intergrowth of plagioclase in clinopyroxene. Olivine 5%, 0.5-1.0 mm anhedral grains, associated with clinopyroxene/plagioclase intergrowths. Plagioclase 30%, up to 5 mm, An₆₀₋₇₀. Lath-shaped and equant. Clinopyroxene 40%, 1-6 mm augite. Irregular crystals, both enclosing plagioclase and as intergranular grains between gabbroic and ophitic fragments. Mesostasis, microlites etc., 10%. Clays and zeolites 10-15%. Zeolites apparently replacing plagioclase.

SECTION 3: DOMINANT LITHOLOGY: DOLERITE, grading to coarse dolerite or GABBRO.

Macroscopic Description

Pieces 1 and 2: dolerite as in previous sections. Medium-gray (N5), medium-grained aphyric, moderately altered and more altered around veins to mostly quartz and epidote.

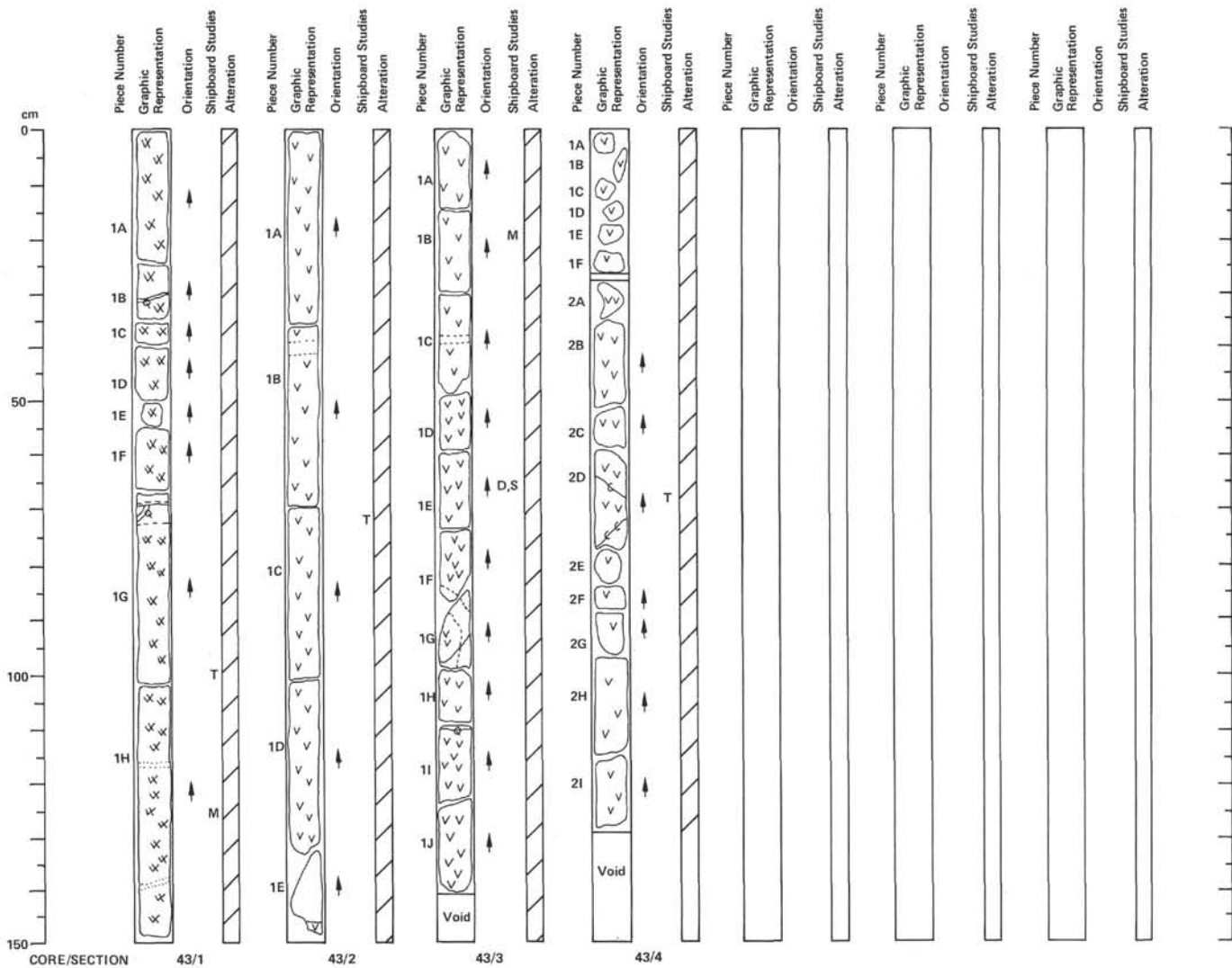
Pieces 3-5: are coarser-grained, approaching gabbroic texture with large clinopyroxene and plagioclase crystals up to 1-3 mm long. Contact in Piece 3B zone of plagioclase and clinopyroxene phyric basalt-dolerite ends in base of Piece 5B.

TS 93 cm, Piece 3B: altered dolerite, sampled adjacent to a zeolite vein. Sub-ophitic to intergranular texture. No olivine seen. Plagioclase 40%, 0.5-2.5 mm, An₆₀₋₆₅ lath-shaped. Clinopyroxene 20%, up to 4 mm, augite, irregular, isolated crystals sub-ophitically enclosing plagioclase laths, also intergranular. Magnetite 1%, up to 0.5 mm. Ilmenite 1%, up to 0.5 mm. Clays and zeolites 35%, probably replacing mesostasis (and possibly olivine?) between large clinopyroxene and plagioclase intergrowths.

SECTION 4: DOMINANT LITHOLOGY: COARSE DOLERITE OR GABBRO.

Macroscopic Description

Medium gray (N5) or equigranular coarse dolerite to gabbro, moderately weathered. Large, 1-3 mm clinopyroxene and plagioclase phenocrysts. Veins are siliceous with little or no calcite.



64-478-43

Depth 364.5 to 374.0 m

SECTION 1: DOMINANT LITHOLOGY: coarse-grained DOLERITE OR GABBRO (microgabbro).

Macroscopic Description

Medium gray (N5) coarse-grained clinopyroxene, plagioclase and olivine-bearing dolerite with moderate alteration. Important to note that discrete aphyric zones occur at ~70 cm, ~116 cm, and 138 cm, sometimes associated with veining (siliceous). Rock shows very little fracturing.

1.5–3 mm clinopyroxene, fractured anhedral to subhedral phenocrysts enclosing plagioclase laths (–An₅₅), surrounded by small plagioclase laths and some clinopyroxene and olivine with clay-zeolite alteration products (10%) in intergranular boundaries and after clinopyroxene. Abundant opaques. Ilmenite has layering of trellis-type magnetite.

SECTION 2: DOMINANT LITHOLOGY: DOLERITE.

Macroscopic Description

Medium gray (N5) microgabbro-gabbro-containing clinopyroxene and plagioclase and olivine. Zones of aphyric basalt in the top of Piece 1B and mostly Piece 1E. The aphyric zones contain small olivine(?) phenocrysts. Rock is continuation of textural gradations (increasing grain size) seen through last few cores.

TS 70 cm, Piece 1E: subophitic dolerite with 1–3 mm tabulate laths of plagioclase, with strong zoning. Subophitically including many small (0.5–1 mm) anhedral clinopyroxene (10%) and olivines (~7%) in a matrix of clinopyroxene and olivine microcrysts and small plagioclase laths and minor disseminated opaques (3%). Abundant clay and zeolite minerals (~10%), brown to brownish green in color and calcite (~5%) filling small veinlets.

SECTION 3: DOMINANT LITHOLOGY: DOLERITE.

Macroscopic Description

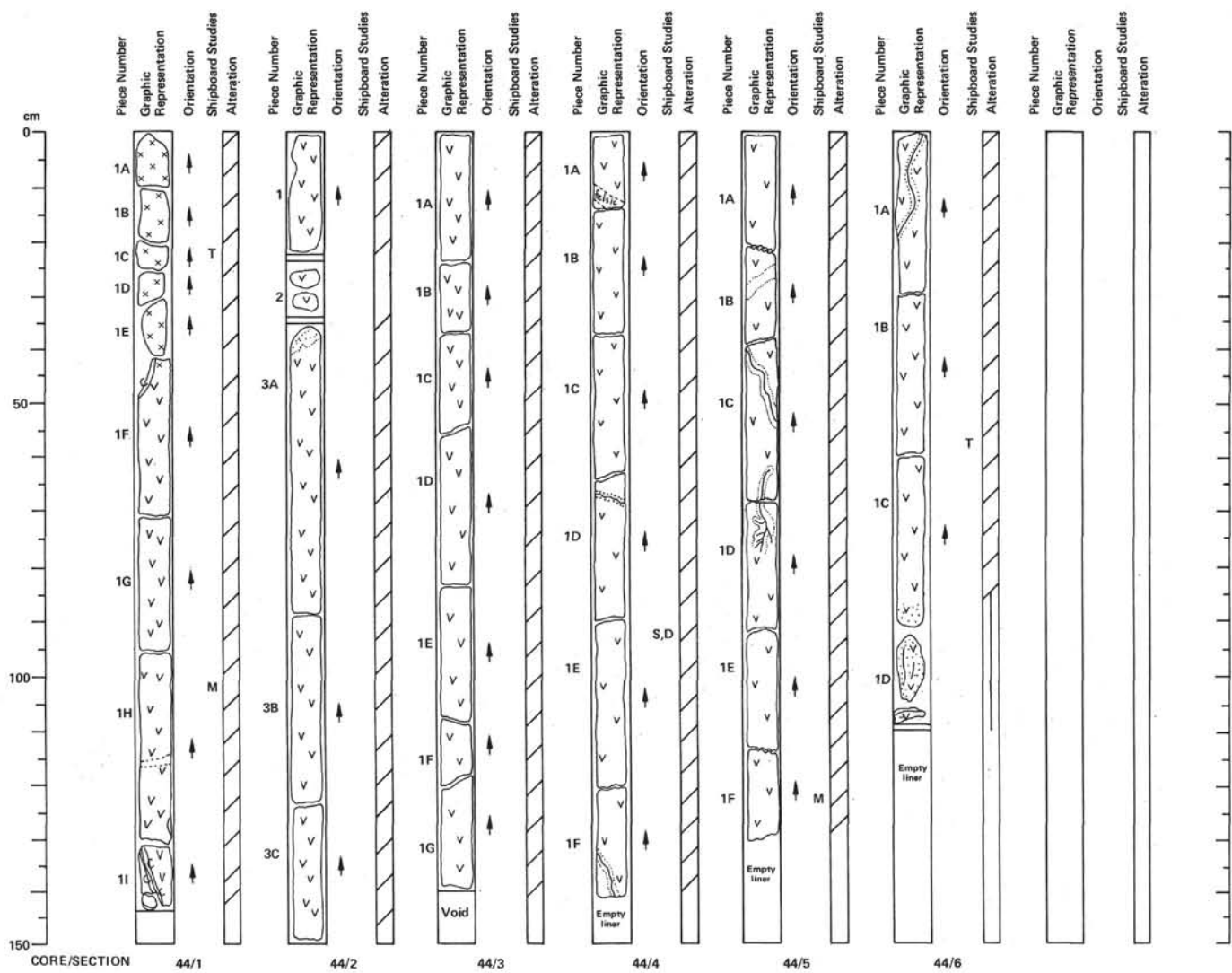
Medium gray (N5) clinopyroxene-plagioclase and olivine grains, 1–2 mm in size. Two zones of aphyric basalt in Piece 1C which continue through 1F and 1G. These zones are also present in sections above this and they are light gray (N7) in color. Massive texture with only rare fractures, one small vein runs across the top of Piece 1I.

SECTION 4: DOMINANT LITHOLOGY: DOLERITE.

Macroscopic Description

Same as Section 3 of this core, except Piece 2 which is an aphyric BASALT zone with thin CALCITE VEINS (<1 mm). All other veins in this sill are filled principally by silicate and clay.

TS 68 cm, Piece 2D: subophitic with plagioclase phenocrysts (~15%) in a matrix of clinopyroxene (30%), plagioclase (25%), olivine (10%), and opaques (~5%). Moderate to slightly altered with 10% clays and ~5% calcite vein fillings. Plagioclase phenocrysts show strong zoning and some reverse zoning.



64-478-44

Depth 374.0 to 383.0 m

SECTION 1: DOMINANT LITHOLOGY: MICROGABBRO TO DOLERITE from 40 cm.

Macroscopic Description

Pieces 1A to 1E: similar to base of Core 42, moderately weathered gabbro with clinopyroxene, olivine, and plagioclase components. Pieces 1F to base: rock becomes significantly fresher and lighter in color, light to medium light gray (N6–N7) and finer-grained, hence to doleritic. Veining rare, calcitic.

A small aphanitic zone occurs ~116 cm.

Piece 1E has large vein on the side filled with coarse pyrite.

TS 25 cm, Piece 1C: coarse DOLERITE to microgabbro with ophitic texture predominates with large (1–3 mm) fresh clinopyroxene enclosing (1–4.5 mm) plagioclase laths ($\sim A_{0.40}$) in a matrix of coarse-grained intersertal clinopyroxene and plagioclase ($\sim 15\%$) with $\sim 5\%$ disseminated opaques, mostly magnetite. Abundant clay and zeolite minerals ($\sim 20\%$) that are dark brownish green and appear in inter-grain boundaries and replacing large clinopyroxene crystals. No olivine seen.

SECTION 2: DOMINANT LITHOLOGY: DOLERITE.

Macroscopic Description

Medium light gray (N6), equigranular. Continuation of Section 1 dolerite, fairly fresh without veins or fractures.

SECTION 3: DOMINANT LITHOLOGY: DOLERITE.

Macroscopic Description

Same as Section 2.

SECTION 4: DOMINANT LITHOLOGY: coarse APHYRIC DOLERITE.

Macroscopic Description

Medium gray (N5) to light brownish gray (5YR 6/1) aphyric dolerite, consisting of inequigranular plagioclase laths (up to 2 mm long) and subordinate pyroxene and olivine. Mafics tend to be concentrated in narrow zones (2–3 mm) surrounding more felsic zones, up to 1.5 cm across. This gives a rather polygonal appearance to the cut surfaces (see diagram Core 45, Section 5).

The rocks are altered, with tinted feldspars and occasional blebs of white silica. Reaction rims around vein probably mafic-free.

SECTION 5: DOMINANT LITHOLOGY: coarse APHYRIC DOLERITE.

Macroscopic Description

Medium gray to light brownish gray (N5–5YR 6/1) aphyric dolerite, consisting of approximately equigranular plagioclase laths (up to 2 mm long) and subordinate pyroxene and olivine. Mafics tend to be concentrated in a narrow zone around more felsic areas approximately 1.5 cm in diameter.

Rock is altered, with altered feldspars and occasional blebs of white silica or zeolites reaction rims around veins.

SECTION 6: DOMINANT LITHOLOGY: APHYRIC DOLERITE.

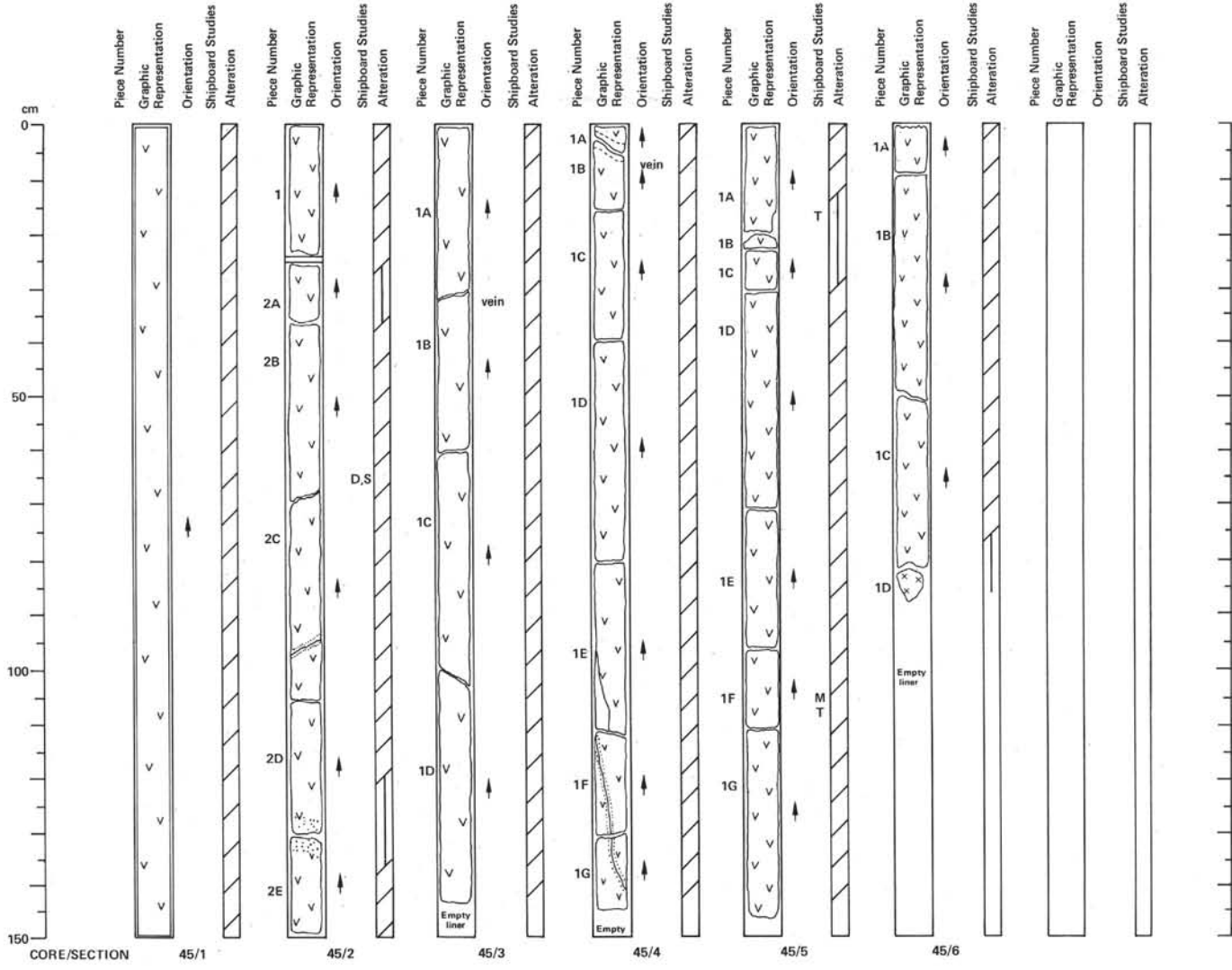
Macroscopic Description

Medium gray to light brownish gray (N5–5YR 6/1) aphyric dolerite, consisting of approximately equigranular plagioclase laths (up to 2 mm) and subordinate pyroxene and olivine(?). Mafics concentrated in narrow zones around more felsic areas approximately 1.5 cm in diameter.

Rock is altered, with altered feldspars and occasional blebs of white silica or zeolites.

TS 58 cm, Piece 1B: ophitic to subophitic ALTERED DOLERITE, with large ($\sim 1\text{--}4$ mm) clinopyroxene subhedral to anhedral phenocrysts, optically enclosing 0.5–1.5 mm tabulate plagioclase and

albite laths ($\sim A_{0.60}$). Occasional subophitic texture. Matrix has small fragments (anhedral) of clinopyroxene ($\sim 10\%$) and small plagioclase laths ($\sim 25\%$) with disseminated opaques (magnetite and ilmenite) ($\sim 5\%$) with abundant clay ($\sim 15\%$) and zeolite ($\sim 15\%$) as alteration products. Plagioclase phenocrysts are mostly normally zoned. No olivine observed.



64-478-45

Depth: 383.0 to 392.0 m

SECTION 1: DOMINANT LITHOLOGY: APHYRIC DOLERITE.

Macroscopic Description

This section forms part of a 186.5 cm length of dolerite, returned to Scripps unbroken. The section was not sliced. The drilled surfaces shows identical characteristics to the preceding core, and to the following section.

SECTION 2: DOMINANT LITHOLOGY: APHYRIC DOLERITE.

Macroscopic Description

Medium gray (N5) to light brownish gray (5YR 6/1) medium grained aphyric dolerite. Contains clinopyroxene (~15%) which is altered in part to a green color; plagioclase (~70%) and olivine (~5%). The rock has a mottled or blotchy appearance, similar to previous cores of this hole, due to segregation of mafics from fine-grained felsic patches.

Alteration in Pieces 2A and 2D-2E severe, resulting in considerable replacement of minerals (zeolitization and silicification).

Piece 1 is part of a 186.5 cm length of core sent uncut to Scripps.

SECTION 3: DOMINANT LITHOLOGY: APHYRIC DOLERITE.

Macroscopic Description

Medium gray (N5) to light brownish gray (5YR 6/1) medium grained aphyric dolerite. Clinopyroxene ~15%, up to 2 mm; plagioclase ~70%, up to 2 mm; and olivine ~5%, <1 mm.

The rock has a mottled or blotchy appearance, similar to Sections 1 and 2, due to segregation of mafics from finer-grained felsic patches.

The feldspars in the lower part of the section are amorphous white rather than translucent, and probably quite altered, and the clinopyroxene appears to be altered.

SECTION 4: DOMINANT LITHOLOGY: APHYRIC DOLERITE.

Macroscopic Description

Medium gray (N5) to light brownish gray (5YR 6/1) medium grained aphyric dolerite. Clinopyroxene ~15%, up to 2 mm; plagioclase ~70%, up to 2 mm; and olivine ~5%, <1 mm.

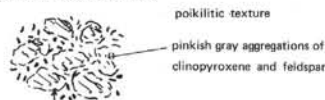
The rock has a mottled or blotchy appearance similar to Sections 1 and 2, due to segregation of mafics from finer-grained felsic patches. Severe zeolitization around vein in Pieces 1A and 1B.

SECTION 5: DOMINANT LITHOLOGY: APHYRIC DOLERITE.

Macroscopic Description

Medium gray (N5) to light brownish gray (5YR 6/1) medium grained aphyric dolerite.

Blotchy appearance due to segregation and irregular distribution of mafic and felsic components:



dark green clays, and olivine, and green-tinted feldspars in interstices

This pattern has been observed throughout most of previous cores in dolerite.

TS 6 cm, Piece 1A: poikilitic texture to subophitic. Areas of layer (~0.5-5 mm) clinopyroxene, anhedral to coarsely subhedral, enclosing 0.5-1.5 mm plagioclase laths (~An₆₀). Areas of poikilitic clinopyroxene separated by weathered areas filled with clay and zeolite minerals, part of which result from the breakdown of clinopyroxene. Small opaques are disseminated throughout (~5%). Approximately 40% of plagioclase, 15% clinopyroxene crystals; 25% clays; and 15% zeolites. At the edge of some poikilitic clinopyroxene crystals the texture becomes ophitic and is thought to result from weathering and breakdown of the clinopyroxene grain periphery.

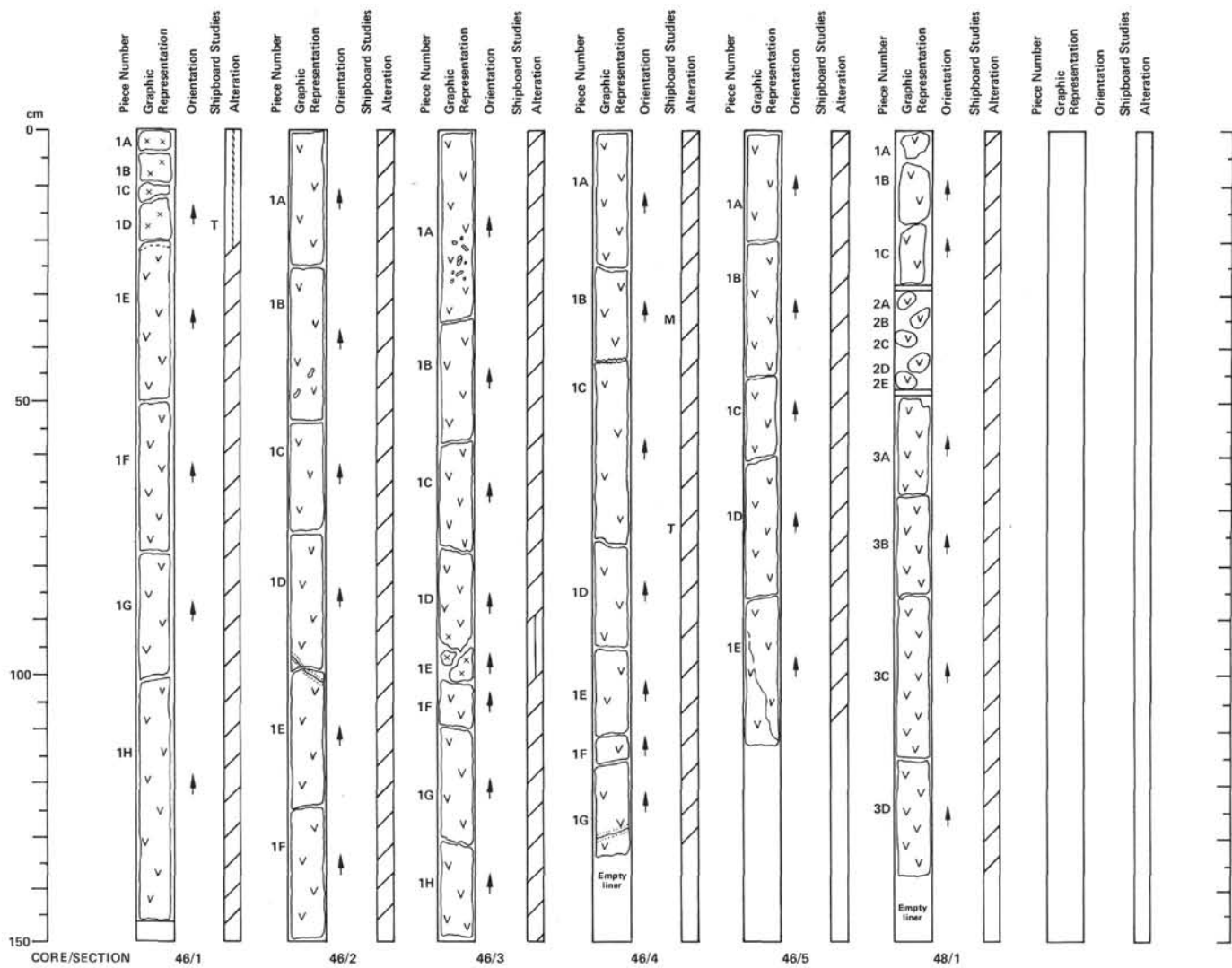
SECTION 6: DOMINANT LITHOLOGY: APHYRIC DOLERITE.

Macroscopic Description

Medium gray (N5) is light brownish gray (5YR 6/1) medium grained aphyric dolerite.

Poikilitic or blotchy appearance as in Section 5. Same textures and minerals. Very slight alteration.

TS 108 cm, Piece 1F: ophitic to some poikilitic texture ~15% clinopyroxene phenocrysts, optically to poikilitically enclosing plagioclase (~20%) laths (~An₄₅) in a matrix of anhedral clinopyroxene (~10%). Small plagioclase (~30%) with minor opaques (~15%) and clay and zeolites in intergranular boundaries and after clinopyroxene. Eight percent olivine occurs interstitial to clinopyroxene, anhedral <1 mm.



64-478-46

Depth: 392.0 to 401.0 m

SECTION 1: DOMINANT LITHOLOGY: APHYRIC DOLERITE.

Macroscopic Description

Pieces 1A–1D: coarse-grained dark brownish gray (5YR 6/1) (aphyric) gabbro. Consists of plagioclase, clinopyroxene, olivine and zeolites. Badly altered. Large (5–10 mm) pinkish aggregates may be pyroxene-feldspar intergrowths as they appear to have a crystalline structure, unlike the felsic patches noted in the core above and sections below.

Pieces 1I–1H: medium-grained dark brownish gray (N5 to 5YR 6/1) aphyric dolerite. Identical to cores above (45 and lower). Poikilitic segregation of mafics from felsics gives rock a patchy appearance. Zeolites and amorphous (?) silica present.

TS 18 cm, Piece 1D: ophitic coarse dolerite to microgabbro with large (2–5 mm) clinopyroxene crystals optically or poikilitically enclosing smaller (~1–2 mm) plagioclase (~An₄₄) surrounded by smaller plagioclase laths and minor but large 0.25–0.75 mm opaques and anhedral clinopyroxene, probably fragments of larger, now altered phenocrysts. Areas of ophitic texture in some instances very well preserved with little alteration, however slide shows ~10% clays (brown to greenish brown) and ~5% zeolite minerals in intergranular boundaries and in some cases after clinopyroxene. Very minor olivine < 1%, 0.5 mm rounded grains.

SECTION 2: DOMINANT LITHOLOGY: APHYRIC DOLERITE.

Macroscopic Description

Continuation of previous section, medium-grained, aphyric, medium gray to medium brownish gray (5YR 6/1) dolerite, plagioclase, pyroxene, and olivine. Segregation of mafics has caused blotchy appearance to the rock (poikilitic texture). Zeolite filled cavities in Piece 1B.

SECTION 3: DOMINANT LITHOLOGY: APHYRIC DOLERITE.

Macroscopic Description

Medium-grained, medium gray (N5) to medium light brownish gray (5YR 6/1) aphyric dolerite. More coarse-grained, almost gabbroic interval at 93–101 cm.

Dominant minerals are pyroxene, plagioclase, and olivine. Blotchy appearance recorded in previous sections still present (poikilitic texture). May be due to growth of 1–1.5 cm intergranular crystals of feldspar in pyroxene. Alteration moderate but appears to be decreasing. Veining noticeably less in the core than in previous ones.

Zeolites- or silica-filled cavities in Pieces 1A and 1D/1E. Gabbroic section has numerous empty cavities, perhaps due to hydrothermal dissolution of fine groundmass.

SECTION 4: DOMINANT LITHOLOGY: APHYRIC DOLERITE.

Macroscopic Description

Medium-grained, medium gray (N5) aphyric dolerite. Grain size ~1–1.5 mm. Comprises slightly altered feldspar, and fresher clinopyroxene and olivine. Occasional small (~1 mm) amorphous white blebs of silica and zeolite.

TS 75 cm, Piece 1C: Large clinopyroxene (~20%) (0.5–4 mm) mostly broken, anhedral to subhedral fragments, ophitic; containing plagioclase laths (0.5–1.5 mm) (~An₅₀) (30%). In places the texture more intergranular with the small plagioclase laths (~35%) predominantly with scattered fragment (anhedral) of clinopyroxene and small olivines, anhedral (~5%) in the matrix. Most clinopyroxene and plagioclase is fresh; some (~18%) alteration present in clay and zeolites that occur along grain boundaries. Small opaques (<5%) minor and appear to be associated with altered clinopyroxene.

SECTION 5: DOMINANT LITHOLOGY: APHYRIC DOLERITE.

Macroscopic Description

Medium-grained, medium gray (N5) aphyric dolerite, grain size 1–1.5 mm, comprising slightly altered feldspar, and fresher clino-

pyroxene and olivine. Occasional small amorphous white blebs of silica or zeolite, and fine, white veins of silica or zeolites. Larger poikiloblastic pyroxene enclosing feldspar produce blotchy appearance.

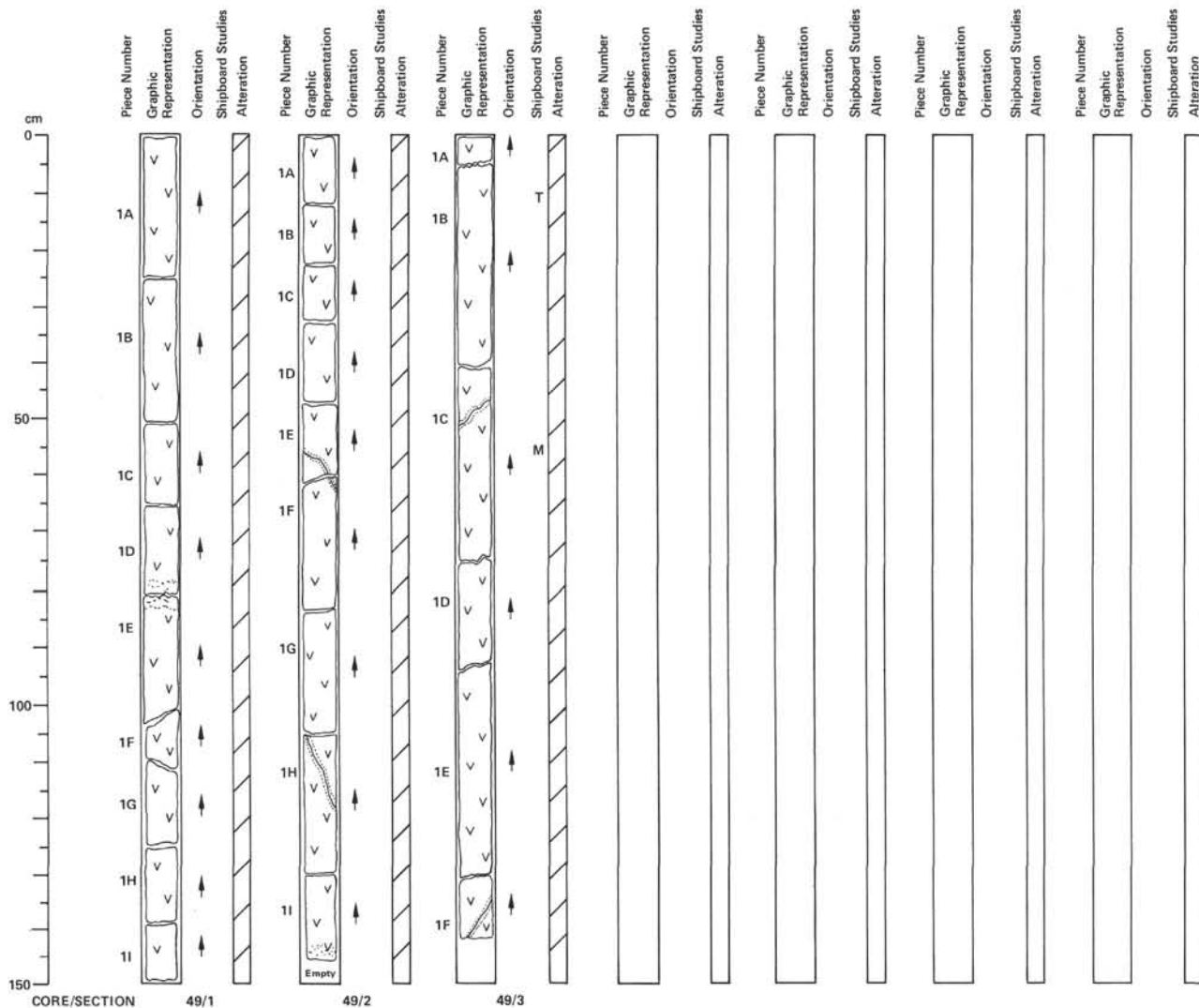
64-478-48

Depth 410.0 to 412.0 m

SECTION 1: DOMINANT LITHOLOGY: APHYRIC DOLERITE.

Macroscopic Description

Medium-grained, medium gray (N5) aphyric dolerite. Grain size 1–1.5 mm, comprising slightly altered feldspar, and fresher clinopyroxene and olivine. Similar to Core 46.



64-478-49

Depth 412.0 to 419.0 m

SECTION 1: DOMINANT LITHOLOGY: APHYRIC DOLERITE.

Macroscopic Description

Medium-grained, aphyric, medium gray (N4/N5) dolerite. Blotchy appearance (noted on an earlier core) seems to be due to ophitic textures, the pale felsic portions being 1–1.5 cm wide pale green pyroxene crystals optically enclosing small plagioclase laths (poikilitic texture). These larger, irregular pyroxene crystals are surrounded by dark green pyroxene, plagioclase and ore.

Alteration appears to be less than in previous cores, although there are still some minor, amorphous blebs of silica or zeolite. A vein separating Pieces 1D and 1E has caused considerable recrystallization of these pieces for a distance of 2 cm either side of the vein.

SECTION 2: DOMINANT LITHOLOGY: APHYRIC DOLERITE.

Macroscopic Description

Continuation of, and identical to, previous section. Altered, with development of silica zeolites, at base of section. Veins in Pieces 1E–1F and 1H, contain silica and/or zeolites. No calcite.

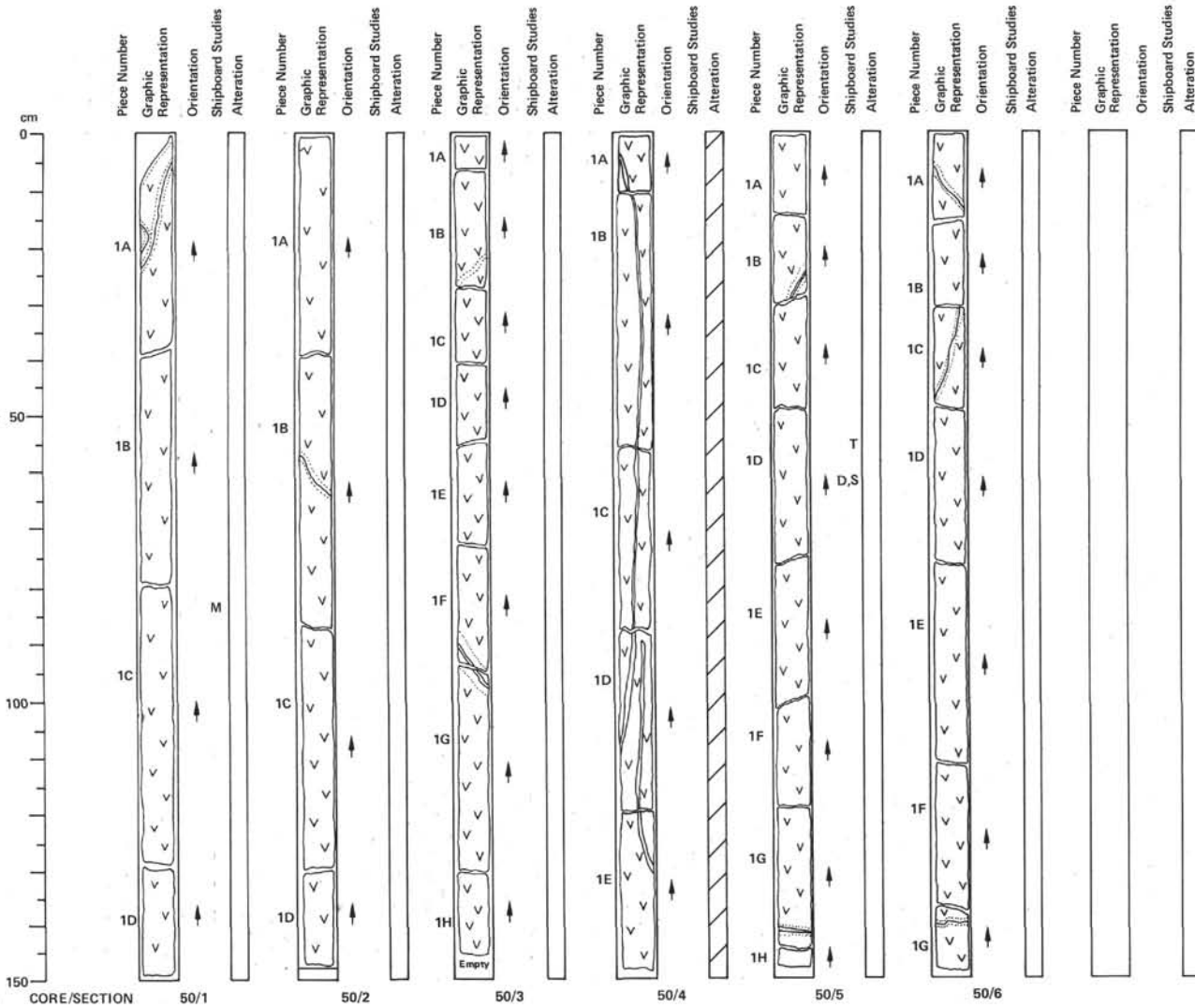
SECTION 3: DOMINANT LITHOLOGY: APHYRIC DOLERITE

Macroscopic Description

Continuation of, and identical to, dolerite in Sections 1 and 2, perhaps rather more fresh.

Veins in Pieces 1C and 1F consists of zeolite and/or silica – no carbonate detected.

TS 10 cm, Piece 1B: subophitic to ophitic intergranular texture. Large clinopyroxene (up to ~4 mm) optically enclosing smaller plagioclase (0.4–1.5 mm). Commonly texture is subophitic with clinopyroxene fragments surrounded by plagioclase. Minor olivine ~5%, anhedral, subrounded by clay minerals. Clinopyroxene phenocrysts are optically continuous aggregates although some groundmass clinopyroxene is present in anhedral to subhedral intergranular crystals in a plagioclase matrix. Minor opaques (~2–3%) up to 1 mm in size which is fragmented and some skeletal (ilmenite). Rock is fresh with only ~5% interstitial clay minerals. Plagioclase and clinopyroxene equals ~45%.



64-478-50 Depth 419.0 to 428.0 m

SECTION 1: DOMINANT LITHOLOGY: APHYRIC DOLERITE.

Macroscopic Description
Medium gray (N5) to medium dark gray (N4) medium-grained aphyric dolerite. Inequigranular, with 1–1.5 cm diameter pinkish gray, rounded, anhedral, diffuse crystals of pyroxene (subophitically enclosing plagioclase–poikilitic texture) in a matrix of feldspar, dark pyroxene, ore, and olivine. Fresher than in previous cores, but extensive veining in Piece 1A with silica and/or zeolite, no carbonate.

SECTION 2: DOMINANT LITHOLOGY: DOLERITE.

Macroscopic Description
Essentially identical to Cora 50, Section 1. Very diffuse white vein in Piece 1B at 58–63 cm.

SECTION 3: DOMINANT LITHOLOGY: DOLERITE.

Macroscopic Description
Inequigranular dolerite, aphyric, medium gray to medium dark gray (N5–N4), comprising large brown gray irregular pyroxene with plagioclase, dark green pyroxene, zircon and opaques. Essentially identical to previous 2 sections. Fresh appearance, with a good 'ring' indicative of freshness. Minor veining in Pieces 1B and 1F–G (not calcite).

SECTION 4: DOMINANT LITHOLOGY: DOLERITE.

Macroscopic Description
Same rock type as previous section. However, there are two veins running almost the length of this section. Width ranges from about 3–5 mm, and contains aphanitic, pale gray minerals (not calcite). Reaction between vein and country rock is considerable, with accentuation of dark minerals causing a speckled appearance adjacent to the vein. This is very similar to what was seen in some earlier cores.

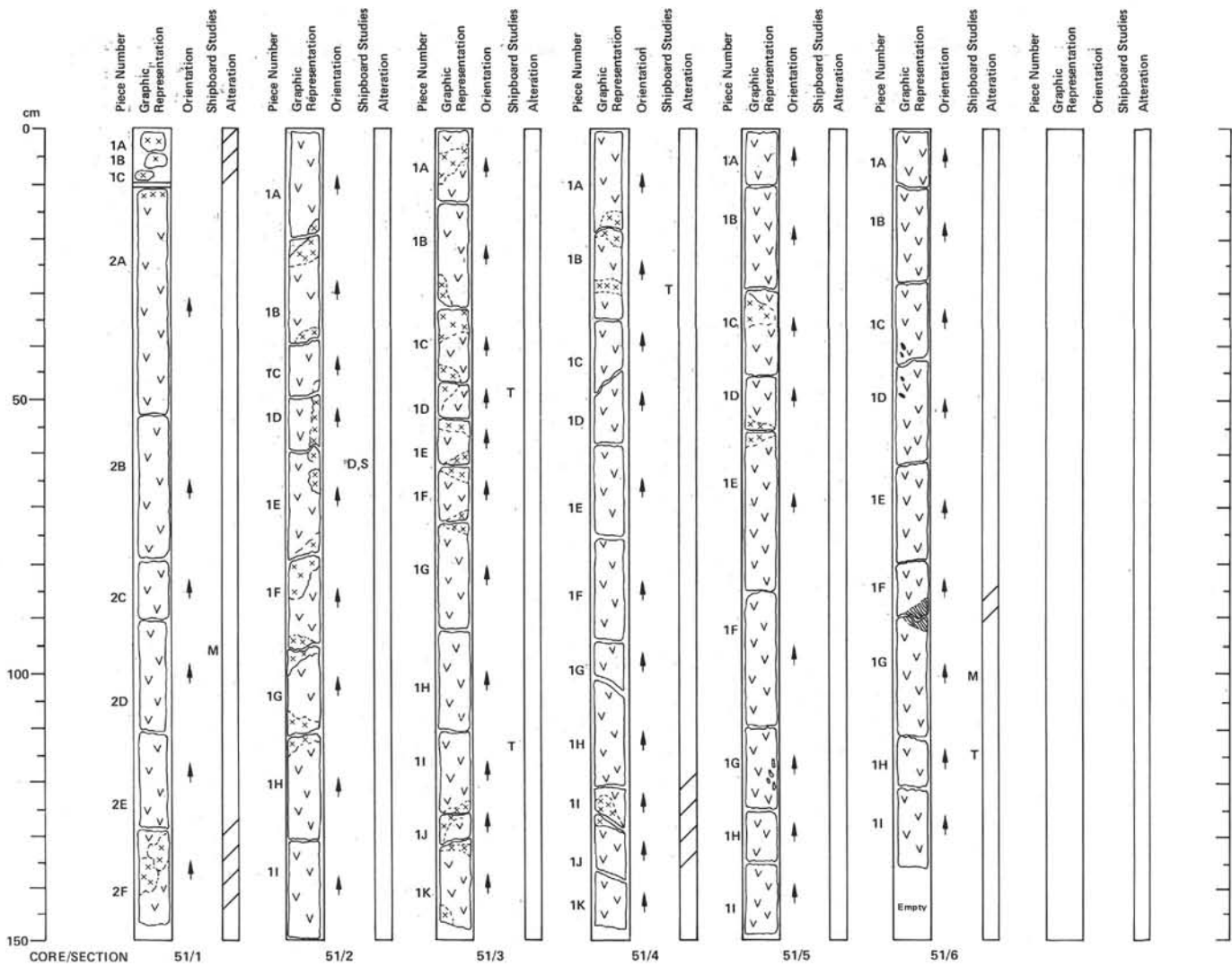
SECTION 5: DOMINANT LITHOLOGY: DOLERITE.

Macroscopic Description
Essentially identical to Section 3, Two minor veins in Pieces 1B and 1G (not calcite – probably silica and/or zeolites).

TS 55 cm, Piece 1D: ophitic & intergranular texture with large (up to 5 mm) clinopyroxene phenocrysts with some poikilitically embayed plagioclase (~An₅₅₋₆₀) and rare olivine crystals. Approximately 50% plagioclase 0.3–2 mm in size, 80% clinopyroxene in large phenocrysts and smaller intergranular crystals. Minor ~5% olivine in matrix and sometimes as inclusions in clinopyroxene phenocrysts. Minor opaques < ~1%. Rock is fresh with only ~5% interstitial clay minerals partially replacing olivines.

SECTION 6: DOMINANT LITHOLOGY: DOLERITE.

Macroscopic Description
Essentially identical to Section 3, Minor veins in Pieces 1A, B and 1G (silica and/or zeolites, but not calcite).



64-478-51

Depth 418.0 to 437.0 m

SECTION 1: DOMINANT LITHOLOGY: DOLERITE

Macroscopic Description

Medium gray (N5), aphyric, medium-grained but strongly inequigranular dolerite.

Poikilitic texture, with 1–1.5 cm diameter crystals of gray brown colored pyroxene optically enclosing plagioclase. The large pyroxenes are rounded in shape, anhedral, and separated by dark green pyroxene, plagioclase, olivine, and ores.

Weathering very slight alteration.

Pieces 1A, B, and C: pebbles of pyroxene gabbro. Crystals of dark pyroxene up to 1 cm optically enclose plagioclase laths (1–4 mm long), gabbro occurs in top of Piece 2A, 130–140 cm. Similar gabbroic inclusions found inside dolerite. There they are dominantly felsic (80% plagioclase, <20% clinopyroxene).

SECTION 2: DOMINANT LITHOLOGY: POIKILITIC DOLERITE with GABBRO XENOLITHS.

Macroscopic Description

Medium gray (N5), aphyric medium-grained, poikilitic dolerite. Similar to that in Section 1.

However, the dolerite contains abundant xenoliths, of plagioclase-clinopyroxene gabbro, up to 10 cm across.

SECTION 3: DOMINANT LITHOLOGY: POIKILITIC DOLERITE with GABBRO XENOLITHS.

Macroscopic Description

Poikilitic dolerite similar to that in Section 1, about 20% of the rock, however, comprise coarse-grained xenoliths of pyroxene-feldspar gabbro. Cavities in the xenoliths contain acicular zeolites in addition to cryptocrystalline silica. In general both rock types are quite fresh.

TS 48 cm, Piece 1D: gabbro xenolith in dolerite sill, ophitic texture in mesostasis (10%). Xenolith comprises ~ 55%, 1–10 mm, clinopyroxene phenocrysts optically enclosing plagioclase laths 30%, (–0.5–3 mm) with 10% clay and zeolite minerals as a mesostasis. Distinct ilmenite laths up to 1 mm long (–3%) also occurs in the mesostasis.

TS 111 cm, Piece 1I: ophitic to intergranular texture with large 1–6 mm clinopyroxene optically enclosing 0.5–1.5 mm laths of plagioclase and olivine microphenocrysts (0.5–1 mm). Approximately 10% olivine to 50% plagioclase, ~ 30% clinopyroxene and ~5% opaques. Magnetite (Ti-rich) with ~5% clay minerals in interstices and possibly after olivine. Dolerite host is somewhat fresher than xenoliths.

SECTION 4: DOMINANT LITHOLOGY: POIKILITIC DOLERITE with GABBRO XENOLITHS.

Macroscopic Description

Medium-grained, inequigranular, aphyric, medium gray (N4/N5) to poikilitic dolerite. Similar to that in Section 1.

Contains approximately 5% 5–10 cm wide xenoliths of pyroxene-feldspar gabbro. These xenoliths have zeolite-lined or filled cavities.

TS 30 cm, Piece 1B: gabbro xenolith in dolerite host — ophitic to subophitic texture — large 1–4 mm clinopyroxene (–15%) optically enclosing 0.2–1 mm plagioclase laths (30% and clinopyroxene and plagioclase (1–3 mm) subophitically intergrown, plagioclase subophitic phenocrysts (–30%), plagioclase matrix (–30%), with 5% clinopyroxene and olivine grains and abundant opaques. Opaques include long needles of ilmenite (up to 6 mm), clay and zeolite minerals (10%) in intergrain boundaries and after clinopyroxene. Zeolite is clear and fibrous.

SECTION 5: DOMINANT LITHOLOGY: POIKILITIC DOLERITE with GABBRO XENOLITHS.

Macroscopic Description

Essentially similar to previous section, but with fewer gabbro xenoliths. Amorphous silica- or zeolite-filled cavities (–2 mm across) in Piece 1G (117–120 cm).

SECTION 6: DOMINANT LITHOLOGY: POIKILITIC DOLERITE.

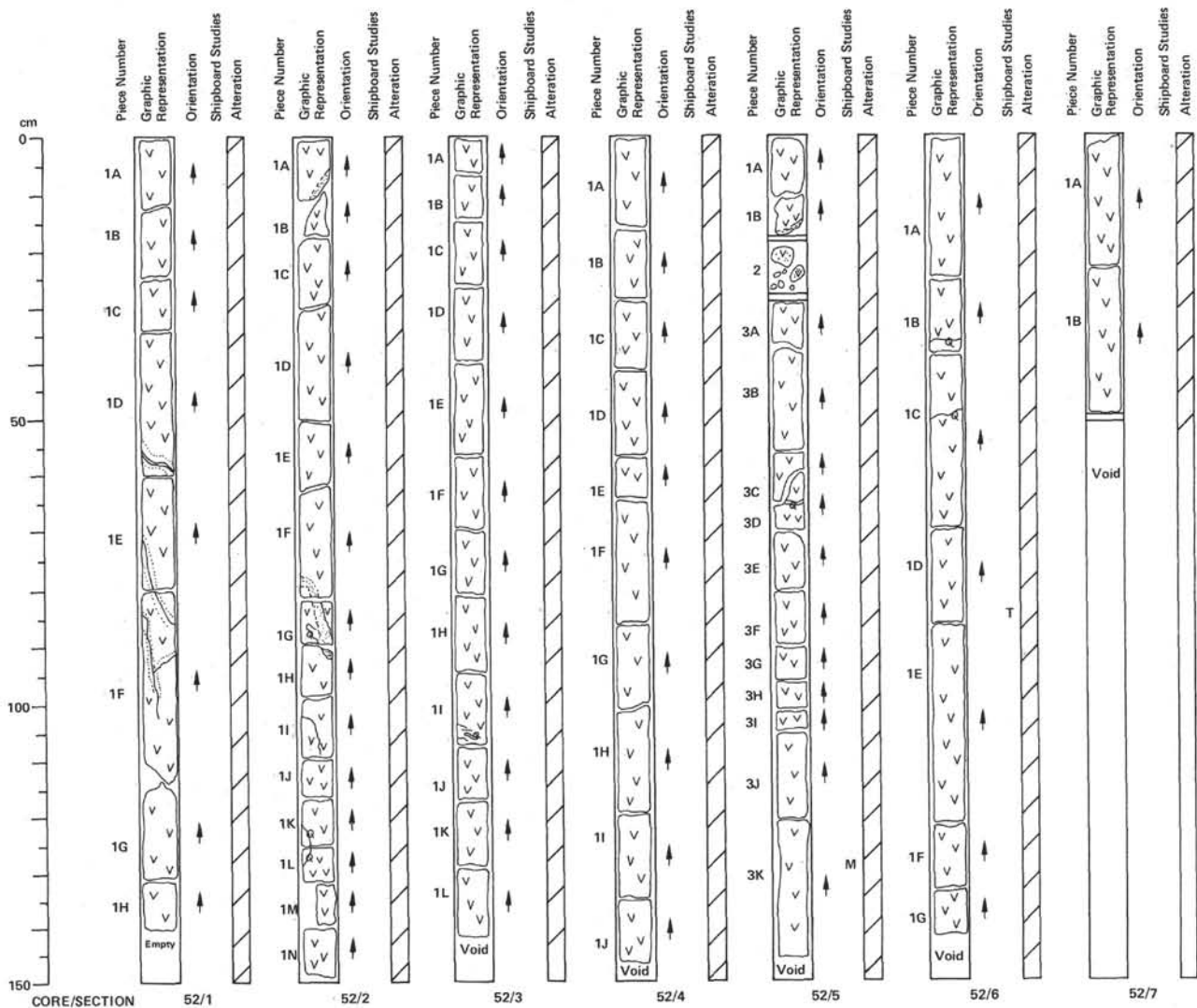
Macroscopic Description

Medium gray (N5) to medium dark gray (N4) aphyric, medium-grained, inequigranular, poikilitic dolerite.

Poikiloblastic crystals of pinish gray pyroxene, subophitically enclosing plagioclase, are surrounded by white feldspar, dark green pyroxene, olivine and opaques. Textures and mineralogy very similar to those in preceding cores and sections.

Alteration restricted to development of occasional bleb of amorphous silica and/or zeolites, especially in the 87–91 cm interval where fibrous zeolites are clearly seen.

TS 113 cm, Piece 1H: ophitic texture. Clinopyroxene (35%) with large, 1–5 mm optically continuous aggregates enclosing smaller plagioclase (–55%), 1–3 mm laths with some anhedral olivine (–4%) mostly altered to clay and minor opaques (< 1%). Clay is 5% and occurs in intergranular spaces replacing olivine and some feldspars.



64-478-52

Depth 437.0 to 446.0 m

SECTION 1: DOMINANT LITHOLOGY: POIKILITIC DOLERITE.**Macroscopic Description**

Medium dark gray to dark gray (N4 to N3) medium-grained, aphyric, inequigranular-poikilitic dolerite. Similar to that in Core 51 but no gabbro xenoliths, and there is more alteration.

Large, anhedral (1–1.5 cm) pinkish gray pyroxene crystals optically enclose plagioclase, and are surrounded by plagioclase green pyroxene, olivine and ores.

Extensive amorphous-silica and zeolite veint in several pieces.

SECTION 2: DOMINANT LITHOLOGY: DOLERITE.**Macroscopic Description**

Medium dark gray (N4 to N5) medium-grained aphyric poikilitic(?) dolerite. Large clinopyroxene enclosing plagioclase and olivine, moderately altered, one large quartz and zeolite vein cuts through Pieces 1F, 1G, and 1H. Section seems richer in olivine. Clinopyroxene, anhedral crystals, poikilitically enclosed after mineral phases, except for more abundant olivine. Section is similar to Section 1.

SECTION 3: DOMINANT LITHOLOGY: DOLERITE.**Macroscopic Description**

Medium dark gray (N5), homogeneous, unfractured, clinopyroxene, poikilitic. Same as Sections 1 and 2 with little veining, one small silicic vein in Piece 1I.

SECTION 4: DOMINANT LITHOLOGY: DOLERITE.**Macroscopic Description**

Homogeneous, medium dark gray (N4 to N5). Similar in all respects to Sections 1–3. No veining and unfractured. Appears slightly less altered and poikilitic mottling is less pronounced.

SECTION 5: DOMINANT LITHOLOGY: FINE-GRAINED DOLERITE.**Macroscopic Description**

Dolerite is more homogeneous and less mottled, finer-grained, lighter color, medium to medium light gray (N5–N6). Still clinopyroxene-plagioclase and olivine major components. More unaltered zone at base of Piece 1B and 2.

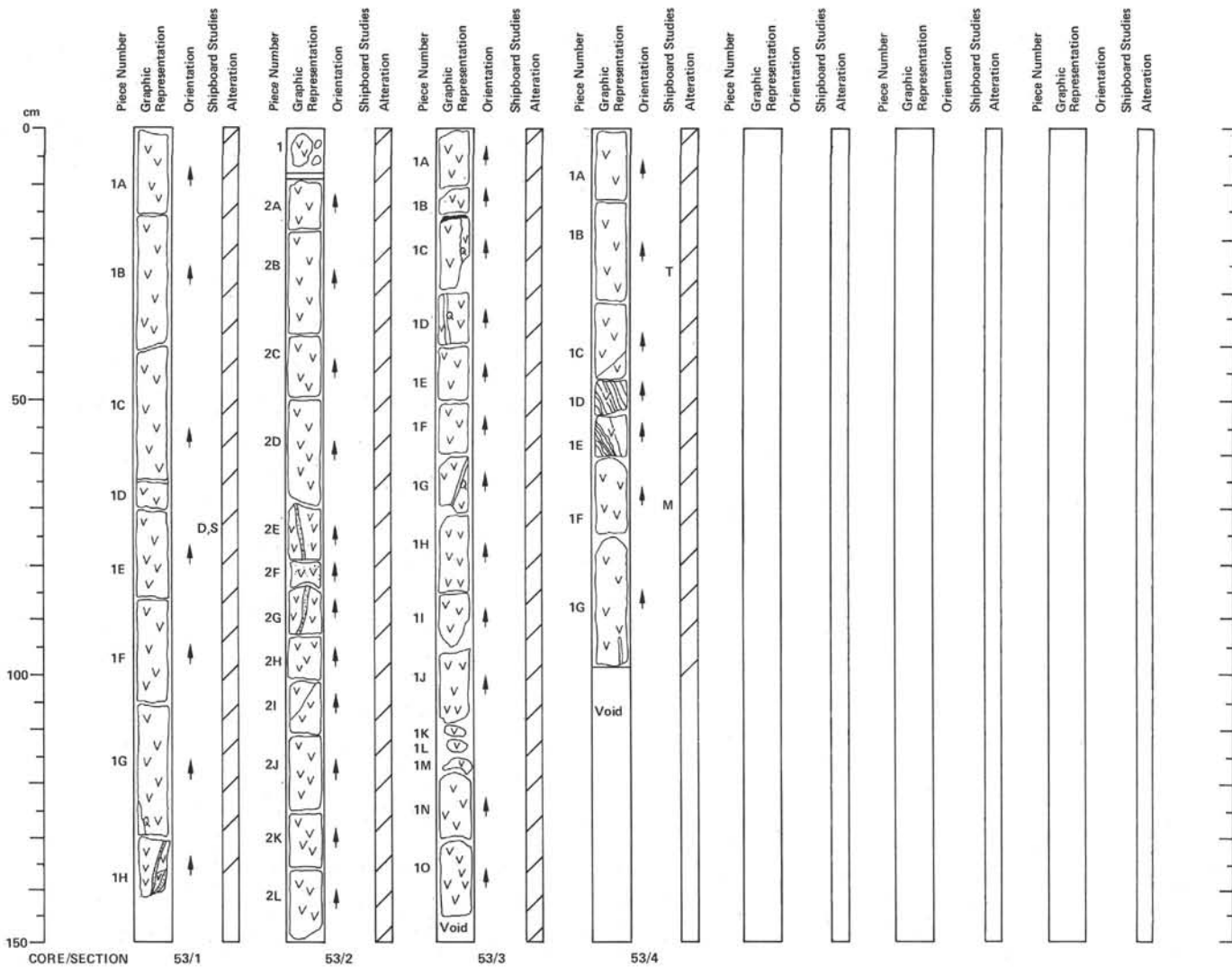
SECTION 6: DOMINANT LITHOLOGY: FINE-GRAINED DOLERITE.**Macroscopic Description**

Medium gray (N5) homogeneous, without veins or fractures. Similar to Section 5. Minor mottling, Piece 1E has some olivine segregation.

TS 85 cm, Piece 1D: subophitic to intergranular dolerite. Plagioclase phenocrysts (40%), 0.5–1.5 mm, partially enclose clinopyroxene (20%), 0.3–3 mm. Groundmass clinopyroxene and olivine (5%); minor opaques (3%) magnetite and ilmenite. 30% interstitial clay mineral alteration in mesostasis and groundmass olivines.

SECTION 7: DOMINANT LITHOLOGY: DOLERITE.**Macroscopic Description**

Same as Section 6, medium gray (N6), homogeneous without fractures or veins, minor mottling. Mottling has decreased progressively from the top of Core 52.



64-478-53

Depth 446.0 to 455.0 m

SECTION 1: DOMINANT LITHOLOGY: FINE-GRAINED DOLERITE.

Macroscopic Description

Homogeneous, fine grained, aphyric, minor mottling as seen in Core 52. Rock without fractures. One minor vein (Piece 1H) with silica and green clay.

SECTION 2: DOMINANT LITHOLOGY: DOLERITE.

Macroscopic Description

Same as Section 1 except more silica and clay-filled veins; moderately altered, slightly more than Section 1. Piece 2F, medium light gray (N6) split along the surface of a vein.

SECTION 3: DOMINANT LITHOLOGY: DOLERITE.

Macroscopic Description

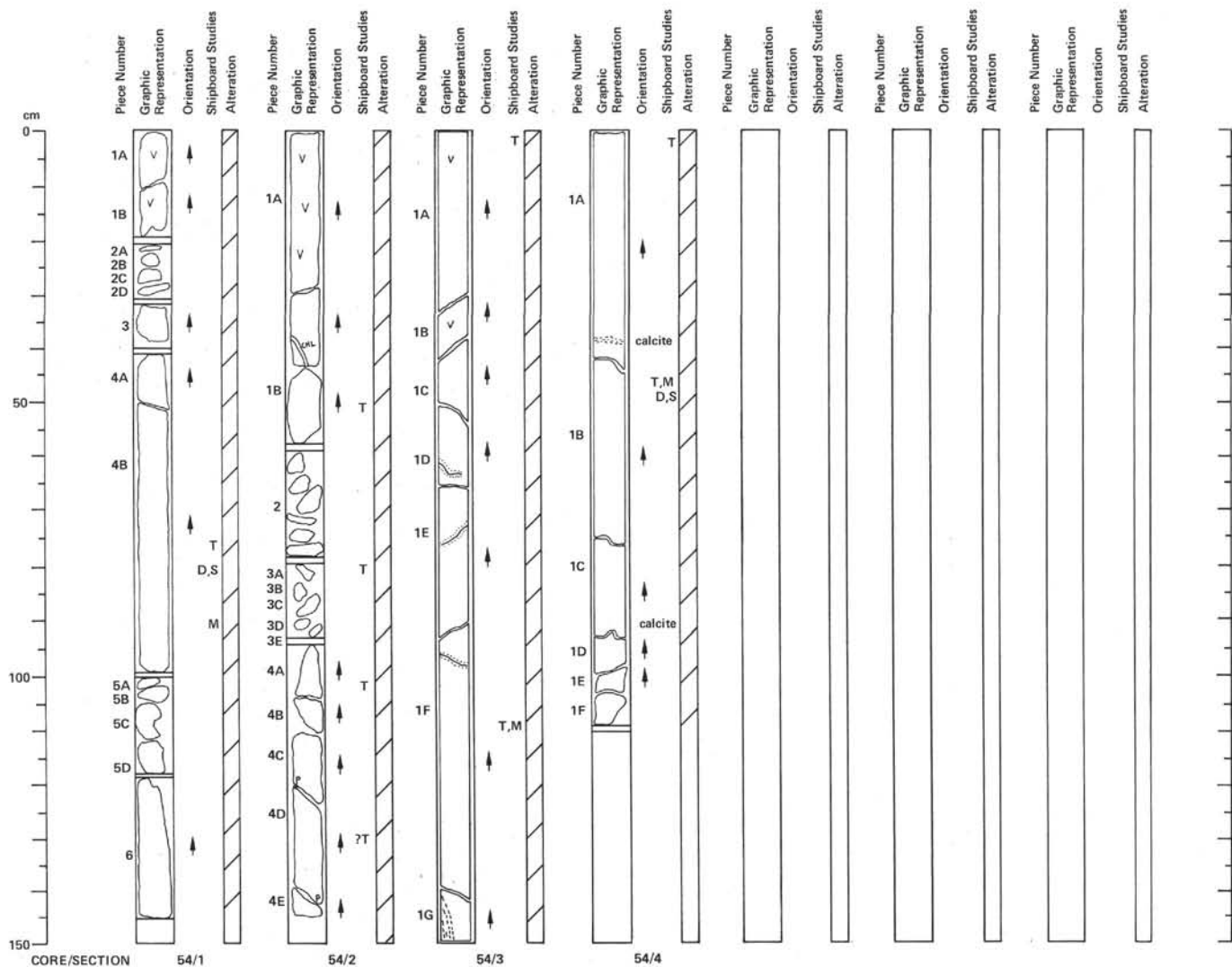
Same as Section 2, medium gray (N6), fine-grained, homogeneous with rare veins. Pieces 1D to 1G, not fractured. Piece 1M to 1O appear slightly finer-grained than rest of section. Minor veins contain calcite.

SECTION 4: DOMINANT LITHOLOGY: DOLERITE.

Macroscopic Description

Similar to Section 3, fine-grained, aphyric, medium gray to medium light gray (N5 to N6), dolerite with extensive microfracturing in Piece 1D which continues into Pieces 1E and 1C.

TS 28 cm, Piece 1B: intergranular texture, ~50% plagioclase (~An 55-60), 0.3-1.5 mm laths with 30% clinopyroxene (0.2-1.5 mm) irregular to anhedral phenocrysts and minor opaques (~4% [skeletal-ilmenite to cuboid-magnetite with mesostasis of 20% clay minerals (brownish colors)] and mica (biotite) 5%.



SECTION 1: DOMINANT LITHOLOGY: coarse aphyric BASALT (OR DOLERITE).**Macroscopic Description**

Medium gray (N5) aphyric basalt. Grain size progressively decreases through section.

Piece 1A: feldspar, 1–4 mm long, 0.5–1 mm wide laths in a dark clinopyroxene and olivine matrix.

Piece 6: feldspars do not exceed 1.5 mm in length, and are less than 0.5 mm wide. Matrix same as in Piece 1A.

The rock at the top of this section, and throughout the rest of the core, is different from that in Core 53. The latter has a fine-grained, fresh doleritic appearance, whereas this section has a speckled appearance, with altered feldspar laths lying in dark green clinopyroxene/olivine matrix. Rough proportions: clinopyroxene and olivine 50% and feldspar 50%.

The proportion of feldspar appears to increase down the section. Fractures are lined with green clay.

TS 76 cm, Piece 4B: BASALT. Intersertal texture of small clinopyroxene and olivine (10%, 0.5 mm) micropheocrysts in a matrix of small (30%, 0.3 mm) plagioclase laths and altered, brownish to greenish clay, glass (45%) with minor opaques.

SECTION 2: DOMINANT LITHOLOGY: 0–80 cm APHYRIC BASALT, 80–95 cm CONTACT ZONE, and 95–145 cm APHYRIC BASALT.**Macroscopic Description**

0–80 cm: very fine-grained aphyric medium light gray basalt. Grain size generally much less than 0.5 mm. Clay minerals notably abundant. A continuation of Section 1. Chlorite vein in Piece 1A. Bottom part of this interval becomes fragmented (Piece 2).

80–95 cm: small fragments comprising aphanitic greenish gray (5G 6/1) basalt (Pieces 3B–3E). Rare smectite-lined vesicles or cavities. Piece 1A contains contact between aphanitic basalt (continuation of 0–80 cm) and more coarsely crystalline basalt (90–140 cm).

95–140 cm: medium gray (N5) fine-grained aphyric basalt. Pieces 4A and 4B have 1–2 mm very elongate randomly orientated feldspar laths, but in Pieces 4C, D, and E the feldspars are less well-developed. Mafics all replaced by chloritic material?

Contact in interval 80–95 cm: upper unit (0–80 cm) appears to be chilled against lower unit (95–145 cm), with possible regrowth of feldspars in lower unit. See thin section description.

Pyrite in Pieces 4C and D along fractures.

TS 50 cm, Piece 1B: APHYRIC BASALT with intersertal to intergranular texture. No olivine seen. Plagioclase 25%, 0.1–0.5 mm, small laths. Clinopyroxene 20%, 0.1–0.6 mm, augite, small intergranular crystals and large ophitic crystals enclose plagioclase. Magnetite and ilmenite 5%, 0.1 mm, anhedral. Badly altered, much clay lost during thin section preparation.

TS 82 cm, Piece 3A: BASALT contact, equigranular, fine-grained. Phenocrysts: olivine (5%), 0.1–0.3 mm, anhedral; plagioclase (3%), 0.5 mm, blocky, zoned; clinopyroxene (10%), 0.1–0.3 mm, anhedral. Groundmass: mesostasis (60%). Badly altered (30%) to clay or zeolite.

TS 100 cm, Piece 4A: aphyric intergranular to intersertal BASALT. Plagioclase (30%), 0.2–1.0 mm, elongate laths Ang_{60-65} . Clinopyroxene (30%), 0.3–1.0 mm, augite, irregular optically continuous minerals, some large poikilitic with plagioclase. Mesostasis (40%), highly altered to clay or zeolite. Similar to 50 cm.

TS 130 cm, Piece 4D: sparsely phyrlic, intersertal to intergranular BASALT from sill interior. Phenocrysts plagioclase (1%), 1 mm, anhedral, resorbed. Groundmass: plagioclase (35%), 0.3–1.5 mm, laths. Clinopyroxene (30%), 0.2–0.6 mm, augite with some larger poikilitic crystals enclosing plagioclase. Magnetite (1%), 0.3 mm, cuboid

elongate. Vesicles (1%), 1.0–1.5 mm, random, calcite-filled, spherical, highly* altered (30%); calcite in mesostasis, green clay alteration of clinopyroxene.

SECTION 3: DOMINANT LITHOLOGY: APHYRIC BASALT.**Macroscopic Description**

Medium light gray (N6) medium-grained aphyric basalt. The light coloration of the rock is probably mainly due to alteration, but feldspar appears to be a major component with altered mafics. Feldspars are white, opaque. Grain size less than 2 mm, generally 0.5–1.0 mm.

Occasional veins contain calcite, and several fractures are coated with pyrites. The rock matrix is also speckled with pyrites.

A coarser-grained area occurs in Piece 1G, but this may be due to alteration rather than due to a primary process.

TS 1 cm, Piece 1A: sparsely PLAGIOCLASE-PHYRIC BASALT intergranular to intersertal texture. Phenocrysts: plagioclase ~1%, 2.5–3.0 mm, lath shaped, zoned and resorbed. Composition could not be determined. Groundmass: no olivine seen. Plagioclase 30%, 0.2–1.0 mm, Ang_{60-65} , lath-shaped. Clinopyroxene 20%, 0.2–0.6 mm, 7augite, anhedral. Approximately equidimensional with an intergranular to plagioclase. The mesostasis and some pyroxene has been replaced by clay minerals. There are some disseminated pyrite crystals in a vein.

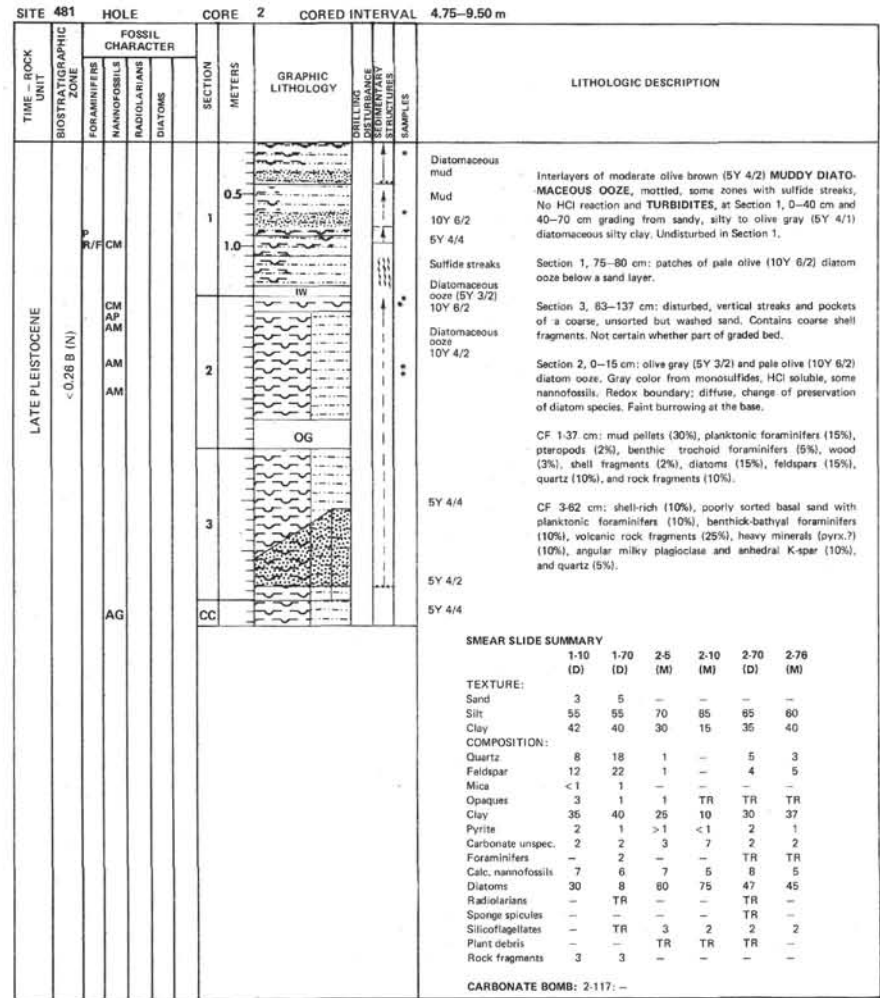
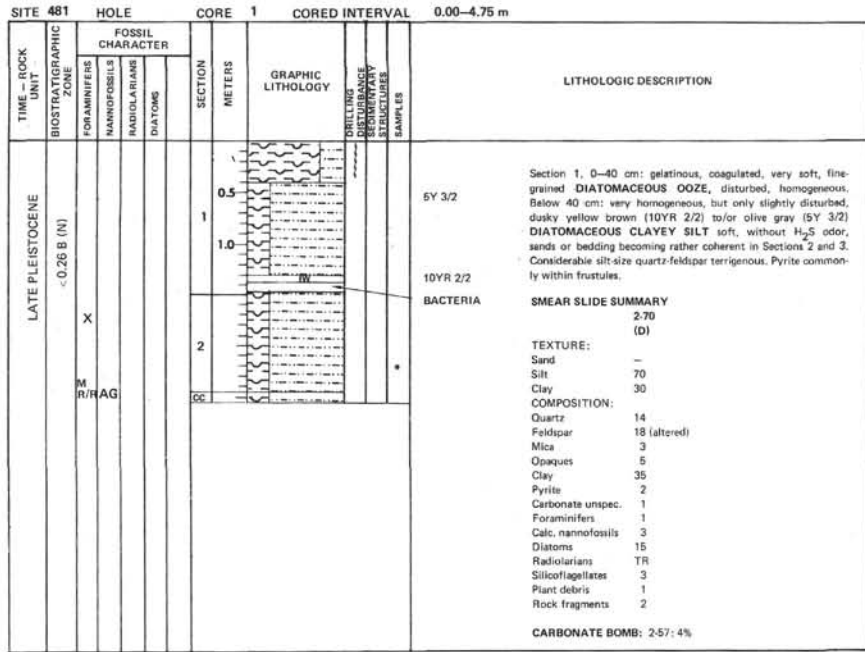
TS 110 cm, Piece 1F: determined during preparation.

SECTION 4: DOMINANT LITHOLOGY: APHYRIC BASALT.**Macroscopic Description**

Medium gray (N5) medium-grained aphyric basalt. A continuation of Section 3. However, the basalt becomes progressively more mafic towards the base of the section (N5/6 at top, N4 at bottom). Texturally and mineralogically this section look very similar to Section 1. Pyrites and calcite are again present. Calcite at 40 cm and Piece 1D.

TS 2 cm, Piece 1A: see below, similar to Piece 1B.

TS 50 cm, Piece 1B: intersertal to aphyric basalt, anhedral, small clinopyroxene (5%) laths and smaller olivine (0.1–0.3 mm) and clinopyroxene in mesostasis of small plagioclase laths (15%), 0.5 mm, and altered glass (60%) with clays and zeolites.



SITE 481		HOLE		CORE 3		CORED INTERVAL		9.50-14.25 m	
TIME - ROCK UNIT	BIOSTRATIGRAPHIC ZONE	FOSSIL CHARACTER			SECTION METERS	GRAPHIC LITHOLOGY	DRILLING APPROPRIATE SEDIMENTARY STRUCTURES SAMPLES	LITHOLOGIC DESCRIPTION	
		FORAMINIFERS	NANNOFOSSILS	RADIOLARIANS					
LATE PLEISTOCENE	<0.26 B (N)				1			5Y 4/2 Fibrous organic	
		P C/C			1.0			5Y 4/4	
					2			Muddy diatomaceous ooze Wood	Section 1, 65 cm: clump of fibrous organic material (crustacean?). Section 2, 51-58 cm: minor shell bits.
		AM			3				
	M C/F	AM			CC				

SITE 481		HOLE		CORE 4		CORED INTERVAL		14.25-19.00 m	
TIME - ROCK UNIT	BIOSTRATIGRAPHIC ZONE	FOSSIL CHARACTER			SECTION METERS	GRAPHIC LITHOLOGY	DRILLING APPROPRIATE SEDIMENTARY STRUCTURES SAMPLES	LITHOLOGIC DESCRIPTION	
		FORAMINIFERS	NANNOFOSSILS	RADIOLARIANS					
LATE PLEISTOCENE	<0.26 B (N)				1			Moderate dark olive (5Y 4/4, 4/3) Dark phase	
		P A C/G/M			1.0			5Y 4/4, 4/3	Shell fragments
		AM			CC				

SMEAR SLIDE SUMMARY
1-50 (D)

TEXTURE:
Sand -
Silt 55
Clay 45

COMPOSITION:
Quartz 2
Feldspar TR
Heavy minerals TR
Clay 45
Opauques TR
Pyrite 1
Carbonate unsp. 1
Foraminif. TR
Calc. nannofossils 8
Diatoms 40
Radiolarians TR
Sponge spicules TR
Silicoflagellates 2
Rock fragments 2

CARBONATE BOMB: 1-85: 13%

Note: Site 481, Core 5, 19.00-23.75 m: No Recovery.

SITE 481		HOLE		CORE 6		CORED INTERVAL		23.25-28.50 m	
TIME - ROCK UNIT	BIOSTRATIGRAPHIC ZONE	FOSSIL CHARACTER			SECTION METERS	GRAPHIC LITHOLOGY	DRILLING LOG	DIAPHRAGM SAMPLES	LITHOLOGIC DESCRIPTION
		FORAMINIFERS	NANNOFOSSILS	RADIOLARIANS					
PLEISTOCENE	IN 20/ANN 21	AG	C/F	CC	1				5Y 4/2 In Core-Catcher: disturbed mud with gaseous-spongy texture MUDDY DIATOM OOZE , moderate olive brown (5Y 4/2) with a patch of olive gray (5Y 3/2) ooze. Strong H ₂ S odor, faint HCl reaction.

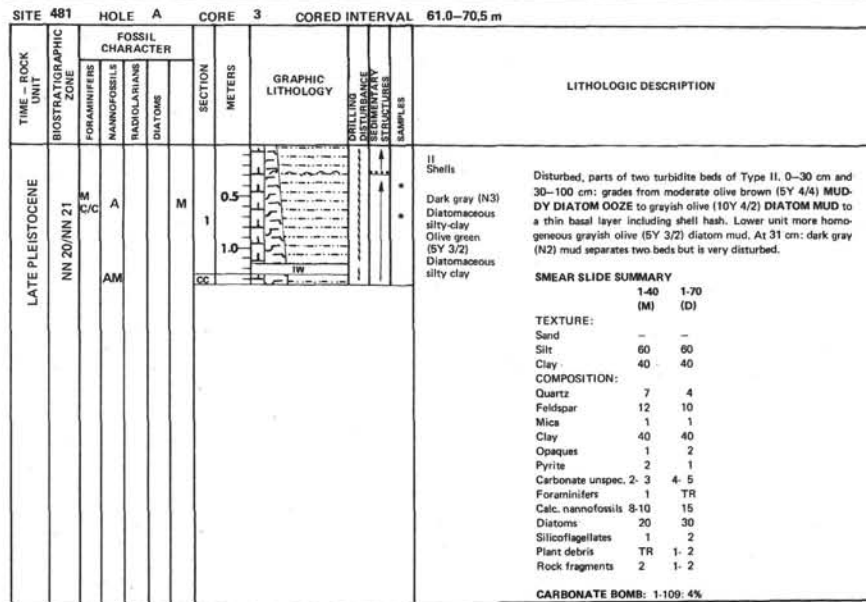
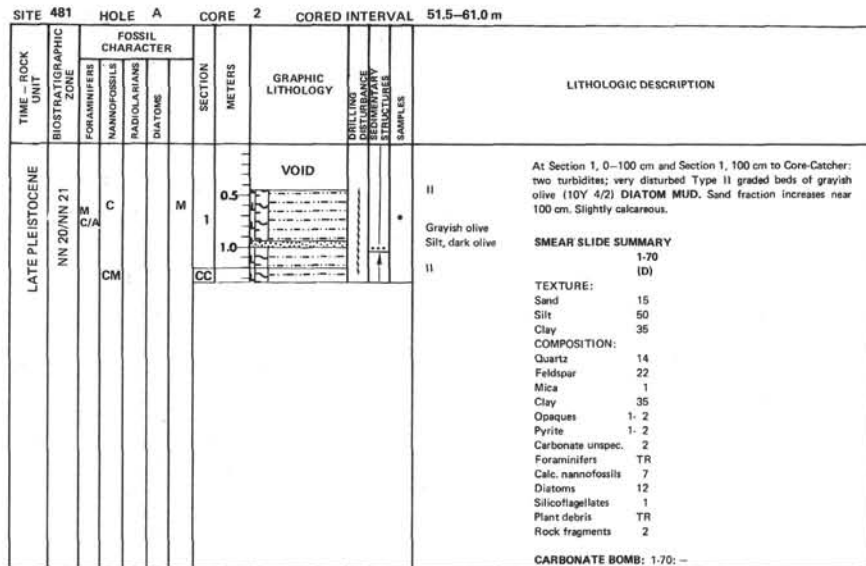
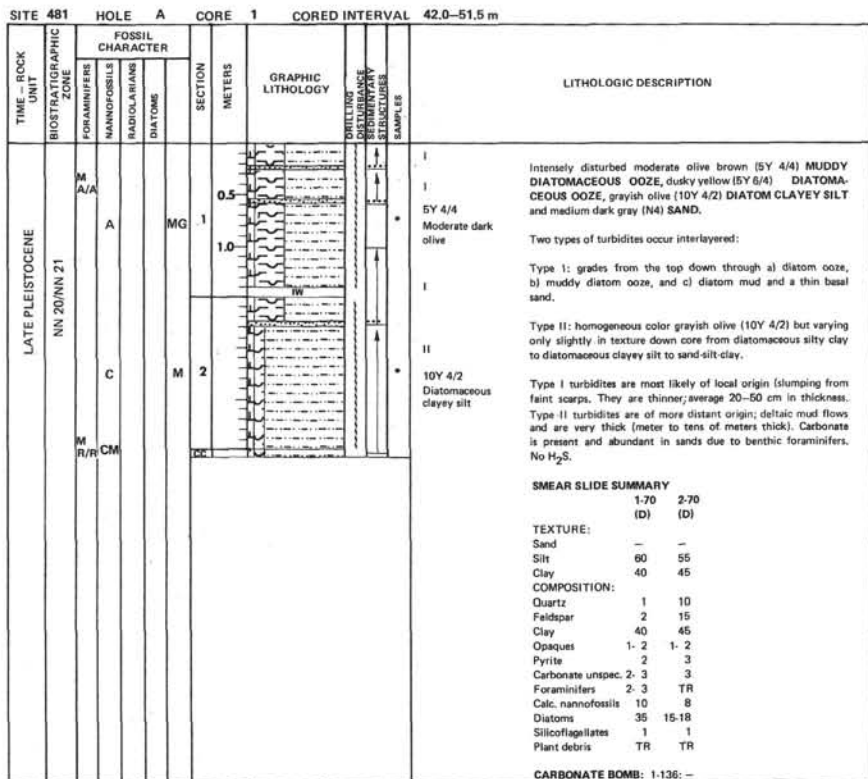
SITE 481		HOLE		CORE 7		CORED INTERVAL		28.50-33.25 m																																																												
TIME - ROCK UNIT	BIOSTRATIGRAPHIC ZONE	FOSSIL CHARACTER			SECTION METERS	GRAPHIC LITHOLOGY	DRILLING LOG	DIAPHRAGM SAMPLES	LITHOLOGIC DESCRIPTION																																																											
		FORAMINIFERS	NANNOFOSSILS	RADIOLARIANS						DIATOMS																																																										
LATE PLEISTOCENE	<0.26 B (N)	CM	R/R	P	1				5Y 3/2 5Y 4/4 Moderate dark olive 5Y 4/4 Interlayers: mainly 1) moderate olive brown (5Y 4/4) MUDDY DIATOMACEOUS OOZE , homogeneous, mottled in lighter and darker shades, with faint HCl reaction, scattered single shell fragments, burrowed. 2) Light olive gray (5Y 5/2) MUDDY DIATOM OOZE TO DIATOM MUD . Graded beds, have thin sandy basal layer. Surface shows gas pimples. More terrigenous. Upper contacts heavily burrowed and embayed. 3) At Section 2, 90-100 cm coarse sandy mud with a thin layer of pale olive (10Y 6/2) diatom ooze above. At Section 3, 30-34 cm two coarse gray (N4) sand separated by thin lutite.																																																											
					2				Diatomaceous silt (10Y 6/2)																																																											
					3				5Y 4/4																																																											
					CC																																																															
SMEAR SLIDE SUMMARY <table border="1"> <thead> <tr> <th></th> <th>1-20 (D)</th> <th>2-70 (D)</th> </tr> </thead> <tbody> <tr> <td>TEXTURE:</td> <td></td> <td></td> </tr> <tr> <td>Sand</td> <td>-</td> <td>-</td> </tr> <tr> <td>Silt</td> <td>60</td> <td>50</td> </tr> <tr> <td>Clay</td> <td>40</td> <td>50</td> </tr> <tr> <td>COMPOSITION:</td> <td></td> <td></td> </tr> <tr> <td>Quartz</td> <td>4</td> <td>10</td> </tr> <tr> <td>Feldspar</td> <td>5</td> <td>12</td> </tr> <tr> <td>Mica</td> <td>TR</td> <td>TR</td> </tr> <tr> <td>Heavy minerals</td> <td>1</td> <td>-</td> </tr> <tr> <td>Clay</td> <td>40</td> <td>45</td> </tr> <tr> <td>Opacues</td> <td>-</td> <td>3</td> </tr> <tr> <td>Pyrite</td> <td>1-2</td> <td>2</td> </tr> <tr> <td>Carbonate unspc.</td> <td>3</td> <td>1</td> </tr> <tr> <td>Foraminifers</td> <td>1</td> <td>1</td> </tr> <tr> <td>Calc. nanofossils</td> <td>15</td> <td>8</td> </tr> <tr> <td>Diatoms</td> <td>30</td> <td>25</td> </tr> <tr> <td>Silicoflagellates</td> <td>1</td> <td>1</td> </tr> <tr> <td>Plant debris</td> <td>-</td> <td>TR</td> </tr> <tr> <td>Rock fragments</td> <td>-</td> <td>2</td> </tr> </tbody> </table> CARBONATE BOMB: 2-136: 5.5%										1-20 (D)	2-70 (D)	TEXTURE:			Sand	-	-	Silt	60	50	Clay	40	50	COMPOSITION:			Quartz	4	10	Feldspar	5	12	Mica	TR	TR	Heavy minerals	1	-	Clay	40	45	Opacues	-	3	Pyrite	1-2	2	Carbonate unspc.	3	1	Foraminifers	1	1	Calc. nanofossils	15	8	Diatoms	30	25	Silicoflagellates	1	1	Plant debris	-	TR	Rock fragments	-	2
	1-20 (D)	2-70 (D)																																																																		
TEXTURE:																																																																				
Sand	-	-																																																																		
Silt	60	50																																																																		
Clay	40	50																																																																		
COMPOSITION:																																																																				
Quartz	4	10																																																																		
Feldspar	5	12																																																																		
Mica	TR	TR																																																																		
Heavy minerals	1	-																																																																		
Clay	40	45																																																																		
Opacues	-	3																																																																		
Pyrite	1-2	2																																																																		
Carbonate unspc.	3	1																																																																		
Foraminifers	1	1																																																																		
Calc. nanofossils	15	8																																																																		
Diatoms	30	25																																																																		
Silicoflagellates	1	1																																																																		
Plant debris	-	TR																																																																		
Rock fragments	-	2																																																																		

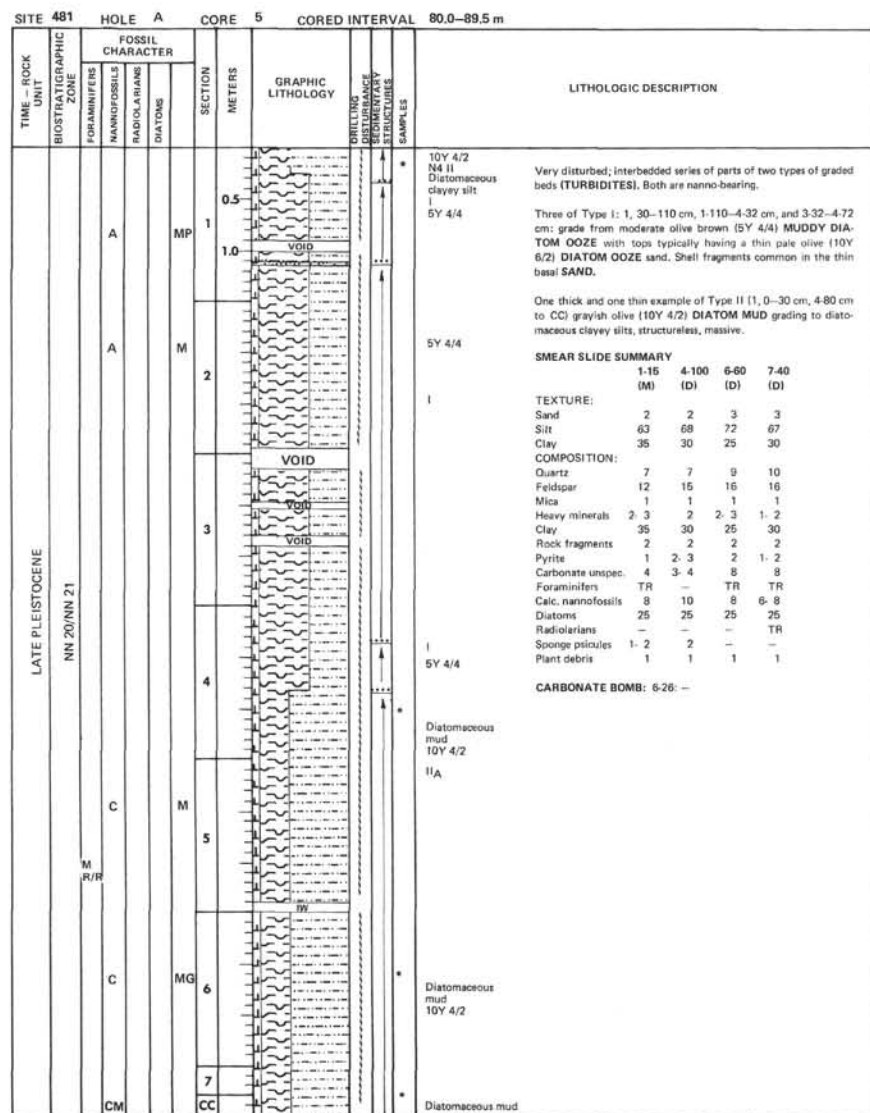
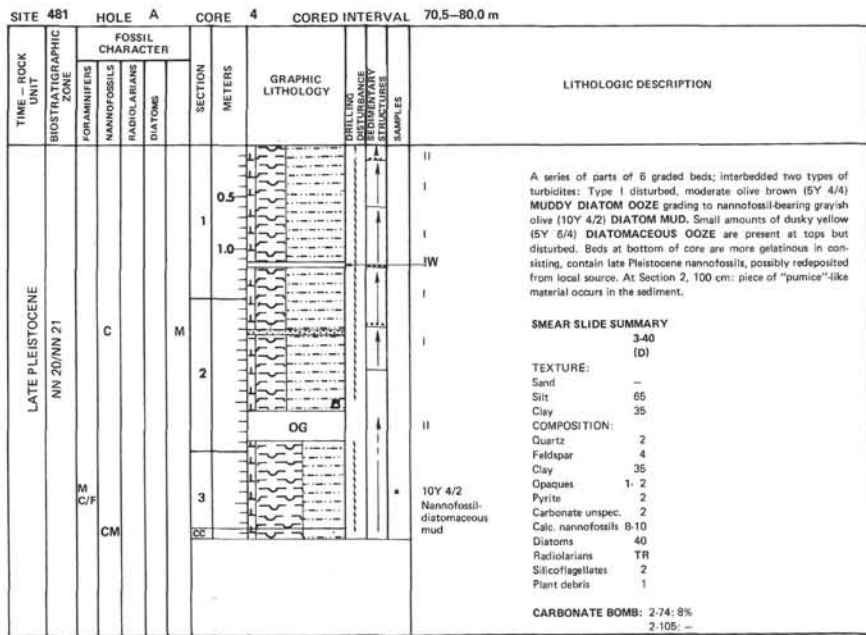
SITE 481		HOLE		CORE 8		CORED INTERVAL		33.25-38.00 m																																																																																															
TIME - ROCK UNIT	BIOSTRATIGRAPHIC ZONE	FOSSIL CHARACTER			SECTION METERS	GRAPHIC LITHOLOGY	DRILLING LOG	DIAPHRAGM SAMPLES	LITHOLOGIC DESCRIPTION																																																																																														
		FORAMINIFERS	NANNOFOSSILS	RADIOLARIANS						DIATOMS																																																																																													
LATE PLEISTOCENE	<0.26 B (N)	C/M/G	A	P	0.5				5Y 3/2 Disturbance: minor; multiple alternating redeposited beds with little intercalated host sediment. All slightly calcareous. A) MUDDY DIATOMACEOUS OOZE TURBIDITES , moderate olive brown (5Y 4/4) which have a thin basal sand and thin pale olive (10Y 6/2) DIATOM OOZE top (Section 1, 20-30 cm, Section 2, 48-85 cm, and Section 3, 30-67 cm and 120 cm+).																																																																																														
					1				B) Light olive gray (5Y 5/2) DIATOM MUD TURBIDITE very fine-grained without basal sand. Homogeneous, smooth surface, but graded.																																																																																														
					2				C) At Section 1, 50 cm to Section 2, 50 cm; diatom mud MASS FLOW with 2 large convolute folds, limestone bits, shell fragments, and a complete pecten. Faint irregular layering at the base Section 2, 50 cm.																																																																																														
					3				D) Rare; host lithology, moderate olive brown (5Y 4/4) MUDDY DIATOM OOZE with some darker zones. Mottled, burrowed, and commonly streaked with iron sulfide and faint bedding. Not laminated.																																																																																														
					CC																																																																																																		
SMEAR SLIDE SUMMARY <table border="1"> <thead> <tr> <th></th> <th>1-115 (M)</th> <th>2-10 (M)</th> <th>3-3 (M)</th> <th>3-70 (D)</th> </tr> </thead> <tbody> <tr> <td>TEXTURE:</td> <td></td> <td></td> <td></td> <td></td> </tr> <tr> <td>Sand</td> <td>-</td> <td>70</td> <td>-</td> <td>-</td> </tr> <tr> <td>Silt</td> <td>60</td> <td>30</td> <td>-</td> <td>55</td> </tr> <tr> <td>Clay</td> <td>40</td> <td>-</td> <td>-</td> <td>45</td> </tr> <tr> <td>COMPOSITION:</td> <td></td> <td></td> <td></td> <td></td> </tr> <tr> <td>Quartz</td> <td>1</td> <td>50</td> <td>3</td> <td>3</td> </tr> <tr> <td>Feldspar</td> <td>TR</td> <td>50</td> <td>5</td> <td>2</td> </tr> <tr> <td>Mica</td> <td>TR</td> <td>-</td> <td>1</td> <td>-</td> </tr> <tr> <td>Clay</td> <td>40</td> <td>-</td> <td>85</td> <td>25</td> </tr> <tr> <td>Opacues</td> <td>1</td> <td>-</td> <td>2</td> <td>-</td> </tr> <tr> <td>Pyrite</td> <td>1</td> <td>-</td> <td>-</td> <td>2</td> </tr> <tr> <td>Carbonate unspc.</td> <td>-</td> <td>-</td> <td>-</td> <td>3</td> </tr> <tr> <td>Foraminifers</td> <td>-</td> <td>-</td> <td>-</td> <td>2</td> </tr> <tr> <td>Calc. nanofossils</td> <td>55</td> <td>-</td> <td>-</td> <td>20</td> </tr> <tr> <td>Diatoms</td> <td>4</td> <td>-</td> <td>2-3</td> <td>40</td> </tr> <tr> <td>Sponge spicules</td> <td>TR</td> <td>-</td> <td>-</td> <td>-</td> </tr> <tr> <td>Silicoflagellates</td> <td>TR</td> <td>-</td> <td>-</td> <td>1</td> </tr> <tr> <td>Plant debris</td> <td>-</td> <td>-</td> <td>1-2</td> <td>1-2</td> </tr> </tbody> </table> CARBONATE BOMB: 2-110: -										1-115 (M)	2-10 (M)	3-3 (M)	3-70 (D)	TEXTURE:					Sand	-	70	-	-	Silt	60	30	-	55	Clay	40	-	-	45	COMPOSITION:					Quartz	1	50	3	3	Feldspar	TR	50	5	2	Mica	TR	-	1	-	Clay	40	-	85	25	Opacues	1	-	2	-	Pyrite	1	-	-	2	Carbonate unspc.	-	-	-	3	Foraminifers	-	-	-	2	Calc. nanofossils	55	-	-	20	Diatoms	4	-	2-3	40	Sponge spicules	TR	-	-	-	Silicoflagellates	TR	-	-	1	Plant debris	-	-	1-2	1-2
	1-115 (M)	2-10 (M)	3-3 (M)	3-70 (D)																																																																																																			
TEXTURE:																																																																																																							
Sand	-	70	-	-																																																																																																			
Silt	60	30	-	55																																																																																																			
Clay	40	-	-	45																																																																																																			
COMPOSITION:																																																																																																							
Quartz	1	50	3	3																																																																																																			
Feldspar	TR	50	5	2																																																																																																			
Mica	TR	-	1	-																																																																																																			
Clay	40	-	85	25																																																																																																			
Opacues	1	-	2	-																																																																																																			
Pyrite	1	-	-	2																																																																																																			
Carbonate unspc.	-	-	-	3																																																																																																			
Foraminifers	-	-	-	2																																																																																																			
Calc. nanofossils	55	-	-	20																																																																																																			
Diatoms	4	-	2-3	40																																																																																																			
Sponge spicules	TR	-	-	-																																																																																																			
Silicoflagellates	TR	-	-	1																																																																																																			
Plant debris	-	-	1-2	1-2																																																																																																			

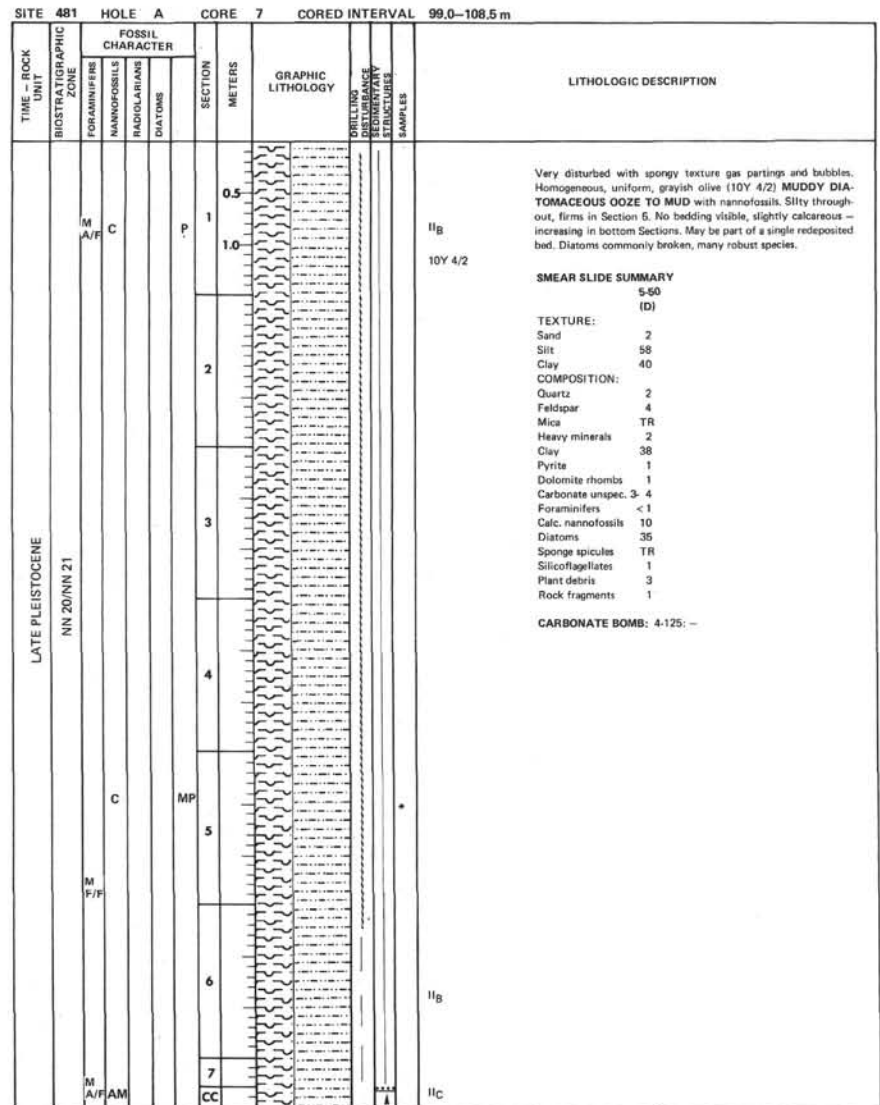
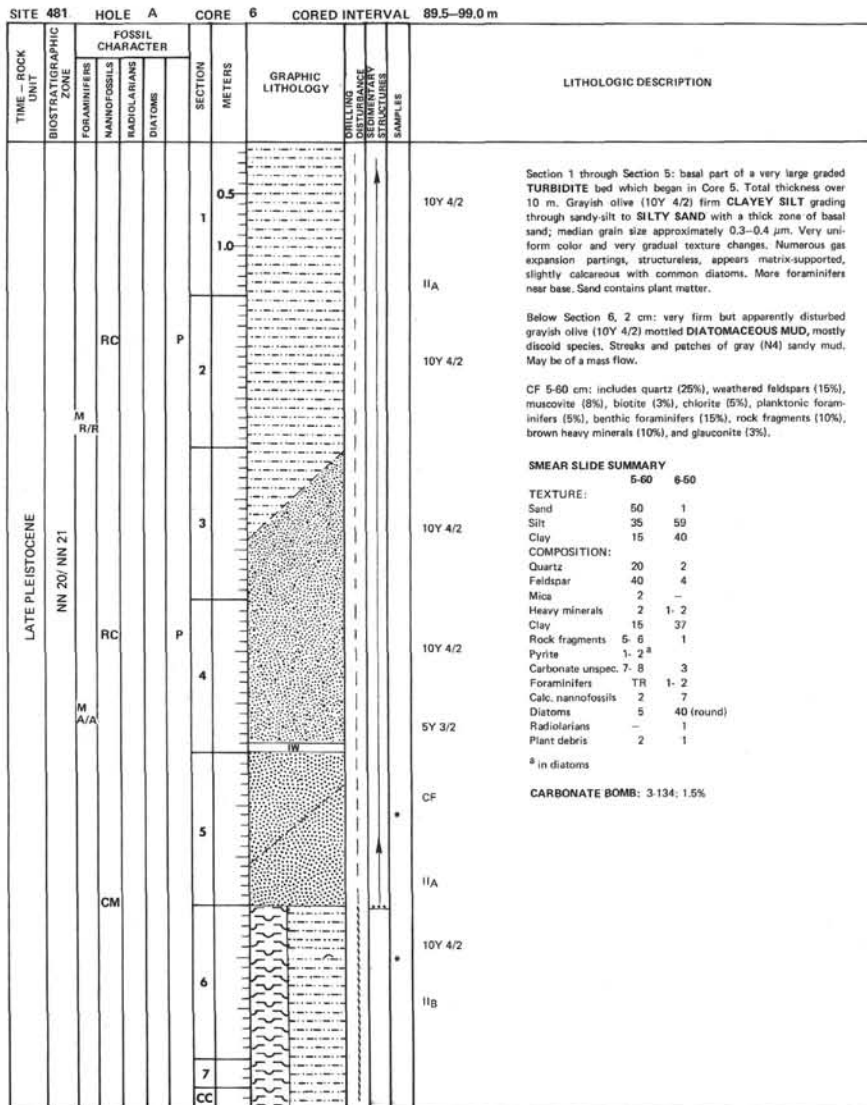
SITE 481		HOLE		CORE 9		CORED INTERVAL 38.00-42.75 m	
TIME - ROCK UNIT	BIOSTRATIGRAPHIC ZONE	FOSSIL CHARACTER			SECTION METERS	GRAPHIC LITHOLOGY	LITHOLOGIC DESCRIPTION
		FORAMINIFERS	NANNOFOSSILS	RADIOLARIANS			
LATE PLEISTOCENE	<0.45 B (N)	P			0.5		Section 1, 0-80 cm: disturbed mixture of MUDDY NANNOFOSSIL BEARING DIATOMACEOUS OOZE , shell bits with pockets of gray clay. Some cavings are apparently present. Section 1, 80 cm to CC: homogeneous moderate olive brown (5Y 4/4) MUDDY DIATOM OOZE which may be part of a redeposited bed.
		A/C			1.0		
		CM					* Nannofossil-diatomaceous ooze
		AM					
					2		
					CC		
SMEAR SLIDE SUMMARY 1-85 TEXTURE: Sand <1 Silt 55 Clay 45 COMPOSITION: Quartz 7 Feldspar 5 Mica 1 Clay 30 Pyrite 3 Carbonate unspec. TR Foraminifers TR Calc. nannofossils 15 Diatoms 35 Silicoflagellates 2 Plant debris 5 CARBONATE BOMB: 1-141; 3%							

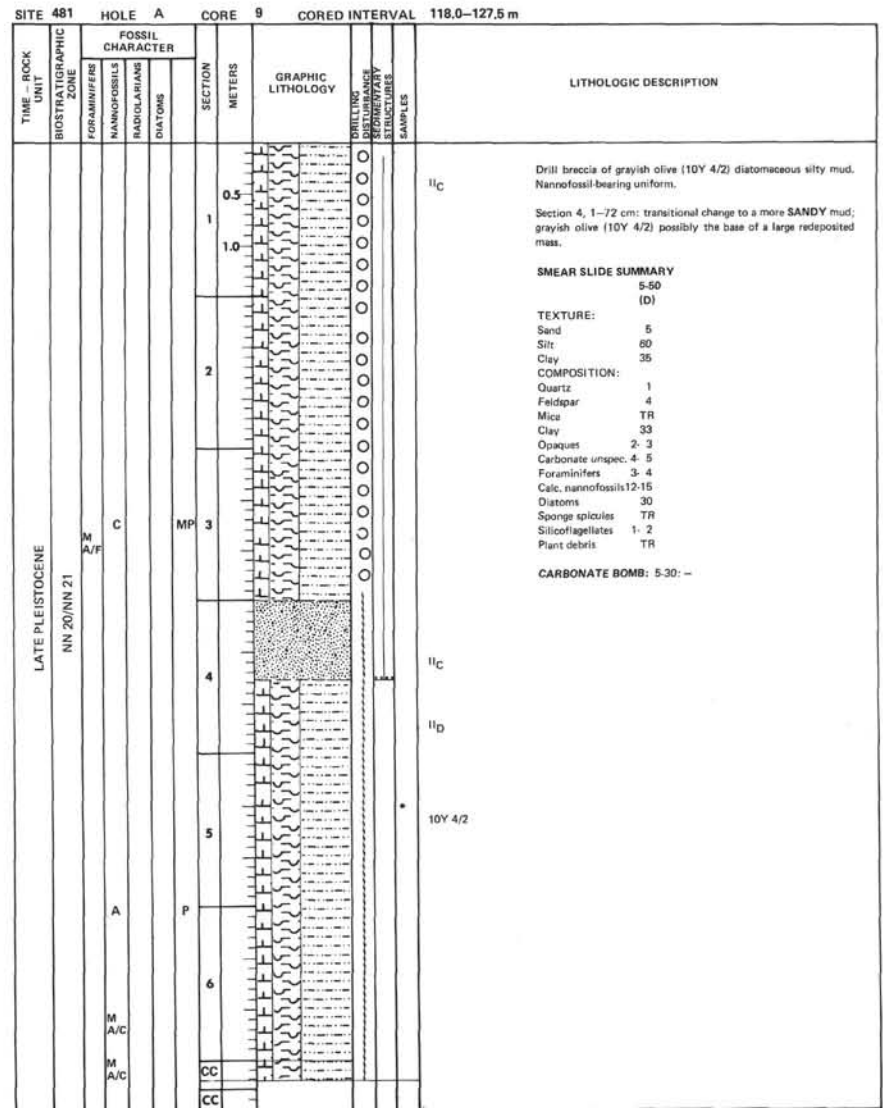
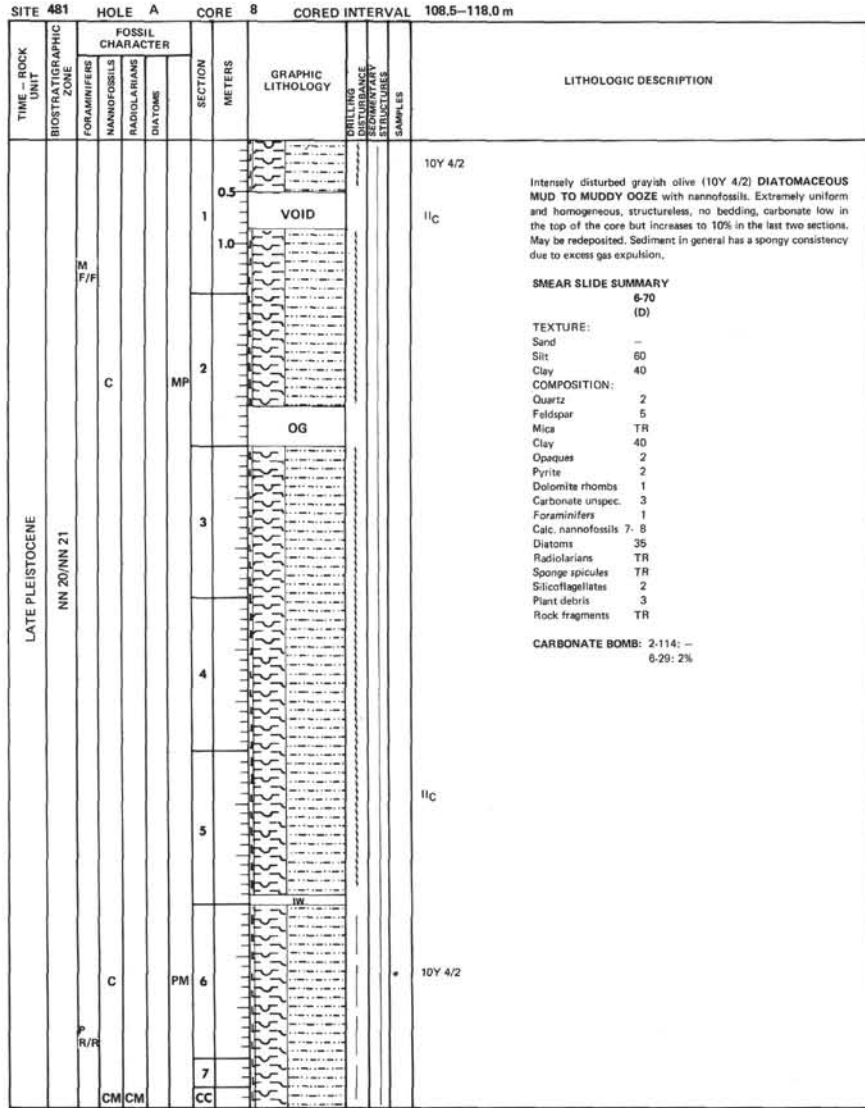
SITE 481		HOLE		CORE 10		CORED INTERVAL 42.75-47.50 m																																																																																																
TIME - ROCK UNIT	BIOSTRATIGRAPHIC ZONE	FOSSIL CHARACTER			SECTION METERS	GRAPHIC LITHOLOGY	LITHOLOGIC DESCRIPTION																																																																																															
		FORAMINIFERS	NANNOFOSSILS	RADIOLARIANS				DIATOMS																																																																																														
LATE PLEISTOCENE	<0.45 B (N)				0.5		Host sediment Nannofossil-diatomaceous ooze 5Y 4/4 TYPE I: turbidite (example 1.50 to 2.20 cm) MUDDY DIATOMACEOUS OOZE , moderate olive brown (5Y 4/4), more calcareous, and foraminifer specks increase down toward a very thin sand laminal base, with benthic, 5Y 3/2 bathyal foraminifers.																																																																																															
		AM			1.0																																																																																																	
		M					5Y 4/4 TYPE II: light olive gray (5Y 5/2) SILTY DIATOM MUD , grades evenly to a silty sand base, structureless, except some gas pimples which form on the surface. Gray (N4) sands are feldspar and rock fragment rich, burrowed or thin light clay top Section 3, 70 cm to bottom continuing on in Core 11.																																																																																															
		C/A/AM			2																																																																																																	
							Host sediment Top of turbidite Quartz-feldspathic diatomaceous silt Middle of turbidite Silty clay Bottom of turbidite Sandy silt 5Y 3/2 SMEAR SLIDE SUMMARY <table border="1"> <thead> <tr> <th></th> <th>1-60</th> <th>2-98</th> <th>2-130</th> <th>3-26</th> </tr> <tr> <th>TEXTURE:</th> <th>(D)</th> <th>(M)</th> <th>(M)</th> <th>(CF)</th> </tr> </thead> <tbody> <tr> <td>Sand</td> <td>-</td> <td>-</td> <td>-</td> <td>40</td> </tr> <tr> <td>Silt</td> <td>70</td> <td>90</td> <td>30</td> <td>60</td> </tr> <tr> <td>Clay</td> <td>30</td> <td>10</td> <td>70</td> <td>-</td> </tr> <tr> <td>COMPOSITION:</td> <td></td> <td></td> <td></td> <td></td> </tr> <tr> <td>Quartz</td> <td>3</td> <td>20</td> <td>15</td> <td>40</td> </tr> <tr> <td>Feldspar</td> <td>2</td> <td>30</td> <td>5</td> <td>60</td> </tr> <tr> <td>Heavy minerals</td> <td>-</td> <td>-</td> <td>1</td> <td>-</td> </tr> <tr> <td>Clay</td> <td>10</td> <td>5</td> <td>58</td> <td>-</td> </tr> <tr> <td>Pyrite</td> <td>2</td> <td>10</td> <td>2</td> <td>TR</td> </tr> <tr> <td>Carbonate unspec.</td> <td>TR</td> <td>1-2</td> <td>1-2</td> <td>-</td> </tr> <tr> <td>Foraminifers</td> <td>-</td> <td>-</td> <td>-</td> <td>TR</td> </tr> <tr> <td>Calc. nannofossils</td> <td>20</td> <td>2-3</td> <td>2-3</td> <td>-</td> </tr> <tr> <td>Diatoms</td> <td>60</td> <td>20</td> <td>12</td> <td>-</td> </tr> <tr> <td>Sponge spicules</td> <td>-</td> <td>-</td> <td>-</td> <td>TR</td> </tr> <tr> <td>Silicoflagellates</td> <td>TR</td> <td>-</td> <td>TR</td> <td>-</td> </tr> <tr> <td>Plant debris</td> <td>1-2</td> <td>10</td> <td>3</td> <td>-</td> </tr> <tr> <td>Red-brown stained grains</td> <td>-</td> <td>-</td> <td>-</td> <td>TR</td> </tr> </tbody> </table>		1-60	2-98	2-130	3-26	TEXTURE:	(D)	(M)	(M)	(CF)	Sand	-	-	-	40	Silt	70	90	30	60	Clay	30	10	70	-	COMPOSITION:					Quartz	3	20	15	40	Feldspar	2	30	5	60	Heavy minerals	-	-	1	-	Clay	10	5	58	-	Pyrite	2	10	2	TR	Carbonate unspec.	TR	1-2	1-2	-	Foraminifers	-	-	-	TR	Calc. nannofossils	20	2-3	2-3	-	Diatoms	60	20	12	-	Sponge spicules	-	-	-	TR	Silicoflagellates	TR	-	TR	-	Plant debris	1-2	10	3	-	Red-brown stained grains	-	-	-	TR
	1-60	2-98	2-130	3-26																																																																																																		
TEXTURE:	(D)	(M)	(M)	(CF)																																																																																																		
Sand	-	-	-	40																																																																																																		
Silt	70	90	30	60																																																																																																		
Clay	30	10	70	-																																																																																																		
COMPOSITION:																																																																																																						
Quartz	3	20	15	40																																																																																																		
Feldspar	2	30	5	60																																																																																																		
Heavy minerals	-	-	1	-																																																																																																		
Clay	10	5	58	-																																																																																																		
Pyrite	2	10	2	TR																																																																																																		
Carbonate unspec.	TR	1-2	1-2	-																																																																																																		
Foraminifers	-	-	-	TR																																																																																																		
Calc. nannofossils	20	2-3	2-3	-																																																																																																		
Diatoms	60	20	12	-																																																																																																		
Sponge spicules	-	-	-	TR																																																																																																		
Silicoflagellates	TR	-	TR	-																																																																																																		
Plant debris	1-2	10	3	-																																																																																																		
Red-brown stained grains	-	-	-	TR																																																																																																		
					3																																																																																																	
					CC																																																																																																	
CARBONATE BOMB: 3-103; -																																																																																																						

SITE 481		HOLE		CORE 11		CORED INTERVAL 47.50-52.25 m			
TIME - ROCK UNIT	BIOSTRATIGRAPHIC ZONE	FOSSIL CHARACTER			SECTION METERS	GRAPHIC LITHOLOGY	DRILLING LOG SEGMENTARY STRUCTURES SAMPLES	LITHOLOGIC DESCRIPTION	
		FORAMINIFERS	NANNOFOSSILS	RADIOLARIANS					DIATOMS
LATE PLEISTOCENE	NN 20/NN 21	AM			0.5		5Y 3/2	<p>Section 1, 0-20 cm: drillavings downhole; mud. Entire core comprises the mid-section of a large (about 11 m thick) TURBIDITE BED. Begins in Core 10, Section 3, 45 cm with very thin diatomaceous clay grading continuous through Core 11 without loss as seen on GRAPE density profiles. Grades faintly downward from light olive gray (5Y 3/2) diatomaceous silty clay to gray (N4) sandy silt, very uniform, structureless, homogeneous, without burrows, mottling or layering. Slight increase in HCl reaction down core due to foraminifera. No H₂S odor. Terrigenous clastics feldspar-rich, volcanic rock fragments, scattered wood fragments. Sorting poor, but grain supported near bottom.</p> <p>SMEAR SLIDE SUMMARY</p> <p>3-20 (D)</p> <p>TEXTURE:</p> <p>Sand - Silt 60 Clay 40</p> <p>COMPOSITION:</p> <p>Quartz 14 Feldspar 25 Clay 30 Pyrite 2 Carbonate unspec. TR Foraminifera TR Calc. nannofossils 10 Diatoms 20 Plant debris 3</p> <p>CARBONATE BOMB: 1-121: 2.5%</p>	
		A M/G			1.0		2		N4
		M	M/C/C						3
		M/A/AG			CC				



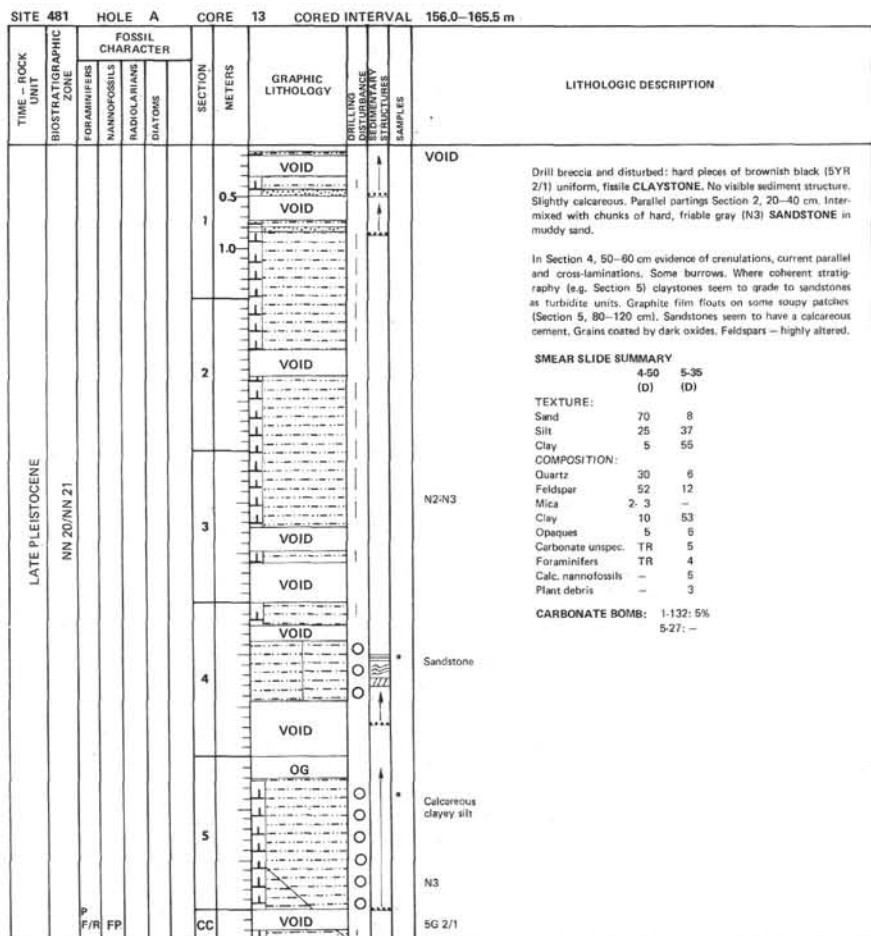
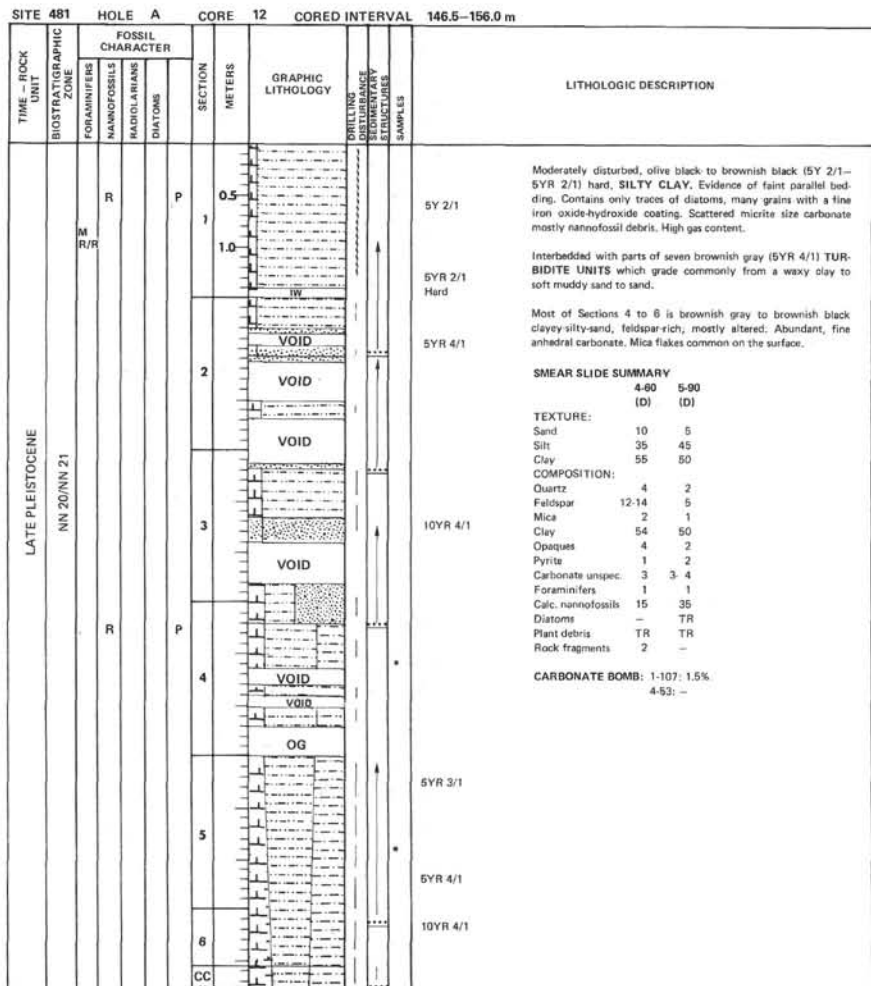




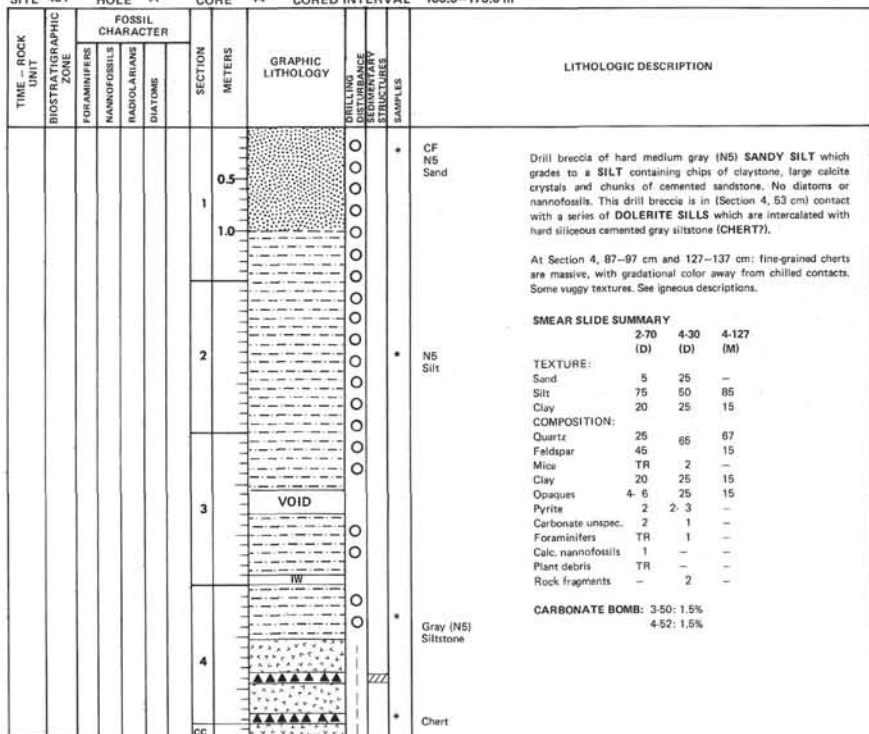


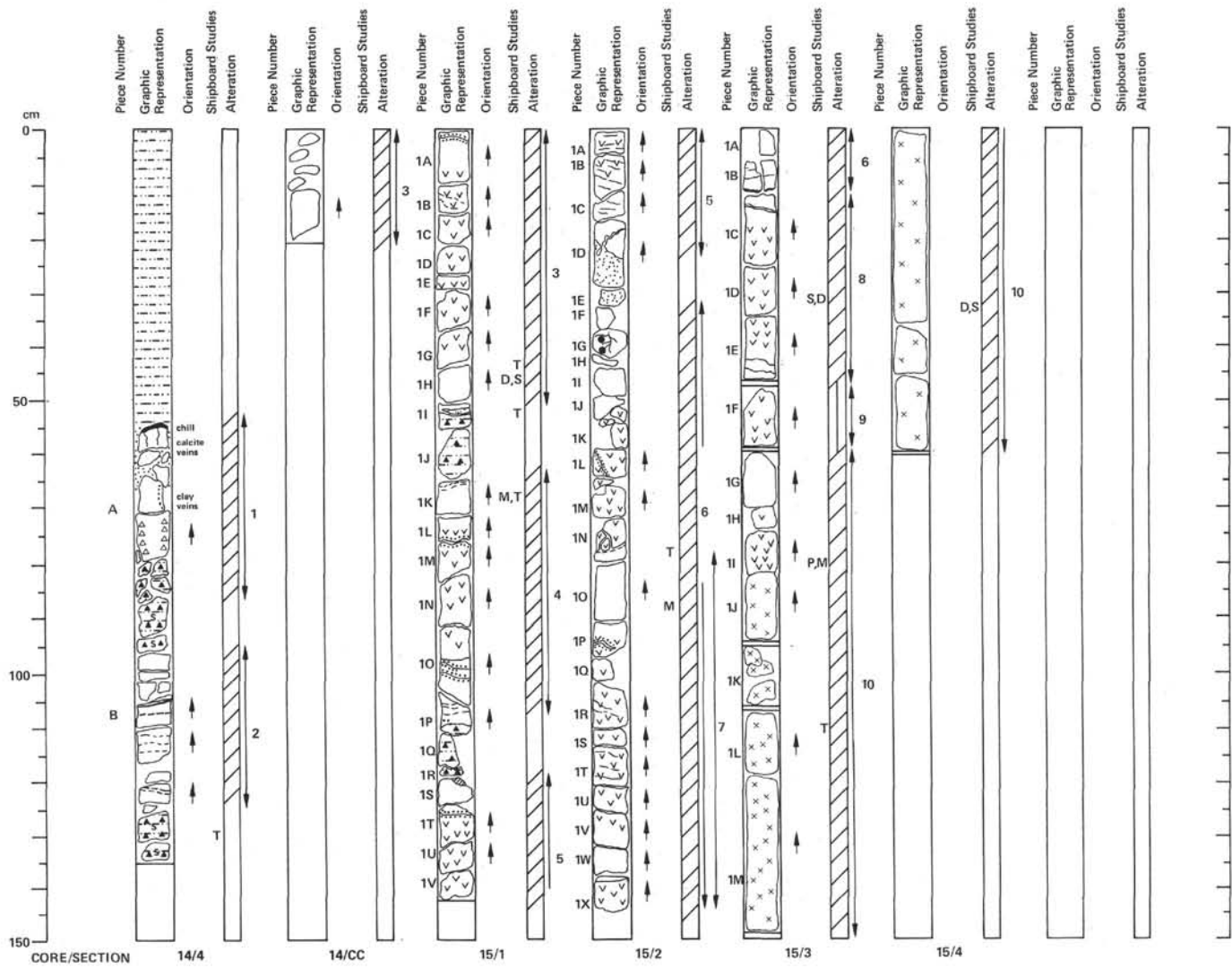
SITE 481 HOLE A CORE 10 CORED INTERVAL 127.5-137.0 m										
TIME - ROCK UNIT	BIOSTRATIGRAPHIC ZONE	FOSSIL CHARACTER			SECTION METERS	GRAPHIC LITHOLOGY	DRILLING DISTURBANCE BY STRUCTURES	SAMPLES	LITHOLOGIC DESCRIPTION	
		FORAMINIFERS	NANNOFOSSILS	RADIOLARIANS						
LATE PLEISTOCENE	NN 20/NN 21	M A/C	C	M	0.5				Drill breccia of olive gray (5Y 3/2) DIATOMACEOUS MUD with minor amounts of gray SAND and occurrence of more chips of hard gray olive (10Y 4/2) clayey silt. Sediment appears to become firmer. Diatoms unaltered. Nannofossils decrease slightly and gas pockets are common. Turbidites, if any, cannot be differentiated.	
					1					
					1.0					
					VOID					
					2					
3	M	TW	M	3				Extremely disturbed by drilling but core seems to be a mixture of three lithologies: A) Mostly olive gray (5Y 3/2) DIATOMACEOUS MUD. B) Minor amounts of gray (N4) SAND. C) Harder, dark brownish-olive black diatomaceous claystone chips within Sections 4 to 6.		
4										
5	C		M	5				SMEAR SLIDE SUMMARY 4-40 TEXTURE: Sand 10 Silt 40 Clay 50 COMPOSITION: Quartz 5 Feldspar 11 Clay 50 Opales 2 Pyrite 2-3 Carbonate unspec. 1-2 Foraminifers 1 Calc. nannofossils 5 Diatoms 20 Radiolarians TR Silicoflagellates 1 Plant debris 1-2 CARBONATE BOMB: 2-104; 1%		
6	CM		CC							

SITE 481 HOLE A CORE 11 CORED INTERVAL 137.0-146.5 m										
TIME - ROCK UNIT	BIOSTRATIGRAPHIC ZONE	FOSSIL CHARACTER			SECTION METERS	GRAPHIC LITHOLOGY	DRILLING DISTURBANCE BY STRUCTURES	SAMPLES	LITHOLOGIC DESCRIPTION	
		FORAMINIFERS	NANNOFOSSILS	RADIOLARIANS						
LATE PLEISTOCENE	NN 20/NN 21	M C/F	R	MP	0.5				Intensely disturbed, uniform and gassy, olive black (5Y 2/1) to olive gray (5Y 3/2) SILTY CLAY. Clays are fissile and color darkens. Slightly calcareous, increases with depth. Diatoms mostly robust types, decrease in abundance. Many particles have Fe-oxy-hydroxide coatings.	
					1					
					1.0					
					2					
					3					
4	P	VOID	MP	4				At Section 3, 95-100 cm and 120-130 cm, and Section 4, 10-20 cm: basal, graded parts of 3 sandy TURBIDITES with moderate olive brown diatomaceous mud, nannofossil-bearing near their tops.		
5										
6	CC			6				SMEAR SLIDE SUMMARY 3-115 3-140 (D) (M) TEXTURE: Sand 2 3 Silt 23 37 Clay 75 60 COMPOSITION: Quartz 3-4 1 Feldspar 7 2-3 Clay 75 60 Opales 1-2 1 Pyrite 2 2-3 Carbonate unspec. 5 3-4 Foraminifers TR 1 Calc. nannofossils 2-3 10 Diatoms 2 15 Sponge spicules TR - Plant debris TR - Rock fragments TR - CARBONATE BOMB: 3-144: -		
7										



SITE 481 HOLE A CORE 14 CORED INTERVAL 165.5-175.0 m





64-481A-14

Depth: 166.5 to 175.0 m

SECTION 4: DOMINANT LITHOLOGY: Contact zone — black mudstone with BASALT.

Macroscopic Description

0–55 cm: dark gray (N5) SILTY MUDSTONE

55–56 cm: QUENCHED BASALT. Unit 1 — not glassy. Two–three selvage of devitrified glass at 55 cm. Two–three mm irregular black patches; 10% of rock probably alteration zones. Basalt is aphyric, aphanitic. N5–N6 clay. Minor clay (plus rare calcite) veining, normal and parallel to contact.

86–95 cm: BROWN CHERTS with baked appearance. Intercalated sediment.

96–124 cm: Unit 2 — aphanitic to fine-grained medium gray BASALT. Veined (one calcite). Grain-size gradational from aphanitic to fine-grained to aphanitic, indicating chilling against intercalated sediment.

Below 125 cm: BROWN CHERT, with baked contact at upper margin. Color gradation and cavities.

TS at 57 cm (sampled just below chill margin): BASALT (80%) to altered basalt glass with small (0.5–1.0 mm) plagioclase microlites (An_{50}) (3%) set in a matrix of glass. Tiny (0.05–0.3 mm) plagioclase laths (7%) and anhedral clinopyroxene (3%, 0.5 mm). Small opaques (2%, <0.1 mm), carbonate (3%), zeolite (2%), and some clay along intergranular spaces and veinlets.

CORE-CATCHER: DOMINANT LITHOLOGY: Coarse-grained BASALT, a dolerite.

Macroscopic Description

Medium gray (N4/N5), medium- to coarse-grained BASALT (grain-size 1–2 mm). Intrusive Unit 3 — feldspars green tinted and indicating alteration. Development of fibrous texture in altered minerals; chlorite⁷, aphyric, pyroxenes appear fresh.

64-481A-15

Depth 175.0 to 184.5 m

SECTION 1: DOMINANT LITHOLOGY: BASALT and DOLERITE. Intrusive Units 3, 4, and 5 with intercalations of CERTIFIED SEDIMENT.

Macroscopic Description

0–8 cm (Piece 1A): medium light gray (N6) (dry) basalt grading into dolerite at bottom. Aphyric. Pyroxene and plagioclase. Slight alteration to clay minerals. One–two mm (light gray) vein filled with ?clays and zeolites (no calcite).

8–35 cm (Pieces 1B–1F): similar to basal portion of Piece 1A — doleritic. Aphyric, increasing in grain-size to maximum of approximately 2–3 mm in Piece 1F. Minor veins common, but no calcite.

35–51 cm (Pieces 1G–1I): gradational from dolerite to aphanitic (chilled) basalt in 1I, where sediment-basalt contact is preserved. Again, aphyric — rather altered.

51–64 (Pieces 1I–1J): olive gray CHERTY SILTSTONE

65–109 cm (Pieces 1K–1P): veined aphyric basalt, grading from aphanitic adjacent to sediment to doleritic in center (1L–1O). Similar to Unit 1, 1A–1I (veined without calcite).

109–118 cm (Pieces 1P–1R): medium light gray CHERTY SILTSTONE
118–142 cm (Pieces 1S–1V): Intrusive Unit 5 — aphyric medium gray (N5) basalt (fine-grained in Piece 1S) to dolerite (1T–1V). Grain-size progressively increases from 1S–1V, latter comprising of clinopyroxene and plagioclase (up to 2 mm laths). Veined but without calcite.

TS 44 cm (Piece 1G): BASALT sparsely porphyritic, intersertal to intergranular texture. Small (0.5–1.0 mm) tabulate plagioclase laths (2%) and olivine (1%) in mesostasis. Comprising 30% skeletal laths of plagioclase (0.1–5 mm) and 20% intergranular clinopyroxene with 1% anhedral intergranular opaques and 50% intersertal mesostasis with green clays.

TS 50 cm (Piece 1I): Contact zone; hyalopilitic basalt below contact and chilled pilotaxitic basalt vein in contact with chertified sediments. Groundmass: 85% basaltic glass; only minor alteration restricted to intergranular spaces and microfractures; 2% plagioclase microlites (An_{50}) and 1/2% each clinopyroxene and olivine microphenocrysts, mostly fresh although some corrosion. Some plagioclase quenched. Opaques concentrated along flow lines, in chilled vein and adjacent to sediment contact.

TS 68 cm (Piece 1K): Hyalopilitic basalt with 30% plagioclase (An_{40}) laths and microlites, in a mesostasis of 5% each clinopyroxene and olivine (fresh, small <0.4 mm) and minor (1%) opaques, 10% greenish clay and zeolites, and 49% fresh to slightly altered basaltic glass. Occasional patches that approach pilotaxitic texture with coarsely aligned plagioclase laths.

SECTION 2: DOMINANT LITHOLOGY: APHYRIC BASALT and DOLERITE. Parts of 3 (5, 6, and 7) intrusive units present. Unit 7 intruded into 6, distinguished by chilled, aphanitic margins. Intercalated sediment.

Macroscopic Description

Intrusive Unit 5 (Pieces 1A–1D): medium light gray (N6) aphyric dolerite (Piece 1A) grading to aphanitic basalt (1D) at contact with light gray siltstone. Continuation of base of Section 1. Sediment stringer cuts through basalt. Numerous veins cut basalt and dolerite (none contains calcite) — probably all zeolite/silica/clay mineral filled.

Pieces 1D–1E: intercalated sediment. Light gray siltstone, siliceous, baked. Shows deformation of sediment beds.

Intrusive Unit 6 (Pieces 1F–1N): medium gray to medium light gray (N5–N6) aphyric* basalt grading from aphanitic in Piece 1F, to doleritic (grain-size up to 2 mm) in Piece 1N. Veins and fractures lined with fibrous zeolites.

*Chilled portion has numerous 1–2 mm laths of feldspar (?micro-phenocrysts).

Piece 1N: contact zone between dolerite (upper) and aphanitic, dark gray (N4–N3) quenched basalt, which intrudes dolerite. Continues in Section 3.

Intrusive Unit 7 (Pieces 1N–1X): from aphanitic chill zone in 1N, the aphyric basalt progressively coarsens to a dolerite in Pieces 1P–1V. Alteration of the doleritic portion is moderate, especially adjacent to zeolite(?) filled veins.

Piece 1X: well-preserved contact zone. Quenched, aphanitic basalt in upper part of pieces, chilled against aphyric dolerite (grain-size approximately 2 mm; altered).

TS 76 cm (Piece 1N): contact zone between intrusive Unit 6 and later intruded Unit 7. BASALT below contact with spherulitic grading into intergranular texture. Five percent elongate plagioclase laths with sharp borders occur in chilled margin. Matrix is 25% skeletal plagioclase (0.6 mm) and 30% clinopyroxene (0.1 to 0.4 mm). Mesostasis comprises 30% olivine, clinopyroxene and plagioclase with glass, along with 13% clay; both intergranular and as pseudomorph after olivine. Plagioclase in the groundmass is fine (0.3–0.6 mm) in relation to contact distance. Some pilotaxitic flow texture. A spherulitic zone grades laterally into a viriolitic basalt. Dolerite host above contact is intergranular to supophitic.

SECTION 3: DOMINANT LITHOLOGY: DOLERITE grading to GABBRO. Parts of intrusive Units 6, 8, 9, and 10 present, but without intercalated sediment.

Macroscopic Description

Piece 1A: medium-grained, medium gray (N5) basalt with 1–2 mm long PLAGIOCLASE LATHS. Texturally distinct from coarse dolerite at base of previous section, but may be a chill zone of intrusive Unit 6 (it is very similar to Pieces 1F–1H of Section 2).

Piece 1B: continuation of Piece 1A, grading to aphanitic, with a chilled

margin on its lower surface. Plagioclase phenocrysts not seen in chill zone, so probably groundmass phases.

Unit 8 (Pieces 1C–1E): medium gray (N5), grading from aphanitic aphyric basalt at upper part of Piece 1C, through doleritic in Piece 1D, and back to aphanitic in bottom part of Piece 1E. Recognized as possibly one intrusive unit. Narrow veins appear to be zeolite-filled (no calcite).

Unit 9 (Piece 1F — should be Piece 2, but wrongly labelled): medium-grained greenish gray aphyric dolerite. Clinopyroxene, plagioclase (altered to greenish color), grains up to 3 mm long. Moderate to severe alteration: the rock appears permeated by clay minerals and water.

Unit 10 (Piece 1G): aphyric medium gray (N6) basalt grading from aphanitic in the upper part, to coarse-grained in the lower part. Greenish tint indicates alteration — probably by clay minerals.

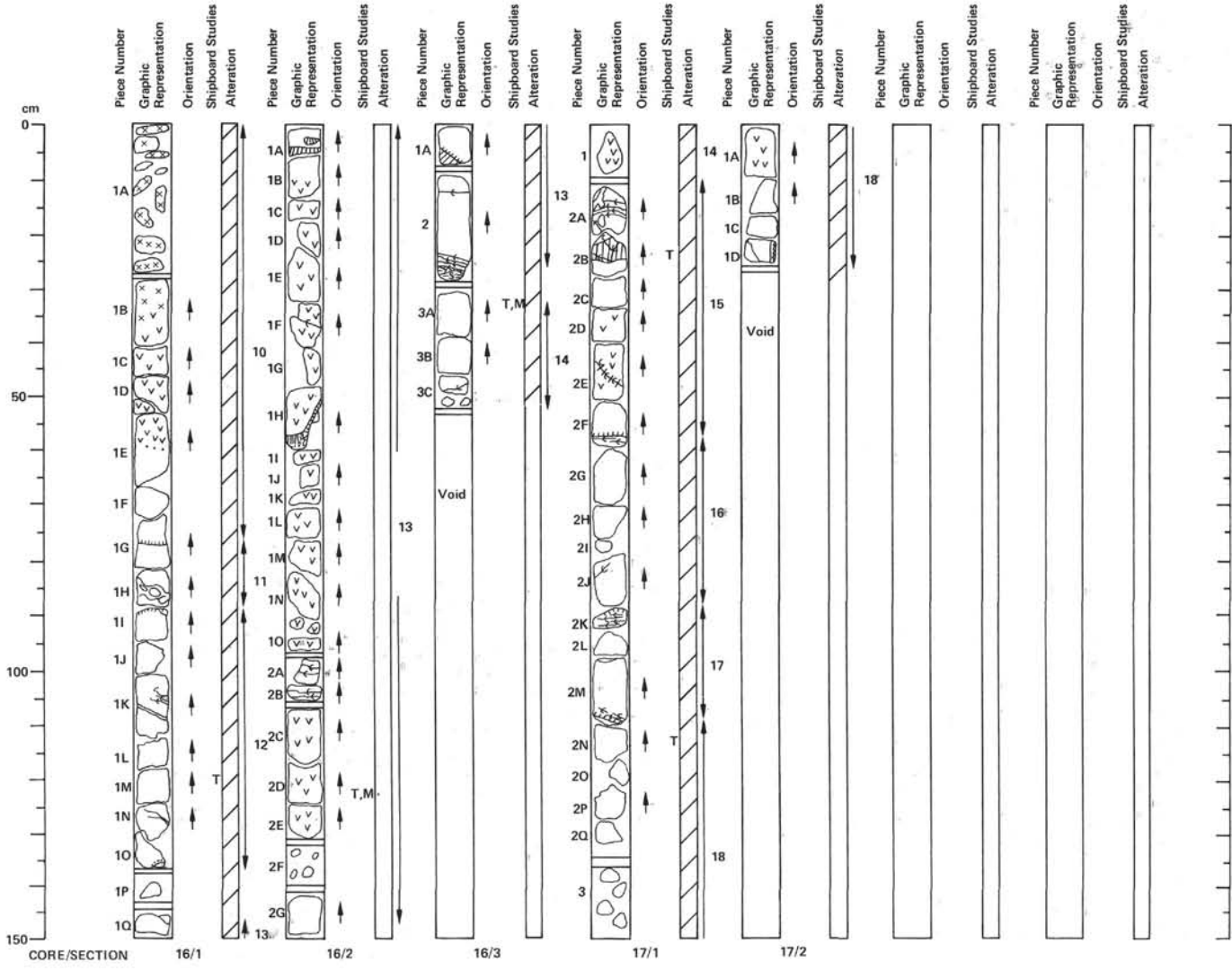
Pieces 1H–1N: coarse basalt of Piece 1G increases in grain-size through Pieces 1H to 1J, to form a GABBROIC rock. Inequigranular, comprising green pyroxene (1–3 mm prismatic crystals), green-tinted (altered) plagioclase (up to 3 mm long) and ores. No olivine seen. Alteration products abundant — small (?diktytaxitic) cavities contain up to 2 mm fibrous clay minerals and zeolites. No veining in the unit.

TS 114 cm (Piece 1L): GABBRO with ophitic texture, 15% large (0.5 to 4 cm) clinopyroxene aggregates optically enclose plagioclase (An_{40}) phenocrysts (40%). Five percent sub- to anhedral olivines, some having corroded margins, occur with plagioclase aggregates. Not very weathered, 1 to 2 mm pockets of mesostasis, occur between ophitic patches. Rock is very fresh with only 5% alteration products and about 1% reddish brown pseudomorph mineral after olivine or clinopyroxene.

SECTION 4: DOMINANT LITHOLOGY: gabbro.

Macroscopic Description

Coarse-grained gabbro. Prismatic crystals of green clinopyroxene up to 30 mm long, with smaller pyroxene and plagioclase grains inbetween. Plagioclase appears altered, but pyroxene looks fresh. Numerous 1–2 mm diktytaxitic cavities containing fibrous zeolites with or without clay minerals. Continuation of Section 3.



64-481A-16

Depth 184.5 to 194.0 m

SECTION 1: DOMINANT LITHOLOGY: GABBRO – grading quickly to DOLERITE to medium-grained plagioclase phyric BASALT. Parts of intrusive Units 10, 11, 12, and 13 with baked intercalation between Units 11/12 and 12/13.

Macroscopic Description

Unit 10 (0–37 cm): gabbro similar to Core 15, Section 4
37–63 cm: dolerite transition to medium-grained basalt with calcite or clay-filled veins
63–77 cm: gray (N5) basalt grading to aphyric basalt and a 2 mm chill zone contact with a clinopyroxene and plagioclase phyric basalt occurring below 77 cm
77–79 cm: approximately 2 cm weathering of contact zone
Top of Unit 11 (79–91 cm): gradual change from clinopyroxene to plagioclase-phyric basalt
91–94 cm: cherty sediment intercalation
94–150 cm: medium light gray (N6) plagioclase-phyric basalt
140–142 cm: cherty sediment intercalated as Pieces 1P and 1Q

SECTION 2: DOMINANT LITHOLOGY: DOLERITE and minor fine grained plagioclase-phyric BASALT. Section considered one intrusive Unit 13. Cut in two places by small chilled basalt veins (at 5–6 cm, 50–60 cm).

Macroscopic Description

Continuation of intrusive Unit 13 from the base of Core 16. Fine-grained, aphyric basalt with chilled basalt veinlet and splotch in Piece 1A. A gradual change to fine- to medium-grained dolerite through remainder of section. Another chilled basalt vein occurs in Piece 1H and small bits of interlayered aphanitic basalt with calcite vein-filling occur in Pieces 2A and 2B.

TS 122 cm (Piece 2D): Coarse dolerite to microgabbro. Texture subophitic. Thin section in poor condition. Contains 1–3 mm tabular plagioclase laths; 1–2 mm irregular, intergranular to subophitic clinopyroxene; small cuboid to anhedral magnetites with clay minerals after olivine. Due to preparation losses, mineral percentages were not estimated.

SECTION 3: DOMINANT LITHOLOGY: Aphyric to sparsely plagioclase-phyric BASALT. Includes parts of intrusive Units 13 and 14 with intercalated CHERTY sediments. Chilled contacts in Piece 1A; base of Piece 2.

Macroscopic Description

0–26 cm: weathered aphanitic medium gray (N6) basalt from the basal part intrusive Unit 13. Piece 1A has a rim of chilled basalt, possibly part of a vein
26–31 cm: contact zone of the base of Unit 13, preserved intact, with a transition to a 1.5 cm thick piece of chertified sediment, dark olive gray.
31–52 cm: Unit 14. No baking at upper contact. Medium gray (N5) aphyric to sparsely plagioclase phyric (small-laths) basalt. Narrow calcite-filled veins cut Piece 3B.

TS 32 cm (Piece 3A): Coarse-grained basalt. Seriate, intergranular to intersertal texture. Five percent, 1–2 mm plagioclase, lath-shaped to tabular, many resorbed. Matrix: 40% plagioclase, skeletal to small laths (0.5–2 mm), 20% clinopyroxene, granular to anhedral intergranular, 2% elongate dendritic ilmenite, 35% clay and zeolite alteration replacing intergranular mesostasis and as pseudomorphs after olivine.

64-481A-17

Depth: 194.0 to 103.5 m

SECTION 1: DOMINANT LITHOLOGY: aphyric BASALT with minor fine-grained dolerite. Intercalated sediment and chilled contacts at 10, 23, 58, 87 and 109 cm, separating parts of 5 intrusive units.

Macroscopic Description

Piece 1: fine dolerite could be part of mid-Unit 14 but no contacts recovered

10–57 cm: Unit 15, medium gray (N5) aphanitic BASALT, tiny plagioclase laths with chertified sediment blebs. Unit 15 becomes slightly doleritic between 35 and 50 cm. In Piece 2A fine subparallel calcite veins characteristic of chilled contacts. Piece 2B has a 4 cm chilled basalt vein cutting through the fine dolerite host of Unit 15.

Unit 16: same rock type as Unit 15. Top contact at 56 cm and bottom contact at approximately 87 cm. Top contact has faint traces of chertified sediments.

Unit 17 (87–107 cm): medium gray (N5) aphanitic basalt with minor, tiny plagioclase laths and minor, very thin calcite veins.

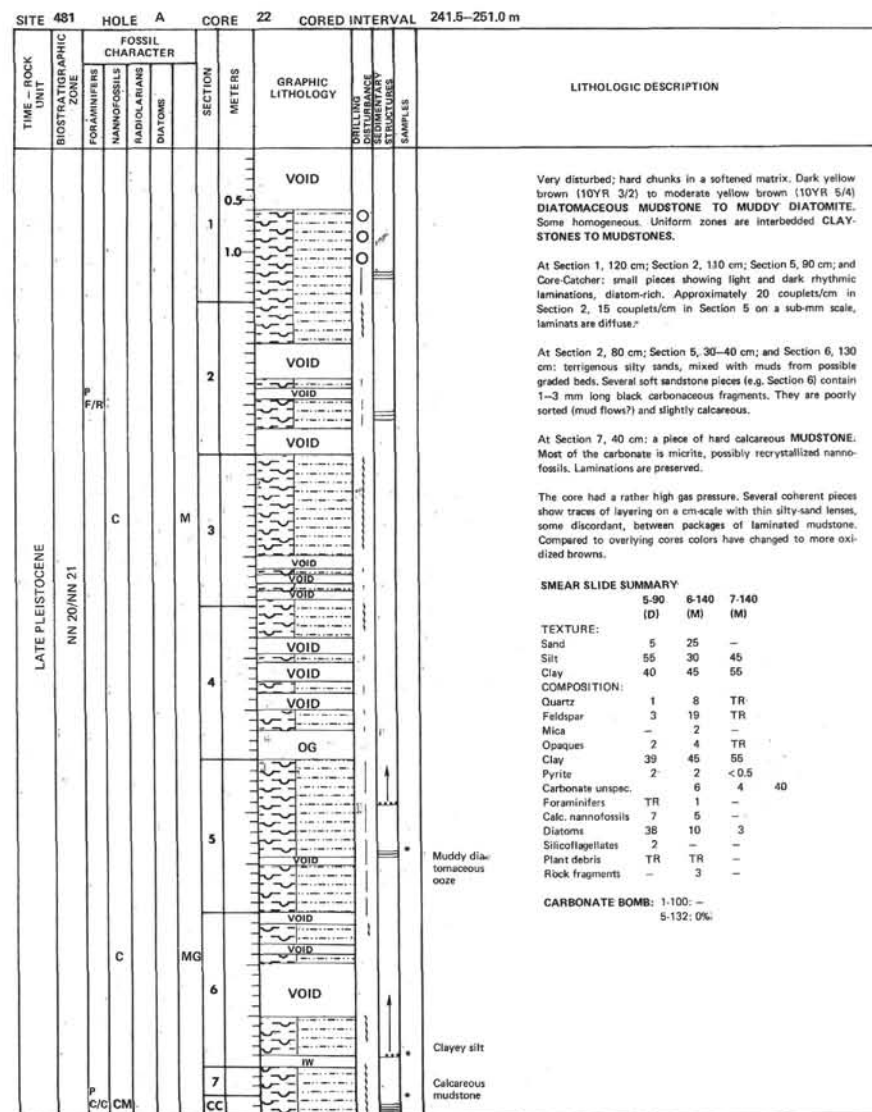
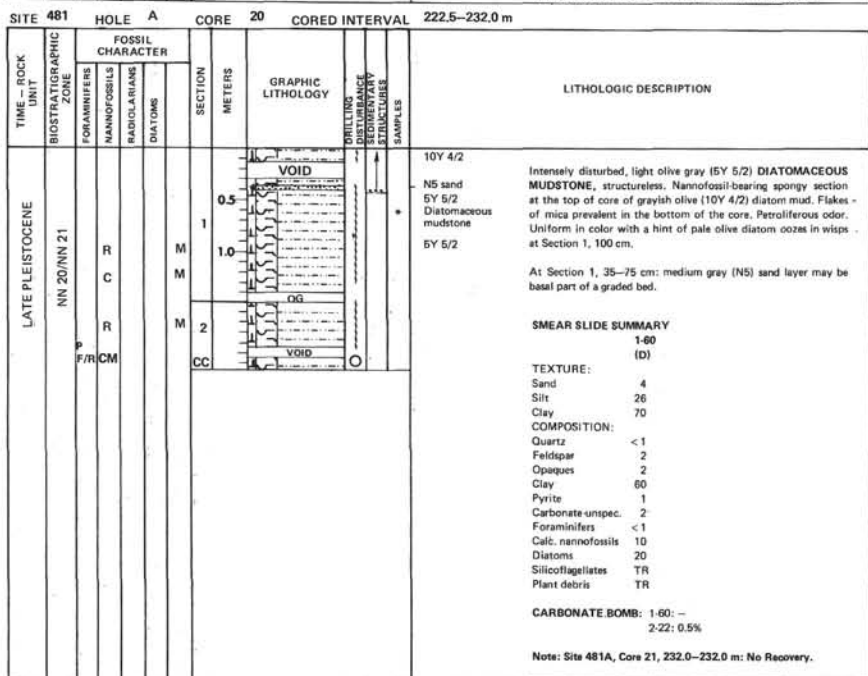
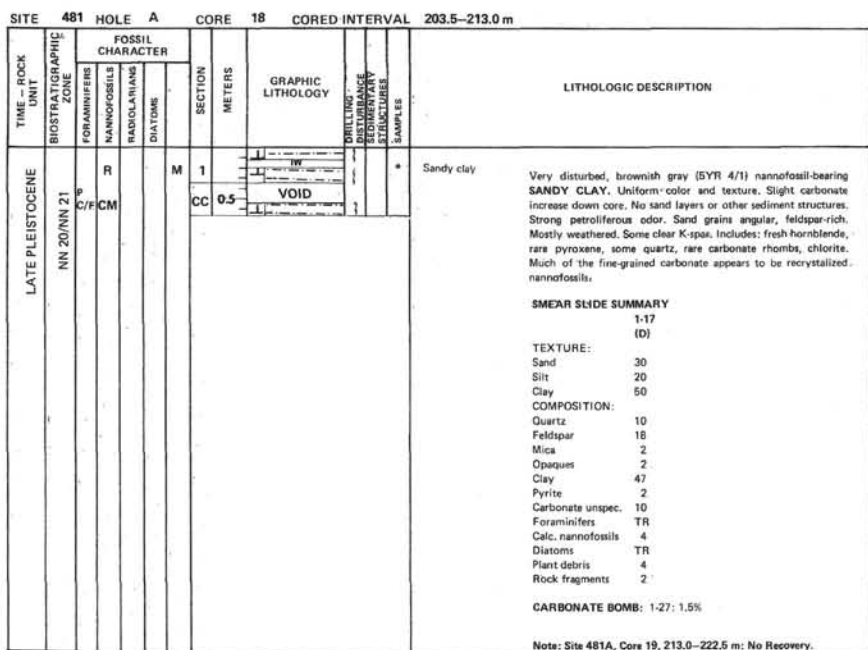
Unit 18 (107 cm to base): N5, fine-grained basalt to base; plagioclase laths are more frequent but smaller.

Pyrite concentrations at 98 cm, Piece 2M. Sediment – Pieces 2A and 2K.

SECTION 2: DOMINANT LITHOLOGY: fine-grained DOLERITE grading to BASALT.

Macroscopic Description

Medium gray (N5) fine-grained dolerite to medium gray (N5) basalt. Still part of Unit 18. Piece 1A is slightly coarser than other pieces. Possible that grain-size decreases from here to the base of Unit 18, which although not recovered would occur within the next low 50 cm.

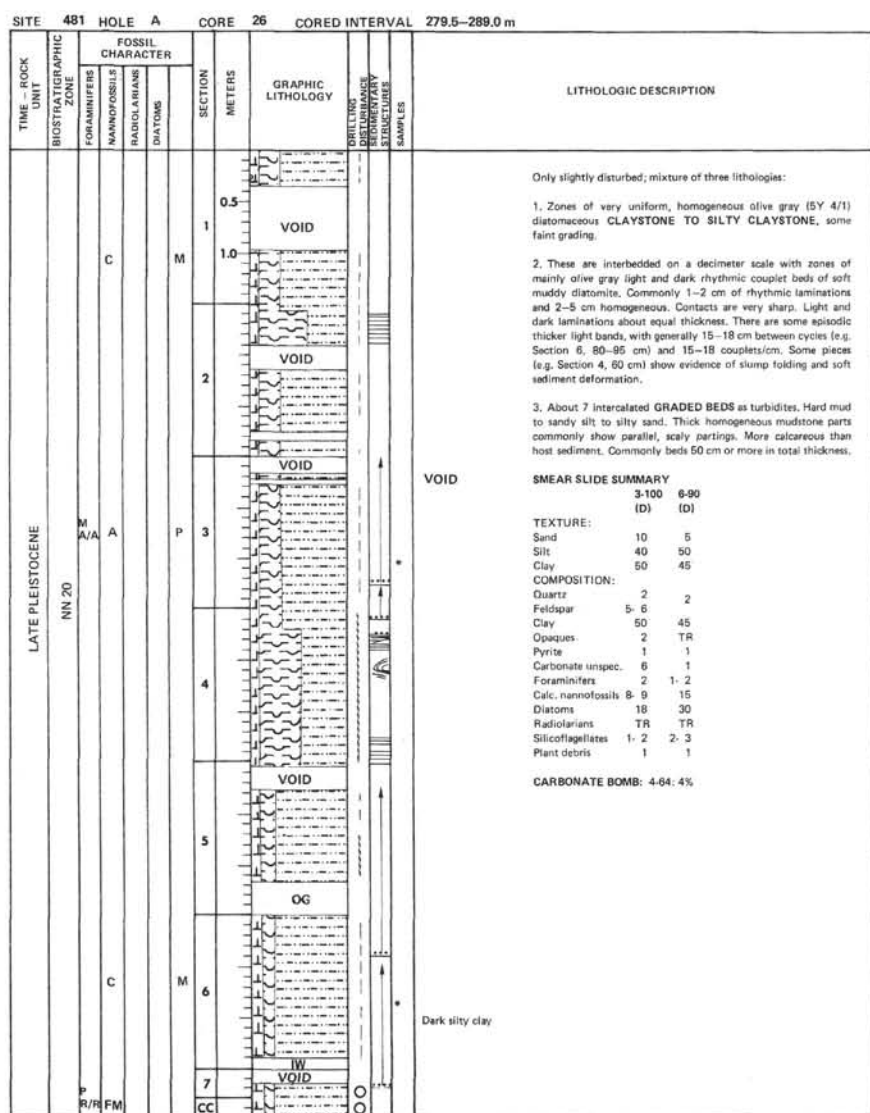
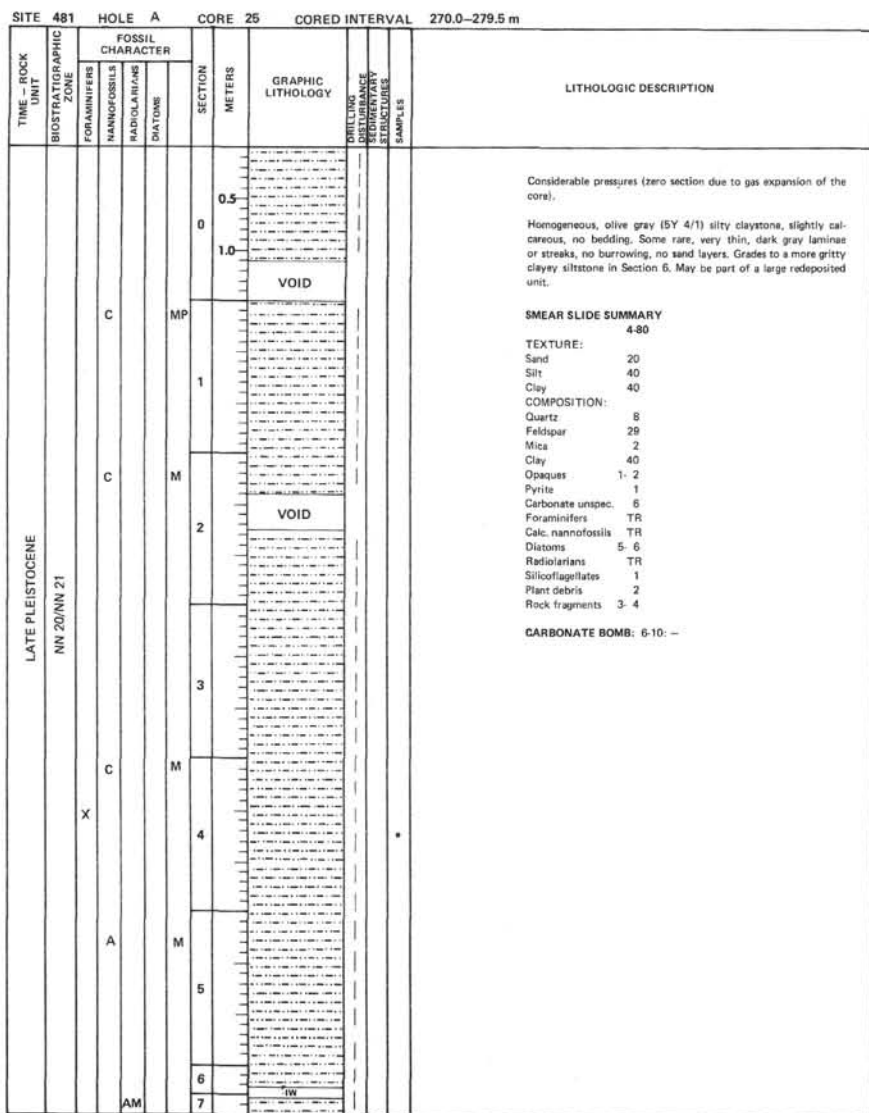


SITE 481 HOLE A CORE 23 CORED INTERVAL 251.0-260.5 m

TIME - ROCK UNIT	BIOSTRATIGRAPHIC ZONE	FOSSIL CHARACTER			SECTION METERS	GRAPHIC LITHOLOGY	DRILLING DISTURBANCE SEDIMENTARY STRUCTURES SAMPLES	LITHOLOGIC DESCRIPTION
		FORAMINIFERS	NANNOFOSSILS	RADIOLARIANS				
LATE PLEISTOCENE	NN 20/NN 21	R			1		<p>Clayey silt</p> <p>Disturbed; uniform and homogeneous, light olive gray (5Y 5/4) hard clayey siltstone. No carbonate reaction, diatoms mostly fragments.</p> <p>SMEAR SLIDE SUMMARY 1-26 (D)</p> <p>TEXTURE: Sand - Silt 55 Clay 45</p> <p>COMPOSITION: Quartz 11 Feldspar 19 Mica 1 Heavy minerals 2 Clay 45 Pyrite 2 Opques 2 Carbonate unspec. 2 Foraminifers TR Calc. nannofossils 5 Diatoms 10 Radiolarians TR Plant debris 3 Rock fragments 2</p> <p>CARBONATE BOMB: 1-11: -</p>	

SITE 481 HOLE A CORE 24 CORED INTERVAL 260.5-270.0 m

TIME - ROCK UNIT	BIOSTRATIGRAPHIC ZONE	FOSSIL CHARACTER			SECTION METERS	GRAPHIC LITHOLOGY	DRILLING DISTURBANCE SEDIMENTARY STRUCTURES SAMPLES	LITHOLOGIC DESCRIPTION
		FORAMINIFERS	NANNOFOSSILS	RADIOLARIANS				
LATE PLEISTOCENE	NN 20/NN 21				1		<p>Moderately disturbed mixture of redeposited and host lithologies:</p> <p>At Section 1 to Section 2, 10 cm: olive gray (5Y 4/1 to 6/1) MUDDY SAND, some chunks of calcareous cemented sandstone mixed with traces of laminated mud.</p> <p>At Section 2, 10 cm to Section 3, 150 cm: interlayered zones of laminated and bioturbated DIATOMACEOUS MUDSTONE burrows on a cm-scale. Some slightly sandy, homogeneous beds (e.g. Section 3, 103 cm). Intermittent zones of dark olive-black (5Y 2/1) (e.g. Section 3, 22-24 cm) scattered, dusky yellow laminae.</p> <p>At Section 4 to Core-Catcher: very uniform, homogeneous chunks of olive gray (5Y 4/1) SILTY CLAYSTONE, slightly calcareous. No mottling, sand or burrowing. Some slightly graded portions towards the base. Gas pressure strong.</p> <p>SMEAR SLIDE SUMMARY 2-90 (D) 2-113 (M)</p> <p>TEXTURE: Sand 4 2 Silt 46 58 Clay 50 40</p> <p>COMPOSITION: Quartz 5 3 Feldspar 10 6 Opques 3 2 Clay 47 40 Pyrite 3 2 Carbonate unspec. 6 6 Foraminifers - TR Calc. nannofossils 7 12 Diatoms 15 25 Radiolarians TR TR Sponge spicules TR - Silicoflagellates 2 2 Plant debris 2 1</p> <p>CARBONATE BOMB: 3-126: 2%</p>	
					2		<p>Diatomaceous clayey silt</p>	
					3		<p>Diatomaceous silty clay</p>	
					4			
					5			
					6			
					7			
					CC			



TIME - ROCK UNIT	BIOSTRATIGRAPHIC ZONE	FOSSIL CHARACTER			SECTION METERS	GRAPHIC LITHOLOGY	DRILLING DISTURBANCE (SPALLS, HOLES, ETC.)	CORRECTION SAMPLES	LITHOLOGIC DESCRIPTION
		FORAMINIFERS	NANNOFOSSILS	RADIOLARIANS					
		DIATOMS							
LATE PLEISTOCENE	NN 20/NN 21	P R/R	C	P	1	VOID		Homogeneous massive olive gray (5Y 4/1) CLAYEY SILTSTONE. Diatoms are rare, mostly fragmented, mostly terrigenous, silts, no sand, no laminae or bedding visible. Increased amounts of land derived organics. Carbonate as elastic and micrite size nanofossil debris.	
					1.0	VOID			
					2	VOID		VOID SMEAR SLIDE SUMMARY 3-70 (D) TEXTURE: Sand 4 Silt 50 Clay 46 COMPOSITION: Quartz 6 Feldspar 18 Mica 1 Clay 44 Opaque 2 Carbonate unsp. 5-4 Foraminifers TR Calc. nanofossils 10 Diatoms 10 Radiolarians TR Silicoflagellates 1 Plant debris 4 CARBONATE BOMB: 3-61: -	
					3	VOID		Silty clay	
					4	VOID			
					5	VOID			
					6	VOID			
					7	W OG			

TIME - ROCK UNIT	BIOSTRATIGRAPHIC ZONE	FOSSIL CHARACTER			SECTION METERS	GRAPHIC LITHOLOGY	DRILLING DISTURBANCE (SPALLS, HOLES, ETC.)	CORRECTION SAMPLES	LITHOLOGIC DESCRIPTION
		FORAMINIFERS	NANNOFOSSILS	RADIOLARIANS					
		DIATOMS							
LATE PLEISTOCENE	NN 20/NN 21	A		M	1	VOID		Slightly disturbed, Uniform, olive gray (5Y 4/1) CLAYEY SILTSTONE, diatomaceous. Slightly calcareous, gas partings common.	
					1.0	VOID		Sections 6 and 7: contain some mud chips showing rhythmic laminations and bedding defined by a few wavy laminae of land derived organic matter. Some scattered, rafted, larger carbonate chips. Some laminated diatomite fragments seem to be flattened mud clasts in a mud supported matrix. Core may be part of redeposited unit (mud flow?).	
					2	VOID		SMEAR SLIDE SUMMARY 3-70 TEXTURE: Sand 5 Silt 56 Clay 40 COMPOSITION: Quartz 6 Feldspar 15 Mica 2-3 Clay 41 Opaque 3 Pyrite 2 Carbonate unsp. 5 Foraminifers TR Calc. nanofossils 8-9 Diatoms 12 Radiolarians TR Silicoflagellates 2 Fish remains TR Plant debris 4 CARBONATE BOMB: 3-131: 2.5%	
					3	VOID			
					4	VOID			
					5	VOID			
					6	VOID			
					7	W CC			

TIME - ROCK UNIT	FOSSIL CHARACTER					SECTION METERS	GRAPHIC LITHOLOGY	DRAWING DISTURBANCE STRUCTURE SAMPLES	LITHOLOGIC DESCRIPTION																																																														
	BIOSTRATIGRAPHIC ZONE	FORAMINIFERS	NANNOFOSSILS	RADIOLIARIANS	DIATOMS																																																																		
LATE PLEISTOCENE	NN 20/NN 21					0.5 1 1.0	VOID																																																																
		C						Clayey silt	Base part of large MUD FLOW: scattered polygenetic angular, soft mudstone clasts in a mud-supported matrix of uniform, olive gray (5Y 4/1) SAND-CLAY-SILT. Grades to coarser at the bottom of the core. Slightly calcareous mud clasts include lensoid pieces having rhythmic couplets of diatom oozes; scattered shelly hash; olive brown (5Y 5/8) clay.																																																														
		M						Clayey silt	At Section 1, 110 cm there is a fracture seam, lined with a halo of dark gray (N2).																																																														
<p>SMEAR SLIDE SUMMARY</p> <table border="1"> <thead> <tr> <th></th> <th>1-42 (M)</th> <th>1-129 (M)</th> </tr> </thead> <tbody> <tr> <td>TEXTURE:</td> <td></td> <td></td> </tr> <tr> <td>Sand</td> <td>—</td> <td>7</td> </tr> <tr> <td>Silt</td> <td>50</td> <td>46</td> </tr> <tr> <td>Clay</td> <td>50</td> <td>47</td> </tr> <tr> <td>COMPOSITION:</td> <td></td> <td></td> </tr> <tr> <td>Quartz</td> <td>1</td> <td>5</td> </tr> <tr> <td>Feldspar</td> <td>—</td> <td>15</td> </tr> <tr> <td>Mica</td> <td>1</td> <td>1-2</td> </tr> <tr> <td>Clay</td> <td>47</td> <td>47</td> </tr> <tr> <td>Volcanic glass</td> <td>—</td> <td>TR (hyolite)</td> </tr> <tr> <td>Opaques</td> <td>1-2</td> <td>4</td> </tr> <tr> <td>Pyrite</td> <td>1</td> <td>2</td> </tr> <tr> <td>Carbonate unspec.</td> <td>8</td> <td>10</td> </tr> <tr> <td>Foraminifers</td> <td>1</td> <td>1</td> </tr> <tr> <td>Calc. nannofossils</td> <td>10</td> <td>3-4</td> </tr> <tr> <td>Diatoms</td> <td>25</td> <td>5</td> </tr> <tr> <td>Radiolarians</td> <td>1</td> <td>TR</td> </tr> <tr> <td>Silicoflagellates</td> <td>2-3</td> <td>1</td> </tr> <tr> <td>Plant debris</td> <td>—</td> <td>TR</td> </tr> <tr> <td>Rock fragments</td> <td>—</td> <td>2</td> </tr> </tbody> </table> <p>CARBONATE BOMB: 1-133: —</p>										1-42 (M)	1-129 (M)	TEXTURE:			Sand	—	7	Silt	50	46	Clay	50	47	COMPOSITION:			Quartz	1	5	Feldspar	—	15	Mica	1	1-2	Clay	47	47	Volcanic glass	—	TR (hyolite)	Opaques	1-2	4	Pyrite	1	2	Carbonate unspec.	8	10	Foraminifers	1	1	Calc. nannofossils	10	3-4	Diatoms	25	5	Radiolarians	1	TR	Silicoflagellates	2-3	1	Plant debris	—	TR	Rock fragments	—	2
	1-42 (M)	1-129 (M)																																																																					
TEXTURE:																																																																							
Sand	—	7																																																																					
Silt	50	46																																																																					
Clay	50	47																																																																					
COMPOSITION:																																																																							
Quartz	1	5																																																																					
Feldspar	—	15																																																																					
Mica	1	1-2																																																																					
Clay	47	47																																																																					
Volcanic glass	—	TR (hyolite)																																																																					
Opaques	1-2	4																																																																					
Pyrite	1	2																																																																					
Carbonate unspec.	8	10																																																																					
Foraminifers	1	1																																																																					
Calc. nannofossils	10	3-4																																																																					
Diatoms	25	5																																																																					
Radiolarians	1	TR																																																																					
Silicoflagellates	2-3	1																																																																					
Plant debris	—	TR																																																																					
Rock fragments	—	2																																																																					

TIME - ROCK UNIT	FOSSIL CHARACTER					SECTION METERS	GRAPHIC LITHOLOGY	DRAWING DISTURBANCE STRUCTURE SAMPLES	LITHOLOGIC DESCRIPTION																																																																																																																														
	BIOSTRATIGRAPHIC ZONE	FORAMINIFERS	NANNOFOSSILS	RADIOLIARIANS	DIATOMS																																																																																																																																		
LATE PLEISTOCENE	NN 20/NN 21					0.5 1 2 3 4 5 6	VOID		21 couplets/cm																																																																																																																														
		M C/F						Clayey silt	Mixture of two interbedded lithologies:																																																																																																																														
		C					VOID	Clayey silt	1. Zones with rhythmically laminated couplets of light and darker hard DIATOMACEOUS MUD TO MUDDY DIATOMITE. Light olive gray (5Y 4/2) and pale olive (10Y 6/2). Contacts sharp, 19-22 couplets/cm. Most laminated beds 5-8 cm thick; total 131 cm in core.																																																																																																																														
		M A/F					VOID	Clayey silt	At Section 5, 90-96 cm: just below turbidite base, discordant terminated deformed laminations from soft sediment deformation.																																																																																																																														
		CM					VOID	Clayey silt	At Section 5, 100 cm: light bluish gray (5B 6/1) clay interlayer.																																																																																																																														
							VOID	Clayey silt	At Section 1, 47 cm: a thin cm-band of yellow-gray (5Y 7/2) diatomite; abundant silicoflagellates, fragile diatoms.																																																																																																																														
							VOID	Clayey silt	2. Most of core is thick beds (60-100 cm) homogeneous, massive to graded DIATOMACEOUS MUDSTONE TO MUDDY SAND. TURBIDITES. Upper parts show darker shaly partings. Muddy, coarse basal portion lighter olive brown (5Y 5/6) (e.g. Section 3.70-90 cm).																																																																																																																														
							VOID	Clayey silt	At Section 4, 130-140 cm and Section 5, 0-10 cm: discordant sub-vertical seams are filled with a black (Mn?) clay. Also occurs along bedding plane (Section 4, 47 cm).																																																																																																																														
							VOID	Clayey silt	5Y 3/2 Sand																																																																																																																														
							VOID	Clayey silt	SMEAR SLIDE SUMMARY																																																																																																																														
							VOID	Clayey silt	<table border="1"> <thead> <tr> <th></th> <th>1-47 (M)</th> <th>2-70 (D)</th> <th>4-67 (M)</th> <th>5-22 (M)</th> <th>5-22 (M)</th> </tr> <tr> <th></th> <th></th> <th></th> <th></th> <th>(gray)</th> <th>(light)</th> </tr> </thead> <tbody> <tr> <td>TEXTURE:</td> <td></td> <td></td> <td></td> <td></td> <td></td> </tr> <tr> <td>Sand</td> <td>—</td> <td>5</td> <td>—</td> <td>20</td> <td>—</td> </tr> <tr> <td>Silt</td> <td>70</td> <td>65</td> <td>55</td> <td>50</td> <td>70</td> </tr> <tr> <td>Clay</td> <td>30</td> <td>30</td> <td>45</td> <td>30</td> <td>30</td> </tr> <tr> <td>COMPOSITION:</td> <td></td> <td></td> <td></td> <td></td> <td></td> </tr> <tr> <td>Quartz</td> <td>TR</td> <td>3</td> <td>2</td> <td>15</td> <td>1-2</td> </tr> <tr> <td>Feldspar</td> <td>—</td> <td>7</td> <td>—</td> <td>38</td> <td>—</td> </tr> <tr> <td>Mica</td> <td>—</td> <td>—</td> <td>—</td> <td>1-2</td> <td>—</td> </tr> <tr> <td>Clay</td> <td>25</td> <td>30</td> <td>25</td> <td>27</td> <td>28</td> </tr> <tr> <td>Opaques</td> <td>TR</td> <td>2</td> <td>1</td> <td>4</td> <td>1</td> </tr> <tr> <td>Pyrite</td> <td>TR</td> <td>1</td> <td>1</td> <td>3</td> <td>1</td> </tr> <tr> <td>Carbonate unspec.</td> <td>2</td> <td>3-4</td> <td>10</td> <td>3</td> <td>35</td> </tr> <tr> <td>Foraminifers</td> <td>—</td> <td>1</td> <td>1</td> <td>TR</td> <td>—</td> </tr> <tr> <td>Calc. nannofossils</td> <td>4</td> <td>8-10</td> <td>12</td> <td>3-4</td> <td>10</td> </tr> <tr> <td>Diatoms</td> <td>85</td> <td>40</td> <td>50</td> <td>2</td> <td>20</td> </tr> <tr> <td>Radiolarians</td> <td>—</td> <td>—</td> <td>TR</td> <td>—</td> <td>—</td> </tr> <tr> <td>Silicoflagellates</td> <td>4</td> <td>3</td> <td>1</td> <td>TR</td> <td>1-2</td> </tr> <tr> <td>Plant debris</td> <td>—</td> <td>—</td> <td>—</td> <td>—</td> <td>1</td> </tr> <tr> <td>Rock fragments</td> <td>—</td> <td>—</td> <td>—</td> <td>2</td> <td>—</td> </tr> </tbody> </table>		1-47 (M)	2-70 (D)	4-67 (M)	5-22 (M)	5-22 (M)					(gray)	(light)	TEXTURE:						Sand	—	5	—	20	—	Silt	70	65	55	50	70	Clay	30	30	45	30	30	COMPOSITION:						Quartz	TR	3	2	15	1-2	Feldspar	—	7	—	38	—	Mica	—	—	—	1-2	—	Clay	25	30	25	27	28	Opaques	TR	2	1	4	1	Pyrite	TR	1	1	3	1	Carbonate unspec.	2	3-4	10	3	35	Foraminifers	—	1	1	TR	—	Calc. nannofossils	4	8-10	12	3-4	10	Diatoms	85	40	50	2	20	Radiolarians	—	—	TR	—	—	Silicoflagellates	4	3	1	TR	1-2	Plant debris	—	—	—	—	1	Rock fragments	—	—	—	2	—
	1-47 (M)	2-70 (D)	4-67 (M)	5-22 (M)	5-22 (M)																																																																																																																																		
				(gray)	(light)																																																																																																																																		
TEXTURE:																																																																																																																																							
Sand	—	5	—	20	—																																																																																																																																		
Silt	70	65	55	50	70																																																																																																																																		
Clay	30	30	45	30	30																																																																																																																																		
COMPOSITION:																																																																																																																																							
Quartz	TR	3	2	15	1-2																																																																																																																																		
Feldspar	—	7	—	38	—																																																																																																																																		
Mica	—	—	—	1-2	—																																																																																																																																		
Clay	25	30	25	27	28																																																																																																																																		
Opaques	TR	2	1	4	1																																																																																																																																		
Pyrite	TR	1	1	3	1																																																																																																																																		
Carbonate unspec.	2	3-4	10	3	35																																																																																																																																		
Foraminifers	—	1	1	TR	—																																																																																																																																		
Calc. nannofossils	4	8-10	12	3-4	10																																																																																																																																		
Diatoms	85	40	50	2	20																																																																																																																																		
Radiolarians	—	—	TR	—	—																																																																																																																																		
Silicoflagellates	4	3	1	TR	1-2																																																																																																																																		
Plant debris	—	—	—	—	1																																																																																																																																		
Rock fragments	—	—	—	2	—																																																																																																																																		
							VOID	Clayey silt	CARBONATE BOMB: 2-137: 6.5% 4-120: — 5-46: 2% 6-46: 3.5%																																																																																																																														
							VOID	Clayey silt	OG																																																																																																																														
							VOID	Clayey silt	iw																																																																																																																														
							VOID	Clayey silt	PM																																																																																																																														
							VOID	Clayey silt	CM																																																																																																																														
							VOID	Clayey silt	CC																																																																																																																														

SITE 481 HOLE A CORE 31 CORED INTERVAL 327.0-336.5 m

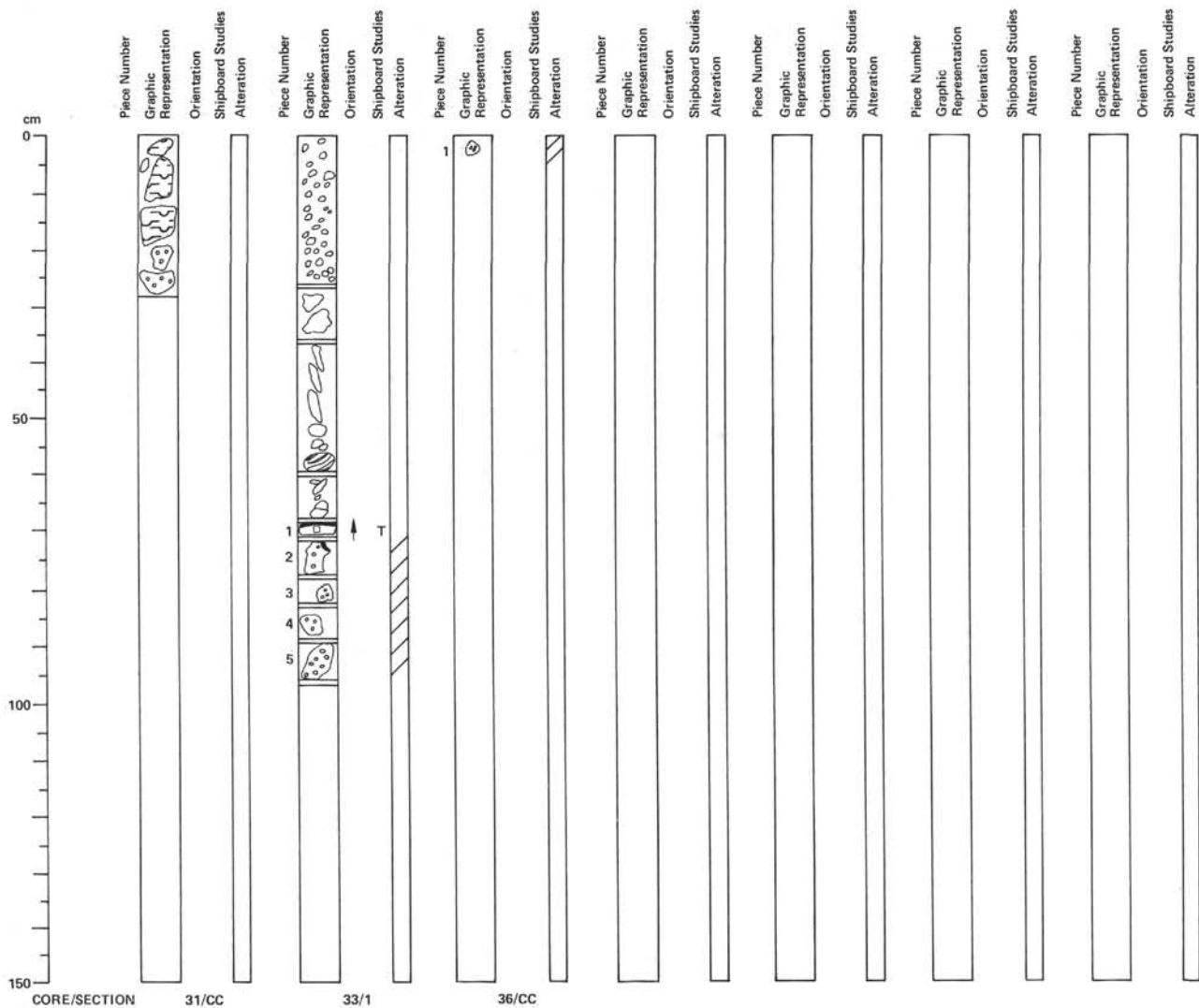
TIME - ROCK UNIT	BIOSTRATIGRAPHIC ZONE	FOSSIL CHARACTER			SECTION METERS	GRAPHIC LITHOLOGY	DRILLING DISTURBANCE	STERNALITY	SAMPLES	LITHOLOGIC DESCRIPTION
		FORAMINIFERS	NANNOFOSSILS	RADIOLARIANS						
LATE PLEISTOCENE	NN 207									<p>Drill breccia of light olive gray (5Y 4/2) chips of MUDDY DIATOMITE. Homogeneous, massive.</p> <p>Core-Catcher: yellowish gray (5Y 6/2) muddy diatomites with discontinuous laminations, homogeneous center part. Diatom frustules pristine.</p> <p>Some chunks of softer material above 2 pieces of VESICULAR BASALT with zeolite filled vesicles. Appears to be close to but not at the sediment-basalt contact. Sediment does not appear baked.</p> <p>SMEAR SLIDE SUMMARY 1-139 (D)</p> <p>TEXTURE: Sand 3 Silt 52 Clay 45</p> <p>COMPOSITION: Quartz 1 Feldspar 3 Clay 44 Opacues 2 Pyrite 2 Carbonate unsp. 5 Foraminifers TR Diatoms 3-4 Diatoms 35 Radiolarians 1 Sponge spicules TR Silicoflagellates 2 Plant debris 1</p> <p>CARBONATE BOMB: CC: 4%</p> <p>Note: Site 481A, Core 32, 336.5-346.0 m: No Recovery.</p>
					VOID				VOID Silty clay	

SITE 481 HOLE A CORE 33 CORED INTERVAL 346.0-355.5 m

TIME - ROCK UNIT	BIOSTRATIGRAPHIC ZONE	FOSSIL CHARACTER			SECTION METERS	GRAPHIC LITHOLOGY	DRILLING DISTURBANCE	STERNALITY	SAMPLES	LITHOLOGIC DESCRIPTION
		FORAMINIFERS	NANNOFOSSILS	RADIOLARIANS						
										<p>Partly drill breccia at contact zone with vesicular basalt sill.</p> <p>Dark gray (N3) CLAYSTONE; some scattered calcite crystals. Several pieces with light gray (N7) claystone rims. Several show thin parallel, rhythmic laminations but without diatoms. Some of siliceous grains appear authigenic-microplitic chert. Contains thin laths (zeolite?).</p> <p>At 68 cm: contact with VESICULAR BASALT. Five pieces, some vesicles pyrite or zeolite-filled. Piece 1 has thin glassy rind preserved.</p> <p>SMEAR SLIDE SUMMARY 1-60 (D) (M)</p> <p>TEXTURE: Sand - - Silt 20 20 Clay 80 80</p> <p>COMPOSITION: Quartz 7-8 15 Feldspar 6-7 3-4 Mica - 1 Clay 70 70 Opacues 1 TR Pyrite 1 1 Zeolite 75 78 Carbonate unsp. 3-4 1 Fish remains 2 -</p> <p>CARBONATE BOMB: 1-20: 0%</p> <p>Note: Site 481A, Core 34, 355.5-365.0 m: No Recovery. Site 481A, Core 35, 365.0-374.5 m: No Recovery.</p>
									Dark gray claystone N7 Claystone	

SITE 481 HOLE A CORE 36 CORED INTERVAL 366.0-374.5 m

TIME - ROCK UNIT	BIOSTRATIGRAPHIC ZONE	FOSSIL CHARACTER			SECTION METERS	GRAPHIC LITHOLOGY	DRILLING DISTURBANCE	STERNALITY	SAMPLES	LITHOLOGIC DESCRIPTION
		FORAMINIFERS	NANNOFOSSILS	RADIOLARIANS						
										Small piece of vesicular basalt.
										Note: Site 481A, Core 37, 374.5-384.0 m: NO RECOVERY.



64-481A-31

Depth: 327.0 to 336.5 m

CORE-CATCHER: DOMINANT LITHOLOGY: vesicular BASALT

Macroscopic Description

Two pieces (rounded cobbles) fresh medium gray (N5), aphyric medium-grained BASALT.

About 15% basalt comprises irregular vesicles, lined with pale gray to white zeolite. One contains calcite; the other pyrite.

0–20 cm: intercalated sediment, diatom ooze. Olive gray (varved) silty clays, apparently unbacked, but no indication of the distance of sediments from basalts in actual sequence. Diatoms fresh, probable downhole cavings.

64-481A-33

Depth: 346.0 to 355.5 m

SECTION 1: DOMINANT LITHOLOGY: BASALT with sediment.

Macroscopic Description

0–35 cm: fragmented (by drilling) black claystones and mudstones

35–68 cm: pieces of black and brown mudstones and varved claystones and clays

68–70 cm: aphanitic basalt with rare plagioclase phenocrysts (approximately 5 mm long), and chilled margin of ropy-textured devitrified glass

71–95 cm: 4 rounded pieces of vesicular, practically aphyric, fine-grained to aphanitic medium gray (N5) to medium dark gray (N4) basalt. Fresh. Vesicles 1–5 mm, spherical and irregular. Fillings include zeolite, calcite and pyrite. Flow textures visible in basalt adjacent to chill margins.

TS 69 cm (Piece 1): basalt with chilled margin. Pilotaxitic texture. Devitrified glass 95%, shows wheat-sheave structures and plagioclase spherulites plus (2%) 0.2–3 mm plagioclase laths (An₄₀) surrounded by glass. Less than 1% clay and zeolite alteration, mostly pseudomorphs after clinopyroxene and olivine. Some tiny clinopyroxene and olivine anhedral grains occur within plagioclase spherulites.

TS 90 cm (Piece 5): hyalopilitic vesicular (5%) basalt. Fifteen percent plagioclase phenocrysts and microlites (0.1–1.0 mm). Mesostasis includes 65% glass, only slightly altered, and cryptocrystalline clinopyroxene and plagioclase with possible olivine. Two percent olivine and 3% clinopyroxene microcrysts, anhedral dispersed in mesostasis. Three percent opaques with pilotaxitic texture of tiny ilmenite laths. Elliptical to spherule vesicles; irregular with thin lining of greenish clay.

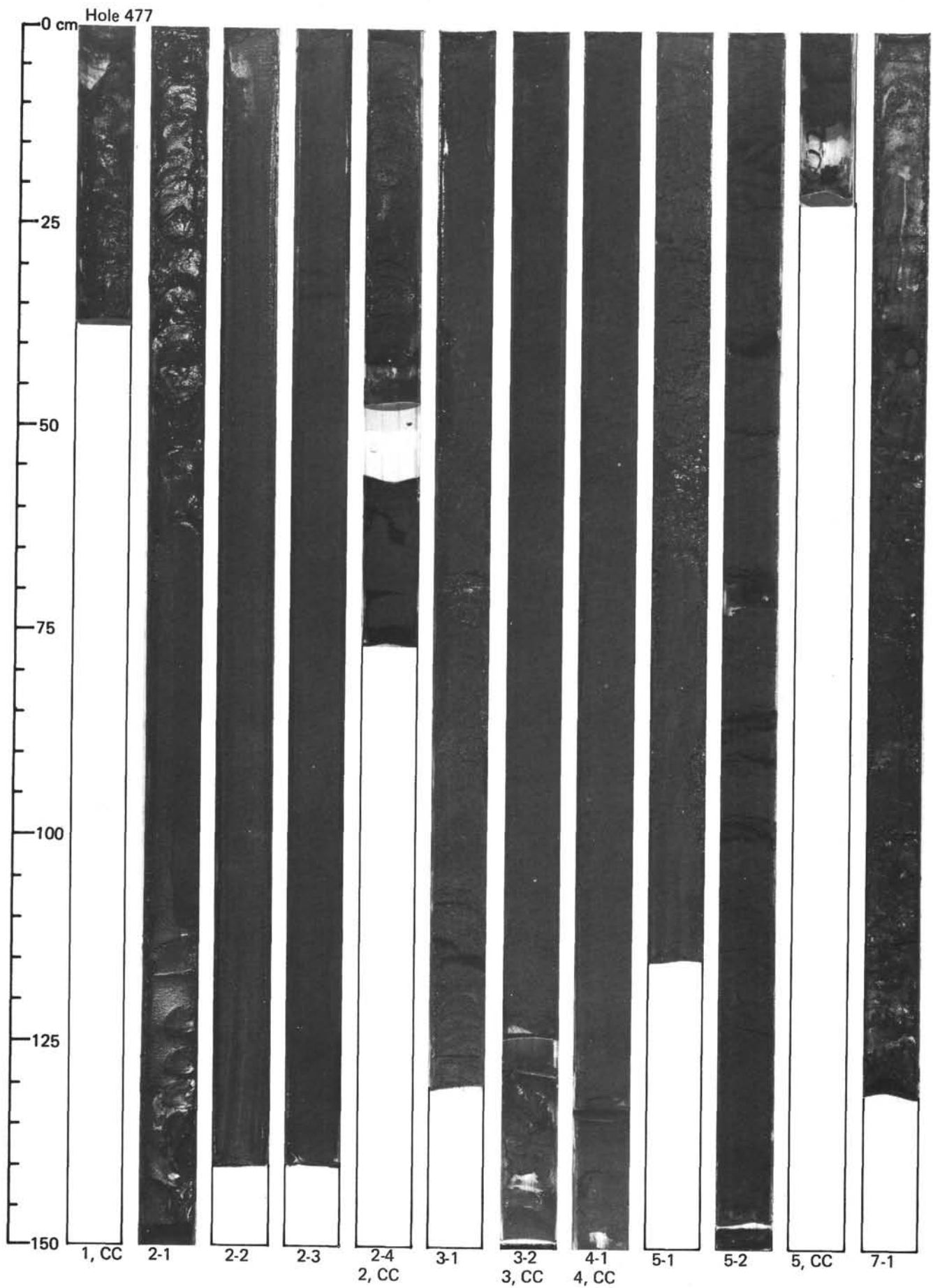
64-481A-36

Depth: 366.0 to 374.5 m

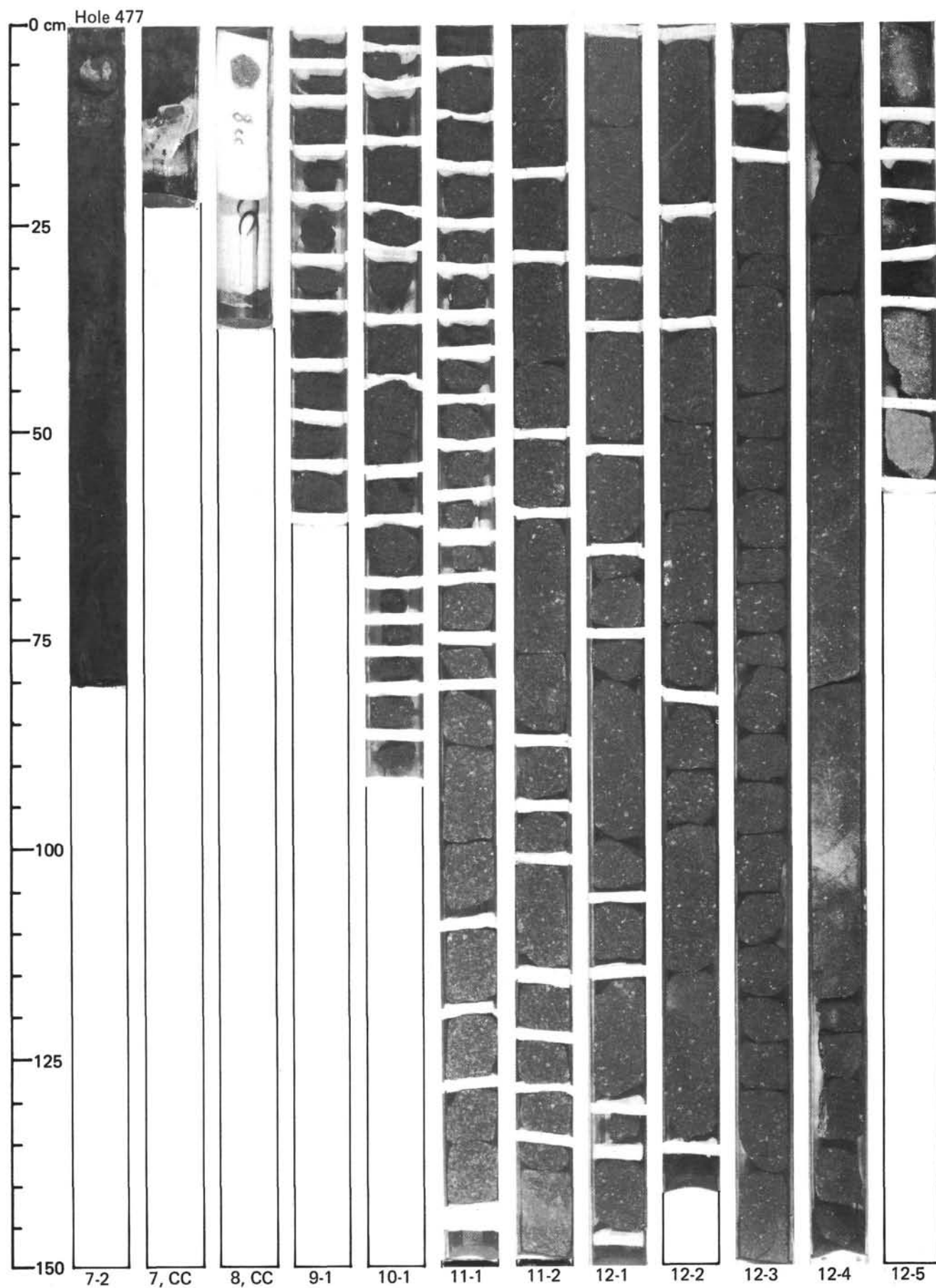
CORE-CATCHER: DOMINANT LITHOLOGY: aphyric BASALT

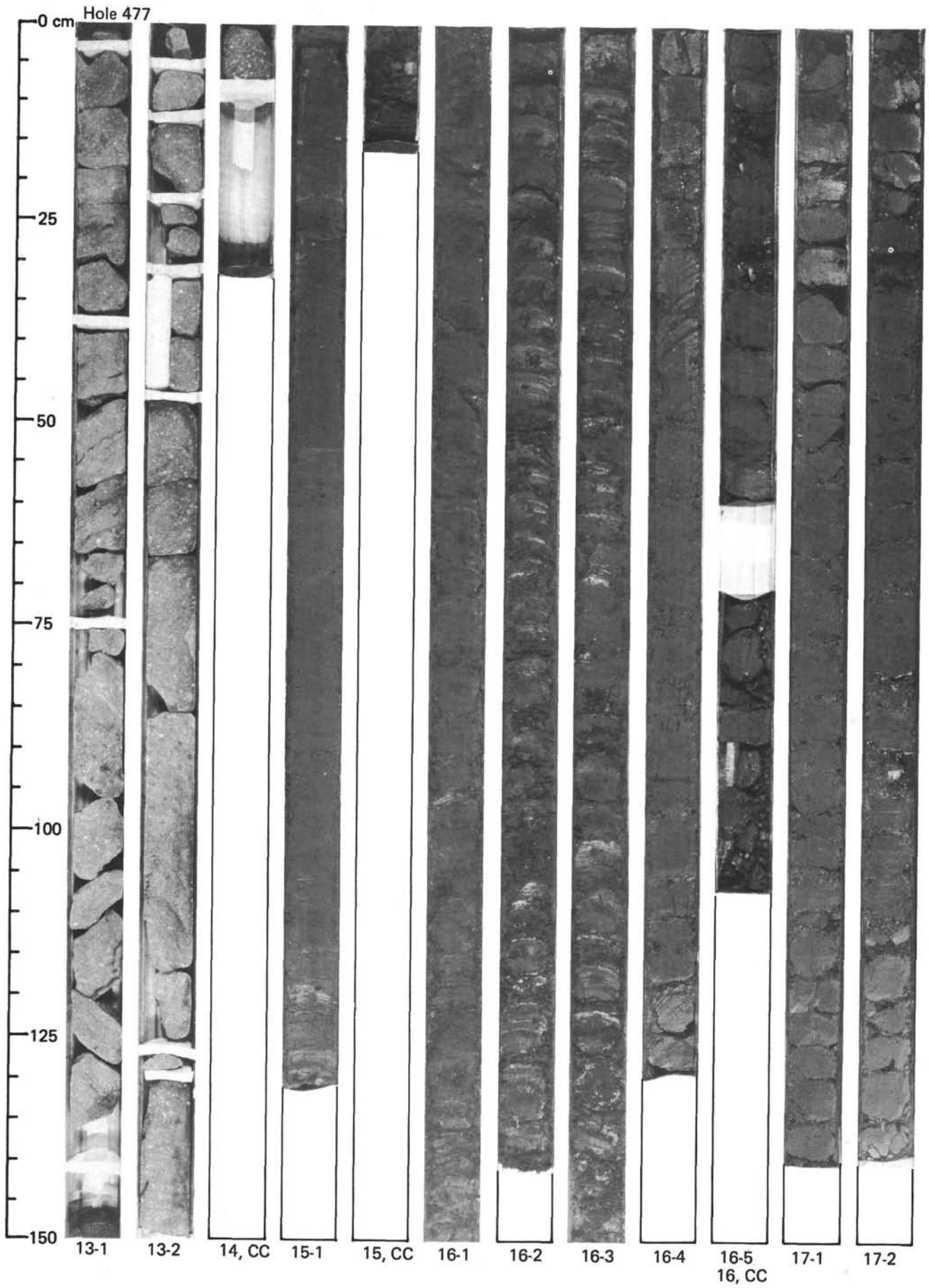
Macroscopic Description

Medium to dark gray (N5) fine-grained basalt fragment recovered in Core-Catcher. Has small < 1 mm vesicles.

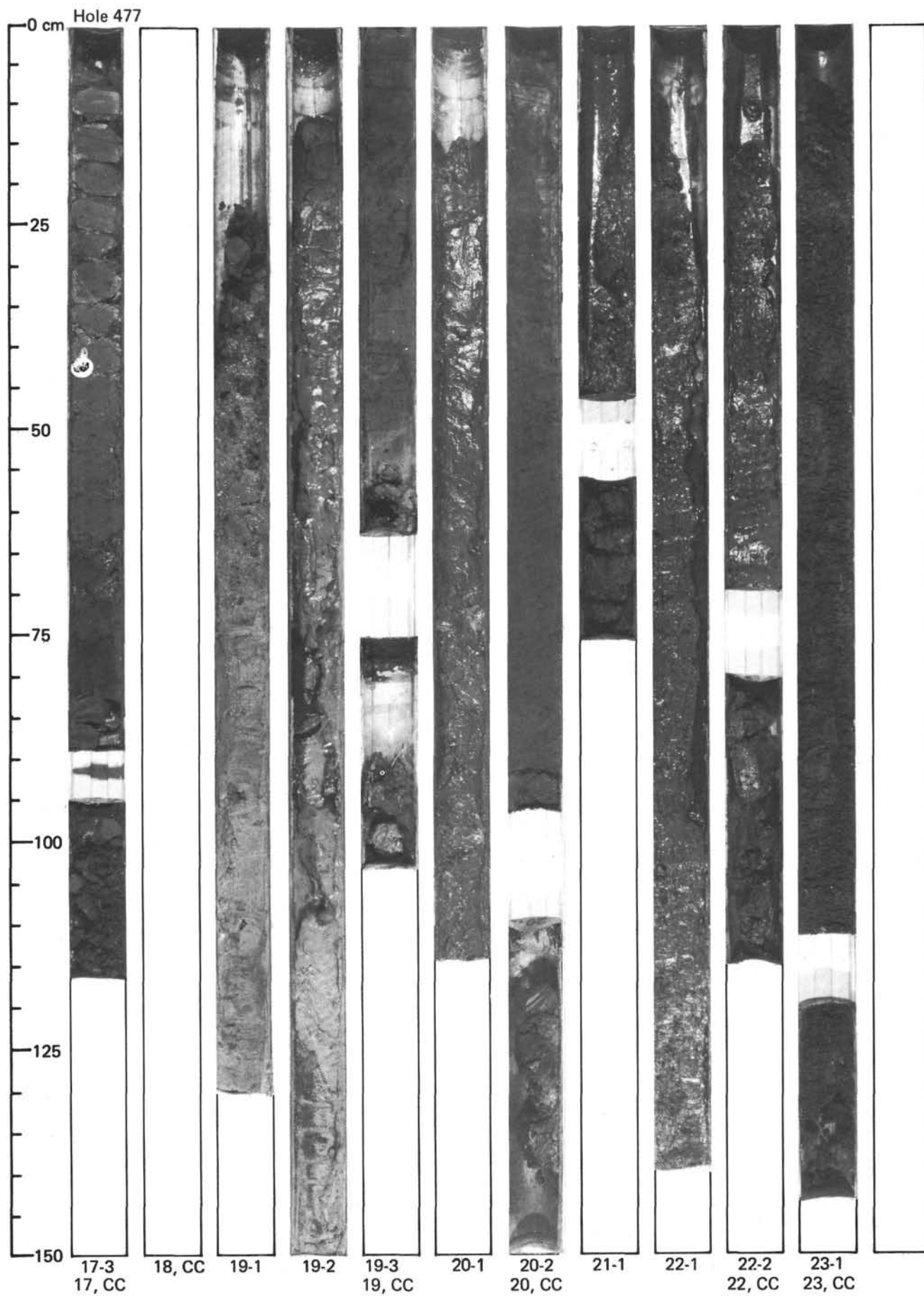


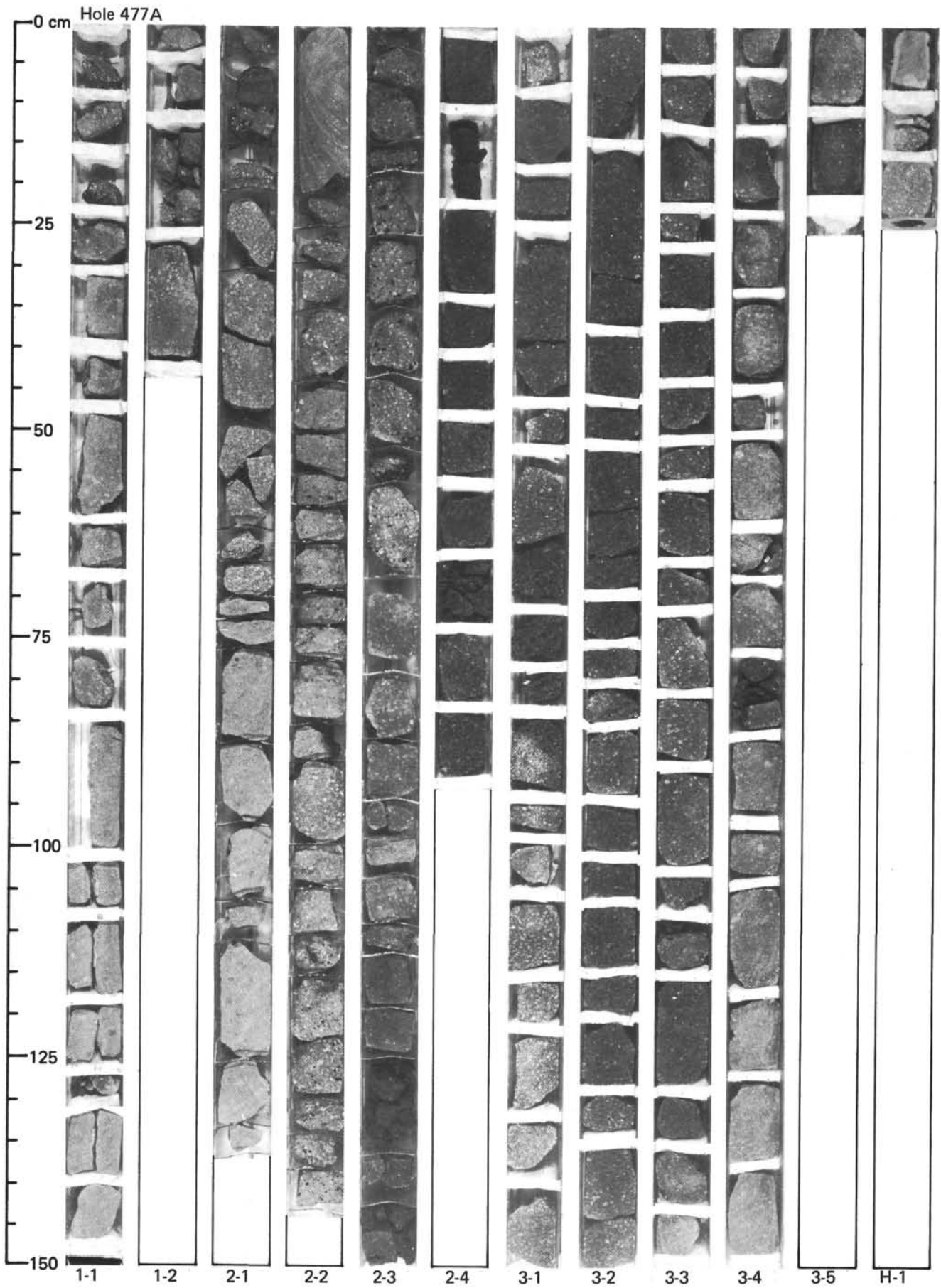
GUAYMAS BASIN SITES



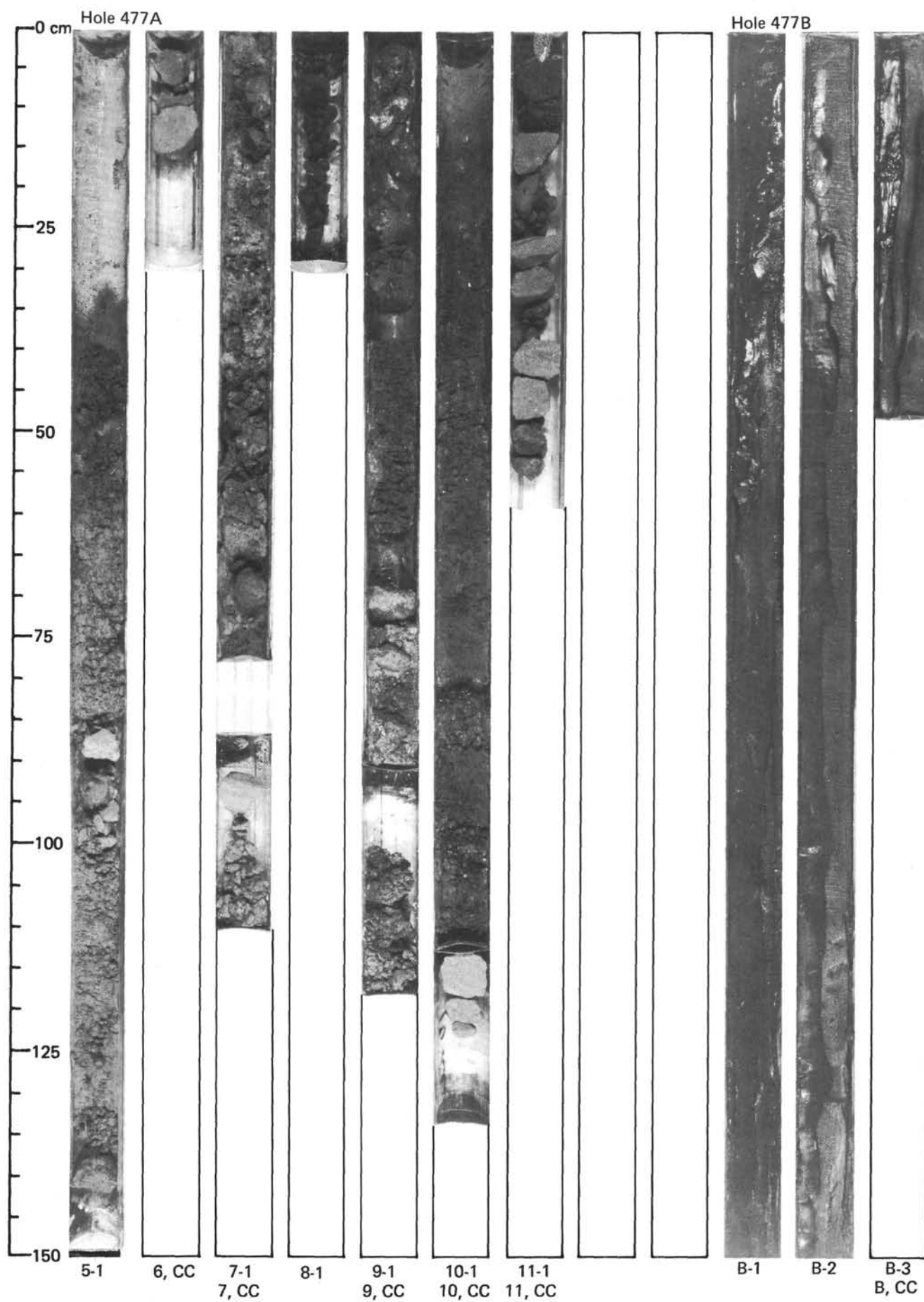


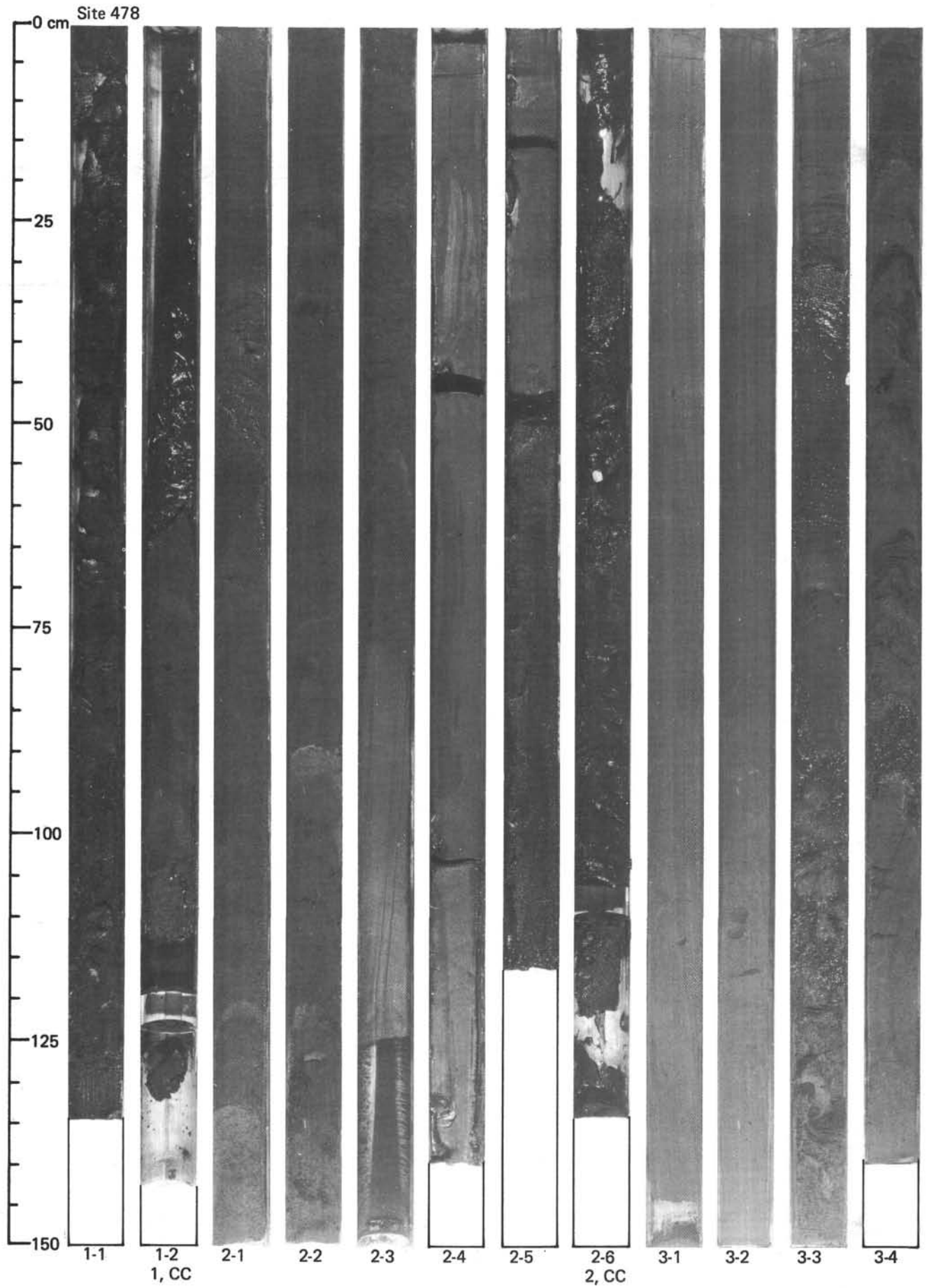
GUAYMAS BASIN SITES



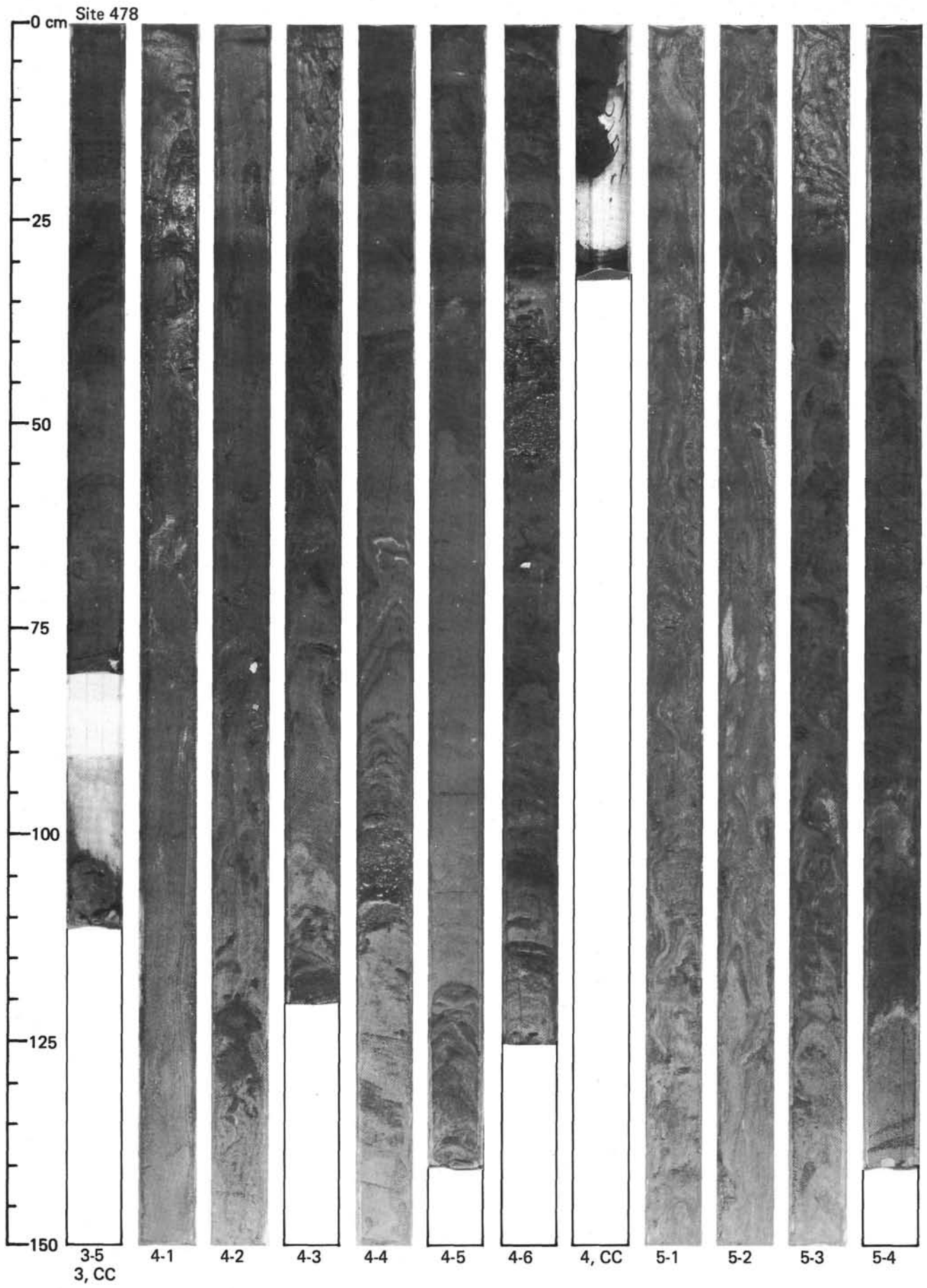


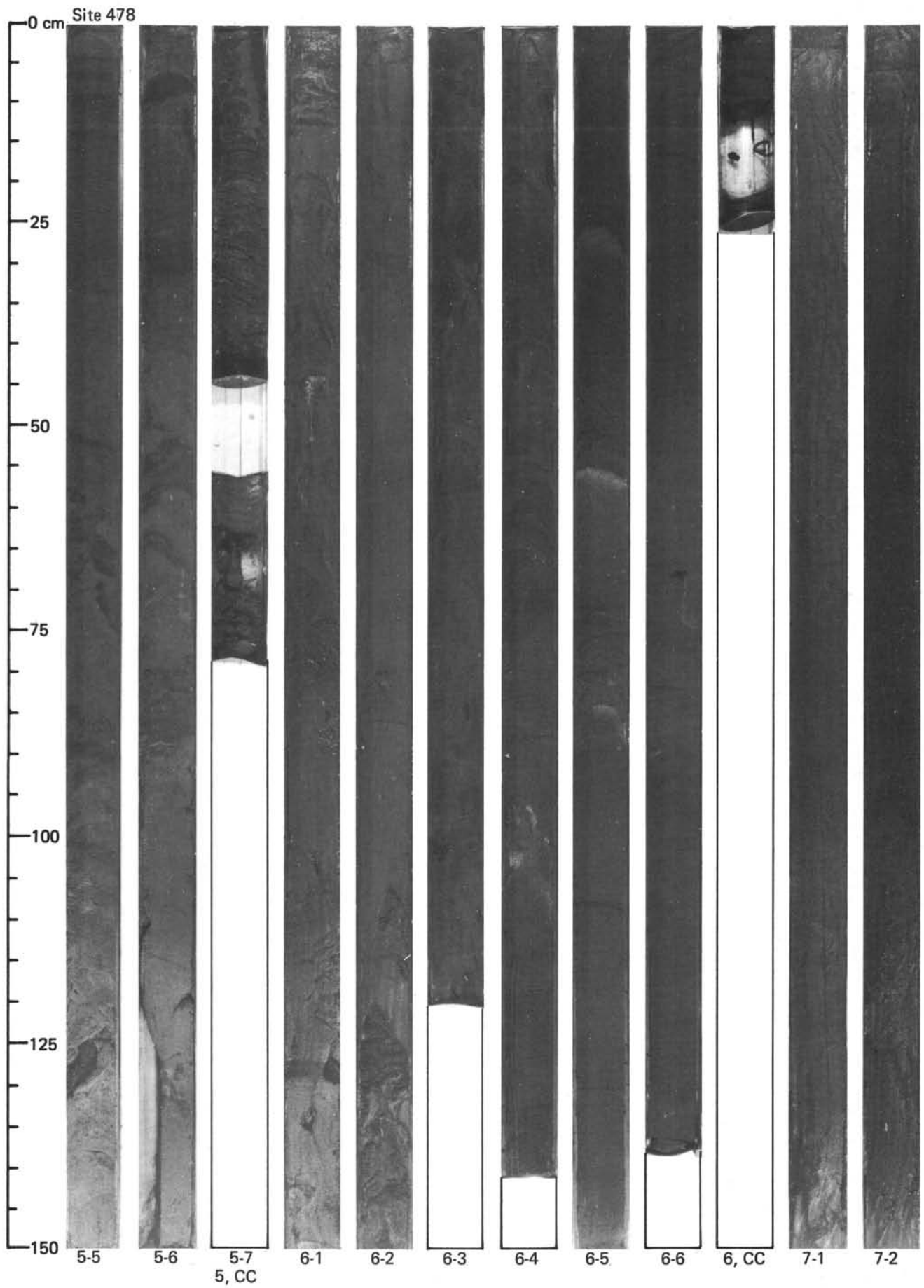
GUAYMAS BASIN SITES



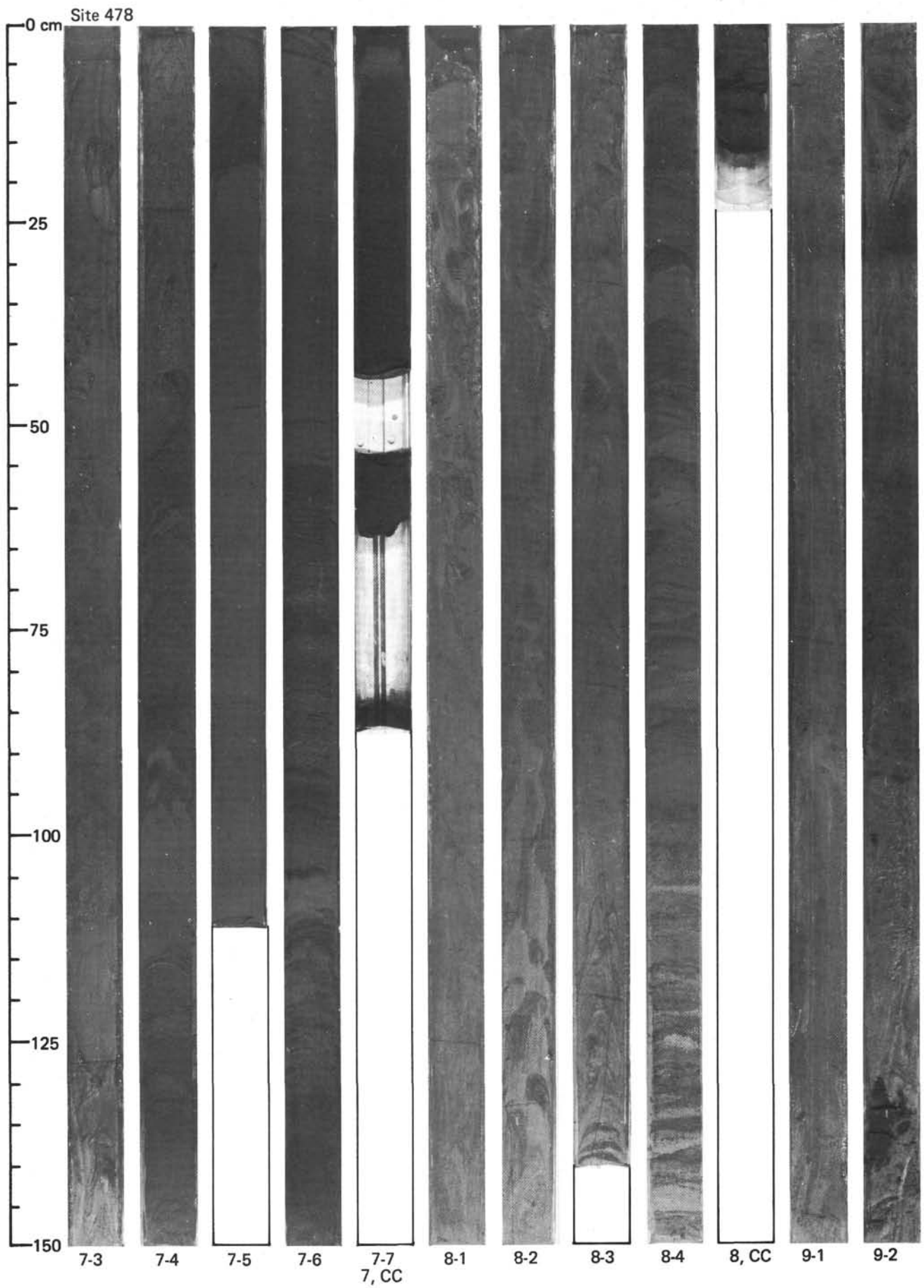


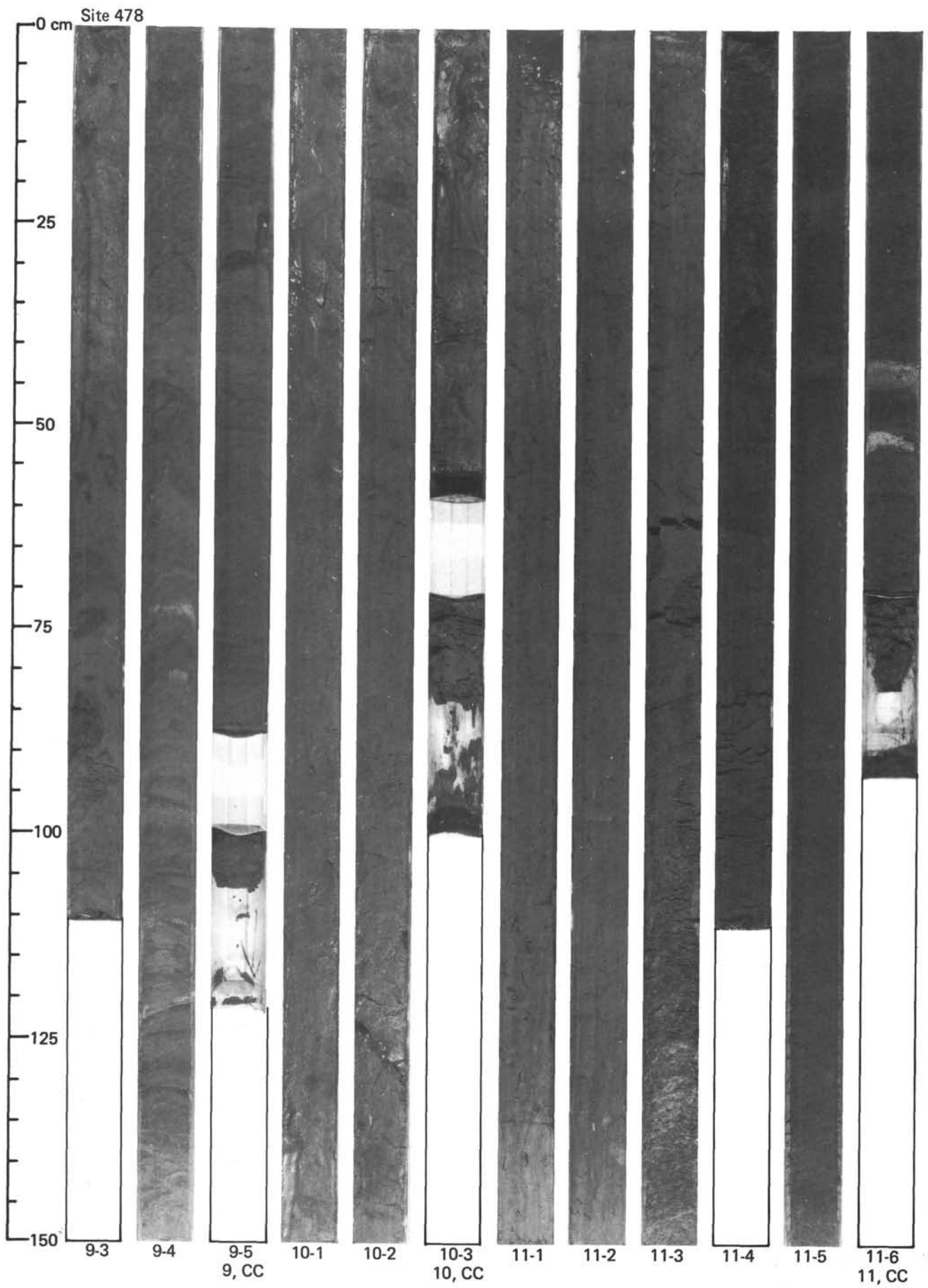
GUAYMAS BASIN SITES



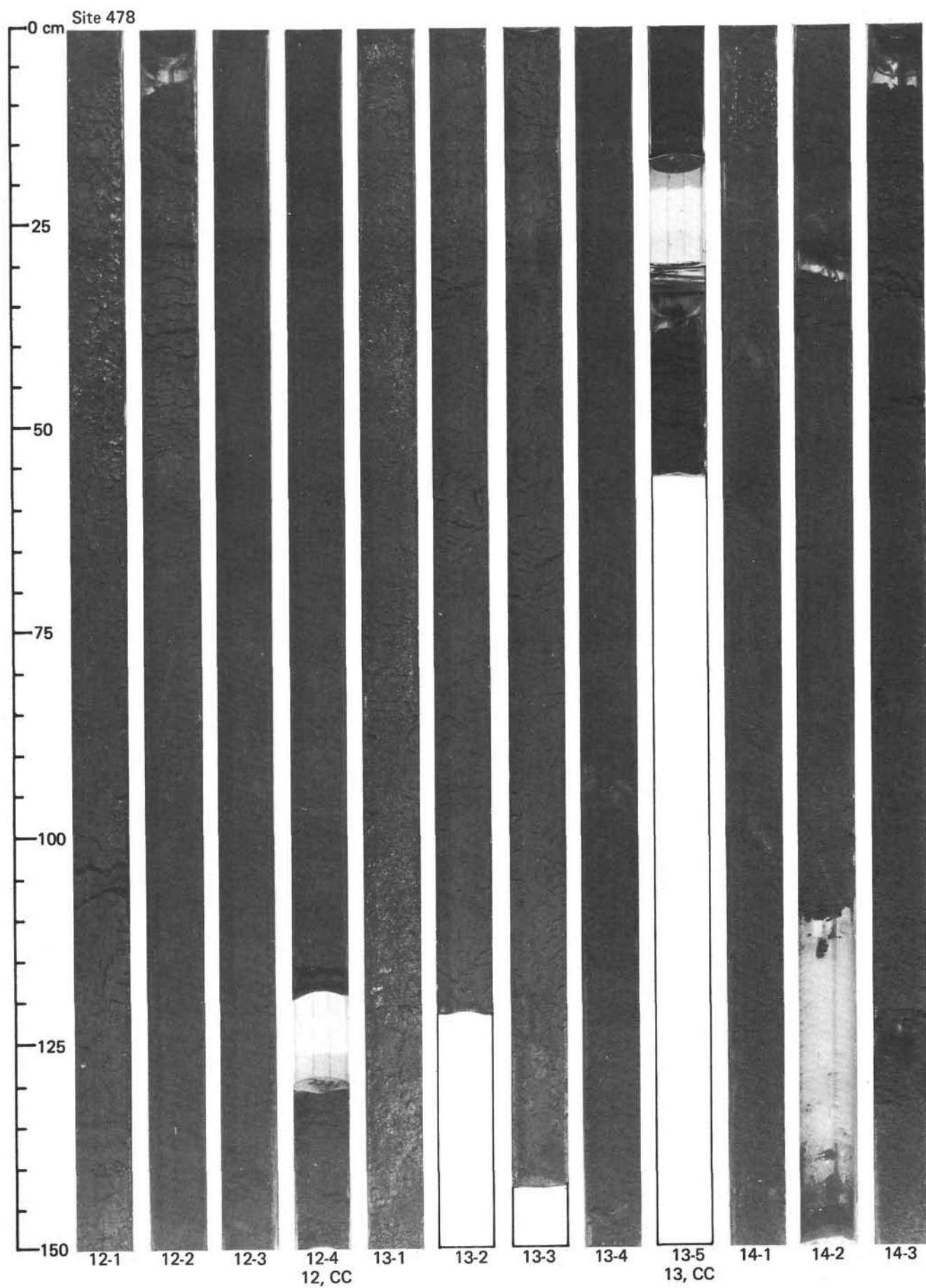


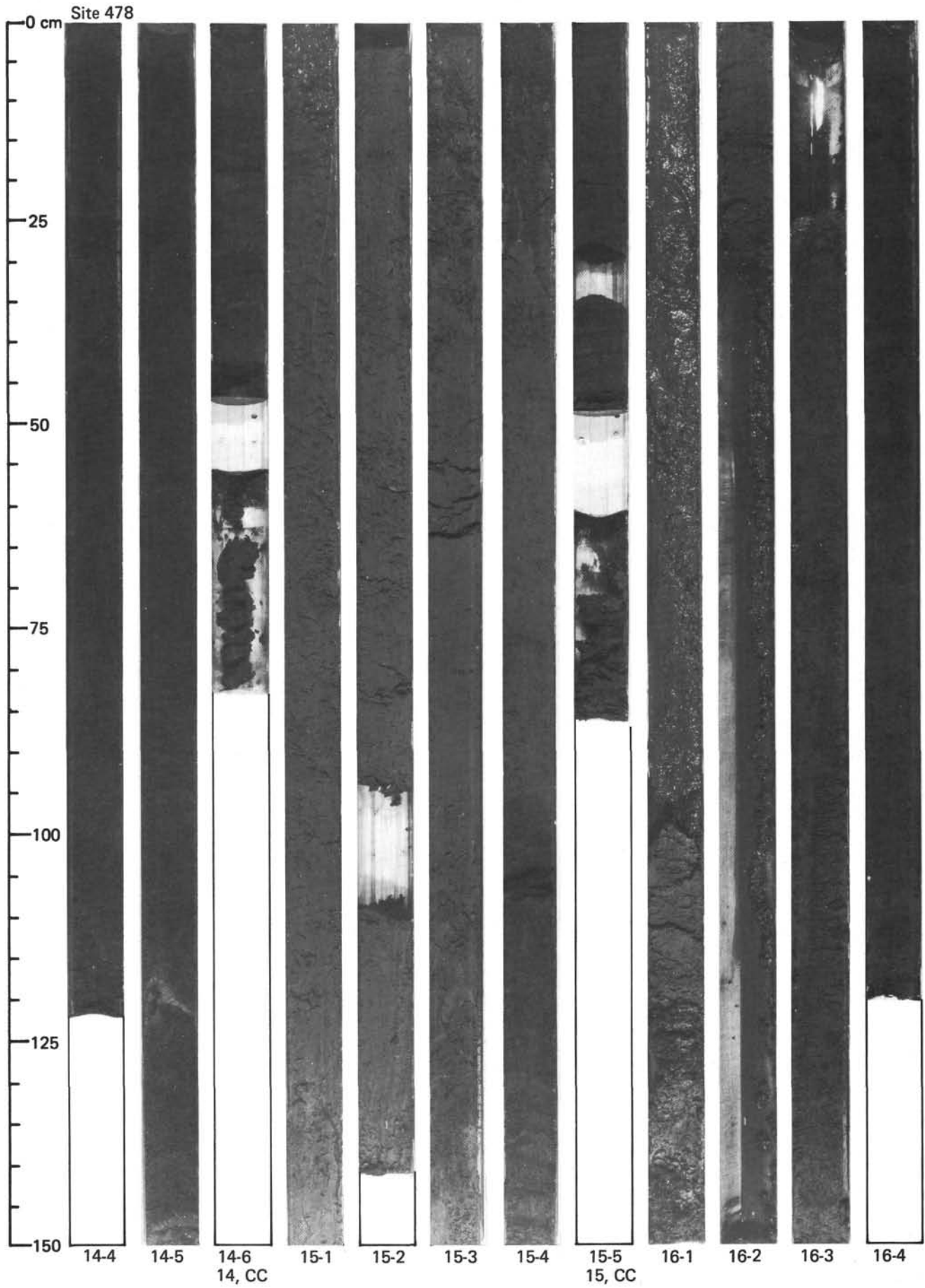
GUAYMAS BASIN SITES



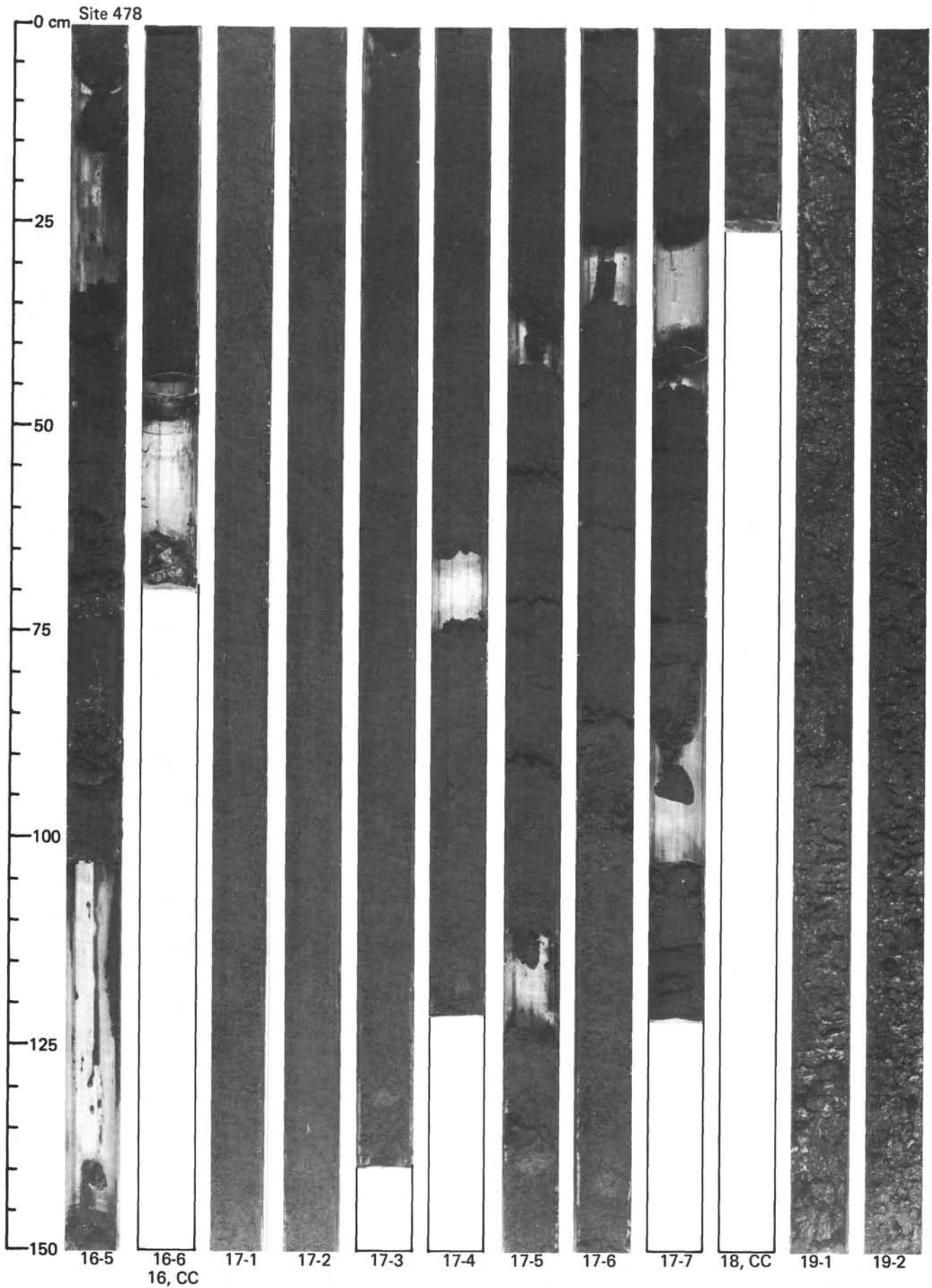


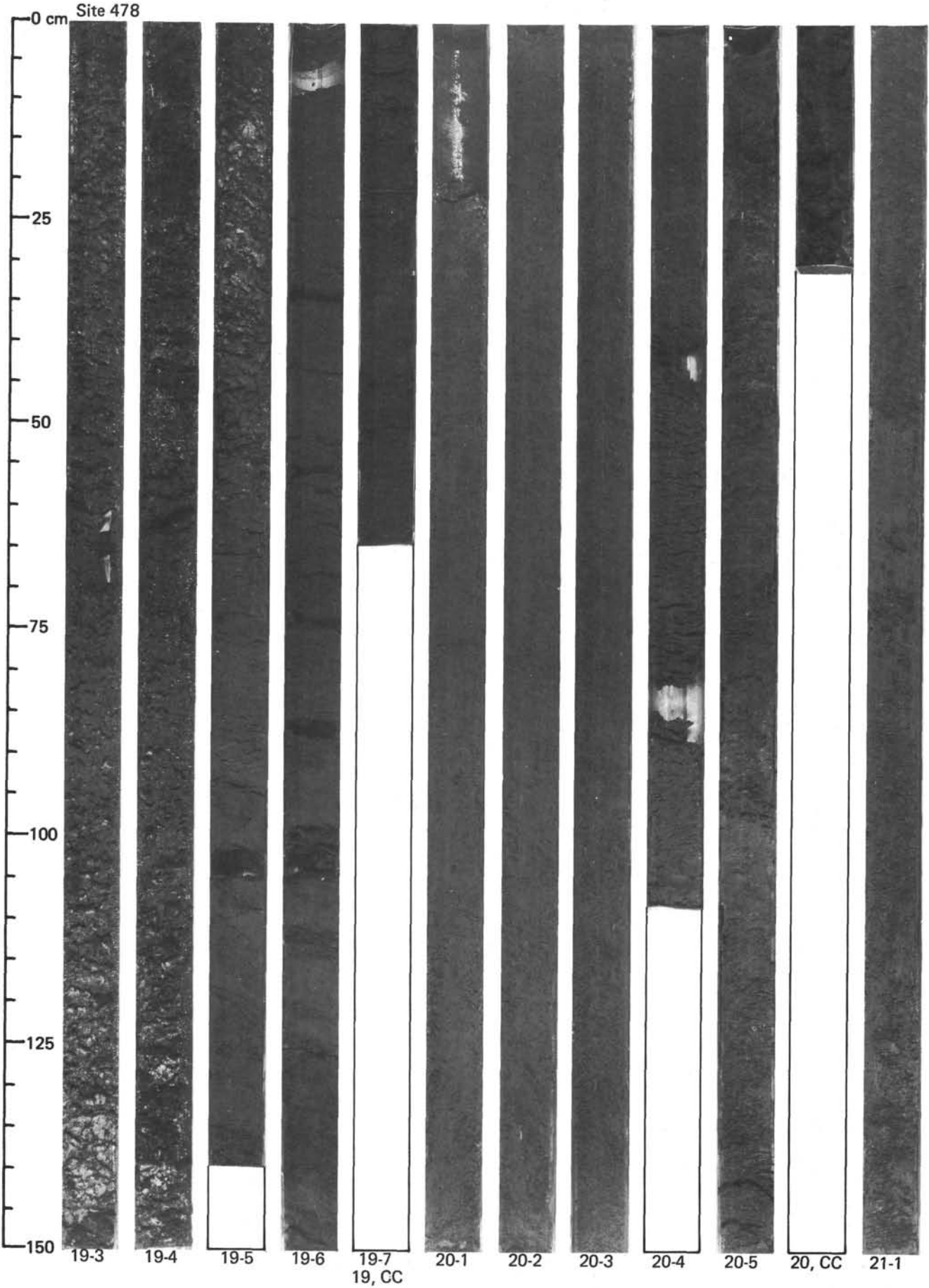
GUAYMAS BASIN SITES



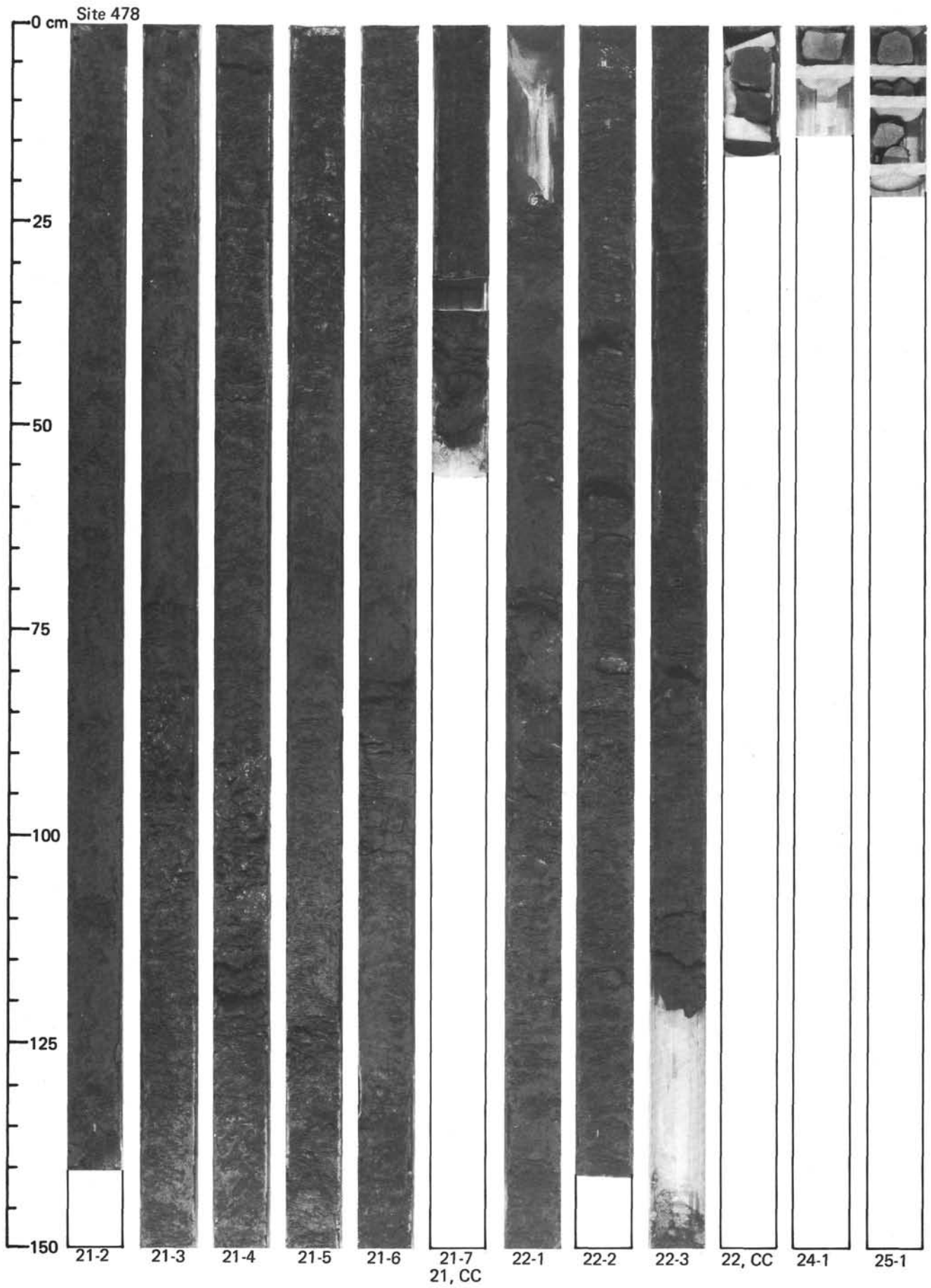


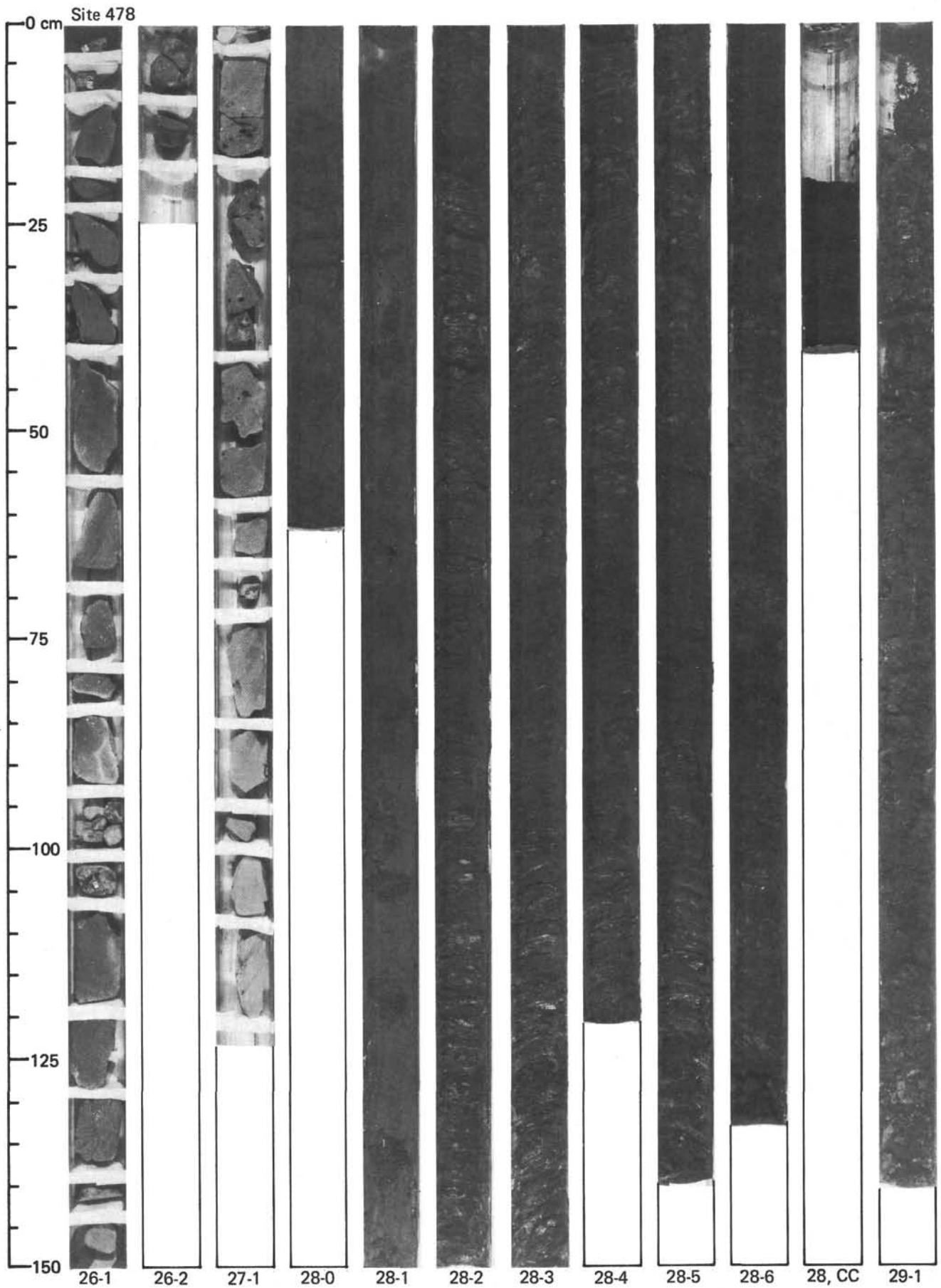
GUAYMAS BASIN SITES



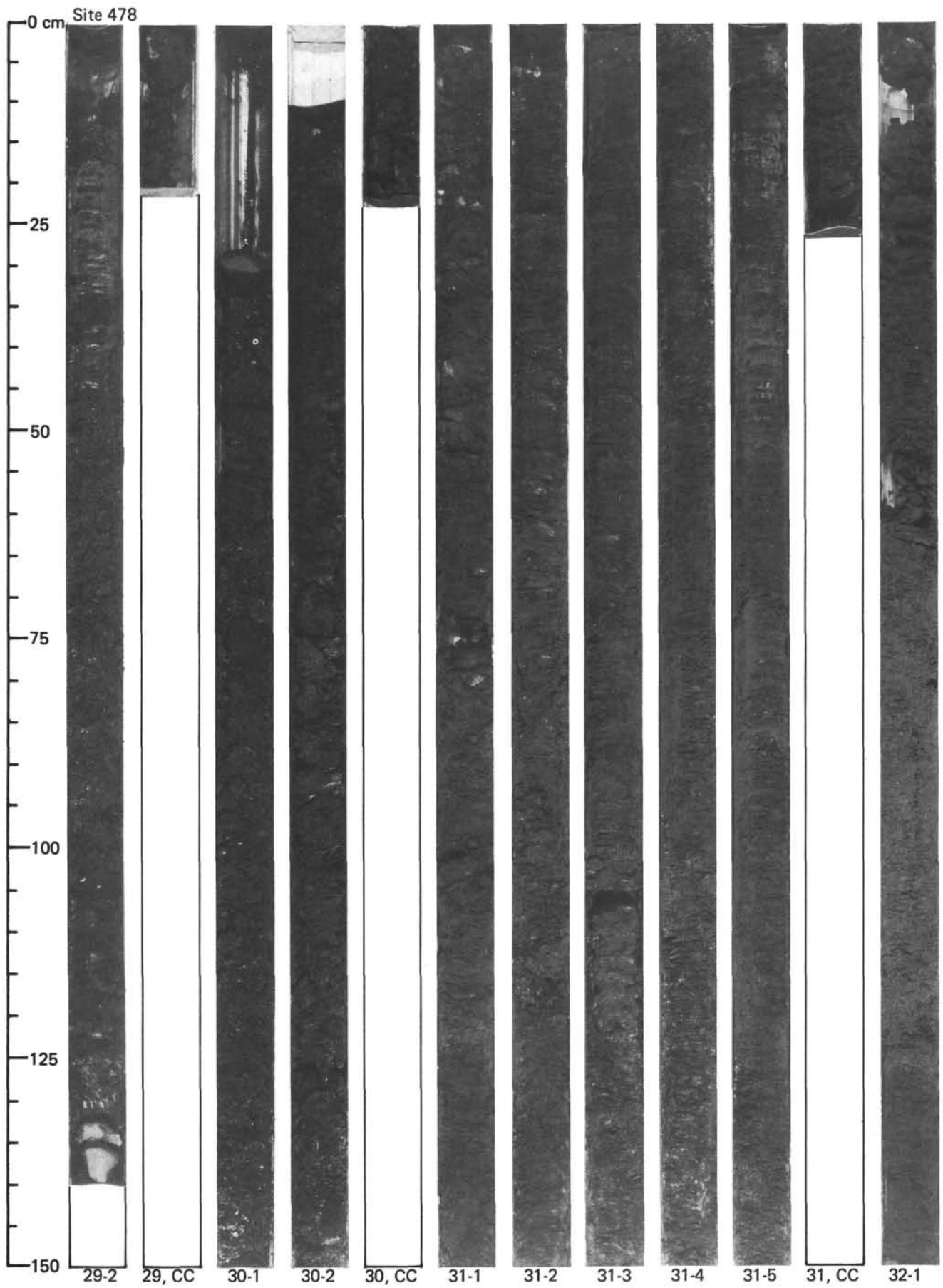


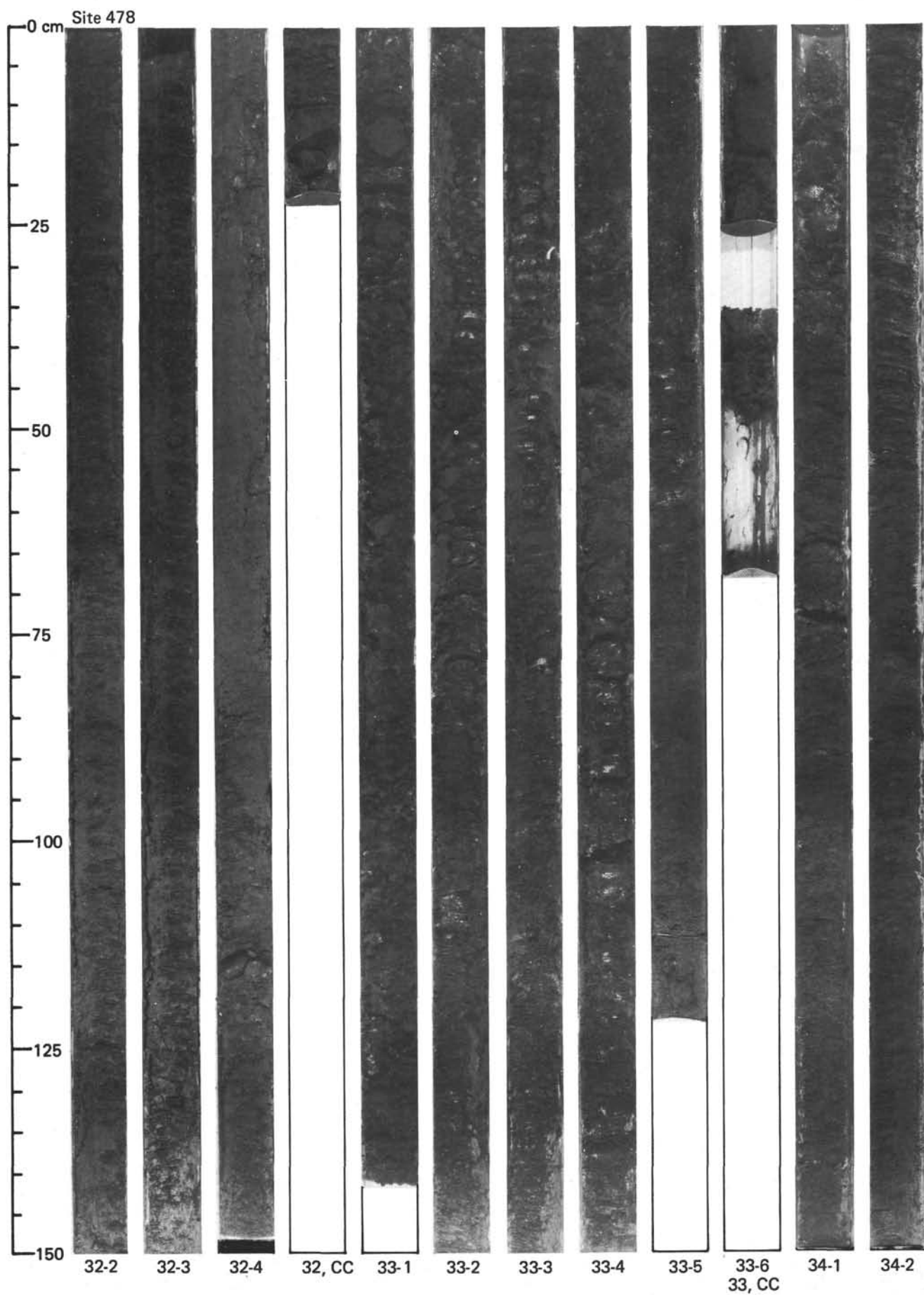
GUAYMAS BASIN SITES



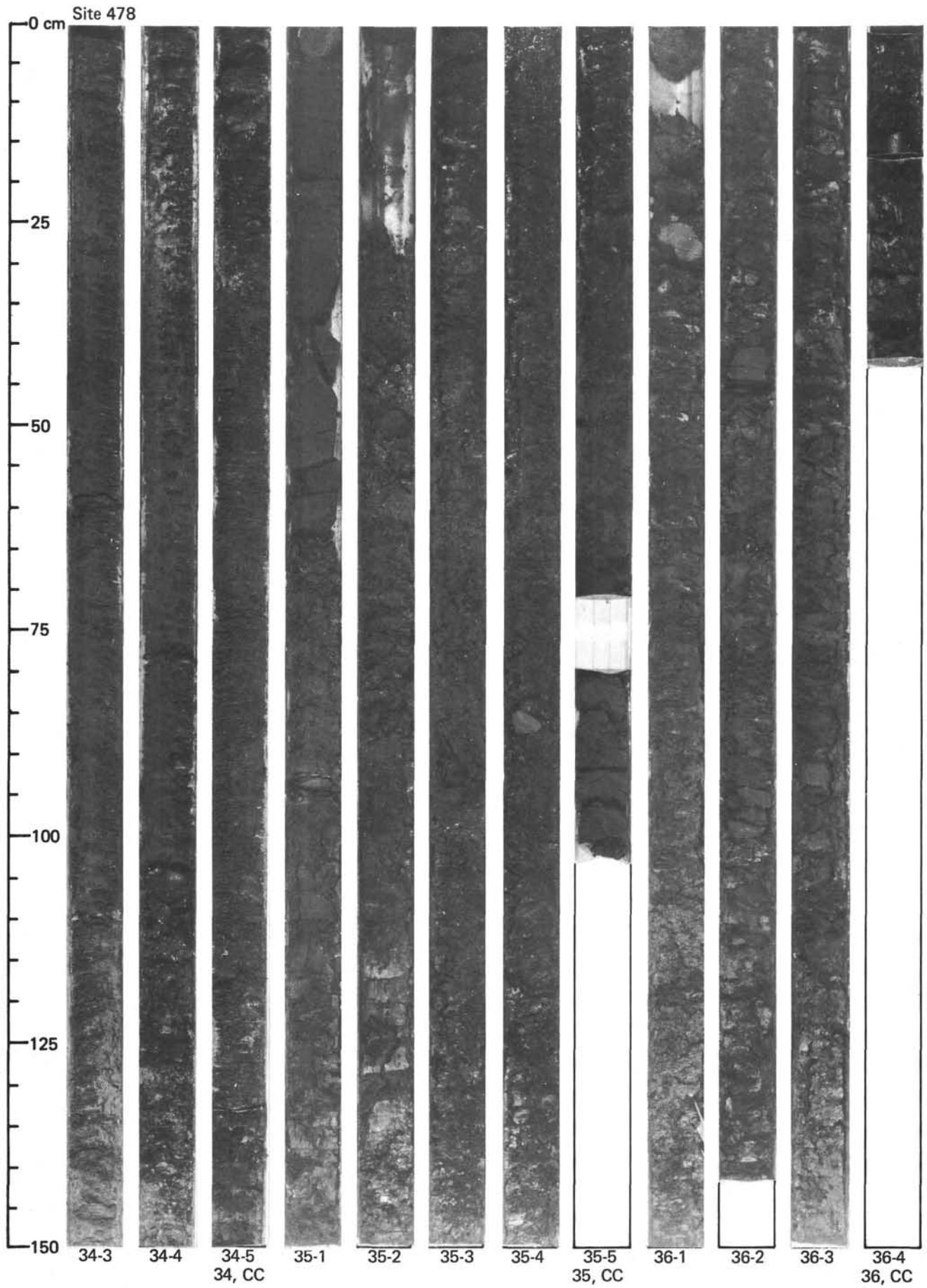


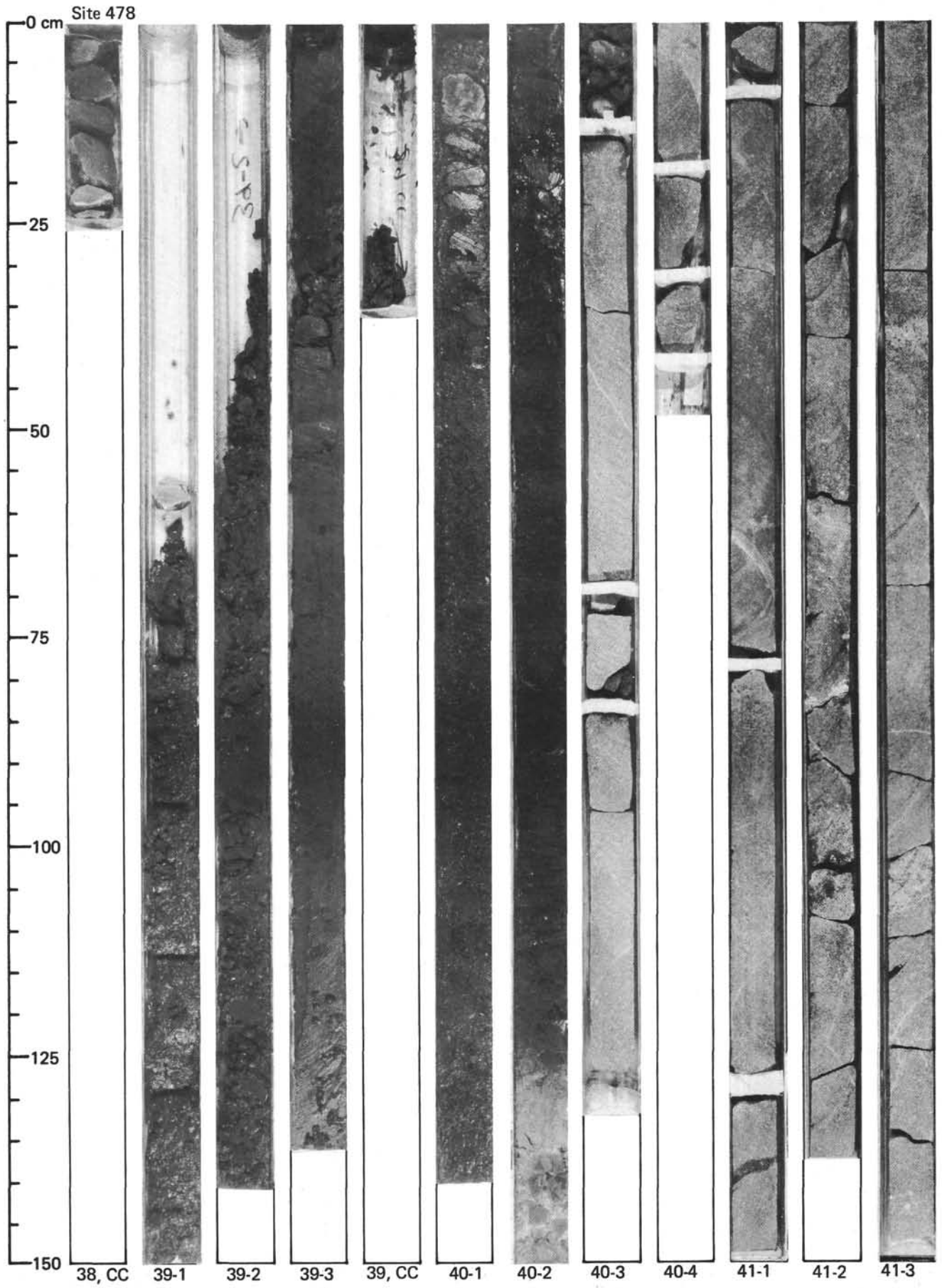
GUAYMAS BASIN SITES



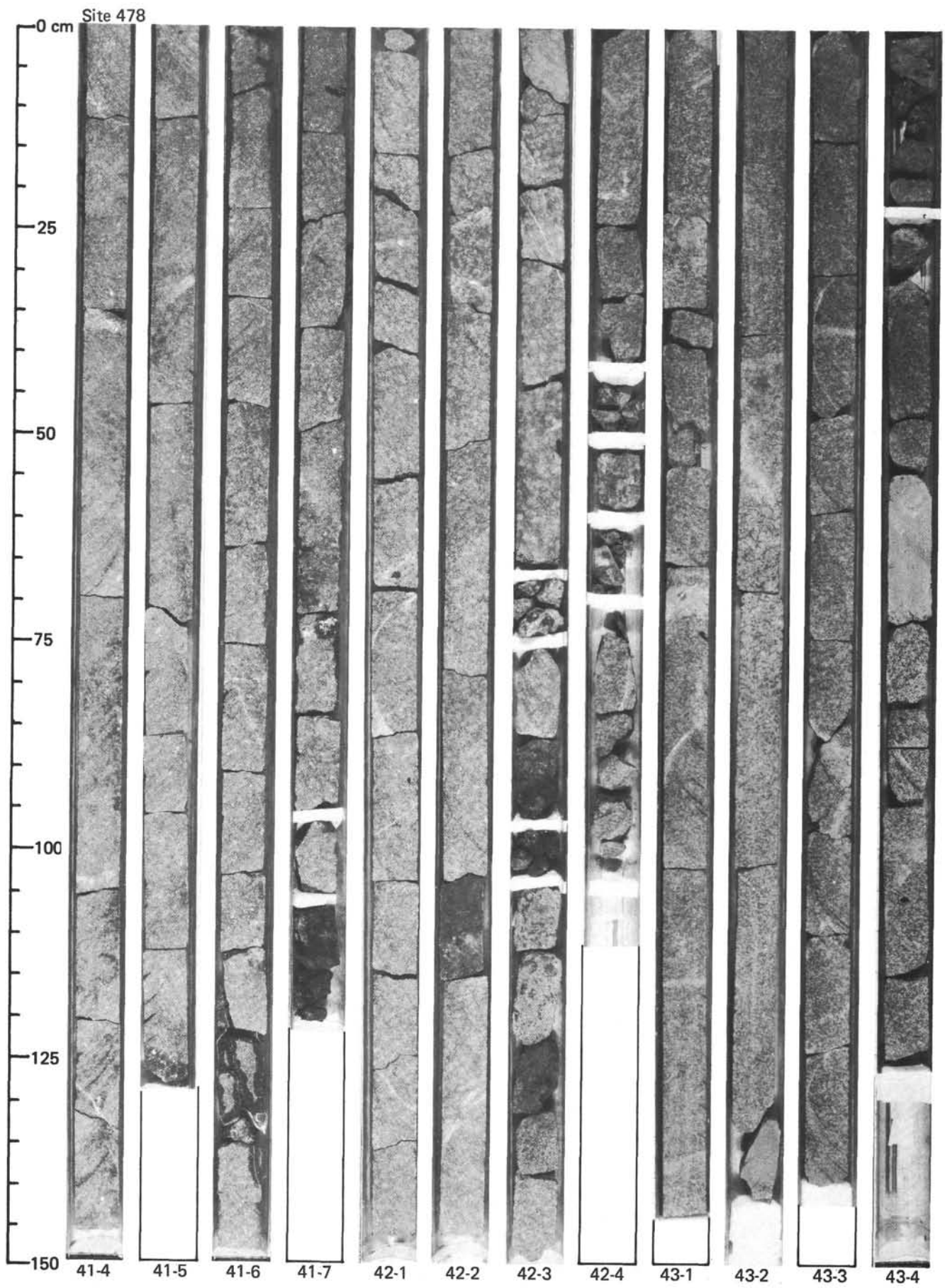


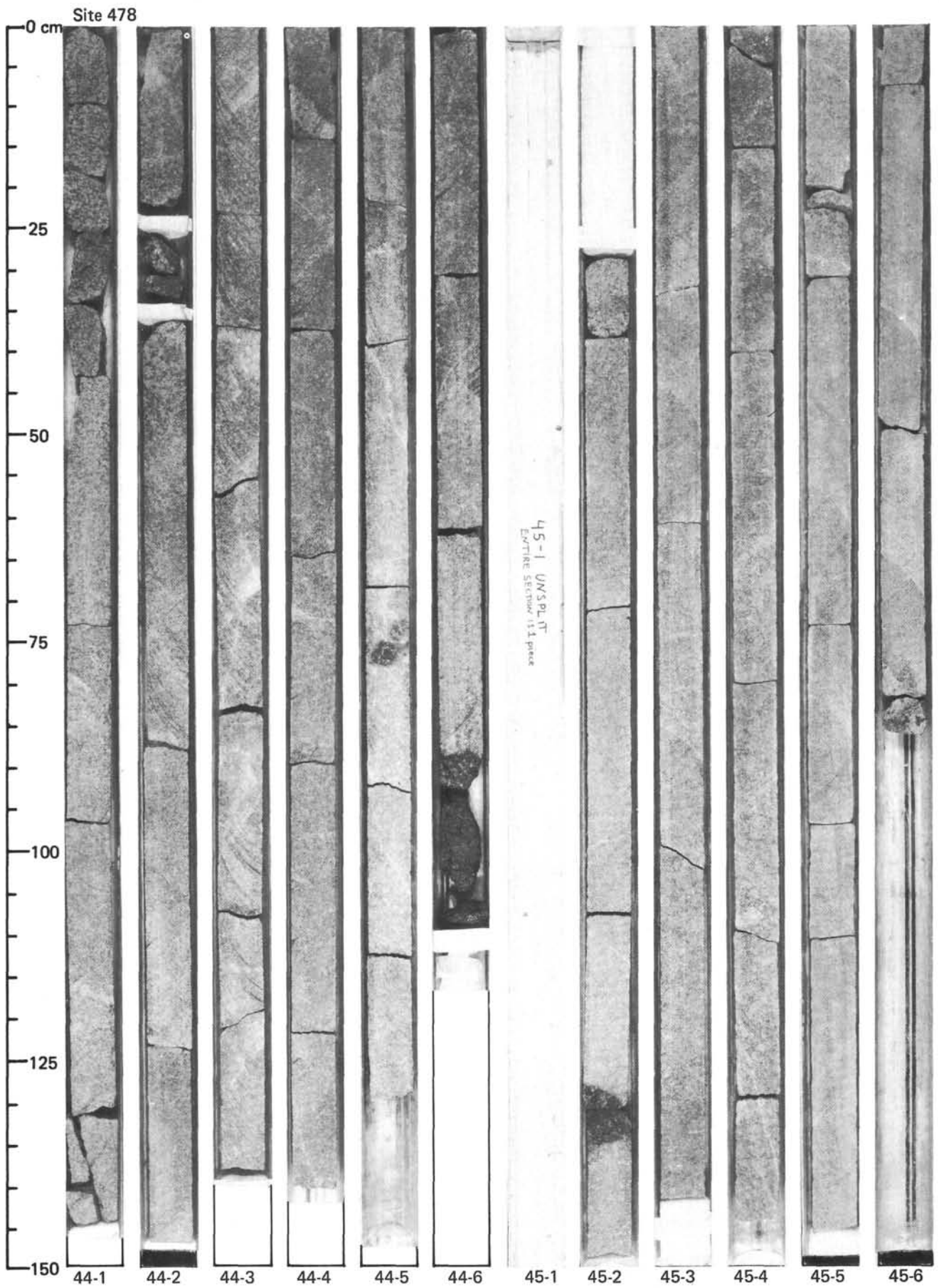
GUAYMAS BASIN SITES



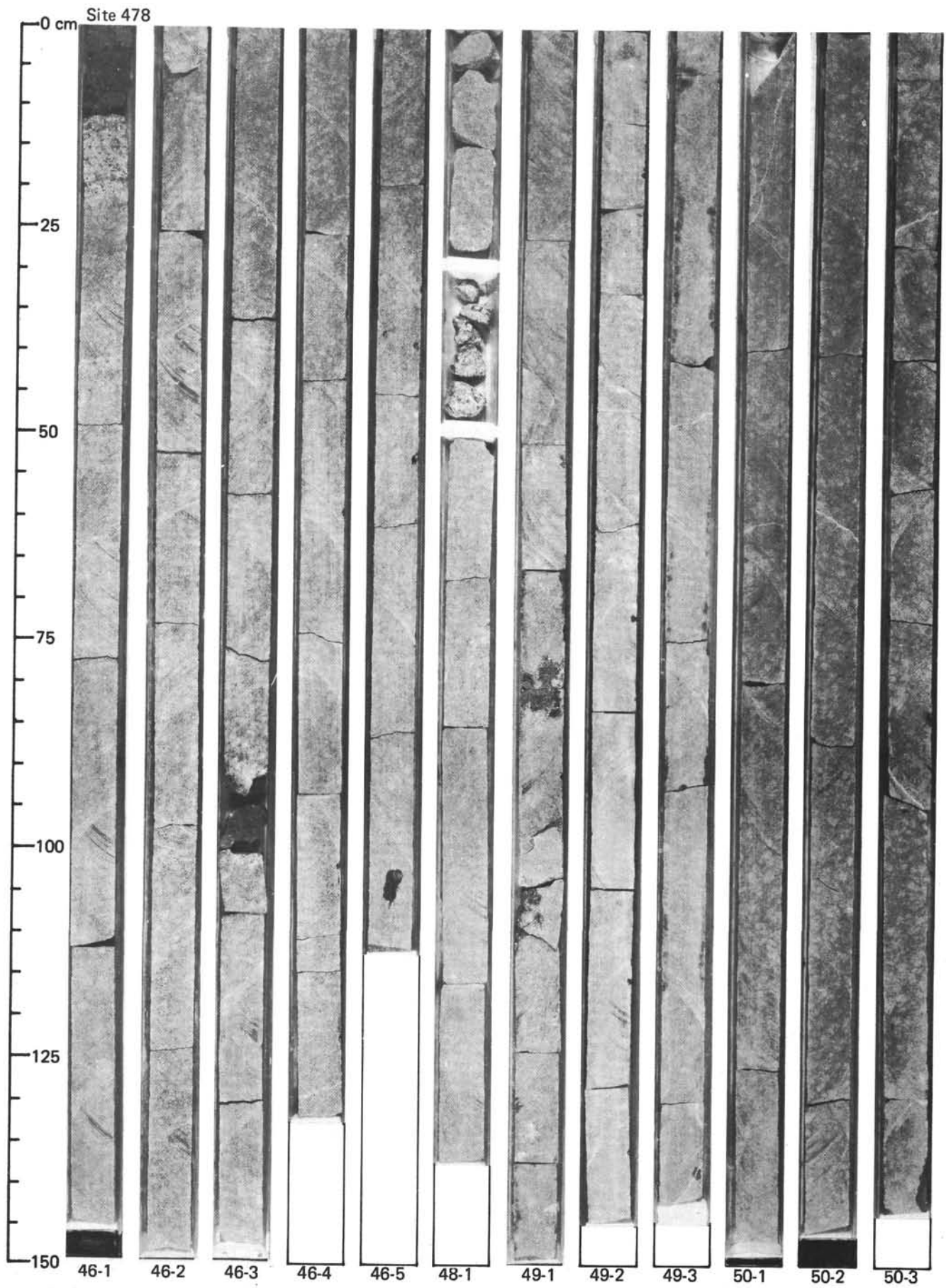


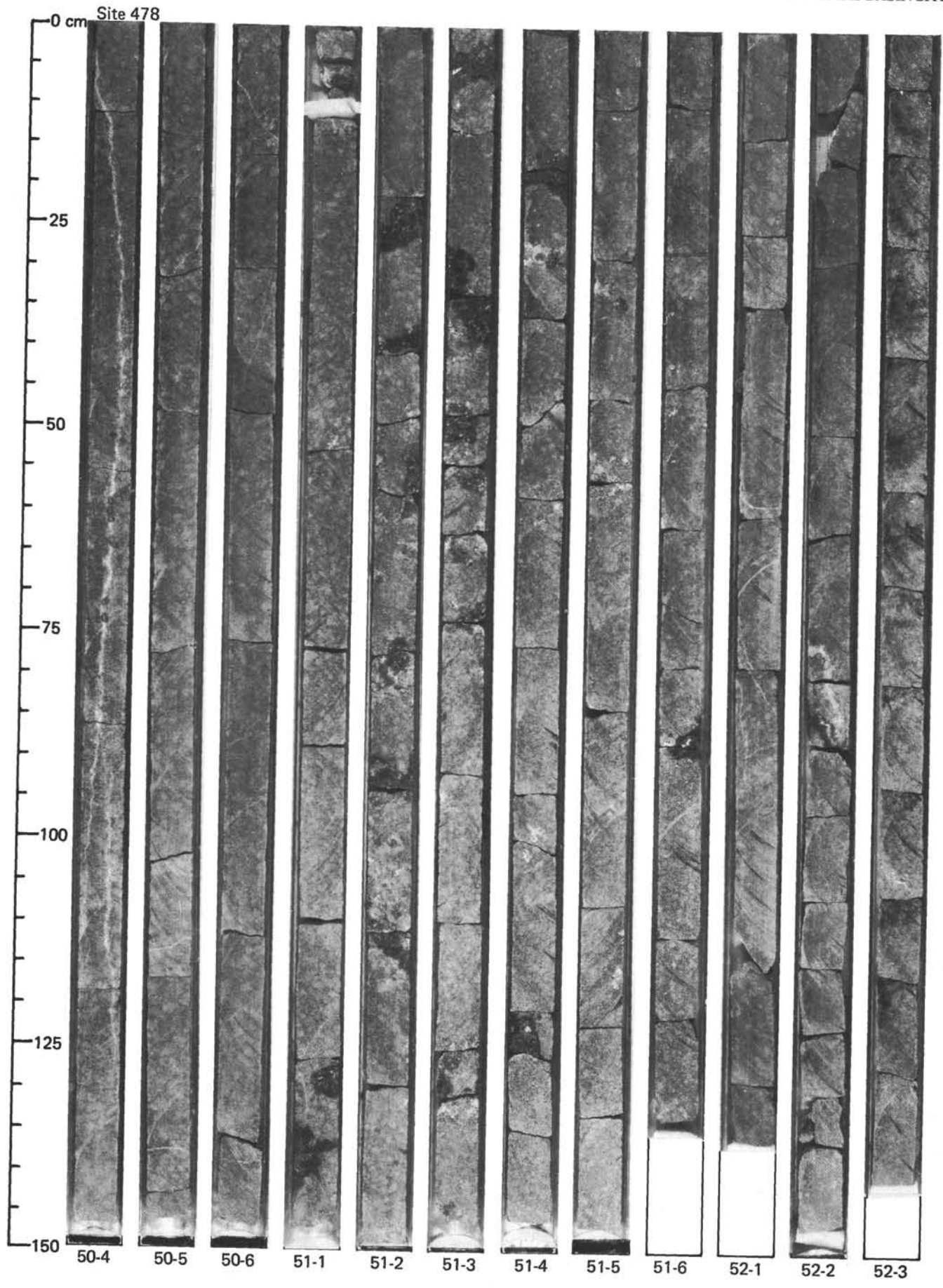
GUAYMAS BASIN SITES



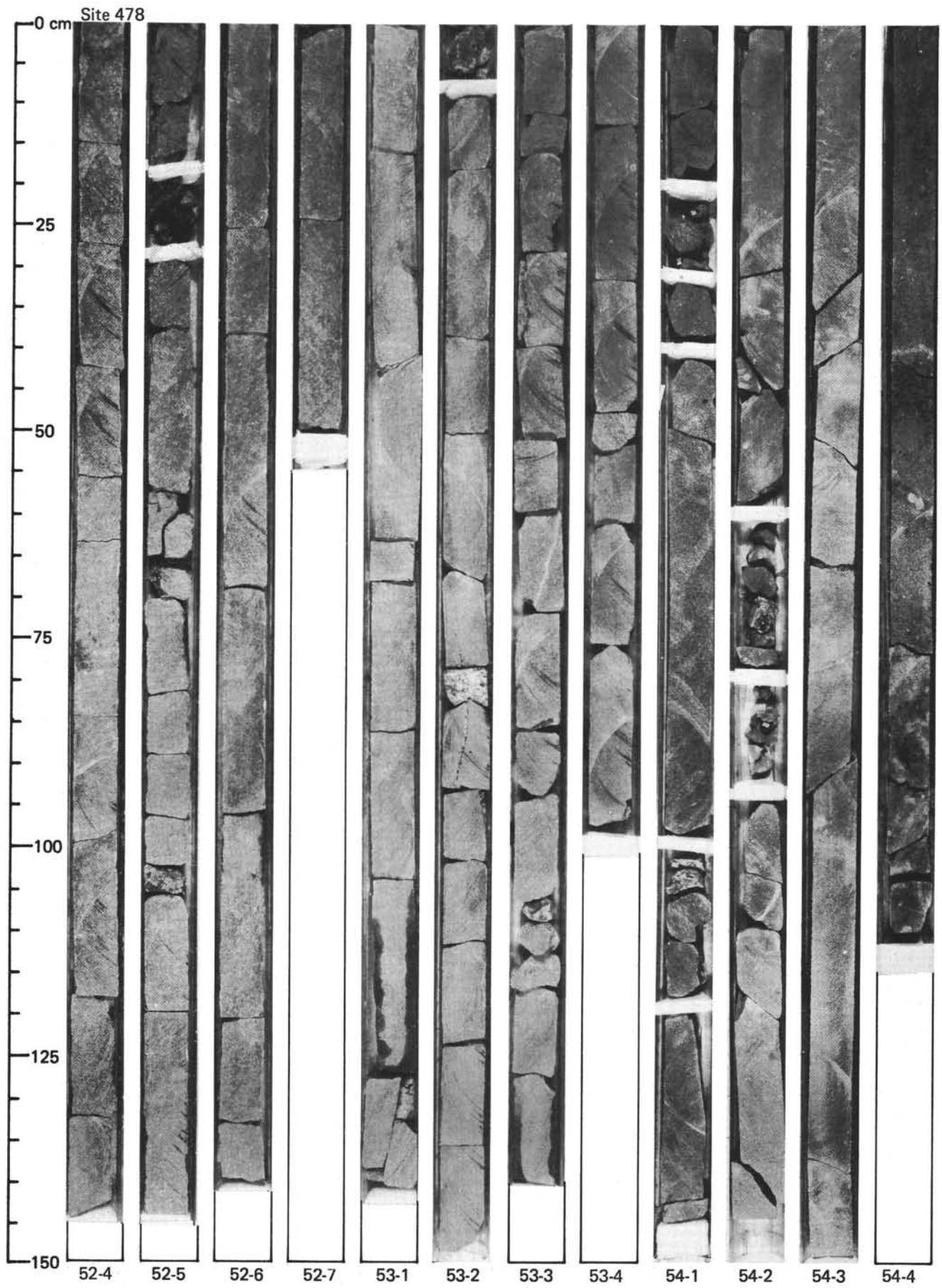


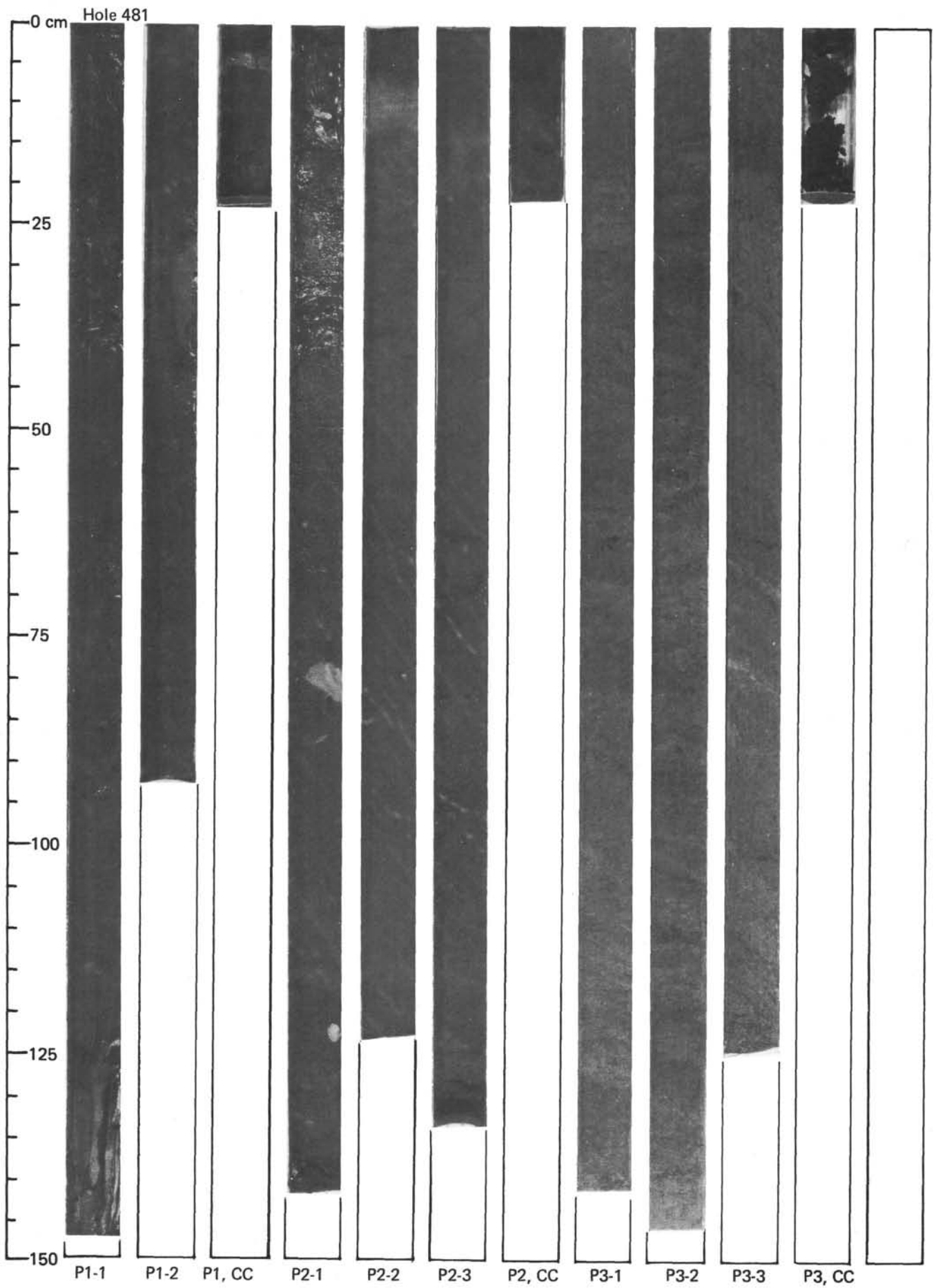
GUAYMAS BASIN SITES



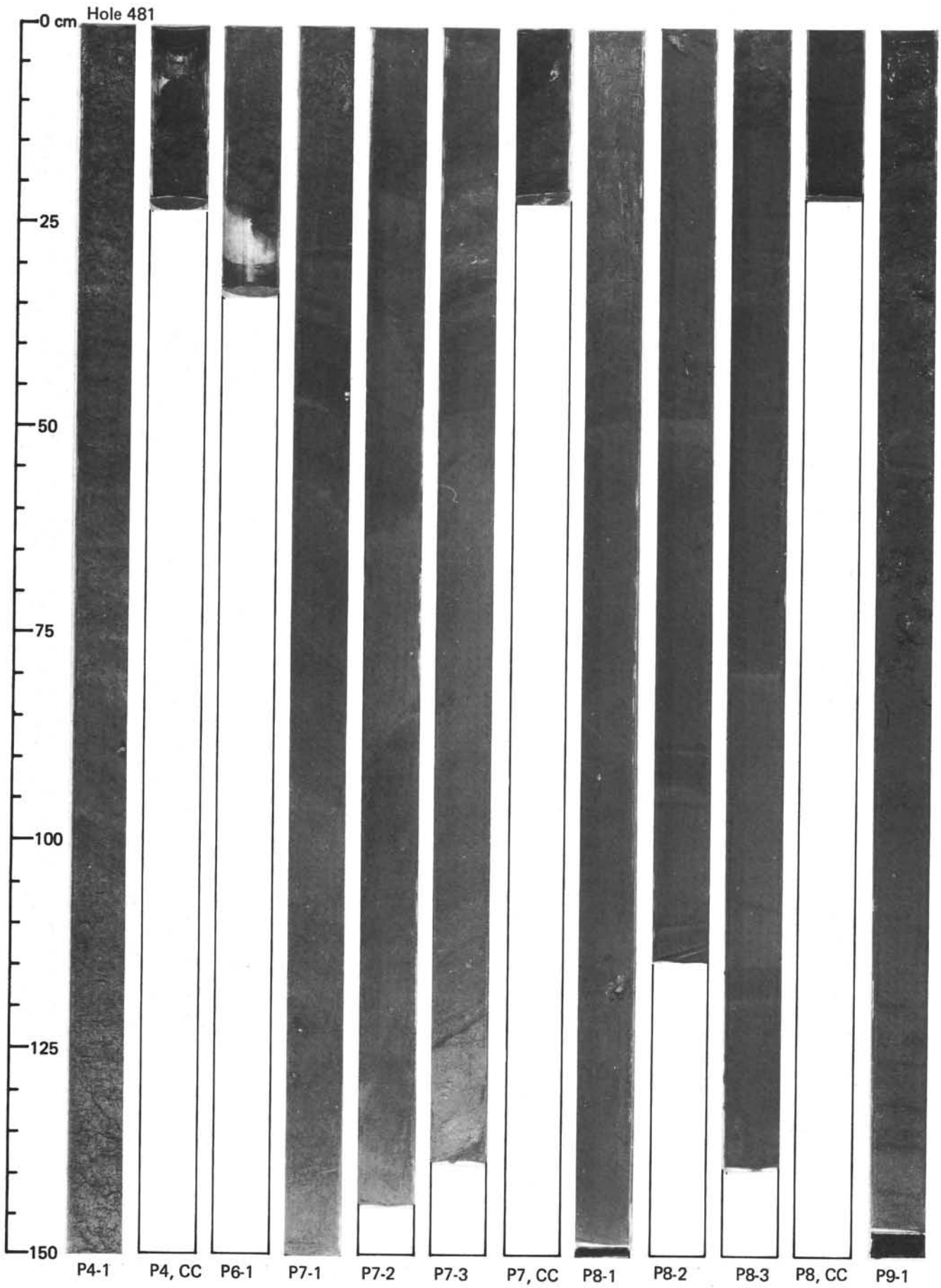


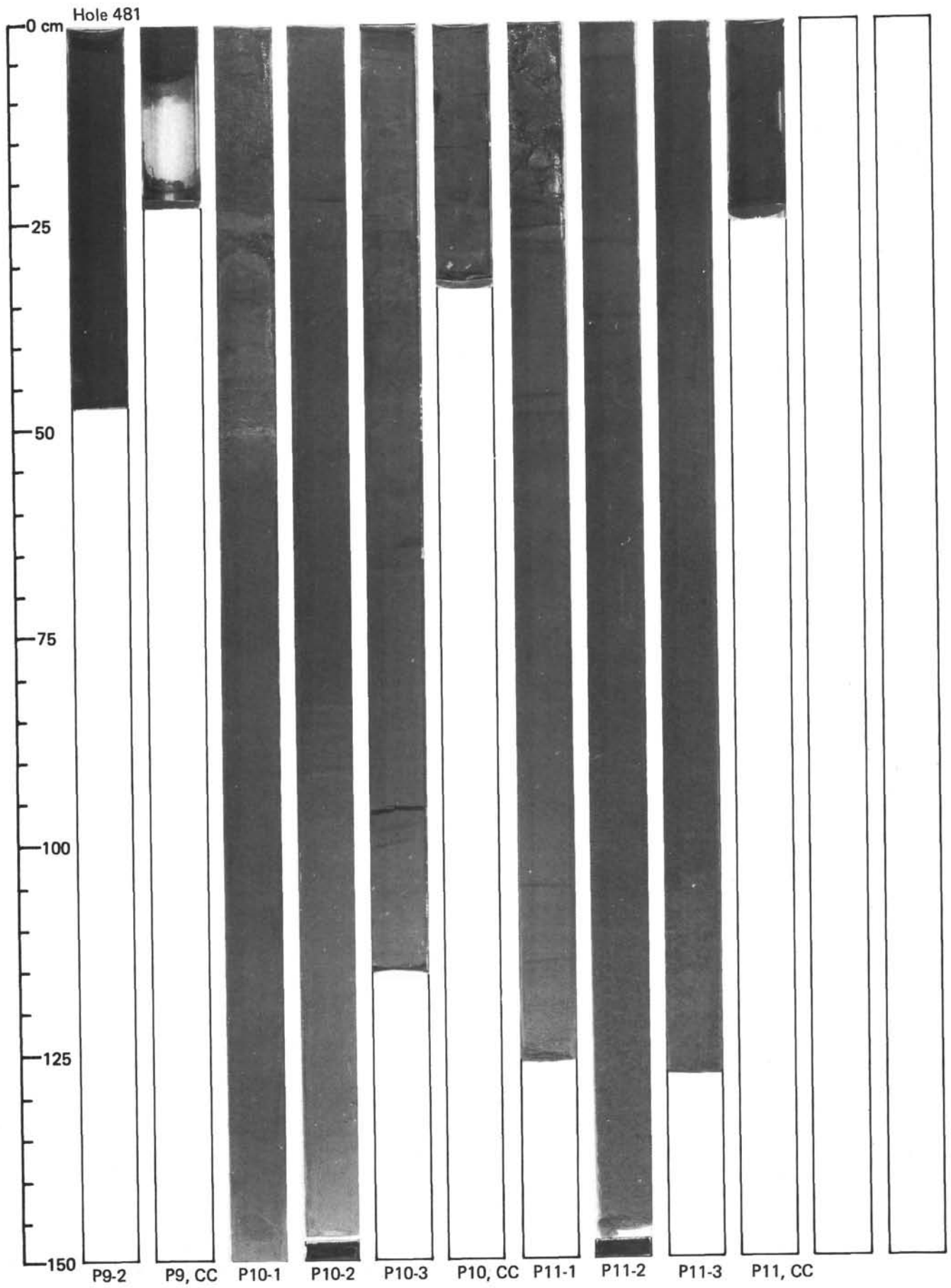
GUAYMAS BASIN SITES



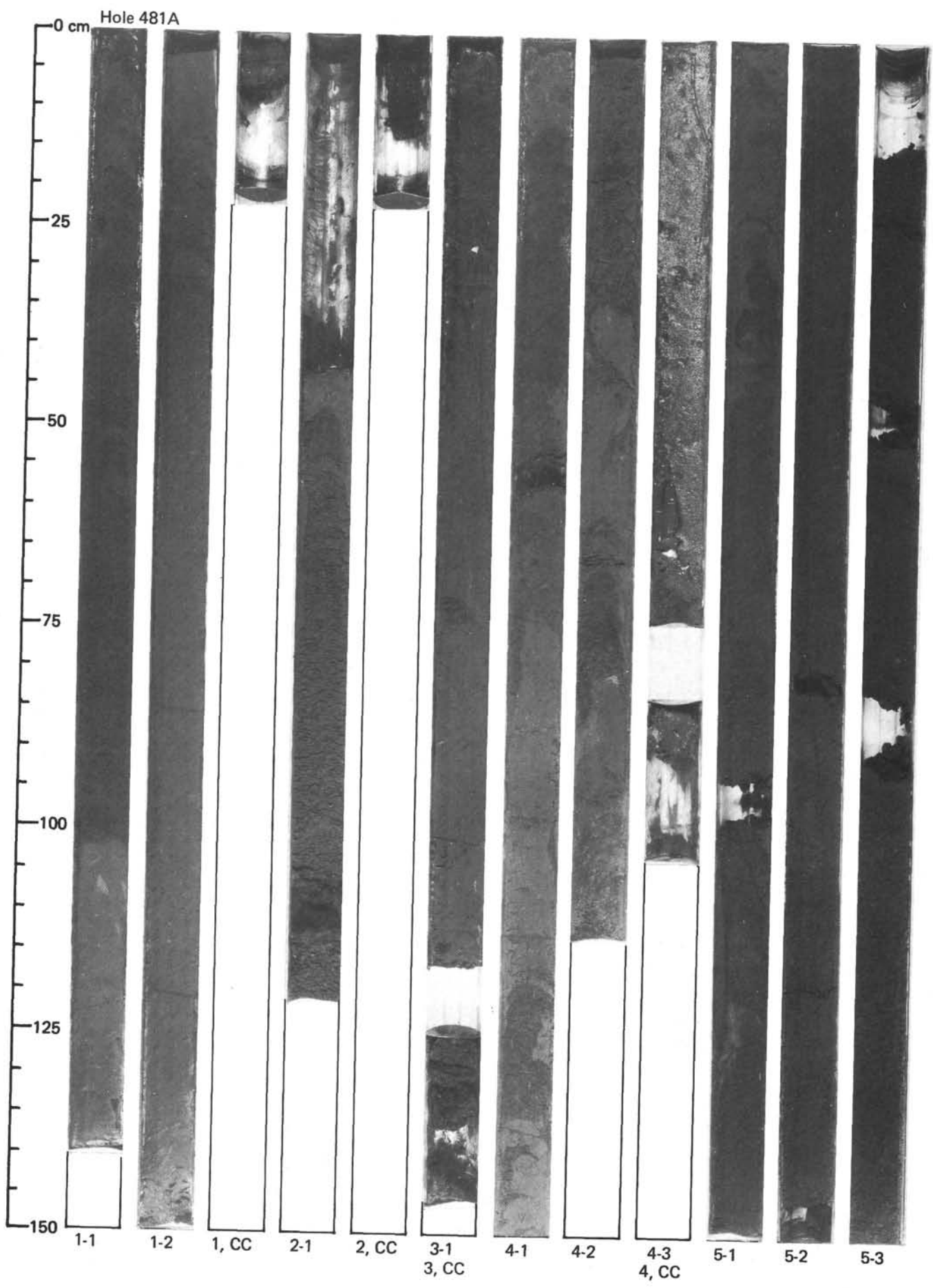


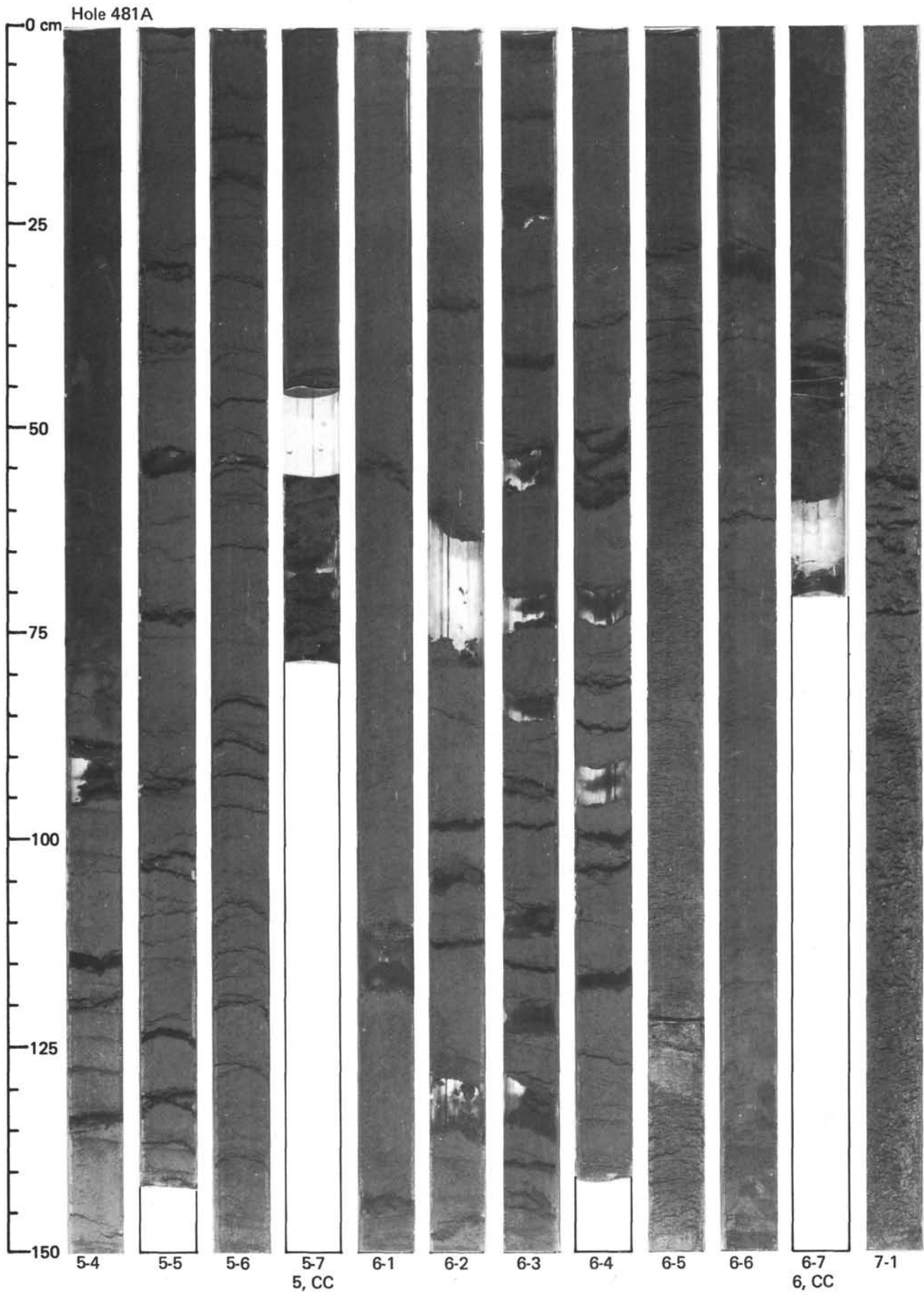
GUAYMAS BASIN SITES



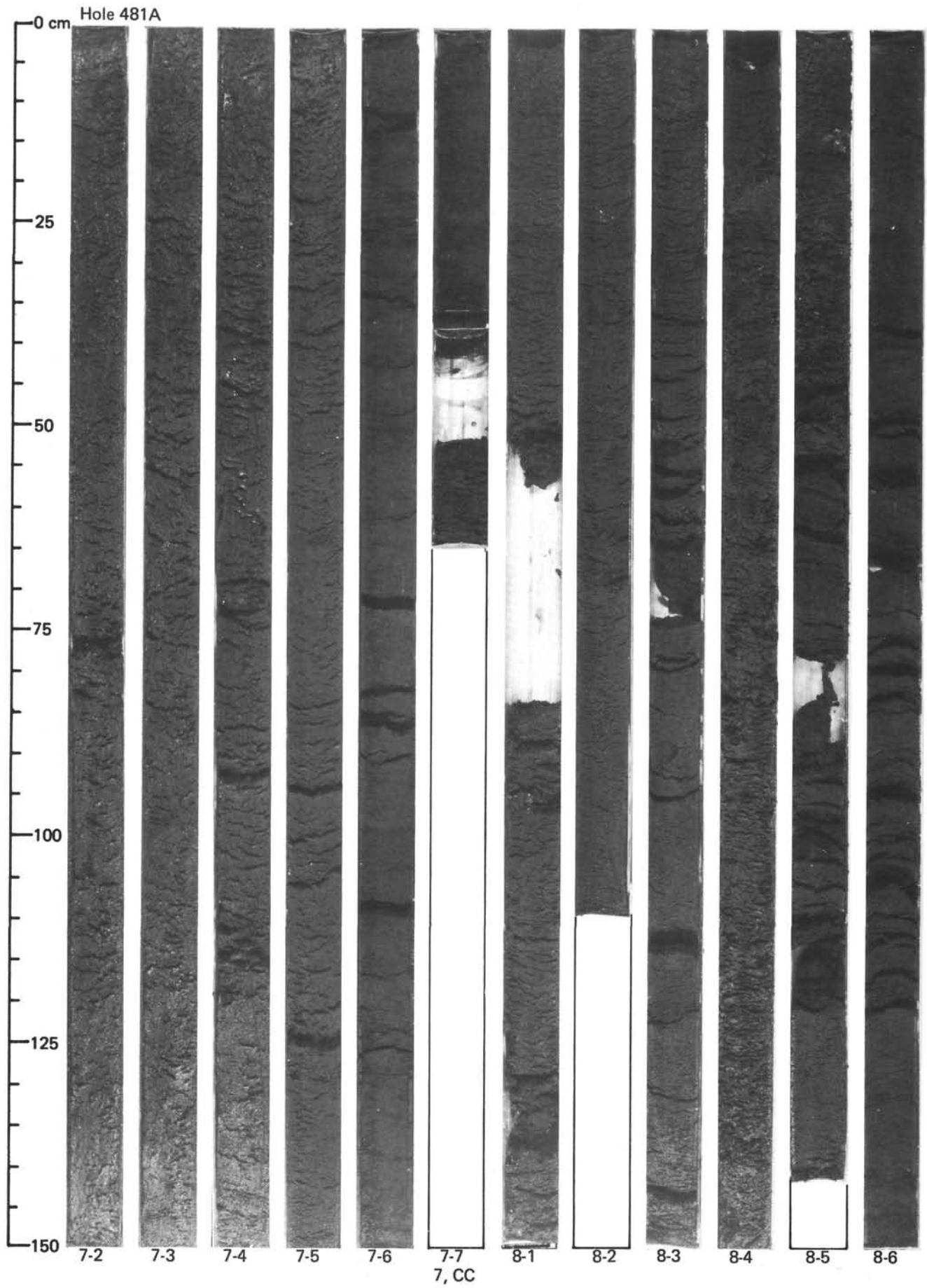


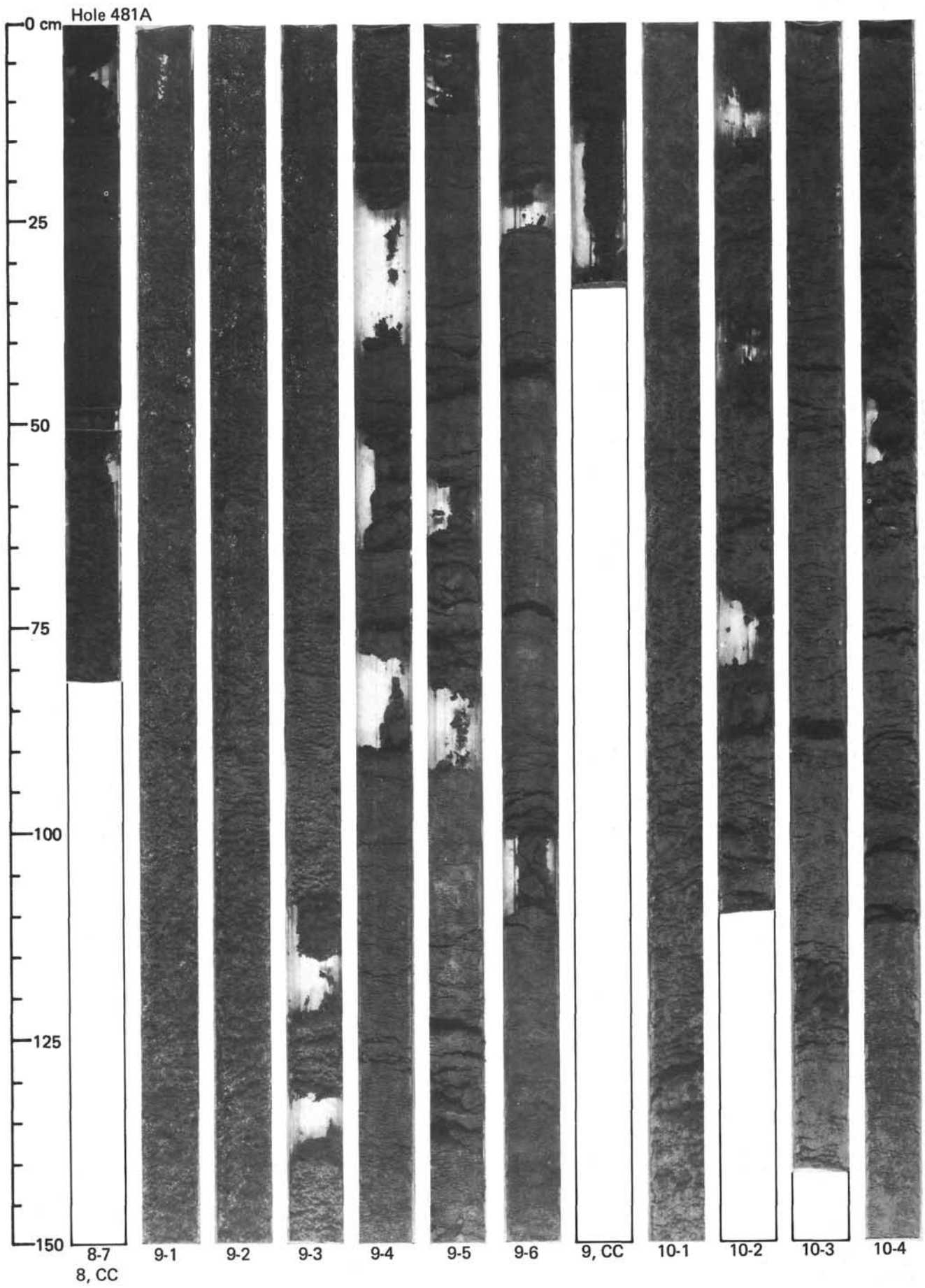
GUAYMAS BASIN SITES



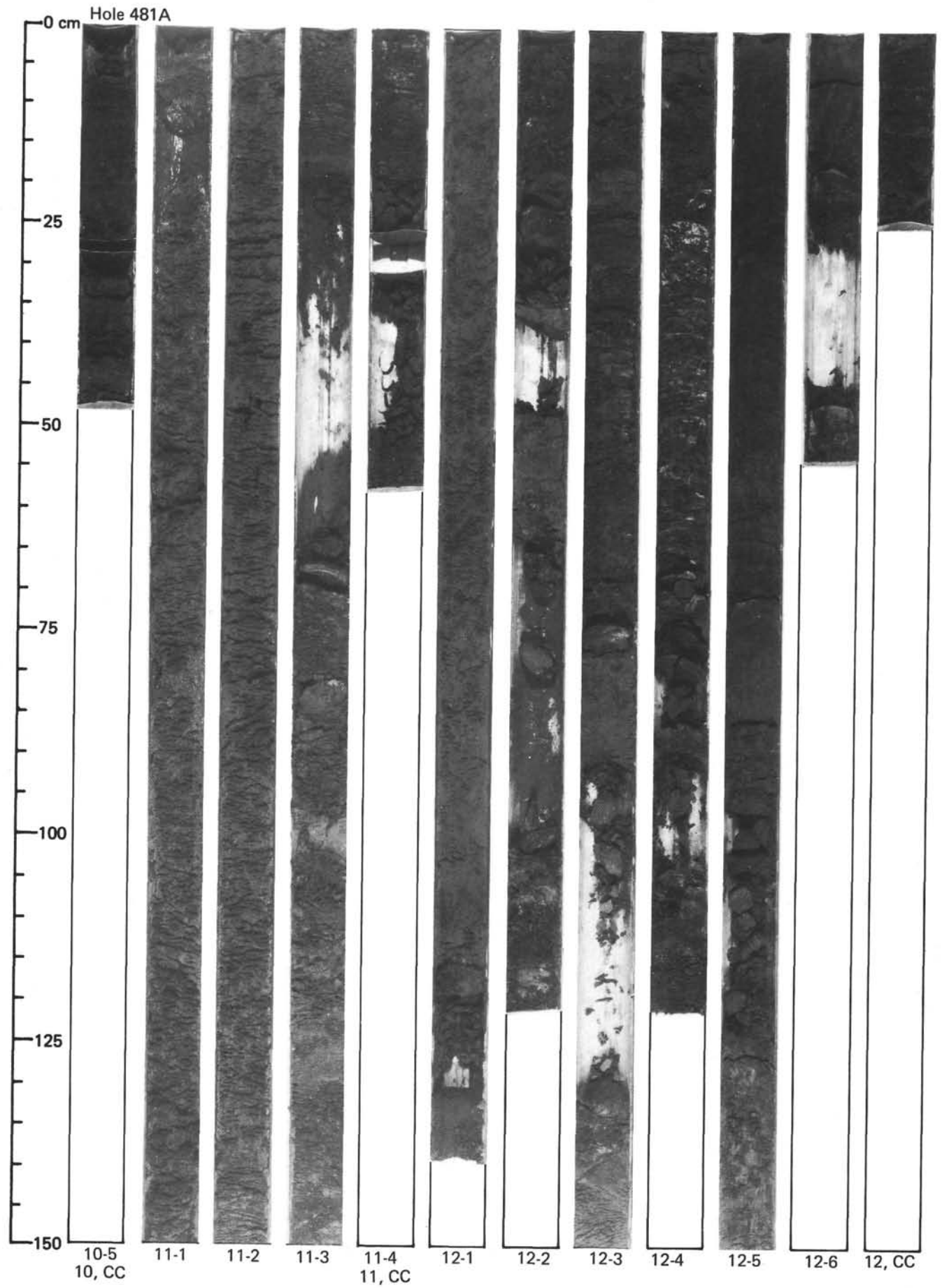


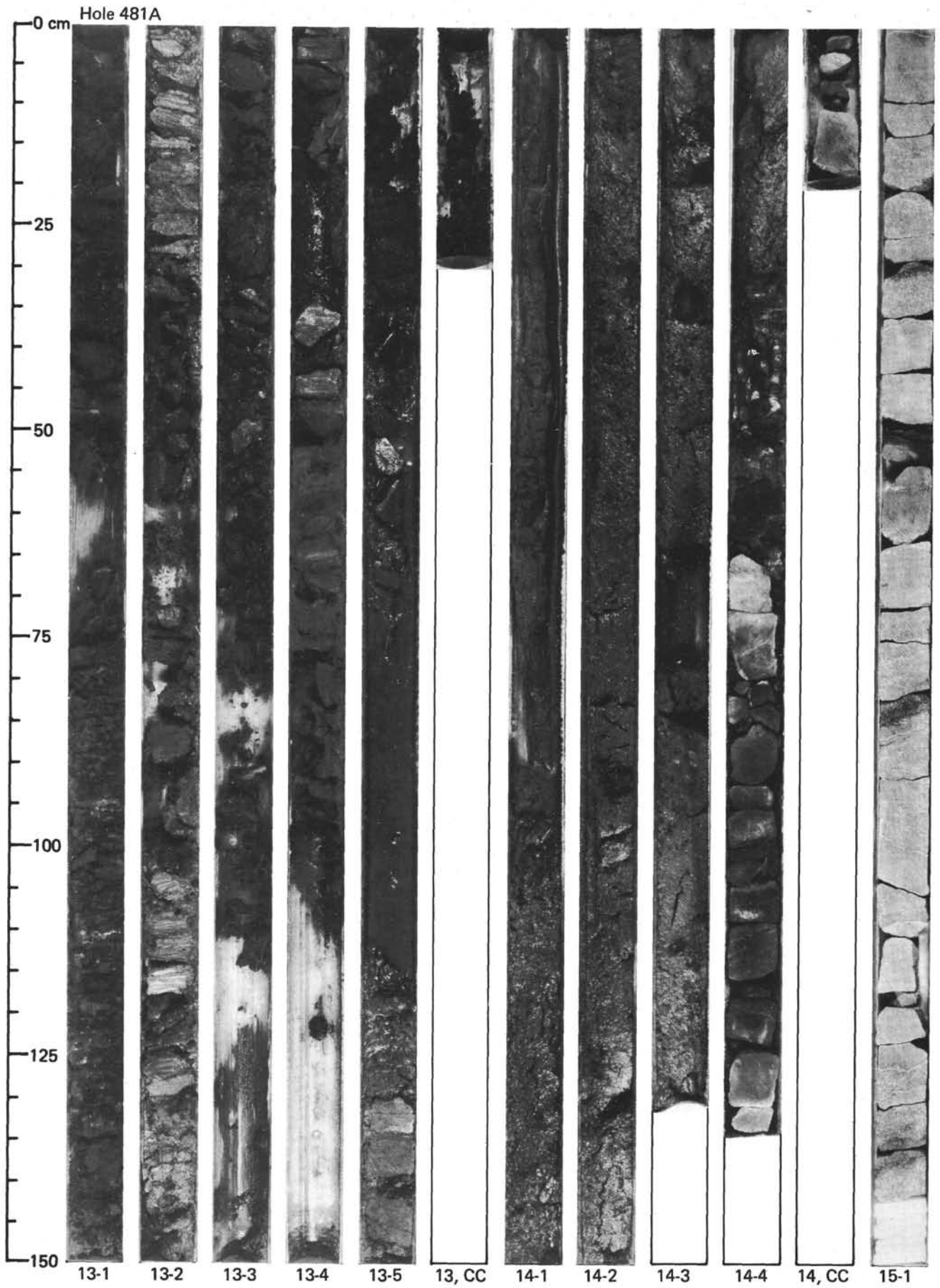
GUAYMAS BASIN SITES



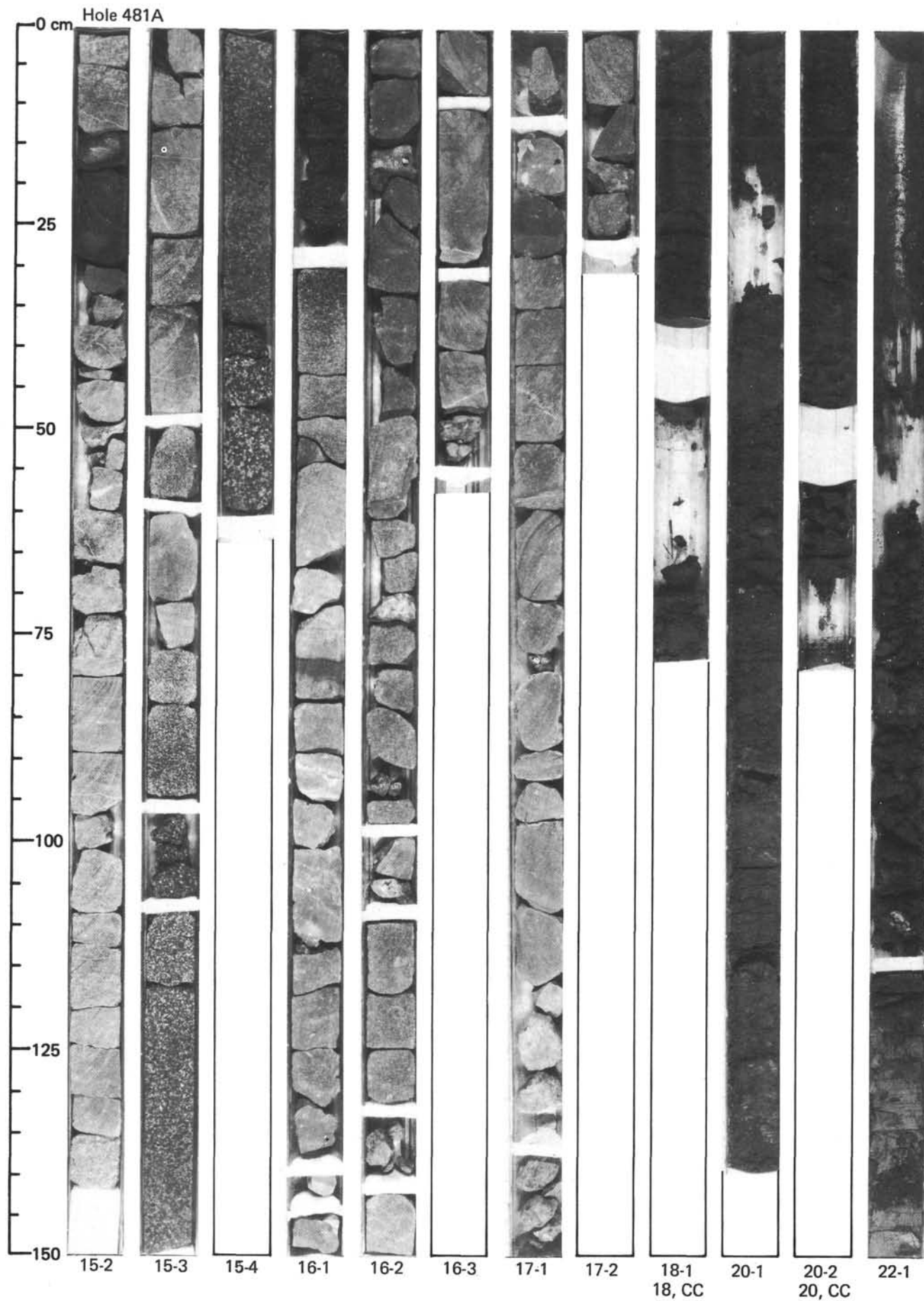


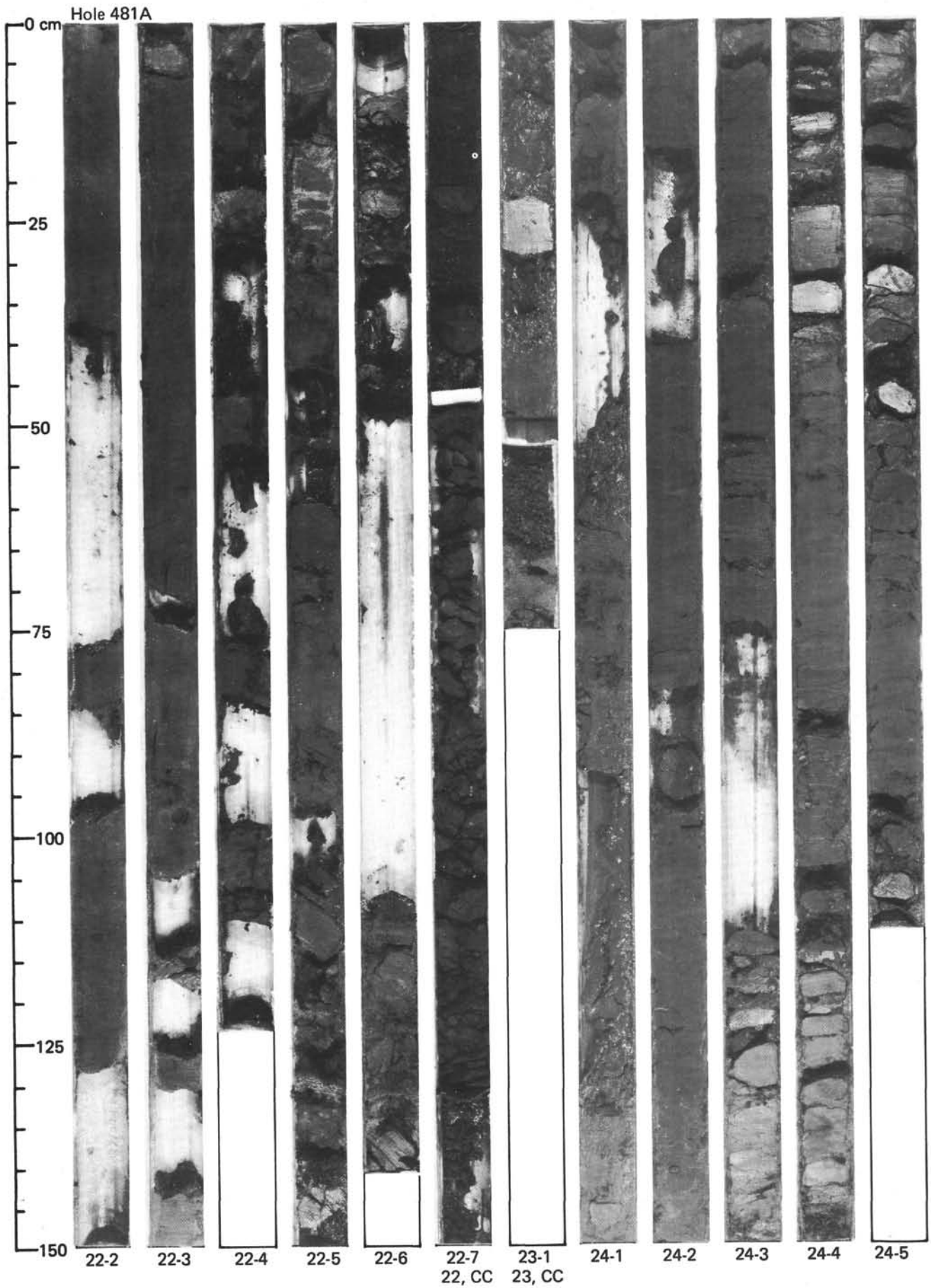
GUAYMAS BASIN SITES



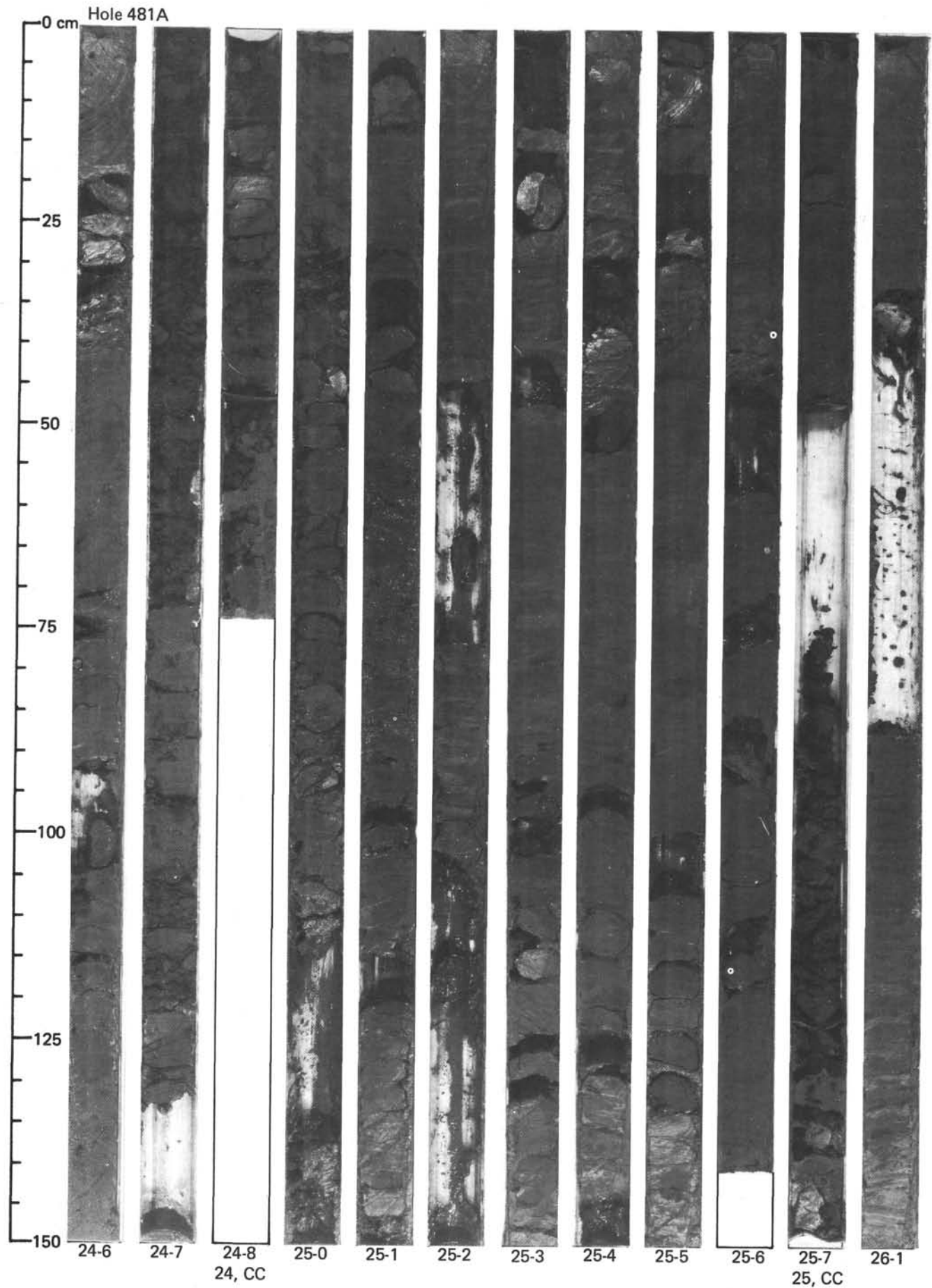


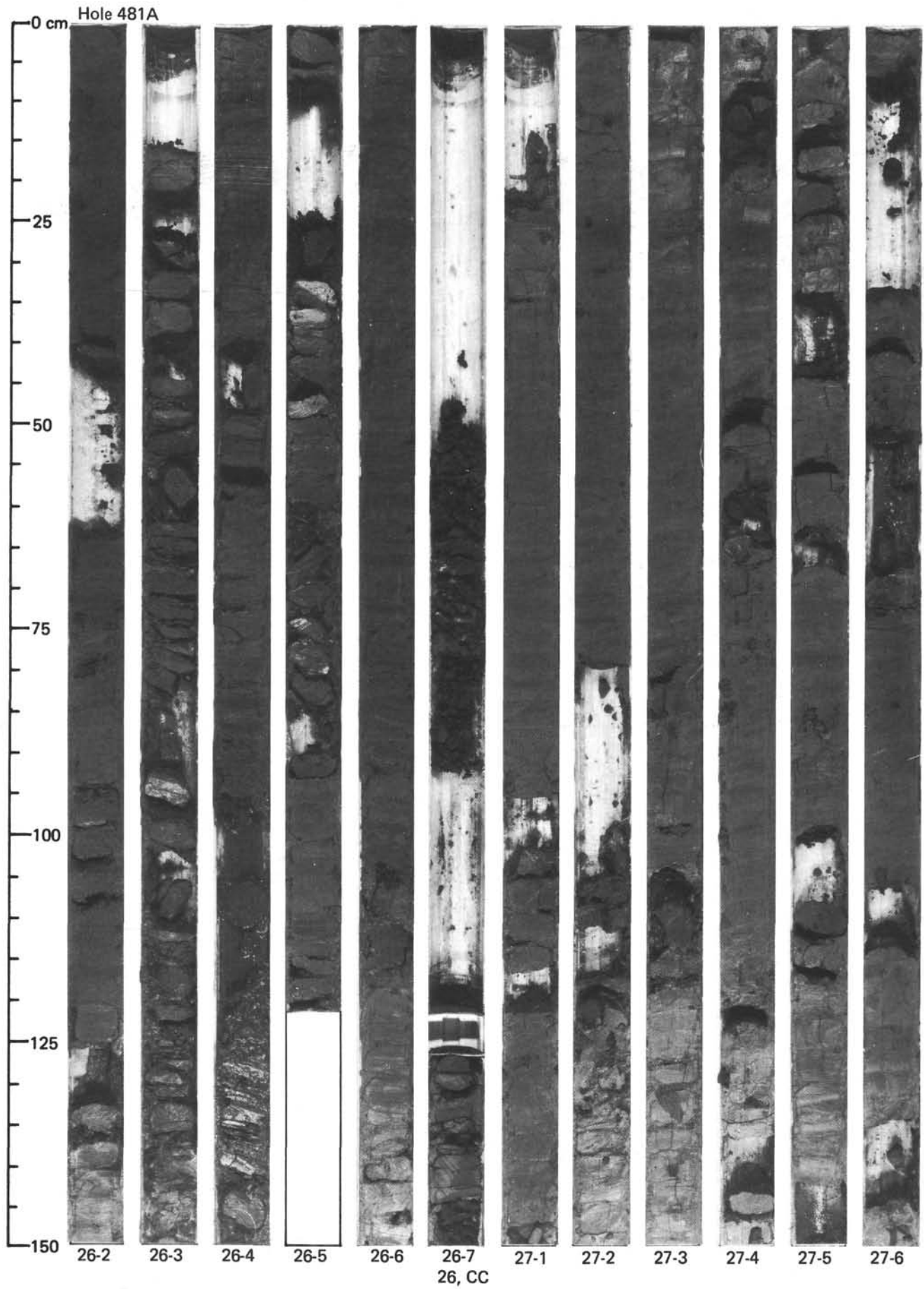
GUAYMAS BASIN SITES





GUAYMAS BASIN SITES





GUAYMAS BASIN SITES

